ANALYSIS OF THREE-DIMENSIONAL TALL BUILDING STRUCTURES

by

HRAND KHACHATOORIAN, B.Sc.

A thesis presented for the degree of

Doctor of Philosophy

of the University of Glasgow

Department of Civil Engineering, May 1984

University of Glasgow.

DEDICATED TO MY PARENTS

ACKNOWLEDGEMENTS

The author wishes to express his gratitude and appreciation to Professor A. Coull, Regius Professor of Civil Engineering, University of Glasgow, for his supervision, guidance, encouragement and invaluable advice during the course of study and throughout the preparation of this thesis.

Grateful thanks are also due to:-

Professor H.B. Sutherland, Cormack Professor of Civil Engineering, for his help and general advice on various occasions.

My colleagues, Dr. M. Memon, Dr. A. Al-Manasser, Mr. J. Tubman, Mr. J. Burns, Mr. J. Baird, Mr. C.K.Wong and Mr. D. Ponniah for their company and useful discussions.

University of Glasgow and the Committee of Vice-Chancellors and Principals of the Universities of the United Kingdom for their support regarding the partial fulfilment of my tuition fees.

Mrs. A. Baran for her neat typing of the manuscript.

My parents for their moral and financial assistance throughout my education, without which this work would not have been possible.

Last but not least to my brothers for their encouragement and continuous interest regarding my education.

SYNOPSIS

The elastic analyses of three-dimensional symmetric and asymmetric structures consisting of various load bearing elements have been presented in this thesis.

Based on the continuous connection technique, closed-form solutions have been presented for the particular cases of uniform symmetric cross-wall and wall-frame structures subjected to distributed lateral loads. A modification to the continuum method of analysis of wall-frame structures has been made to allow the base flexibility of the two components to be included.

The analyses have been extended to structures consisting of cores, coupled shear walls and rigidly-jointed framework assemblies, and also to structures which consist of two different sets of coupled shear walls, cores and frames.

Based on the folded plate theory and the continuum approach solutions have been presented for asymmetric partially closed core structures subjected to torsional loading. Transformations have been derived to enable a symmetrical building structure subjected to torsion to be analysed as an equivalent plane structure subjected to in-plane bending forces.

An approximate method of analysis has been presented for asymmetric structures subjected to bending and torsional loading. In order to examine the validity and accuracy of the methods presented three example structures which were analysed previously by various investigators have been considered. Finally, a parameter study has been carried out to assess the relative importance of the various structural parameters.

C O N T E N T S

C H A P T E R 1

INTRODUCTION

CHAPTER 1

INTRODUCTION

1.1 General

Buildings in general can be regarded as one of the most significant signs of civilization. In the past, engineers and architects have designed and constructed buildings which have related closely to the cultural, social and economic needs of their era. In fact buildings are often described as expressing the power and socio-economic development of any society[1], and this is clearly the reason why ancient Egyptian, Persian, Greek and Roman designers planned some of the most magnificent monumental structures built some hundreds, or thousands, of years ago.

Although various forms of buildings have been designed by engineers throughout the centuries, the designing and erection of tall buildings in a systematic and scientific way is almost wholly a 20th century development.

The socioeconomic developments in industrialised nations, especially the United States, have increasingly required the construction of tall apartment and office buildings in urban areas. This is due to increase in population and postwar affluence on one hand, and scarcity and high costs of land on the other. As a result, a large number of tall buildings have been constructed to meet these social and economic demands.

While there is no general agreement as to what constitutes a tall building, from the structural engineer's point of view, a tall building is one whose planning, or design, or operation and use is influenced by the quality of "tallness". Thus it is not the absolute height nor number of storeys that counts.[2]

After the second world war the need for more economic and safer tall building structures has encouraged engineers throughout the world to look for new philosophies and strategies for designing tall buildings. Up to that time, most buildings were designed in a conventional way; that is, structural engineers connected columns and beams together to create a structural grid for resisting lateral forces in both directions as well as innate gravitational loads. In such a rigid-frame type of system, the building's resistance to lateral forces stemmed from the rigidity of the column-beam connections[3], Fig. 1.1 . A large number of research activities together with the greater refinement in analysis which the computer has allowed, has led to the development of new structural systems and a re-examination of the more conventional structural forms aimed at achieving greater efficiency with respect to lateral load resisting functions.

The structural units which may be adopted for providing lateral stiffness to buildings are essentially frames, cores, shear walls or their combinations, in conjunction with the

floor systems. The basis of the classification is the mode of deformation of the system when subjected to lateral loading. Frames deform in a predominantly shear mode, Fig. 1.2(a), while single walls deform in an essentially bending mode as illustrated in Fig. 1.2(b). When the two units are constrained to deflect together by the stiff floor slabs, considerable redistribution of lateral forces occurs throughout the height of the building with heavy interactions near the top and bottom, Fig. 1.2(c).

Any of the structural units mentioned above, singly or in combination , form a structural system. However, each of these systems tends to be more suitable for a particular range of height from an economic point of view. Table 1.1 presents a preliminary guide to the selection of a structural system[4].

The selection of an appropriate system for a specific height of building helps the structural engineer to utilize his building materials more efficiently and hence reduce the building costs. For example, for a sixty storey building, the cost difference between a rigid-frame system against a more suitable structural system (i.e. tube in tube) is very large indeed. The former would require roughly double the amount of steel.

Figs. 1.3(a), 1.3(b) and 1.3(c) show typical plan layouts of shear wall, shear wall-frame and coupled shear wall

core-frame systems for tall buildings.

1.2 Review of Previous Research

In the past two decades a large number of methods for the analysis of tall building structures have been presented, many of which have found application in the design office. Some of the methods presented are applicable to the elastic analysis of tall buildings, while some are suitable for the elasto-plastic analysis of such buildings. Since this thesis is concerned with the elastic analysis of tall building structures, the publications considered for the literature review relate only to the elastic analysis of these structures.

The most important methods developed and in use for the analysis of the structural units present in a tall building are; the frame analogy method, the finite element method and the continuous connection technique.

The frame analogy method is simply an extension of the stiffness method of analysis of conventional frames. The wall is analysed as a frame, except that the finite width of the wall is incorporated by stiff arms connecting the ends of the beams to the centroidal axes of the wall, and the beams are assumed to be infinitely stiff from the neutral axis of the wall to the edge of the actual opening. The method can take into account changes in wall thickness,

storey height, opening sizes, and concrete elasticity at various locations within the height of the building. Any combination of load cases can be considered. A solution may be derived by standard matrix procedures using any of the widely available computer framework programs.

The technique appears to have been used first by MacLeod[5,6] in the analysis of coupled shear wall structures. Further developments were due to Kratky and Puri[7] who developed a subroutine to modify a standard framework program, thereby achieving the same result, and Schwaighofer and Microys[8] who used a framework analysis program that incorporates a variable member stiffness subroutine.

In the finite element method of analysis, the continuous structure is divided into a mesh of two-dimensional elements connected at their nodes. Simplified assumptions are made for the mode of deformation or stress distribution in each element, from which the stiffness matrix corresponding to the nodes is established. Then by combining these element stiffnesses, the total stiffness matrix for the structure is formed. Following the same procedure to that for a frame analysis a solution for the nodal displacements and forces may be achieved. This method is well established and has generally been used for checking accuracy of the results obtained by other techniques. The finite element method is highly versatile in that variations in geometry and loading can be taken into account but a digital computer is a pre-

requisite for this method. The finite element method is not suitable for the analysis of the overall three-dimensional structures because of its time and cost limitations. However, it is particularly useful for the detailed analysis of localized stresses and displacements in complex situations.

The continuous connection technique is probably the only method suitable for hand calculations and it can easily be programmed for small computers. In the case of coupled shear walls, the usual assumptions of the continuous technique are that the discrete set of connecting beams or floor slabs may be replaced by an equivalent continuous medium of same overall stiffness. Since both walls are assumed to deflect equally at all heights, so their slopes are the same, and hence the connecting beams deflect with a point of contraflexure at mid-span. If the connecting medium is then assumed 'cut' at the line of contraflexure , the only forces acting at that position are shear flow and axial force intensities per unit height. The behaviour of the structure may be expressed by a second order differential equation. Closed-form solutions may be achieved for standard load cases, enabling the complete distribution of forces and deflections to be determined for the uniform coupled shear walls.

The continuous technique has been used by many investigators, for the analysis of two-dimensional systems.

It was first applied to the approximate analysis of coupled shear walls by Beck[9] who used the shear forces in the connecting medium as the statically indeterminate function and treated the single case of uniform coupled shear walls on rigid foundation, subjected to a uniformly distributed lateral load. More comprehensive studies were followed by Rosman[10,11] who derived solutions for a wall with two symmetric bands of openings, with various conditions of support at the lower end (piers on rigid basement, on separate foundations, and on various forms of column supports). Two loading cases, a uniform wind pressure, and a point load at the top of the building were considered.

Using the continuum approach Coull and Choudhury[12,13,14] developed closed-form solutions based on vertical cantilever beam concepts and presented curves for rapid calculation of the stresses, maximum deflections, axial forces in connecting beams and shear forces in any system of coupled shear walls subjected to uniformly distributed, and concentrated point loads at the top. The basic analysis was then extended by Coull and Puri to cover the cases where the wall thickness [15] and cross-sections[16] are variable. There are relatively few published works available which deal with foundation deformation criteria in tall buildings; perhaps the most readily available and convenient are those developed by Tso and Chan[17], and Coull[18] who presented an analysis for coupled shear walls supported on

elastic foundations and subjected to the simple lateral load cases of a uniformly and triangularly distributed load and a point load at the top. Coull[19] also considered the effects of a finite differential settlement between the foundations of two coupled shear walls.

Many investigators presented simplified theories for the analysis of three-dimensional symmetric structures which may be reduced to equivalent plane systems. Based on the continuous connection technique, Heidebrecht and Stafford Smith[20] devised a method for the analysis of symmetric structures consisting of shear walls and rigidly-jointed frame assemblies. The method is suitable for the static analysis of uniform and non-uniform planar structures, and for dynamic analysis of uniform structures.

Using the continuum approach, Coull[21] presented a method for the analysis of regular symmetric structures consisting of coupled shear walls and cores. He considered the shear flow intensity in the connecting beams of the coupled shear walls as the unknown variable. The solution for the shear flow was then used to determine the deflections and the internal forces. Stafford Smith and Abergel[22] presented a method for the analysis of structures of the form considered by Coull[21]. In their analysis coupled shear walls and cores were transformed into a single coupled shear wall with modified parameters. Expressions were given for the horizontal deflections and the internal forces. Arvidsson[23] devised a method for structures consisting of coupled shear

walls and frames. His method is based on the continuum approach and the complementary energy theory, and a solution was obtained by Euler's formula.

Despite a large amount of research carried out on the behaviour of tall building structures, published studies which deal with the analysis of three-dimensional systems are few in number. In an asymmetric structure which consists of different load bearing units, such as independent and coupled shear walls, rigidly-jointed frameworks, and open box-type cores, lateral forces resulting from wind and/or earthquake action produce both lateral and torsional displacements. Relatively little work has been done in this particular area, and the problem is further complicated if warping of the core assemblies due to the in-plane deformations of the floor slabs are considered.

In many current structural forms of tall buildings, the lateral resistance of the structure is provided entirely or partly by the central core which contains the lift shafts, stair wells and other service ducts. Due to an asymmetry of the structural layout or to an eccentric alignment of lateral loads torsional as well as bending deformations may be induced in the core walls.

The torsional analysis of core structures has been presented by many investigators. Based on Vlasov's theory and stiffness matrix analysis Stafford Smith and Taranath[24]

devised a method in which particular attention was paid to the warping displacements and the associated stresses which accompany torsional displacements. The basic features of the theory relating the rotations, bimoments and warping stresses were presented, neglecting the effect of the connecting beams and the floor slabs. The method was then extended to include the effects of the connecting members. Tso and Biswas[25] presented a method of analysis which was based on Vlasov's theory and continuous connection technique. The governing differential equation was obtained by equilibrium consideration of the internal and applied torques.

Based on the folded plate theory, Tawfik[26] presented a method in which the core was considered as an assembly of vertical panels rigidly connected along their edges, the influence of openings in any of the panels was included by the use of the continuous connection technique.

A comprehensive report describing various numerical methods for analysis of three-dimensional structure up to 1972 was presented by Stamato[27]. The methods presented assumed linear elastic behaviour of the structural members and were classified into three categories; continuous methods, simplified discrete methods, and refined discrete methods. Using a stiffness matrix analysis Clough and King[28] devised a method for the multistorey frame structures. The

method of analysis was intended to be programmed for solution by a digital computer and the basic features of the program written for the IBM 7090 were described. Winkur and Gluck[29] presented a method which considered the structure subdivided into main structural units for which the separate in-plane stiffness matrices were determined. Equations were formulated for the combinations of the units to the equilibrium of the floors with respect to translations along a pair of arbitrary orthogonal horizontal axes, and the rotation about an arbitrary vertical axis. Their solution gave values for the translations and rotation of each floor, and hence in-plane displacements of each unit, from which the unit actions were determined. Stamato and Mancini[30] presented a method which was based on the continuous approach and matrix analysis. In the analysis frame assemblies were replaced by equivalent shear cantilevers. Solutions were derived for the deflection rotation and the internal forces. Wynhoven and Adams[31] analysed three-dimensional wall-frame structures by employing slope-deflection equations to formulate equations of equilibrium for the structure. These equations were then arranged in matrix form and solved for the unknown displacements by using a modified Gauss Elimination technique. In a further study using model structures they[32] considered the influence of torsional displacements throughout the structure.

An approximate analysis for the asymmetric wall-frame structures which is based on decoupling of the coupled

torsion-bending differential equations of equilibrium was developed by Rutenburg and Heidenbrecht[33]. The equilibrium equations were decoupled by using an orthogonal transformation. The deformations and stress resultants in the wall and frame assemblies were obtained by combining the respective coefficients which had been tabulated from the solved decoupled equations.

Using an approximate frame analysis Mortelmans, Roeck and Van Gemert[34], and Haris[35] devised methods for the approximate analysis of high-rise buildings which consist of wall and frame assemblies; the former method leads to a system of four simultaneous linear equations, which can be solved with a pocket calculator, while the latter is an approximate stiffness method which requires a computer for analysis.

Coull and Irwin[36] presented an approximate method for the torsional analysis of three-dimensional structures consisting of parallel assemblies of coupled shear walls and core elements. In this method the continuum technique is used to determine the flexibility matrix of each assembly, and by inversion the stiffness matrix is obtained. After determining the component stiffness matrices the complete structure is solved by matrix analysis.

A simplified method of analysis of three-dimensional buildings whose structure consists essentially of parallel

systems of shear wall assemblies and box-core elements was presented by Coull and Adams[37]. In this method it was assumed that the load distribution on each element could be represented with sufficient accuracy by a polynomial in the height coordinate. Due to ill-conditioning of the matrices involved this assumption led to errors at higher and lower storey levels of the building. The method was later extended by Coull and Mohammed[38] to include rigidly jointed frames in the analysis, and in order to obtain more accurate results a top concentrated interactive force was added to the polynomial load distribution on each assembly.

The first international symposium on tall buildings was held in the Department of Civil Engineering, University of Southampton[39] in April 1966. Since then a number of regional conferances and symposia have been held all over the world. A major event was the International Conference on Planning and Design of Tall buildings which took place at Lehigh[2] University in August 1972. These conferences produced several valuable papers on the design and analysis of tall building. A very useful collection of papers was published by the American Concrete Institute[40] and more recently a comprehensive series of monographs on the planning and design of tall buildings was published by the American Society of Civil Engineers[1].

1.3 Reasons for Present Study

Most of the studies on the three-dimensional analysis of tall buildings are related either to the flexural behaviour of symmetrical systems or the torsion-bending analysis of structures with relatively simple structural layouts. However, many of these methods require the use of a computer, and may also require special programming. Few of the methods presented are suitable for rapid hand calculation by practising engineers in the preliminary proportioning of components at the initial stages of the design process. As a result, methods of analysis which are less dependent on large scale computers are highly desirable.

1.4 Scope of the Thesis

This thesis is devoted to the "exact" analyses of three-dimensional symmetric and asymmetric structures, which consist of combinations of different load bearing elements, such as shear walls, coupled shear walls, cores, and rigidly-jointed frameworks, subjected to lateral forces which produce bending and torsion. By using the continuous medium approach, and representing a frame by an equivalent shear cantilever, closed-form solutions to the problems are possible. Closed-form solutions may be achieved for standard load cases, enabling the complete distribution of forces and deflections to be determined and design curves to be produced.

In chapter 2, the analysis of coupled shear wall-core and wall-frame symmetrical structures subjected to bending have been considered. Frames have been represented by equivalent shear cantilevers and the effects of shearing deformations which occur in the frame at the base level, and the base shear which results have been investigated. Two numerical examples have been considered.

In chapter 3, the analysis of symmetrical structures consisting of assemblies of identical coupled shear walls, cores, and frames subjected to bending has been studied. In order to illustrate the typical behaviour of such systems a numerical example has been considered.

In chapter 4, the analysis of symmetrical structures consisting of two different groups of coupled shear walls and cores subjected to bending has been considered. The analysis has then been extended to include framework assemblies. The typical behaviour of such structures has been demonstrated by a numerical example.

Chapter 5 describes the torsional analysis of symmetric and asymmetric core structures. The folded plate and continuum techniques have been used for the analysis.

Chapter 6 includes the torsional analysis of symmetric coupled shear wall structures, shear wall-core structures, and shear wall-core-frame structures. The torsional

analysis of symmetric structures consisting of shear walls, coupled shear walls, cores and frames has then been formulated.

In chapter 7, the analysis of asymmetric structures consisting of parallel assemblies of cores, shear walls and frames subjected to bending and torsion has been considered. The analysis has then been extended to include frame assemblies in two orthogonal directions.

Chapter 8 describes comparison of the results from present analysis with other published works, and a numerical parameter studies together with relevant discussions.

Chapter 9 includes the conclusions drawn from the above studies and suggestions for future work.

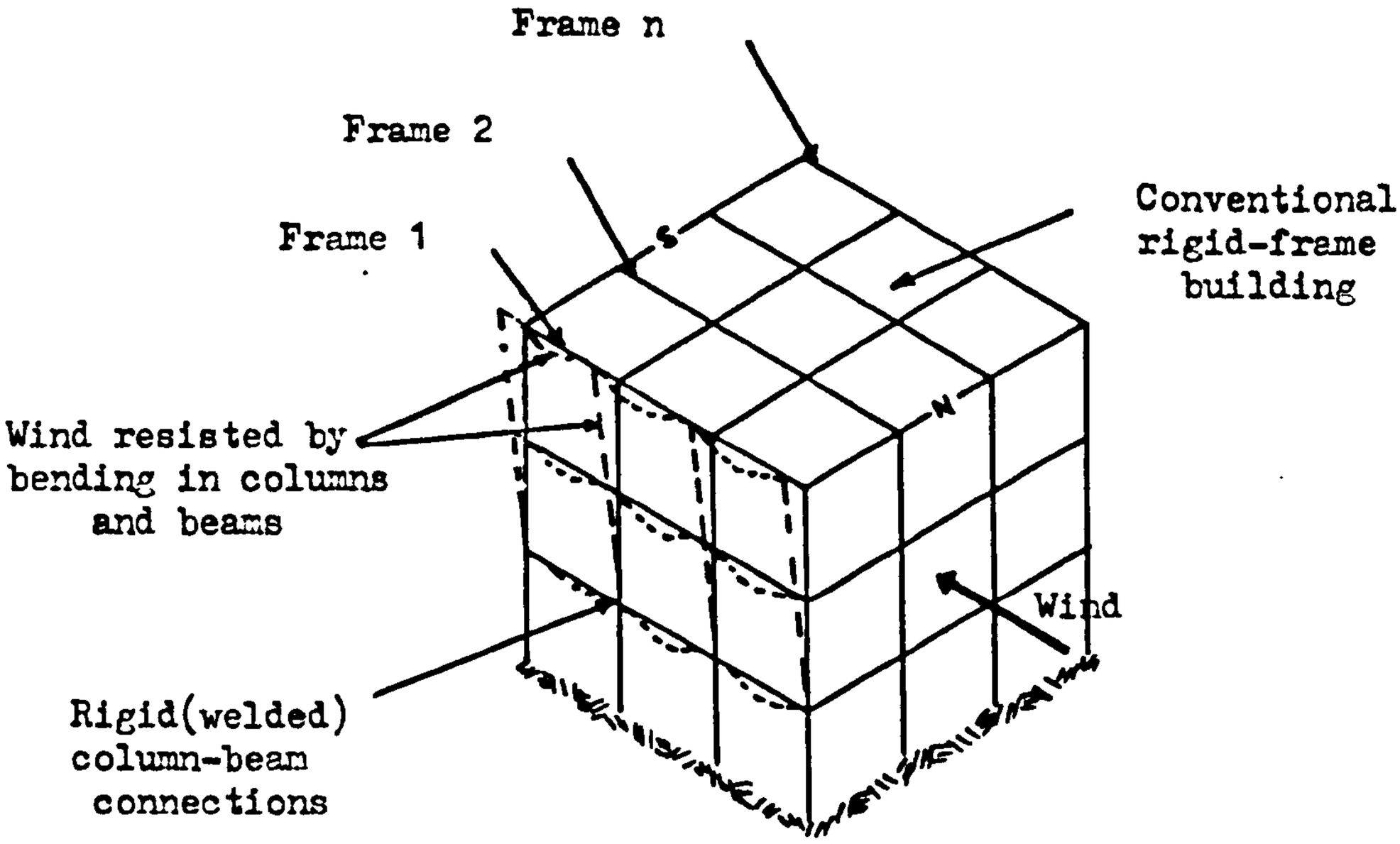

Years ago,most steel-frame high-rise buildings resisted wind forces with a rigid frame system: winds were resisted by bending in columns and beams. But "bending" is a poor way to tap a structural members strength. Better to fashion a structural system so only axial compression and tension forces are imposed on members, as is done in buildings with X-braced cores or perimeter tubes.

Fig.1.1

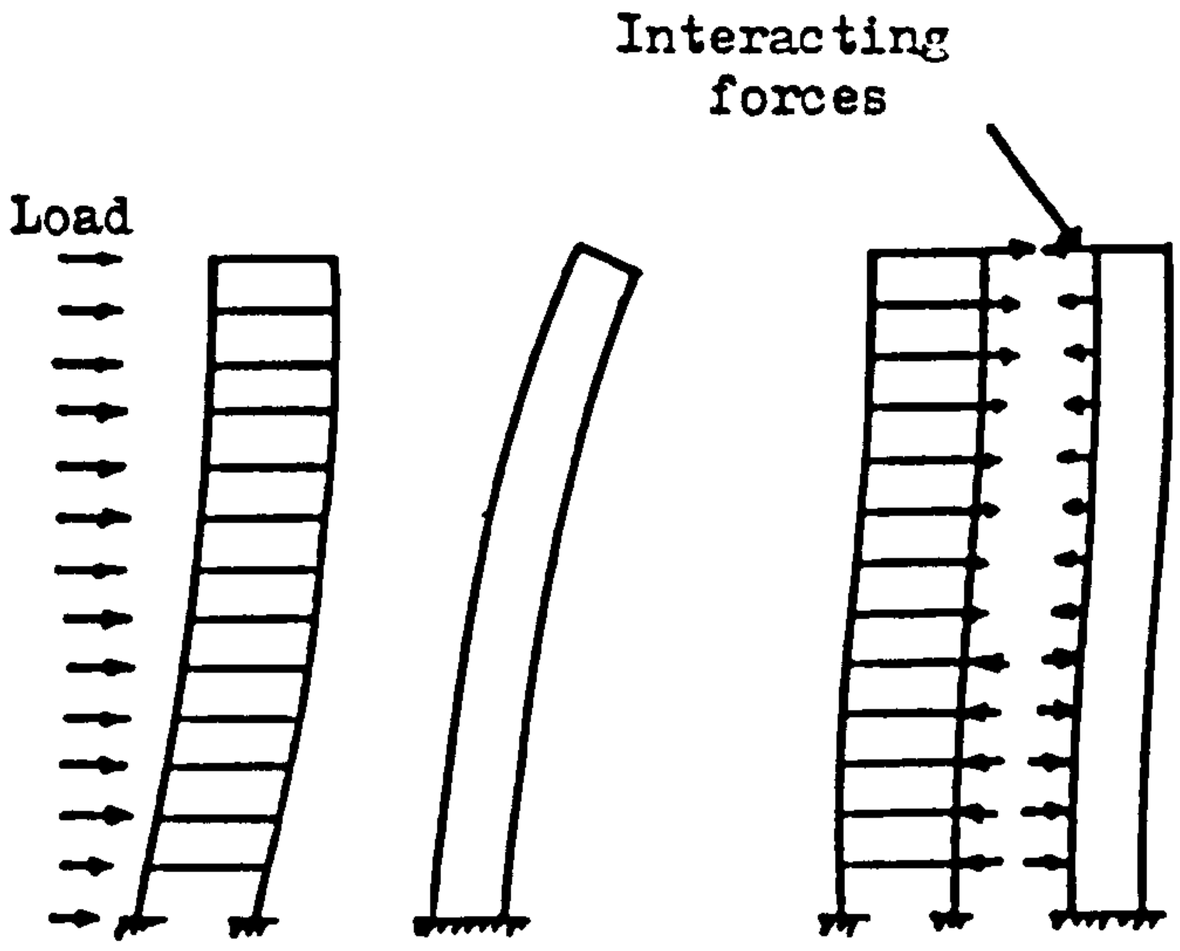

(a) Rigid frame shear mode deformation

(b) Shear wall bending mode deformation

(c) Interconnected frame and shear wall(equal deflections at each storey level)

Fig.1.2

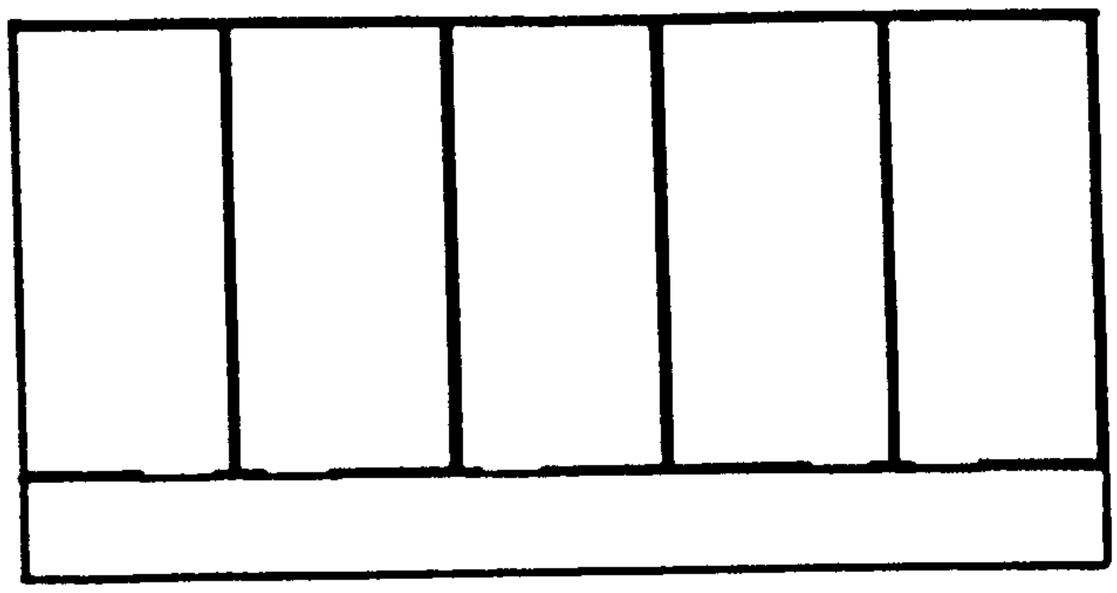

No openings in walls: access from outside

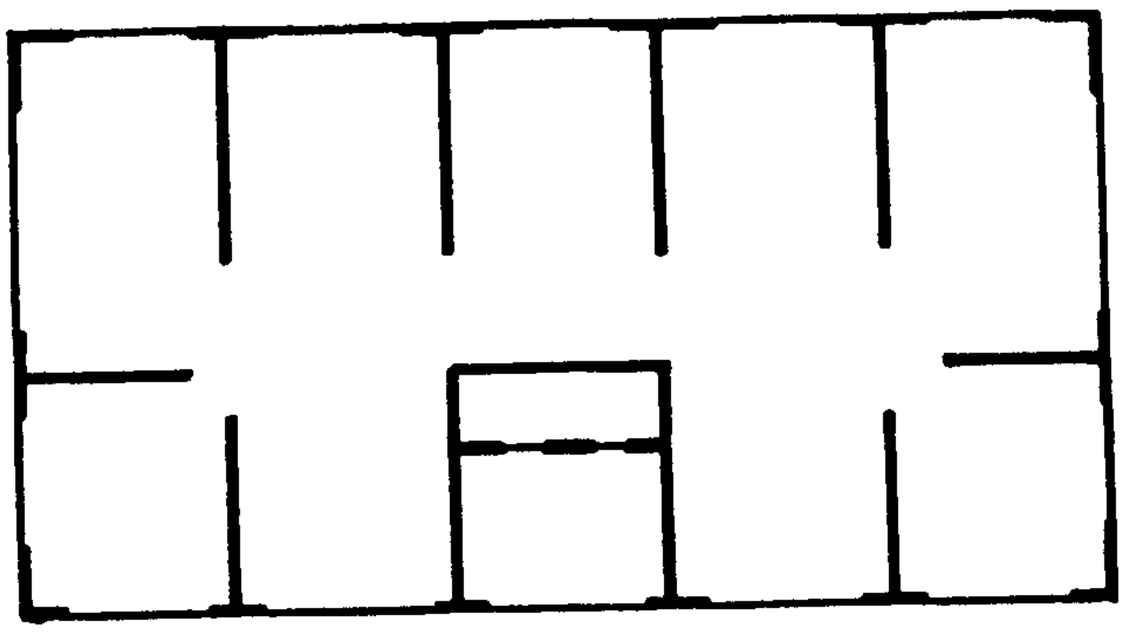

Coupled walls

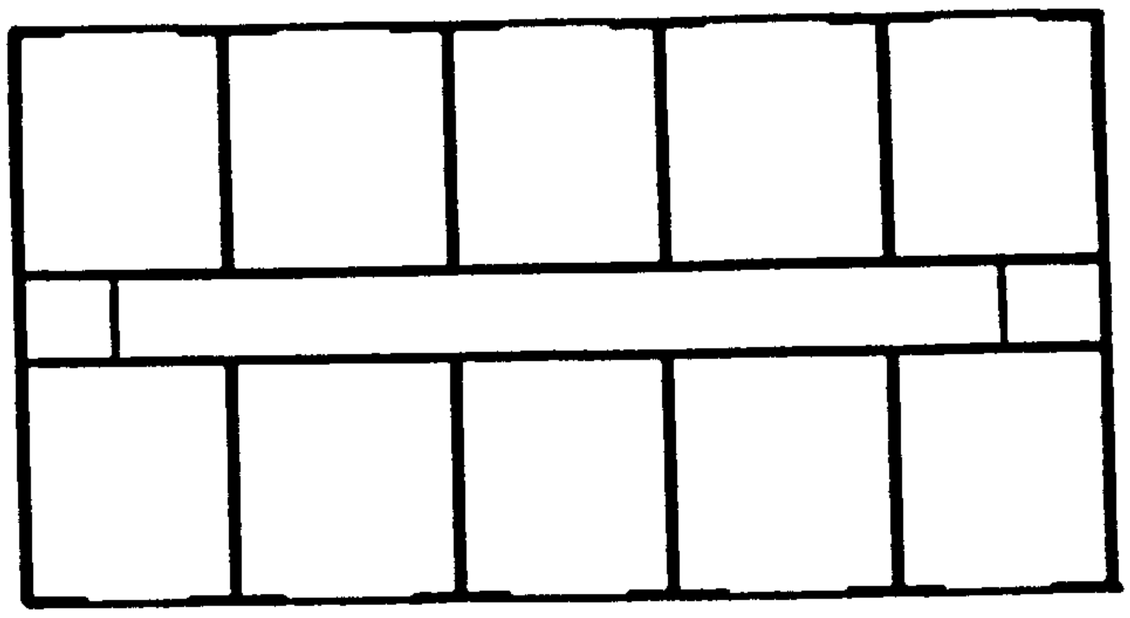

Longitudinal corridor walls

Fig.1.3(a) Typical layouts of shear walls

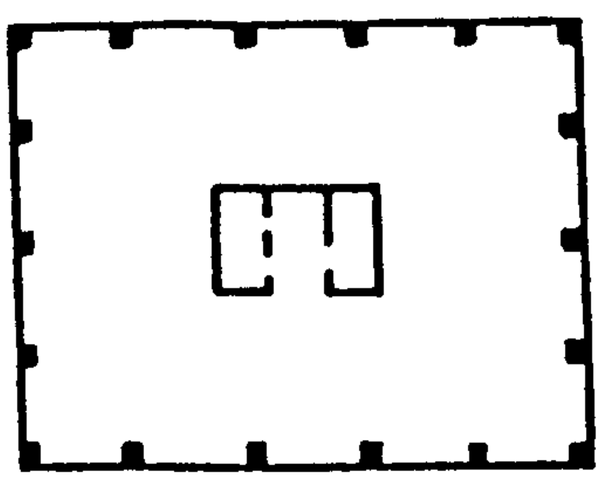

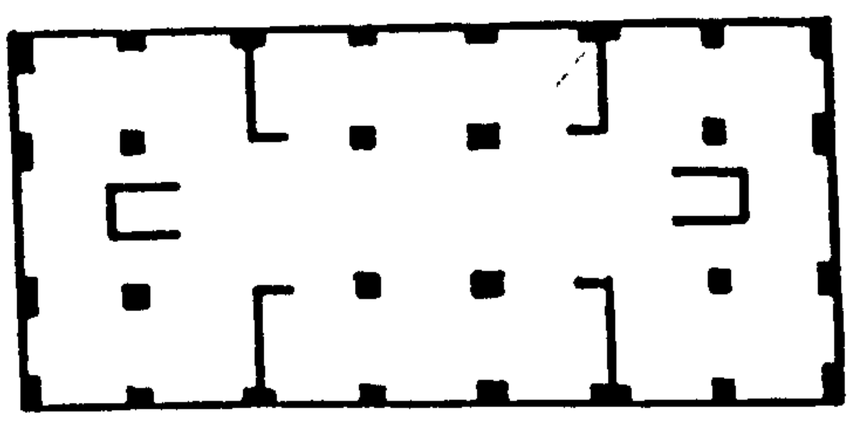

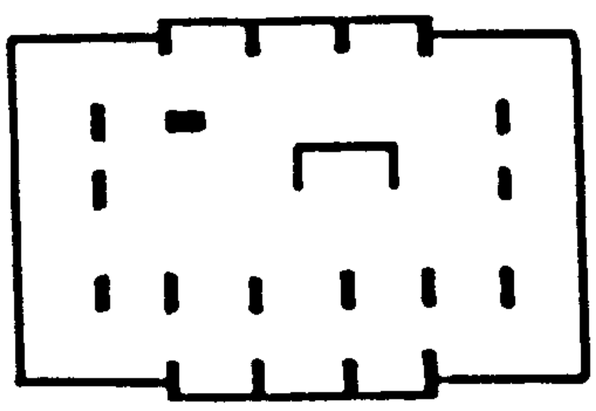

Fig.1.3(b) Typical layouts of high-rise buildings with shear wall-frame interaction

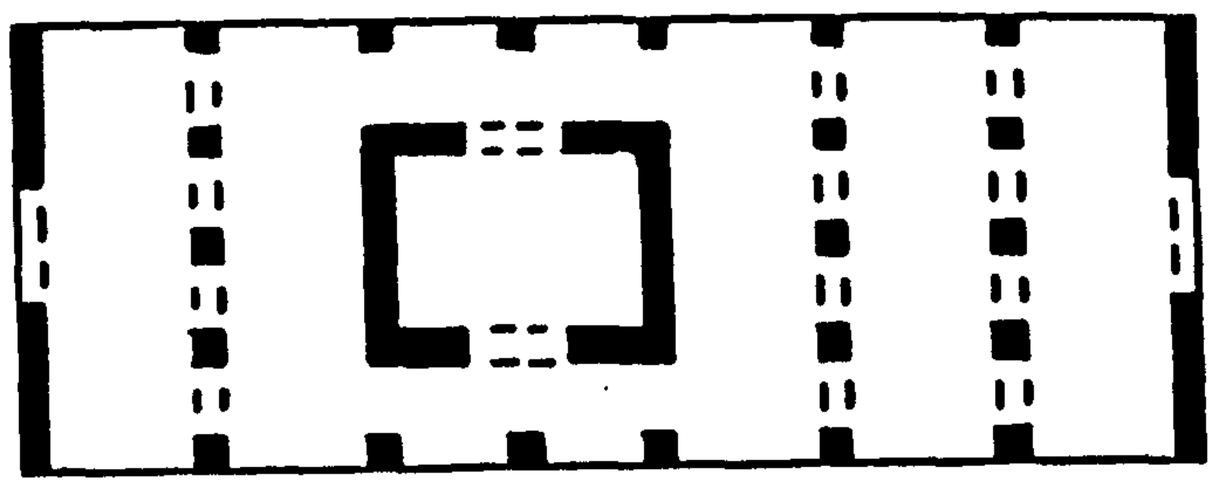

Fig.1.3(c) Typical layout of a high-rise building with coupled shear wall-core-frame interaction

GUIDE TO SELECTION OF STRUCTURAL SYSTEMS

Structural system	Section in report	Number of storey's		Seismic behaviour
		Office buildings	Apartment buildings, etc.	
Frame	5.2	Up to 15	Up to 20	Very good
Shear wall(egg-crate)	5.3		Up to 150	Good
Staggered wall beam	5.4		Up to 40	Good
Shear walls acting with frames	5.5	Up to 40	Up to 70	Good
Single framed tube	5.6	Up to 40	Up to 60	Very good
Tube-in-tube	5.7	Up to 80	Up to 100	Good

Table 1

C H A P T E R 2

BENDING ANALYSIS OF SYMMETRIC COUPLED SHEAR WALL-CORE, AND WALL-FRAME STRUCTURES

NOTATION

A_1, A_2	cross-sectional areas of coupled walls
b	clear span between coupled walls
E	elastic modulus
h	storey height
H	total height
I_i	second moment of area of wall i (i = 1,2,3)
I	$I_1 + I_2 + I_3$
I_c	second moment of area of connecting beams
l	distance between centroidal axes of coupled walls
M_i	bending moment in wall i (i = 1,2,3)
M	static applied moment
N	axial force in coupled walls
n_i	axial force in connecting media (i = 1,2)
Q_i	concentrated interactive forces (i = 1,2)
q	shear force intensity in connecting medium of coupled shear walls
S_i	shear force in wall i (i = 1,2,3)
ω	uniformly distributed lateral force intensity
y	lateral deflection
α, β	structural parameters
k	parameter αH
ξ	non-dimensional height (x/H)
ϕ_1	axial force function
ϕ_2	shear flow function in connecting beams
ϕ_3	axial force function in coupled walls
ϕ_4	top deflection function

ϕ_5, ϕ_6	maximum moment functions in coupled walls and core respectively
GA	effective shearing rigidity of shear cantilever
S_w	shear force in shear wall
S_f	shear force in frame
M_w	bending moment in shear wall
M_f	bending moment in frame
θ	base slope
A_w	effective shear area of shear wall
GA_w	shearing rigidity of shear wall
ϕ	shearing rigidity ratio
S_o	base shear
M_o	base moment
x	height above base

CHAPTER 2

BENDING ANALYSES OF SYMMETRIC COUPLED SHEAR WALL-CORE, AND WALL-FRAME STRUCTURES

2.1 Introduction

In many tall building structures the resistance to lateral forces is provided by coupled shear walls, core and frame assemblies. Careful arrangement of these elements in a tall building can also provide the architectural functions of dividing and enclosing space, and providing fire and acoustic insulation between dwellings. When these assemblies are subjected to distributed lateral loads, their modes of behaviour are different. A cantilever core or an independent shear wall deforms in a bending mode, a frame in a shear mode, and a coupled shear wall system bends with a reversal of curvature in the higher levels. However, in a typical tall building structure these elements are constrained to act together by floor slabs, and, as a result, when subjected to lateral forces a considerable redistribution of load may occur throughout the height of the building.

If the structural layout and the loading are symmetrical the three-dimensional structure may be replaced by an equivalent plane system in which the various load bearing elements are connected together in series by pin-ended rigid links.[20,21] The links simulate the actions of the

floor slabs, which are assumed rigid in their own plane but flexible out of plane.

In this chapter, analyses are presented for symmetrical coupled shear wall-core and wall-frame structures by using the continuous connection technique.

To simplify the analysis it is assumed that a frame assembly may be replaced by an equivalent shear cantilever which has the same effective stiffness. Closed-form solutions may be achieved for standard load cases, enabling the complete distribution of forces and deflections to be determined rapidly. In order to demonstrate the typical structural response of such systems, two numerical examples are considered. In the analysis of symmetrical wall-frame structures, the shear cantilever representation of frame elements is discussed in detail, and an extension to the analysis is presented to allow shearing deformations of both walls and frames at ground level to be included, and allow an assessment to be made of the shears carried by the frame.

2.2 Analysis of regular symmetric coupled shear wall-core Structures

Consider a three-dimensional regular symmetric structure which consists of assemblies of identical coupled shear walls, box cores and floor slabs, as shown in Fig. 2.1(a). Due to the high in plane rigidity of the floor slabs, it is assumed that each horizontal section of the structure

undergoes only a rigid body movement. A simplified analysis can then be presented by replacing the three-dimensional structure by an equivalent plane system, in which, the various elements are constrained to act in series by a set of pin-ended rigid members, which are assumed to simulate the actions of the floor slabs. Fig. 2.1(b) shows the plane system which is used for the initial analysis.

2.2.1 Assumptions

The following assumptions are made for the analysis:

(i) The coupled shear walls have uniform sectional properties, spacing and dimensions throughout the height and are rigidly built in at the base.

(ii) The coupling beams have uniform sectional properties, spacing and flexural rigidities.

(iii) The independent shear wall or box core has uniform sectional properties and dimensions throughout the height of the building and is rigidly fixed at the base.

(iv) The axial deformations in the connecting beams are negligible and the coupled shear wall and core assemblies deflect equally. Hence, the coupling beams deflect with a point of contraflexure at their mid-span.

2.2.2 Analysis

Consider initially the plane system shown in Fig.21(c). The basic idea of the continuum approach is the replacement of the discrete set of connecting beams of flexural rigidity EI_c by an equivalent continuous system of laminas of flexural rigidity $EI_{c/h}$ per unit height. If a vertical cut is now made at the line of contraflexure in the continuous medium (Fig. 2.1(d)), the only forces present at that position are shear and axial forces of intensity q and n_1 per unit height respectively. Under the action of external and internal forces, there is no relative vertical movement at the cut section. Therefore, at any height x, the compatibility equation may be shown to be

$$l\frac{dy}{dx} - \frac{b^3h}{12EI_c}\,q - \frac{1}{E}\left(\frac{1}{A_1}+\frac{1}{A_2}\right)\int_0^x\int_\eta^H q(\lambda)\,d\lambda\,d\eta = 0 \qquad (2.1)$$

The three terms in equation (2.1) are, the relative displacement due to bending of the walls under external load, the deflection due to bending and shear of the cantilevered lamina, and the relative displacement of the walls due to axial forces, respectively.

In equation (2.1)

l = distance between wall centroids

b = clear span of the coupling beams

h = storey height

E = Young's modulus

I_c = second moment of area of the coupling beams

A_1, A_2 = Cross-sectional areas of the walls

x = height above base

λ, η = auxiliary variables

y = horizontal deflection

In a similar manner, the set of discrete rigid pin-ended links between the coupled walls and the core element is replaced by a continuous medium which transmits an axial force of intensity n_2 per unit height. The equivalent structure and the loading pattern is shown in Fig. 2.1(d). The respective moment-curvature relationships at any height x for the coupled shear walls and core in Fig. 2.1(c) are

$$EI_1 \frac{d^2y}{dx^2} = M_1 = M - (\frac{b}{2} + d_1) \int_x^H q(\lambda)\, d(\lambda) - M_{a1} \qquad (2.2)$$

$$EI_2 \frac{d^2y}{dx^2} = M_2 = -(\frac{b}{2} + d_2) \int_x^H q(\lambda)\, d(\lambda) + M_{a1} - M_{a2} \qquad (2.3)$$

$$EI_3 \frac{d^2y}{dx^2} = M_3 = M_{a2} \qquad (2.4)$$

where d_1 and d_2 are the distances from the 'cut' section to the centroidal axis of the coupled walls (Fig. 2.1(d));

I_1, I_2 and I_3 are the second moments of area of wall 1, 2 and 3; M is the static applied moment, and M_{a1} and M_{a2} are the moments due to the axial forces in the two connecting media, given by

$$M = P\,(H - x) + \frac{1}{2}\,\omega\,(H - x)^2 + \frac{1}{6}\,\frac{u}{H}\,(H - x)^2(2\,H + x) \qquad (2.5)$$

$$M_{a1} = \int_x^H n_1(\lambda)\,(\lambda - x)\,d\lambda + Q_1\,(H - x) \qquad (2.6)$$

$$M_{a2} = \int_x^H n_2(\lambda)\,(\lambda - x)\,d\lambda + Q_2\,(H - x) \qquad (2.7)$$

Q_1 and Q_2 are the concentrated interactive forces which generally exist at the top of the connecting media as shown in Fig. 2.1(d), and

P = concentrated point load at the top of the structure

ω = uniformly distributed load intensity

u = triangularly distributed load intensity

On addition of equations (2.2), (2.3) and (2.4) the overall moment-curvature relationship is given by

$$EI\left(\frac{d^2y}{dx^2}\right) = M - 1\int_x^H q\,(\lambda)\,d\lambda \qquad (2.8)$$

where $I = I_1 + I_2 + I_3$

Differentiation of equation (2.8) with respect to x yields an expression for the shear flow q, given by

$$q = \frac{1}{l} \left(- \frac{dM}{dx} + EI \frac{d^3y}{dx^3}\right) \qquad (2.9)$$

Thus

$$\frac{dq}{dx} = \frac{1}{l} \left(- \frac{d^2M}{dx^2} + EI \frac{d^4y}{dx^4}\right) \qquad (2.10)$$

On differentiating equation (2.1) with respect to x, and substituting for $\frac{dq}{dx}$ and $\int_x^H q(\lambda)\, d\lambda$ from equations (2.10) and (2.8), the governing differential equation becomes

$$\frac{d^4y}{dx^4} - \alpha^2 \frac{d^2y}{dx^2} = \frac{1}{EI} \left[\frac{d^2M}{dx^2} - (\alpha^2 - \beta^2)\, M\right] \qquad (2.11)$$

where

$$\beta^2 = \frac{12 I_c l^2}{b^3 h I}$$

$$\alpha^2 = \beta^2 \left(1 + \frac{AI}{A_1 A_2 l^2}\right)$$

$$A = A_1 + A_2$$

The general solution of equation (2.11) is obtained by adding the complementary function and the particular integral solutions of the equation, and may be expressed in the form

$$y = C_o + C_1 x + C_2 \sinh \alpha x + C_3 \cosh \alpha x + y_{PI} \quad (2.12)$$

where C_o, C_1, C_2 and C_3 are constants of integration and y_{PI} is the particular integral solution. These quantities may be determined from the necessary boundary conditions and the specific loading pattern.

Boundary Conditions

The constants C_o, C_1, C_2 and C_3 may be determined by considering the top and bottom boundary conditions for the system. If the structure is rigidly built in at the base, $x = o$, then

$$y = o \quad \text{and} \quad \frac{dy}{dx} = o \quad (2.13)$$

At the top of the structure, there are no axial forces and bending moments. Thus, at $x = H$

$$\frac{d^2y}{dx^2} = o \quad (2.14)$$

From equations (2.1) and (2.13) it can be deduced that

q = o at x = o, hence from equation (2.9), at x = o

$$\frac{d^3y}{dx^3} = \frac{1}{EI} \frac{dM(o)}{dx} \qquad (2.15)$$

Uniformly Distributed Wind Loading

The differential equation (2.11) may be solved for the three standard load cases, the only essential difference being in the particular integral solution. However, in order to obtain a solution, consider the particular case of a uniformly distributed wind loading of intensity ω per unit height. In that case,

$$M = \frac{1}{2}\omega(H - x)^2 \qquad (2.16)$$

$$\frac{dM}{dx} = -\omega(H - x)$$

$$\frac{d^2M}{dx^2} = \omega$$

On substituting for M and $\frac{d^2M}{dx^2}$ in equation (2.11), it becomes

$$\frac{d^4y}{dx^4} - \alpha^2 \frac{d^2y}{dx^2} = \frac{\omega}{EI}\left[1 - \frac{1}{2}(\alpha^2 - \beta^2)(H - x)^2\right] \qquad (2.17)$$

The simplest particular integral part of the general solution then becomes

$$y_{PI} = \frac{-\omega}{4\alpha^2 EI}\left[\frac{2\beta^2}{\alpha^2} - (\alpha^2-\beta^2)\,H^2\right]x^2 - \frac{\omega H}{6\alpha^2 EI}(\alpha^2-\beta^2)\,x^3 + \frac{\omega}{24\alpha^2 EI}(\alpha^2-\beta^2)\,x^4 \qquad (2.18)$$

On substituting for the particular integral function in equation (2.12) the general solution becomes

$$y = C_o + C_1 x - \frac{\omega}{4\alpha^2 EI}\left[\frac{2\beta^2}{\alpha^2} - (\alpha^2-\beta^2)\,H^2\right]x^2 - \frac{\omega H}{6\alpha^2 EI}(\alpha^2-\beta^2)\,x^3 + \frac{\omega}{24\alpha^2 EI}(\alpha^2-\beta^2)\,x^4 + C_2 \sinh\alpha x + C_3 \cosh\alpha x \qquad (2.19)$$

Using the boundary conditions (2.13) to (2.15) the integration constants C_o, C_1, C_2 and C_3 may be found to be

$$C_o = -\frac{\omega\beta^2}{\alpha^6 EI \cosh\alpha H}(1+\alpha H \sinh\alpha H)$$

$$C_1 = \frac{\omega H}{EI}\frac{\beta^2}{\alpha^4}$$

$$C_2 = -\frac{\omega H}{EI}\frac{\beta^2}{\alpha^5} \qquad (2.20)$$

$$C_3 = \frac{\omega\beta^2}{\alpha^6 EI \cosh\alpha H}(1+\alpha H \sinh\alpha H)$$

Then, on substituting for (C_o)-(C_3) into equation (2.19), the general solution becomes

$$y = \frac{\omega H^4}{EI}\left\{\frac{1}{24}\left(1-\frac{\beta^2}{\alpha^2}\right)\left[(1-\xi)^4+4\xi-1\right]+\frac{\beta^2}{\alpha^2 K^2}\left[\left(\xi-\frac{\xi^2}{2}\right)-\frac{1+k\sinh k-\cosh k\,\xi-k\sinh k\,(1-\xi)}{k^2\cosh k}\right]\right\} \quad (2.21)$$

where

$$\xi = \frac{x}{H} \quad (2.22)$$

$$k = \alpha H$$

ξ and k are the non-dimensional height and stiffness variables respectively, and are used to emphasize the dependence of the solution on these two variables.

On differentiating equation (2.8) with respect to x and substituting for the deflection and moment functions from equations (2.16) and (2.21), the shear flow q in the connecting medium becomes

$$q = \frac{\omega\beta^2 H}{l\alpha^2}\left[1-\xi+\frac{\sinh k\xi-k\cosh k\,(1-\xi)}{k\cosh k}\right] \quad (2.23)$$

The axial force N in each coupled wall at any height x is given by

$$N = \int_x^H q\,(\lambda)\,d\lambda \qquad (2.24)$$

On substituting for shear flow q from equation (2.23) into equation (2.24) the axial force N becomes

$$N = \frac{\omega \beta^2 H^2}{1 \alpha^2} \left[\frac{1}{2}(1-\xi)^2 + \frac{\cosh k - \cosh k\xi - k \sinh k\,(1-\xi)}{k^2 \cosh k} \right] \qquad (2.25)$$

The moments in the walls can be obtained by considering equations (2.2), (2.3), (2.4) and (2.8) and are given by

$$M_i = \frac{I_i}{I}\,(M - 1\,N) \qquad (2.26)$$

where i = 1, 2 and 3 for walls 1, 2 and 3 respectively.

From equations (2.2), (2.4), (2.8) and (2.24), M_{a1} and M_{a2} are given by

$$M_{a1} = \left(1 - \frac{I_1}{I}\right) M + \left(\frac{I_1}{I} 1 - \frac{b}{2} - d_1\right) N \qquad (2.27)$$

$$M_{a2} = \frac{I_3}{I}\,(M - 1\,N) \qquad (2.28)$$

On differentiating equations (2.7) and (2.8) twice with respect to x, the distribution of axial force intensities

in the connecting media become

$$n_1 = \frac{d^2 M_{a1}}{dx^2} \qquad (2.29)$$

$$n_2 = \frac{d^2 M_{a2}}{dx^2} \qquad (2.30)$$

Hence, on substituting for M_{a1} and M_{a2} from equations (2.27) and (2.28) into equations (2.29) and (2.30), the axial force distributions n_1 and n_2 become

$$n_1 = \omega \left[\left(1 - \frac{I_1}{I}\right) - \frac{\beta^2}{\alpha^2_1} \left(\frac{I_1}{I} 1 - \frac{b}{2} - d_1\right) \phi_1 \right] \qquad (2.31)$$

and

$$n_2 = \frac{\omega I_3}{I} \left[1 + \frac{\beta^2}{\alpha^2} \phi_1 \right] \qquad (2.32)$$

where the axial force function ϕ_1 is

$$\phi_1 = \frac{1}{\cosh k} \left[\cosh k\xi + k \sinh k (1 - \xi) \right] - 1 \qquad (2.33)$$

The lateral force distributions in walls 1, 2 and 3 are then given by $\omega - n_1$, $n_1 - n_2$ and n_2 respectively.

A consideration of equations (2.31) and (2.32) demonstrates the possible errors involved in an assumption

commonly made in design that the externally applied loads are distributed between the walls in proportion to their flexural rigidities. The axial force function ϕ_1 can therefore be thought of, as a lateral force redistribution factor.

The variation of axial force function ϕ_1 for a range of values of stiffness variable k is illustrated in Fig. 2.2 .It can be deduced that coupled shear walls carry a larger proportion of the lateral loads in the upper levels and less in the lower levels. The curves also indicate that as the stiffness variable k increases, the redistribution of lateral loads between coupled shear walls and core elements becomes more significant at lower levels.

The shear forces in the coupled shear walls and core assemblies may be found by considering the conditions of equilibrium of a small vertical element of each structural unit (Fig. 2.1(e)). For the coupled shear walls, the shear forces S_1 and S_2 are

$$S_1 = -\frac{dM_1}{dx} + (\frac{b}{2} + d_1)q \qquad (2.34)$$

$$S_2 = -\frac{dM_2}{dx} + (\frac{b}{2} + d_2)q \qquad (2.35)$$

and, for the independent wall or box core, the shear force S_3 is

$$S_3 = -\frac{dM_3}{dx} \qquad (2.36)$$

Hence, on substituting for q, M_1, M_2 and M_3 from equations (2.23) and (2.26) into equations (2.34) - (2.36), the shear forces S_1, S_2 and S_3 become

$$S_1 = \omega H\left\{\frac{I_1}{I}(1-\xi) - \frac{\beta^2}{l\alpha^2}\left(\frac{I_1}{I}l - \frac{b}{2} - d_1\right)\left[(1-\xi) + \frac{\sinh k\xi - k\cosh k(1-\xi)}{k\cosh k}\right]\right\} \quad (2.37)$$

$$S_2 = \omega H\left\{\frac{I_2}{I}(1-\xi) - \frac{\beta^2}{l\alpha^2}\left(\frac{I_2}{I}l - \frac{b}{2} - d_2\right)\left[(1-\xi) + \frac{\sinh k\xi - k\cosh k(1-\xi)}{k\cosh k}\right]\right\} \quad (2.38)$$

$$S_3 = \frac{I_3}{I}\omega H\left\{(1-\xi) - \frac{\beta^2}{\alpha^2}\left[(1-\xi) + \frac{\sinh k\xi - k\cosh k(1-\xi)}{k\cosh k}\right]\right\} \quad (2.39)$$

At the base, $\xi = o$, the shear forces become

$$S_1 = \frac{I_1}{I}\omega H$$

$$S_2 = \frac{I_2}{I}\omega H$$

$$S_3 = \frac{I_3}{I}\omega H$$

i.e. irrespective of the relative stiffness of the coupled wall element, the base shear in the individual wall is always proportional to the flexural rigidity.

From equations (2.37) - (2.39) it is found that shear forces exist at the top of the structure in the various elements. These shear forces can only be caused by concentrated interactive forces at the top of each connecting medium, as shown in Fig. 2.1(d), such that

$$S_1(H) = -Q_1, \qquad S_2(H) = Q_1 - Q_2, \qquad S_3(H) = Q_2$$

Hence,

$$Q_1 = \omega H \left(\frac{I_1}{I}\right) 1 - \frac{b}{2} - d_1) \left[\frac{\beta^2}{\alpha^2 1} \left(\frac{\sinh k - k}{k \cosh k}\right)\right] \qquad (2.40)$$

$$Q_2 = -\frac{I_3}{I} \omega H \frac{\beta^2}{\alpha^2} \left(\frac{\sinh k - k}{k \cosh k}\right) \qquad (2.41)$$

Figs. 2.3 and 2.4 illustrate the variations at any level of the shear flow function ϕ_2 in the connecting beams, and the axial force function ϕ_3 in each coupled wall respectively.

Hence

$$q = \omega H \frac{\beta^2}{1\alpha^2} \phi_2$$

$$N = \omega H^2 \frac{\beta^2}{1\alpha^2} \phi_3 \qquad (2.42)$$

and ϕ_2 and ϕ_3 are given by

$$\phi_2 = 1 - \xi + \frac{\sinh k\xi - k \cosh k (1 - \xi)}{k \cosh k} \qquad (2.43)$$

$$\phi_3 = \frac{1}{2}(1 - \xi)^2 + \frac{\cosh k - \cosh k\xi - k \sinh k (1 - \xi)}{k^2 \cosh k} \qquad (2.44)$$

The maximum deflection which occurs at the top of the structure and the maximum moments which are present at the base of each assembly can be determined using equations (2.21) and (2.26). Hence

$$y_{max} = \frac{\omega H^4}{EI} \phi_4$$

$$M_{1+2}{}_{max} = \frac{1}{2} \omega H^2 \phi_5 \qquad (2.45)$$

$$M_{3}{}_{max} = \frac{1}{2} \omega H^2 \phi_6$$

where

$$\phi_4 = \frac{1}{8}(1 - \frac{1}{\mu}) + \frac{1}{\mu k^2} (\frac{1}{2} - \frac{1 + k \sinh k - \cosh k}{k^2 \cosh k}) \qquad (2.46)$$

$$\phi_5 = \frac{I_{1+2}}{I}\left[1 - \frac{2}{\mu} (\frac{1}{2} - \frac{1 + k \sinh k - \cosh k)}{k^2 \cosh k}\right] \qquad (2.47)$$

$$\phi_6 = \frac{I_3}{I} \left[1 - \frac{2}{\mu} (\frac{1}{2} - \frac{1 + k \sinh k - \cosh k)}{k^2 \cosh k}\right] \qquad (2.48)$$

and

$$\mu = \frac{\alpha^2}{\beta^2}$$

Figs. 2.5, 2.6 and 2.7 show the forms of functions ϕ_4, ϕ_5 and ϕ_6 for a range of values of the stiffness parameter k.

2.2.3 Application to three-dimensional structures

The analysis developed may be applied to three-dimensional regular symmetric structures consisting of box cores and a number of identical coupled shear walls, such as those in Fig. 2.8. If it is assumed that the lateral loads acting on the building have a resultant which acts as a vertical line load at the axis of symmetry of the structure, no rotation will occur and all assemblies will undergo the same lateral deflection at any level. The three-dimensional structure may then be replaced by an equivalent two dimensional system, which is obtained by assembling the parallel units in series with rigid pin-ended connecting links at each floor level as shown in Fig. 2.1(b). As the coupled shear walls are identical, the structure may be replaced by a simpler equivalent plane system in which the stiffness of a single coupled shear wall element is the sum of the stiffness of individual coupled shear wall assemblies (Fig. 2.1(c)). The summation is simply performed by adding the relevant areas and second moment of areas of walls and connecting beams, i.e. if there are n coupled walls, the values of I_1, I_2, A_1, A_2 and I_c in the formulae must be replaced by nI_1, nI_2 and so on. Similarly, the stiffness of the core element in the equivalent plane system may be obtained by adding

the flexural rigidities of all core assemblies. The equivalent plane system may then be analysed using the formulae developed in section (2.2.2). The loads and corresponding forces are divided equally among individual elements, and between the core units in proportion to their flexural rigidities. The common deflection may be obtained directly from equation (2.21).

2.2.4 Numerical example

The floor plan for this example is shown in Fig. 2.9. This thirty storey structure consists of two end U-shape cores and five pairs of coupled shear walls. The relevant structural data are: storey height = 2.5 m; total building height = 75 m ; for each core, $I = 19.75\ m^5$; for coupled shear walls, $I_1 = I_2 = 3.6 m^4$, $A_1 = A_2 = 1.2\ m^2$, $I_c = 10.67 \times 10^{-4}\ m^4$, b = 2 m, l = 8 m, $E = 21 \times 10^6\ k^N/_{m^2}$. The relevant structural parameters are then: $\alpha H = 4.61$, $\beta H = 3.91$.

The lateral deflections and internal forces in different assemblies may be found from the formulae presented in section 2.2.2 . The distributions may be expressed in terms of a series of functures F_1 to F_9 as follows,

$$y = \frac{\omega H^4}{EI} F_1, \qquad q = \omega H F_2 , \qquad N = \left(\frac{\omega H^2}{2}\right) F_3$$

$$M_1 = M_2 = \frac{1}{2}\left(\frac{\omega H^2}{2}\right)F_4 , \qquad M_3 = \left(\frac{\omega H^2}{2}\right)F_5$$

$$L.D_3 = \omega F_6 , \qquad L.D_{1+2} = \omega F_7$$

$$S_3 = \omega H F_9 , \qquad S_1 = S_2 = \frac{1}{2}\omega H F_8$$

where

L.D = Lateral load distribution in the various elements equal to $\omega - n_2$ and n_2 in coupled shear walls and core respectively.

The distributions of lateral deflection and internal forces are shown in Figs. 2.10 - 2.18. The magnitudes of the top concentrated interactive forces Q_1 and Q_2 may be determined from equations (2.40) - (2.41) and are found to be: $Q_1 = 0.037\omega H$, $Q_2 = 0.074\ \omega H$, that is 3.7% and 7.4% of the total lateral load respectively.

A commonly adopted design rule is to assume that lateral forces are distributed among the various assemblies uniformly, such that the resulting deflections at the top of the structure are equal. The lateral load distributions which would occur then are shown by broken lines in Figs. 2.17 and 2.18. The corresponding distributions of the axial force forces in the coupled shear walls, bending moments and shear forces in the two components are shown by broken

lines in Figs. 2.12 to 2.14, 2.17 and 2.18 respectively. It is clearly indicated that considerable errors may arise if these simple design procedures are used.

2.3 Replacement of rigidly-jointed frame by equivalent shear cantilever.

A laterally loaded frame element deforms in a predominantly shearing mode as a result of the racking action in each storey, produced by the bending of the columns in double curvature. In order to achieve a simplified generalised analysis, the overall mode of behaviour of the complete frame may be simulated by replacing the frame by an equivalent shear cantilever of shearing rigidity GA, and infinite flexural rigidity. The axial deformations of the columns under the action of lateral forces are then assumed to be negligible.

In order to produce a correct distribution of lateral forces, the shearing rigidity of the equivalent cantilever must be chosen so that the horizontal displacement of both frame and cantilever must be the same when subjected to the same shear force.

Consider the single storey segment of a frame panel shown in Fig. 2.19(a). In particular cases where the columns are closely spaced, and the beams relatively deep, the finite size of the joint relative to the free column

height and beam span should be taken into account. This may be done by assuming that short rigid arms exist at each node, of width equal to the width of the column, and of height equal to the depth of the beams.

It is assumed that the columns are constrained to deflect equally at each floor level due to the high in-plane rigidity of the floor slabs, and that the beams deflect with a point of contraflexure at their mid-span position. It is further assumed that the columns bend with points of contraflexure at their mid-height positions. The forces on the frame segment, and effective boundary conditions, are then as shown in Fig. 2.19(c).

If a horizontal shear force Q is applied at the node D, the resulting horizontal deformation Δ may readily be calculated from the moment-deformation characteristics of the frame segment.

For an equivalent shear cantilever element of the same bay width, subjected to the same shearing force Q, (Fig.2.19(b)), the load-displacement relationship is,

$$\Delta = \frac{Q}{GA} h$$

On equating the two relationships, it is found that the effective shearing rigidity GA becomes

$$GA = \frac{1}{Z} \frac{12EI_h}{e^2} \left(1 + \frac{t_2}{e}\right)$$

where
$$Z = 1 + \frac{2I_h \left(1 + {}^{t_2}/_{e}\right)^2}{e\left[\frac{I_{d_1}}{l_1}\left(1 + \frac{t_1}{l_1}\right)^2 + \frac{I_{d_2}}{l_2}\left(1 + \frac{t_1}{l_2}\right)^2\right]}$$

in which I_h = second moment of area of column, h = storey height, I_{d_1} and I_{d_2} are the second moments of area of the adjacent beams of total lengths d_1 and d_2 respectively, t_1 and t_2 are the length and height of the rigid arms, and

$$e = h - t_2$$

$$l_1 = d_1 - t_1$$

$$l_2 = d_2 - t_1$$

This relationship is applicable also to an exterior column if the second moment of area of one of the beams is taken to be zero. The total shear stiffness of the equivalent cantilever is then equal to the sum of the individual GA values of the bays.

If, as is frequently the case with tall buildings,

$I_{d_1} = I_{d_2} = I_d$, and $d_1 = d_2 = d$, or $l_1 = l_2 = l = d - t_1$

$$GA = \frac{1}{Z_1} \frac{12EI_h}{e^2} \left(1 + \frac{t_2}{e}\right)$$

$$\text{where } Z_1 = 1 + \frac{l}{e}\ \frac{I_h(1 + {}^{t_2}/_e)^2}{I_d(1 + {}^{t_1}/_l)^2}$$

If the spans of the beams and heights of the columns are relatively large in comparison with the joint dimensions, t_1 and t_2 may be taken to be zero in the above expressions.

2.4 Analysis of symmetric shear wall-frame structures

Consider a three-dimensional symmetric structure which consists of assemblies of independent shear walls or box cores and rigidly-jointed frames, constrained to act together by the floor slabs, as shown in Fig. 2.20(a). Due to the high in-plane rigidity of the floor slabs, it is again assumed that each horizontal section of the structure undergoes only a rigid body movement. On replacing the three-dimensional structure by an equivalent plane system as described in section 2.2, a simplified analysis may be achieved. Fig. 2.20(b) shows the plane system which is used for the initial analysis.

2.4.1 Analysis

Consider the structure shown in Fig. 2.20(b). The set of discrete pin-ended links between the shear wall and the frame can be replaced by a continuous medium which transmits an axial force of intensity n_3 per unit height. The equivalent structure and the loading pattern are shown in Fig. 2.20(c).

The shear force-displacement characteristics of the constituent wall and frame components may be expressed as,

$$S_w = - EI \frac{d^3y}{dx^3} \qquad (2.49)$$

$$S_f = GA \frac{dy}{dx} \qquad (2.50)$$

where S_w and S_f are the shear forces on the wall and frame, EI and GA are the flexural and equivalent shearing rigidities of the wall and frame, and y is the lateral deflection.

The moment-curvature relationship for the shear wall is

$$EI \frac{d^2y}{dx^2} = M_w = M - M_{aj} \qquad (2.51)$$

where M_w is the moment on the wall, M is the static applied moment and M_{aj} is the moment due to the axial forces in the connecting medium.

The equations governing the behaviour of the structure, referring to Fig. 2.20(c) are

$$EI \frac{d^4y}{dx^4} = \frac{d^2M}{dx^2} - n_j \qquad (2.52)$$

$$- GA \frac{d^2y}{dx^2} = n_j \qquad (2.53)$$

On adding equations (2.52) and (2.53), the governing differential equation becomes

$$\frac{d^4y}{dx^4} - \alpha^2 \frac{d^2y}{dx^2} = \frac{1}{EI} \frac{d^2M}{dx^2} \qquad (2.54)$$

where $\alpha^2 = \frac{GA}{EI}$

The solution of the differential equation (2.54) consists of two parts, complementary function and the particular integral and is given by

$$y = A_o + A_1 x + A_2 \sinh \alpha x + A_3 \cosh \alpha x + y_{PI} \qquad (2.55)$$

where A_i ($i = 0 - 3$) are constants of integration and y_{PI} is the particular integral solution. These quantities may be obtained from the boundary conditions and the loading pattern.

Boundary Conditions

For a conventional structure which is fixed at the base and free at the top, the four boundary conditions required for a complete solution are

$$\text{At } x = 0, \qquad y = 0, \qquad \frac{dy}{dx} = 0 \qquad (2.56)$$

$$\text{At } x = H, \qquad M = S = 0 \qquad (2.57)$$

where M and S are the externally applied bending moment and shear force respectively.

Equations (2.57) may be expressed in terms of the lateral deflection y as

$$\frac{d^2y}{dx^2} = 0 \ , \qquad GA \frac{dy}{dx} - EI \frac{d^3y}{dx^3} = 0 \qquad (2.58)$$

In the particular case of a top concentrated applied lateral load, used in equivalent static earthquake loadings, the top shear S(H) will be put equal to the applied load P, and the boundary condition (2.58) becomes

$$P = S(H) = GA \frac{dy}{dx} - EI \frac{d^3y}{dx^3}$$

Uniformly distributed wind loading

The differential equation (2.54) may be solved for the three standard load cases. However, in order to obtain a solution, the case of a uniformly distributed wind loading of intensity ω per unit height is again considered. The applied static moment and its derivations are given by equations (2.16) and on substituting for $\frac{d^2M}{dx^2}$ in equation (2.54), it becomes

$$\frac{d^4y}{dx^4} - \alpha^2 \frac{d^2y}{dx^2} = \frac{\omega}{EI} \qquad (2.59)$$

The simplest particular integral then becomes

$$y_{PI} = - \frac{\omega}{2\alpha^2 EI} x^2 \qquad (2.60)$$

On substituting y_{PI} in equation (2.55) the general solution becomes

$$y = A_o + A_1 x - \frac{\omega}{2\alpha^2 EI} x^2 + A_2 \sinh\alpha x + A_3 \cosh\alpha x \qquad (2.61)$$

The integration constant A_i (i = 0 -3) may be found using the boundary conditions (2.56) - (2.57), to be

$$A_o = - \frac{\omega}{EI\alpha^4 \cosh\alpha H} (\alpha H \sinh\alpha H + 1)$$

$$A_1 = \frac{\omega H}{\alpha^2 EI}$$

$$A_2 = \frac{-\omega H}{\alpha^3 EI} \qquad (2.62)$$

$$A_3 = \frac{\omega}{EI\alpha^4 \cosh\alpha H} (\alpha H \sinh\alpha H + 1)$$

Then, on substituting for (A_o) - (A_3) into equation (2.61), the general solution becomes

$$y = \frac{\omega H^4}{EI\ k^4} \left\{ \left(\frac{k \sinh k + 1}{\cosh k}\right) (\cosh k\xi - 1) - k \sinh k\xi + k^2\left(\xi - \frac{1}{2}\xi^2\right) \right\} \qquad (2.63)$$

where ξ and k are as defined in equations (2.22)

The shear force on the wall and frame may be obtained by substituting for the deflection from (2.63) into equations (2.49)-(2.50) and are given by

$$S_w = \omega H\left[-\left(\frac{k \sinh k + 1}{k \cosh k}\right) \sinh k\xi + \cosh k\xi\right] \quad (2.64)$$

$$S_f = \omega H \left[\left(\frac{k \sinh k + 1}{k \cosh k}\right) \sinh k\xi - \cosh k\xi + (1 - \xi)\right] \quad (2.65)$$

On substituting for the deflection from equation (2.63) into equation (2.51) the moment in the shear wall becomes

$$M_w = \frac{\omega H^2}{k^2}\left[\left(\frac{k \sinh k + 1}{\cosh k}\right) \cosh k\xi - k \sinh k\xi - 1\right] \quad (2.66)$$

The moment in the frame is then given by

$$M_f = M - M_w \quad (2.67)$$

$$= \frac{\omega H^2}{k^2}\left[\frac{1}{2} k^2 (1 - \xi)^2 - \left(\frac{k \sinh k + 1}{\cosh k}\right) \cosh k\xi + k \sinh k\xi + 1\right] \quad (2.68)$$

From equations (2.53) and (2.63) the axial force distribution becomes

$$n_3 = -\omega\left[\left(\frac{k \sinh k + 1}{\cosh k}\right) \cosh k\xi - k \sinh k\xi - 1\right] \quad (2.69)$$

As before (section 2.2.2), the concentrated interactive force at the top of the connecting medium is given by

$$Q_3 = -S_w(H) \qquad (2.70)$$

Hence, from equation (2.64), Q_3 becomes

$$Q_3 = \left[-\left(\frac{k \sinh k + 1}{k \cosh k}\right) \quad \sinh k + \cosh k \right] \qquad (2.71)$$

Figs. 2.21 - 2.26 show the variations at any height of the deflection and the internal force functions (P_1)-(P_6) where

$$y = \frac{\omega H^4}{EI} P_1, \qquad S_w = \omega H P_2 , \qquad S_f = \omega H P_3$$

$$M_w = \frac{\omega H^2}{2} P_4 , \qquad M_f = \frac{\omega H^2}{2} P_5, \qquad n = -\omega P_6 \qquad (2.72)$$

Application to three-dimensional structures

Using the same procedure as explained in section 2.2.3, the analysis presented may be applied to three-dimensional symmetric structures consisting of independent shear walls or box cores and rigidly jointed framework assemblies, i.e. if there are n frames the value of GA must be replaced by $\sum_{i=1}^{n} (GA)_i$

2.4.2 Numerical example

The floor plan for this example is shown in Fig.2.27. This thirty storey structure consists of two central cores

and six rigidly jointed frame assemblies. The relevant structural data are: storey height h = 2.5 m; total building height H = 75m ; for each core, I = 1.86 m^4; for each frame the dimensions of the columns are 0.35m x 0.35 m , and beams are 0.35 m thick and 0.37 m deep, then GA= 6 x 10^4 (each frame), E = 21 x 10^6 $kM/_m2$. The relevant structural parameter αH becomes: αH = 5.09.

The distribution of deflections and internal forces are shown in Fig. 2.28 - 2.33. The magnitude of the top concentrated interactive force Q_3 may be determined from equation (2.71) or from Figs. 2.28 - 2.29, and is found to be: Q_3 = 0.184ωH or 18.4% of the total lateral load. In Figs. 2.29 to 2.33 broken lines show the results obtained by using the commonly adopted design procedure mentioned in section (2.4.4).

2.4.3 Inclusion of base flexibility of wall-frame components in the general analysis

The use of the second boundary condition of equation (2.56) in association with (2.50) reveals that the shear force S_f in the frame at the base of the structure is always zero, irrespective of the relative stiffness of the two components, and the flexural wall element will carry the total horizontal shear at the foundation level.

In many structures, because of load redistribution throughout the height, the flexural element does carry a very large proportion of the applied shear at the base level. However, for frames which are relatively much stiffer than slender walls, the error involved in the analysis may become significant.

The difficulty arises with the basic continuum approach, in which two independent components with disimilar load-deformation characteristics are constrained to deflect equally at all points on the height. This difficulty does not arise with discrete methods of analysis, since the local bending of the frame columns over the first storey height induces shears at the base level.

At the top of the structure, a fictitious concentrated axial load is found to exist at the top of the continuous linking medium, which allows an equal and opposite shear force Q_3 to exist in both frame and wall, and ensures that the slope at the top of the frame is not zero. The total shear force is of course zero in the absence of any applied concentrated horizontal load.

Modified analysis

In order to allow a shearing deformation of the frame to exist at ground level, it is assumed that the shearing deflections of the wall are no longer neglected near the base where shearing stresses are high. Since both

components are assumed to deflect equally, the base slope Θ is then given by

$$\text{At } x = 0 , \quad \Theta = \frac{dy}{dx} = \frac{S_w}{GA_w} = \frac{S_f}{GA} \tag{2.73}$$

where GA_w is the shearing rigidity of the wall, with A_w being the effective shear area.

Since the applied shear S is equal to the sum of the individual shears in the components, the alternative base condition becomes

$$\Theta = \frac{dy}{dx} = \frac{S}{GA_w + GA} \tag{2.74}$$

In order to compare the results with those obtained by the earlier analysis (2.4.2), the particular case is considered of a uniformly distributed lateral load of intensity ω per unit height. Then, at any level the applied shear force and bending moment are,

$$S = \omega H(1 - \xi) , \qquad M = \frac{\omega H^2}{2} (1 - \xi)^2 \tag{2.75}$$

On substituting equation (2.75) into (2.54), and using the modified boundary conditions, the solution becomes

$$y = \frac{\omega H^4}{EI(k)^4} \left\{ \left(\frac{\phi k \sinh k + 1}{\cosh k} \right) (\cosh k\xi - 1) - \phi k \sinh k\xi + k^2 \left(\xi - \frac{\xi^2}{2} \right) \right\} \tag{2.76}$$

in which ϕ is the shearing rigidity ratio,

$$\phi = \frac{GA_w}{GA_w + GA} \qquad (2.77)$$

Except for the introduction of the parameter ϕ, equation (2.76) is similar to the solution obtained in section (2.4.2), and the two solutions are identical when $\phi = 1$.

The corresponding expressions for bending moments and shearing forces in the wall component become

$$\frac{M_w}{M_o} = \frac{2}{k^2}\left[\left(\frac{\phi\, k \sinh k + 1}{\cosh k}\right)\cosh k\xi - \phi\, k \sinh k\xi - 1\right] \qquad (2.78)$$

and

$$\frac{S_w}{S_o} = \frac{1}{k}\left[\phi\, k \cosh k\xi - \left(\frac{\phi\, k \sinh k + 1}{\cosh k}\right)\sinh k\xi\right] \qquad (2.79)$$

For convenience, the moments and shears have been expressed in terms of the maximum total applied moment M_o and shear S_o at the base. The expressions again become identical to the earlier solutions (2.4.2) in the particular case when $\phi = 1$.

The moments and shears on the frame component follow from equilibrium conditions to be

$$\frac{M_f}{M_o} = (1 - \xi)^2 - \frac{M_w}{M_o} \qquad (2.80)$$

$$\frac{S_f}{S_o} = (1 - \xi) - \frac{S_w}{S_o} \qquad (2.81)$$

Numerical results

In order to illustrate quantitatively the influence of the shearing flexibility at ground level, the variations of the most significant structural actions with relative stiffness parameter k, for the complete range of values of the shearing ratio ϕ, from zero to unity, have been evaluated, although the extreme value of zero has clearly no physical significance. Figs. 2.34, 2.35 and 2.36 show respectively, in non-dimensional form, the variations of the maximum base wall moment $M_w(o)$, the maximum basic frame moment $M_f(o)$, and the frame and wall top shear force $S_f(H)$ ($= - S_w(H)$), equal to the concentrated interactive connecting force.

It is unnecessary to illustrate the variations of the maximum base wall shear force $S_w(o)$ and frame shear force $S_f(o)$ since these are given by the simple expressions

$$\frac{S_w(o)}{S_o} = \phi \quad , \qquad \frac{S_f(o)}{S_o} = 1 - \phi \qquad (2.82)$$

Equation (2.82) shows that the values of the base shears are directly dependent on the shearing stiffness ratio ϕ, but are independent of the relative stiffness k. However, the influence of ϕ on the base moment $M_w(o)$ and $M_f(o)$, and the top shears $S_w(H)$ and $S_f(H)$ varies with k, being greatest at lowest values of the relative stiffness parameter.

The direct influence of the ratio ϕ on the maximum top deflection y(H) is more difficult to illustrate simply, since the value of the function in equation (2.76) tends to be dominated by the term $1/k4$, which varies from being extremely large to extremely small as k increases from 0 to 10, which is a reasonable range of values for the quoted structures. Thus the function in the main external brackets only of equation (2.76) is used in Fig. 2.37, which shows the variation of $y(H) \times EI(k)^4/\omega H^4$ with k for the range of values of shearing stiffness ratio ϕ. The curves show that the influence of ϕ on the top deflection is similar at all values of k.

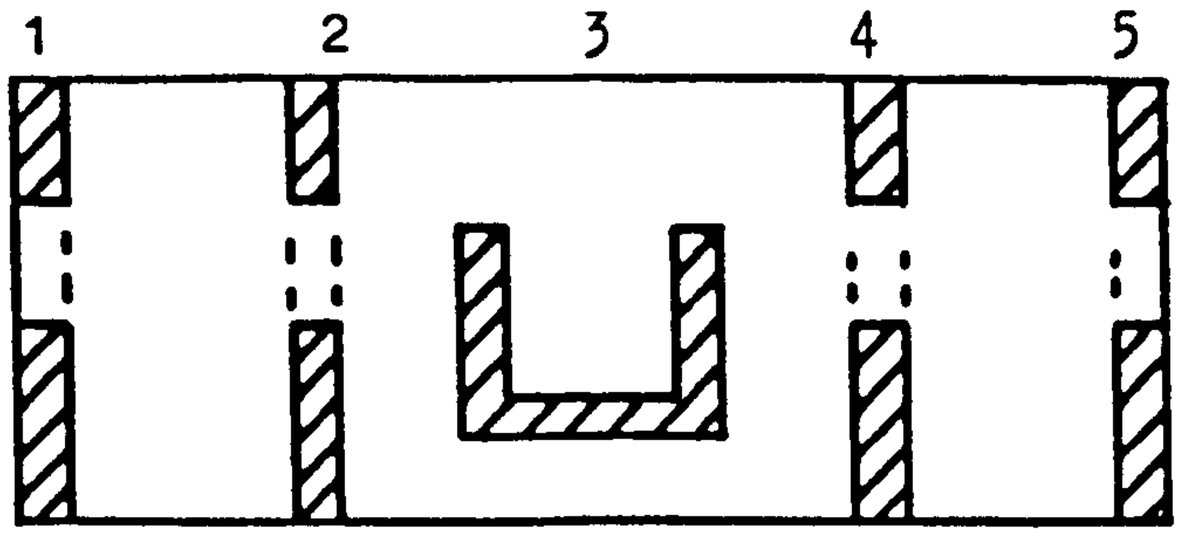

Fig. 2.1(a) Regular symmetric cross-wall structure

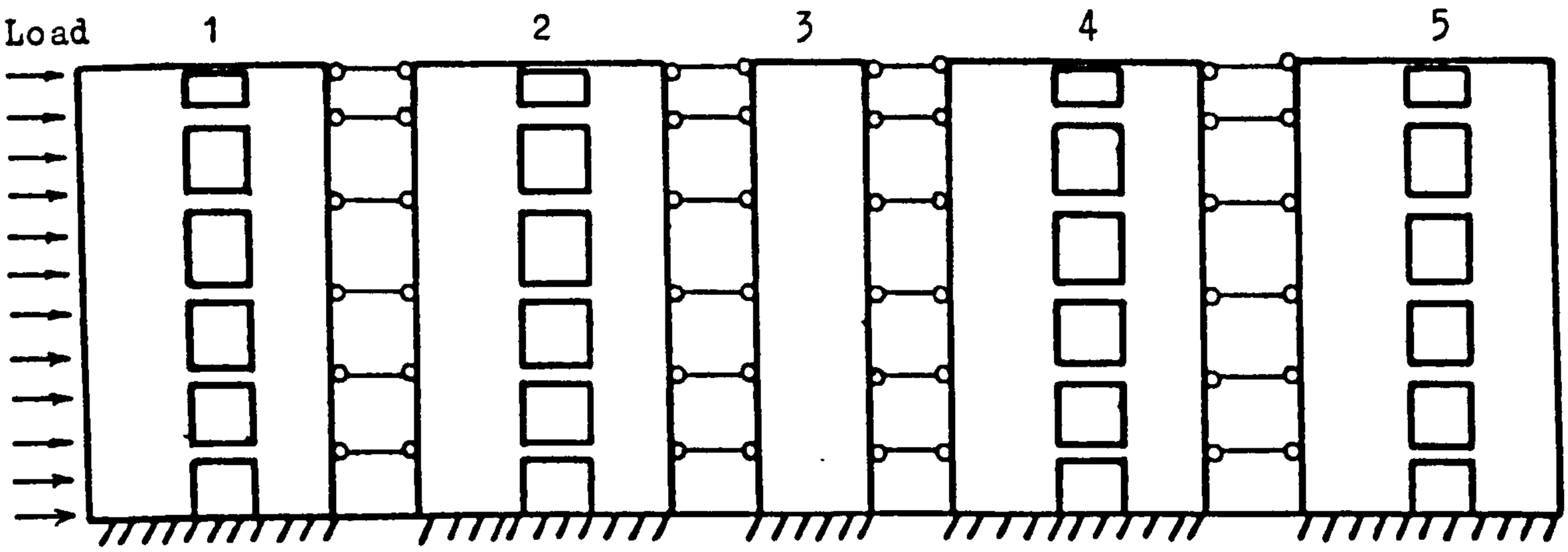

Fig.2.1(b) Replacement of symmetrically loaded structure by equivalent plane system

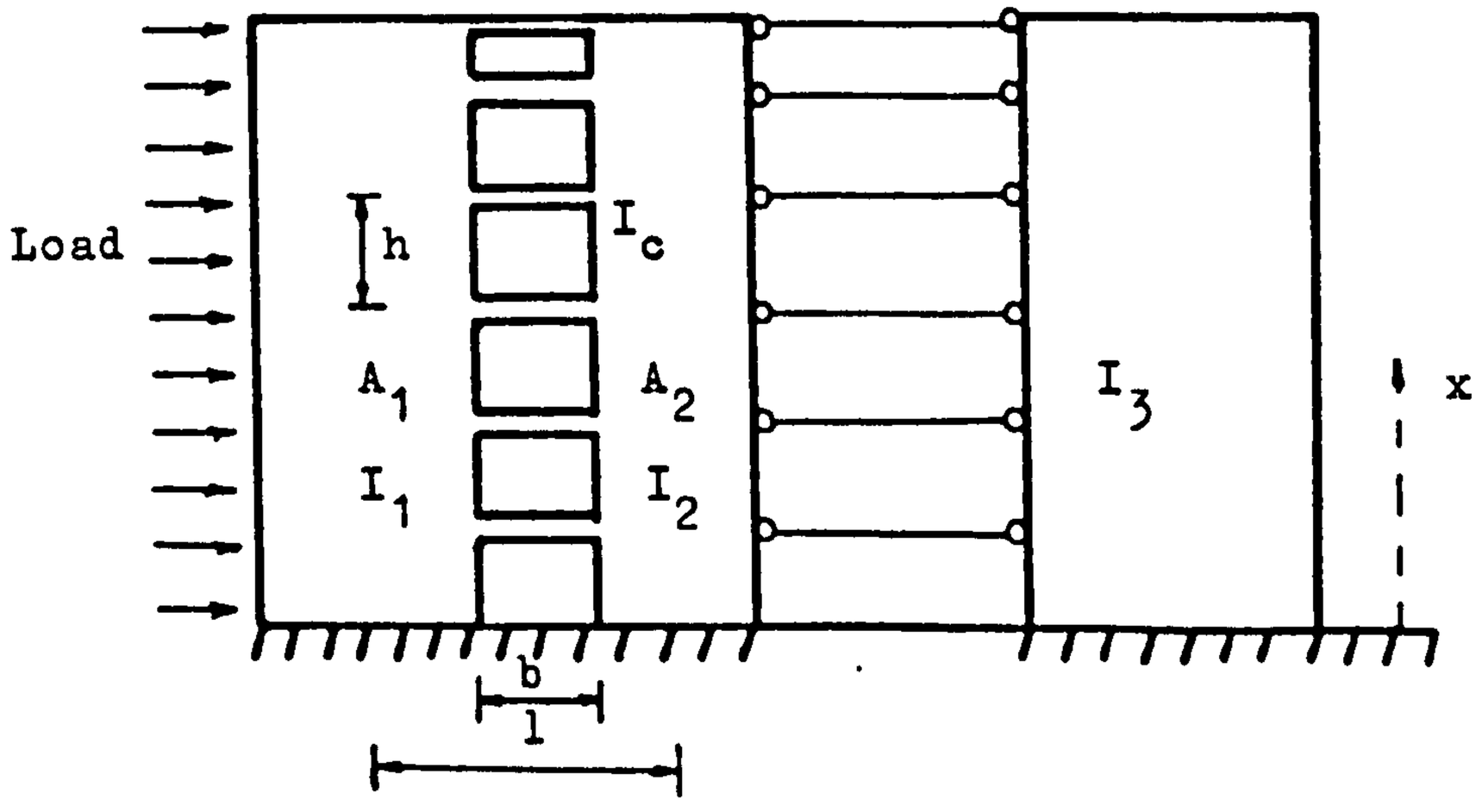

Fig. 2.1(c) Equivalent plane system

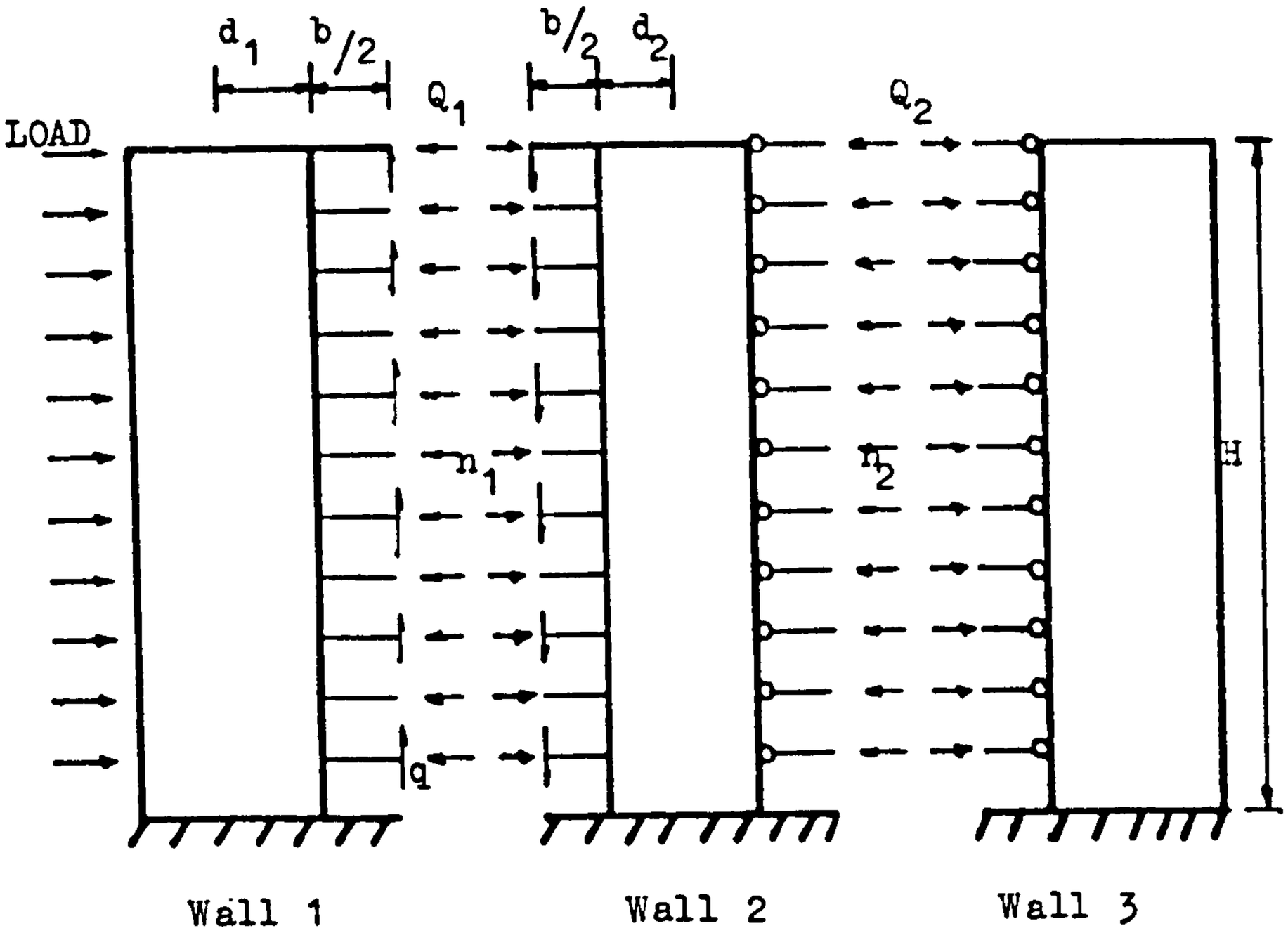

Fig. 2.1(d) Substitute system

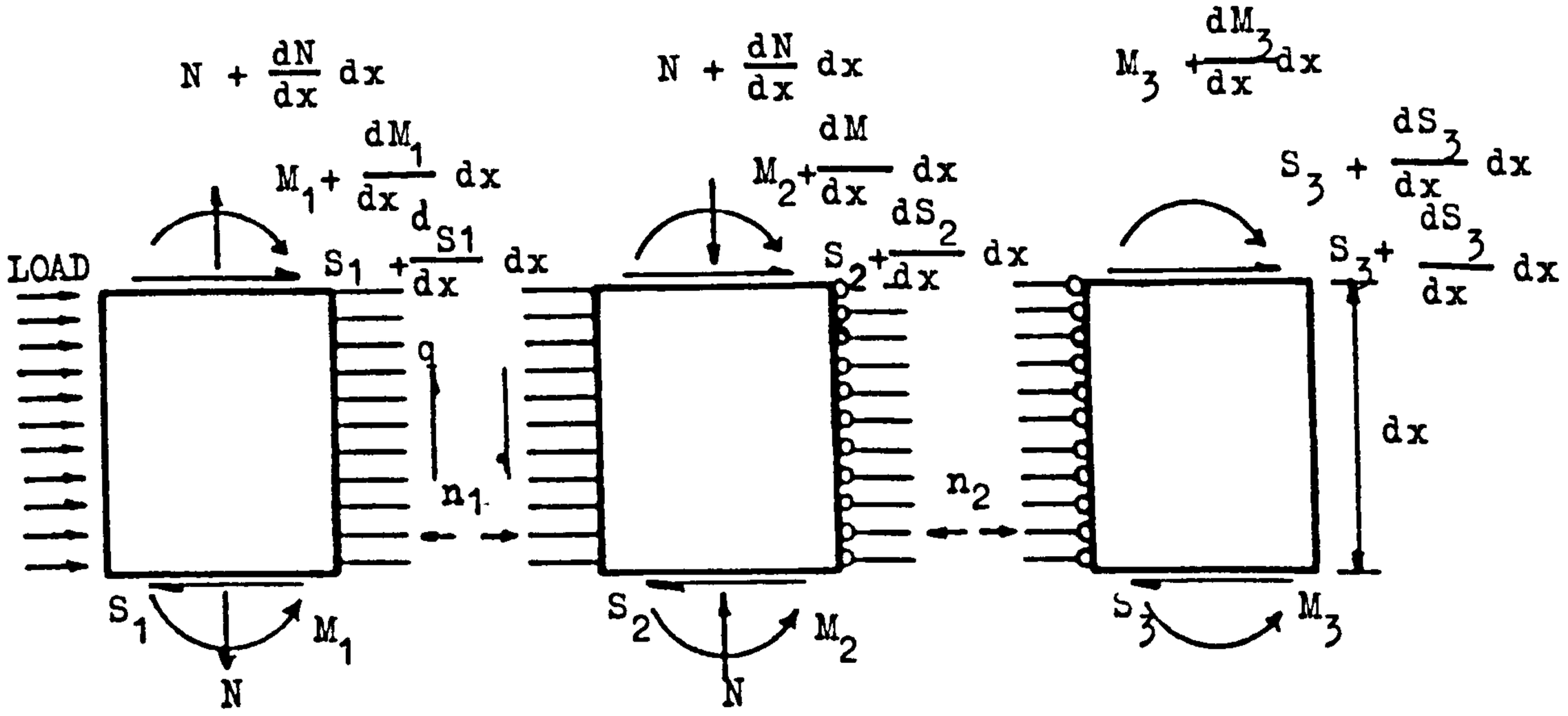

Fig. 2.1(e) Forces on element of substitute equivalent plane structure

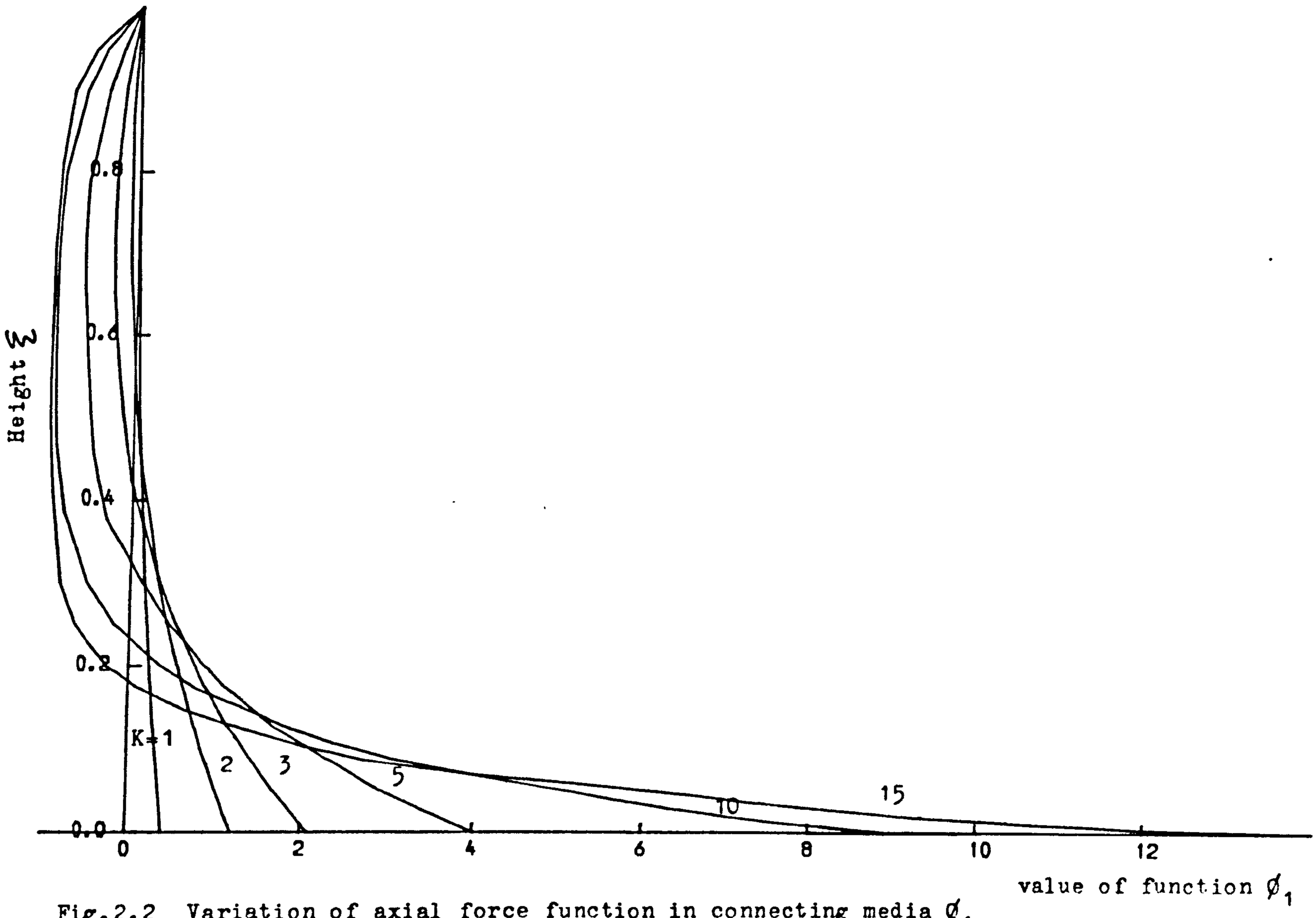

Fig.2.2 Variation of axial force function in connecting media ϕ_1

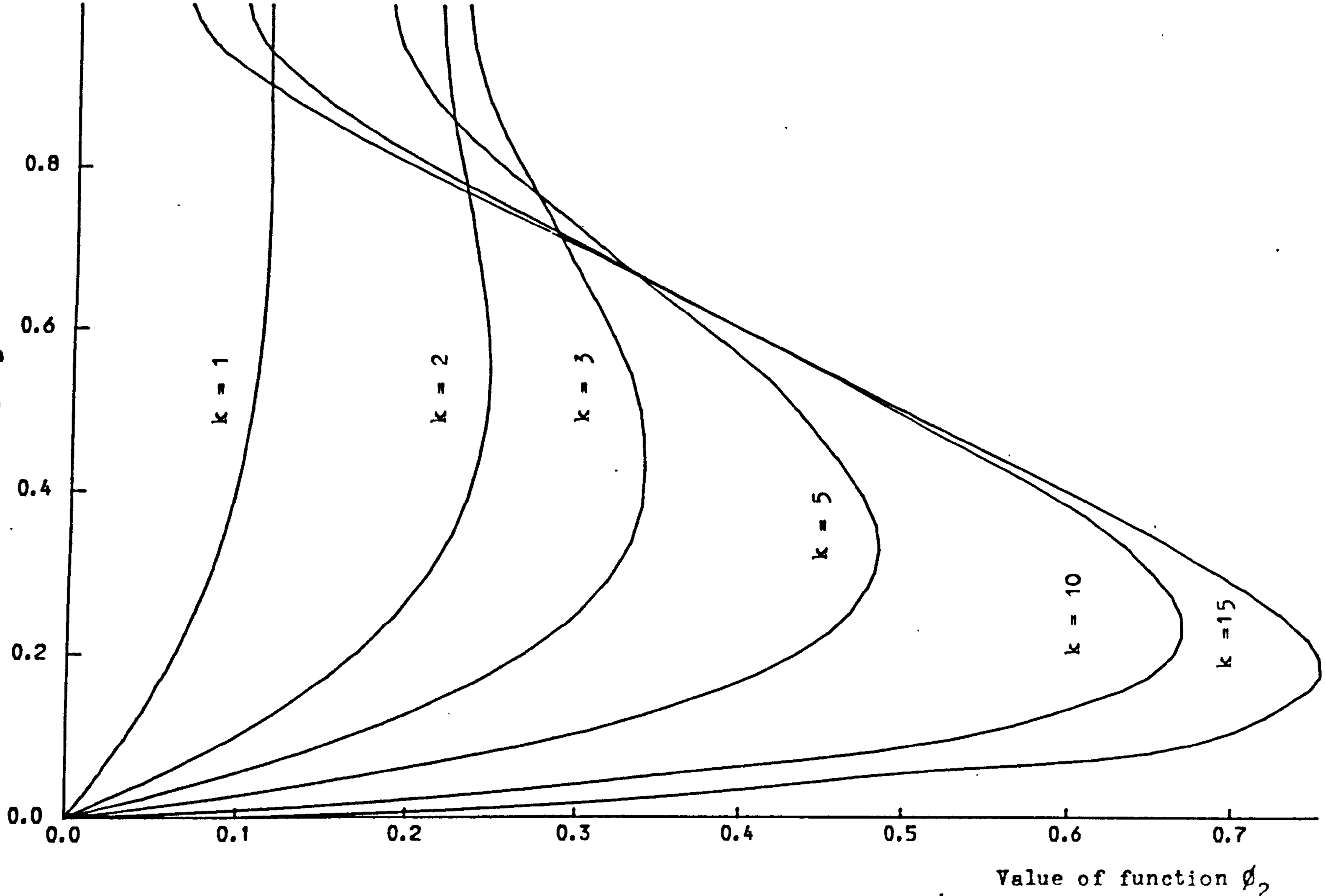

Fig. 2.3 Variation of shear flow function in connecting beams ϕ_2

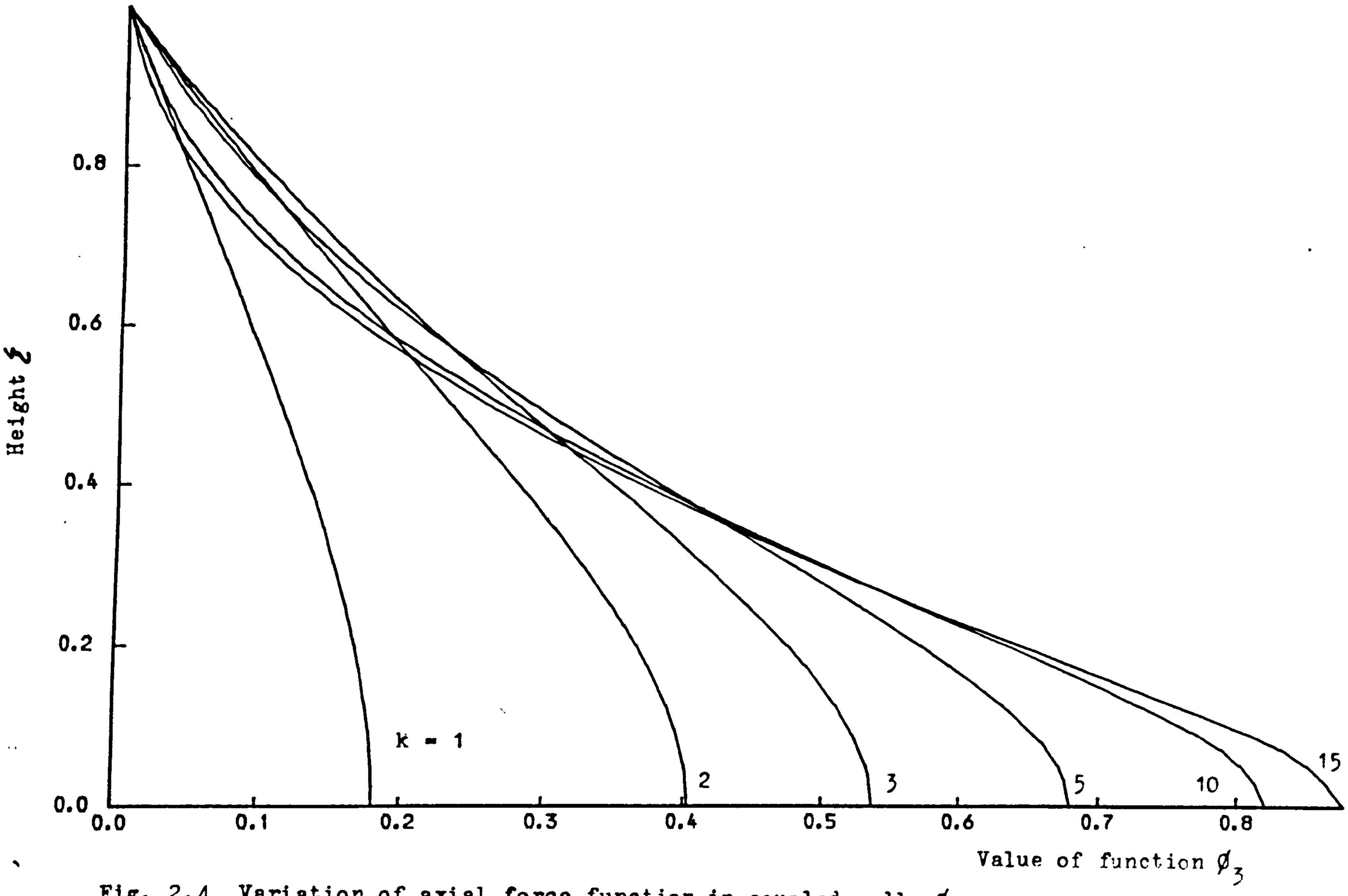

Fig. 2.4 Variation of axial force function in coupled walls ϕ_3

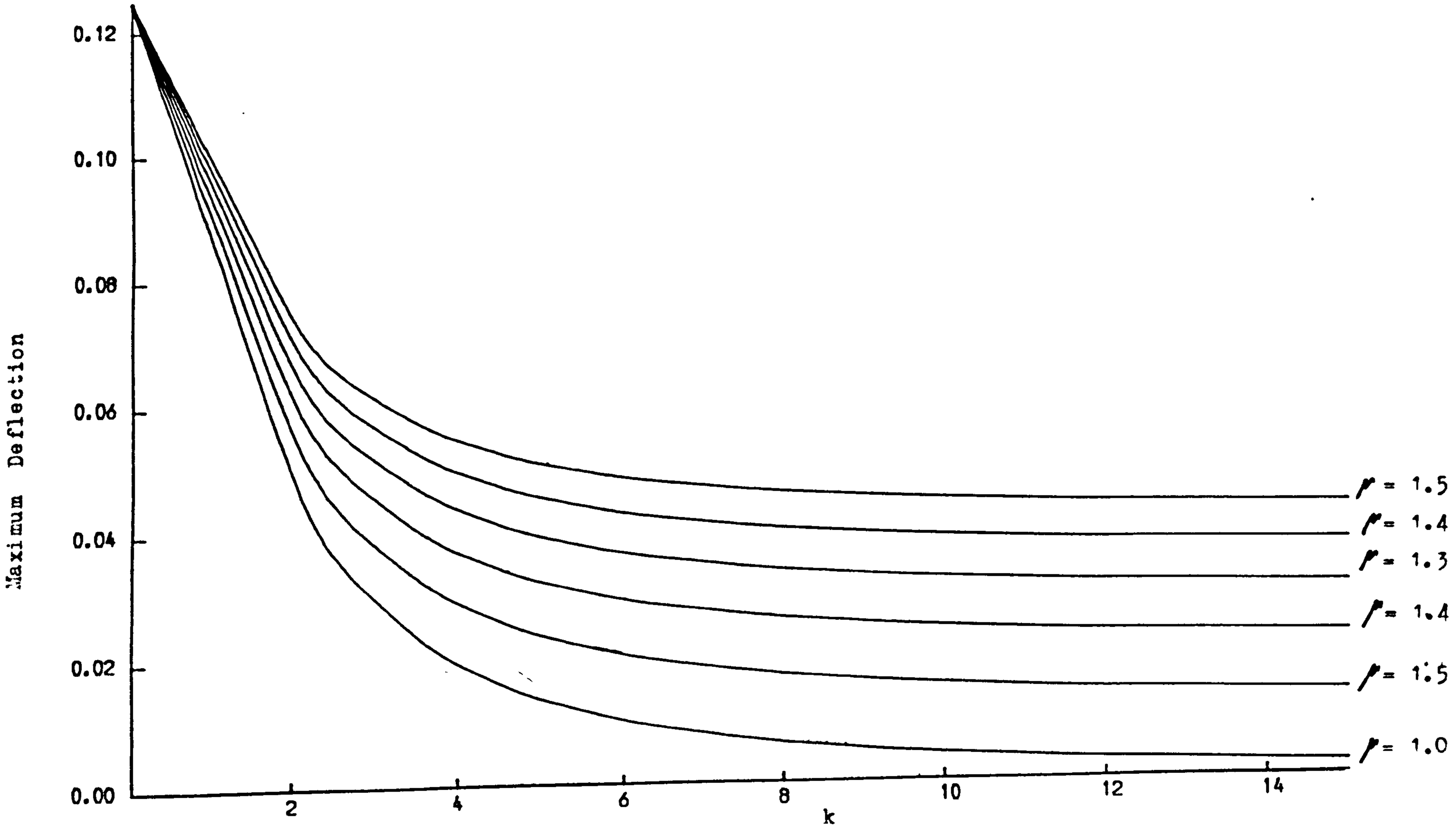

Fig. 2.5 Variation of Deflection Function ϕ_4

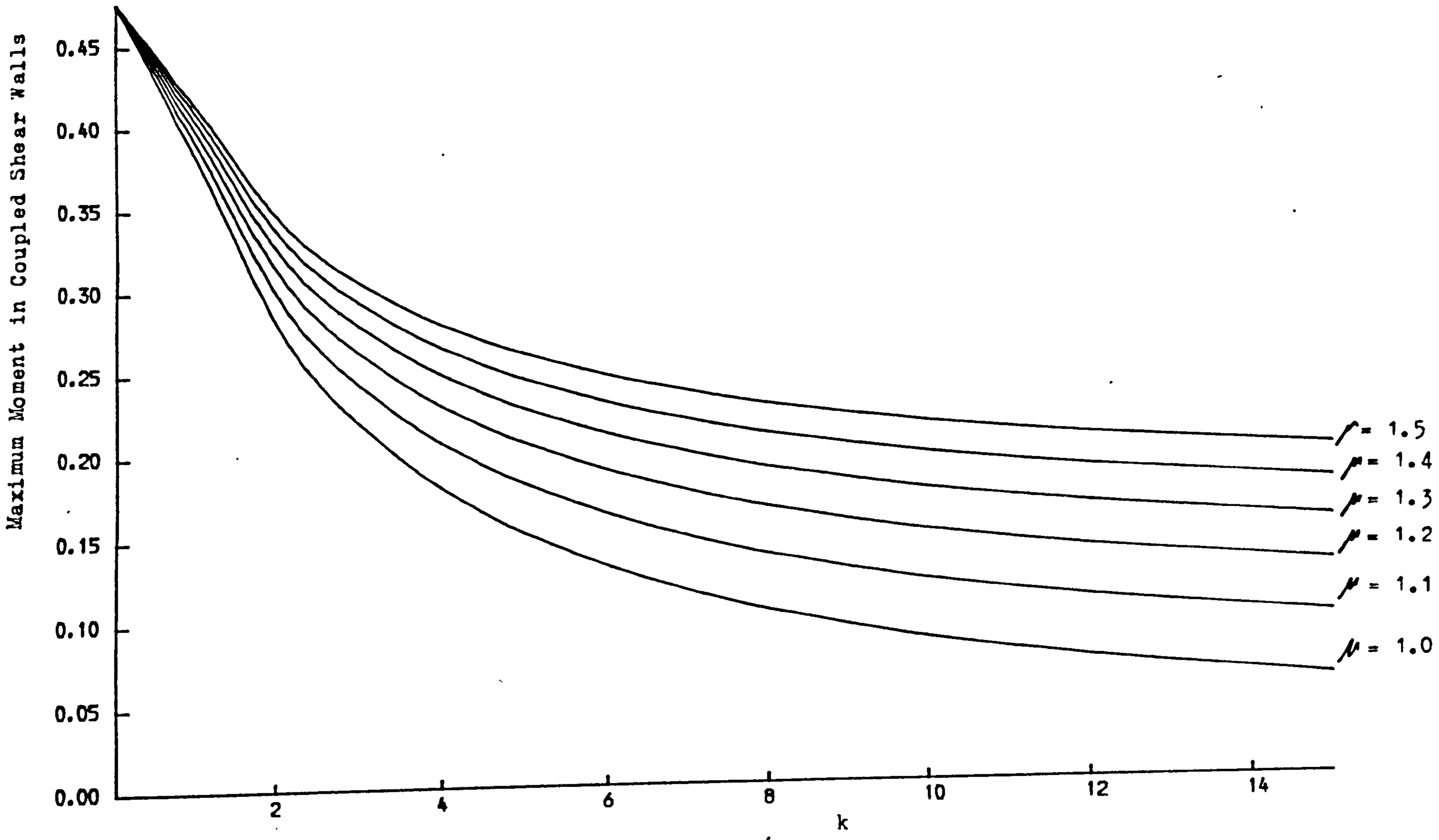

Fig. 2.6 Variation of Maximum Moment Function ϕ_5

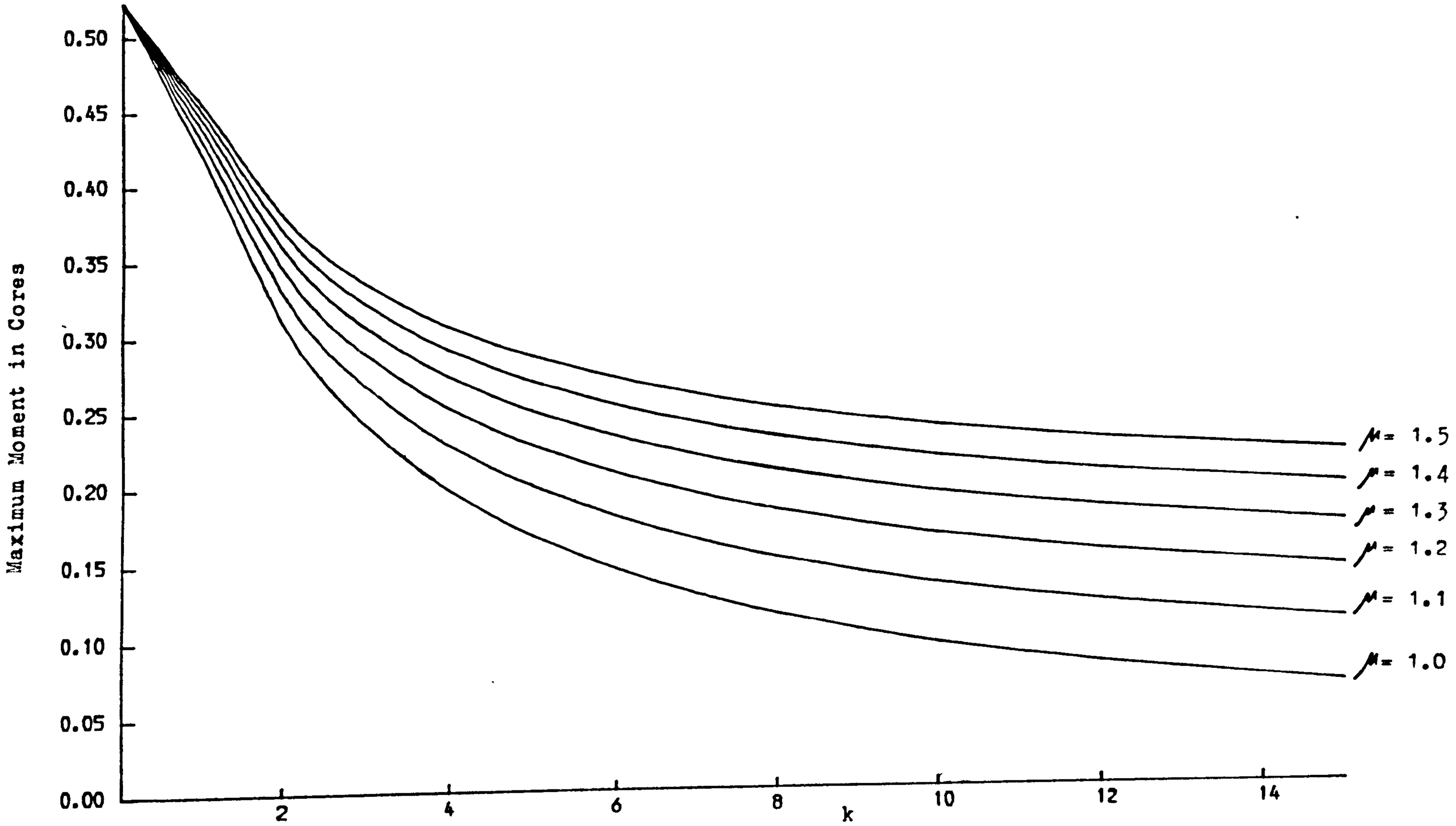

Fig. 2.7 Variation of Maximum Moment Function ϕ_6

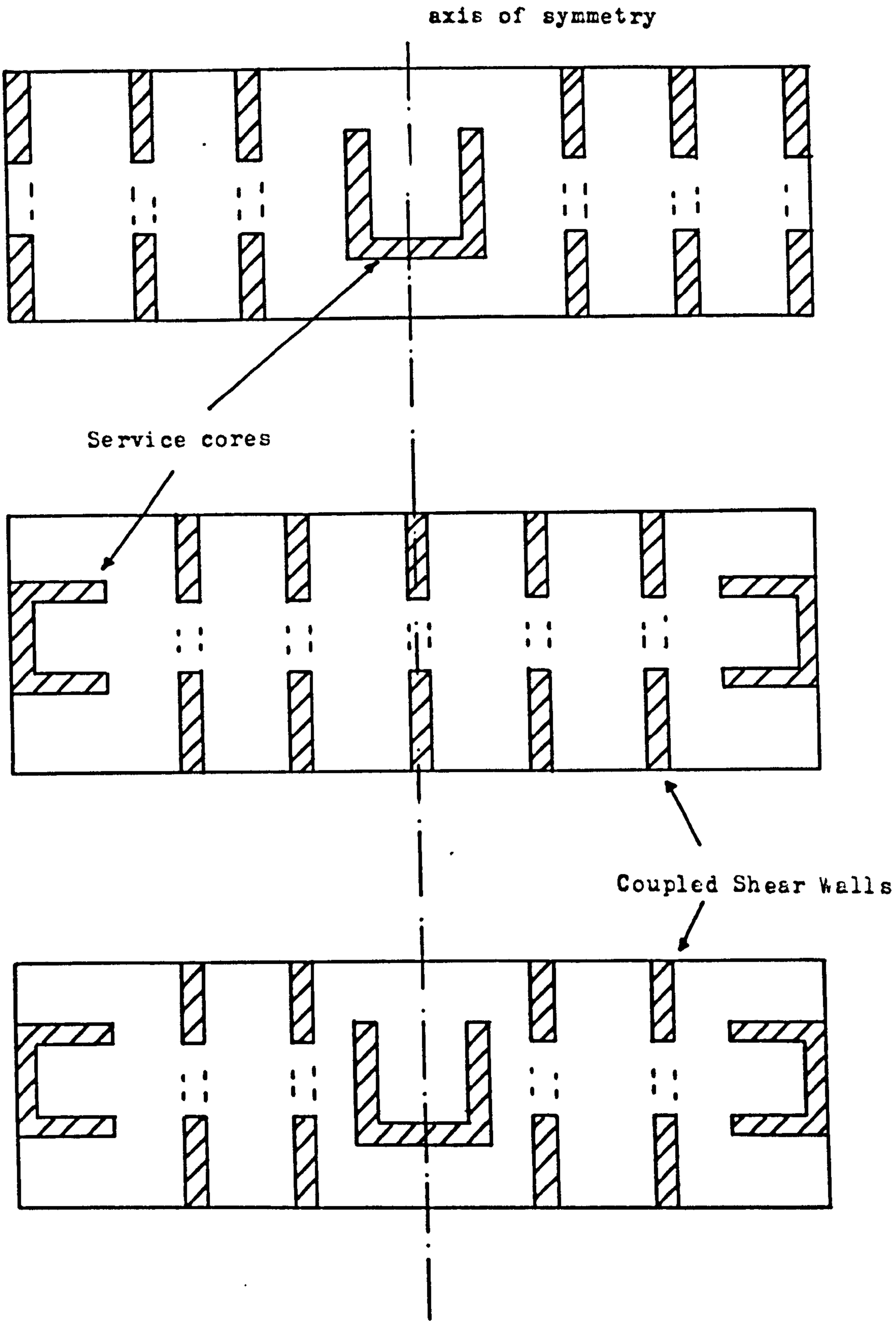

Fig. 2.8 Regular Symmetrical cross-wall structures
Comprising coupled shear walls and service cores

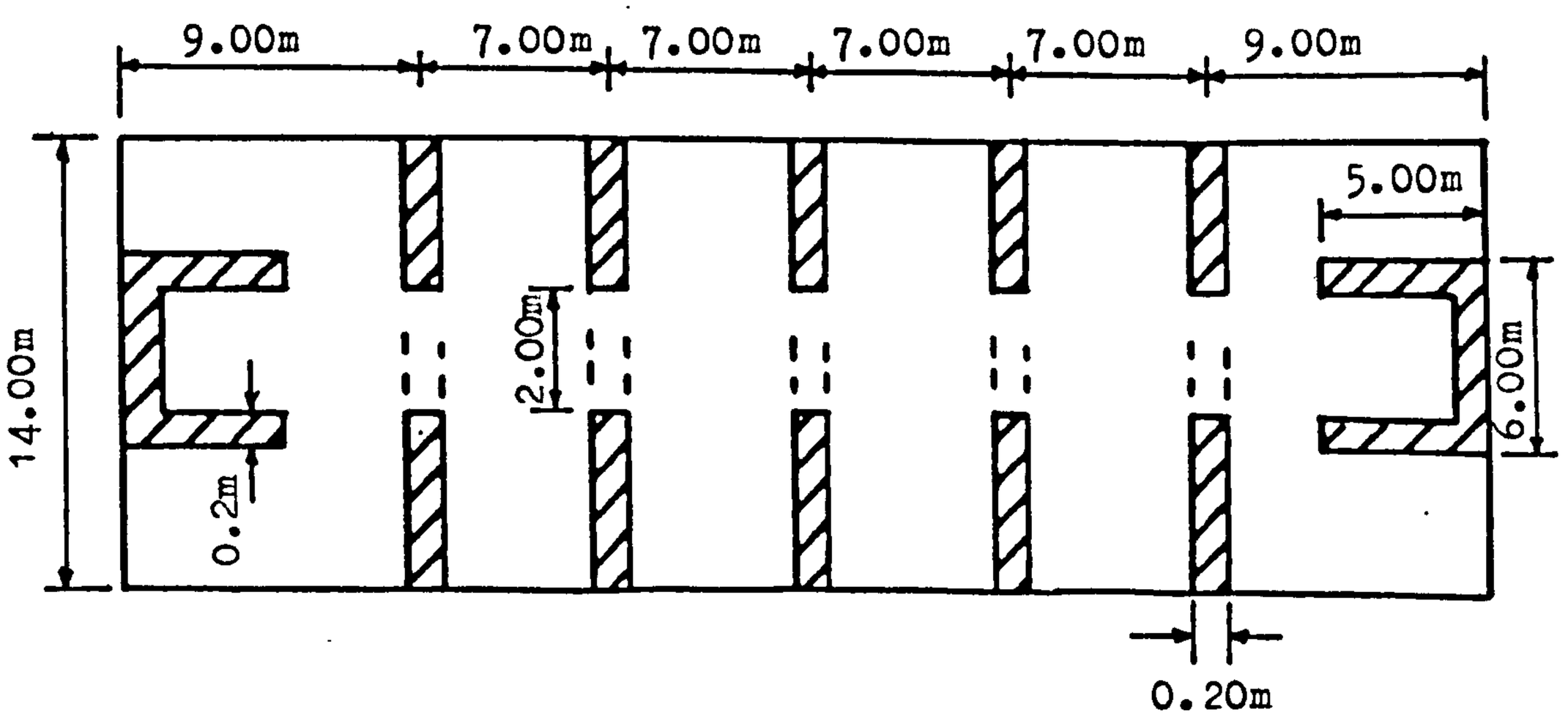

Fig. 2.9 planform of structure for numerical example

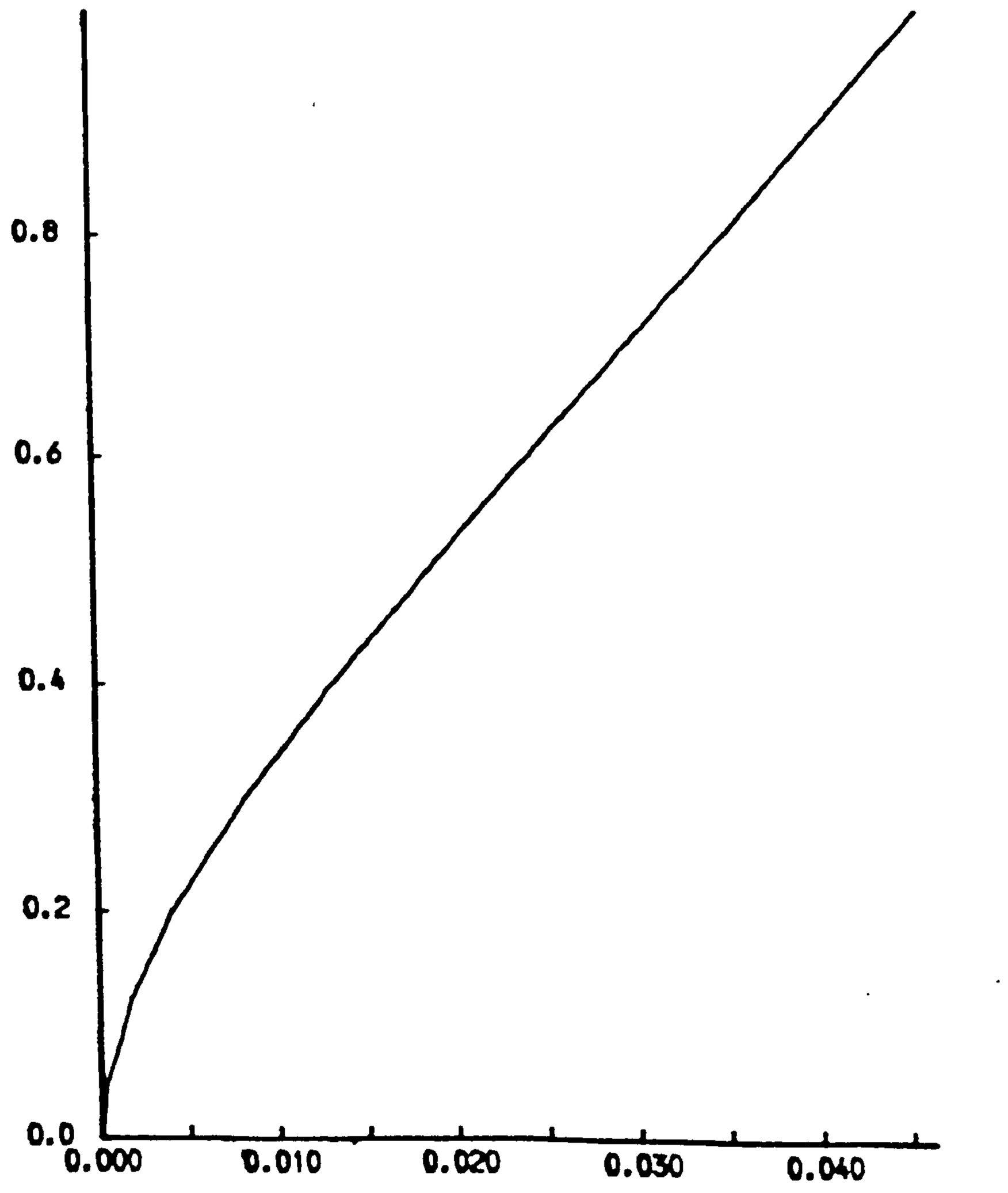

Fig. 2.10 Distribution of lateral deflection variation

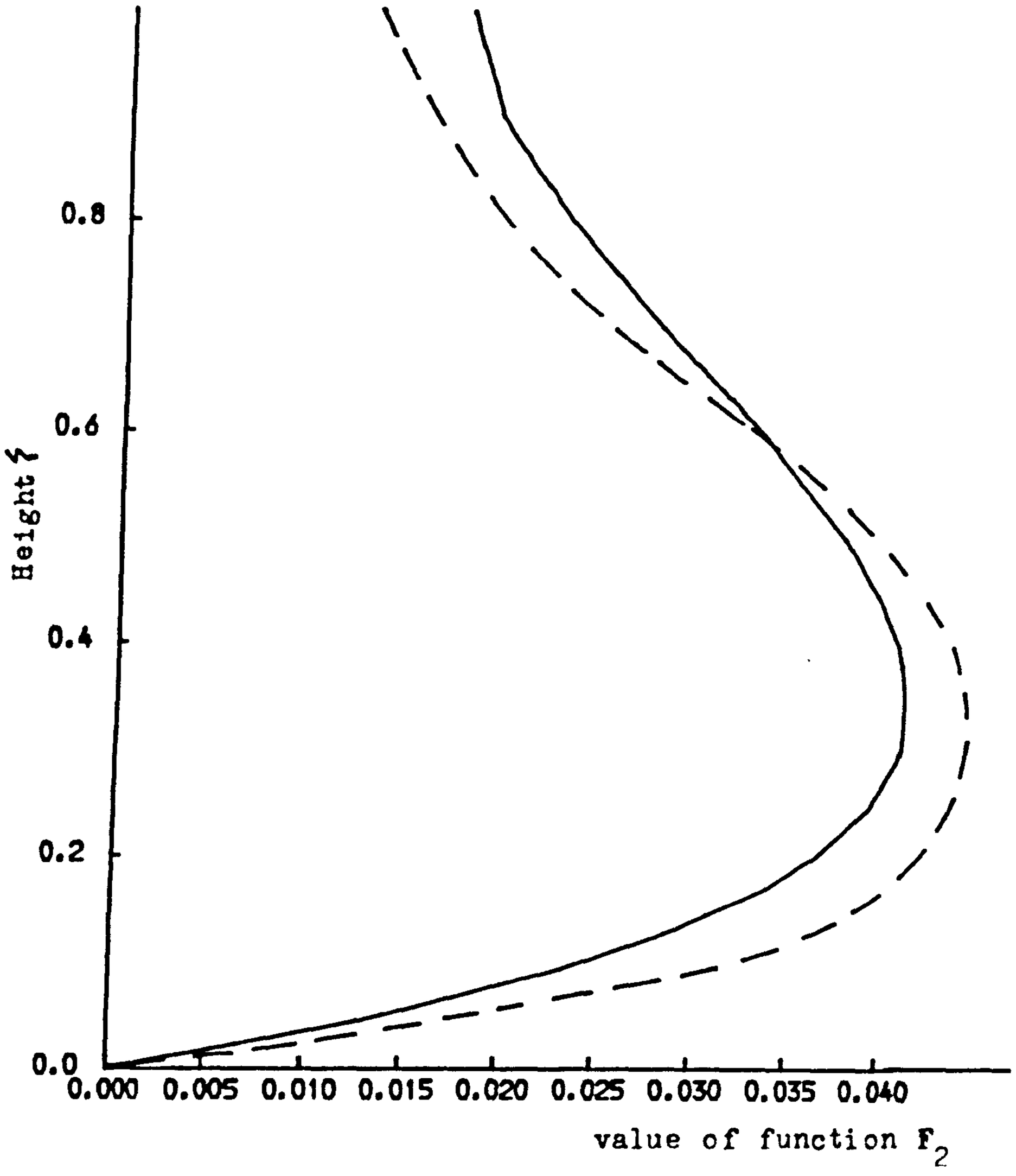

Fig. 2.11 Distribution of shear flow in connecting medium

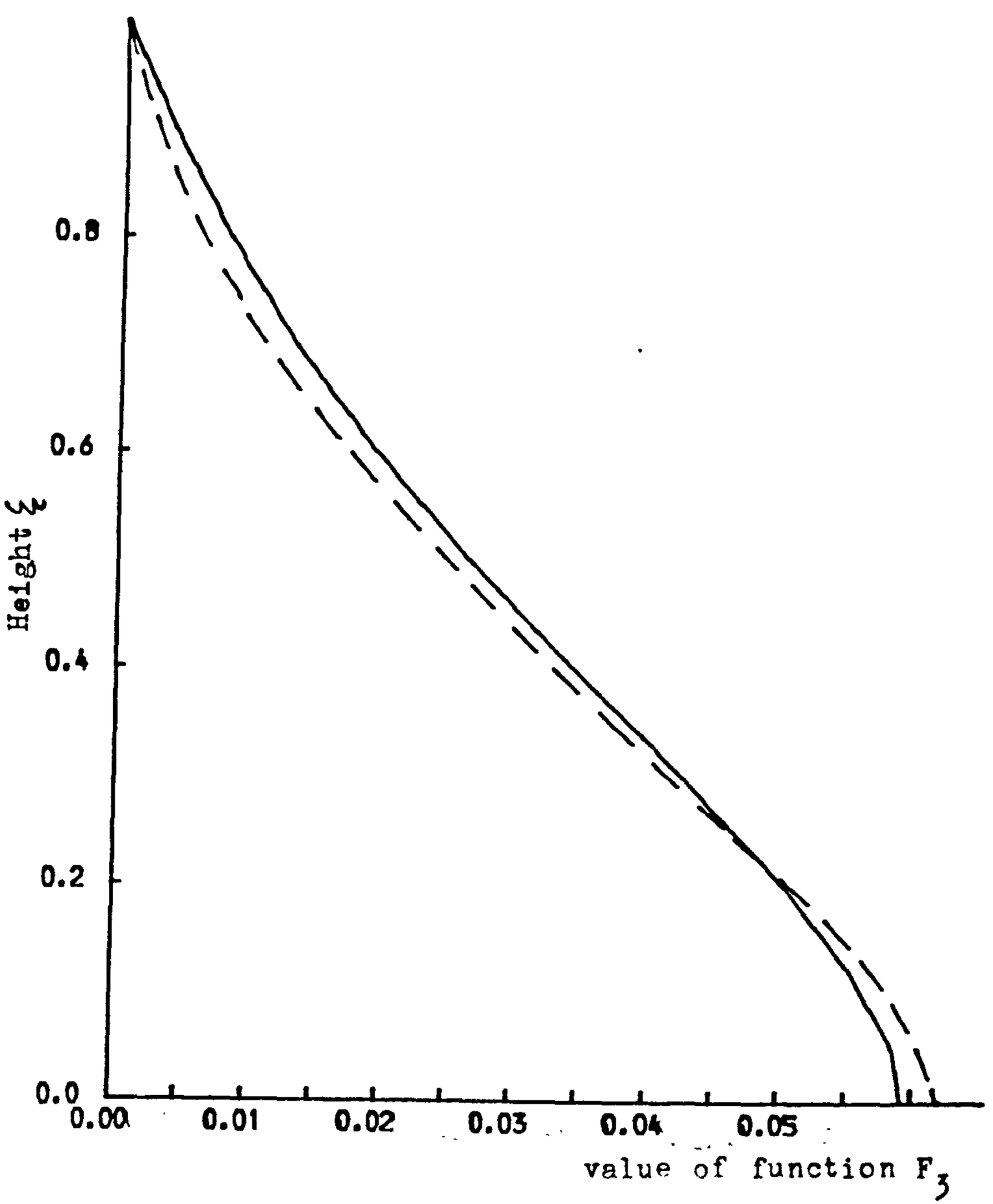

Fig. 2.12 Distribution of axial force in coupled walls

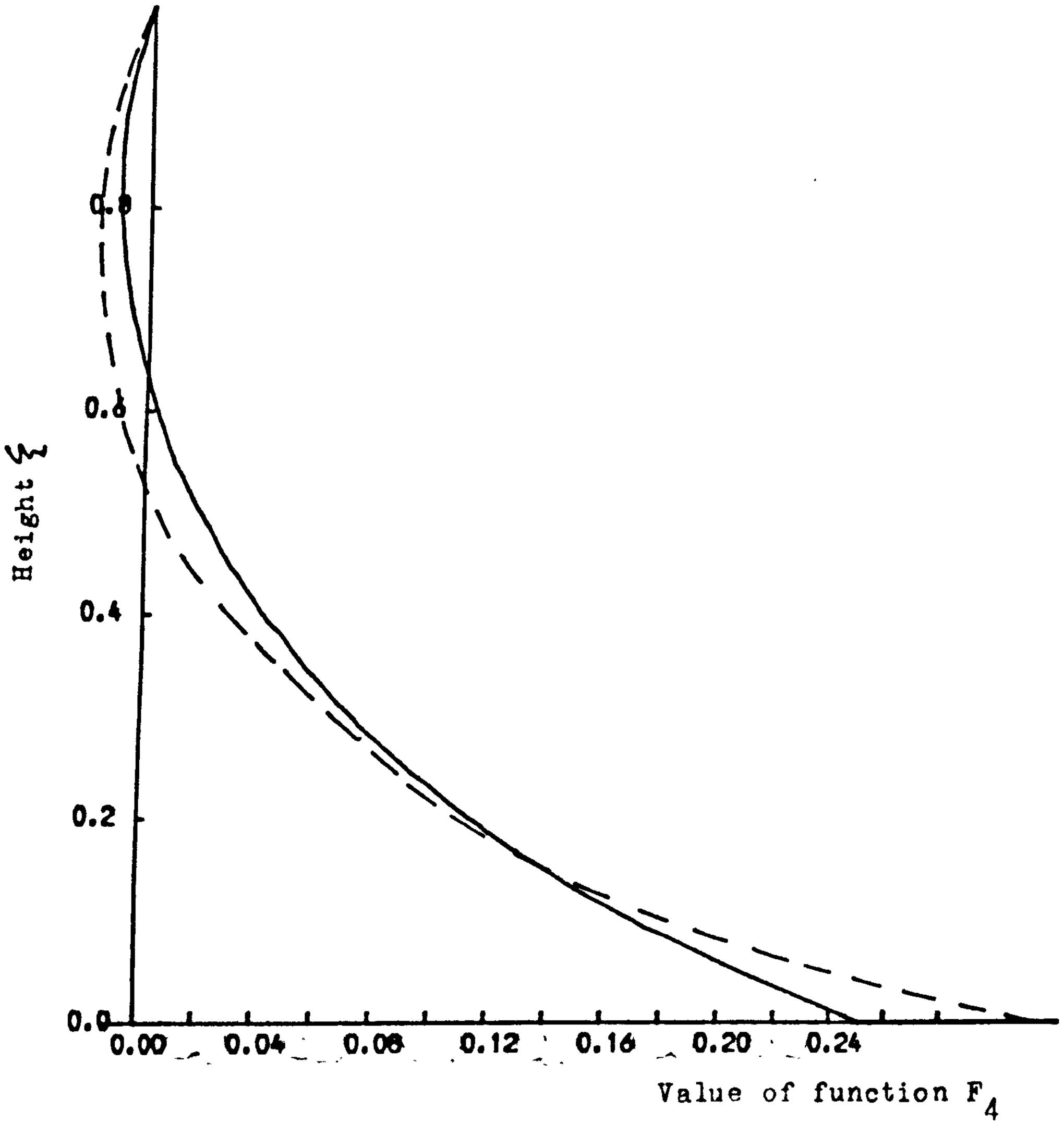

Fig. 2.13 Distribution of total moment in coupled walls

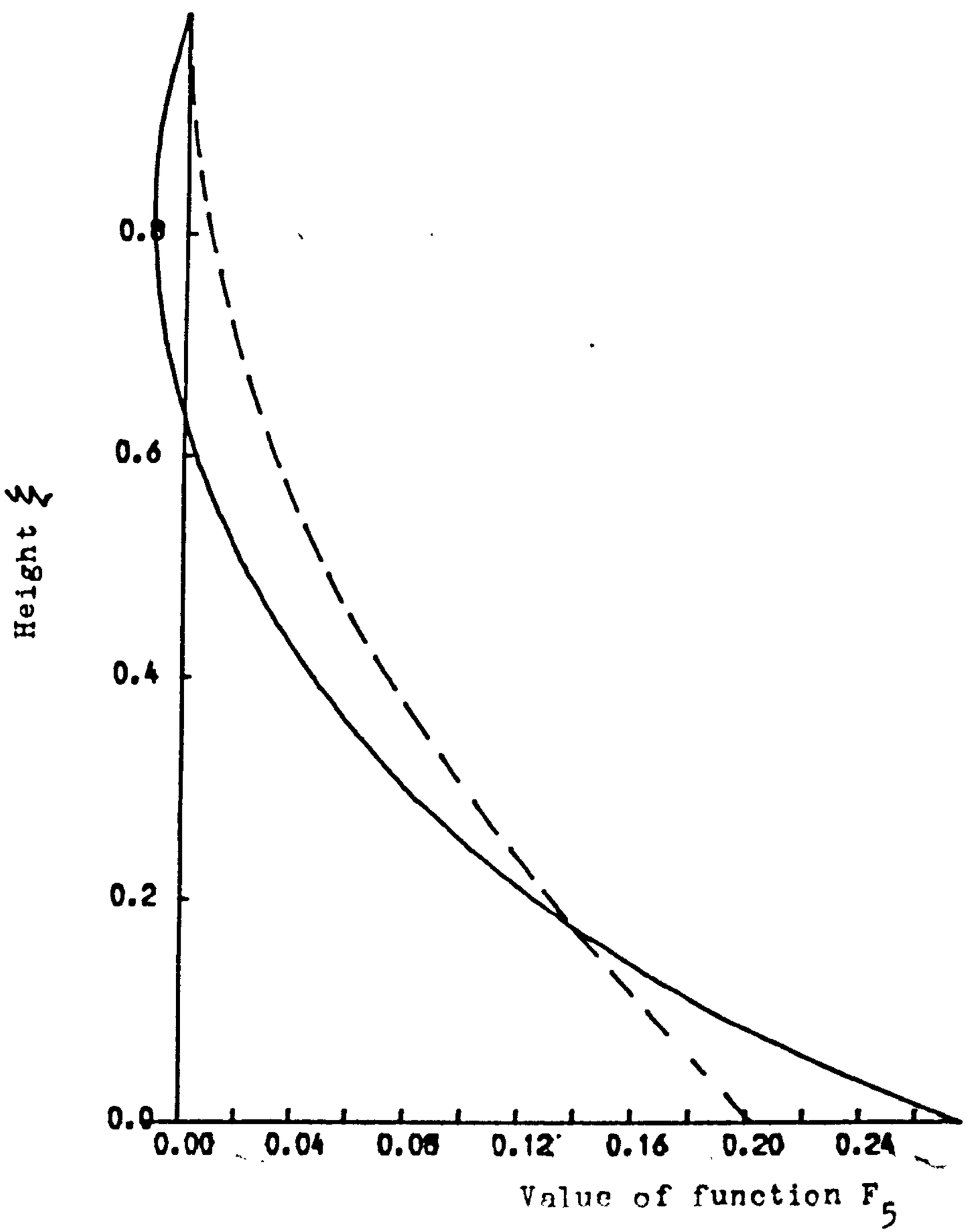

Fig. 2.14 Distribution of totao moment in core

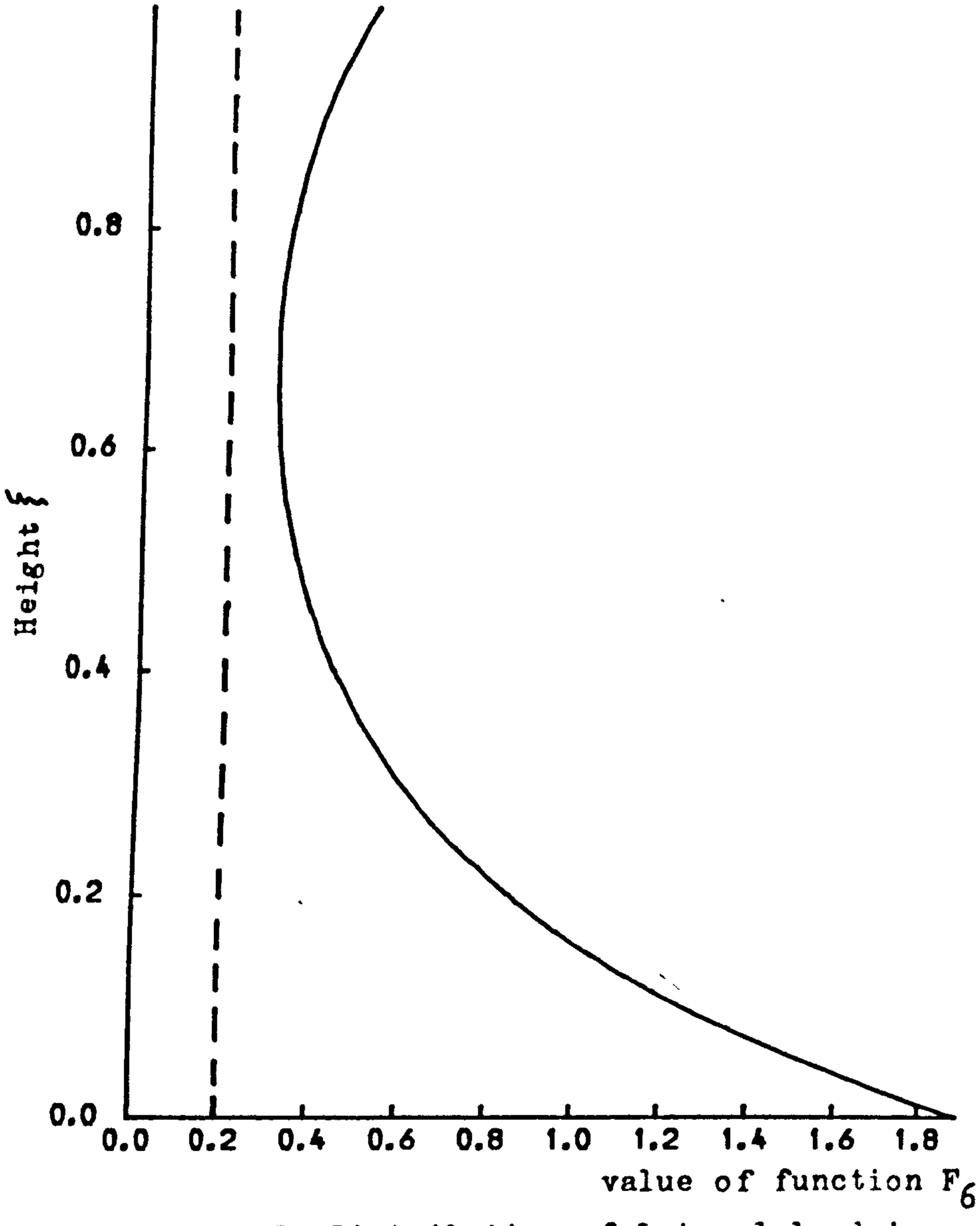

Fig. 2.15 Distribution of Lateral load in core

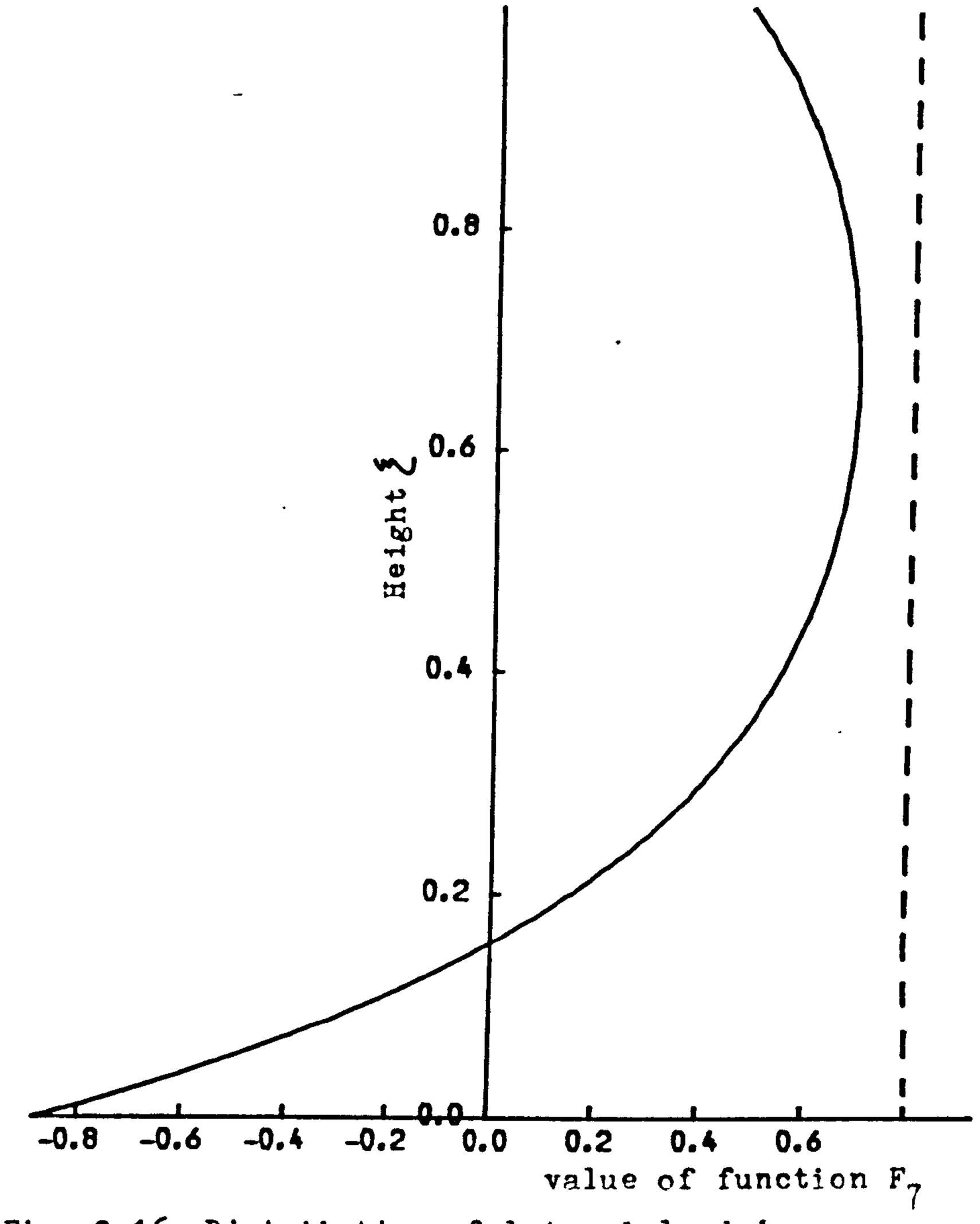

Fig. 2.16 Distribution of lateral load in coupled walls

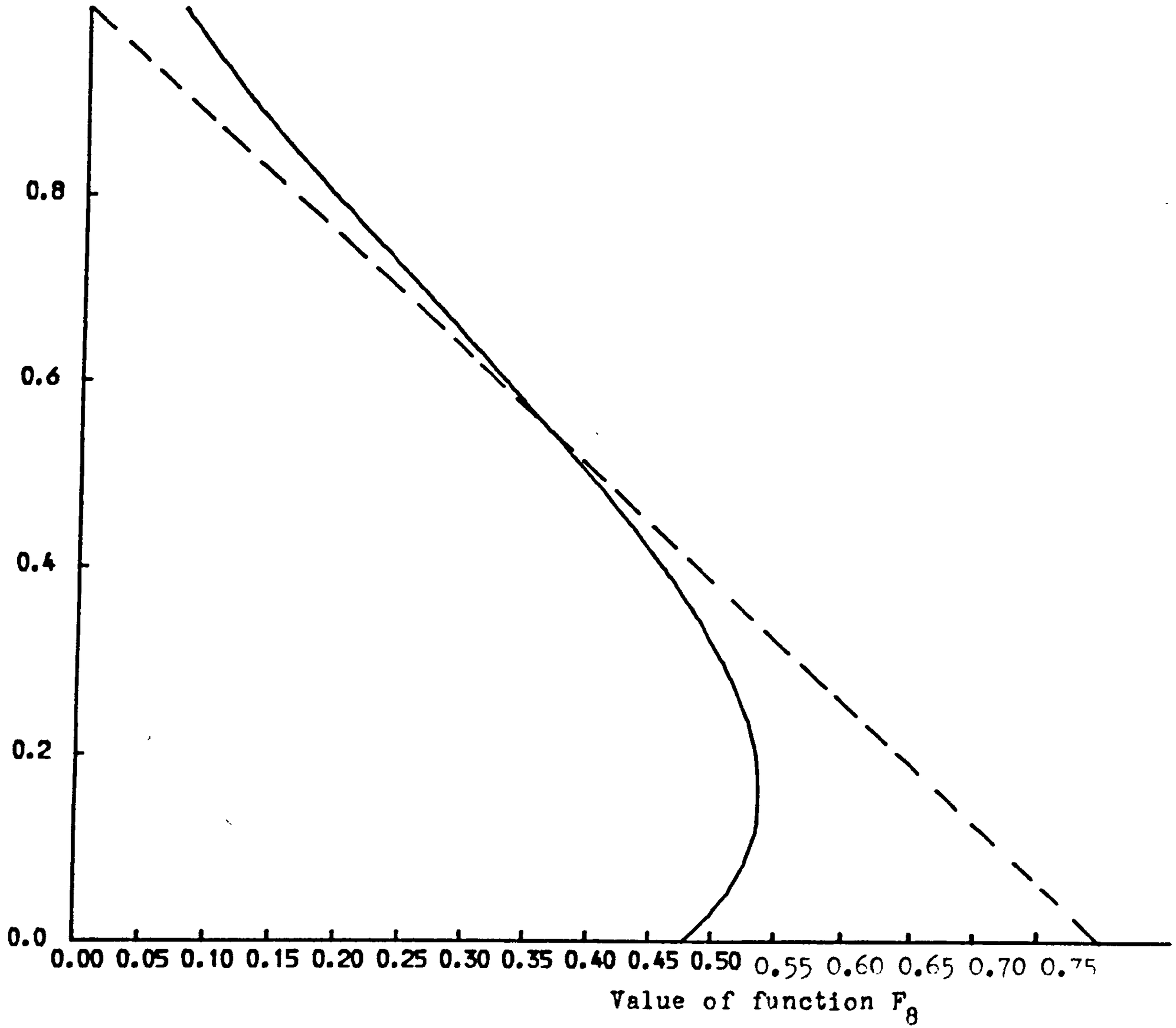

Fig. 2.17 Distribution of total shear force in coupled walls

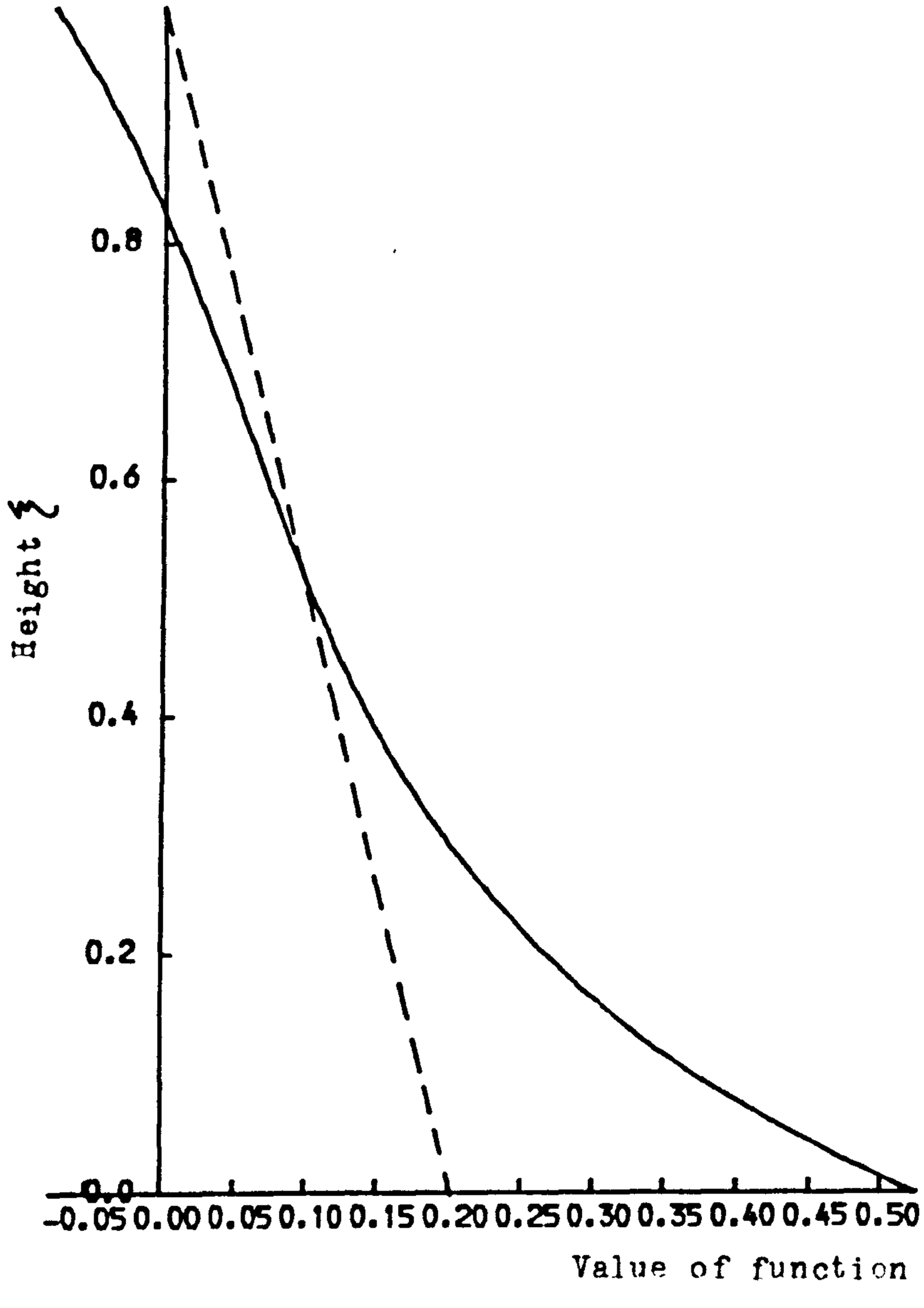

Fig. 2.18 Distribution of total shear force in core

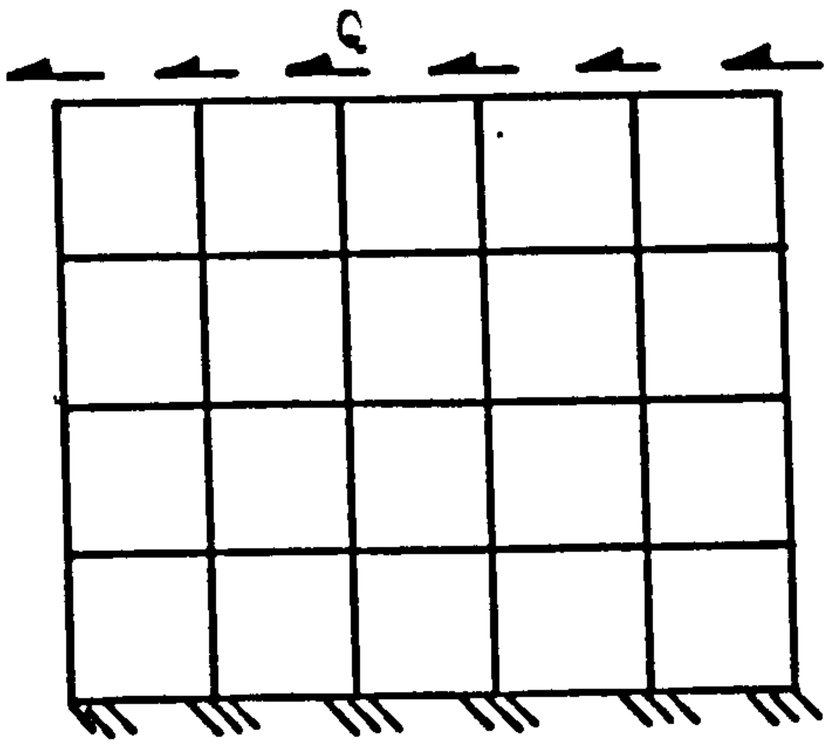

(a)

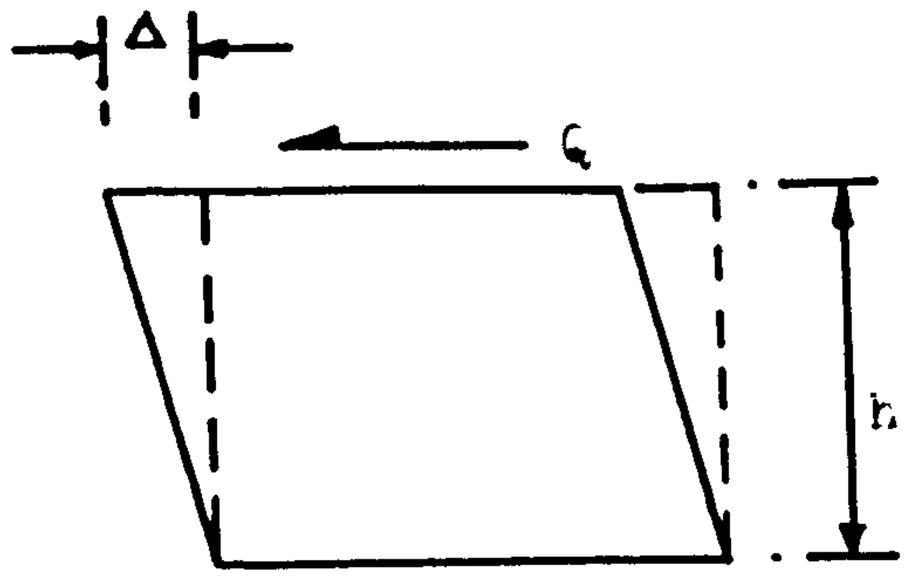

(b)

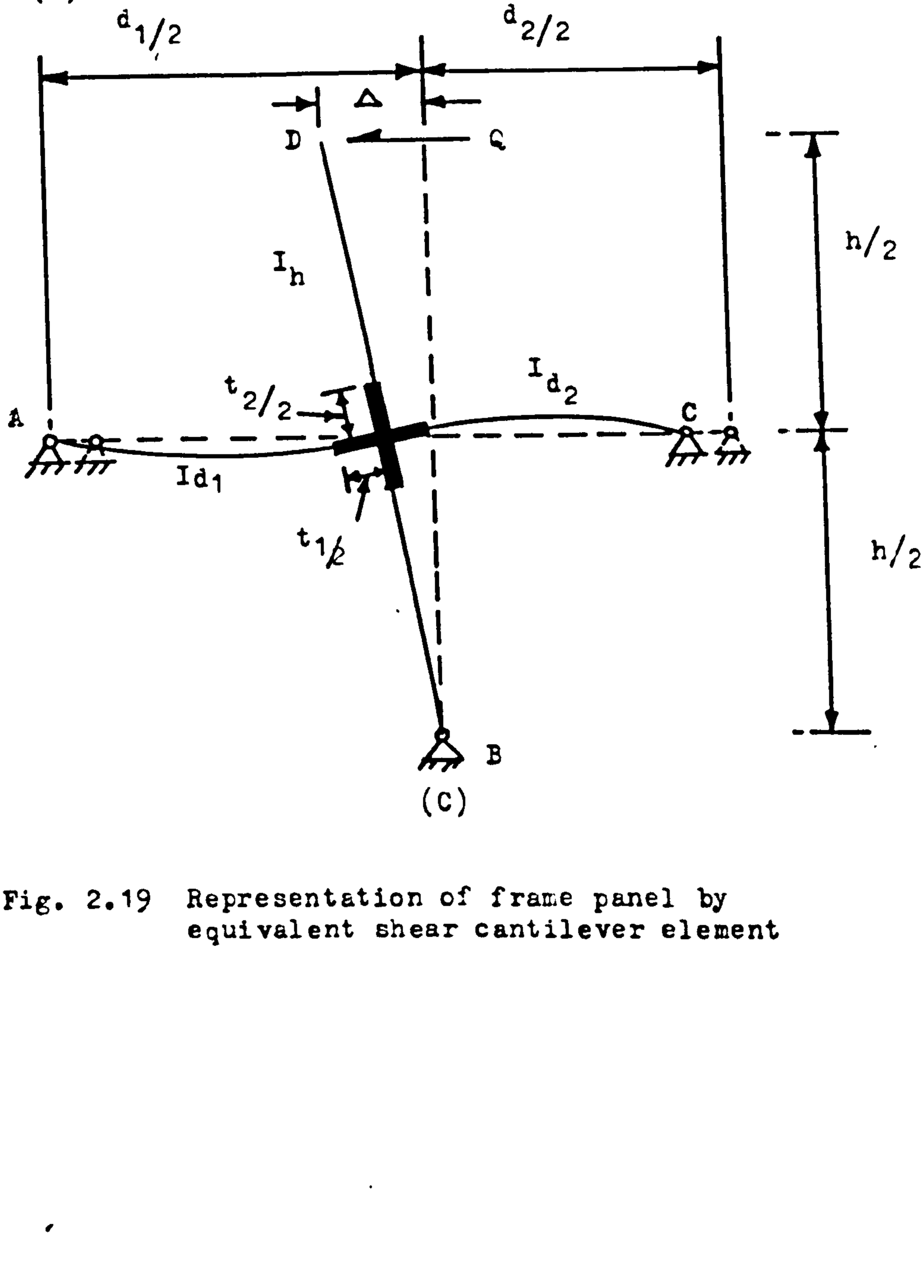

(c)

Fig. 2.19 Representation of frame panel by equivalent shear cantilever element

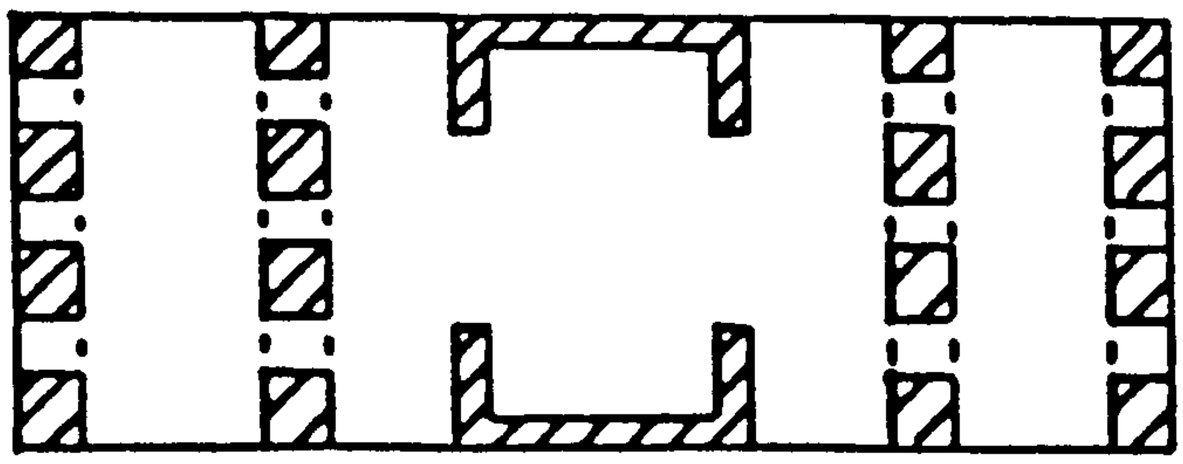

Fig. 2.20(a) Symmetric core-frame structure

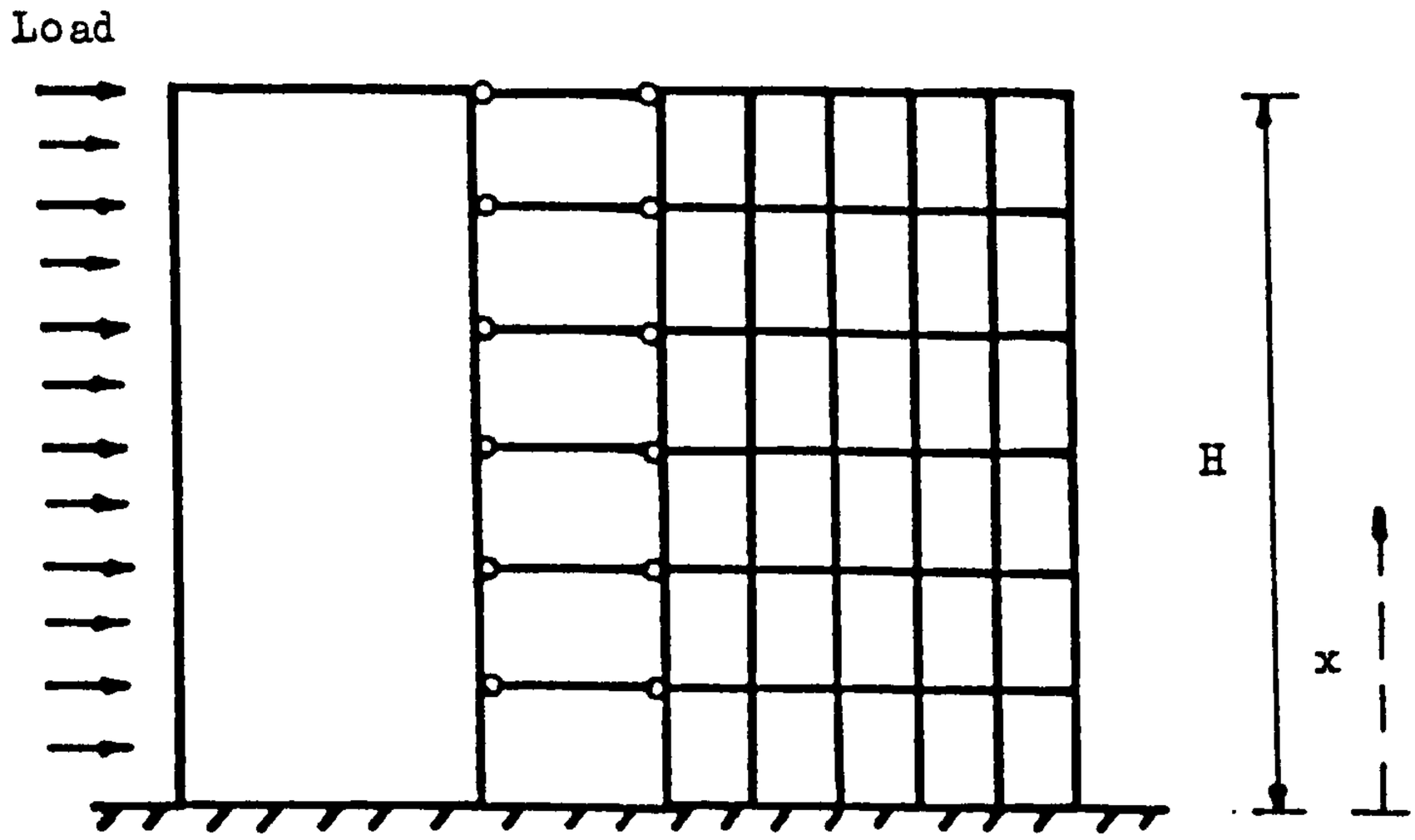

Fig. 2.20(b) Equivalent plane system

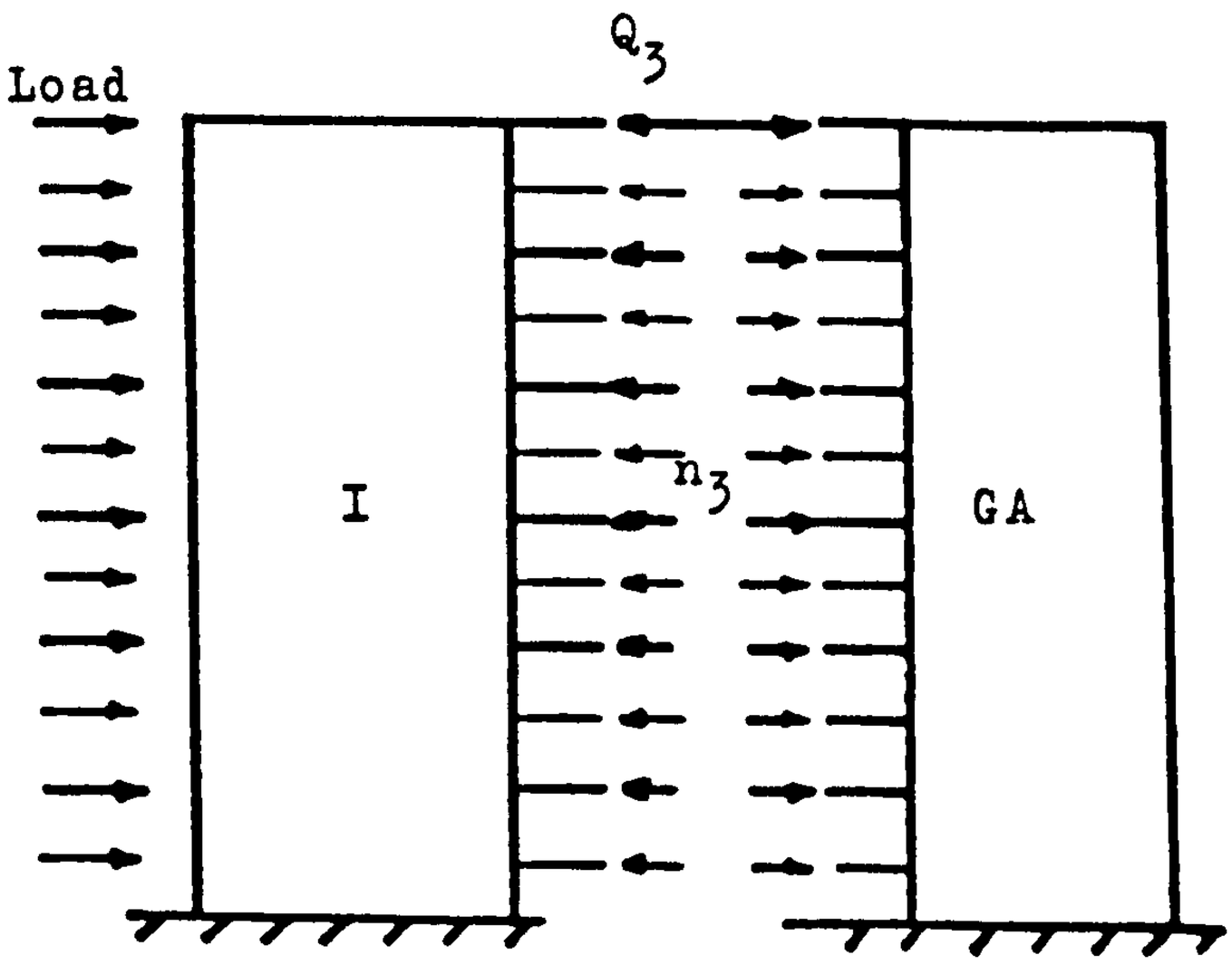

Fig. 2.20(c) Substitute system

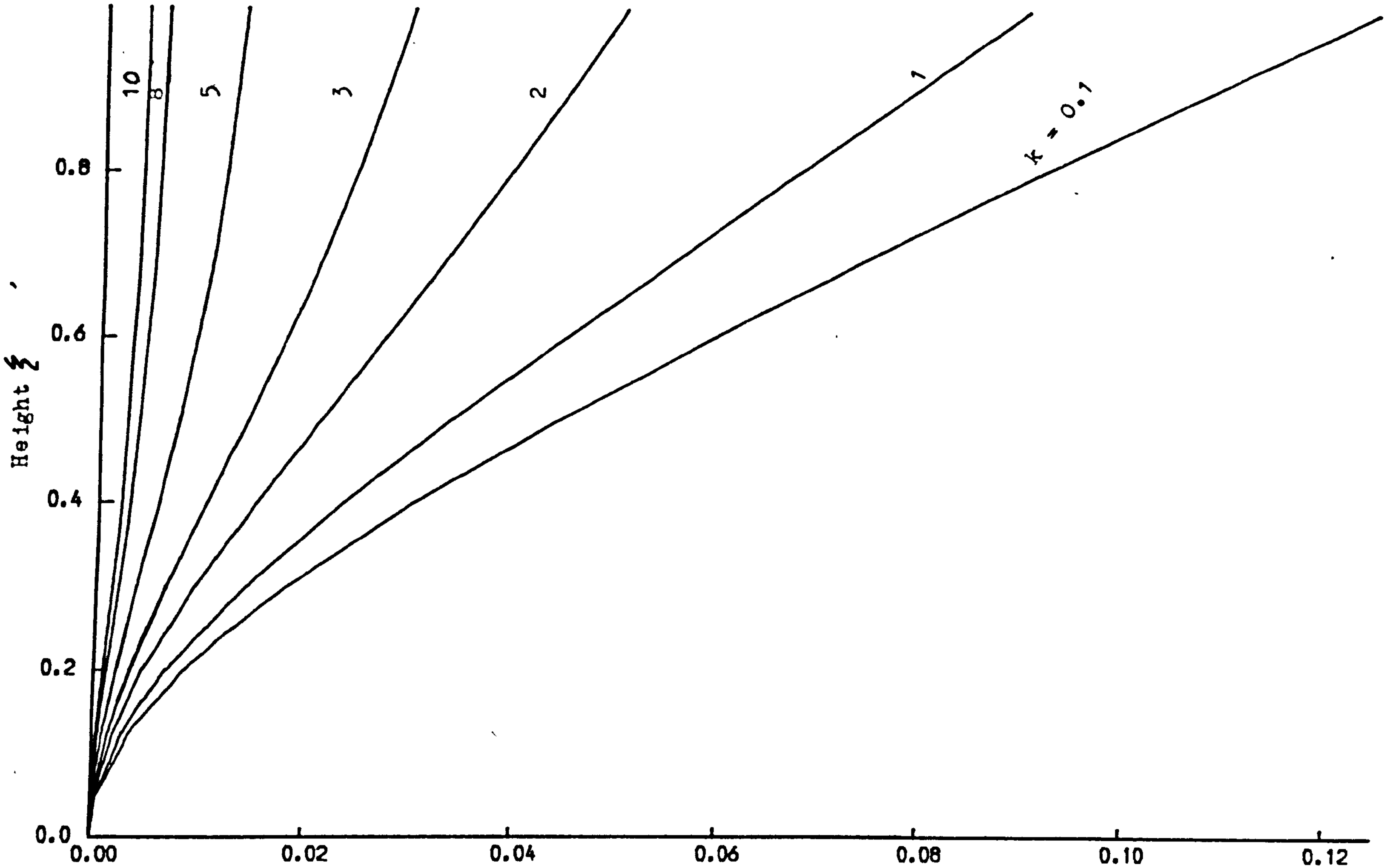

Fig. 2.21 Variation of Deflection Function P_1

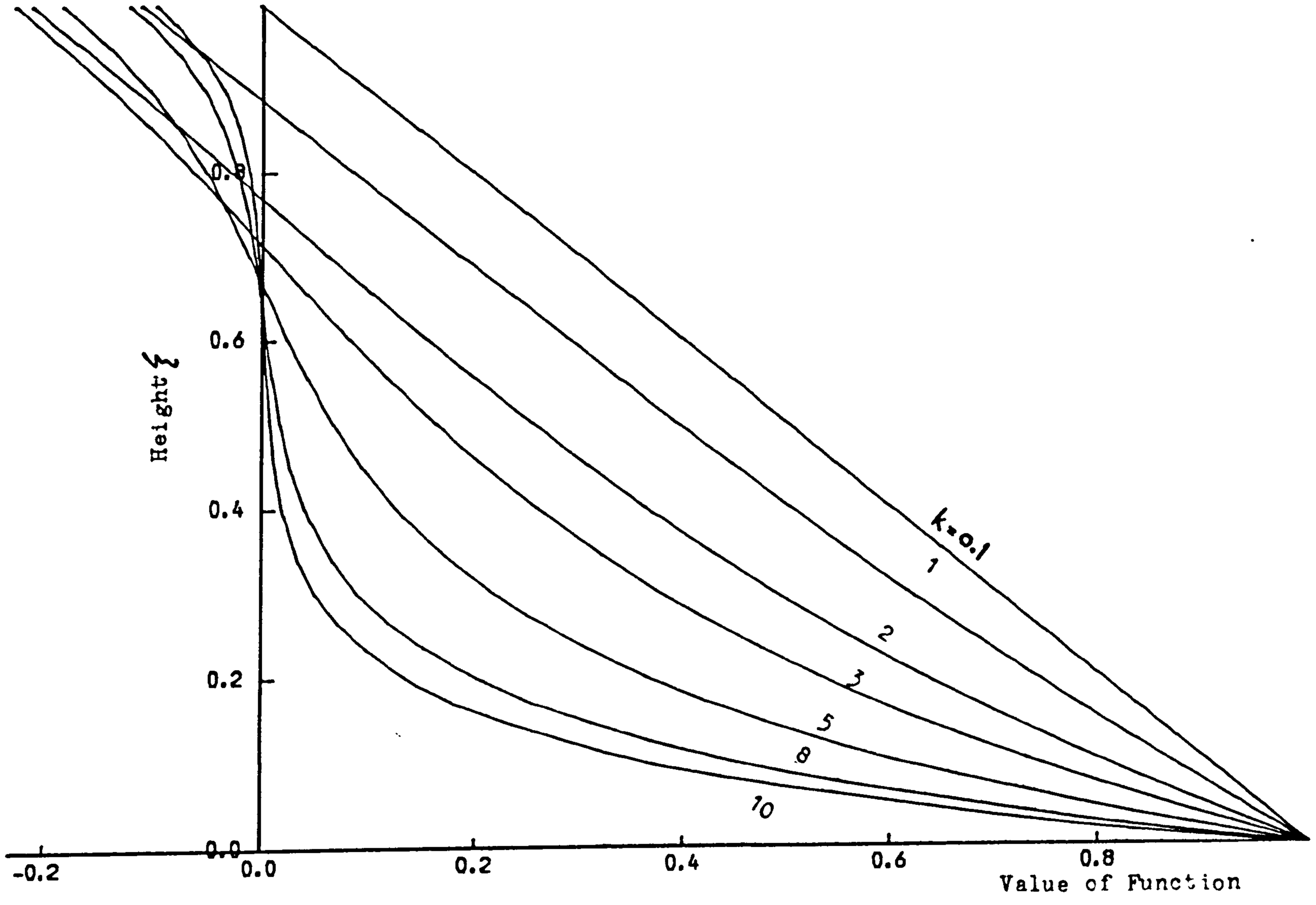

Fig. 2.22 Variation of Shear Force Function in Shear Walls P_2

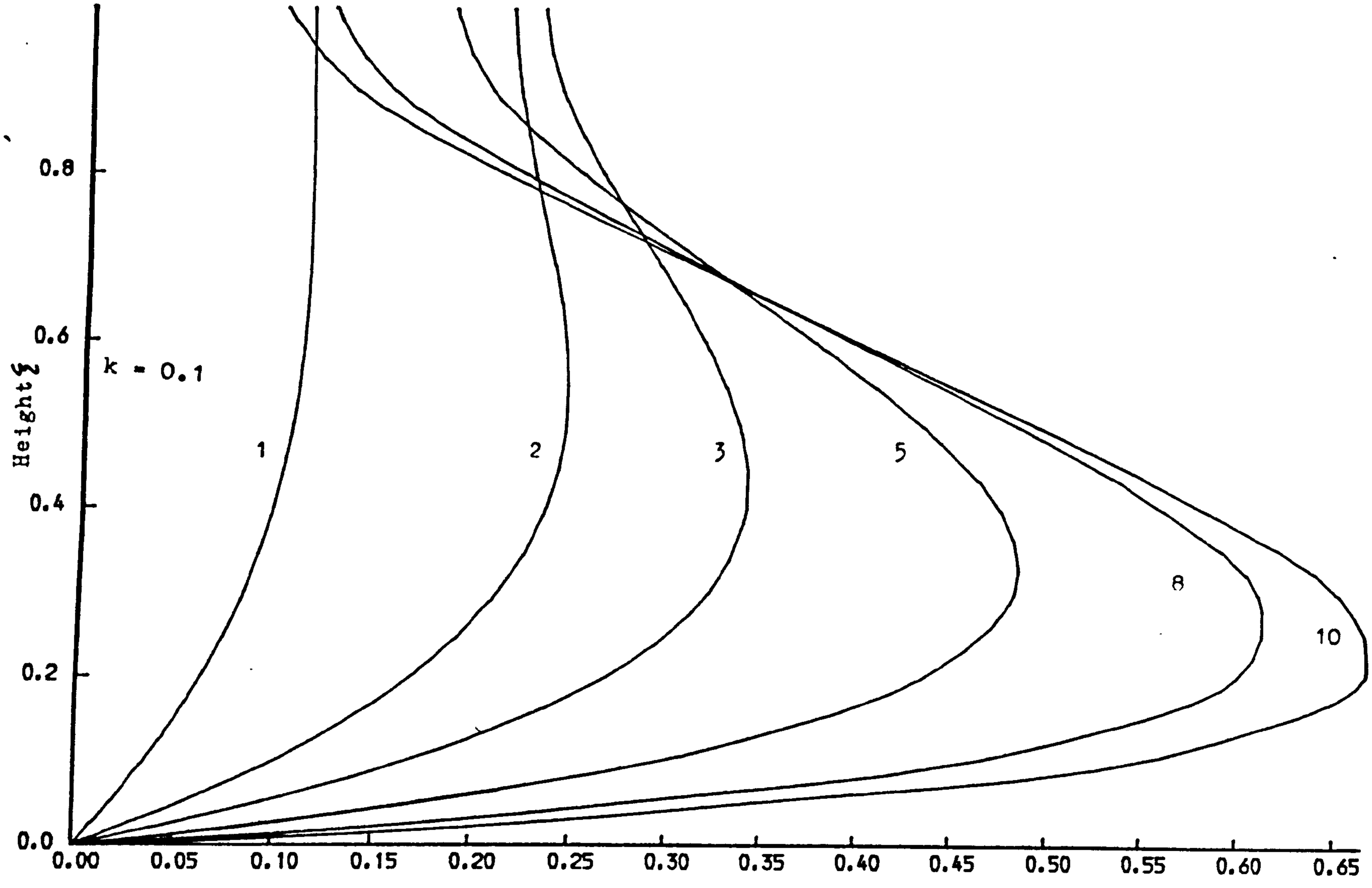

Fig. 2.23 Variation of the Shear Force Function in Frames P_3

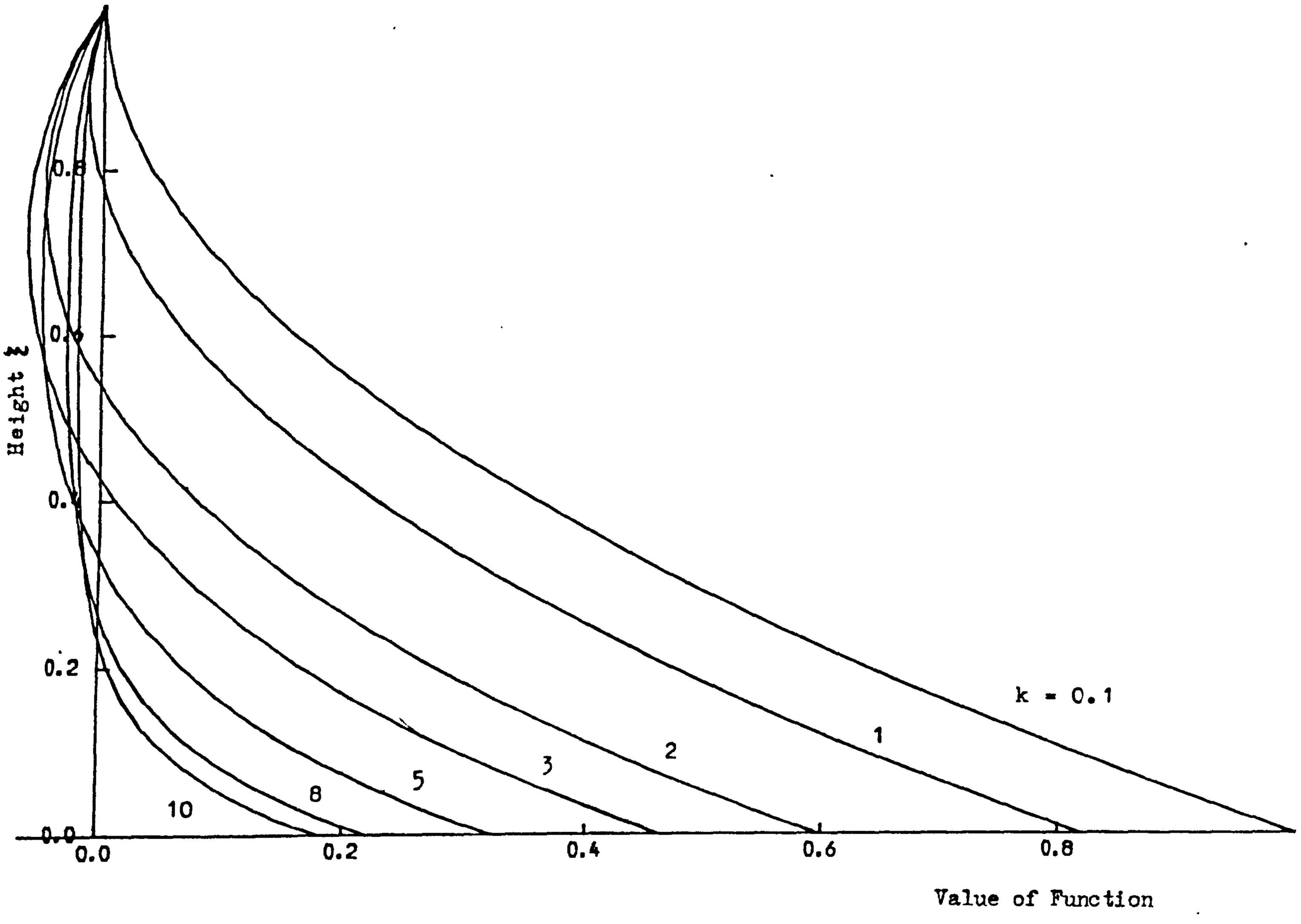

Fig. 2.24 Variation of Moment Function in Shear walls P_4

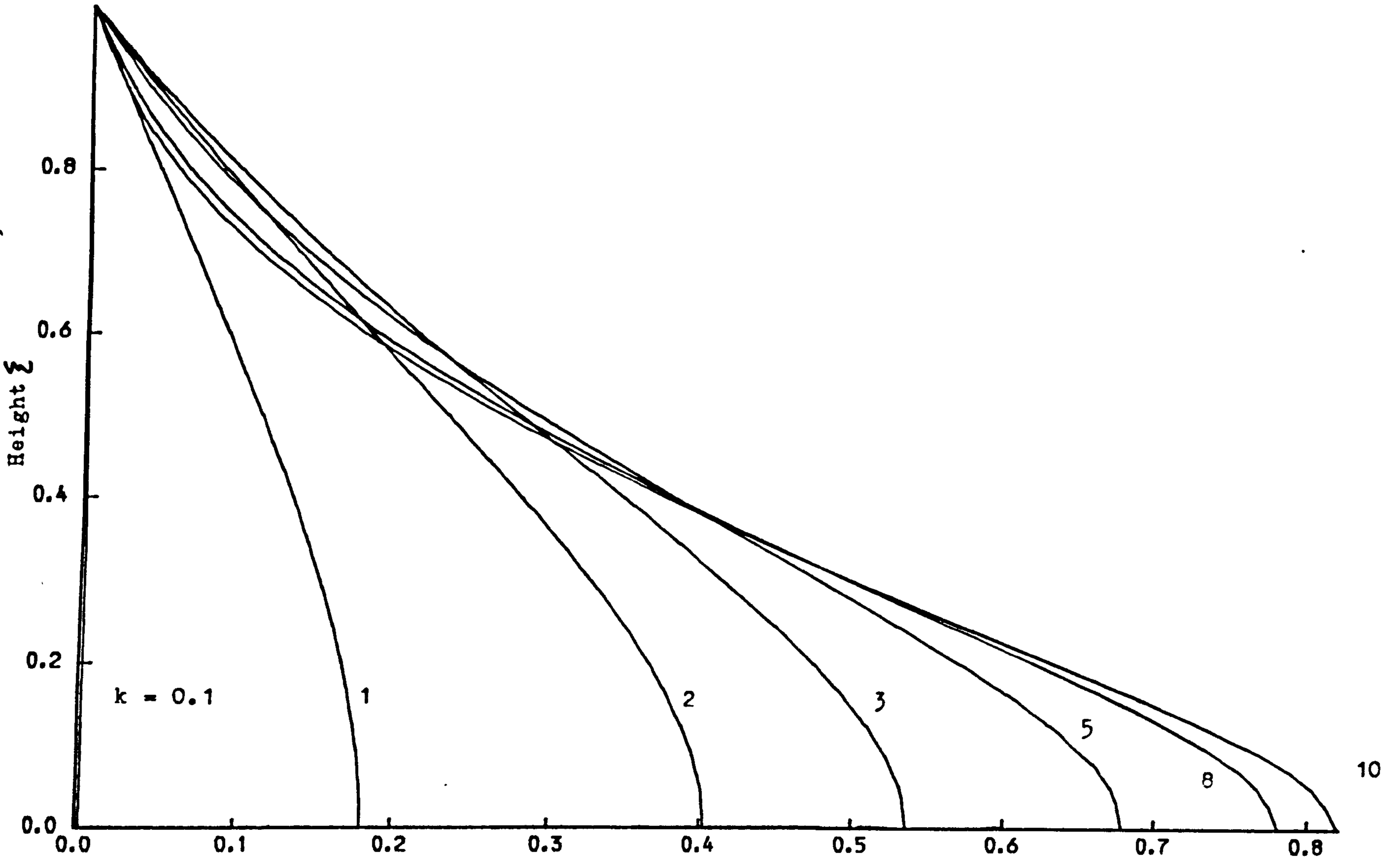

Fig. 2.25 Variation of the Moment Function in Frames P_5

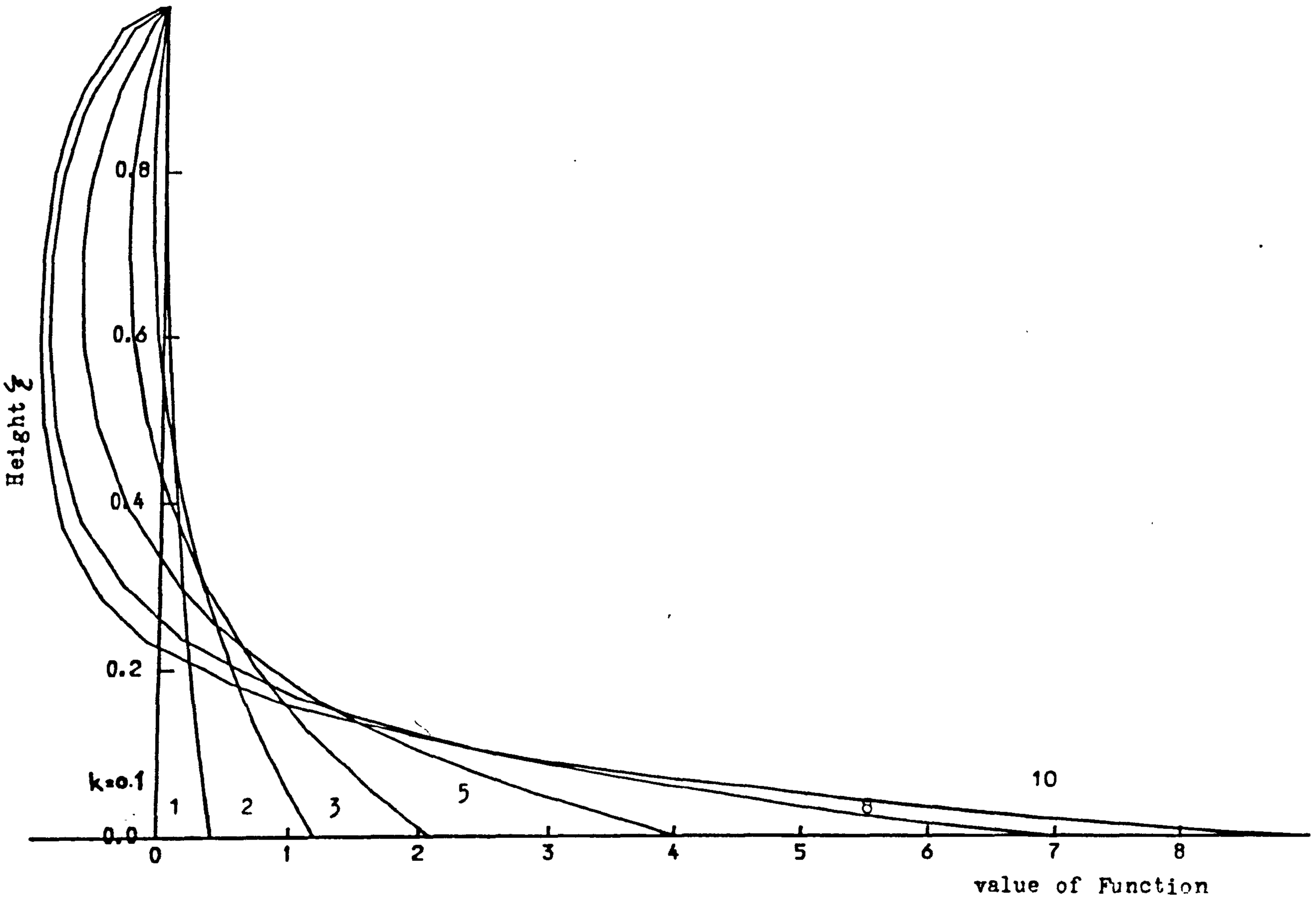

Fig. 2.26 Variation of the Axial Force Function in Connecting Media P_6

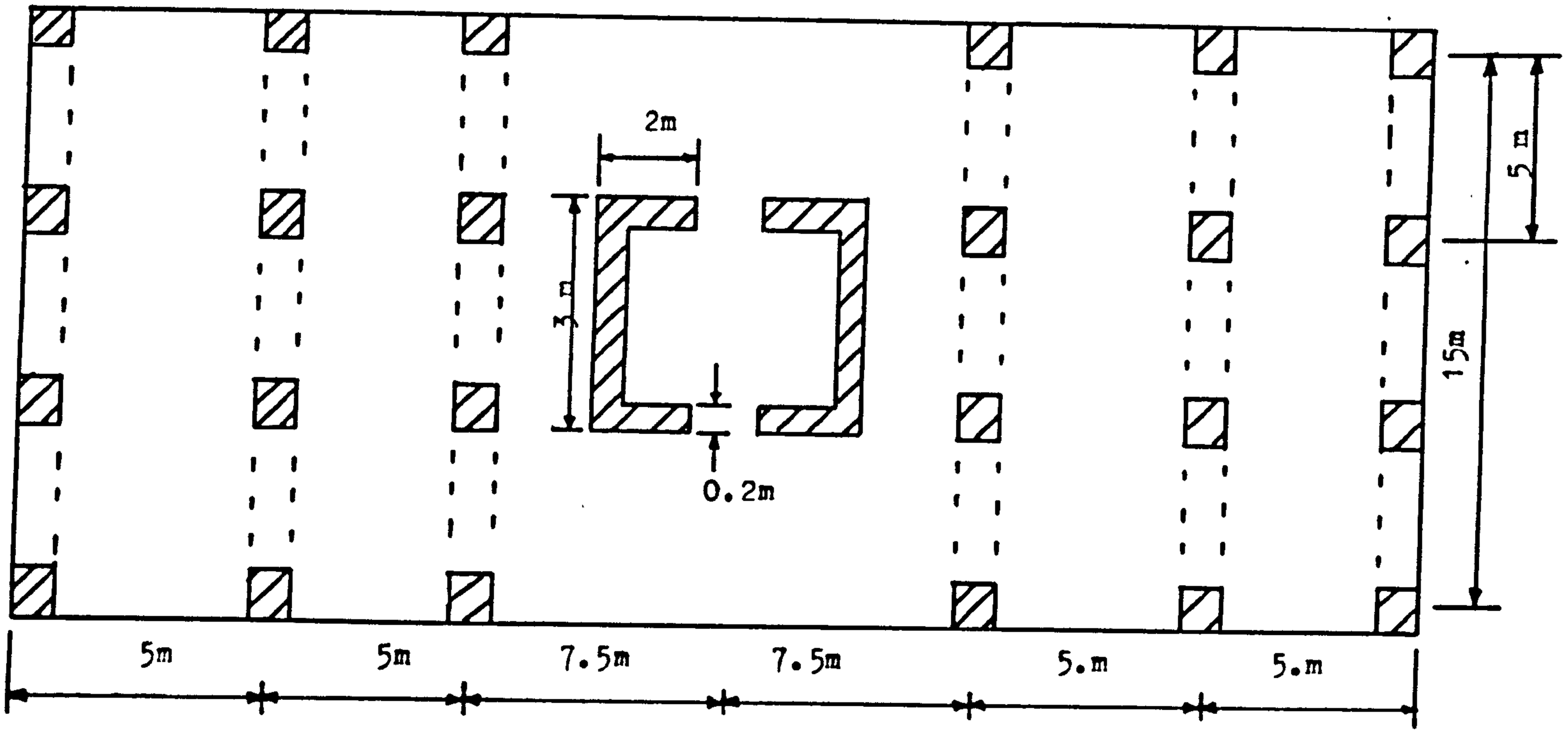

Fig. 2.27 plan form of structure for numerical example

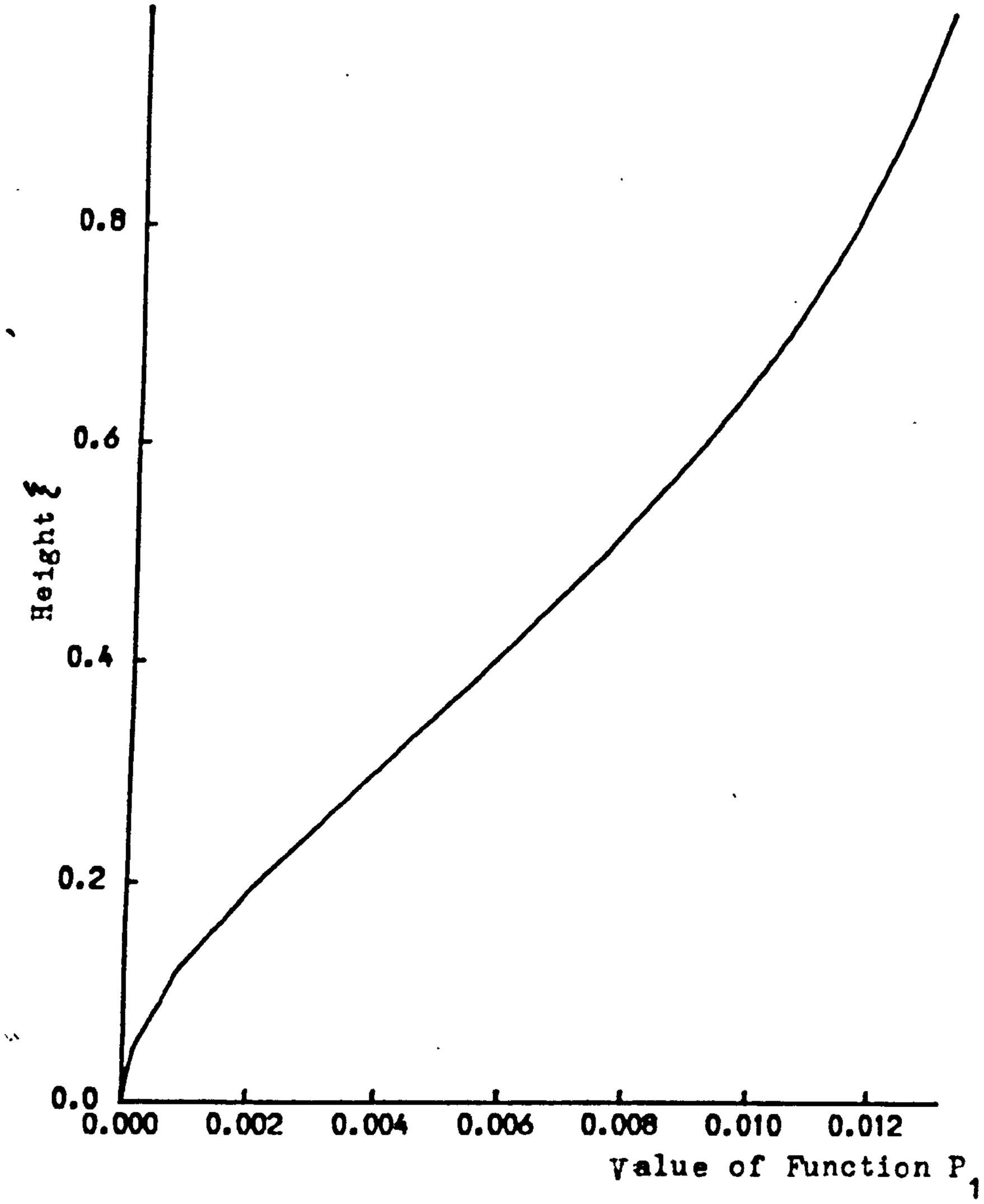

Fig. 2.28 Distribution of lateral deflection

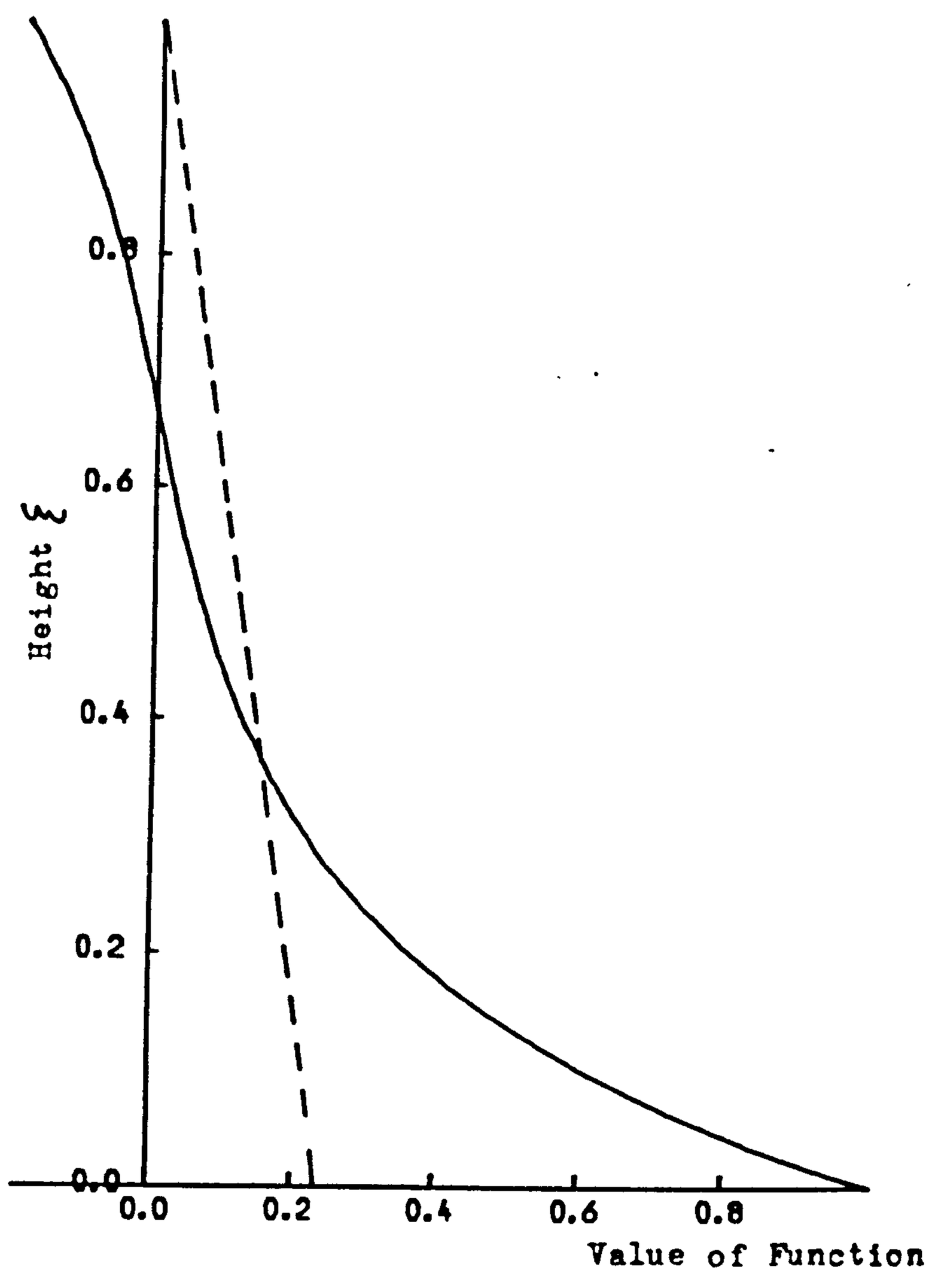

Fig.2.29 Distribution of total shear force in core

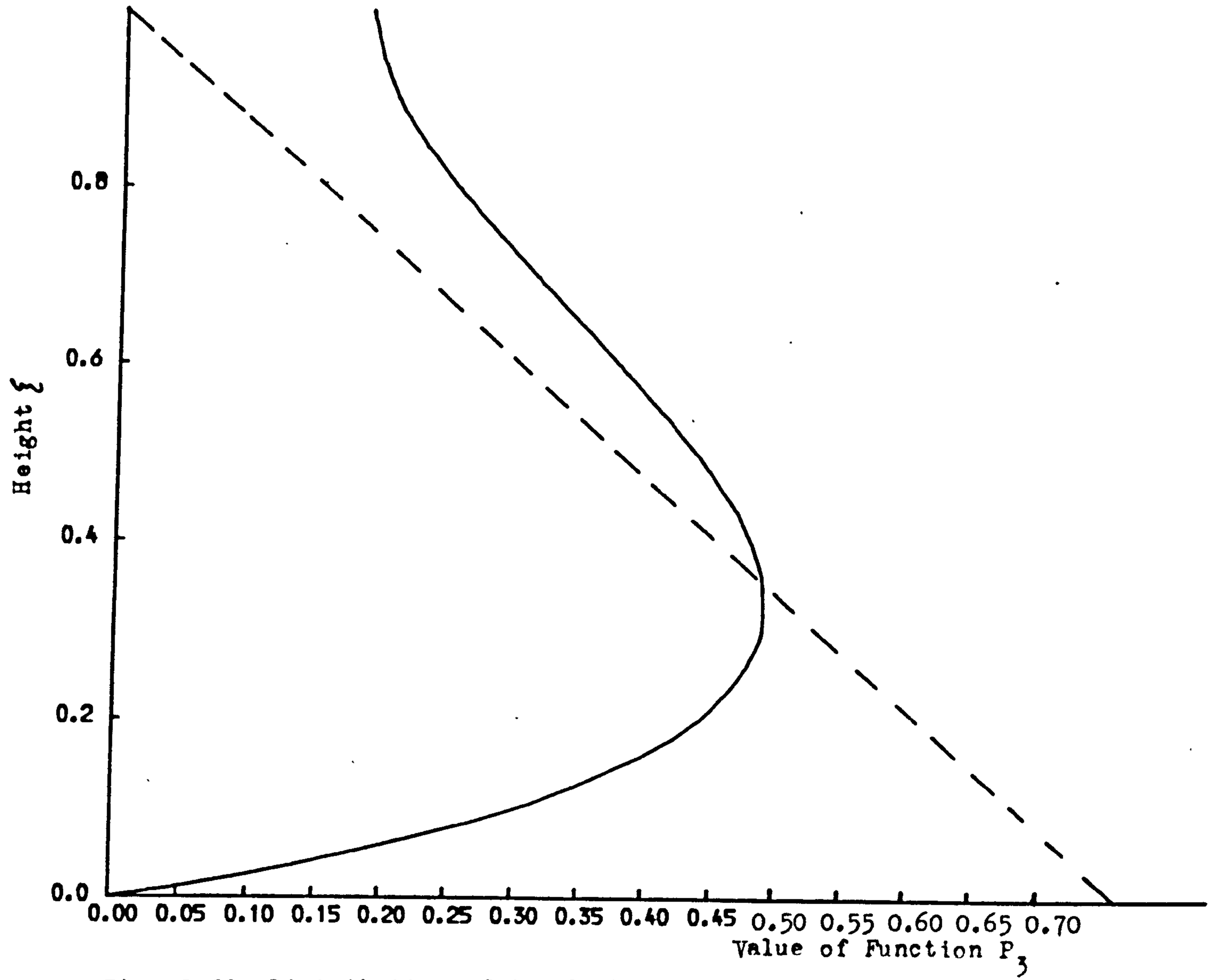

Fig. 2.30 Distribution of total shear force in frames

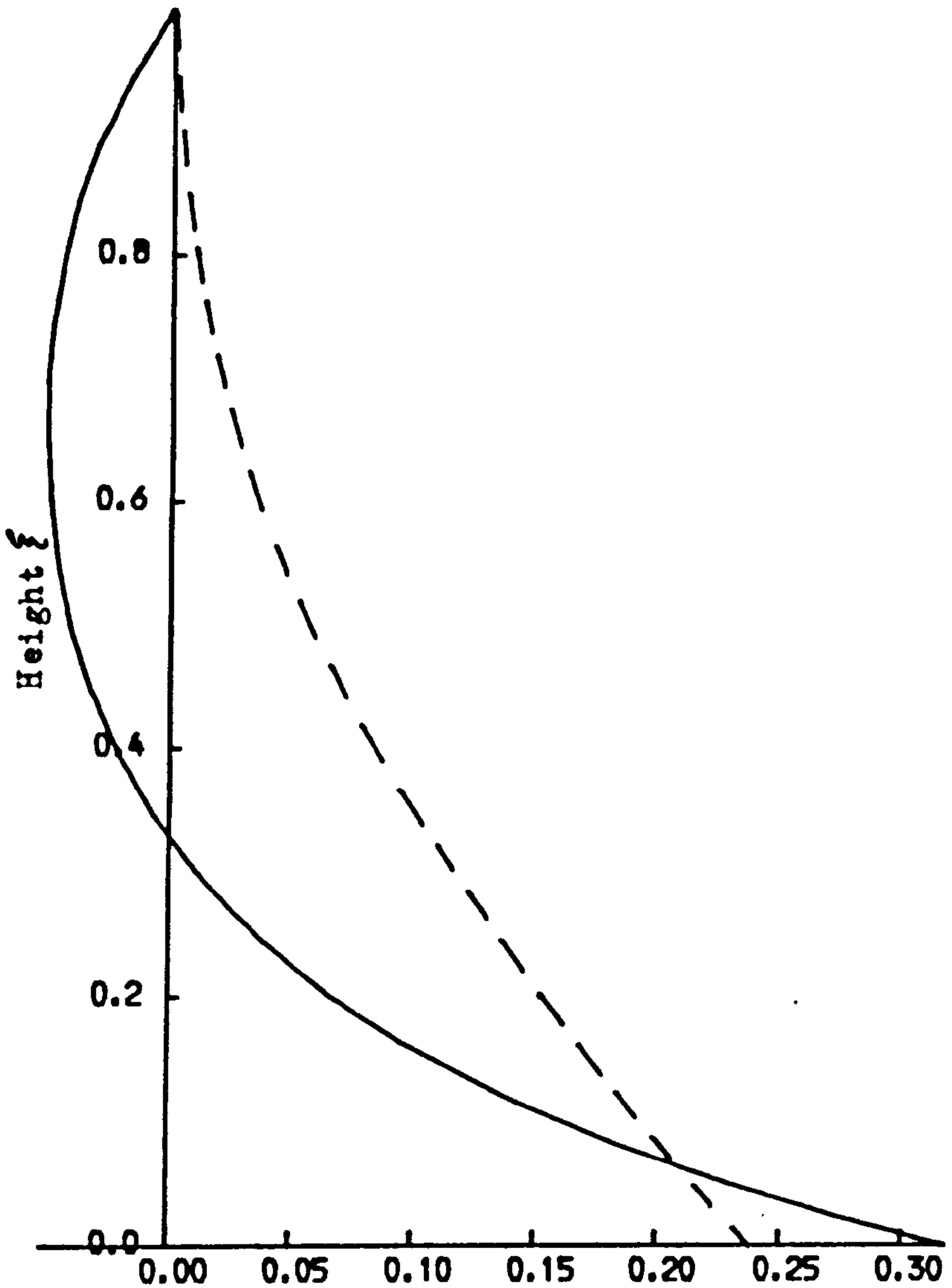

Fig. 2.31 Distribution of total moment in core

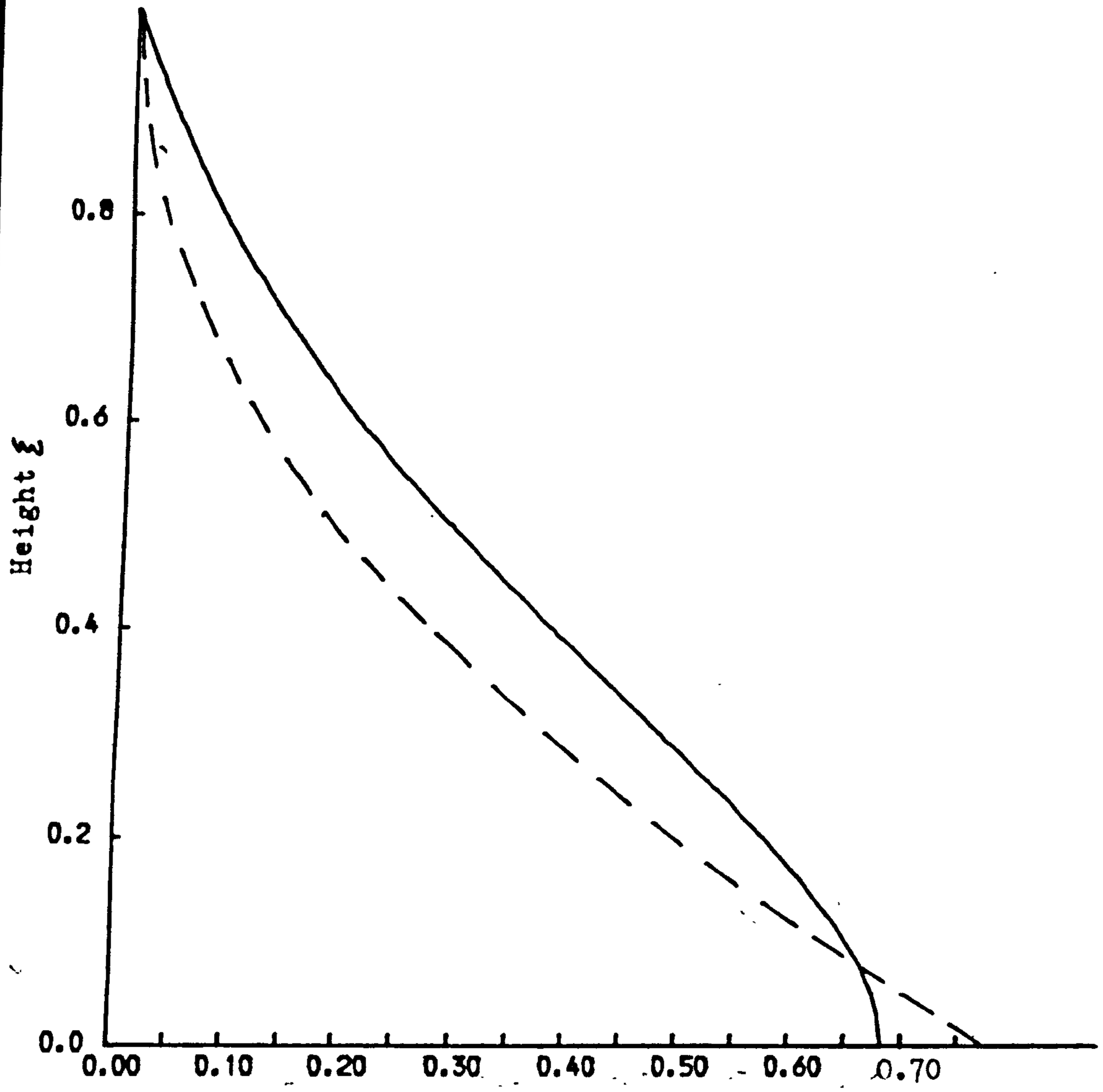

Fig. 2.32 Distribution of total moment in frames

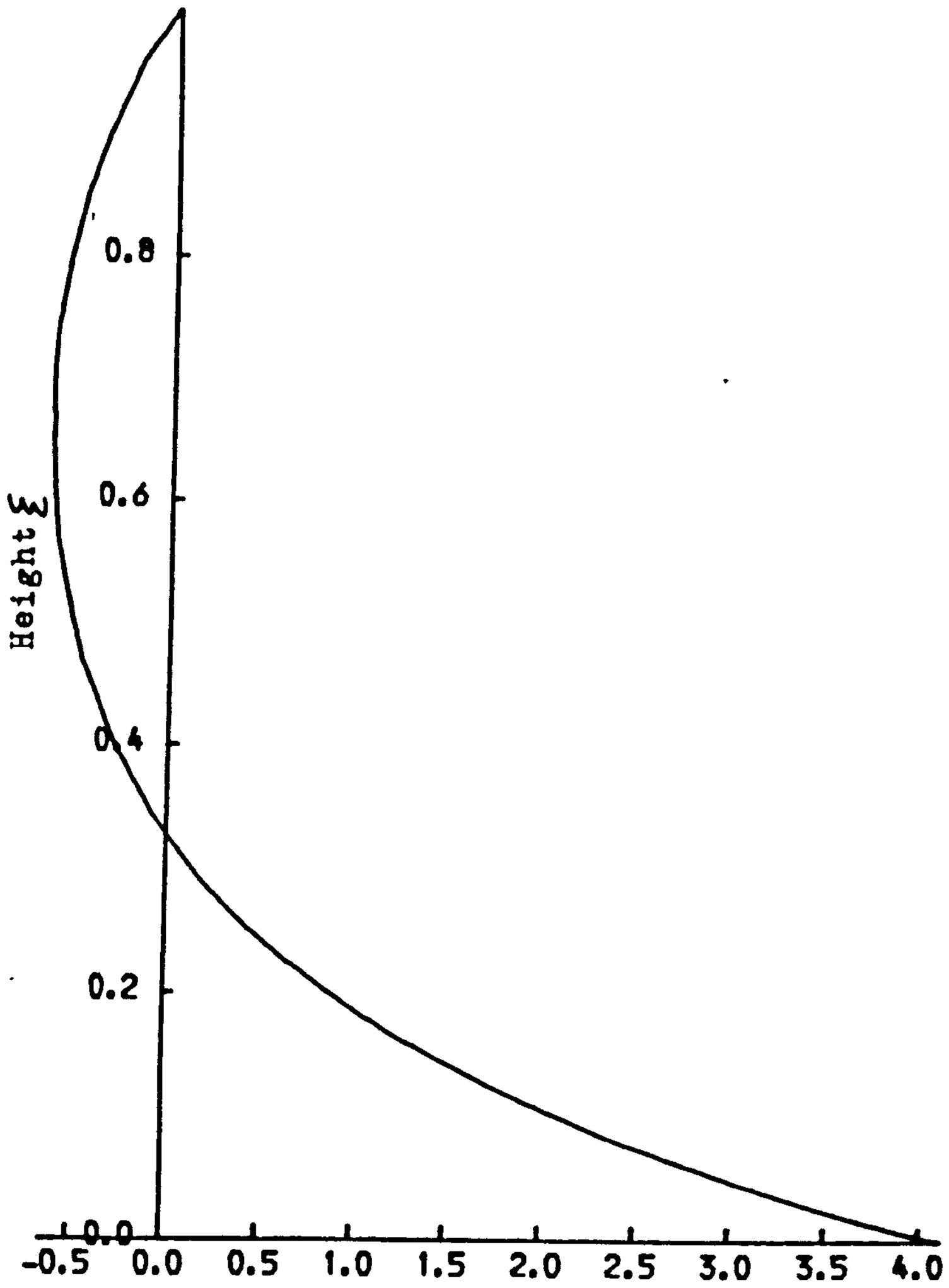

Fig. 2.33 Distribution of the axial force

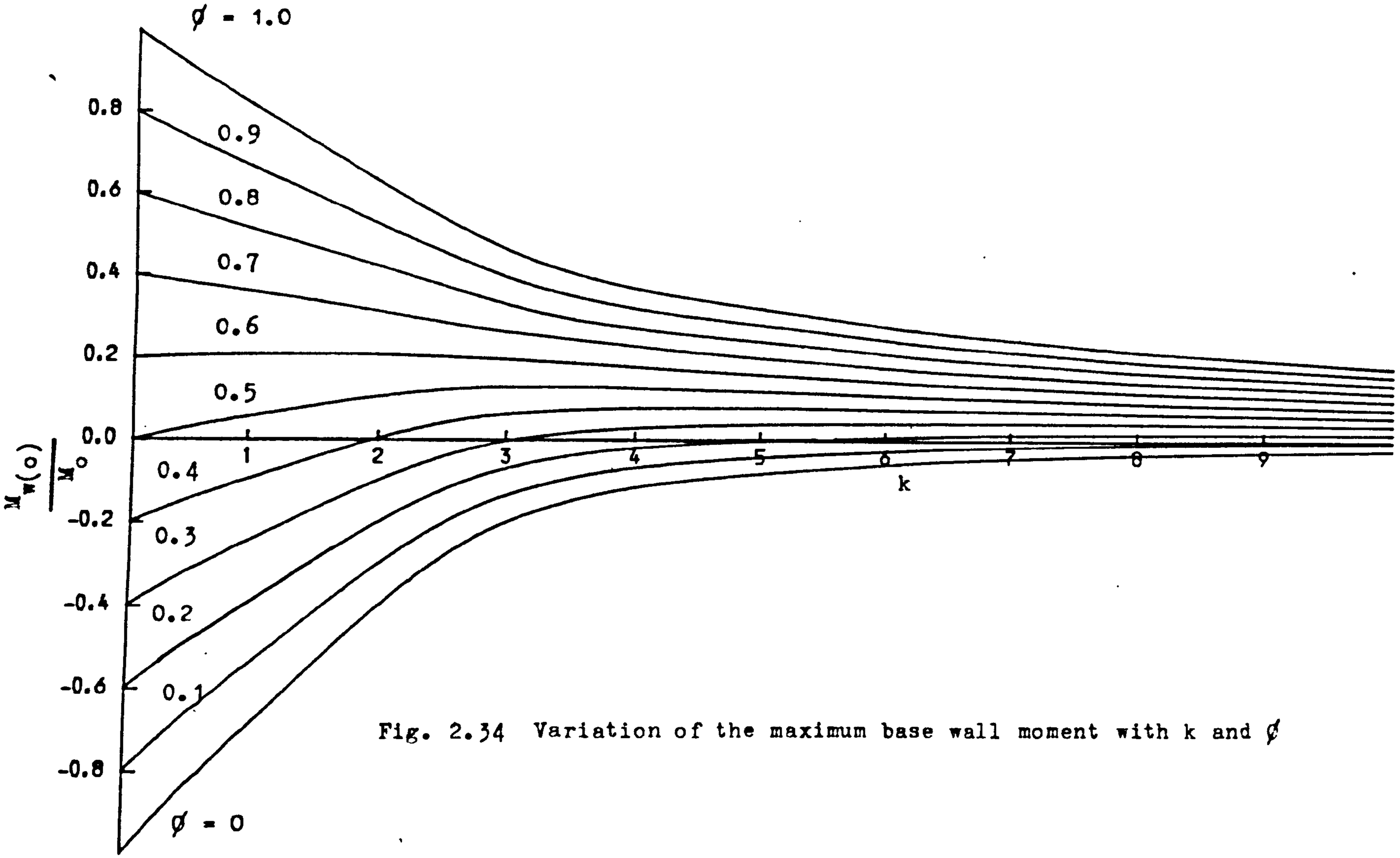

Fig. 2.34 Variation of the maximum base wall moment with k and ϕ

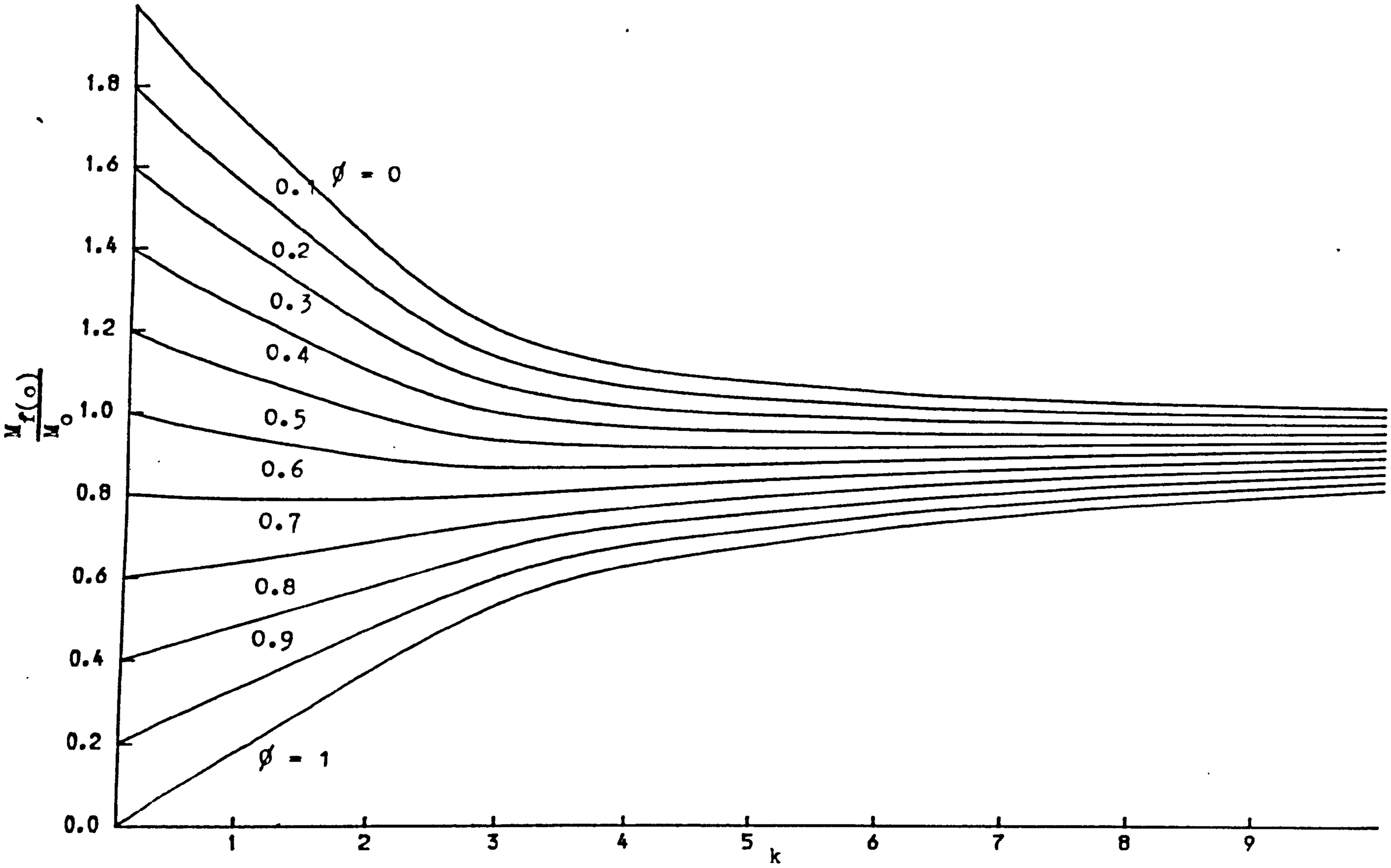

Fig. 2.35 Variation of the maximum base frame moment with k and ϕ

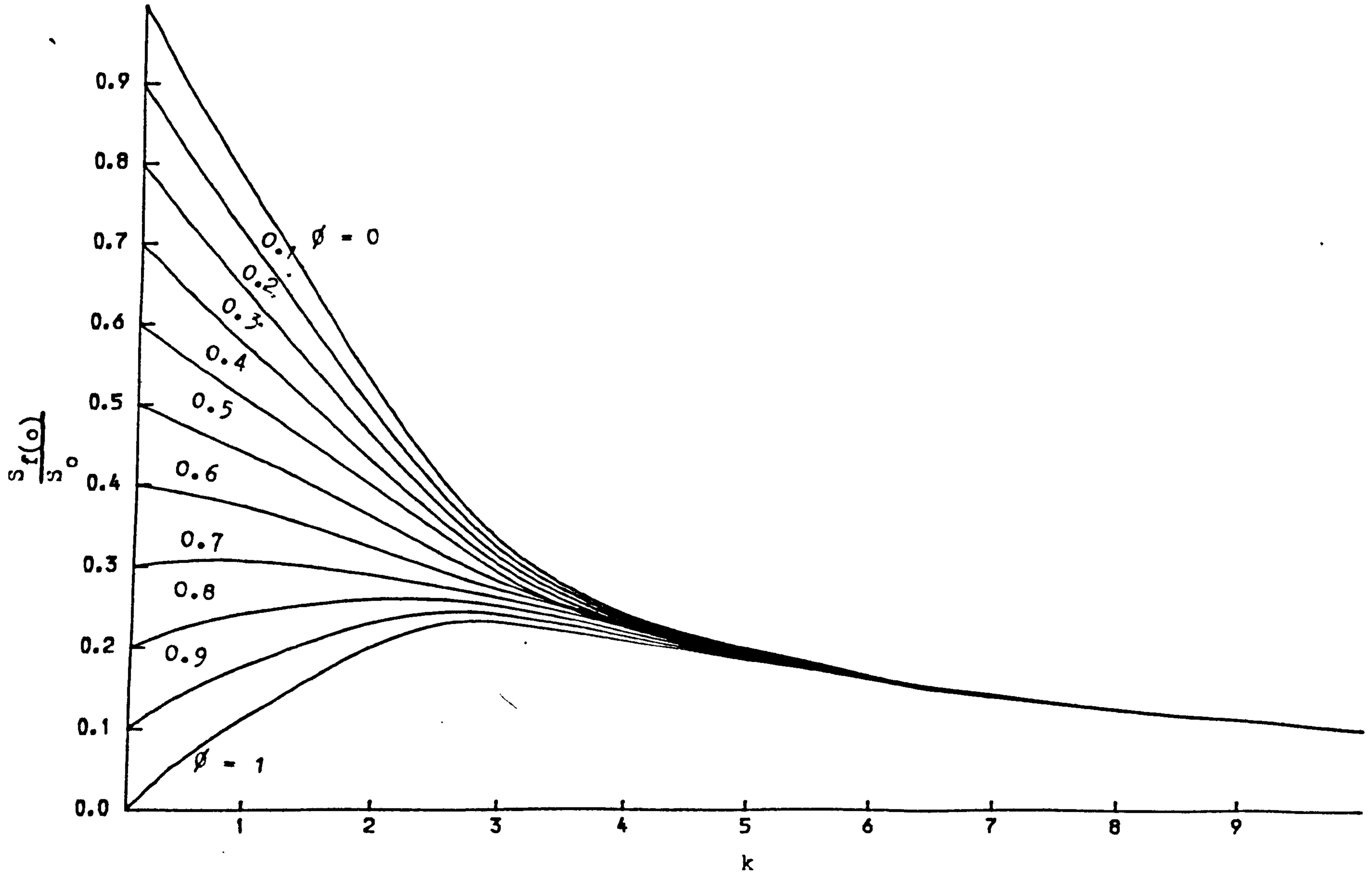

Fig. 2.36 Variation of the frame top shear force with k and Ø

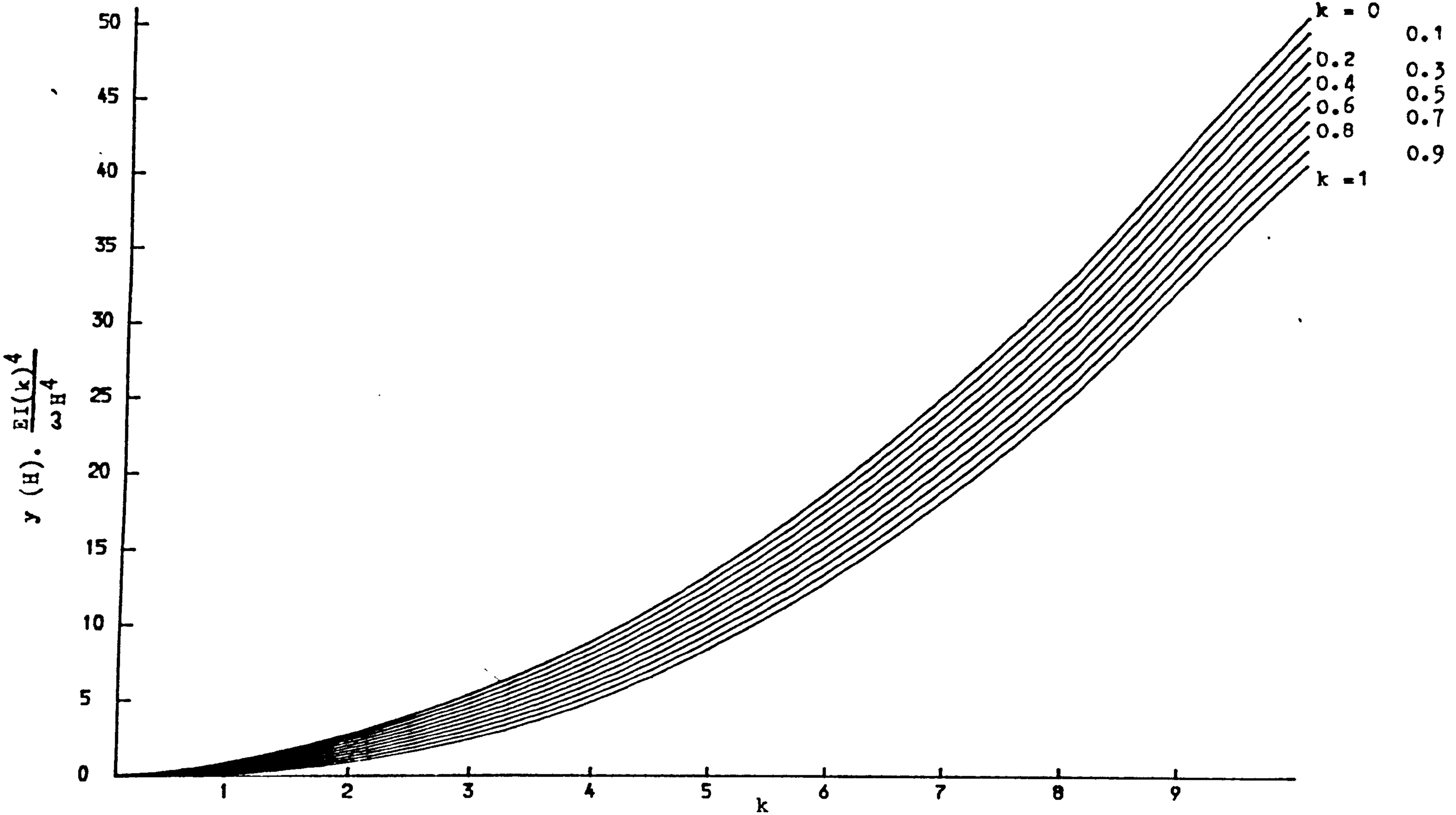

Fig. 2.37 Variation of top deflection function with k and ϕ

C H A P T E R 3

BENDING ANALYSIS OF STRUCTURES CONSISTING OF IDENTICAL COUPLED SHEAR WALLS, CORES AND RIGIDLY-JOINTED FRAME ASSEMBLIES

NOTATION

A_1, A_2	cross-sectional areas of coupled walls.
b	clear span between coupled walls.
E	elastic modulus.
GA	effective shearing rigidity of shear cantilever.
h	storey height.
H	total height.
I_i	second moment of area of wall 'i' (i = 1,2,3)
I	$I_1 + I_2 + I_3$
I_c	second moment of area of connecting beams.
l	distance between centroidal axes of coupled walls.
M_i	bending moment in wall i (i = 1,2,3)
M_4	bending moment carried by frame.
M	applied static moment.
N	axial force in coupled walls.
n_i	axial force intensities in connecting media (i = 1,2,3)
Q_i	concentrated interactive forces (i = 1,2,3)
q	shear force intensity in connecting medium of coupled shear walls.
S_i	shear force in wall i (i = 1,2,3)
S_4	shear force in frame.
ω	uniformly distributed lateral force intensity.
x	height above base.
y	horizontal deflection.
α, β, γ	structural parameters.
ξ	non-dimensional height ($^x/_H$)

Other subsidiary symbols are defined locally in the text.

C H A P T E R 3

BENDING ANALYSIS OF STRUCTURES CONSISTING OF IDENTICAL COUPLED SHEAR WALLS, CORES AND RIGIDLY-JOINTED FRAME ASSEMBLIES

3.1 Introduction

Many tall building structures consist of assemblies of independent and coupled shear walls, cores, and rigidly-jointed frames, constrained to act together by the floor slabs. Fig. 3.1 shows in plan an idealised structure, consisting of three main types of structural assembly, subjected to wind forces.

In this chapter, based on the continuum approach, a general closed-form solution is presented for structures consisting of cores, coupled shear walls and rigidly-jointed frame assemblies.

3.2 Analysis

Consider the action of the plane system of Fig. 3.2(a), consisting of a pair of coupled shear walls linked to a single cantilevered wall which is linked in turn to a rigidly-jointed frame. The single cantilever may be either an independent shear wall or a box core which can be assumed to behave as a simple beam. The axially rigid pin-ended links, which simulate the action of the floor slabs, transmit axial forces only, and

enable the desired load redistribution to take place between components.

In the case of the coupled shear walls, the usual assumptions of the continuum approach are that the discrete set of connecting beams of flexural rigidity EI_c may be replaced by an equivalent connecting medium of flexural rigidity EI_c/h per unit height, if h is the storey height. Since both walls deflect equally, the connecting beams deflect with a point of contraflexure at mid-span. If the connecting medium is then assumed 'cut' at the line of contraflexure (Fig.3.2(b)), the only forces acting at that position are a shear flow of intensity 'q' and an axial force of intensity 'n_1' per unit height. No resultant relative vertical displacement occurs at the cut section, and the compatibility equation at any level 'x' may be shown to be,

$$1\,\frac{dy}{dx} - \frac{qb^3h}{12EI_c} - \frac{1}{E}\left(\frac{1}{A} + \frac{1}{A_2}\right)\int_0^x N\,dx = 0 \qquad (3.1)$$

where the three terms represent respectively the relative displacements due to the slopes of the walls, the deflexions of the connecting beams, and the axial deformations of the walls. The axial force N in each wall is given by

$$N = \int_x^H q\,dx \qquad (3.2)$$

In equation (3.1), y is the horizontal deflexion, l the distance between wall centroids, b the clear span of the beams, and A_1 and A_2 the cross-sectional areas of the walls.

In an analogous manner, it is assumed that the discrete systems of pin-ended links between the three components may be replaced by continuous media transmitting axial forces of intensities n_2 and n_3 per unit height as shown in Fig.3.2(b).

For analytical purposes, the frame component may be replaced by an equivalent continuous shear cantilever to model the predominantly shearing mode of behaviour. The structural behaviour of the shear cantilever is defined by the relationship,

$$\theta = \frac{dy}{dx} = \frac{S_4}{GA} \qquad (3.3)$$

where θ is the shear strain, S_4 is the shear force at any level, and GA is the equivalent shearing rigidity of the framework.

The respective moment-curvature relationships for the coupled walls and core in Fig.3.2(b) are,

$$EI_1 \frac{d^2y}{dx^2} = M_1 = M-(\frac{b}{2} + d_1) N - M_{a1} \qquad (3.4)$$

$$EI_2 \frac{d^2y}{dx^2} = M_2 = -(\frac{b}{2} + d_2) N + M_{a1} - M_{a2} \qquad (3.5)$$

$$EI_3 \frac{d^2y}{dx^2} = M_3 = M_{a2} - M_{a3} \qquad (3.6)$$

where M is the static applied moment and M_{a1}, M_{a2} and M_{a3} are the moments on the walls due to the axial forces in the three sets of connecting beams, given by,

$$M_{a1} = \int_x^H n_1(\lambda)\ (\lambda - x)\ d\lambda + Q_1(H - x) \qquad (3.7)$$

$$M_{a2} = \int_x^H n_2(\lambda)\ (\lambda - x)\ d\lambda + Q_2(H - x) \qquad (3.8)$$

$$M_{a3} = \int_x^H n_3(\lambda)\ (\lambda - x)\ d\lambda + Q_3(H - x) \qquad (3.9)$$

where Q_1, Q_2 and Q_3 are the concentrated forces which exist in the connecting media at the top of the structure,[20,21] (Fig.3.2(b)).

The addition of equations (3.4), (3.5) and (3.6) yield the overall moment-curvature relationship,

$$EI \frac{d^2y}{dx^2} = M - M_{a3} - 1N \qquad (3.10)$$

in which $I = I_1 + I_2 + I_3$

The shear force in the frame component S_4 is,

$$S_4 = \int_x^H n_3 \, dx + Q_3 \qquad (3.11)$$

Substitution of equations (3.7), (3.8), (3.9) and (3.11) into (3.4), (3.5) (3.6) and (3.3) respectively, and differentiating the first three twice and adding to the first differential of the last, yields,

$$EI \frac{d^4y}{dx^4} - GA \frac{d^2y}{dx^2} = \frac{d^2M}{dx^2} + 1\frac{dq}{dx} \qquad (3.12)$$

On eliminating the terms in q and N from equations (3.1), (3.2), (3.10) and (3.12), the governing differential equation finally becomes,

$$\frac{d^6y}{dx^6} - m^2 \frac{d^4y}{dx^4} + n^2 \frac{d^2y}{dx^2} = -\frac{\gamma^2}{EI} \frac{d^2M}{dx^2} + \frac{1}{EI} \frac{d^4M}{dx^4} \qquad (3.13)$$

where

$$m^2 = \alpha^2 + \beta^2 + \gamma^2, \quad n^2 = \alpha^2\gamma^2,$$

$$\alpha^2 = \frac{GA}{EI} \qquad \beta^2 = \frac{12Ic1^2}{b^3hI}$$

$$\gamma^2 = \frac{12Ic}{b^3h} \left(\frac{1}{A_1} + \frac{1}{A_2}\right)$$

The general solution of equation (3.13) for any form of lateral loading may be expressed in the form

$$y = C_0 + C_1 x/H + C_2 \cosh(kx/H) + C_3 \sinh(k\, x/H) + C_4 \cosh(r\ \ x/H) + C_5 \sinh(r\ x/H) + y_{P.I.} \qquad (3.14)$$

where C_i ($i = 0$ to 5) are constants of integration to be determined from the necessary boundary conditions, and y_{PI} is the particular integral solution, that is, any solution for a specified form of applied moment M.

In Equation (3.14),

$$k = pH \text{ and } r = \frac{nH}{p}$$

where $p^2 = \frac{1}{2}\ (m^2 + \sqrt{m^4 - 4n^2})$

and $\frac{n^2}{p^2} = \frac{1}{2}\ (m^2 - \sqrt{m^4 - 4n^2})$

It may readily be shown by inspection of the physical relationships in equation (3.13) that $m^4 \not< 4n^2$, and so the roots of the equation, p and $^n/_p$, are always real (cf. Appendix 1).

Boundary conditions

In order to determine the constants C_i of equation (3.14), it is necessary to derive six independent boundary conditions for the structure.

If the structure is rigidly built in at the base, then

$$\text{At } x = 0 , \quad y = 0 \text{ and } \frac{dy}{dx} = 0 \tag{3.15}$$

At the top, the axial force N and the bending moment in each wall are equal to zero, and so,

$$\text{At } x = H , \quad \frac{d^2y}{dx^2} = 0 \tag{3.16}$$

From equation (2), $\frac{dN}{dx} = -q$

Differentiation of equation (3.10), followed by substitution of equations (3.8), (3.9) and (3.11), gives,

$$EI \frac{d^3y}{dx^3} - GA \frac{dy}{dx} = \frac{dM}{dx} + lq$$

At $x = 0$, the slope $\frac{dy}{dx}$ is zero, and hence, from equation (3.1), q is also zero. Thus, at the base, the following condition holds,

$$\text{At } x = 0 , \quad \frac{d^3y}{dx^3} = \frac{1}{EI} \frac{dM(0)}{dx} \tag{3.17}$$

On differentiating equation (3.1), and using the fact that N and d^2y/dx^2 are each zero at the top, it follows that $d\bar{q}/dx$ is zero also. Hence, from equation (5.12),

$$\text{At } x = H \text{ , } \frac{d^4y}{dx^4} = \frac{1}{EI} \frac{d^2M(H)}{dx^2} \qquad (3.18)$$

On differentiating equation (3.12) and, substituting for d^2q/dx^2 from the derivative of equation (3.1), the remaining boundary condition becomes,

$$\text{At } x = 0 \text{ , } \frac{d^5y}{dx^5} = \frac{1}{EI} \left[\frac{d^3M(0)}{dx^3} + (\alpha^2 + \beta^2) \frac{dM(0)}{dx} \right] \qquad (3.19)$$

It may readily be shown that in the particular cases involving the interaction between two components only, the general equation and boundary conditions reduce to those given in the earlier published solutions.

Uniformly distributed wind loading

In order to achieve a solution, suppose that the particular case is considered of a uniformly distributed wind loading of intensity ω per unit height. In that case,

$$M = \frac{1}{2} \omega (H - x)^2 \qquad (3.20)$$

and

$$\frac{d^2M}{dx^2} = \omega$$

On substituting for the moment function in equation (3.13), the simplest particular integral becomes

$$y_{PI} = -\frac{\omega}{2\alpha^2}\ \frac{x^2}{EI} \tag{3.21}$$

Then on substituting equation (3.14) into the boundary conditions (3.15)-(3.19), and solving for the integration constants, it is found that

$$C_o = -\frac{p^4}{n^2}\ \frac{\omega}{EI\alpha^2\cosh r}\left(\frac{\alpha^2 - p^2}{n^2 - p^4}\right)(r\sinh r + 1) -$$

$$\frac{1}{p^2}\ \frac{\omega}{EI\cosh k}\left(\frac{\gamma^2 - p^2}{n^2 - p^4}\right)(k\sinh k + 1)$$

$$C_1 = \frac{\omega H}{EI\alpha^2}$$

$$C_2 = \frac{1}{p^2}\ \frac{\omega}{EI\cosh k}\left(\frac{\gamma^2 - p^2}{n^2 - p^4}\right)(k\sinh k + 1)$$

$$C_3 = -\frac{\omega H}{pEI}\left(\frac{\gamma^2 - p^2}{n^2 - p^4}\right)$$

$$C_4 = \frac{p^4}{n^2}\ \frac{\omega}{EI\alpha^2\cosh r}\left(\frac{\alpha^2 - p^2}{n^2 - p^4}\right)(r\sinh r + 1)$$

$$C_5 = -\frac{p^3}{n}\ \frac{\omega H}{EI\alpha^2}\left(\frac{\alpha^2 - p^2}{n^2 - p^4}\right)$$

Hence,

$$y = \frac{\omega_H^2}{EI\alpha^2}\left\{(\xi - \frac{1}{2}\xi^2) - \alpha^2\frac{\Theta_1}{\Theta_3}\frac{1}{\Delta_1}\left[1 + k\sinh k - \cosh k\xi - k\sinh k(1-\xi)\right]\right.$$
$$\left. - p^2\frac{\Theta_2}{\Theta_3}\frac{1}{\Delta_2}\left[1 + r\sinh r - \cosh r\xi - r\sinh r(1-\xi)\right]\right\} \quad (3.22)$$

in which

$$\Delta_1 = k^2\cosh k$$

$$\Delta_2 = r^2\cosh r$$

$$\Theta_1 = \gamma^2 - p^2$$

$$\Theta_2 = \alpha^2 - p^2$$

$$\Theta_3 = n^2 - p^4$$

and for convenience, the non-dimensional height $\xi = x/H$ is used. Equation (3.22) emphasises the dependence of the solution on three variables, the height ξ and the relative stiffness parameters k and r.

Substitution of equation (3.22) into the earlier equations yields closed-form solutions for the forces in the various structural components. The shear flow q in the connecting medium becomes

$$q = \frac{\omega\beta^2 pk}{l\Theta_3}\left\{\frac{r}{\Delta_2}\left[\sinh r\xi - r\cosh r(1-\xi)\right] - \frac{k}{\Delta_1}\left[\sinh k\xi - k\cosh k(1-\xi)\right]\right\} \quad (3.23)$$

On substituting for q from equation (3.23) into equation (3.2), the axial force in each coupled wall becomes

$$N = \frac{\omega\beta^2 k^2}{l\theta_3}\left\{\frac{1}{\Delta_2}\left[\cosh r - \cosh r\xi - r\sinh r(1-\xi)\right] - \frac{1}{\Delta_1}\left[\cosh k - \cosh k\xi - k\sinh k(1-\xi)\right]\right\} \quad (3.24)$$

The bending moment M_i in wall i (i = 1,2,3) can be determined by substituting for y from equation (3.22) into equations (3.4) - (3.6) and is given by

$$M_i = \frac{\omega I_i}{\alpha^2 I}\left\{\alpha^2\frac{\theta_1}{\theta_3}\left[\frac{k^2}{\Delta_1}(\cosh k\xi + k\sinh k(1-\xi)) - 1\right] + \frac{p^2\theta_2}{\theta_3}\left[\frac{r^2}{\Delta_2}(\cosh r\xi + r\sinh r(1-\xi)) - 1\right]\right\} \quad (3.25)$$

The moment carried by the frame component M_4, may be obtained from the overall moment equilibrium, i.e.

$$M_1 + M_2 + M_3 + M_4 + Nl = M$$

and is given by

$$M_4 = \frac{1}{2}\omega H^2(1-\xi)^2 + \frac{\omega}{\alpha^2}(1+\beta^2/\gamma^2) - \frac{\omega\alpha^2}{p^2}\frac{\theta_1}{\theta_3}\left\{\frac{k^2}{\Delta_1}\left[\cosh k\xi + k\sinh k(1-\xi)\right]\right\} - \frac{\omega p^4}{n^2}\frac{\theta_2}{\theta_3}\left\{\frac{r^2}{\Delta_2}\left[\cosh r\xi + r\sinh r(1-\xi)\right]\right\} \quad (3.26)$$

A consideration of the conditions of equilibrium of a small vertical element of each wall yields the shear force S_1 and S_2 in the two walls (Fig. 3.3)

$$S_1 = -\frac{dM_1}{dx} + (\frac{b}{2} + d_1)q$$

$$S_2 = -\frac{dM_2}{dx} + (\frac{b}{2} + d_2)q \qquad (3.27)$$

and, for the independent wall and frame, the shear force S_3 and S_4 are

$$S_3 = -\frac{dM_3}{dx} \qquad S_4 = -\frac{dM_4}{dx} \qquad (3.28)$$

Hence, on substituting for q, M_1 (i = 1,2,3) and M_4 from equations (3.23), (3.25) and (3.26) into equations (3.27) -(3.28) the shear force in the walls and frame become

$$S_1 = \left[\frac{\omega I_1}{I} p \frac{\Theta_1}{\Theta_3} - (\frac{b}{2} + d_1)\omega \frac{\beta^2 p}{l\Theta_3}\right]F_1 + \left[-\frac{\omega I_1}{I} \frac{pn\Theta_2}{\alpha^2 \Theta_3} + (\frac{b}{2} + d_1)\omega \frac{\beta^2 p^3}{ln\Theta_3}\right]F_2 \qquad (3.29)$$

$$S_2 = \left[-\omega \frac{I_2}{I} p \frac{\Theta_1}{\Theta_3} - \omega(\frac{b}{2} + d_2) \frac{\beta^2 p}{l\Theta_3}\right]F_1 + \left[-\omega \frac{I_2}{I} \frac{pn}{\alpha^2} \frac{\Theta_2}{\Theta_3} + \omega(\frac{b}{2} + d_2) \frac{\beta^2 p^3}{ln\Theta_3}\right]F_2 \qquad (3.30)$$

$$S_3 = -\frac{\omega I_3}{I} p \frac{\Theta_1}{\Theta_3} F_1 - \omega \frac{I_3}{I} \frac{pn}{\alpha^2} \frac{\Theta_2}{\Theta_3} F_2 \qquad (3.31)$$

$$S_4 = \omega H (1 - \xi) + \frac{\omega \alpha^2}{p} \frac{\Theta_1}{\Theta_3} F_1 + \frac{\omega p^3}{n} \frac{\Theta_2}{\Theta_3} F_2 \qquad (3.32)$$

where the functions F_1 and F_2 are

$$F_1 = (1/\cosh k)\left[\sinh k\xi - k\cosh k\ (1-\xi)\right]$$

$$F_2 = (1/\cosh r)\left[\sinh r\xi - r\cosh r\ (1-\xi)\right] \qquad (3.33)$$

On substituting for M, M_i $(i = 1,2,3)$ and N into equations (3.4) - (3.6), the moments on the walls due to axial forces in the three sets of connecting beams, become

$$M_{a1} = \frac{\omega\beta^2}{ln^2}\left(\frac{b}{2} + d_1\right) + \frac{1}{2}\omega H^2\ (1-\xi)^2 + \frac{\omega}{\alpha^2}\ \frac{I_1}{I}$$

$$- \frac{\omega}{\theta_3}\left[\frac{I_1}{I}\theta_1 + \left(\frac{b}{2} + d_1\right)\frac{\beta^2}{l}\right]F_3 \qquad (3.34)$$

$$- \frac{\omega p^2}{\alpha^2\theta_3}\left[\frac{I_1}{I}\theta_2 - \left(\frac{b}{2} + d_1\right)\frac{\beta^2 p^2}{l\gamma^2}\right]\ F_4$$

$$M_{a2} = \frac{\omega\beta^2}{n^2} + \frac{1}{2}\omega H^2\ (1-\xi)^2 + \frac{\omega}{\alpha^2}\left(\frac{I_1 + I_2}{I}\right)$$

$$- \frac{\omega}{\theta_3}\left[\left(\frac{I_1 + I_2}{I}\right)\theta_1 + \beta^2\right]F_3 \qquad (3.35)$$

$$- \frac{\omega p^2}{\alpha^2\theta_3}\left[\left(\frac{I_1 + I_2}{I}\right)\theta_2 - \frac{\beta^2 p^2}{\gamma^2}\right]F_4$$

$$M_{a3} = \frac{\beta^2\omega}{n^2} + \frac{1}{2}\,\omega_H^2\,(1-\xi)^2 + \frac{\omega}{\alpha^2} - \frac{\omega\alpha^2}{p^2}\,\frac{\Theta_1}{\Theta_3}\,F_3 - \frac{\omega_p^4}{n^2}\,\frac{\Theta_2}{\Theta_3}\,F_4 \qquad (3.36)$$

where the functions F_3 and F_4 are

$$F_3 = (1/\cosh k)\left[\cosh k\xi + k\sinh k\,(1-\xi)\right]$$
$$F_4 = (1/\cosh r)\left[\cosh r\xi + r\sinh r\,(1-\xi)\right] \qquad (3.37)$$

The axial forces in the connecting media follow from equations (3.34) - (3.36), since

$$n_i = \frac{d^2M_{ai}}{dx^2} \quad (i = 1,2,3) \qquad (3.38)$$

and becomes

$$n_1 = \omega - \frac{\omega_p^2}{\Theta_3}\left[\frac{I_1}{I}\Theta_1 + \left(\frac{b}{2} + d_1\right)\frac{\beta^2}{l}\right]F_3 - \frac{\omega\gamma^2}{\Theta_3}\left[\frac{I_1}{I}\Theta_2 - \left(\frac{b}{2} + d_1\right)\frac{\beta^2 p^2}{l\gamma^2}\right]F_4 \qquad (3.39)$$

$$n_2 = \omega - \frac{\omega_p^2}{\Theta_3}\left(\frac{I_1 + I_2}{I}\Theta_1 + \beta^2\right)F_3 - \frac{\omega\gamma^2}{\Theta_3}\left(\frac{I_1 + I_2}{I}\Theta_2 - \frac{\beta^2 p^2}{\gamma^2}\right)F_4 \qquad (3.40)$$

$$n_3 = \omega - \frac{\omega\alpha^2}{\Theta_3} \Theta_1 F_1 - \frac{\omega p^2}{\Theta_3} \Theta_2 F_2 \qquad (3.41)$$

If the expressions for M_1 to M_4 and q are substituted into equations (3.27) and (3.28), it is found that shear forces exist in the various components at the top of the continuous structure. It must again be deduced that these can only be caused by concentrated interactive forces at the top of each connecting medium, as shown in Fig. 3.2(b), such that,

$$S_1(H) = -Q_1 \quad , \quad S_2(H) = Q_1 - Q_2 \quad , \quad S_3(H) = Q_2 - Q_3 \quad ,$$

$$S_4(H) = Q_3$$

These are found to be,

$$Q_1 = \frac{\omega}{p\Theta_3}\left\{\Theta_1\left[\alpha^2 - p^2\,\frac{I_2 + I_3}{I}\right] - \left(\frac{b}{2} + d_2\right)\frac{\beta^2 p^2}{l}\right\}L_1 + \frac{\omega p}{n\Theta_3}\left\{\Theta_2\left[p^2 - \gamma^2\,\frac{I_2 + I_3}{I}\right] + \left(\frac{b}{2} + d_1\right)\frac{\beta^2 p^2}{l}\right\}L_2 \qquad (3.42)$$

$$Q_2 = \frac{\omega\Theta_1}{p\Theta_3}\left(\alpha^2 - \frac{I_3}{I}\,p^2\right)L_1 + \frac{\omega p\Theta_2}{n\Theta_3}\left(p^2 - \frac{I_3}{I}\,\gamma^2\right)L_2 \qquad (3.43)$$

$$Q_3 = -\omega\frac{\alpha^2}{p}\frac{\theta_1}{\theta_3} L_1 + \omega\frac{p^3\theta_2}{n\theta_3} L_2 \qquad (3.44)$$

where

$$L_1 = \frac{1}{\cosh k}(\sinh k - k)$$

$$L_2 = \frac{1}{\cosh r}(\sinh r - r)$$

NUMERICAL EXAMPLE

In order to illustrate the theoretical results, a representative 30-storey structure of the form shown in Fig.3.4is considered. The structure consists of two central U-shaped cores, two pairs of coupled flank shear walls, and four rigidly-jointed frame assemblies. The influence of the two individual central columns in resisting lateral forces is assumed negligible.

The relevant structural data are:

Storey height $h = 2.8$ m

Total building height $H = 84$ m

For each core $I = 1.86\ m^4$

For coupled walls, $I_1 = I_2 = 3.6\ m^4$

$A_1 = A_2 = 1.2\ m^2$

$I_c = 10.67 \times 10^{-4} m^4$

$b = 2$ m $\quad l = 8$ m

$E = 21 \times 10^6\ kN/m^2$

For each frame, $GA = 6 \times 10^4$ kN

The dimensions of the columns are 0.35 m x 0.35 m and the beams are 0.35 m thick and 0.39 m deep.

Then, on adding the properties of the three groups of elements, the relevant structural parameters become,

$\alpha H = 2.11$

$\beta H = 5.34$

$\gamma H = 2.59$

The laternal deflections and internal forces in the different components may be determined from the earlier equations (3.22) to (3.44). Since the coupled shear walls are identical, the forces in each are the same. The distributions may be expressed in terms of series of functions ϕ_1 to ϕ_{12} as follows, related where appropriate to the applied load intensity ω, the total shear ωH, and the total statical moment $\frac{\omega H^2}{2}$. These functions are defined as

$$y = \frac{\omega H^4}{EI} \phi_1$$

$$q = \omega H \phi_2, \quad N = \frac{\omega H^2}{2} \phi_3$$

$$M_1 = M_2 = \frac{1}{2} \left(\frac{\omega H^2}{2}\right) \phi_4, \quad M_3 = \frac{\omega H^2}{2} \phi_5, \quad M_4 = \frac{\omega H^2}{2} \phi_6$$

$$S_1 = S_2 = \frac{1}{2} \omega H \phi_7, \quad S_3 = \omega H \phi_8, \quad S_4 = \omega H \phi_9$$

The lateral load distributions on the coupled shear walls, core and frames are respectively $\omega\phi_{10}$, $\omega\phi_{11}$ and $\omega\phi_{12}$.

The distributions of deflection, internal forces and lateral loads are shown in Figs. 3.5 to 3.17.

The magnitudes of the concentrated interactive forces are found to be

$$Q_1 = 0.0351\,\omega H$$

$$Q_2 = 0.0702\,\omega H$$

$$Q_3 = 0.1003\,\omega H$$

Figs. 3.5 - 3.17 illustrate the general form of structural action which occurs in composite structures of this nature, in which continuous redistributions of lateral forces occur as a result of the different load deflection characteristics of the components. Figs. 3.7 - 3.8 show typical distributions of shear flow and axial forces in a system of laterally loaded coupled shear walls.

Figs. 3.15 - 3.17 indicate that the lateral forces are small in the upper levels of both cores and frames, but they increase rapidly in the lower levels. The lateral forces are carried largely by the coupled shear walls, and are roughly uniform throughout the height, giving rise to a roughly linear distribution of shearing forces as shown in Fig. 3.12. The top concentrated force on the frame has a

magnitude of 10% of the total lateral load, and produces an approximately linear distribution of bending moments throughout the height. The shear force is roughly constant throughout the height, and gives rise to an efficient uniform design. The bending moments in both coupled walls and cores are both small and negative in sense in the upper levels, due to coupling actions of the connecting beams and the top axial forces, but increase rapidly in the lower levels due to the redistribution of lateral forces.

The distribution which would occur in the case of the commonly adopted design procedure discussed earlier are indicated by the broken lines in Figs. 3.7 - 3.17. Although considerable errors still occur in the force actions at different levels, the degree of accuracy is generally better than that obtained with the lateral force distributions, and this lends credibility to the relatively crude design procedure. For completeness, the deflection profiles of the individual elements, obtained by matching deflections at the top only, are shown in Fig. 3.5. The figure illustrates the predominantly shearing nature of the frame deformations, and indicates the load redistribution which is required to ensure that the three components deflect equally at all levels.

Although the curves presented demonstrate the typical forms of structural actions in structures of this nature, the actual magnitudes of the forces in each component

will naturally depend on their relative stiffness.

3.3 Application of the general theory to particular cases

(i) Core structures

For structures consisting of independent shear wall or core units only, the parameters α^2, β^2 and γ^2 in equation (3.13) do not exist and hence this equation becomes

$$\frac{d^6y}{dx^6} = \frac{1}{EI} \frac{d^4M}{dx^4} \qquad (3.45)$$

The general solution of equation (3.45) for uniformly distributed wind loading of intensity ω per unit height is

$$y = a_0 + a_1 x + a_2 x^2 + a_3 x^3 + a_4 x^4 + a_5 x^5 \qquad (3.46)$$

where a_i (i = 0 -5) are constants of integration to be determined from the necessary boundary conditions.

On substituting equation (3.46) into the boundary conditions (3.15) - (3.19), and solving for the integration constants, they become

$$a_0 = 0 \quad , \quad a_1 = 0 \quad , \quad a_2 = \frac{\omega H^2}{4EI}$$

$$a_3 = -\frac{\omega H}{6EI} \quad , \quad a_4 = \frac{\omega}{24EI} \quad , \quad a_5 = 0$$

Hence, the general solution becomes

$$y = \frac{\omega H^4}{EI} \left(\frac{1}{24} \xi^4 - \frac{1}{6} \xi^3 + \frac{1}{4} \xi^2\right) \qquad (3.47)$$

Equation (3.47) is the general solution of any cantilever subjected to uniformly distributed lateral loads.

(ii) Wall-frame structures

For structures consisting of independent shear walls or box cores and rigidly jointed frame work assemblies the parameters β^2 and γ^2 in equation (3.13) do not exist and hence equation (3.13) becomes

$$\frac{d^6y}{dx^6} - \alpha^2 \frac{d^4y}{dx^4} = 0 \qquad (3.48)$$

The general solution of equation (3.48) for uniformly distributed loading of intensity ω per unit height is

$$y = b_o + b_1 x + b_2 x^2 + b_3 x^3 + b_4 \cosh \alpha x + b_5 \sinh \alpha x \qquad (3.49)$$

where b_i (i = 0-5) are constants of integration to be evaluated from the necessary boundary conditions.

On substituting equation (3.49) into the boundary

conditions (3.15) - (3.19), and solving for the integration constants, the general solution becomes as given by equation (2.63)

(iii) Coupled shear wall - core structures

For structures consisting of coupled shear walls and independent wall or core assemblies, the parameter α^2 in equation (3.13) is set equal to zero, and hence equation (3.13) becomes

$$\frac{d^6y}{dx^6} - m^2 \frac{d^4y}{dx^4} = -(m^2 - \beta^2) \frac{\omega}{EI} \qquad (3.50)$$

where $m^2 = \beta^2 + \gamma^2$

The general solution of equation (3.50) for uniformly distributed wind loading of intensity ω per unit height is

$$y = e_o + e_1x + e_2x^2 + e_3x^3 + e_4x^4 + e_5 \cosh mx + e_6 \sinh mx \qquad (3.51)$$

when e_i (i = 0 -6) are constants of integration to be determined from the necessary boundary conditions.

On substituting equation (3.51) into the boundary conditions (3.15) - (3.19), and solving for the integration constants, they become

$$e_o = - \frac{\omega \beta^2}{EIm^6 \cosh mH} \quad (mH \sinh mH + 1)$$

$$e_1 = \frac{\omega \beta^2 H}{m^4 EI}$$

$$e_2 = -\frac{\omega H^2}{4EI} \left(\frac{\beta^2}{m^2} - 1\right) - \frac{\beta^2 \omega}{2EI_m 4}$$

$$e_3 = \frac{\omega H}{6EI} \left(\frac{\beta^2}{m^2} - 1\right)$$

$$e_4 = \frac{\omega}{24EI} \left(1 - \frac{\beta^2}{m^2}\right)$$

$$e_5 = \frac{\omega \beta^2}{EIm^6 \cosh mH} (m H \sinh mH + 1)$$

$$e_6 = - \frac{\omega \beta^2 H}{EIm^5}$$

Hence the general solution becomes

$$y = \frac{\omega H^4}{EI} \left\{ \frac{1}{24} \left(1 - \frac{\beta^2}{m^2}\right) \left[(1 - \xi)^4 + 4\xi - 1\right] + \frac{\beta^2}{m^2 k^2} \left[\left(\xi - \frac{1}{2}\xi^2\right) - \frac{1 + k \sinh k - \cosh k\xi - k \sinh k (1 - \xi)}{k^2 \cosh k} \right] \right\} \quad (3.52)$$

where

$$k = mH$$

$$\xi = x/H$$

Equation (3.52) is the same as equation (2.21) presented in Chapter 2, except that α is replace by m . The internal forces may readily be shown to be the same as the ones presented in Chapter 2.

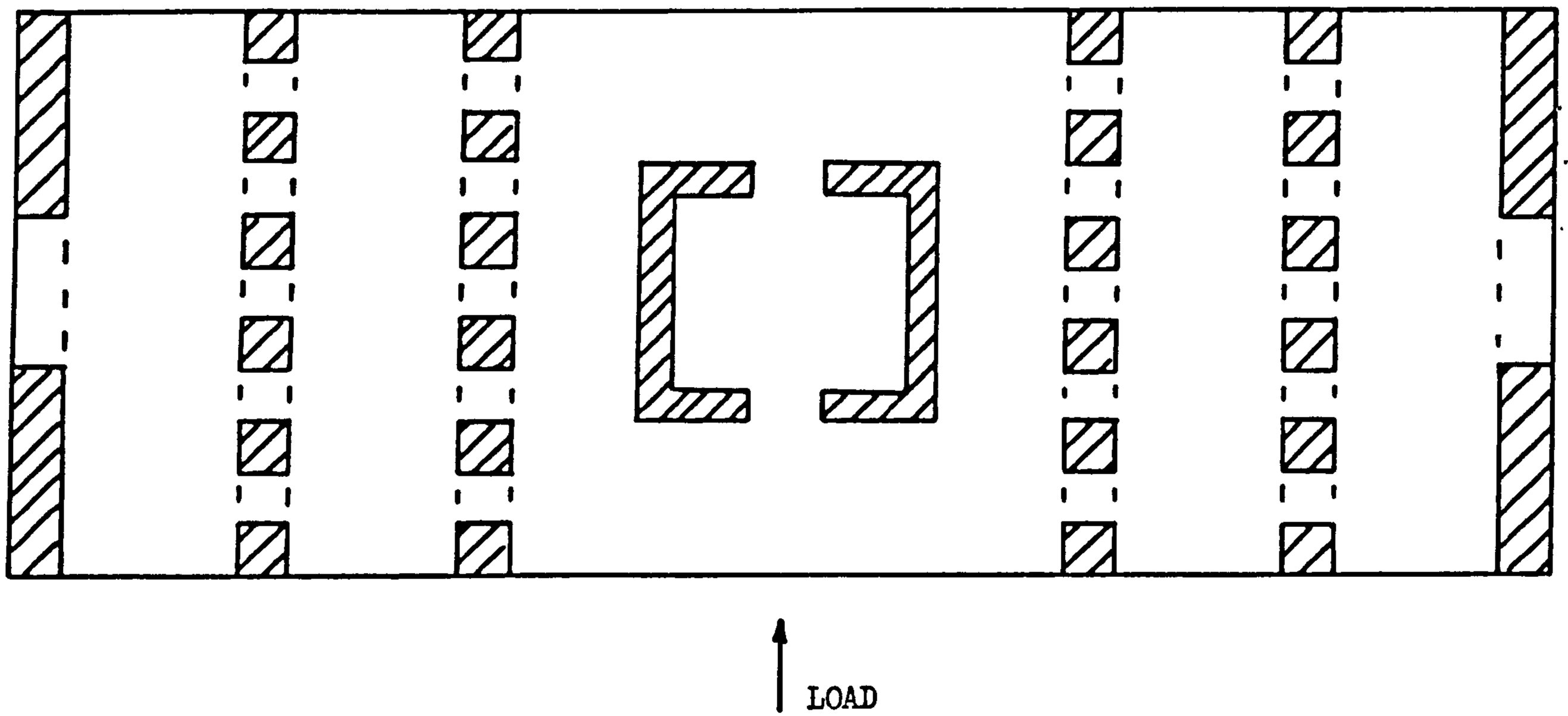

Fig. 3.1 Symmetric structure consisting of coupled shear walls, cores and rigidly-jointed frames.

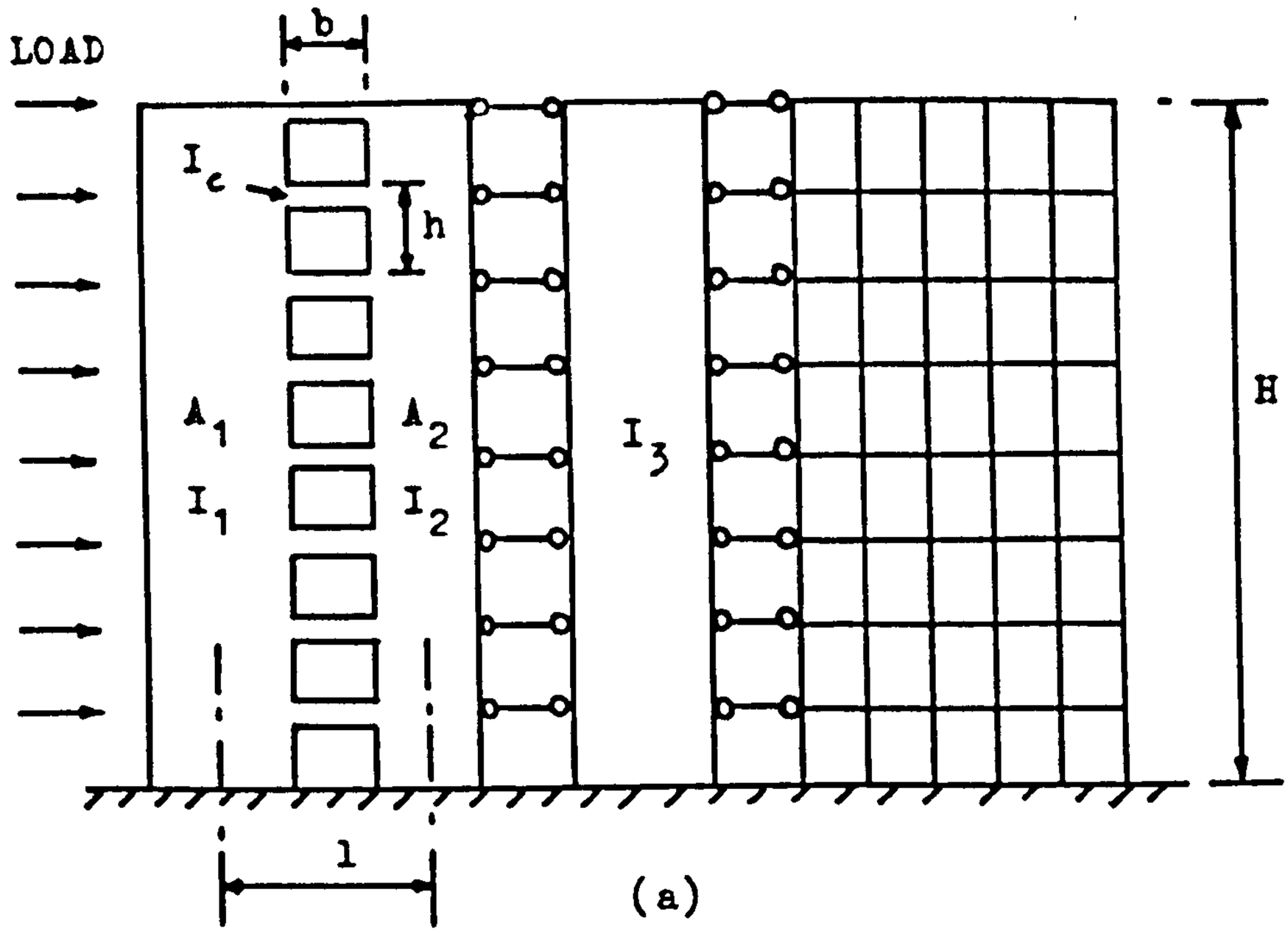

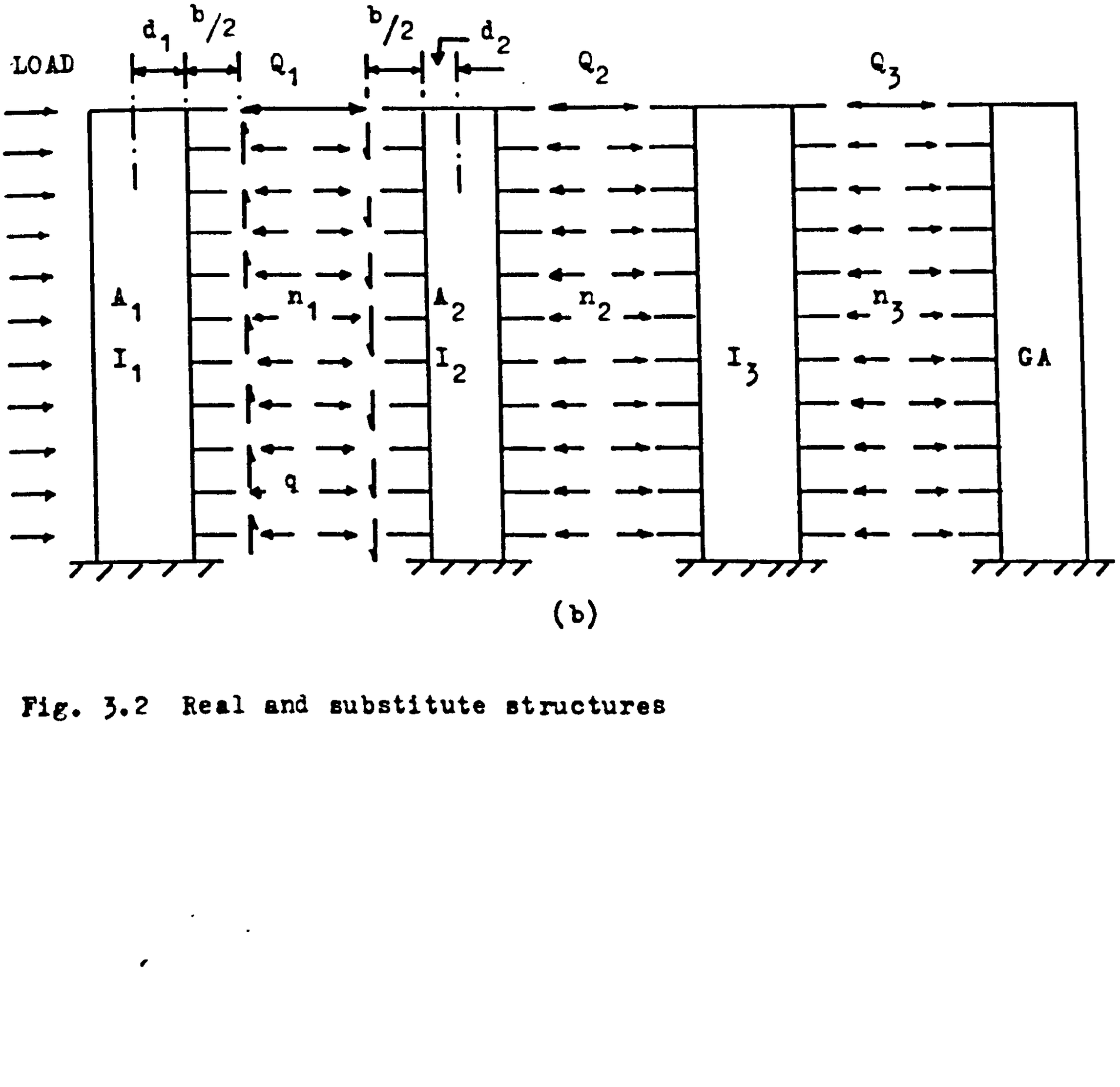

Fig. 3.2 Real and substitute structures

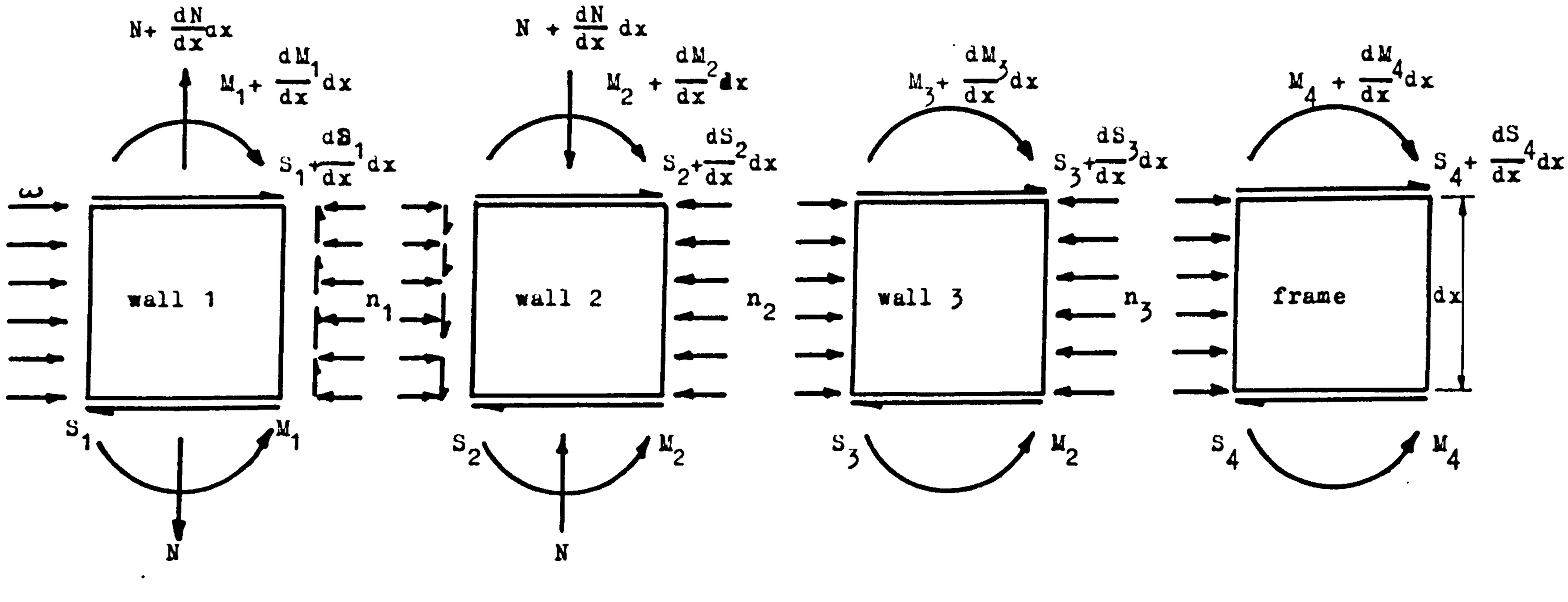

Fig. 3.3 Forces on element of substitute equivalent plane structure

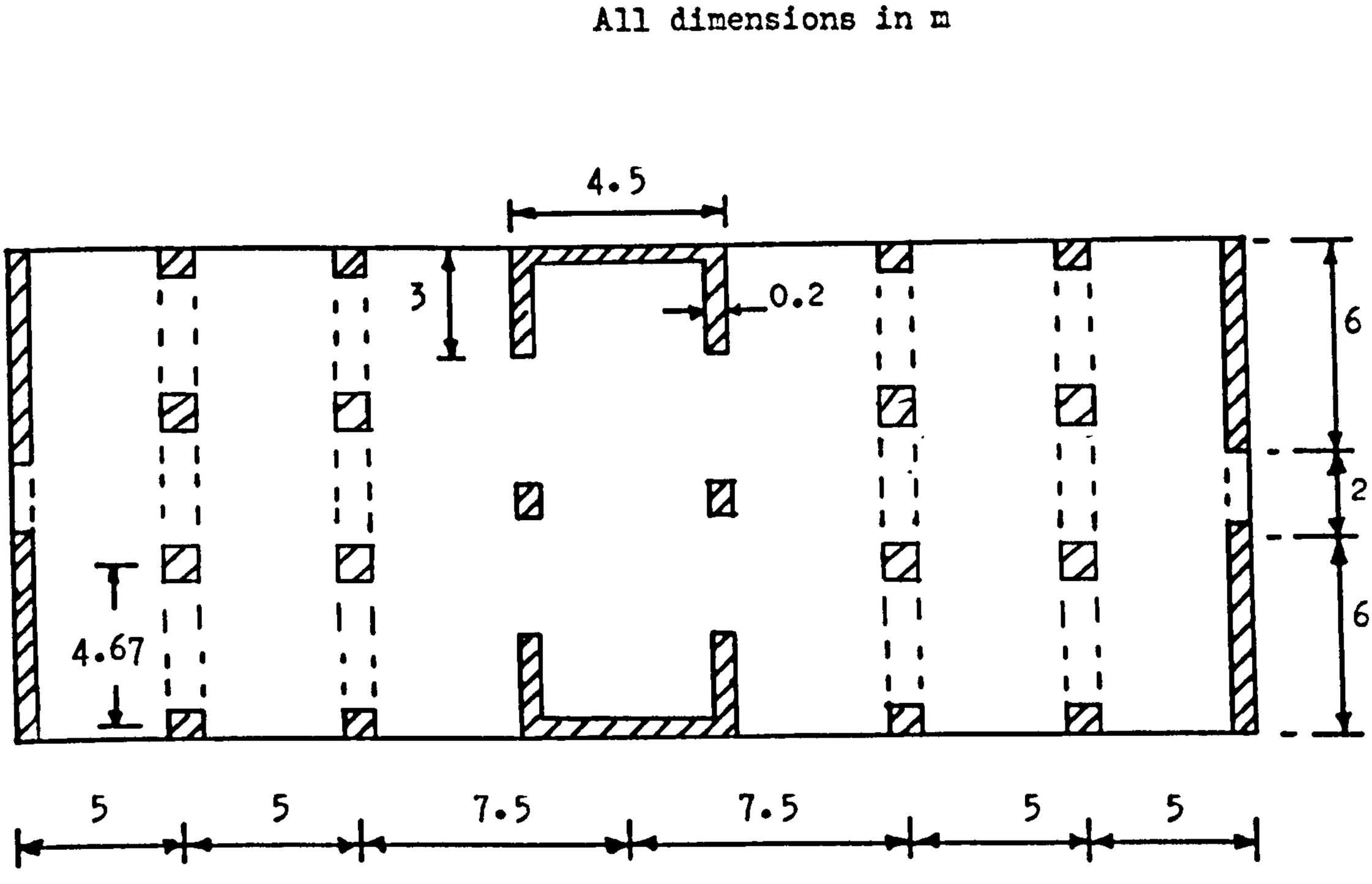

Fig. 3.4 planform of structure for numerical example

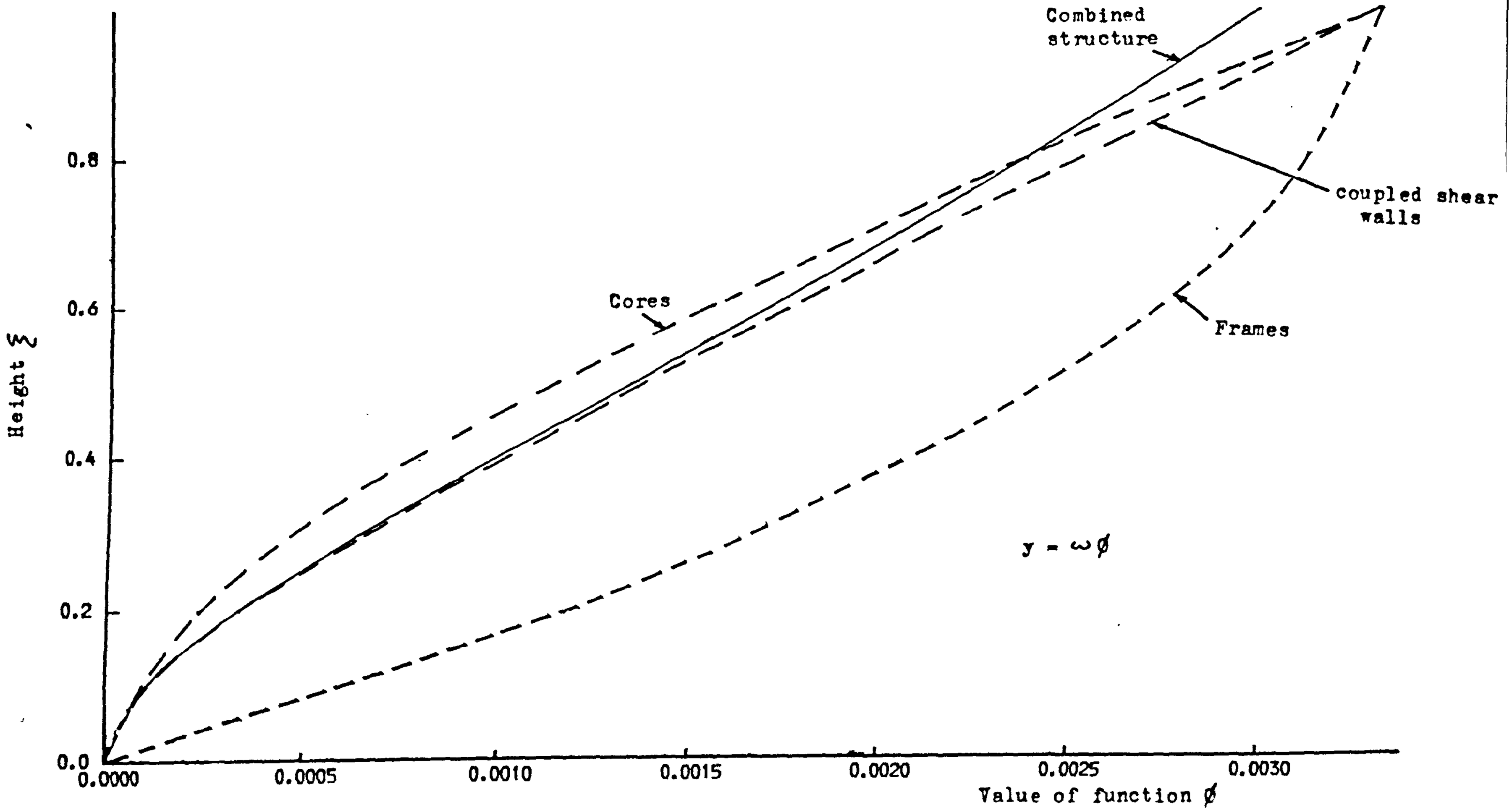

Fig. 3.5 Lateral deflection profiles for shear walls, cores and frames when subjected to distributed loads which produce equal deflections at the top

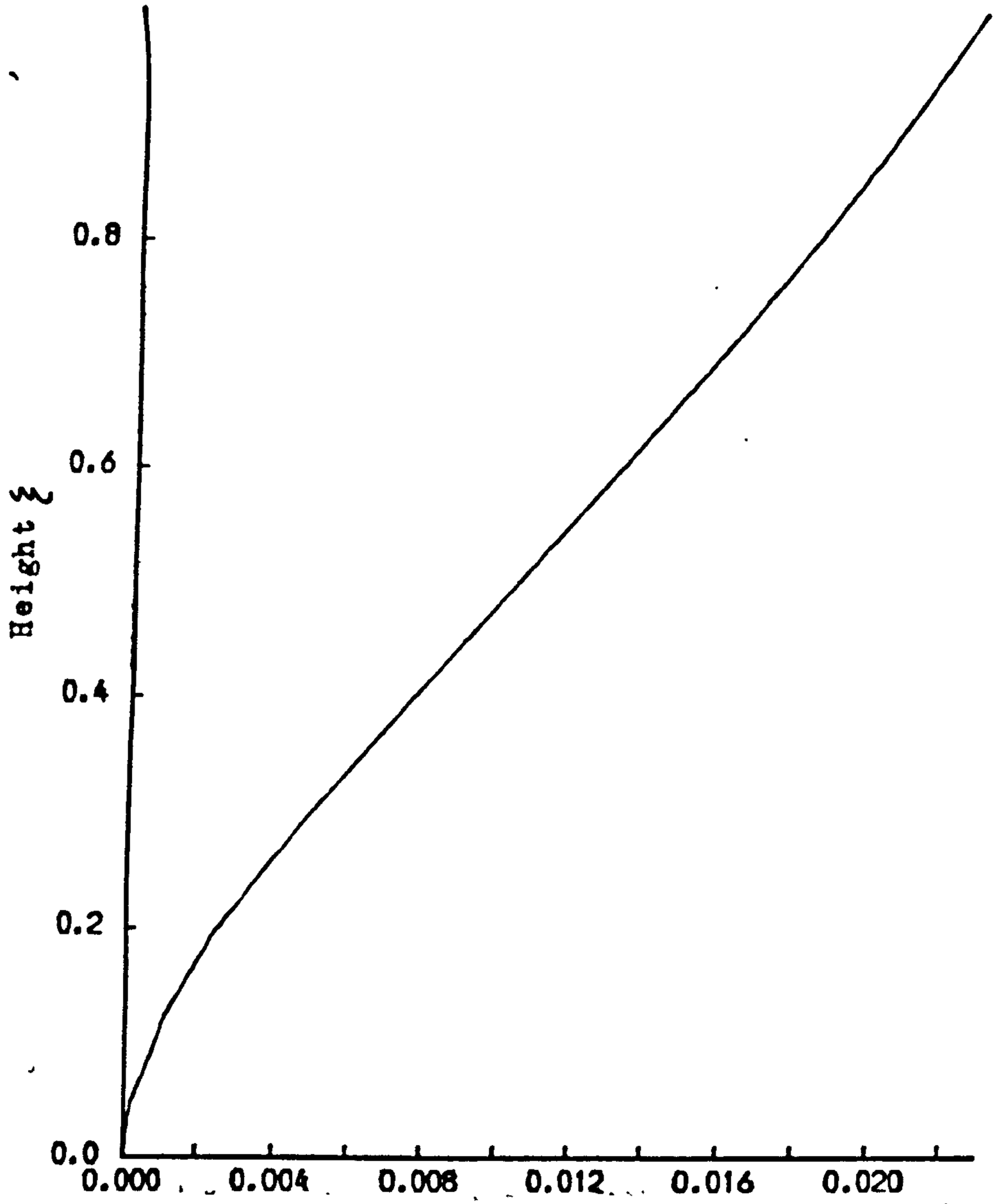

Fig. 3.6 Distribution of lateral deflection

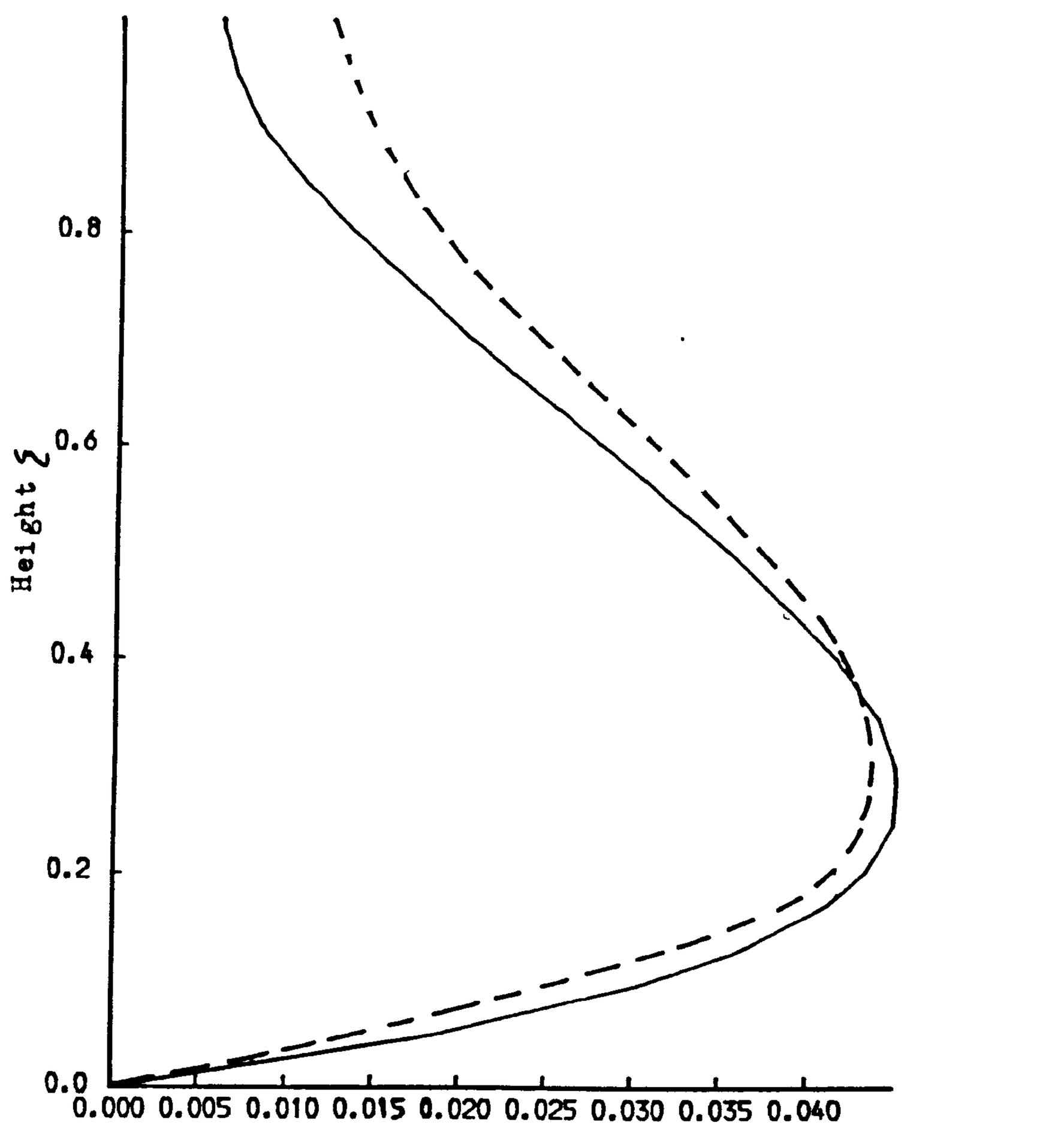

Fig. 3.7 Distribution of shear flow in connecting medium

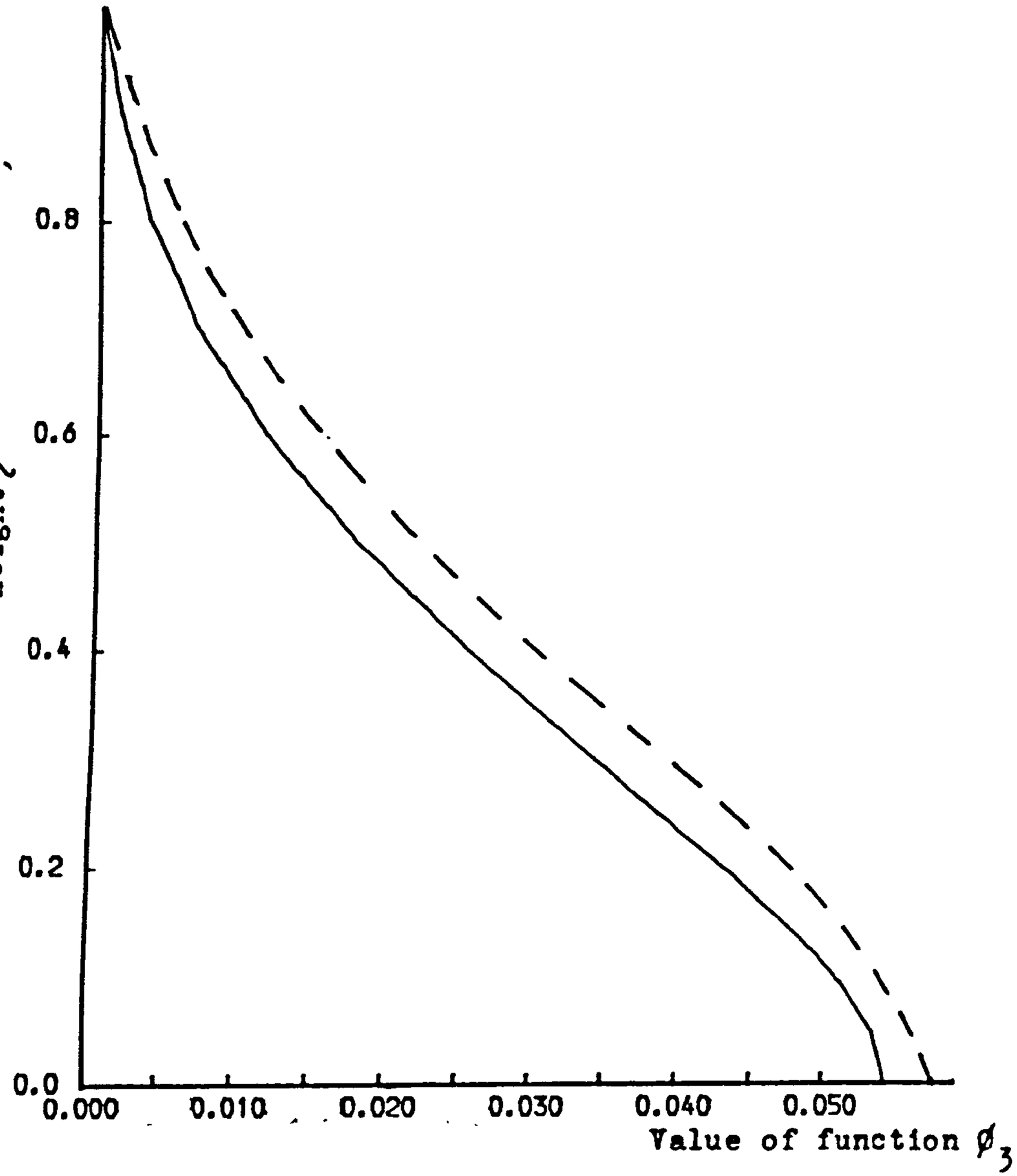

Fig. 3.8 Distribution of axial force in coupled walls

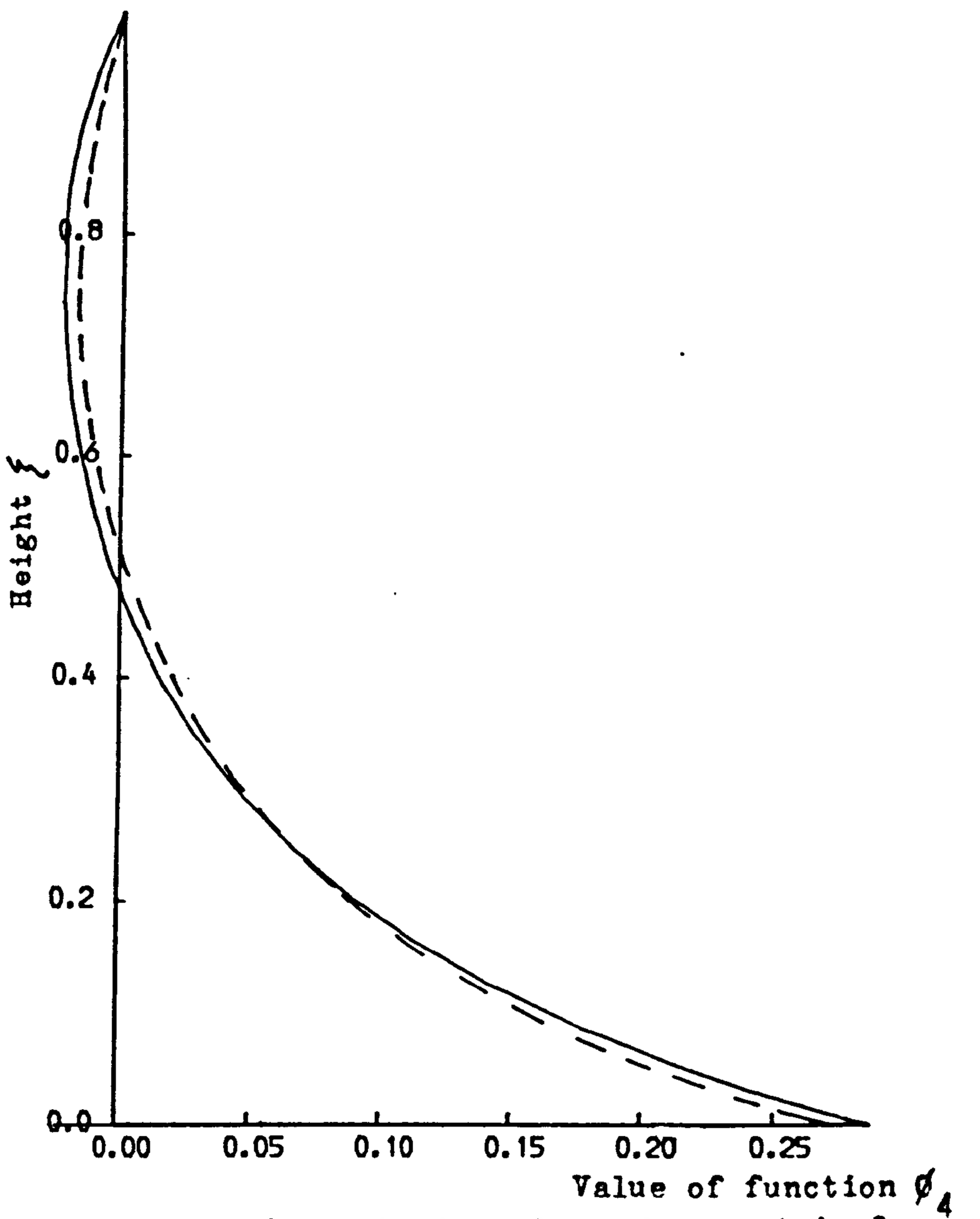

Fig. 3.9 Distribution of total moment in frames

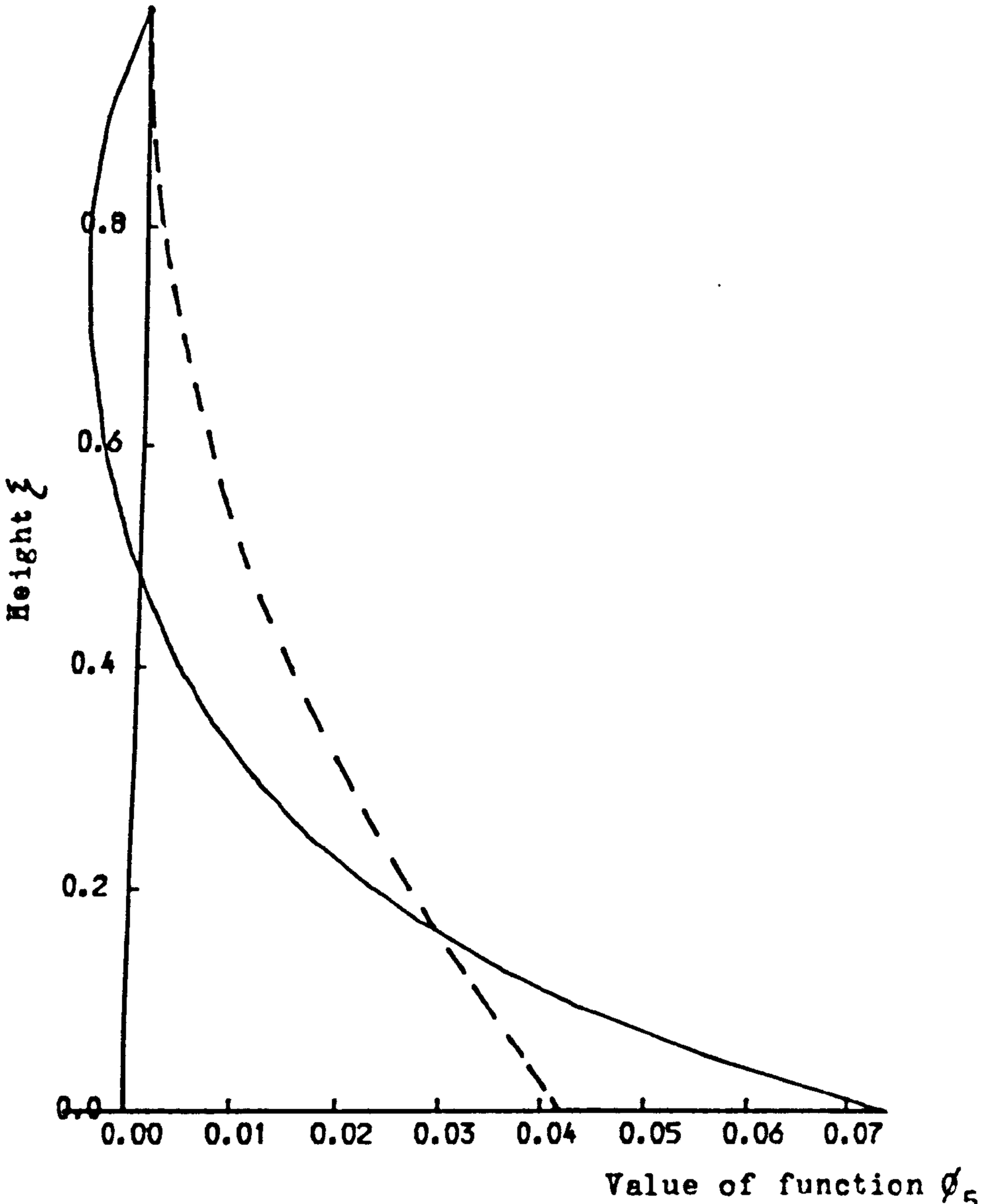

Fig. 3.10 Distribution of total moment in cores

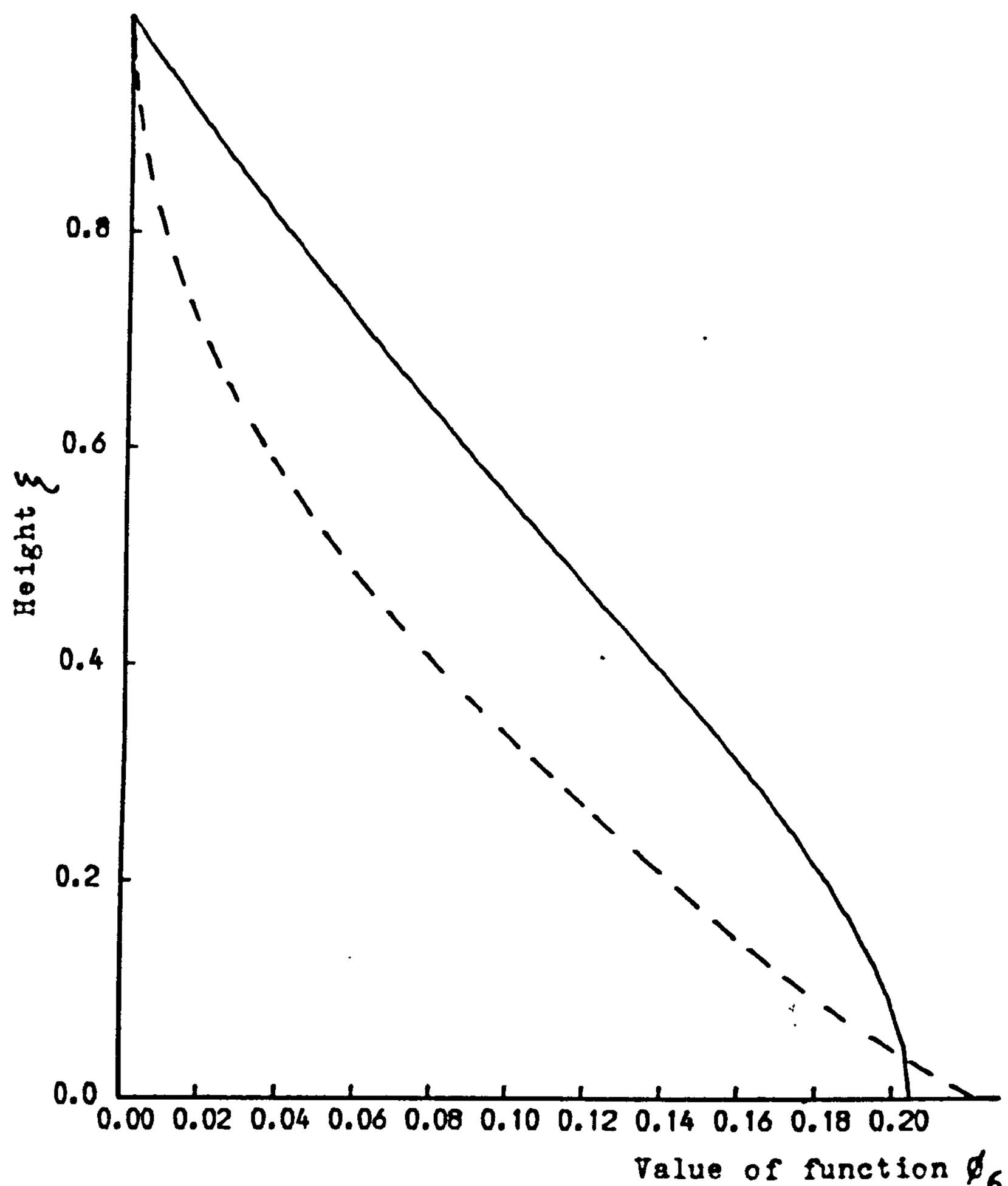

Fig.3.11 Distribution of total moment in coupled shear walls

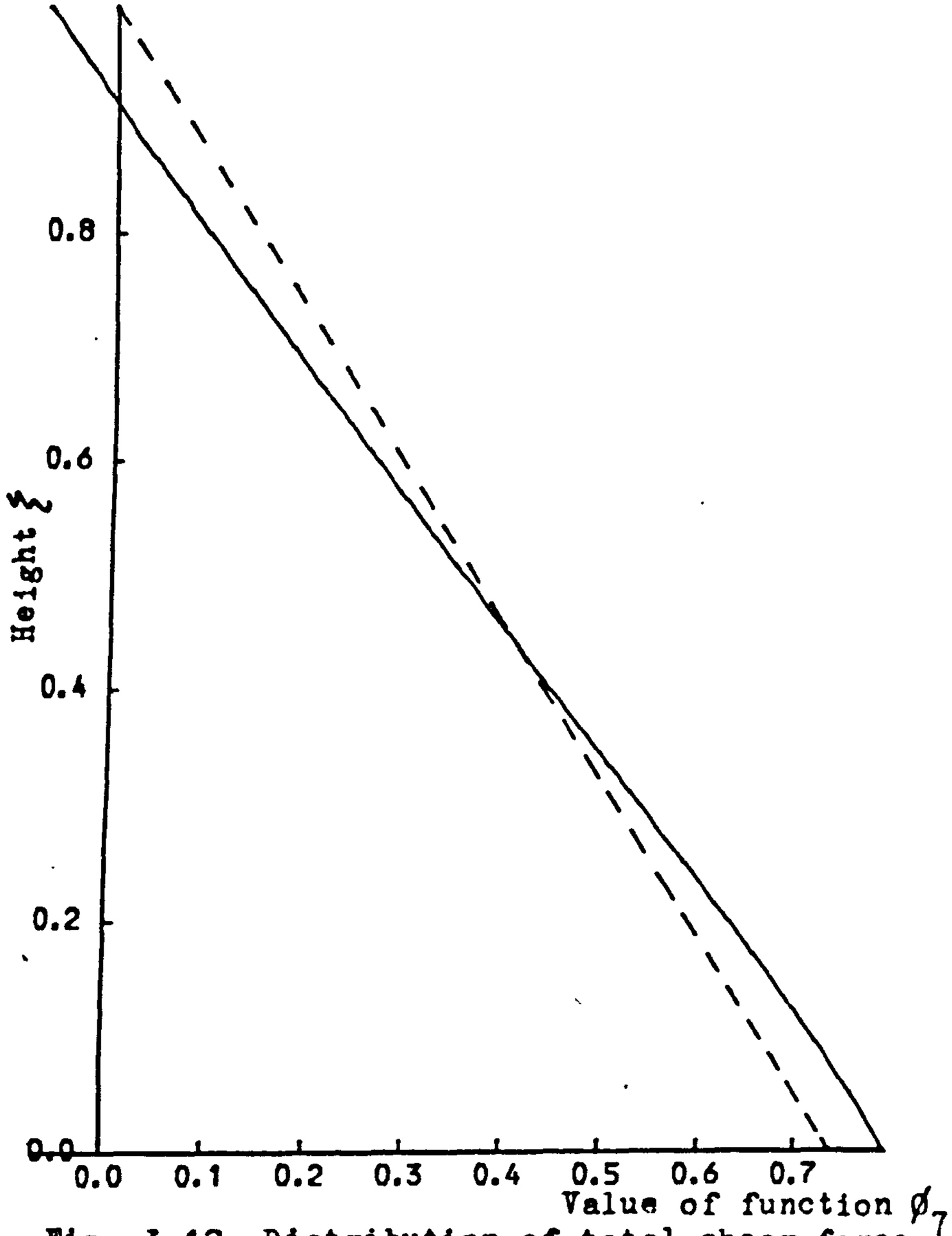

Fig. 3.12 Distribution of total shear force in coupled shear walls

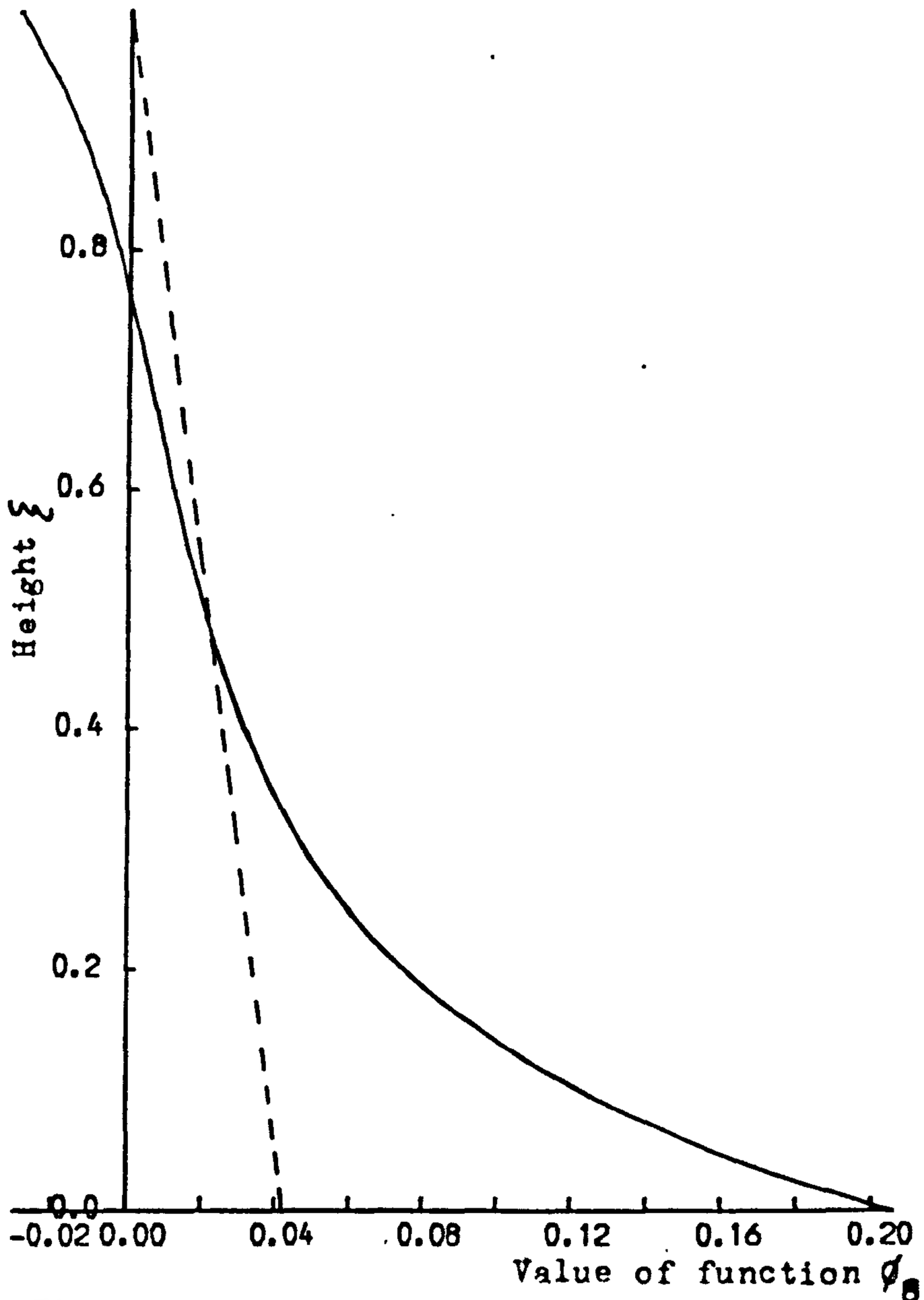

Fig. 3.13 Distribution of total shear force in cores

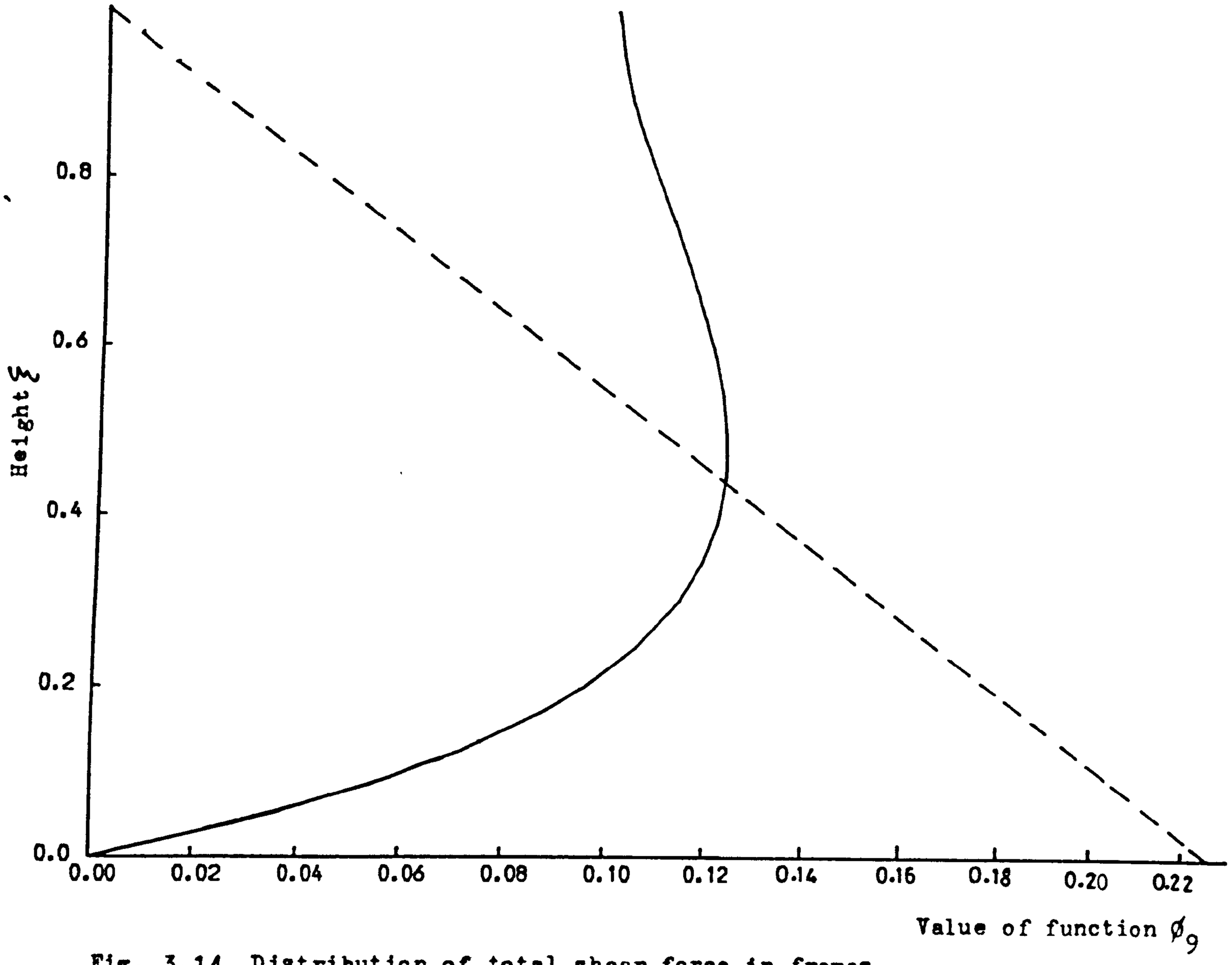

Fig. 3.14 Distribution of total shear force in frames

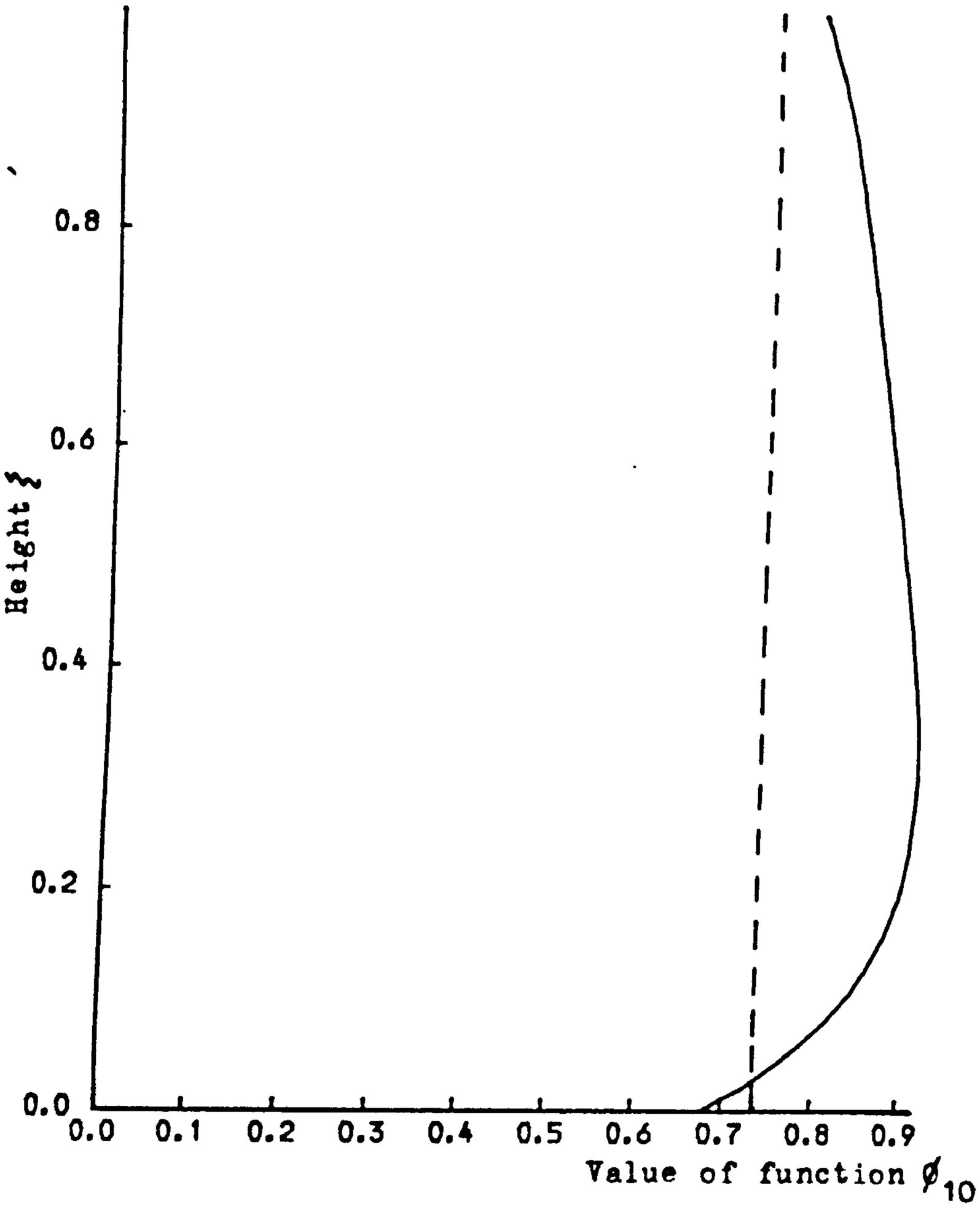

Fig. 3.15 Distribution of lateral loads in coupled shear walls

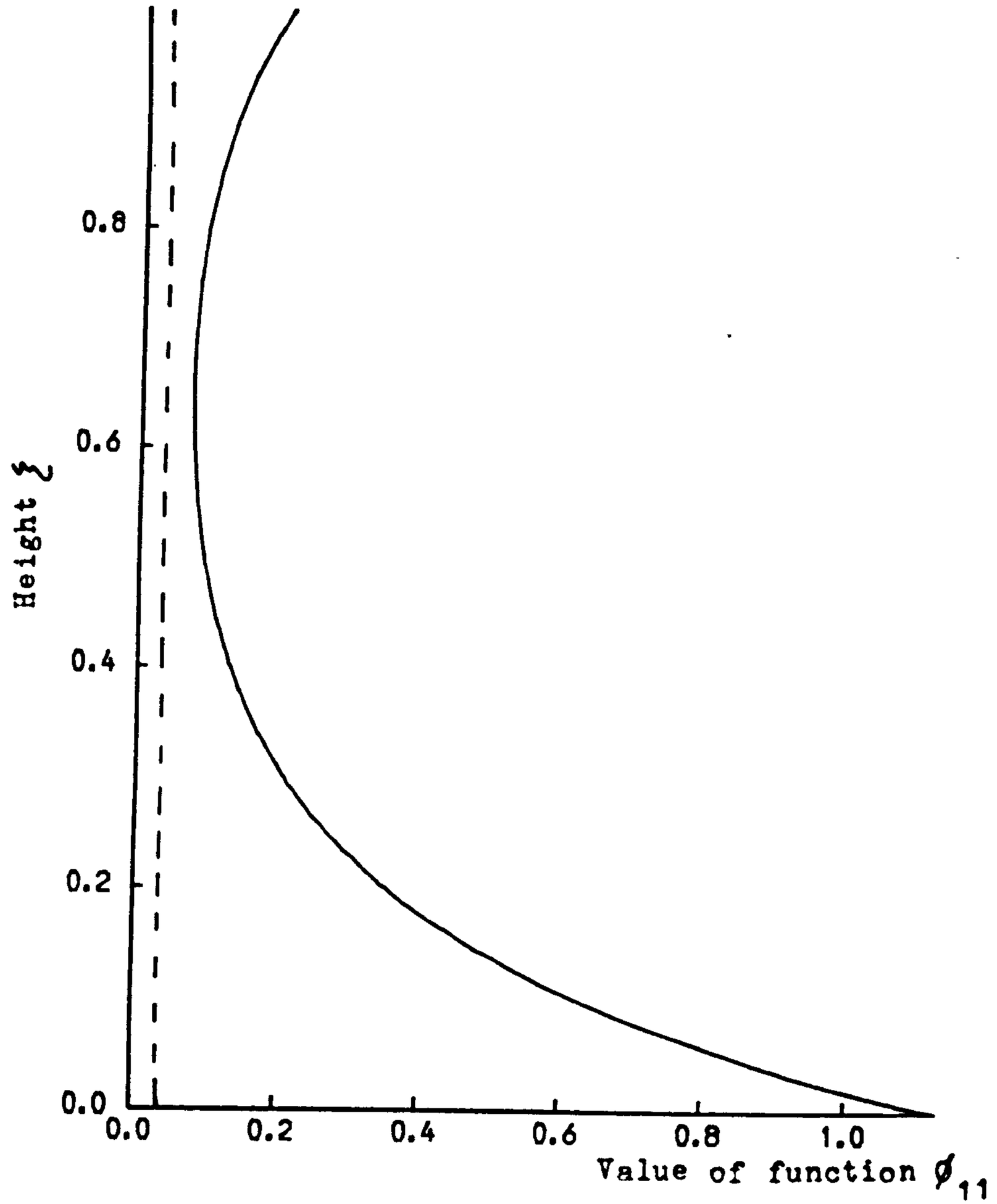

Fig. 3.16 Distribution of lateral loads in cores

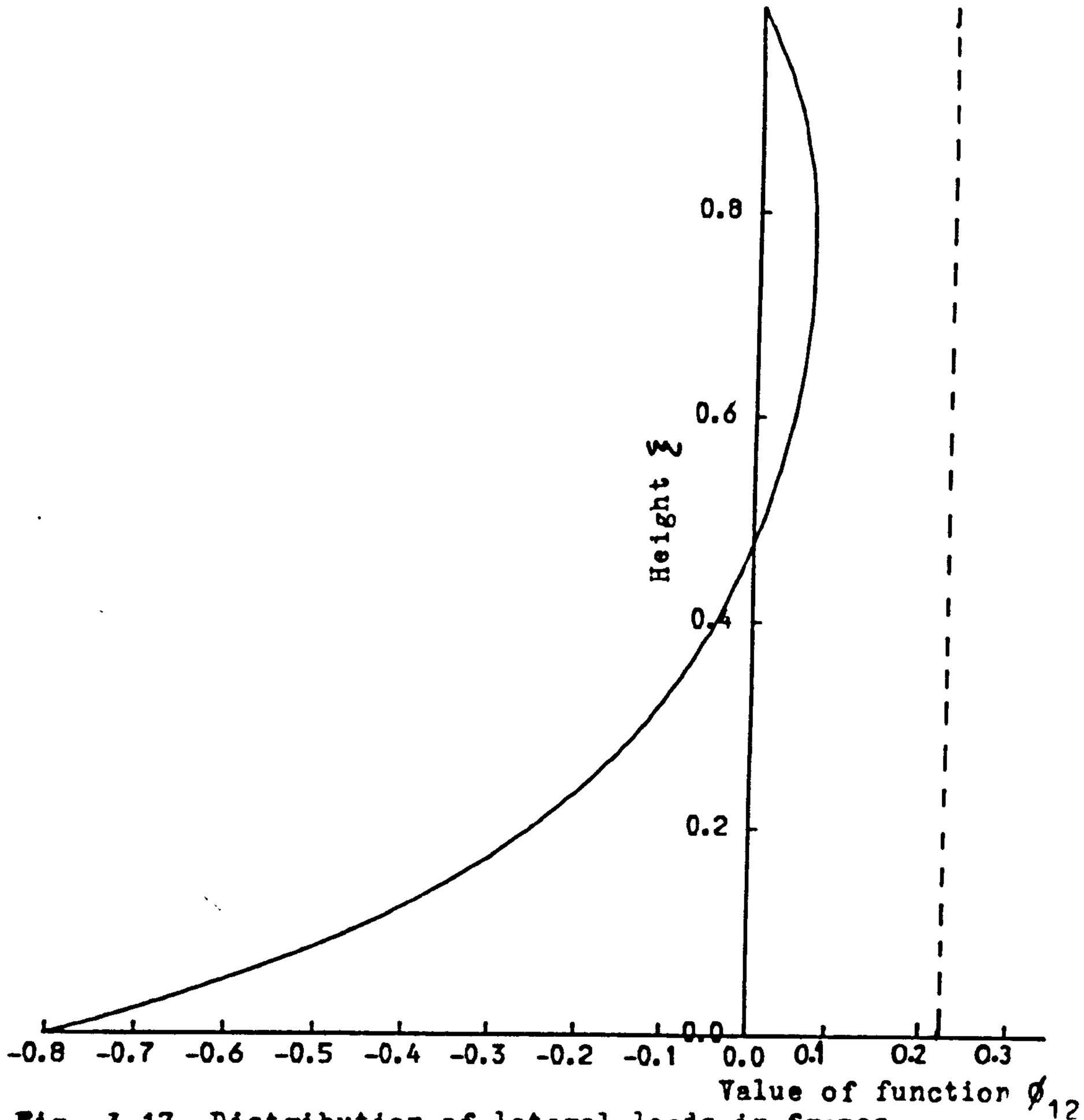

Fig. 3.17 Distribution of lateral loads in frames

C H A P T E R 4

ANALYSES OF THREE-DIMENSIONAL SYMMETRIC STRUCTURES CONSISTING OF SETS OF IDENTICAL COUPLED SHEAR WALL, CORE AND RIGIDLY-JOINTED FRAMEWORK ASSEMBLIES SUBJECTED TO LATERAL LOADS

NOTATION

A_1, A_2, A_3, A_4	cross-sectional areas of walls, 1,2,3 and 4
b_1, b_2	clear spans between coupled walls
E	elastic modulus
GA	effective shearing rigidity of shear cantilever
h	storey height
H	total height
I_i	second moment of area of wall i (i = 1,2,3,4,5)
I	$I_1 + I_2 + I_3 + I_4 + I_5$
I_{c1}, I_{c2}	second moments of area of the connecting beams
l_1, l_2	distances between centroidal axes of coupled walls
M_i	bending moment in wall i (i = 1,2,3,4,5)
M	applied static moment
N_1, N_2	axial forces in coupled walls
n_i	axial force intensities in connecting media (i = 1,2,3,4)
Q_i	concentrated interactive forces (i = 1,2,3,4)
q_1, q_2	shear force intensities in connecting media of coupled shear walls
S_i	shear force in wall i (i = 1,2,3,4,5)
ω	uniformly distributed lateral force intensity
x	height above base
y	horizontal deflection
α, β_1, β_2, γ_1, γ_2	structural parameters
ξ	non-dimensional height (x/H)

CHAPTER 4

ANALYSES OF THREE-DIMENSIONAL SYMMETRIC STRUCTURES CONSISTING OF SETS OF IDENTICAL COUPLED SHEAR WALL, CORE AND RIGIDLY-JOINTED FRAMEWORK ASSEMBLIES SUBJECTED TO LATERAL LOADS

4.1 Introduction

In general, a tall building structure is a complex three-dimensional system consisting of various combinations of interconnected structural assemblies, namely, walls, coupled shear walls, service cores, rigidly-jointed frames and floor systems. When subjected to laterally distributed loads considerable redistribution of lateral forces can occur throughout the height of the building. The load redistribution characteristics of three-dimensional symmetric structures consisting of identical coupled shear walls and cores was discussed in Chapter 2.

In many tall buildings, due to the architectural and structural requirements, it is necessary to use different sets of identical coupled shear walls, service cores and rigidly jointed frame assemblies in conjunction with floor systems. The aim of this chapter is to present an "exact" elastic analysis of three-dimensional symmetrical structures consisting of two different sets of identical coupled shear wall assemblies, service cores and/or

independent shear walls. The analysis is later extended to include rigidly-jointed framework assemblies. A general idealised structural representation of such structures is shown in Fig. 4.1 which depicts a building with central cores. It is assumed that the applied lateral load on the building has a resultant at the same fixed position throughout the height of the building, that is the resultant acts as a vertical line load. If the floor slabs are assumed to be rigid in their own planes, a lateral applied force at any position off the line of symmetry, but parallel to it, may be replaced by a statically equivalent force at the axis of symmetry and a twisting moment about it. The analysis may then be treated as a superposition of a symmetrical pure bending action and a skew-symmetric pure torsional action.

In the case where the resultant of the horizontal load acts as a vertical line load at the axis of symmetry of the building there is no rotation in the horizontal plane and all assemblies will undergo the same horizontal deflection at any level. Hence, the three-dimensional structure may be replaced by an equivalent plane system in which the components are constrained to act in series by rigid pin-ended links as shown in Figs. 4.2 and 4.3. The pin-ended links simulate the action of floor slabs, and are assumed infinitely rigid in plane, but flexible out of plane. The stiffness of the two pairs of coupled shear walls are equal

to the sum of the stiffness of the respective sets of identical coupled shear walls, and the flexural rigidity of the single cantilevered wall is equal to the sum of the flexural rigidities of all the cantilevered service cores and/or independent shear walls in the building.

In the case of skew-symmetric pure torsional action, a technique has been developed (Chapter 6) for transforming the three-dimensional system into an equivalent plane structure consisting of equivalent components constrained to act together by rigid pin-ended links such as those indicated in Figs. 4.2 and 4.3. The plane structure may by analysed using the technique developed for the case of pure bending action, and the forces and deformation subsequently transformed back into the original system.

In some buildings, the service cores are composed of coupled shear walls rather than cantilevered walls. An example of such structures is shown in Fig. 4.4(a). From a structural point of view, these buildings are considered to consist of two different sets of identical coupled shear walls which are symmetrically arranged. Therefore, for the purpose of analysis, the procedure explained above will still apply. Hence, the three dimensional structure may be replaced by the equivalent plane system shown in Fig. 4.4(b).

Finally, by using continuum techniques and representing a frame by an equivalent shear cantilever, closed-form

solutions may be achieved for standard load cases, enabling the complete distribution of forces and deflections to be determined rapidly. A numerical example demonstrates the typical structural behaviour of such systems.

ANALYSIS OF THREE-DIMENSIONAL SYMMETRIC STRUCTURES CONSISTING OF SETS OF IDENTICAL COUPLED SHEAR WALL AND CORE ASSEMBLIES SUBJECTED TO LATERAL LOADS

4.2 Analysis

Consider the action of the plane system of Fig. 4.2, consisting of two different pairs of coupled shear walls linked to a single cantilevered wall. The single cantilever may be either an independent shear wall or a box core which can be assumed to behave as a simple beam. The axially rigid pin-ended links transmit axial forces only, and enable the desired load redistribution to take place between components.

In the case of coupled shear walls as described in earlier chapters the discrete sets of connecting beams of flexural rigidities EI_{c1} and EI_{c2} may be replaced by equivalent connecting media of flexural rigidities $EI_{c1/h}$ and $EI_{c2/h}$ per unit height, if h is the storey height.

The compatibility equations at any level x may be shown to be

$$l_1 \frac{dy}{dx} - \frac{b_1^3 h q_1}{12EI_{c1}} - \frac{1}{E}\left(\frac{1}{A_1} + \frac{1}{A_2}\right) \int_o^x N_1 \, dx = o \qquad (4.1)$$

$$l_2 \frac{dy}{dx} - \frac{b_2^3 h q_2}{12EI_{c2}} - \frac{1}{E}\left(\frac{1}{A_3} + \frac{1}{A_4}\right) \int_o^x N_2 \, dx = o \qquad (4.2)$$

where the three terms in each equation represent respectively the relative displacements due to the slopes of the walls, the deflections of the connecting beams and the axial deformations of the walls. The axial forces N_1 and N_2 in the walls are given by

$$N_1 = \int_x^H q_1 dx \qquad (4.3)$$

$$N_2 = \int_x^H q_2 dx \qquad (4.4)$$

In equations (4.1) and (4.2), y is the horizontal deflection, l_1 and l_2 the distances between wall centroids, b_1 and b_2 the clear spans of the beams and A_1, A_2, A_3 and A_4 the cross-sectional areas of the walls.

In an analogus manner, it is assumed that the discrete system of pin-ended links between the three components may be replaced by continuous media, transmitting axial forces

of intensities n_2 and n_4 per unit height as shown in Fig. 4.5.

The respective moment-curvature relationships for the five walls in Fig. 4.5 are

$$EI_1 \frac{d^2y}{dx^2} = M_1 = M - (\frac{b_1}{2} + d_1) N_1 - M_{a1} \quad (4.5)$$

$$EI_2 \frac{d^2y}{dx^2} = M_2 = - (\frac{b_1}{2} + d_2) N_1 + M_{a1} - M_{a2} \quad (4.6)$$

$$EI_3 \frac{d^3y}{dx^2} = M_3 = - (\frac{b_2}{2} + d_3) N_2 + M_{a2} - M_{a3} \quad (4.7)$$

$$EI_4 \frac{d^2y}{dx^2} = M_4 = - (\frac{b_2}{2} + d_4) N_2 + M_{a3} - M_{a4} \quad (4.8)$$

$$EI_5 \frac{d^2y}{dx^2} = M_5 = M_{a4} \quad (4.9)$$

where M is the static applied moment and M_{a1}, M_{a2}, M_{a3} and M_{a4} are the moments on the walls due to the axial forces in the four sets of connecting beams, given by

$$M_{a1} = \int_x^H n_1(\lambda) (\lambda - x) d\lambda + Q_1 (H - x) \quad (4.10)$$

$$M_{a2} = \int_x^H n_2(\lambda) (\lambda - x) d\lambda + Q_2 (H - x) \quad (4.11)$$

$$M_{a3} = \int_x^H n_3(\lambda) (\lambda - x) d\lambda + Q_3 (H - x) \quad (4.12)$$

$$M_{a4} = \int_x^H n_4(\lambda) (\lambda - x) d\lambda + Q_2 (H - x) \quad (4.13)$$

where Q_1, Q_2, Q_3 and Q_4 are the concentrated forces which exist in the connecting media at the top of the structure, (Fig. 4.5).

The addition of equations (4.5) to (4.9) yields the overall moment curvature relationship

$$EI \frac{d^2y}{dx^2} = M - l_1 N_1 - l_2 N_2 \qquad (4.14)$$

in which

$$I = I_1 + I_2 + I_3 + I_4 + I_5$$

On differentiating equations (4.1) and (4.2) twice, multiplying by l_1 and l_2 respectively and adding them, yields

$$l_1 \frac{d^2q_1}{dx^2} + l_2 \frac{d^2q_2}{dx^2} - l_1\gamma_1^2 q_1 - l_2\gamma_2^2 q_2 = (\beta_1^2 + \beta_2^2) EI \frac{d^3y}{dx^3} \qquad (4.15)$$

$$\beta_1^2 = \frac{12 I_{c1} l_1^2}{b_1^3 h I}$$

$$\beta_2^2 = \frac{12 I_{c2} l_2^2}{b_2^3 h I}$$

$$\gamma_1^2 = \frac{12 I_{c1}}{b_1^3 h} \left(\frac{1}{A_1} + \frac{1}{A_2}\right)$$

$$\gamma_2^2 = \frac{12 I_{c2}}{b_2^3 h} \left(\frac{1}{A_3} + \frac{1}{A_4}\right)$$

Differentiating equation (4.14) thrice, yields

$$l_1 \frac{d^2 q_1}{dx^2} + l_2 \frac{d^2 q_2}{dx^2} = - \frac{d^3 M}{dx^3} + EI \frac{d^5 y}{dx^5} \qquad (4.16)$$

On substituting for the second order derivative terms in q_1 and q_2 from equation (4.15) into (4.16) it becomes

$$EI \frac{d^5 y}{dx^5} - l_1 \gamma_1^{\,2} q_1 - l_2 \gamma_2^{\,2} q_2 - (\beta_1^{\,2} + \beta_2^{\,2}) EI \frac{d^3 y}{dx^3} = \frac{d^3 M}{dx^3} \qquad (4.17)$$

On differentiating equation (4.14) and solving it simultaneously with equation (4.17), the shear flows q_1 and q_2, in the connecting media become

$$q_1 = \frac{EI}{l_1(\gamma_1^{\,2} - \gamma_2^{\,2})} \left[\frac{d^5 y}{dx^5} - (\beta_1^{\,2} + \beta_2^{\,2} + \gamma_2^{\,2}) \frac{d^3 y}{dx^3} - \frac{1}{EI} \frac{d^3 M}{dx^3} + \frac{\gamma_2^{\,2}}{EI} \frac{dM}{dx} \right] \qquad (4.18)$$

$$q_2 = \frac{EI}{l_2(\gamma_2^{\,2} - \gamma_1^{\,2})} \left[\frac{d^5 y}{dx^5} - (\beta_1^{\,2} + \beta_2^{\,2} + \gamma_1^{\,2}) \frac{d^3 y}{dx^3} - \frac{1}{EI} \frac{d^3 M}{dx^3} + \frac{\gamma_1^{\,2}}{EI} \frac{dM}{dx} \right] \qquad (4.19)$$

Back substitution of either of equations (4.18) or (4.19) into (4.1) or (4.2) respectively, yields

$$\frac{d^7y}{dx^7} - m^2 \frac{d^5y}{dx^5} + n^2 \frac{d^3y}{dx^3} = \frac{1}{EI}\left[\frac{d^5M}{dx^5} - (\gamma_1^2 + \gamma_2^2)\frac{d^3M}{dx^3} + \gamma_1^2\gamma_2^2 \frac{dM}{dx}\right] \quad (4.20)$$

where

$$m^2 = \beta_1^2 + \beta_2^2 + \gamma_1^2 + \gamma_2^2$$

$$n^2 = \beta_1^2\gamma_2^2 + \beta_2^2\gamma_1^2 + \gamma_1^2\gamma_2^2$$

On integrating equation (4.20) once, it becomes

$$\frac{d^6y}{dx^6} - m^2 \frac{d^4y}{dx^4} + n^2 \frac{d^2y}{dx^2} = \frac{1}{EI}\left[\frac{d^4M}{dx^4} - (\gamma_1^2 + \gamma_2^2)\frac{d^2M}{dx^2} + \gamma_1^2\gamma_2^2 M\right] + C_1 \quad (4.21)$$

On differentiating equations (4.14) and (4.17) twice and once respectively, hence substituting for the fourth and sixth order differential terms in y (at x = H) into equation (4.21), the integration constant C_1 becomes zero and the governing differential equation finally becomes

$$\frac{d^6y}{dx^6} - m^2 \frac{d^4y}{dx^4} + n^2 \frac{d^2y}{dx^2} = \frac{1}{EI}\left[\frac{d^4M}{dx^4} - (\gamma_1^2 + \gamma_2^2)\frac{d^2M}{dx^2} + \gamma_1^2\gamma_2^2 M\right] \quad (4.22)$$

The general solution of equation (4.22) for any form of lateral loading may be expressed in the form

$$y = C_o + C_1 x/_H + C_2 \cosh(kx/_H) + C_3 \sinh(kx/_H) + C_4 \cosh(r\,x/_H) + C_5 \sinh(rx/_H) + y_{PI} \quad (4.23)$$

where $C_i (i = o - 5)$ are constants of integration to be determined from the necessary boundary conditions, and y_{PI} is the particular integral solution, i.e. any solution for a specific form of applied moment M.

In equation (4.23) $k = PH$ and $r = nH/_p$ where

$$P^2 = \left[m^2 + (m^4 - 4n^2)^{\frac{1}{2}}\right]/2$$

$$n^2/_{p^2} = \left[m^2 - (m^4 - 4n^2)^{\frac{1}{2}}\right]/2$$

It may readily be seen by inspection of the physical relationships in equation (4.22) that $m^4 \not< 4n^2$, and so the roots of the equation, P and $n/_p$, are always real (cf. Appendix 1).

Boundary conditions

In order to determine the constants C_i of equation (4.23), it is necessary to derive six independent boundary conditions for the structure. If the structure is rigidly built at the base, then at x = o

$$y = o \quad \text{and } dy/dx = o \tag{4.24}$$

At the top, the axial forces N_1 and N_2 and the bending moment in each wall are equal to zero, and so, at x = H

$$\frac{d^2y}{dx^2} = o \tag{4.25}$$

From equations (4.3) and (4.4), $\frac{dN_1}{dx} = -q_1$ and $\frac{dN_2}{dx} = -q_2$, and from equations (4.1), (4.2) and (4.24), $q_1 = q_2 = o$ at x = o. Hence, differentiating equation (4.14), and using the fact that dN_1/dx and dN_2/dx are each equal to zero at the base, the following conditions holds at x = o

$$\frac{d^3y}{dx^3} = \frac{1}{EI} \frac{dM}{dx}(o) \tag{4.26}$$

On differentiating equation (4.14) twice, and using the fact that d^2N_1/dx^2 and d^2N_2/dx^2 are each equal to zero at the top, the following condition holds at x = H

$$\frac{d^4y}{dx^4} = \frac{1}{EI}\frac{d^2M}{dx^2} \quad (H) \qquad (4.27)$$

A consideration of equations (4.17) and (4.16) yields the following condition, at x = o

$$\frac{d^5y}{dx^5} = \frac{1}{EI}\left[\frac{d^3M}{dx^3}(o) + (\beta_1^2 + \beta_2^2)\frac{dM}{dx}(o)\right] \qquad (4.28)$$

From a consideration of the above boundary conditions it may be deduced that the sixth order differential equation (4.22) seems to incorporate an element of a rigid body movement (i.e. top and base displacements and a base rotation). It is due to this rigid body movement that there exist four boundary conditions at x = o and two at x = H.

Uniformly distributed wind loading

In order to achieve a solution, suppose that the particular case is considered of a uniformly distributed wind loading of intensity ω per unit height. In that case

$$M = \frac{1}{2}\omega(H - x)^2$$

and

$$\frac{d^2M}{dx^2} = \omega \qquad (4.29)$$

and

$$\frac{d^4M}{dx^4} = o$$

On substituting for the moment function in equation (4.22), the simplest particular integral becomes

$$y_{PI} = \frac{\omega H^4 \gamma_1^2 \gamma_2^2}{24n^2 EI} \left[\left(\frac{x}{H}\right)^4 - 4\left(\frac{x}{H}\right)^3 + \frac{12}{H^2}\left(\frac{m^2}{n^2} + \frac{H^2}{2} - \frac{\gamma_1^2 + \gamma_2^2}{\gamma_1^2 \gamma_2^2}\right)\left(\frac{x}{H}\right)^2 \right] \qquad (4.30)$$

Then on substituting equation (4.23) into boundary conditions (4.24) to (4.28), and solving for the integration constants, it is found that

$$C_1 = (\Delta_3 - m^2\Delta_2)H/n^2$$

$$C_2 = \left[1/(n^2 - p^4)\cosh k\right]\left[(\Delta_1 n^2/p^2 + \Delta_2/H) - (n^2\Delta_2 - p^2\Delta_3)\sinh k/p^3\right]$$

$$C_3 = (n^2\Delta_2 - p^2\Delta_3)/p^3(n^2 - p^4)$$

$$C_4 = \left[-p^5/n^3(n^2 - p^4)\cosh r\right]\left[\frac{n}{p}(\Delta_2/H + p^2\Delta_1) + (\Delta_3 - p^2\Delta_2)\sinh r\right]$$

$$C_5 = p^5(\Delta_3 - p^2\Delta_2)/n^3(n^2 - p^4)$$

$$C_o = -C_2 - C_4$$

89

where

$$\Delta_1 = \frac{\omega}{n^4 EI} (\beta_1^2 \gamma_2^4 + \beta_2^2 \gamma_1^4)$$

$$\Delta_2 = \frac{\omega H}{EI} \left(\frac{\gamma_1^2 \gamma_2^2}{n^2} - 1\right)$$

$$\Delta_3 = - \frac{\omega H}{EI} (\beta_1^2 + \beta_2^2)$$

Then on substituting for (C_o) - (C_5) and y_{PI} into equation (4.23), the general solution becomes

$$y = \frac{(\Delta_3 - m^2 \Delta_2) H}{n^2} \xi$$

$$+ \frac{\omega H^4 \gamma_1^2 \gamma_2^2}{24 n^2 EI} \left[\xi^4 - 4\xi^3 + \frac{12}{H^2} \left(\frac{m^2}{n^2} + \frac{H^2}{2} - \frac{\gamma_1^2 + \gamma_2^2}{\gamma_1^2 \gamma_2^2}\right)\xi^2\right]$$

$$+ \frac{1}{(n^2 - p^4) \cosh k} \left[\left(\frac{\Delta_1 n^2}{p^2} + \frac{\Delta_2}{H}\right)\right.$$

$$\left. - \frac{(n^2 \Delta_2 - p^2 \Delta_3)}{p^3} \times \sinh k\right] (\cosh k\xi - 1)$$

$$+ \frac{n^2 \Delta_2 - p^2 \Delta_3}{p^3 (n^2 - p^4)} \sinh k\xi + \frac{p^5 (\Delta_3 - p^2 \Delta_2)}{n^3 (n^2 - p^4)} \sinh r\xi$$

$$- \frac{p^5}{n^3 (n^2 - p^4) \cosh r} \left[\frac{n}{p}\left(\frac{\Delta_2}{H} + p^2 \Delta_1\right) + (\Delta_3 - p^2 \Delta_2) \sinh r\right]$$

$$(\cosh r\xi - 1)$$

(4.31)

where $\xi = x/H$

ξ is the non-dimensional height variable. Equation (4.31) is dependent on the non-dimensional height ξ, total height H, relative stiffness parameters k and r, and parameters γ_1, γ_2, m, n, p, Δ_1, Δ_2 and Δ_3. These latter parameters are in turn related to k and r.

Substitution of equation (4.31) into the earlier equations yields closed-form solutions for the forces in the various structural components. Using equations (4.18) and (4.19), the shear flows q_1 and q_2 in the connecting media become

$$q_1 = \frac{EI}{l_1(\gamma_1^2 - \gamma_2^2)} \left[\Delta_4 (C_2 \sinh k\xi + C_3 \cosh k\xi) + \Delta_5 (C_4 \sinh r\xi + C_5 \cosh r\xi) + \frac{\omega H \gamma_2^2}{EI} \left(\frac{\gamma_1^2}{n^2} + 1\right)(\xi - 1)\right] \tag{4.32}$$

and

$$q_2 = \frac{EI}{l_2(\gamma_2^2 - \gamma_1^2)} \left[\Delta_6 (C_2 \sinh k\xi + C_3 \cosh k\xi) + \Delta_7 (C_4 \sinh r\xi + C_5 \cosh r\xi) + \frac{\omega H \gamma_1^2}{EI} \left(\frac{\gamma_2^2}{n^2} + 1\right)(\xi - 1)\right] \tag{4.33}$$

in which

$$\Delta_4 = p^3 (p^2 - m^2 + \gamma_1^2)$$

$$\Delta_5 = \frac{n^3}{p^3} (\frac{n^2}{p^2} - m^2 + \gamma_1^2)$$

$$\Delta_6 = p^3 (p^2 - m^2 + \gamma_2^2)$$

$$\Delta_7 = \frac{n^3}{p^3} (\frac{n^2}{p^2} - m^2 + \gamma_2^2)$$

On substituting for q_1 and q_2 from equations (4.32) and (4.33) into equations (4.3) and (4.4), the axial forces in the coupled shear-walls become

$$N_1 = \frac{EI}{l_1(\gamma_1^2 - \gamma_2^2)} \left\{ \frac{\Delta_4}{p} \left[C_2 (\cosh k - \cosh k\xi) + C_3 (\sinh k - \sinh k\xi) \right] + \frac{p\Delta_5}{n} \left[C_4(\cosh r - \cosh r\xi) + C_5(\sinh r - \sinh r\xi) \right] - \frac{1}{2} \frac{\omega H^2 \gamma_2^2}{EI} (\frac{\gamma_1^2}{n^2} + 1) (1 - \xi)^2 \right\} \qquad (4.34)$$

and

$$N_2 = \frac{EI}{l_2 (\gamma_2^2 - \gamma_1^2)} \left\{ \frac{\Delta_6}{p} \left[C_2(\cosh k - \cosh k\xi) + C_3(\sinh k - \sinh k\xi) \right] + \right.$$

$$+ \frac{p\Delta_7}{n}\left[C_4(\cosh hr - \cosh r\xi) + C_5(\sinh hr - \sinh r\xi)\right]$$

$$- \frac{1}{2}\frac{\omega H^2\gamma_1^2}{EI}\left(\frac{\gamma_2^2}{n^2} + 1\right)(1-\xi)^2\Bigg\} \qquad (4.35)$$

The bending moment M_i in wall i (i = 1,2,3,4,5) can be determined by substituting for y from equation (4.23) into equations (4.5) to (4.9) and is given by

$$M_i = EI_i\Bigg\{p^2(C_2\cosh k\xi + C_3\sinh k\xi) + \frac{n^2}{p^2}(C_4\cosh r\xi + C_5\sinh r\xi)$$

$$+ \frac{\omega H^2\gamma_1^2\gamma_2^2}{n^2EI}\left[\frac{1}{2}(1-\xi)^2 + \frac{1}{H^2}\left(\frac{m^2}{n^2} - \frac{\gamma_1^2+\gamma_2^2}{\gamma_1^2\gamma_2^2}\right)\right]\Bigg\} \qquad (4.36)$$

A consideration of the conditions of equilibrium of a small vertical element of each wall (Fig. 4.6) yields the shear forces S_1, S_2, S_3 and S_4 in the four walls (Fig. 4.6)

$$S_1 = -\frac{dM_1}{dx} + \left(\frac{b_1}{2} + d_1\right)q_1$$

$$S_2 = -\frac{dM_1}{dx} + \left(\frac{b_1}{2} + d_2\right)q_1$$

$$S_3 = -\frac{dM_3}{dx} + \left(\frac{b_2}{2} + d_3\right)q_2 \qquad (4.37)$$

$$S_4 = -\frac{dM_4}{dx} + \left(\frac{b_2}{2} + d_4\right)q_2$$

and for the independent wall or core, the shear force S_5 is

$$S_5 = - \frac{dM_5}{dx} \qquad (4.38)$$

Hence, on substituting for q_1, q_2 and M_i $(i = 1,2,3,4,5)$ from equations (4.32), (4.33) and (4.36) into equations (4.37) and (4.38) the shear force in the coupled shear wall and core assemblies may be obtained.

On substituting for M, M_i $(i = 1,2,3,4,5)$, N_1 and N_2 into equations (4.5) to (4.9), the moments in the walls due to axial forces in the four sets of connecting beams may be found. Hence, the axial forces in the connecting media follow from equations (4.10) to (4.13), since

$$n_i = \frac{d^2 M_{ai}}{dx^2} \qquad (i = 1,2,3,4) \qquad (4.39)$$

and becomes

$$n_1 = \omega + (\frac{b_1}{2} + d_1) \frac{dq_1}{dx} - EI_1 \frac{d^4 y}{dx^4} \qquad (4.40)$$

$$n_2 = \omega + l_1 \frac{dq_1}{dx} - EI_{(1+2)} \frac{d^4 y}{dx^4} \qquad (4.41)$$

$$n_3 = n_2 + (\frac{b_2}{2} + d_3) \frac{dq_2}{dx} - EI_3 \frac{d^4 y}{dx^4} \qquad (4.42)$$

$$n_4 = EI_5 \frac{d^4 y}{dx^4} \qquad (4.43)$$

Hence, on substituting for q_1, q_2 and y from equations (4.23), (4.32) and (4.33) into equations (4.40) to (4.43), the axial forces in the connecting media may be found.

If the expressions for M_1 to M_5, q_1 and q_2 are substituted into equations (4.37) and (4.38), it is found that shear forces exist in the various components at the top of the continuous structure. It must be deduced that these can only be caused by concentrated interactive forces at the top of each connecting medium, as shown in Fig. 4.5, such that

$$S_1(H) = - Q_1, \quad S_2(H) = Q_1 - Q_2, \quad S_3(H) = Q_2 - Q_3,$$

$$S_4(H) = Q_3 - Q_4, \quad S_5(H) = Q_4$$

Hence,

$$Q_1 = \frac{dM_1(H)}{dx} - (\frac{b_1}{2} + d_1)\, q_1(H) \qquad (4.44)$$

$$Q_2 = \frac{dM_{1+2}(H)}{dx} - l_1\, q_1(H) \qquad (4.45)$$

$$Q_3 = \frac{dM_{1+2+3}(H)}{dx} - l_1\, q_1(H) - (\frac{b_2}{2} + d_3)\, q_2(H) \qquad (4.46)$$

$$Q_4 = - \frac{dM_5(H)}{dx} \qquad (4.47)$$

The internal force are dependent on the same variables as the deflection y.

4.3 Numerical example

In order to illustrate the theoretical results, a representative 30-storey structure of the form shown in Fig. 4.7 is considered. The structure consists of a central U-shaped core, four pairs of coupled shear walls (A) and two pairs of coupled shear walls (B). Connecting beams are 0.4m deep and of the same width as the walls. The relevant structural data are:

Storey height	$h = 2.8$ m
Total building height	$H = 84$ m
For core	$I = 14.31\ m^4$
For coupled shear walls (A)	$I_1 = I_2 = 3.6\ m^4$
	$A_1 = A_2 = 1.2\ m^2$
	$I_{c1} = 10.67 \times 10^{-4}\ m^4$
	$b_1 = 6$ m
	$l_1 = 12$ m
For coupled shear walls (B)	$I_3 = I_4 = 12.8\ m^4$
	$A_3 = A_4 = 2.4\ m^2$
	$I_{c2} = 16 \times 10^{-4}\ m^4$
	$b_2 = 2$ m
	$l_2 = 10$ m
and	$E = 21 \times 10^6\ KN/m^2$

Then, on adding the properties of the three groups of

elements, the relevant structural parameters for the overall structure become

$\beta_1 H = 0.955$ for set of coupled walls A

$\beta_2 H = 3.581$ for set of coupled walls B

$\gamma_1 H = 0.499$ for set of coupled walls A

$\gamma_2 H = 2.44$ for set of coupled walls B

The lateral deflections and internal forces in the different components may be determined from the earlier equations (4.31) to (4.47).

Since for each group the coupled shear walls are identical, the forces in each are the same. The distributions may be expressed in terms of a series of functions F_1 to F_{14} as follows, related where appropriate to the applied load intensity ω, the total shear force ωH, and the total statical moment $\frac{\omega H^2}{2}$. These functions are defined as

$$y = \frac{\omega H^4}{EI} F_1$$

$$q_1 = \omega H F_2, \quad q_2 = \omega H F_3, \quad N_1 = \frac{\omega H^2}{2} F_4, \quad N_2 = \frac{\omega H^2}{2} F_5$$

$$M_1 = M_2 = \frac{1}{2}\left(\frac{\omega H^2}{2}\right) F_6, \quad M_3 = M_4 = \frac{1}{2}\left(\frac{\omega H^2}{2}\right) F_7, \quad M_5 = \frac{\omega H^2}{2} F_8$$

$$S_1 = S_2 = \frac{1}{2} \omega H F_9, \quad S_3 = S_4 = \frac{1}{2} \omega H F_{10}, \quad S_5 = \omega H F_{11}$$

The lateral load distributions on the two groups of coupled shear walls and core are respectively ωF_{12}, ωF_{13} and ωF_{14}.

The magnitudes of the concentrated interactive forces are found to be

$$Q_1 = 0.00495\,\omega H$$

$$Q_2 = 0.00990\,\omega H$$

$$Q_3 = -0.00715\,\omega H$$

$$Q_4 = -0.02420\,\omega H$$

Figures 4.10 to 4.23 illustrate the general forms of structural actions which occur in composite structures of this nature, in which continuous redistribution of lateral forces occurs as a result of different load-deflection characteristics of the components. Figs. 4.10 to 4.14 show typical distributions of lateral deflection, shear flow and axial forces in the two sets of laterally loaded coupled shear walls.

Figures 4.15 to 4.17 show the distributions of total moments in two sets of coupled shear walls and core assemblies respectively. The bending moments in both ccupled walls and core are both small and negative in sense in the upper levels, owing to the coupling actions of the connecting beams and the top concentrated forces.

Figures 4.18 to 4.20 show the distribution of total shear forces in two sets of coupled shear walls and core assemblies. These indicate that the distribution of shearing forces are roughly linear in the coupled shear walls.

Figures 4.21 to 4.23 indicate that the lateral forces on each assembly (i.e. set of coupled walls A, set of coupled walls B and core) are small in the upper levels of both sets of coupled shear walls and relatively large in the core, but they increase and decrease respectively in the lower levels due to the load redistribution.

A commonly adopted design procedure is to assume that the load distribution on each structural component is uniform and of such a magnitude that the resulting deflections at the top of the structure are equal. The distributions which would occur in that case are indicated by broken lines in Figs. 4.21 to 4.23. The corresponding distributions of the shear flows and axial forces in the two sets of coupled shear walls are shown by the broken lines in Figs. 4.11 to 4.14, and the moments and shear forces in the three components are shown similarly in Figs. 4.15 to 4.20. Although considerable errors still occur in the force actions at different levels, the degree of accuracy is generally better than that obtained with the lateral force distributions and this lends credibility to the relatively crude design

procedure. For completeness, the deflection profiles of the individual elements, obtained by matching deflections at the top only, are shown in Fig. 4.9.

Although the curves presented demonstrate the typical forms of structural actions, the actual magnitudes of the forces in each component will naturally depend on their relative stiffnesses.

ANALYSIS OF THREE-DIMENSIONAL SYMMETRIC STRUCTURES CONSISTING OF SETS OF IDENTICAL COUPLED SHEAR WALL, CORE AND RIGIDLY-JOINTED FRAMES SUBJECTED TO LATERAL LOADS

4.4 Analysis

Many tall building structures consist of assemblies of independent and different sets of identical coupled shear walls, cores, and rigidly jointed-frames, constrained to act together by the floor slabs as shown in Fig. 4.1(b).

Although the mathematical formulation for such structures is considerably harder, the analytical procedure is similar to that described in section 4.2. The plane and equivalent structures are shown in Fig. 4.3 and 4.8 respectively.

The respective moment-curvature relationships for the

coupled shear walls are given by equations (4.5) to (4.8), and for core and frame assemblies they become correspondingly (Fig. 4.8)

$$EI_5 \frac{d^2y}{dx^2} = M_5 = M_{a4} - M_{a5} \qquad (4.48)$$

$$M_6 = M_{a5} \qquad (4.49)$$

where M_{a5} is the moment on the frame due to the axial force n_5 in the connecting medium, given by

$$M_{a5} = \int_x^H n_5 (\lambda)(\lambda - x) \, d\lambda + Q_5(H - x) \qquad (4.50)$$

where Q_5 is the concentrated force which exists in the connecting medium at the top of the structure (Fig. 4.8).

The addition of equations (4.5) to (4.8), (4.48) and (4.49) yields the overall moment-curvature relationship

$$EI \frac{d^2y}{dx^2} + M_6 = M - l_1 N_1 - l_2 N_2 \qquad (4.51)$$

Differentiating equation (4.51) thrice, yields

$$EI \frac{d^5y}{dx^5} - GA \frac{d^3y}{dx^3} = \frac{d^3M}{dx^3} + l_1 \frac{d^2q_1}{dx^2} + l_2 \frac{d^2q_2}{dx^2} \qquad (4.52)$$

On substituting for the second derivative terms in q_1 and q_2 from equation (4.15) into (4.52) it becomes

$$\frac{d^5y}{dx^5} - (\alpha^2 + \beta_1^2 + \beta_2^2) \frac{d^3y}{dx^3} - \frac{l_1\gamma_1^2}{EI} q_1 - \frac{l_2\gamma_2^2}{EI} q_2 = \frac{1}{EI} \frac{d^3M}{dx^3} \qquad (4.53)$$

where $\alpha^2 = GA/EI$, and β_1^2, β_2^2, γ_1^2 and γ_2^2 are as defined in section 4.2.

On differentiating equation (4.51) and solving simultaneously with equation (4.53), the shear force intensities q_1 and q_2 in the connecting media become

$$q_1 = \frac{EI}{l_1(\gamma_1^2 - \gamma_2^2)}\left[\frac{d^5y}{dx^5} - (\alpha^2 + \beta_1^2 + \beta_2^2 + \gamma_2^2)\frac{d^3y}{dx^3} + \alpha^2\gamma_2^2\frac{dy}{dx} - \frac{1}{EI}\frac{d^3M}{dx^3} + \frac{\gamma_2^2}{EI}\frac{dM}{dx}\right] \quad (4.54)$$

$$q_2 = \frac{EI}{l_2(\gamma_2^2 - \gamma_1^2)}\left[\frac{d^5y}{dx^5} - (\alpha^2 + \beta_1^2 + \beta_2^2 + \gamma_1^2)\frac{d^3y}{dx^3} + \alpha^2\gamma_1^2\frac{dy}{dx} - \frac{1}{EI}\frac{d^3M}{dx^3} + \frac{\gamma_1^2}{EI}\frac{dM}{dx}\right] \quad (4.55)$$

Substitution of either of equations (4.54) or (4.55) into (4.1) or (4.2) respectively, yields

$$\frac{d^7y}{dx^7} - m_1^2\frac{d^5y}{dx^5} + n_1^2\frac{d^3y}{dx^3} - p_1^2\frac{dy}{dx} = \frac{1}{EI}\left[\frac{d^5M}{dx^5} - (\gamma_1^2 + \gamma_2^2)\frac{d^3M}{dx^3} + \gamma_1^2\gamma_2^2\frac{dM}{dx}\right] \quad (4.56)$$

where

$$m_1^2 = \alpha^2 + \beta_1^2 + \beta_2^2 + \gamma_1^2 + \gamma_2^2$$

$$n_1^2 = \alpha^2\gamma_1^2 + \alpha^2\gamma_2^2 + \beta_1^2\gamma_2^2 + \beta_2^2\gamma_1^2 + \gamma_1^2\gamma_2^2$$

$$p_1^2 = \alpha^2\gamma_1^2\gamma_2^2$$

A consideration of equation (4.56) might suggest that this equation may be reduced to a sixth order differential equation if integrated once, but due to difficulty involved in finding the integration constant generated this process was ruled out.

The complete solution of the seventh order differential equation is given by the addition of the complementary function and particular integral. The characteristic equation is

$$\lambda^7 - m_1^2\lambda^5 + n_1^2\lambda^3 - p_1^2\lambda = 0 \qquad (4.57)$$

A numerical solution of equation (4.57) yields seven real and/or complex roots, zero, $\pm\lambda_1$, $\pm\lambda_2$ and $\pm\lambda_3$. Hence, the general solution of equation (4.56) for any form of lateral loading may be expressed in the form

$$y = D_0 + D_1 \cosh\lambda_1 x + D_2 \sinh\lambda_1 x + D_3 \cosh\lambda_2 x + D_4 \sinh\lambda_2 x + D_5 \cosh\lambda_3 x + D_6 \sinh\lambda_3 x + y_{PI} \qquad (4.58)$$

where $D_i (i = o - 6)$ are the constants of integration to be determined from the necessary boundary conditions, and y_{PI} is the particular integral solution.

Boundary conditions

The first five boundary conditions are as expressed by equations (4.24) to (4.27). A consideration of equation (4.53) yields the following condition , at x = o

$$\frac{d^5y}{dx^5} = \frac{1}{EI}\left[\frac{d^3M}{dx^3}(o) + (\alpha^2 + \beta_1{}^2 + \beta_2{}^2)\frac{dM}{dx}(o)\right] \quad (4.59)$$

On differentiating equation (4.53) and using the fact that dq_1/dx and dq_2/dx are each equal to zero at the top, the following condition holds, at x = H

$$\frac{d^6y}{dx^6} = \frac{1}{EI}\left[\frac{d^4M}{dx^4}(H) + (\alpha^2 + \beta_1{}^2 + \beta_2{}^2)\frac{d^2M}{dx^2}(H)\right] \quad (4.60)$$

Uniformly distributed wind loading

If a uniformly distributed wind loading of intensity ω per unit height is considered, then

$$M = \frac{1}{2}\omega(H - x)^2$$

and

$$\frac{dM}{dx} = -\omega(H - x)$$

and $$\frac{d^3M}{dx^3} = 0$$

and $$\frac{d^5M}{dx^5} = 0$$

On substituting for the moment function in equation (4.56), the simplest particular integral becomes

$$y_{PI} = \frac{-\gamma_1^2 \gamma_2^2 \omega H^2}{p_1^2 EI} \left[\frac{1}{2} \left(\frac{x}{H}\right)^2 - \left(\frac{x}{H}\right)\right] \qquad (4.61)$$

Then on substituting equation (4.58) into boundary conditions (4.24) to (4.27), (4.59), and (4.60), the constants of integration $D_i (i = o - 6)$ may be obtained. Therefore, for the case of a uniformly distributed load of intensity ω per unit height a closed-form solution for the deflections is possible. On following the same procedure as described in section (4.2), closed-form solutions may be achieved for the moments, shear forces, axial forces in the walls and axial force intensities in the connecting media. As mentioned previously, the characteristic equation regarding the general differential equation can only be solved numerically, hence, a general solution can not be obtained. For any specific structure the parameters m_1^2, n_1^2 and p_1^2 may be calculated and used to solve the general equation (4.56).

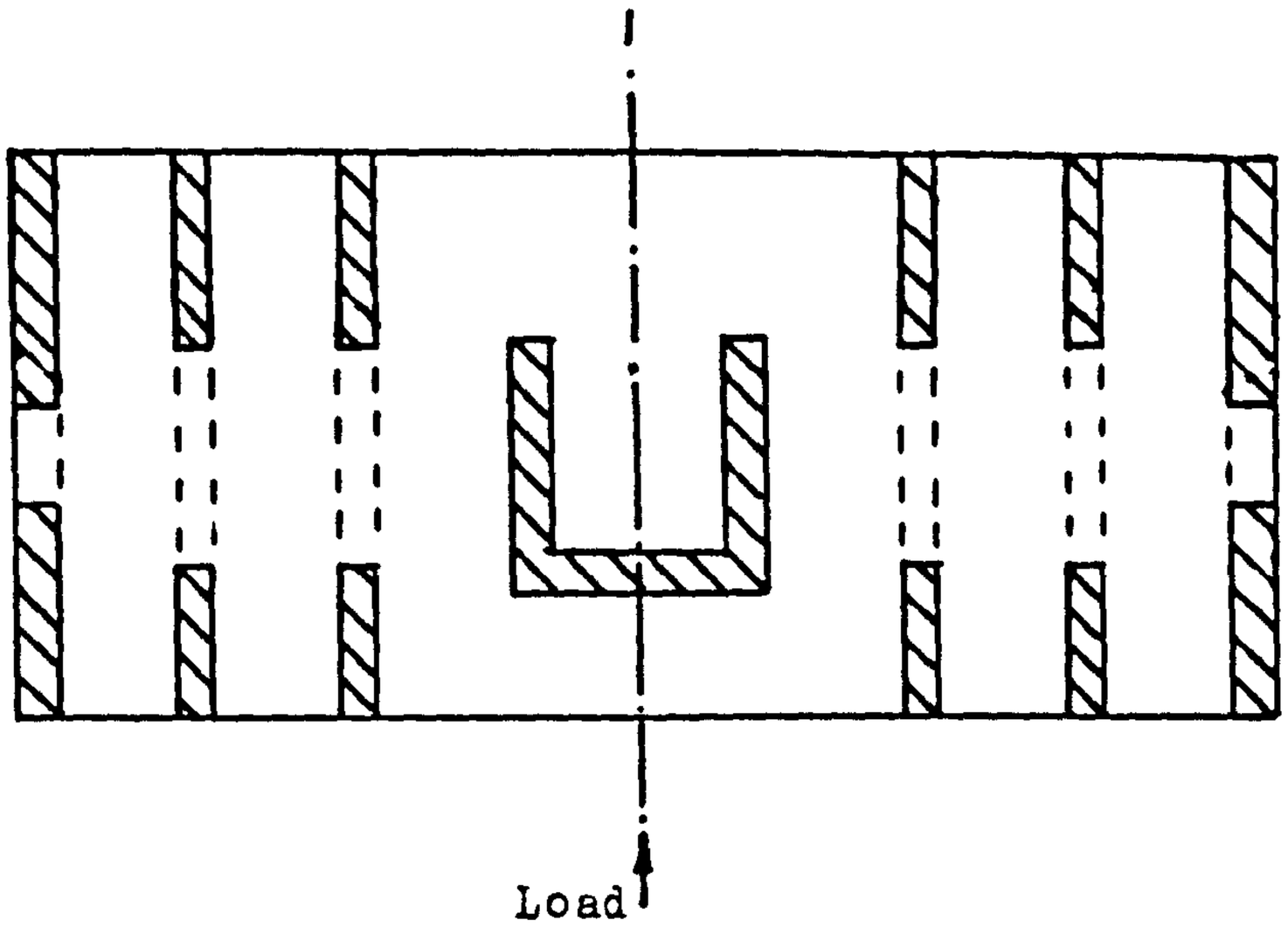

a) Symmetrical structure consisting of two sets of identical coupled shear walls and core

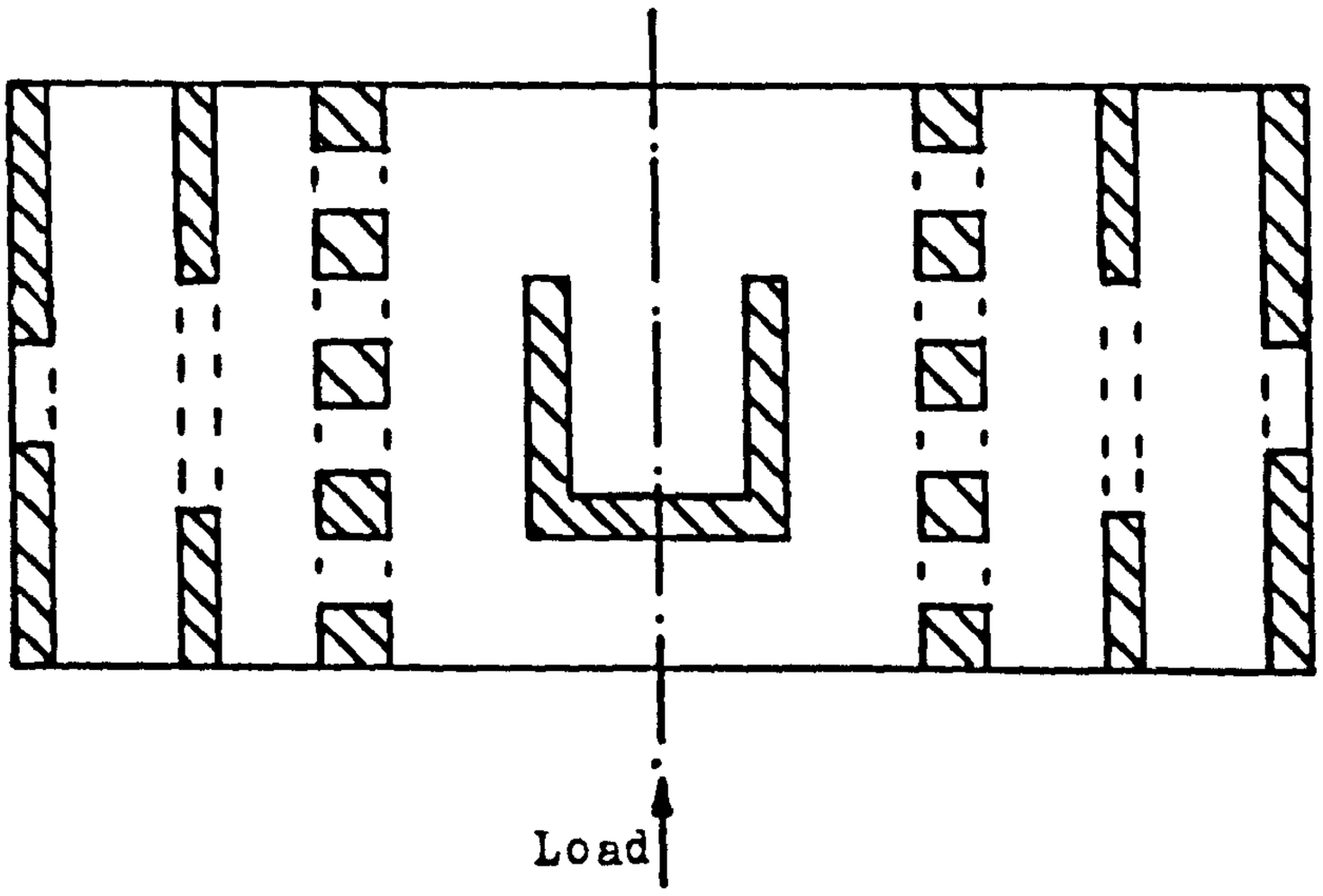

b) Symmetrical structure consisting of two sets of identical coupled shearwalls, core and rigidly-jointed frames

Fig. 4.1

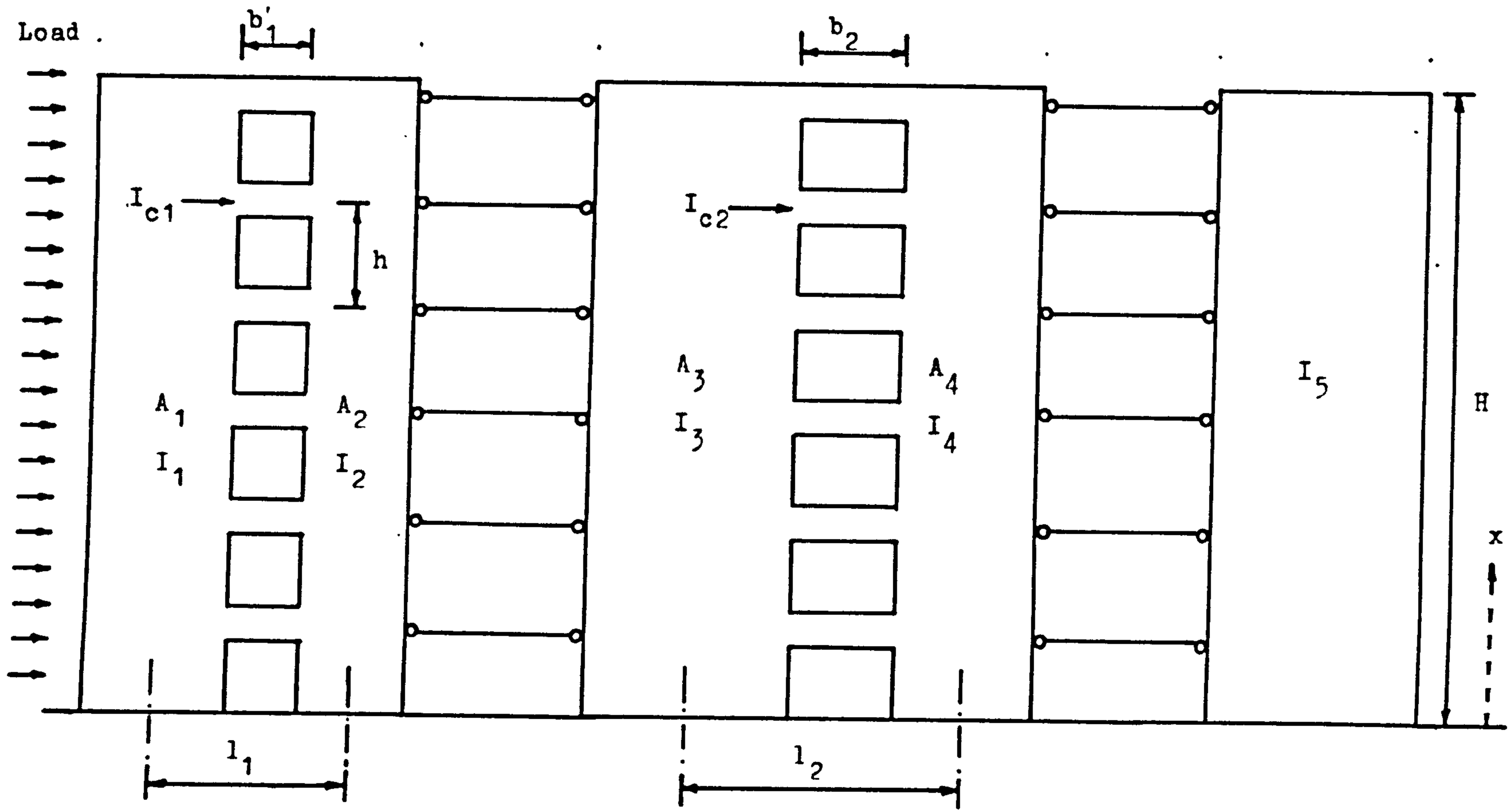

Fig. 4.2 Equivalent plane structure for Fig. 4.1(a)

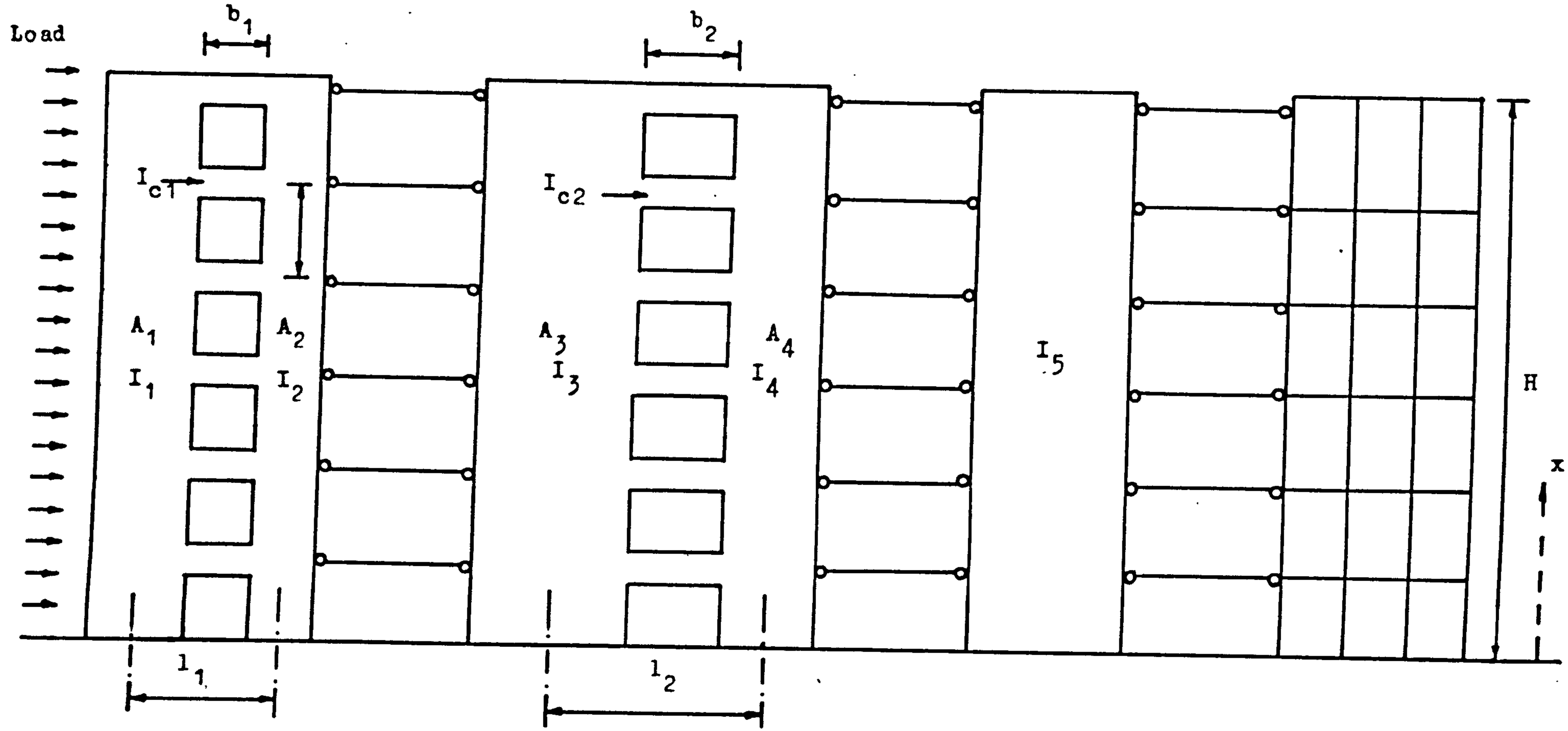

Fig. 4.3 Equivalent plane structure for Fig. 4. 1(b)

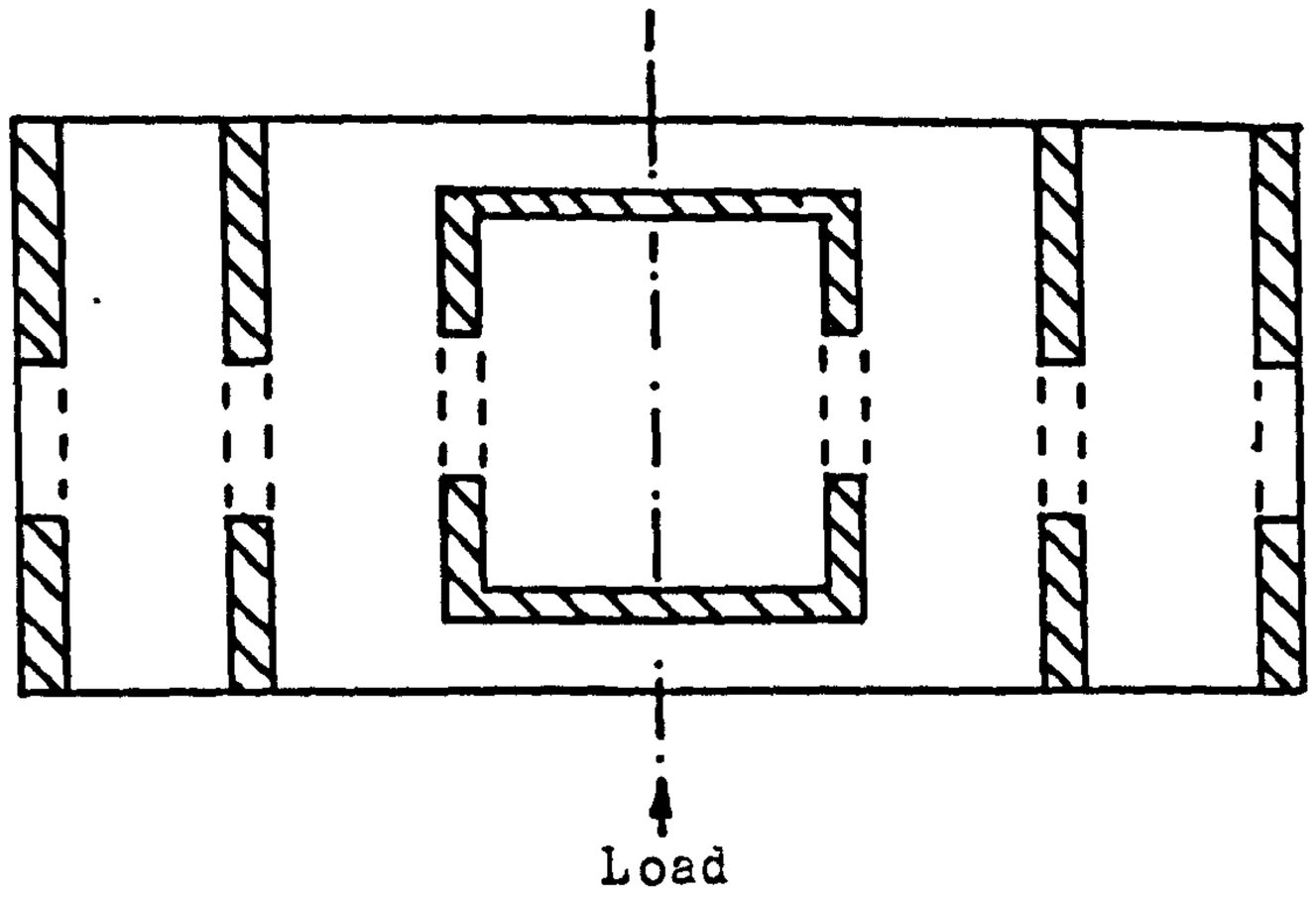

a) Symmetrical structure consisting of two sets of identical coupled shear walls

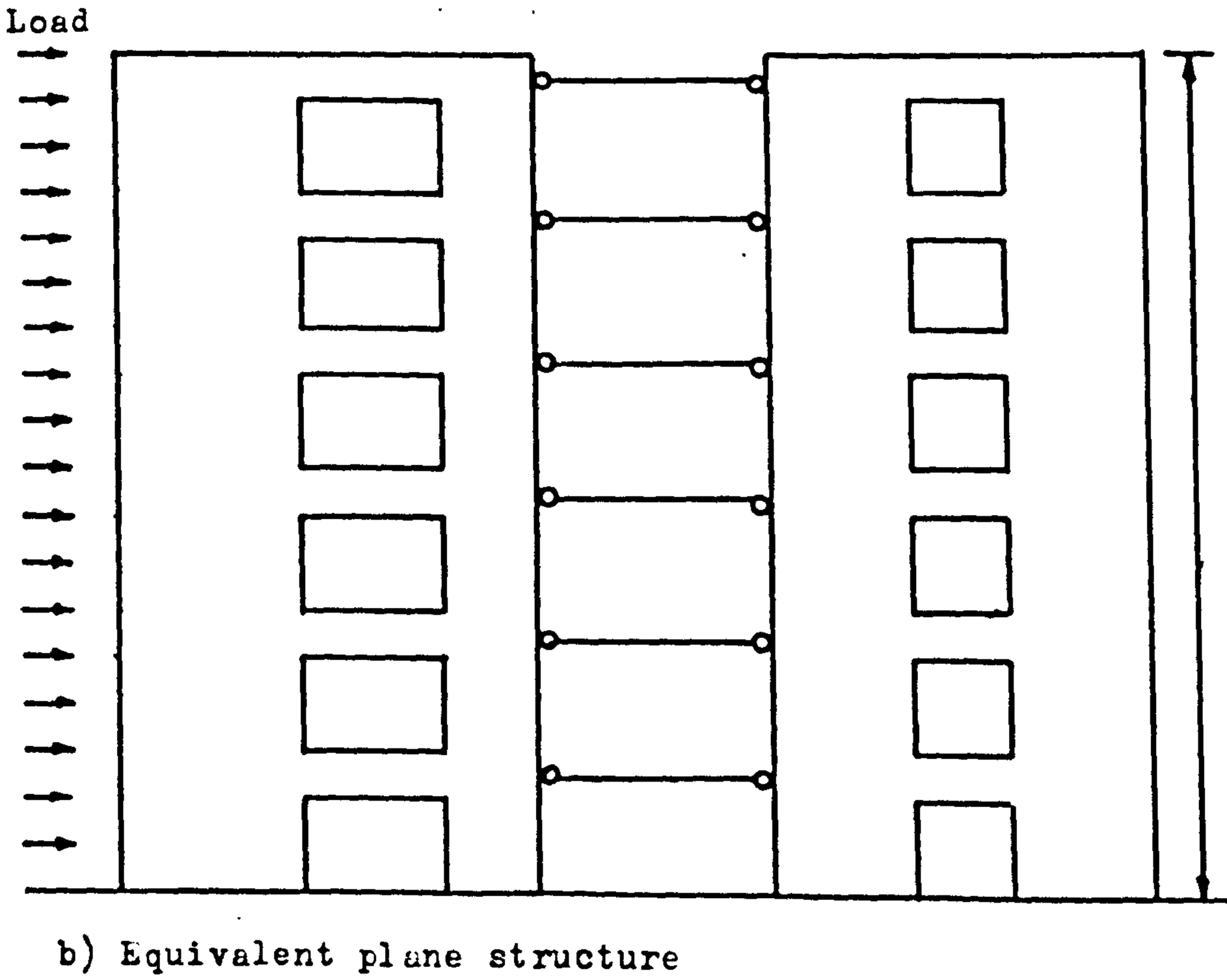

b) Equivalent plane structure

Fig. 4.4

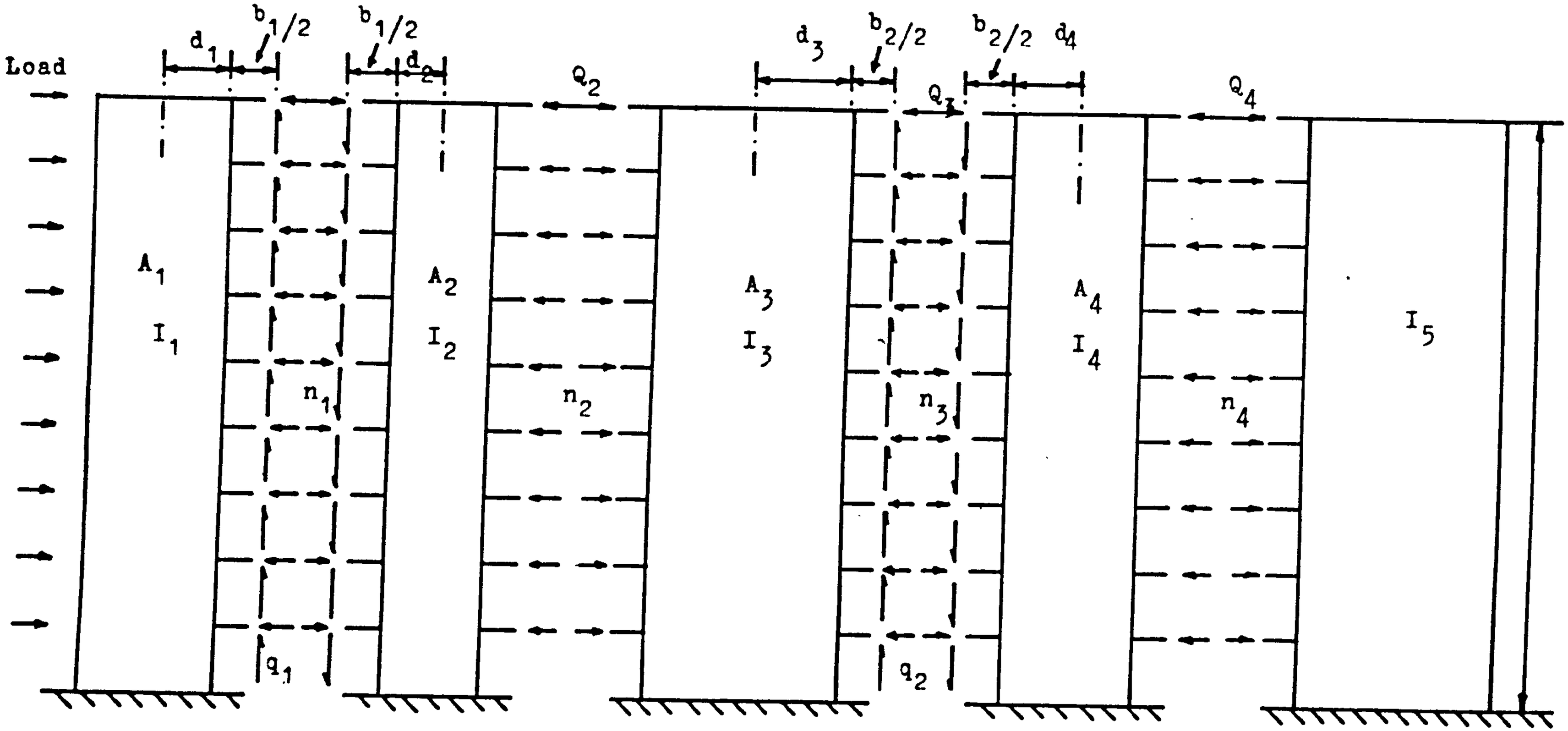

Fig. 4.5 Substitute Structure

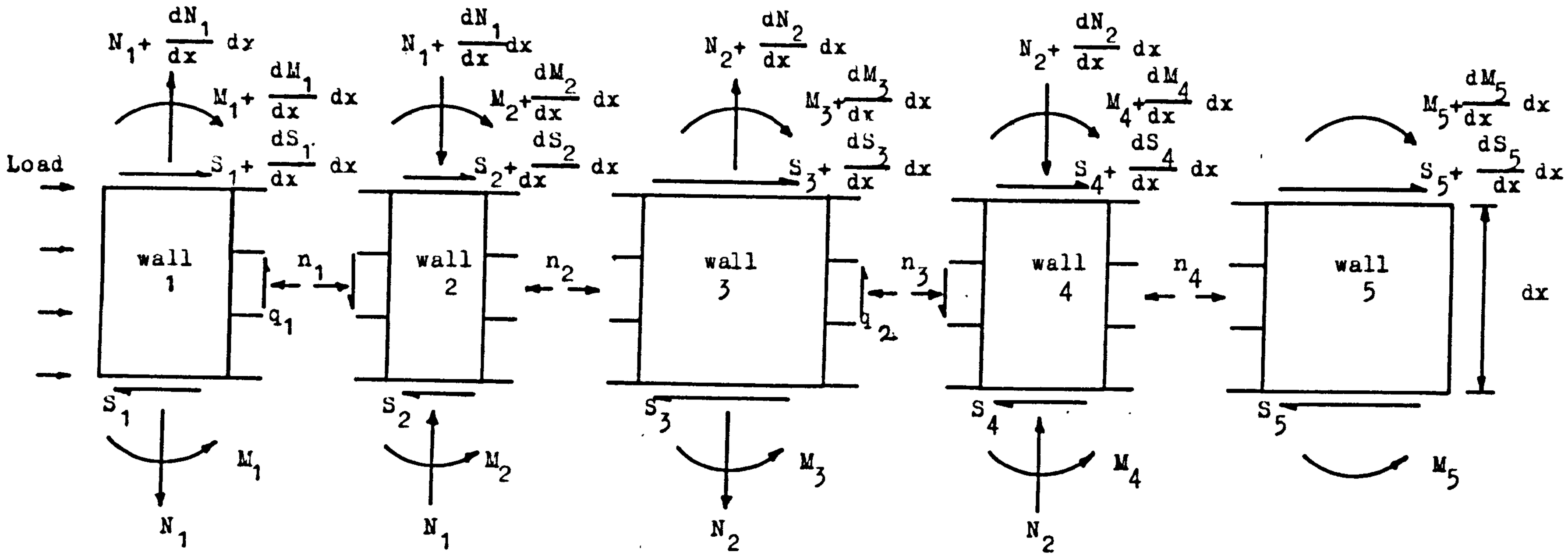

Fig. 4.6 Forces on element of substitute equivalent plane structure

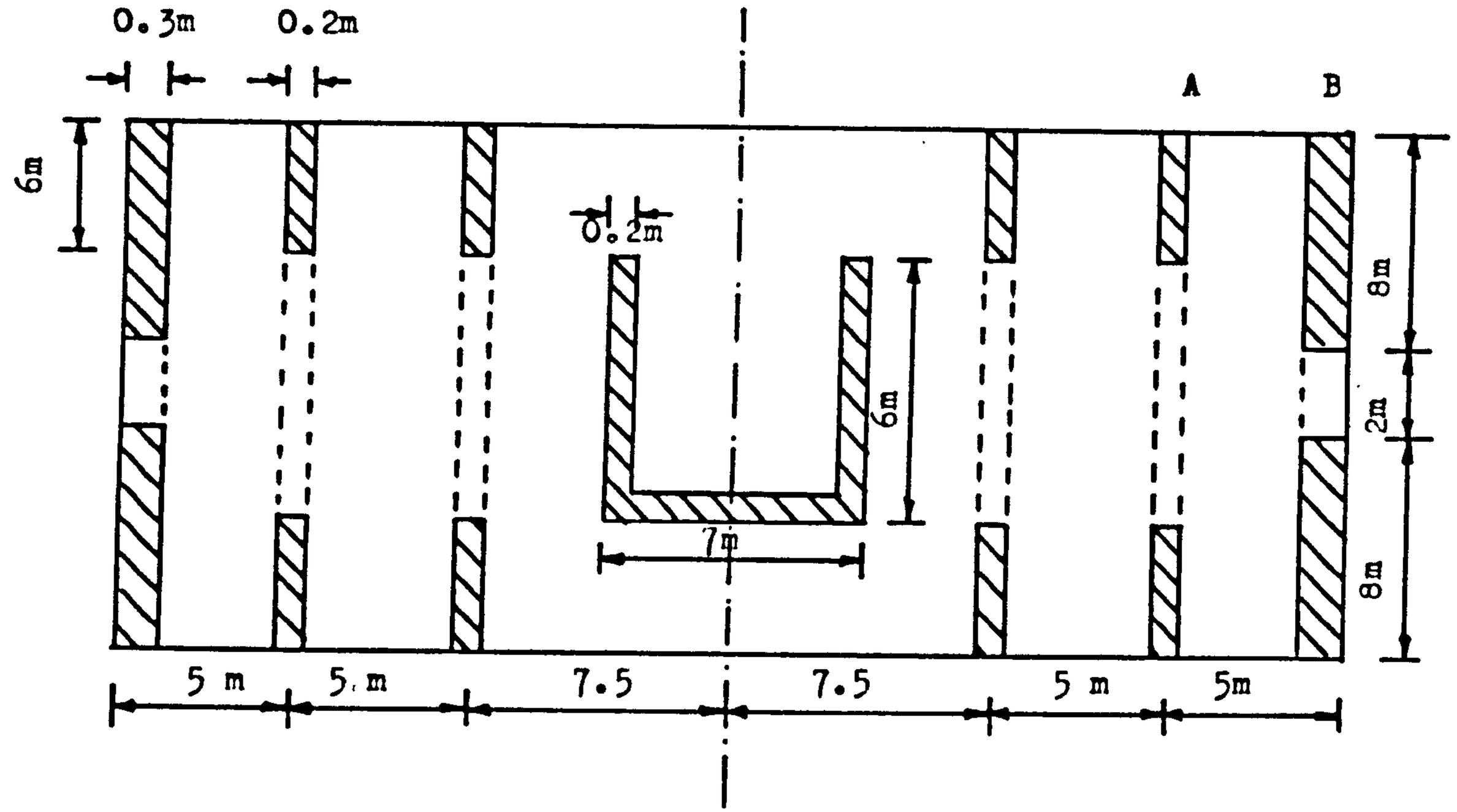

Fig. 4.7 Planform of structure for numerical example

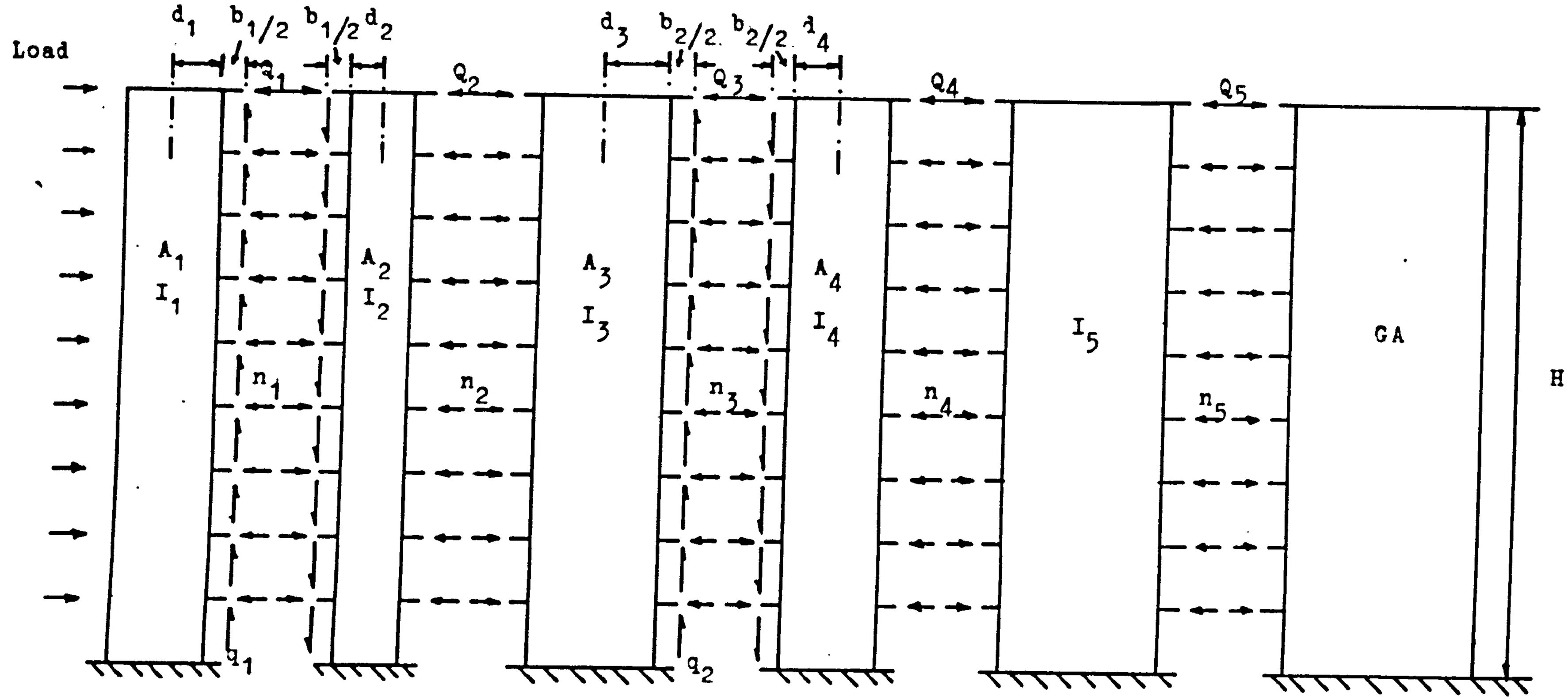

Fig. 4.8 Substitute Structure

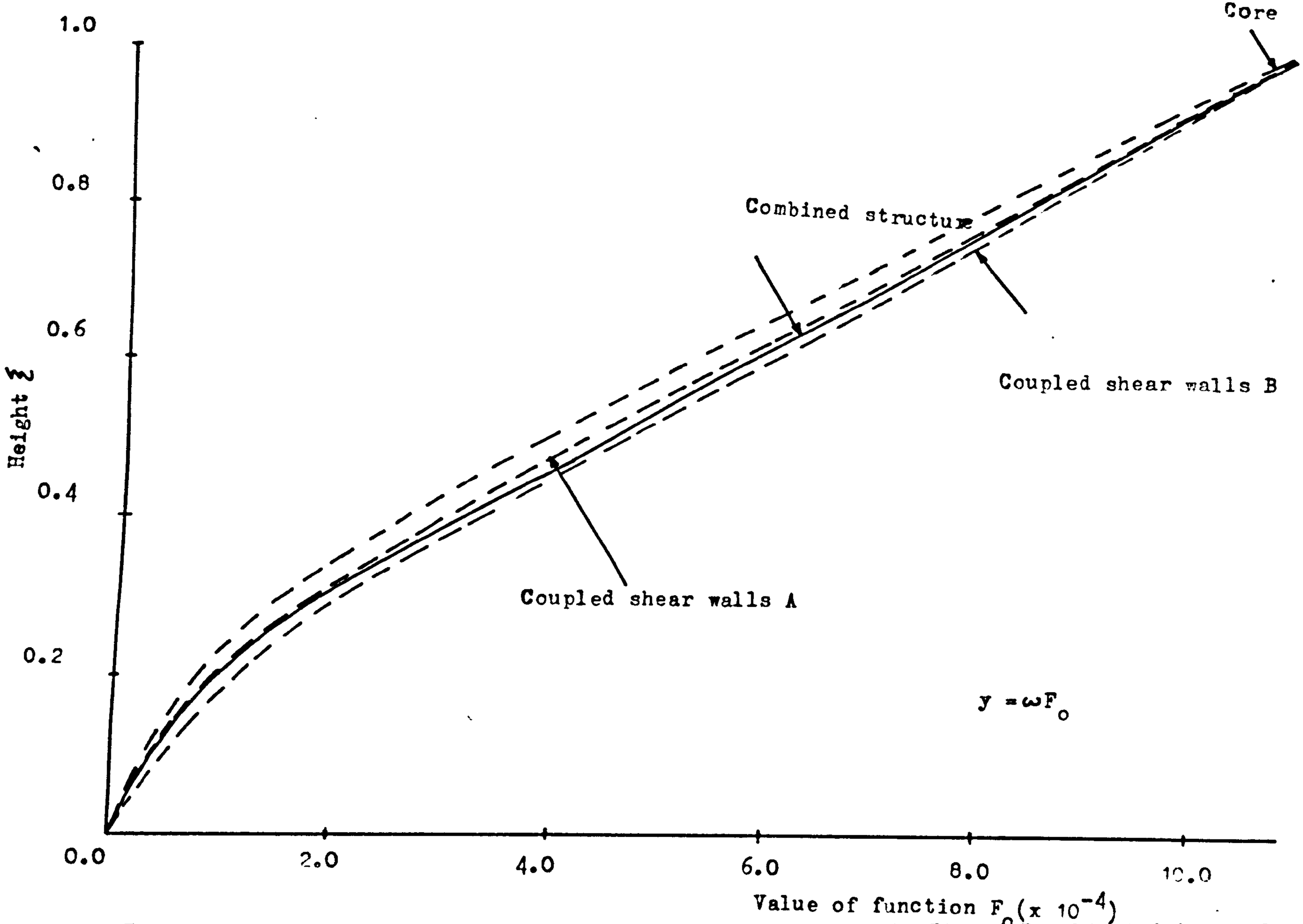

Fig. 4.9 Lateral deflection profiles of structure shown in Fig. 4.7 subjected to uniformly distributed loads which produce equal deflections at the top.

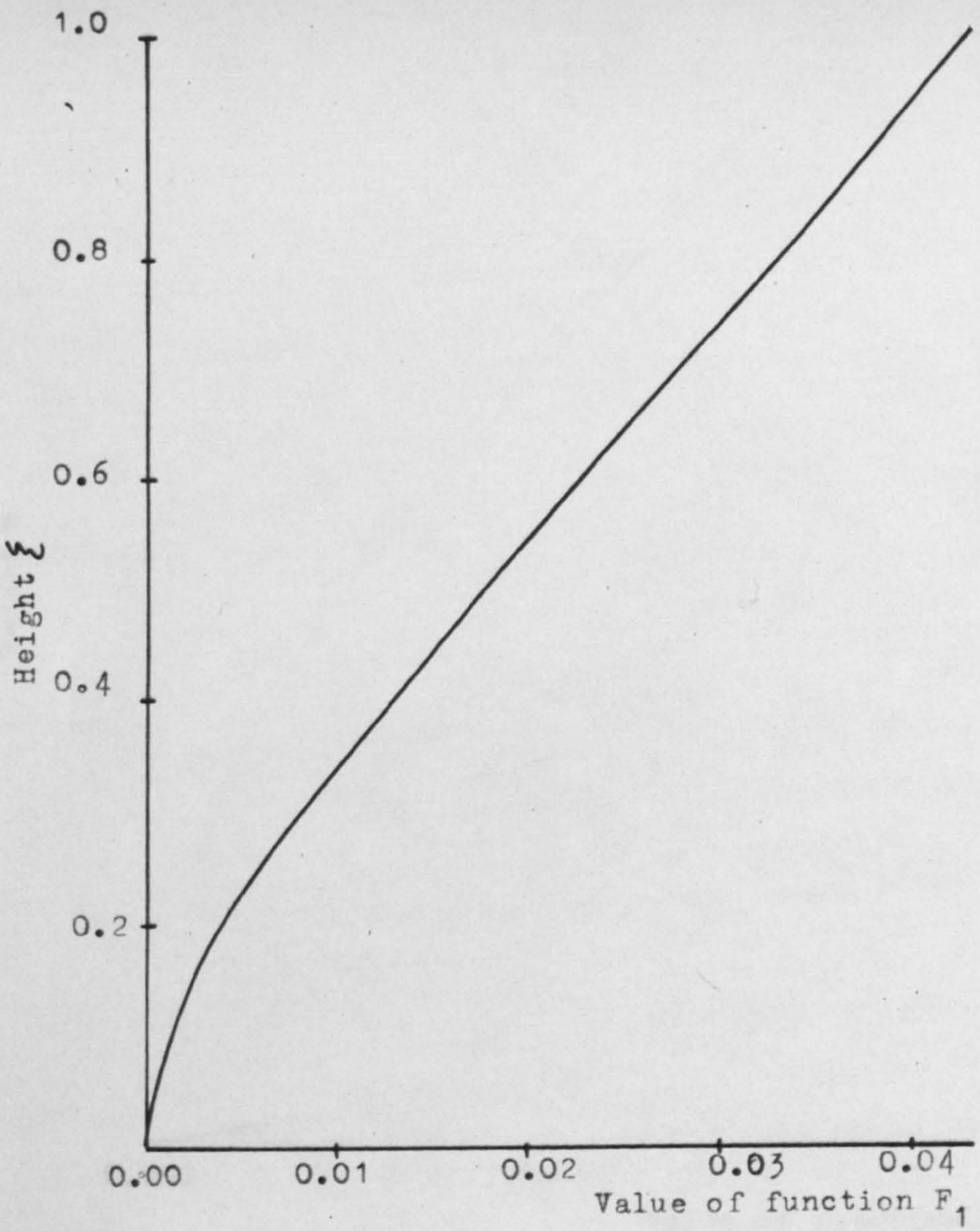

Fig. 4.10 Distribution of lateral deflection

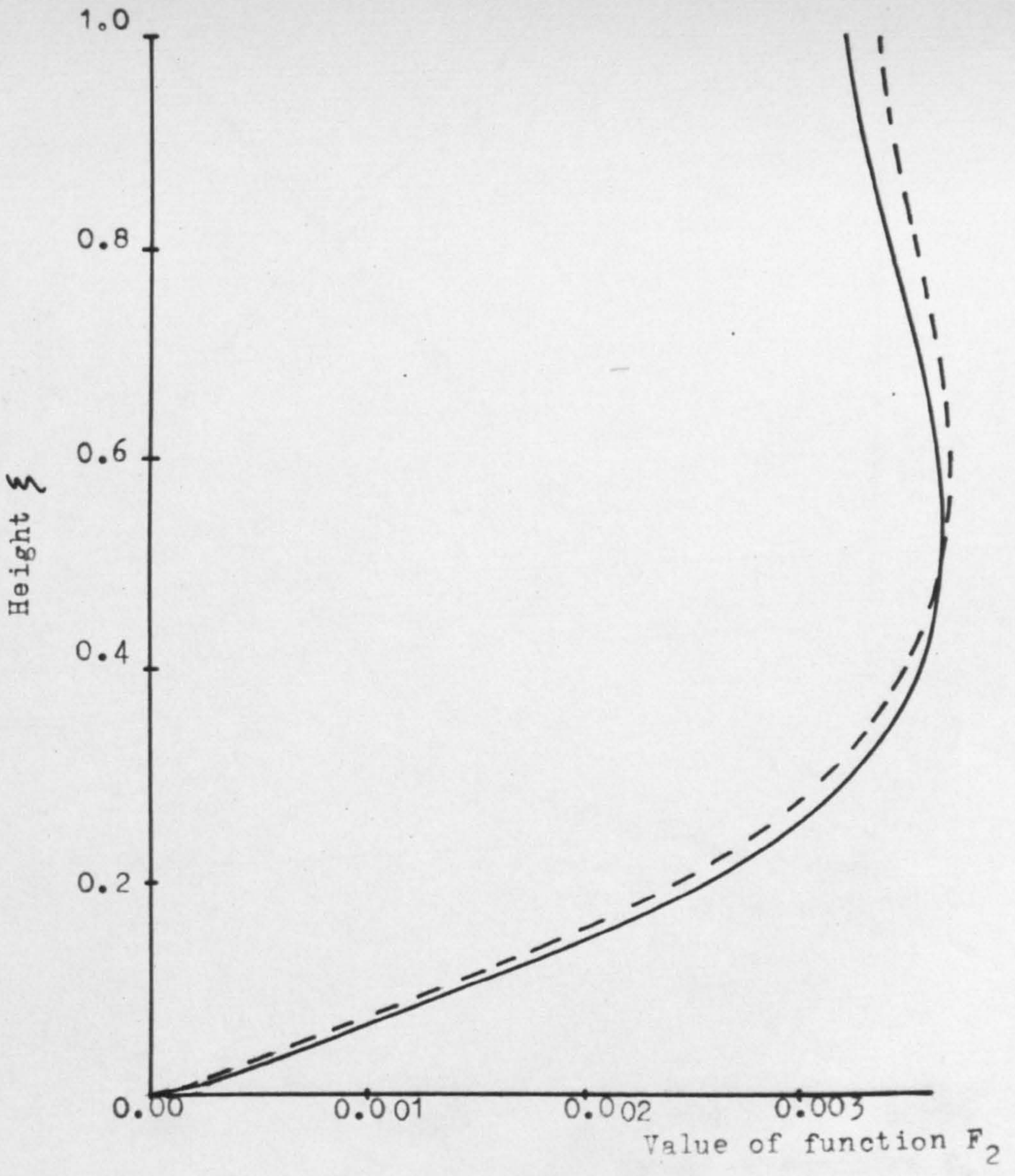

Fig. 4.11 Distribution of shear flow in connecting medium (set of coupled walls A)

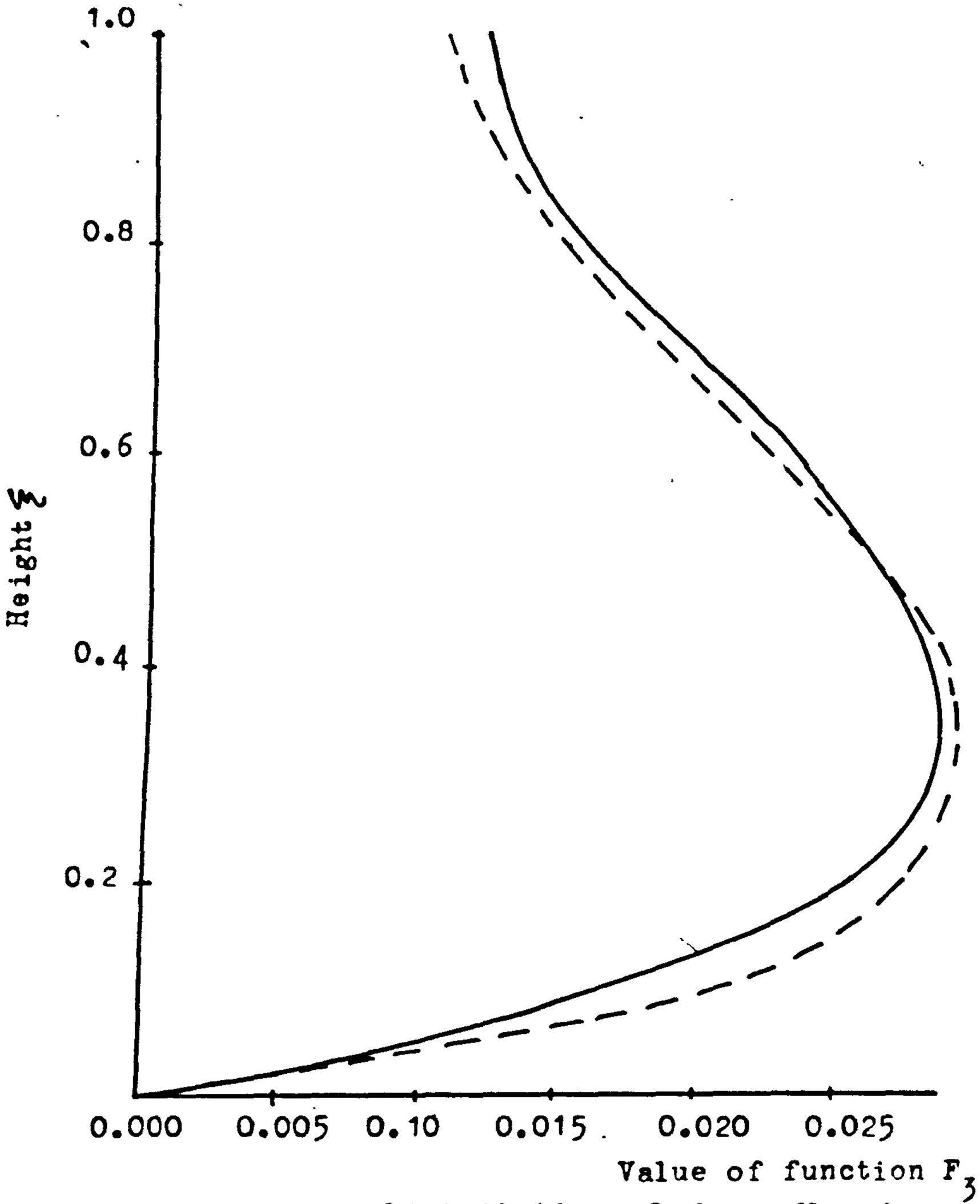

Fig. 4.12 Distribution of shear flow in connecting medium (set of coupled walls B)

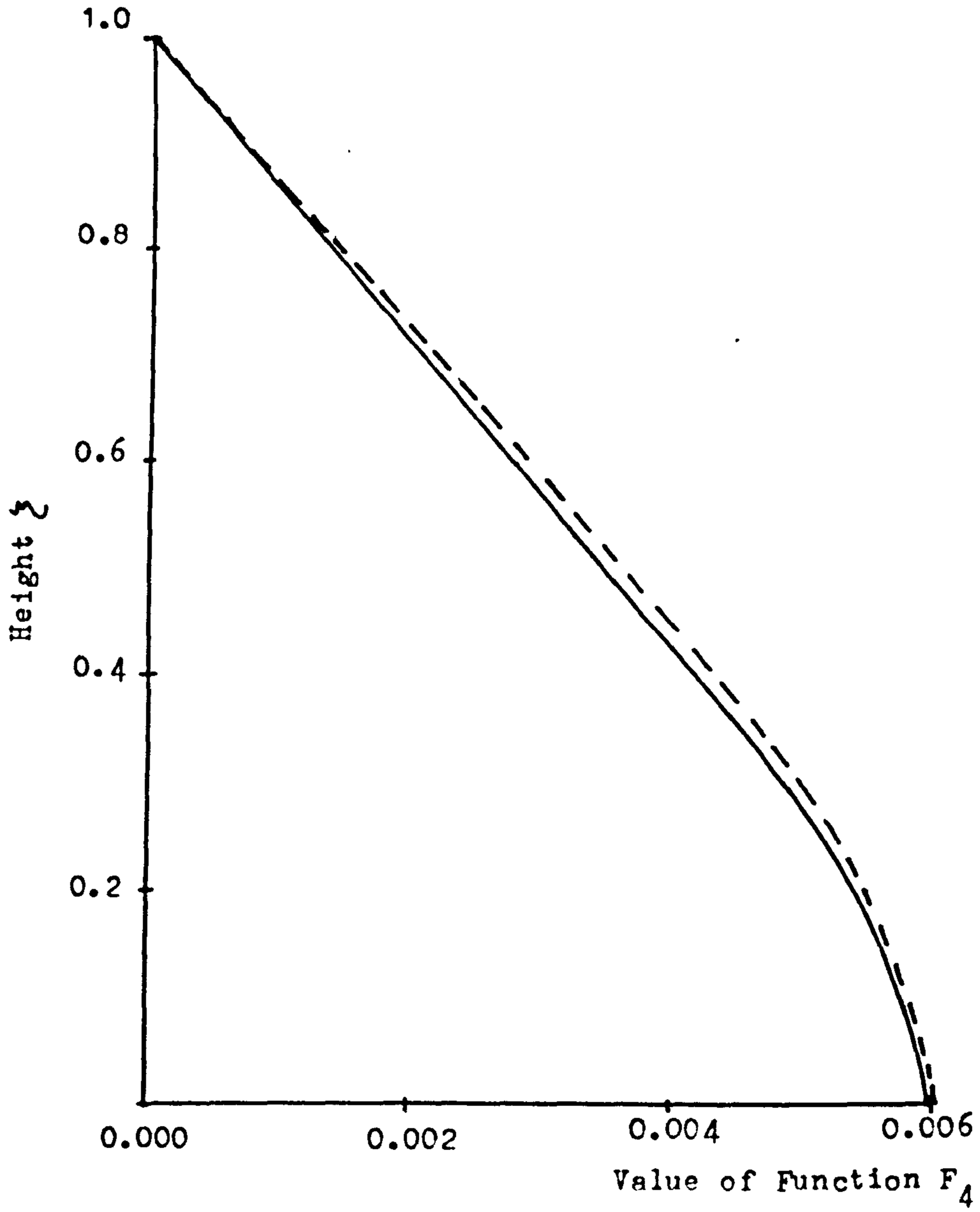

Fig. 4.13 Distribution of oxial force in set of coupled shear walls A

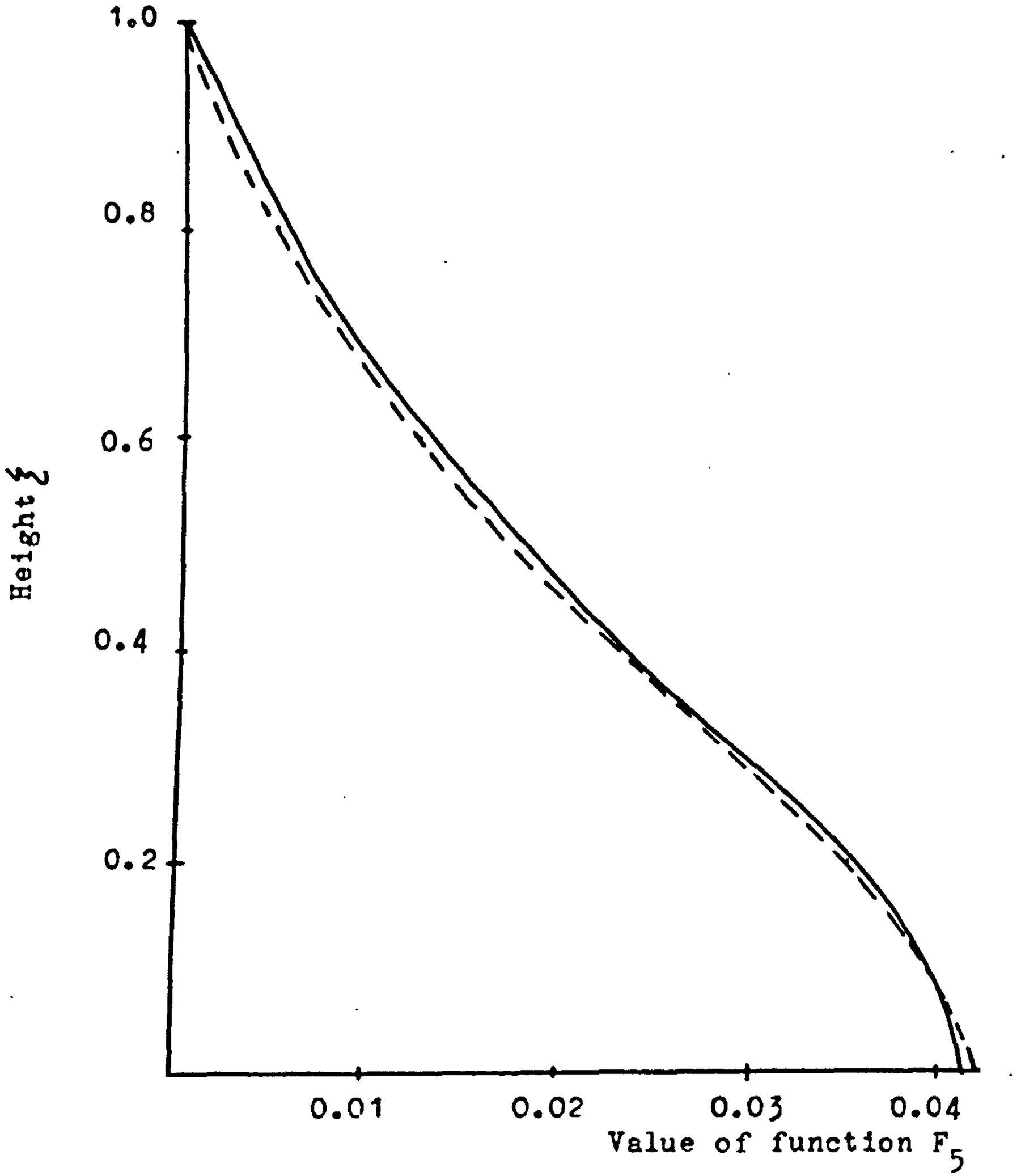

Fig. 4.14 Distribution of axial force in set of coupled shear walls B.

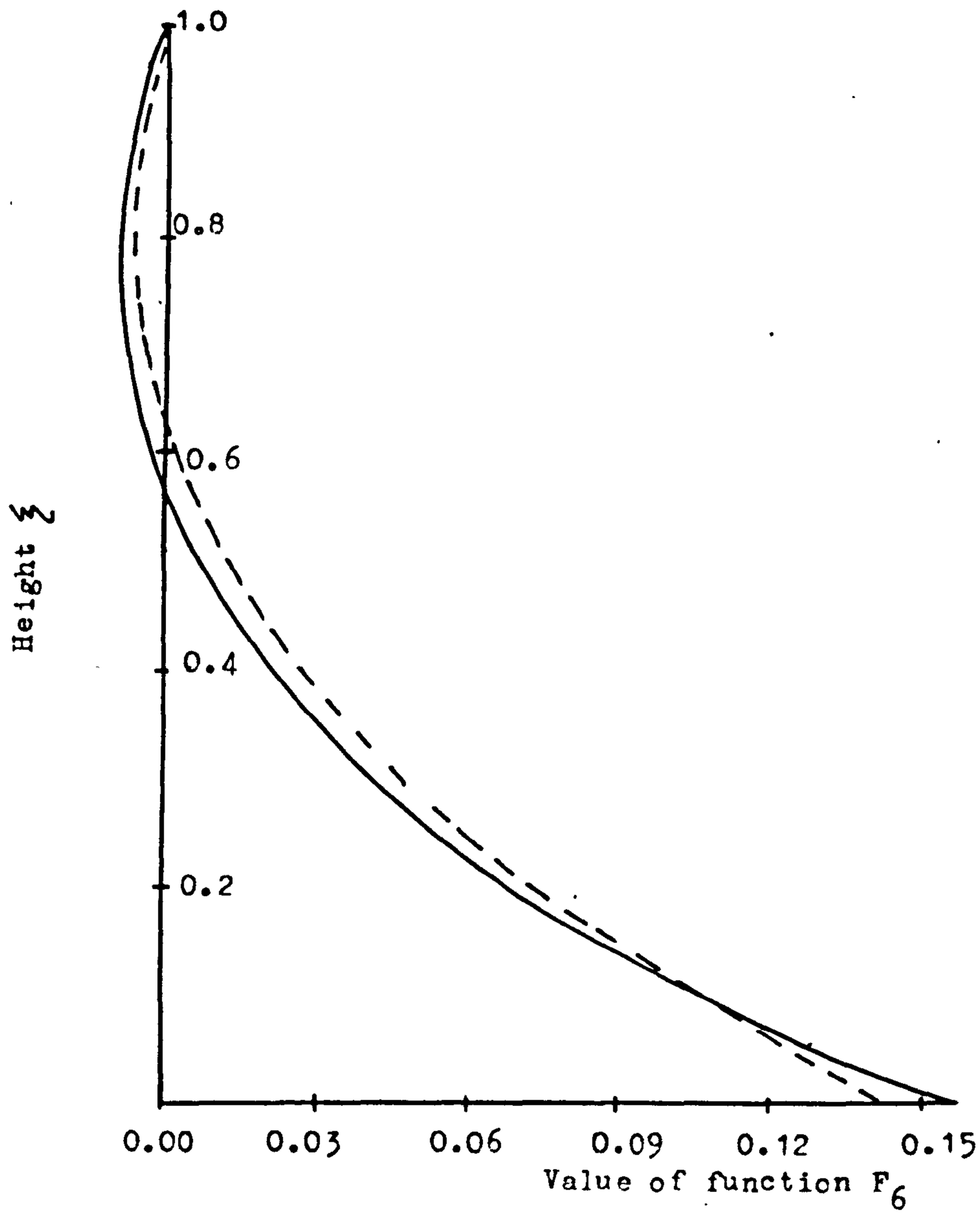

Fig. 4.15 Distribution of total moment in set of coupled shear walls A.

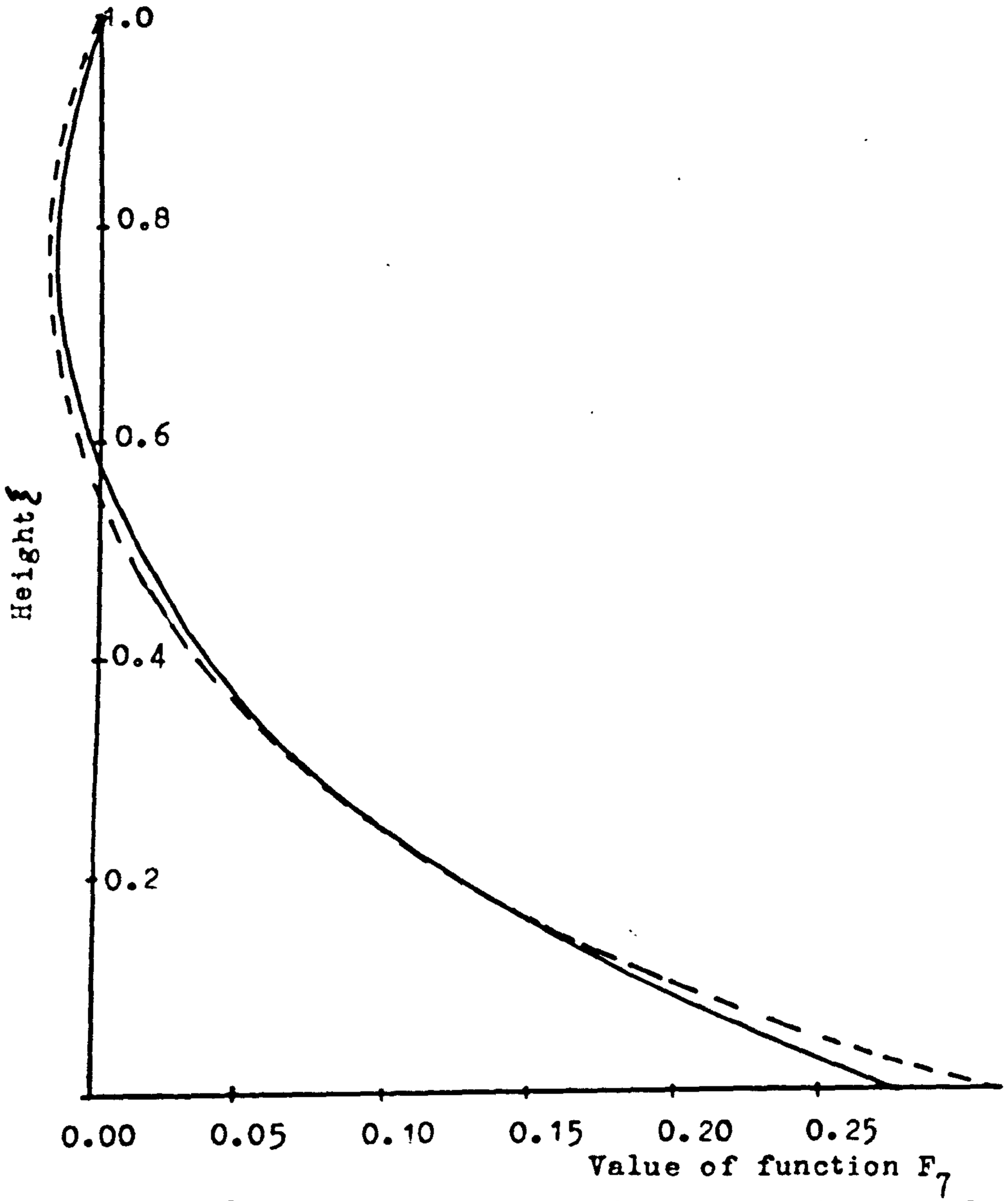

Fig. 4.16 Distribution of total moment in set of coupled shear walls B.

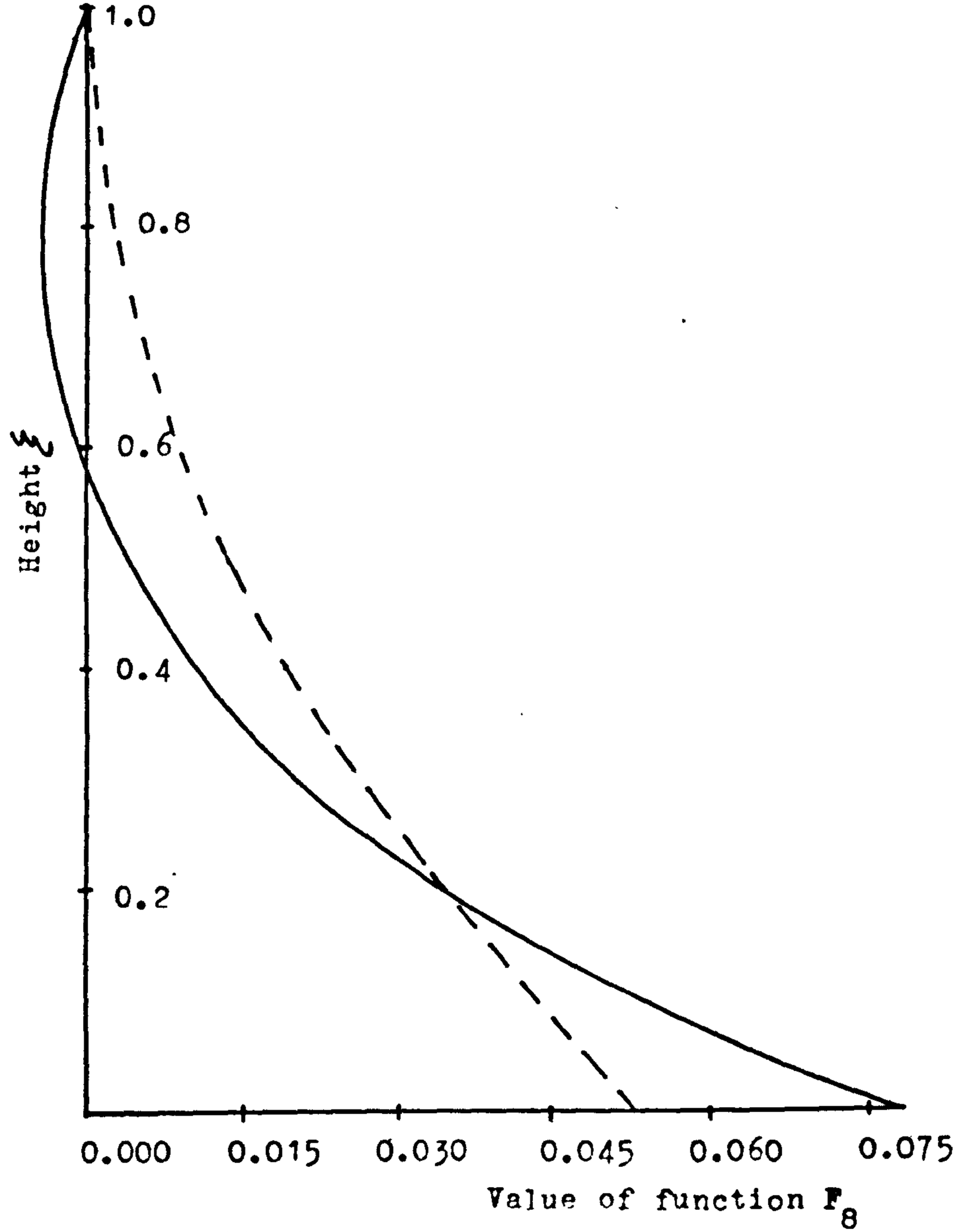

Fig. 4.17 Distribution of total moment in core

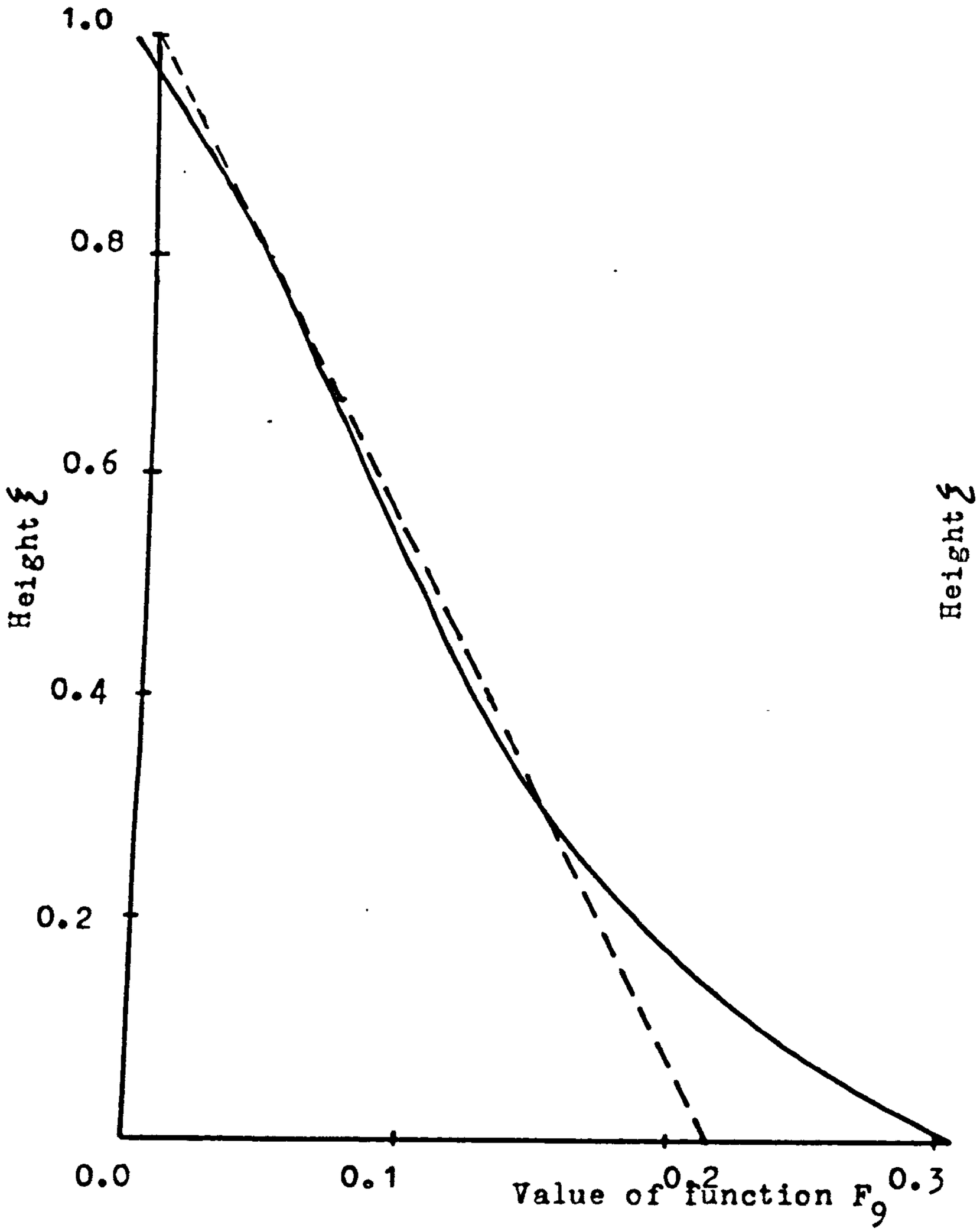

Fig. 4.18 Distribution of total shear force in set of coupled shear walls A

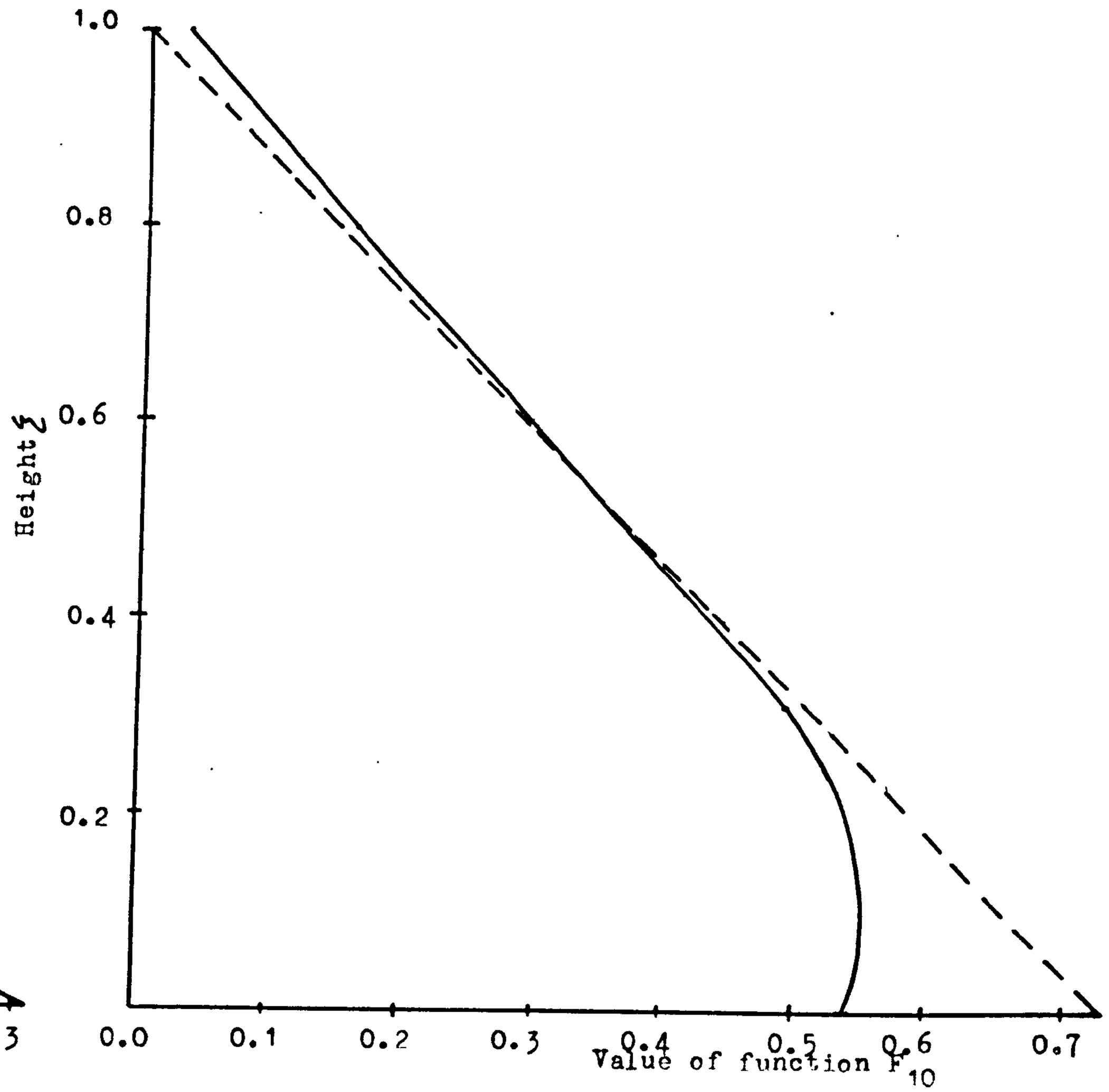

Fig. 4.19 Distribution of total shear force in set of coupled shear walls B.

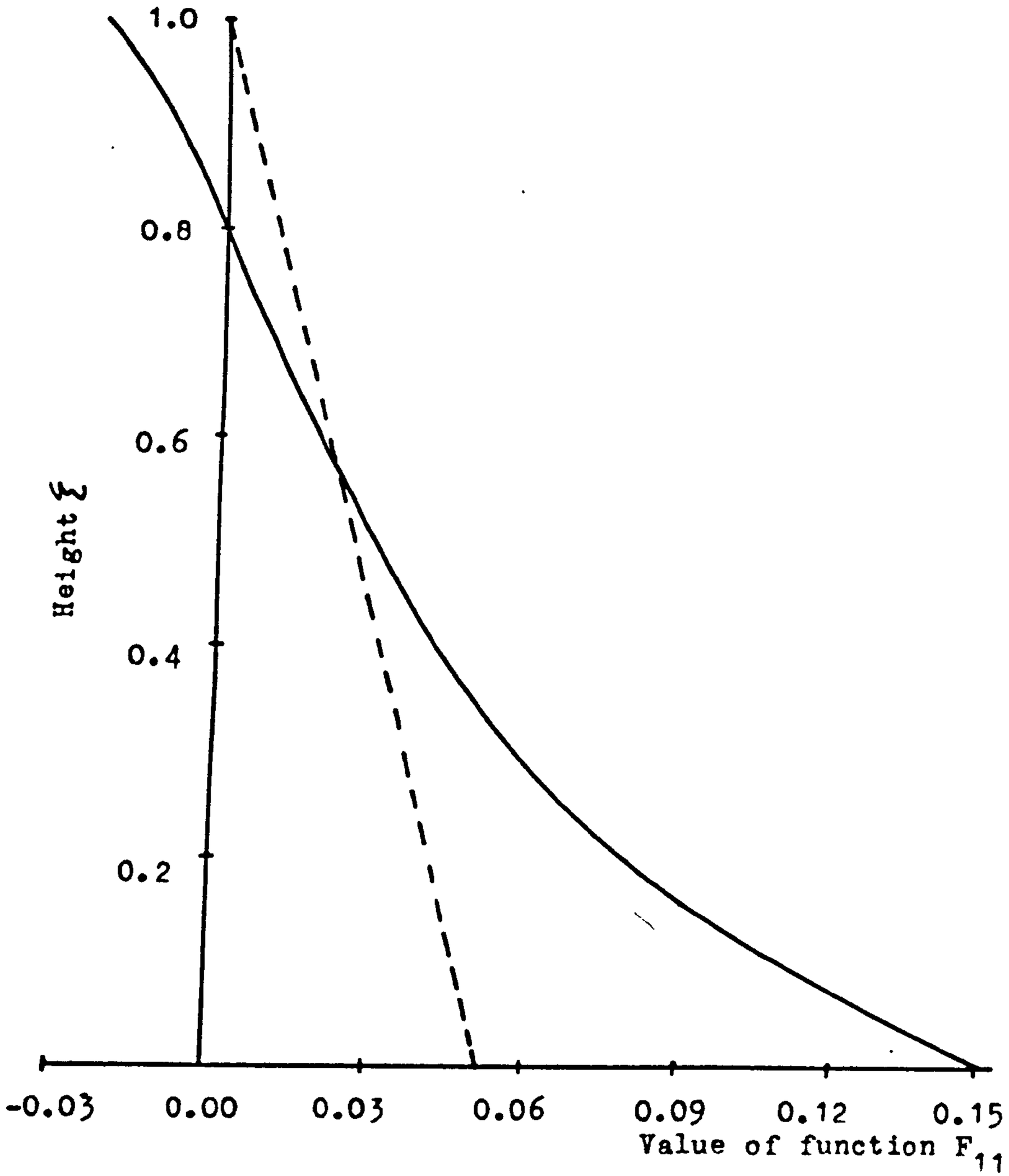

Fig. 4.20 Distribution of total shear force in core

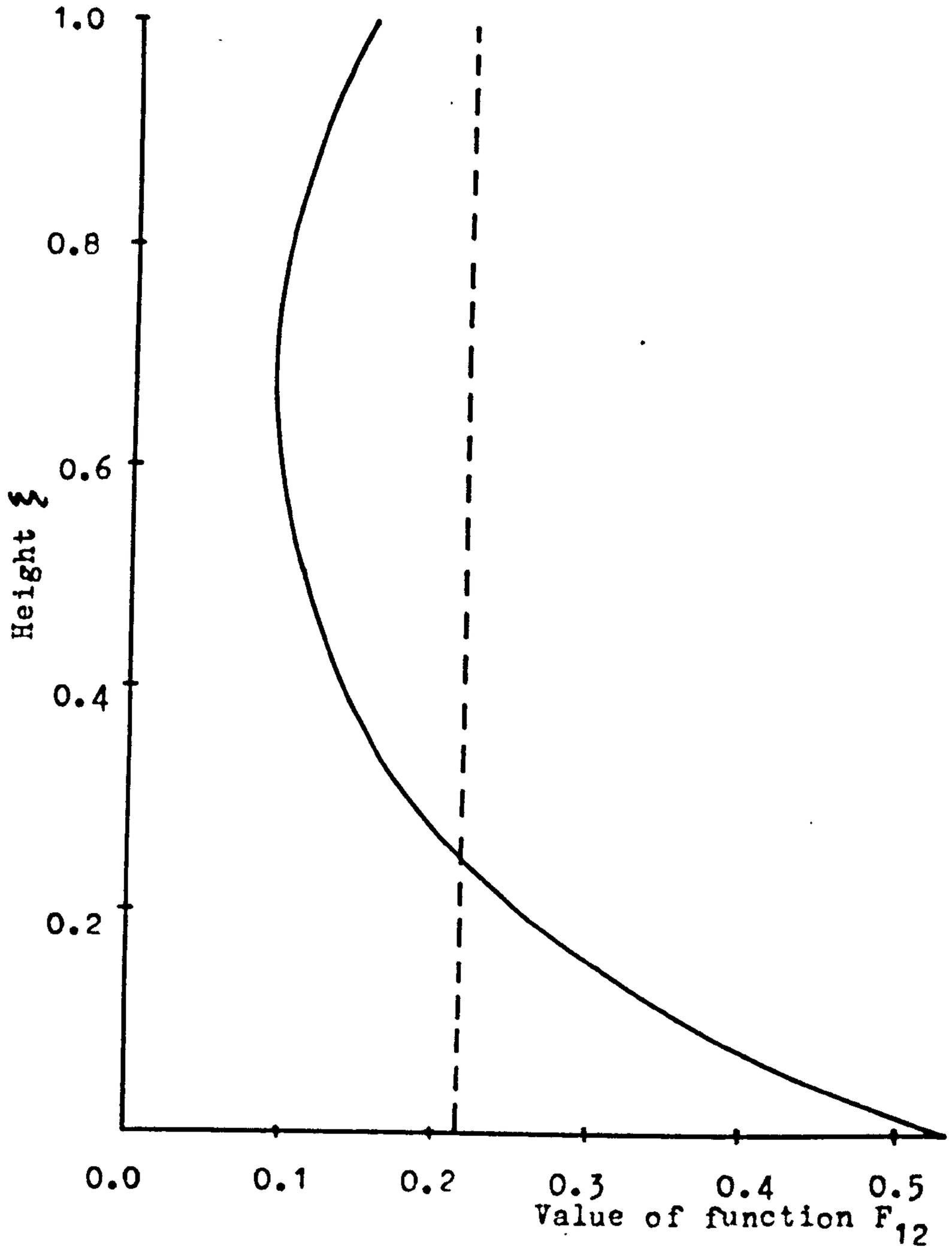

Fig. 4.21 Distribution of lateral forces in set of coupled shear walls A

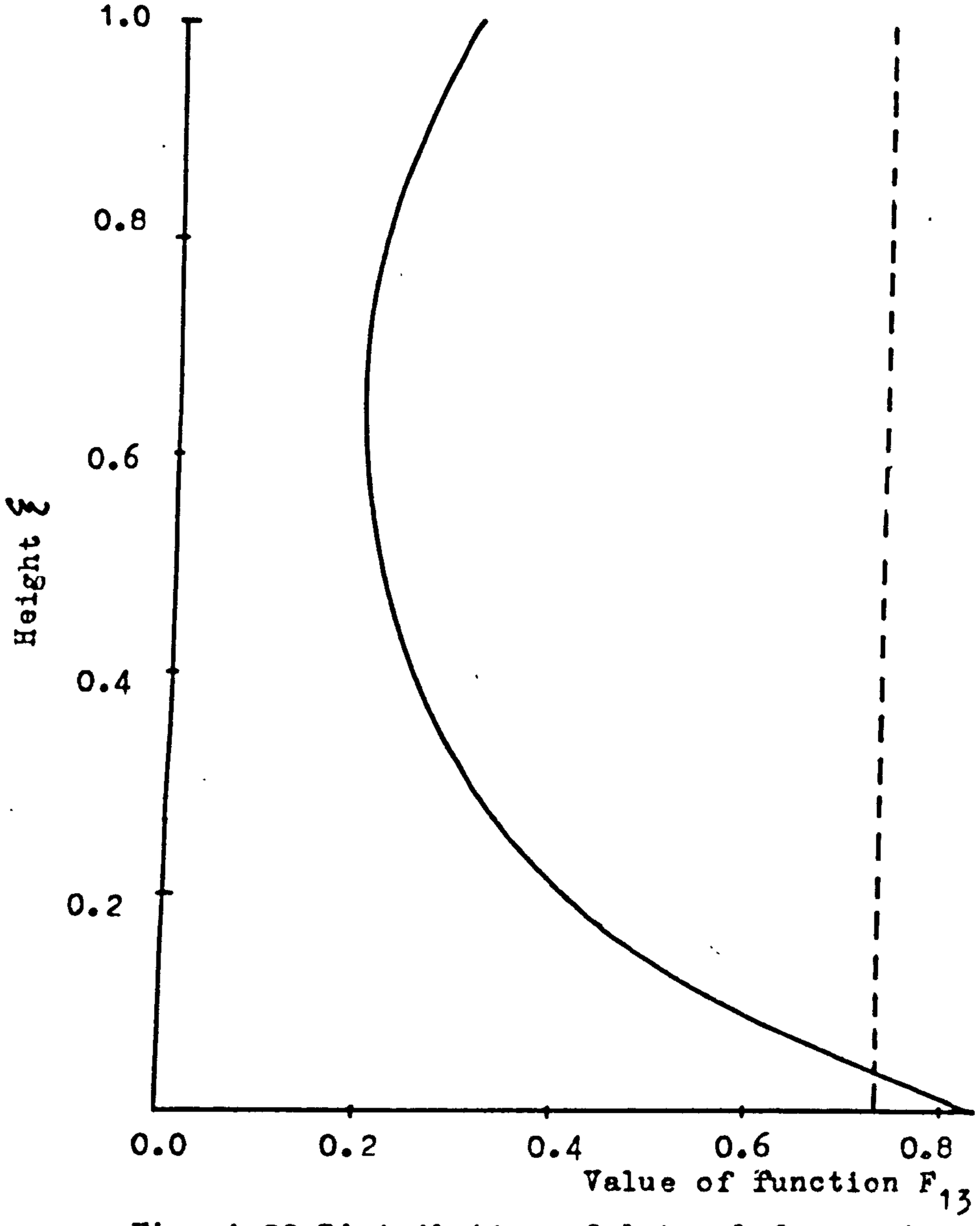

Fig. 4.22 Distribution of lateral forces in set of coupled shear walls B

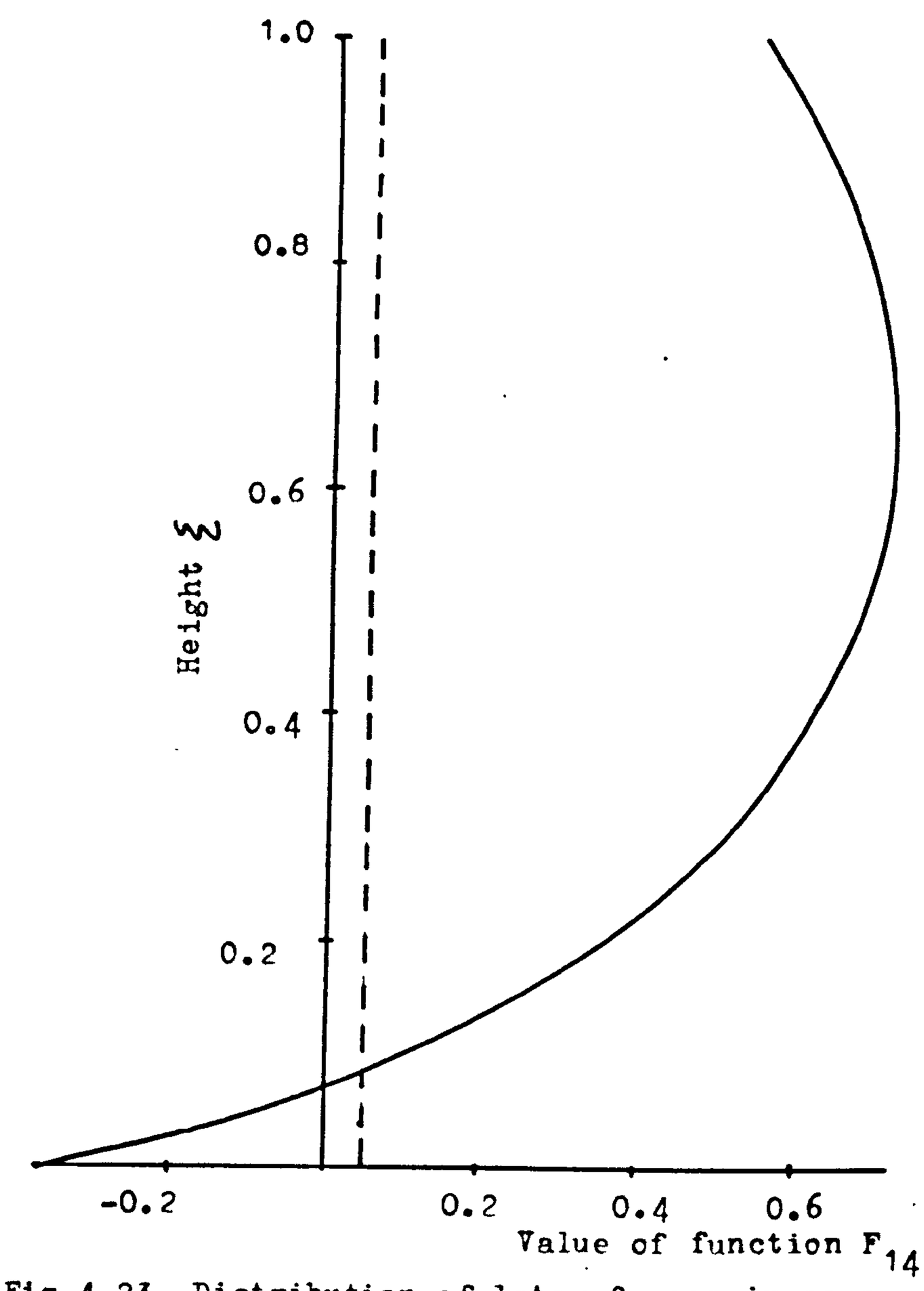

Fig.4.23 Distribution of later forces in core

C H A P T E R 5

ANALYSIS OF CORE STRUCTURES SUBJECTED TO TORSION

NOTATION

A_n	cross-sectional area of wall 'n'
B	core breadth
D	core length
E	modulus of elasticity
G	shear modulus
H	overall core height
h	storey height
I_n	second moment of area of wall 'n' about its local axis
I_c	second moment of area of connecting beams
I_w	core warping moment of inertia
GJ	St. Venant torsional rigidity
M_n	in-plane bending moment in wall 'n'
N_n	normal forces in wall 'n'
q_n	vertical shear flow along line n-n
S_n	horizontal shear force in wall 'n'
T	applied torque at any cross-section
T_w	core warping resistance
T_s	St. Venant torsional resistance
t_o	applied distributed torque
l_n	width of wall 'n'
t_n	thickness of wall 'n'
x, y, z	co-ordinate system
U_n	displacement in x-direction of point 'n'
V_n	displacement in y-direction of point 'n'

W_n	displacement in z-direction of point 'n'
α	structural parameter
k	non-dimensional structural parameter (αH)
ζ	non-dimensional height ($^{x}/_{H}$)
β	connecting medium stiffness constant

C H A P T E R 5

ANALYSIS OF CORE STRUCTURES SUBJECTED TO TORSION

5.1 Introduction

The torsion-bending analysis of symmetrical and asymmetrical structures consisting of coupled shear walls, cores, independent walls and frames are the objects of chapters 6 and 7. Hence, at this stage it is necessary to consider the behaviour of core structures when subjected to torsion. In many recent structural forms of tall buildings, the lateral resistance of the structure to wind or earthquake loading is provided entirely or partly by cores containing lift shafts, stair wells and other service ducts. If twisting is insignificant the core can be analysed as an independent shear wall or a coupled shear wall, as described in previous chapters. However, when the core is located asymmetrically in the building or the loading is eccentric the action of wind or earthquake will induce twisting as well as bending deformations. The need for access to lifts and other services grouped within the core requires it to have an open section, such as the commonly used E, U or H shapes. Usually at every floor level the openings are partly closed by connecting beams or floor slabs. As a consequence of its open section, and the low thickness/width and width/height ratios, a core may be classified as a thin-walled beam. When subjected to torsion, such a member tends to warp as well as bend as shown in Fig. 5.1.

Hence, torsion gives rise not only to the usual St. Venant shear stresses, but also to a system of vertical axial stresses caused by the constraints which prevent free warping of the cross-section. The latter stresses, although usually neglected,may be of such a magnitude as to merit consideration in the design.

The torsional behaviour of perforated core structures subjected to applied torques have been studied by many investigators (eg. (24-26)) and solutions have generally been based on Vlasov's theory of thin-walled beams, in conjunction with a continuous representation, or a stiffness matrix formulation of the connecting lintel beams. So far, hand methods of analysis have been devised for singly and doubly-symmetric open-section walls and computer methods for more complex arrangements. A need exists, therefore, for a continuum method of analysis for asymmetrical open-section shear walls with or without connecting beams which may be used in the appropriate analysis.

In this chapter, a method has been presented for the analysis of asymmetrical and hence, singly symmetrical core structures in tall buildings. The analysis has been achieved by using folded plate theory in conjunction with the continuum technique. In the analysis, the rotation deformation of the structure is used as the unknown variable. The method is suitable for hand calculation, using a desk calculator, and is specially useful in allowing the designer to proportion

members and components at the start of the design process.

5.2 Assumptions

Consider the typical asymmetrical core structure shown in Fig. 5.2(a) subjected to pure torsion.

The following assumptions are made:

(i) The perforated core has uniform sectional properties and dimensions throughout the height of the building and is rigidly fixed at the base.

(ii) Diaphragm action of the floors is assumed, so that the whole structural assembly moves as a rigid body in each horizontal plane.

(iii) The perforated core consists of assemblies of slender vertical plate elements, continuously connected at the corners, undergoing in-plane deformations only.

(iv) The discrete set of connecting beams, of flexural rigidity EI_c at each floor are replaced by an equivalent continuous connecting medium of flexural rigidity $^{EI}c/h$ per unit height.

(v) The walls adjacent to the connecting beams deflect equally in the horizontal plane. Hence, the mid-span positions of the connecting beams are assumed to be points of contraflexue.

(vi) Under the action of the applied twisting moments, the core rotates about a fixed vertical axis Ox through the shear centre of the cross-section (origin O), Fig. 5.2(b).

5.3 Analysis of Asymmetrical core structures

Consider the asymmetrical core structure of Fig. 5.2, where the origin O is assumed to coincide with the shear centre. During twisting, different points on the cross-section suffer different vertical displacements, thus cross-sections which are initially plane are deformed out-of-plane, as shown in Fig. 5.1(b). If this distortion, or 'warping', is constrained at any section, longitudinal stresses parallel to the axis Ox are induced in the core. Hence, the rigid body rotation about the axis Ox will consist of three displacements, V and W in the y and z directions respectively, and angular rotation Θ as shown in Fig. 5.2(b).

The locations of the shear centres for channel cross-sectional shapes are given by Galambos [41]. The position of the shear centre has been determined as if the core was an open-section beam. This is based on the assumption that the connecting beams are shallow lintel beams or floor slabs and the portion in which the horizontal shear will flow is relatively small. However, analyses have been presented which consider the inclusion of connecting beams and the shear deformations of core panels [42,43] which could be

used if required.

Displacements

Consider the displacements of the core structure (Fig.5.2) with its beams cut at their mid-points 1. Since the cross-section of the core structure is restrained in its own plane by the rigid floor slabs, it rotates about the shear centre O. Therefore, a small rotation about the vertical axis Ox yields the following displacements of the significant points (1-5) and centroid of the core (Fig. 5.2(b)), where second order terms in θ are neglected.

$$
\begin{aligned}
W_1 &= W_2 = W_5 = -(e + B)\theta \\
W_3 &= W_4 = -e\theta \\
V_2 &= V_3 = (n-f)\theta \\
V_4 &= V_5 = -(m + f)\theta \\
W_c &= -(e + L)\theta \\
V_c &= -f\theta
\end{aligned}
\qquad (5.1)
$$

where the displacements V and W are in the y and z directions respectively.

Equilibrium conditions

A consideration of the conditions of equilibrium of a small vertical element of each of the five constituent panels, yields the following relationships (Fig. 5.3(a))

For panel 1

$$\frac{dN_1}{dx} + q_1 + q_2 = o$$

$$S_1 = -\left[\frac{dM_1}{dx} - \left(\frac{a+d}{2}\right) q_1 + \frac{d}{2} q_2\right] \qquad (5.2)$$

For panel 2

$$\frac{dN_2}{dx} - q_2 + q_3 = o$$

$$S_2 = -\left[\frac{dM_2}{dx} + (q_2 + q_3) \frac{B}{2}\right] \qquad (5.3)$$

For panel 3

$$\frac{dN_3}{dx} - q_3 + q_4 = o$$

$$S_3 = -\left[\frac{dM_3}{dx} + (q_3 + q_4) \frac{D}{2}\right] \qquad (5.4)$$

For panel 4

$$\frac{dN_4}{dx} - q_4 + q_5 = o$$

$$S_4 = -\left[\frac{dM_4}{dx} + (q_4 + q_5) \frac{B}{2}\right] \qquad (5.5)$$

For panel 5

$$\frac{dN_5}{dx} - q_1 - q_5 = o$$

$$S_5 = -\left[\frac{dM_5}{dx} - \left(\frac{a+c}{2}\right) q_1 + \frac{c}{2} q_5\right] \qquad (5.6)$$

where N_i (i=1-5) and q_i (i=1-5) are the axial forces in panels (1-5) and vertical shear flows at joints (1-5).

Assuming that they behave as relatively slender beams, the moment-curvature relationships for the panels (1-5) become, on using equations (5-1)

$$M_1 = -(e+B)\, EI_1 \frac{d^2\theta}{dx^2}$$

$$M_2 = -(n-f)\, EI_2 \frac{d^2\theta}{dx^2}$$

$$M_3 = e\, EI_3 \frac{d^2\theta}{dx^2} \qquad (5.7)$$

$$M_4 = -(m+f)\, EI_4 \frac{d^2\theta}{dx^2}$$

$$M_5 = -(e+B)\, EI_5 \frac{d^2\theta}{dx^2}$$

where I_i is the appropriate second moment of area for the panel concerned.

Compatibility conditions

The conditions of vertical displacement compatibility between adjacent panels due to bending and axial deformations are,

Along the line of contraflexure 1-1

$$\int_o^x \frac{(a+d)}{2} \frac{M_1}{EI_1} dx + \int_o^x \frac{(a+c)}{2} \frac{M_5}{EI_5} dx - \int_o^x \frac{N_1}{EA_1} dx$$

$$+ \int_o^x \frac{N_5}{EA_5} dx - \frac{1}{\beta E} q_1 = o \qquad (5.8)$$

Along the vertical joint 2-2

$$\int_o^x \frac{(d)}{2} \frac{M_1}{EI_1} dx + \int_o^x \frac{(B)}{2} \frac{M_2}{EI_2} dx + \int_o^x \frac{N_1}{EA_1} dx - \int_o^x \frac{N_2}{EA_2} dx = o \qquad (5.9)$$

Along the vertical joint 3-3

$$\int_o^x \frac{(B)}{2} \frac{M_2}{EI_2} dx + \int_o^x \frac{(D)}{2} \frac{M_3}{EI_3} dx + \int_o^x \frac{N_2}{EA_2} dx - \int_o^x \frac{N_3}{EA_3} dx = 0 \qquad (5.10)$$

Along the vertical joint 4-4

$$\int_o^x \frac{(D)}{2} \frac{M_3}{EI_3} dx + \int_o^x \frac{(B)}{2} \frac{M_4}{EI_4} dx + \int_o^x \frac{N_3}{EA_3} dx - \int_o^x \frac{N_4}{EA_4} dx = 0 \qquad (5.11)$$

Along the vertical joint 5-5

$$\int_o^x \frac{(c)}{2} \frac{M_5}{EI_5} dx + \int_o^x \frac{(B)}{2} \frac{M_4}{EI_4} dx + \int_o^x \frac{N_4}{EA_4} dx - \int_o^x \frac{N_5}{EA_5} dx = 0 \qquad (5.12)$$

The addition of equations (5.8) to (5.12) yields

$$\int_o^x \left(\frac{a}{2} + d\right) \frac{M_1}{EI_1}\,dx + \int_o^x B\,\frac{M_2}{EI_2}\,dx + \int_o^x D\,\frac{M_3}{EI_3}\,dx$$

$$+ \int_o^x B\,\frac{M_4}{EI_4}\,dx + \int_o^x \left(\frac{a}{2} + c\right)\frac{M_5}{EI_5}\,dx - \beta\frac{1}{E}\,q_1 = 0 \qquad (5.13)$$

where $\beta = \frac{12I_c}{a^3h}$, I_c = second moment of area of the connecting beams, a = span of the connecting beams and A_i (i = 1 - 5) are the cross-sectional areas of panels (1-5).

On substituting for the moment functions from equations (5.7) into (5.13), yields

$$q_1 = E\beta P_1 \frac{d\theta}{dx} \qquad (5.14)$$

where $P_1 = 2BD$.

From equations (5.9) to (5.12), the axial forces N_1, N_2, N_3 and N_4 become

$$N_1 = -EA_1\left[\left(\frac{c}{2}\right)\frac{M_5}{EI_5} + B\,\frac{M_4}{EI_4} + D\,\frac{M_3}{EI_3} + B\,\frac{M_2}{EI_2} + \left(\frac{d}{2}\right)\frac{M_1}{EI_1} - \frac{N_5}{EA_5}\right] \qquad (5.15)$$

$$N_2 = -EA_2\left[\left(\frac{c}{2}\right)\frac{M_5}{EI_5} + B\,\frac{M_4}{EI_4} + D\,\frac{M_3}{EI_3} + \left(\frac{B}{2}\right)\frac{M_2}{EI_2} - \frac{N_5}{EA_5}\right]$$

$$N_3 = - EA_3 \left[\frac{(c)}{2} \frac{M_5}{EI_5} + B \frac{M_4}{EI_4} + \frac{(D)}{2} \frac{M_3}{EI_3} - \frac{N_5}{EA_5} \right]$$

$$N_4 = - EA_4 \left[\frac{(c)}{2} \frac{M_5}{EI_5} + \frac{(B)}{2} \frac{M_4}{EI_4} - \frac{N_5}{EA_5} \right]$$

Addition of the equations containing the axial forces and shear flows from (5.2) to (5.6) yields

$$\frac{dN_1}{dx} + \frac{dN_2}{dx} + \frac{dN_3}{dx} + \frac{dN_4}{dx} + \frac{dN_5}{dx} = 0 \qquad (5.16)$$

From the conditions of vertical equilibrium

$$N_1 + N_2 + N_3 + N_4 + N_5 = 0 \qquad (5.17)$$

If the structure is subjected to a direct vertical load the right hand side of equation (5.17) will be equal to that applied load.

On substituting for the axial forces N_1, N_2, N_3 and N_4 from equations (5.15) and the moments M_1, M_2, M_3, M_4 and M_5 from equation (5.7) into (5.17), the axial force N_5 becomes

$$N_5 = - EA_5 (P + c_5) \frac{d^2\theta}{dx^2} \qquad (5.18)$$

A consideration of equations (5.7), (5.15) and (5.18) yields the axial forces N_1, N_2, N_3 and N_4 as

$$N_1 = - EA_1 \ (P - c_2 - c_3 - c_4) \ \frac{d^2\theta}{dx^2} \qquad (5.19)$$

$$N_2 = - EA_2 \ (P - c_3 - c_4) \ \frac{d^2\theta}{dx^2} \qquad (5.20)$$

$$N_3 = - EA_3 \ (P - c_4) \ \frac{d^2\theta}{dx^2} \qquad (5.21)$$

$$N_4 = - EA_4 \ P \ \frac{d^2\theta}{dx^2} \qquad (5.22)$$

where

$$c_1 = \frac{1}{2} \ (e + B) \ (d + 2a + c)$$

$$c_2 = (e + B) \ \frac{d}{2} + (n - f) \ \frac{B}{2}$$

$$c_3 = (n - f) \ \frac{B}{2} - e \ \frac{D}{2}$$

$$c_4 = (m + f) \ \frac{B}{2} - e \ \frac{D}{2}$$

$$c_5 = (e + B) \ \frac{c}{2} + (m + f) \ \frac{B}{2}$$

$$A = A_1 + A_2 + A_3 + A_4 + A_5$$

$$P = \frac{1}{A} \left[A_1 \ (c_2 + c_3 + c_4) + A_2 \ (c_3 + c_4) + A_3 \ c_4 - A_5 \ c_5 \right]$$

Substitution of the axial forces and moments into the appropriate equilibrium conditions (5.2) to (5.6) yields the shear flows at the core corners and the horizontal shear forces S_1 to S_5 as,

$$q_2 = E\beta P_1 \frac{d\theta}{dx} + EP_2 \frac{d^3\theta}{dx^3} \tag{5.23}$$

$$q_3 = E\beta P_1 \frac{d\theta}{dx} + EP_3 \frac{d^3\theta}{dx^3} \tag{5.24}$$

$$q_4 = E\beta P_1 \frac{d\theta}{dx} - EP_4 \frac{d^3\theta}{dx^3} \tag{5.25}$$

$$q_5 = E\beta P_1 \frac{d\theta}{dx} - EP_5 \frac{d^3\theta}{dx^3} \tag{5.26}$$

and

$$S_1 = EP_6 \frac{d^3\theta}{dx^3} - E\beta \left(\frac{a}{2} + d\right) P_1 \frac{d\theta}{dx} \tag{5.27}$$

$$S_2 = EP_7 \frac{d^3\theta}{dx^3} - E\beta BP_1 \frac{d\theta}{dx} \tag{5.28}$$

$$S_3 = EP_8 \frac{d^3\theta}{dx^3} - E\beta DP_1 \frac{d\theta}{dx} \tag{5.29}$$

$$S_4 = EP_9 \frac{d^3\theta}{dx^3} - E\beta BP_1 \frac{d\theta}{dx} \tag{5.30}$$

$$S_5 = EP_{10} \frac{d^3\theta}{dx^3} - E\beta \left(\frac{a}{2} + c\right) P_1 \frac{d\theta}{dx} \tag{5.31}$$

where

$$P_2 = A_1 (P - c_2 - c_3 - c_4)$$

$$P_3 = (A_1 + A_2) (P - c_3 - c_4) - A_1 c_2$$

$$P_4 = (A_4 + A_5) P + A_5 c_5$$

$$P_5 = A_5 (P + c_5)$$

$$P_6 = (e + B) I_1 - A_1 \frac{d}{2} (P - c_2 - c_3 - c_4)$$

$$P_7 = (n - f)\, I_2 - A_1\, B(P - c_2 - c_3 - c_4) - A_2 \frac{B}{2} (P - c_3 - c4)$$

$$P_8 = - eI_3 + \frac{D}{2}\Big[P\,(A_4 + A_5 - A_1 - A_2) + A_1\,(c_2 + c_3 + c_4) + A_2\,(c_3 + c_4) + A_5\, c_5 \Big]$$

$$P_9 = (m + f)\, I_4 + \frac{B}{2P}\,(A_4 + 2A_5) + A_5\, c_5\, B$$

$$P_{10} = (e + B)\, I_5 + A_5 \frac{c}{2}\,(P + c_5)$$

If the core structure is subjected to an applied torque T at any level, its internal torsional resistance will be composed of the warping resistance T_W, and the St. Venant torsional resistance T_S. The warping resistance T_W is produced by the horizontal shear force S_i (i = 1 - 5), and the St. Venant torsional resistance T_S is equal to GJ $\frac{d\theta}{dx}$, where

$$J = \sum_{i=1}^{n} \frac{1}{3}\, l_i t_i^3$$

in which l_i and t_i are the width and the thickness of the wall panel 'i' respectively. For obtaining the St. Venant torsional constant J, the contribution from the connecting beams are again neglected.

The condition of overall equilibrium becomes

$$T = T_W + T_S = - (B + e)\, S_1 - (n - f)\, S_2 + eS_3 - (m + f)\, S_4 - (e + B)\, S_5 + GJ \frac{d\theta}{dx} \qquad (5.32)$$

On substituting for the horizontal shear forces from equations (5.27) to (5.31), equation (5.32) becomes

$$T = EI_\omega \frac{d^3\theta}{dx^3} + GJ_o \frac{d\theta}{dx} \qquad (5.33)$$

where I_ω is the core warping inertia given by

$$I_\omega = (e + B) P_6 + (n - f) P_7 - eP_8 + (m + f) P_9 + (e + B) P_{10}$$

and

$$J_o = \beta \frac{E}{G} P_1^2 + J$$

Equation (5.33) can be expressed in the form

$$\frac{d^3\theta}{dx^3} - \alpha^2 \frac{d\theta}{dx} = - \frac{T}{EI_\omega} \qquad (5.34)$$

where α is the relative stiffness parameter defined as

$$\alpha^2 = \frac{GJ_o}{EI_\omega}$$

5.4 Singly-symmetric core structures

Fig. 5.4 shows an idealized singly-symmetric core structure. The same procedure as described in section (5.3) is applied for the analysis of this particular structure, except in this case

$$f = o$$

$$m = n = \frac{D}{2}$$

$$c = d$$

$$L = \frac{B}{2}$$

Hence, the internal forces are

$$N_1 = EA_1 \gamma_1 \frac{d^2\theta}{dx^2} \tag{5.35}$$

$$N_2 = EA_2 \frac{D}{2} \left(\frac{B}{2} - e\right) \frac{d^2\theta}{dx^2} \tag{5.36}$$

and

$$q_1 = -2\gamma_2 \frac{d\theta}{dx} \tag{5.37}$$

$$q_2 = 2\gamma_2 \frac{d\theta}{dx} - EA_1\gamma_1 \frac{d^3\theta}{dx^3} \tag{5.38}$$

$$q_3 = 2\gamma_2 \frac{d\theta}{dx} - E\left[A_1\gamma_1 + A_2 \frac{D}{2}\left(\frac{B}{2} - e\right)\right] \frac{d^3\theta}{dx^3} \tag{5.39}$$

and

$$S_1 = -\gamma_2 D \frac{d\theta}{dx} + E\left[(e + B) I_1 + A_1 \frac{d}{2} \gamma_1\right] \frac{d^3\theta}{dx^3} \tag{5.40}$$

$$S_2 = -2\gamma_2 B \frac{d\theta}{dx} + E\left[\frac{D}{2} I_2 + A_1\gamma_1 B + A_2 \frac{DB}{4}\left(\frac{B}{2} - e\right)\right] \frac{d^3\theta}{dx^3} \tag{5.41}$$

$$S_3 = -2\gamma_2 D \frac{d\theta}{dx} - E\left[eI_3 - A_1\gamma_1 D - A_2 \frac{D^2}{2}\left(\frac{B}{2} - e\right)\right] \frac{d^3\theta}{dx^3} \tag{5.42}$$

where

$$\gamma_1 = \frac{d}{2}(e + B) + \frac{D}{2}(B - e)$$

$$\gamma_2 = \beta E B D$$

The internal forces in the other panels follow from symmetry of the structure.

If the structure is subjected to an applied moment T at any level, the conditions of overall equilibrium becomes

$$T = T_w + T_S = -2(e + B)\, S_1 - DS_2 + eS_3 + GJ \frac{d\theta}{dx} \qquad (5.43)$$

On substituting for the horizontal shear forces S_i $(i = 1 - 3)$ from equations (5.40) to (5.42) into (5.43), the governing differential equation again becomes

$$- EI_\omega \frac{d^3\theta}{dx^3} + GJ_o \frac{d\theta}{dx} = T \qquad (5.44)$$

where

$$I_\omega = 2\,(e + B)^2\, I_1 + \frac{D}{2}^2 I_2 + e^2 I_3 + 2\, A_1 \gamma_1^2 + A_2 \frac{D}{2}^2 (\frac{B}{2} - e)^2$$

and

$$J_o = 4 \beta \frac{E}{G} B^2 D^2 + J$$

Solution of the governing differential equation

The general solution of the governing differential equation (5.34) for any form of torsional loading may be expressed in the form

$$\theta = C_o + C_1 \cosh \alpha x + C_2 \sinh \alpha x + \theta_{PI} \qquad (5.45)$$

where C_i $(0 - 2)$ are the constants of integration to be determined from the necessary boundary conditions, and θ_{PI} is the particular integral solution for a specific form of applied torque T.

Boundary conditions

In order to determine the constants C_i for equation (5.45), it is necessary to derive three independent boundary conditions for the structure. If the structure is rigidly built in at the base, then at $x = o$

$$\Theta = o \quad \text{and} \quad \frac{d\Theta}{dx} = o \tag{5.46}$$

At the top, the bending moments and axial forces in the wall panels are zero, and so from equations (5.7) and (5.18) to (5.22), at $x = H$

$$\frac{d^2\Theta}{dx^2} = o \tag{5.47}$$

Solution of the governing differential equation

In order to achieve a solution, suppose that the particular case is considered of a uniformly distributed torque of intensity t_o per unit height. In that case

$$T = t_o (H - x) \tag{5.48}$$

On substituting for T in equation (5.34), the simplest particular integral becomes

$$\Theta_{PI} = \frac{t_o}{GJ_o} \left(H x - \frac{x^2}{2}\right) \tag{5.49}$$

Then on substituting equation (5.45) into the boundary conditions (5.46) - (5.47), and solving for the integration constants, the general solution becomes

$$\Theta = \frac{t_o H^2}{GJ_o k^2} \left[\Delta(\cosh k\xi - 1) - k \sinh k\xi + k^2 \left(\xi - \frac{\xi^2}{2}\right) \right] \quad (5.50)$$

where

$$\Delta = \frac{1 + k\sinh k}{\cosh k}$$

and $k = \alpha H$ and $\xi = \frac{x}{H}$

Equation (5.50) emphasizes the dependence of the solution on two variables only the height ξ and the relative stiffness k.

Substitution of equation (5.50) into the earlier equations yields closed-form solutions for internal moments, shear forces, axial forces and corresponding vertical stresses.

Design Curves

Figures 5.5 to 5.8 show design curves for the rotational parameter U_1, and the rotational derivative parameters U_2, U_3 and U_4 for any single cell partially closed core structure subjected to uniformly distributed torque of intensity t_o per unit height.

U_1, U_2, U_3 and U_4 are given by

$$U_1 = \frac{GJ_o k^2}{t_o H^2}\,\theta$$

$$U_2 = \frac{GJ_o k}{t_o H}\left(\frac{d\theta}{dx}\right) \qquad (5.51)$$

$$U_3 = \frac{GJ_o}{t_o}\left(\frac{d^2\theta}{dx^2}\right)$$

$$U_4 = \frac{GJ_o H}{t_o k}\left(\frac{d^3\theta}{dx^3}\right)$$

Once the value of k is known, the values of parameters U_1, U_2, U_3 and U_4 at the desired height can be obtained from the curves, then the rotation and rotational derivatives can be determined.

The curves for rotational parameter U_1 can be used in conjunction with equations (5.1) to determine the displacements of the significant points (1-5), and the centroid of the core structures.

The curves for U_3 can be used together with equations (5.7) and (5.18) to (5.22) to determine the moments M_i and the axial forces N_i (i = 1 - 5) in the panels (1-5) respectively.

The curves for U_2 can be used in conjunction with equation (5.14) to determine the shear flow in the connecting beams (along line of contraflexure 1-1). The shear flows in the vertical joints q_i (i = 2 - 5), and the horizontal shear forces S_i (i = 1 - 5) can be computed by using the curves for U_2 and U_4 together with equations (5.23) to (5.31).

The method of analysis presented may be used to analyse any core structure providing it is open or partially closed by lintel beams, and no s egment is completely closed. In the above analysis the St. Venant torsional constant J has been calculated disregarding the connecting beams. Hence, the actual value of J will be greater than the calculated value. However, this would not have a significant effect on the analysis, as the St. Venant torsional resistance is relatively small compared to the warping resistance.

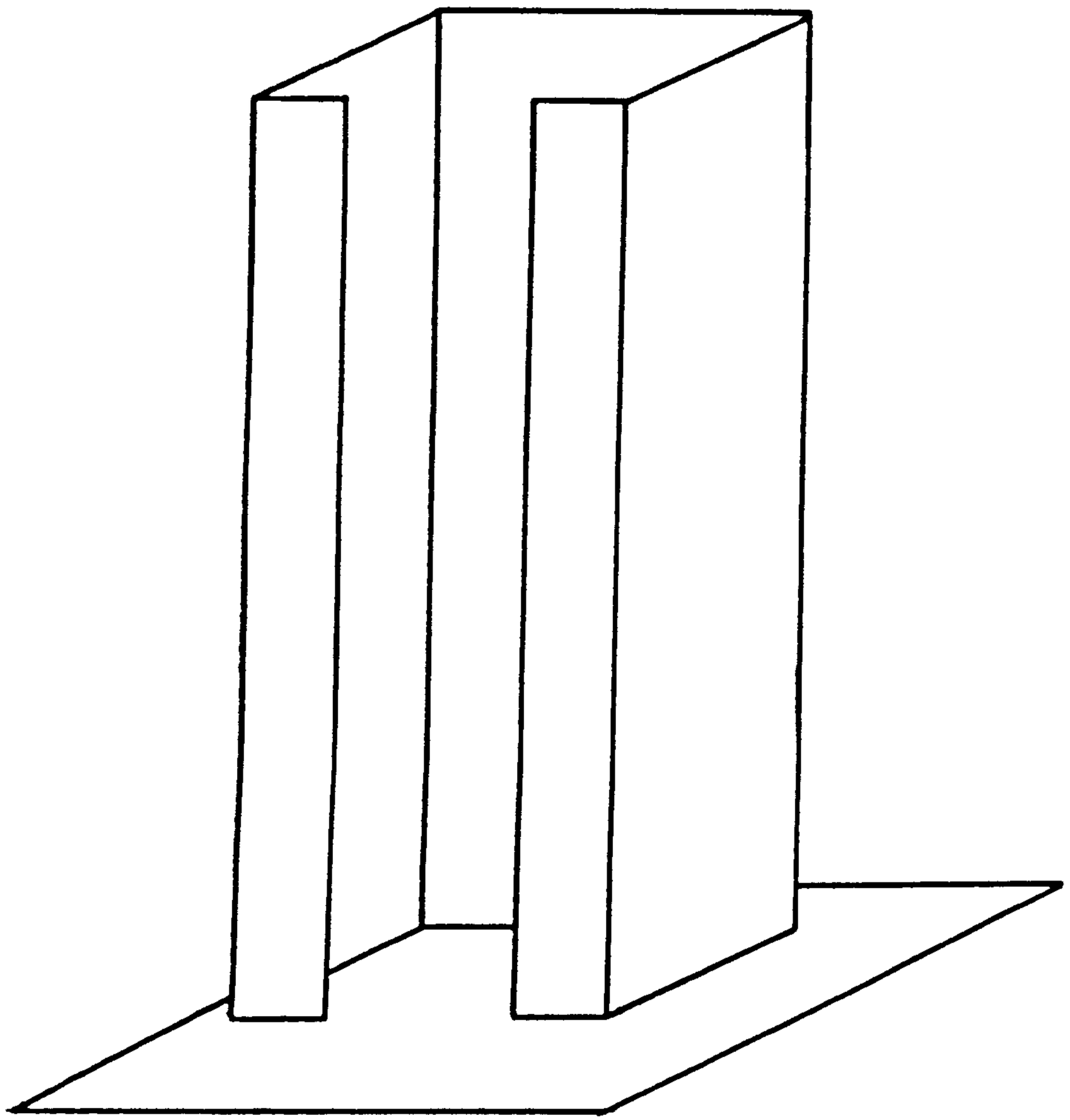

a) Open section core

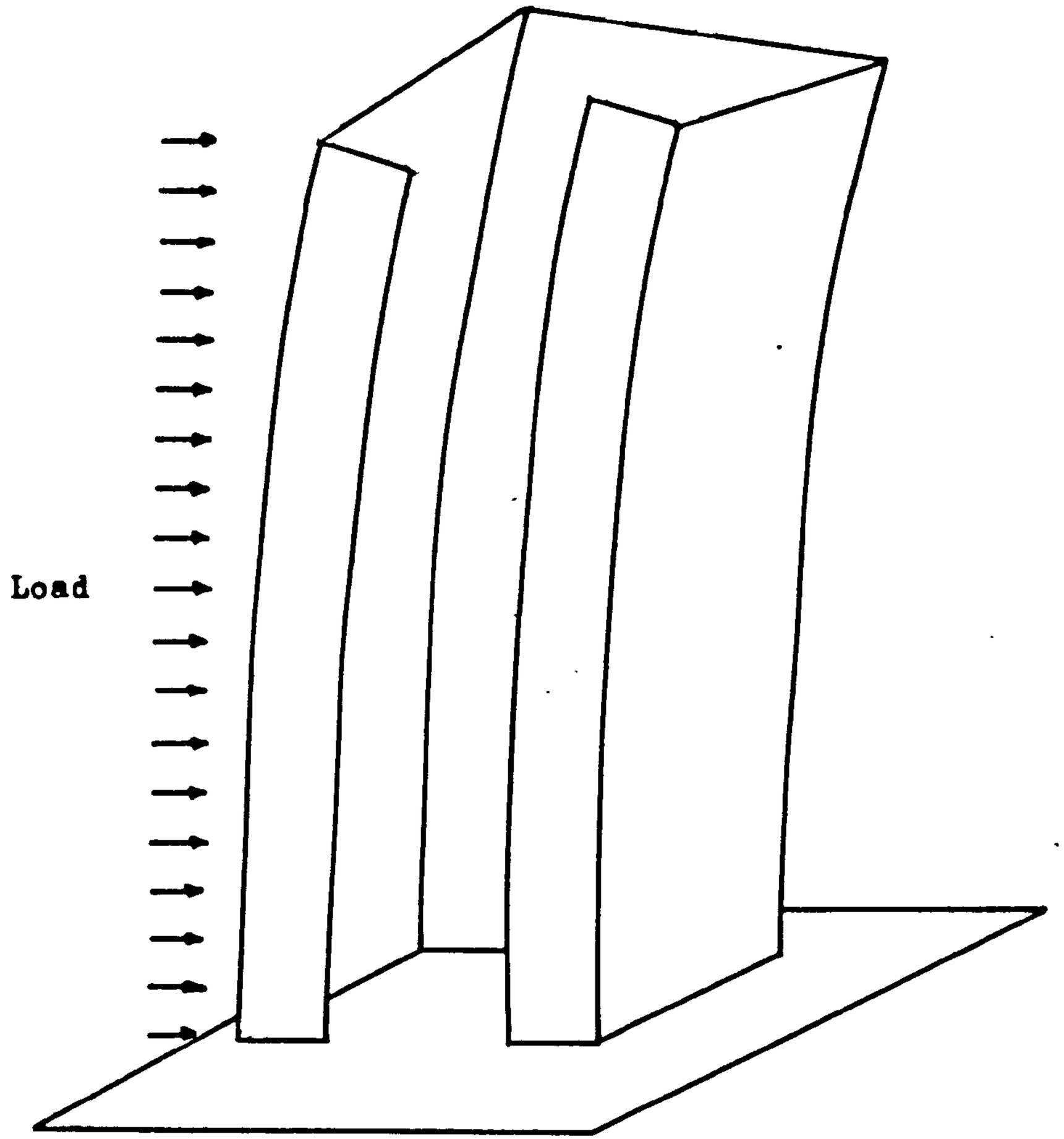

b) Bending and warping resulting from horizontal loading

Fig. 5.1

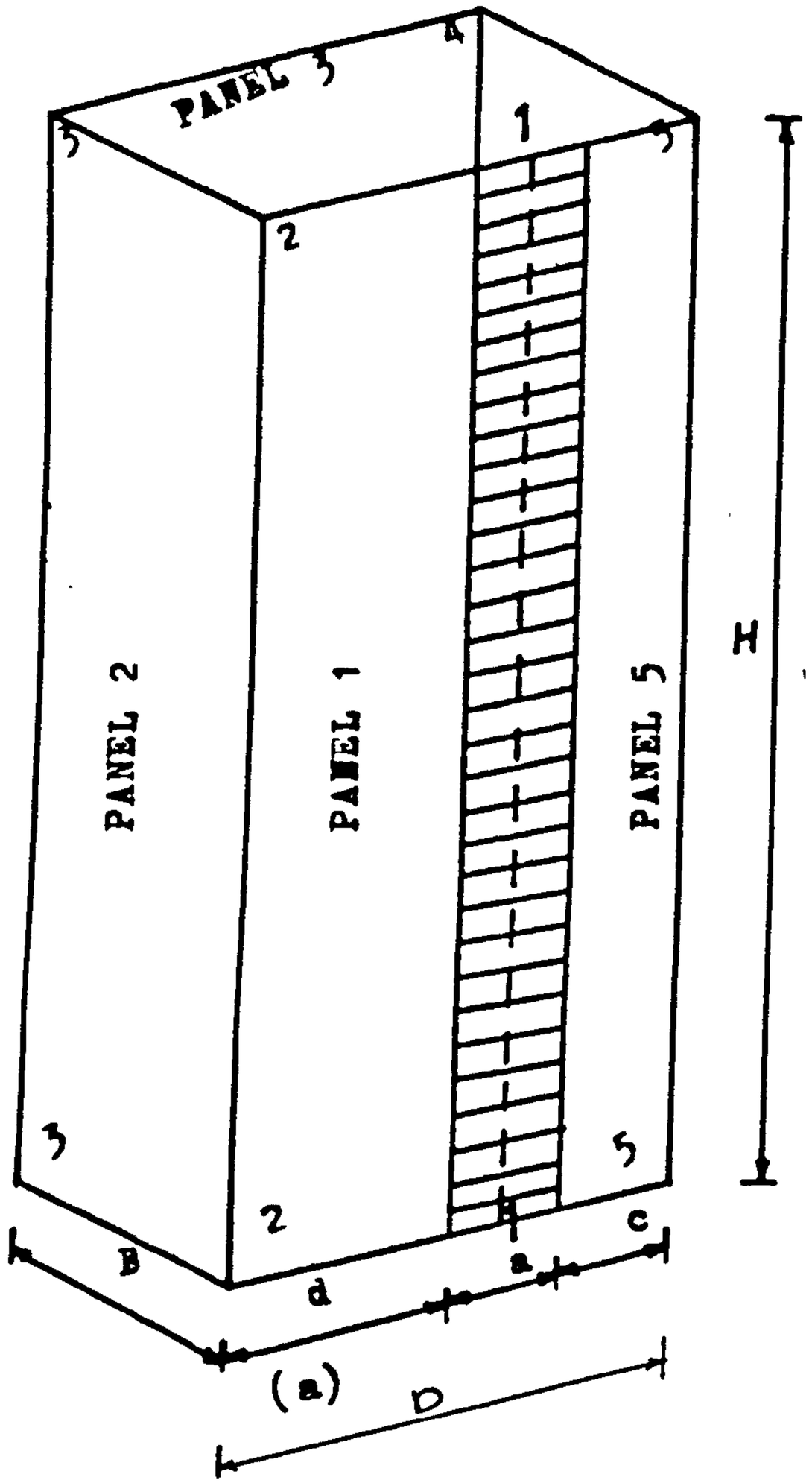

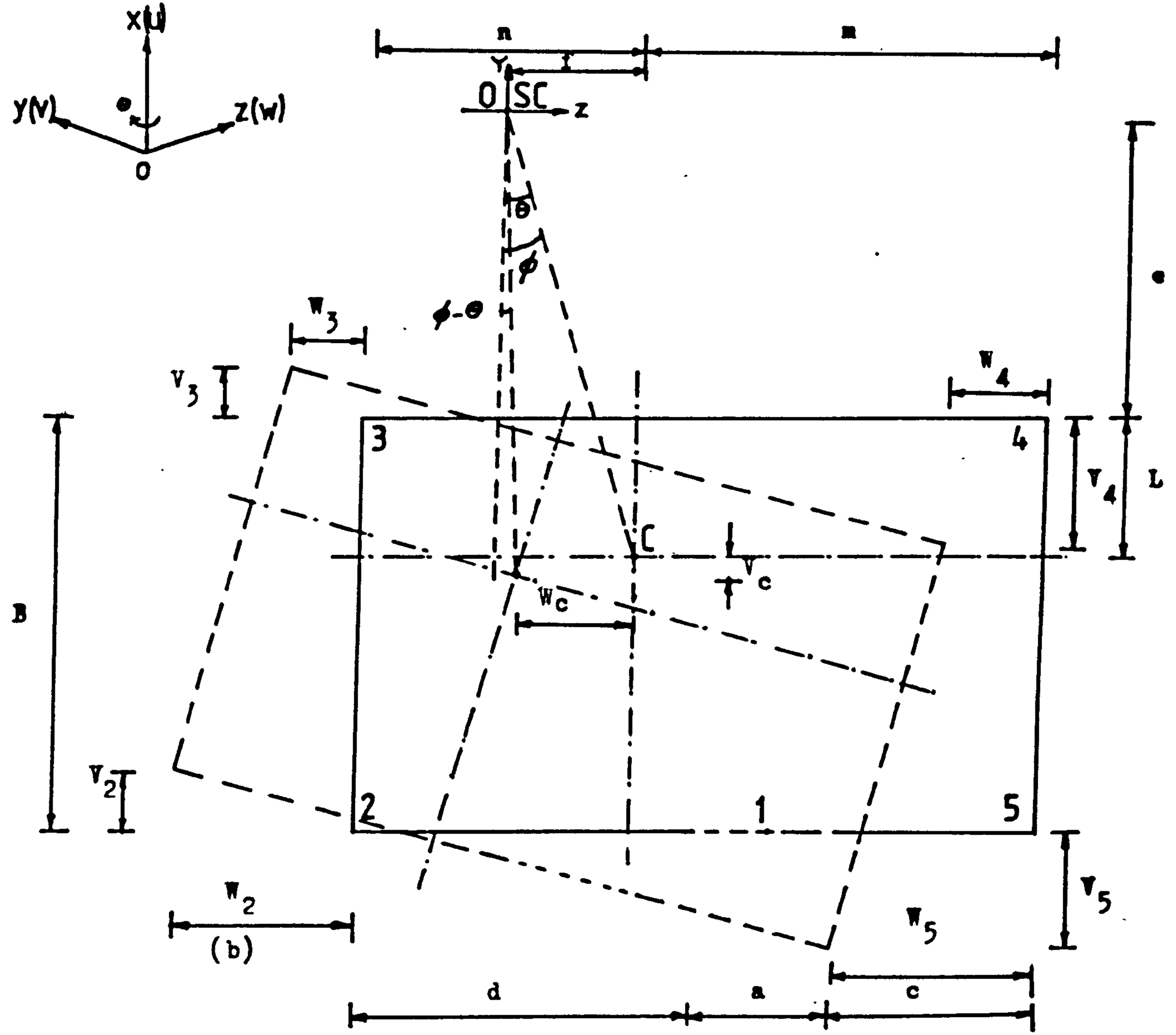

Fig. 5.2 Asymmetrical partially closed core structure

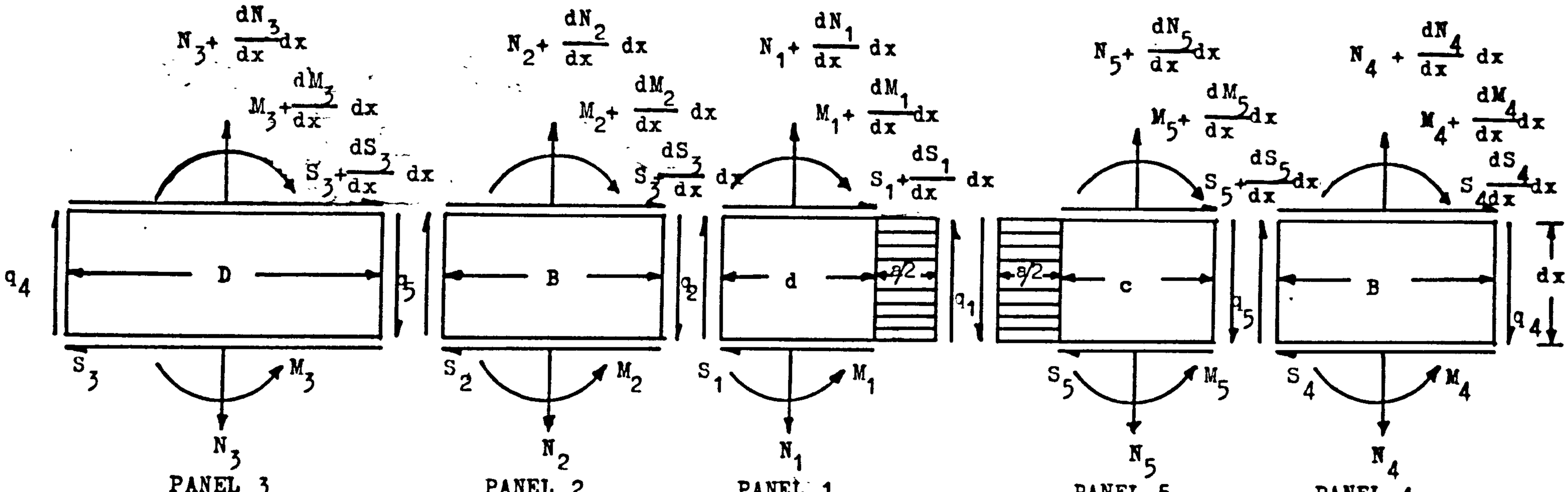

Fig. 5.3(a) Forces on element of core panels

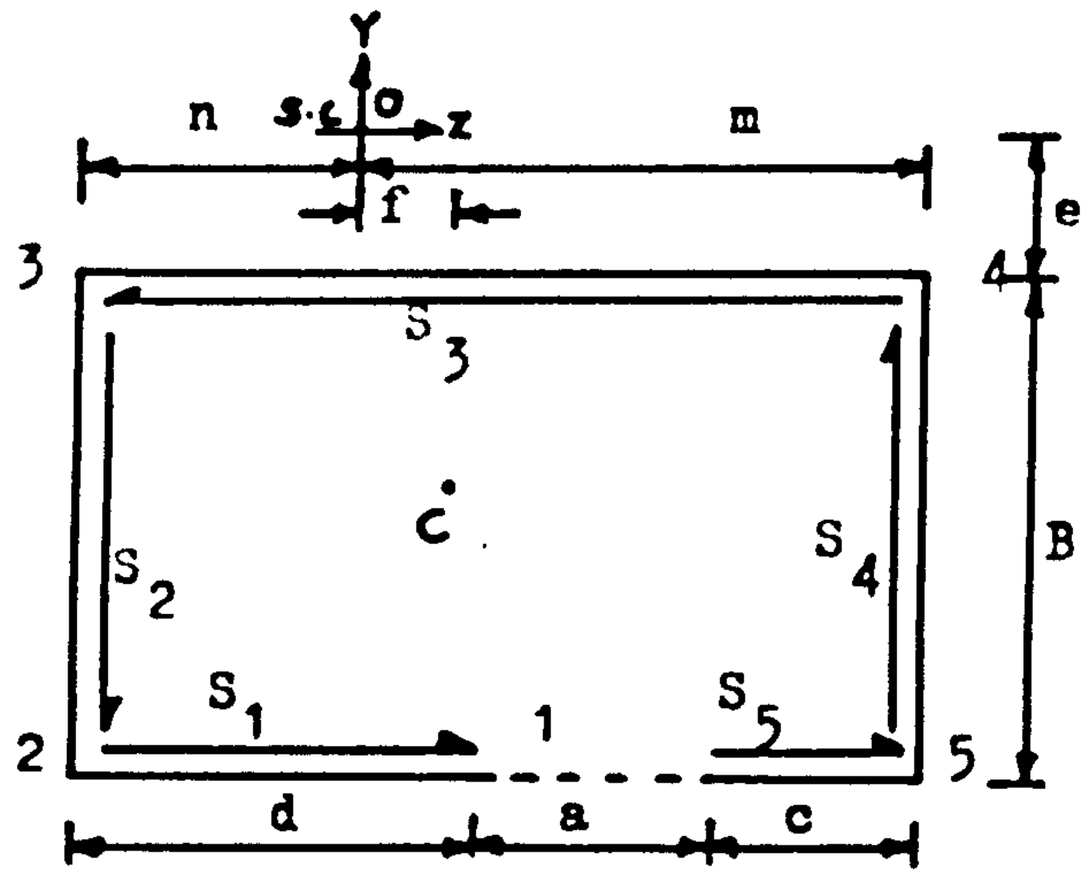

Fig. 5.3(b) Horizontal shear forces in core cross-section

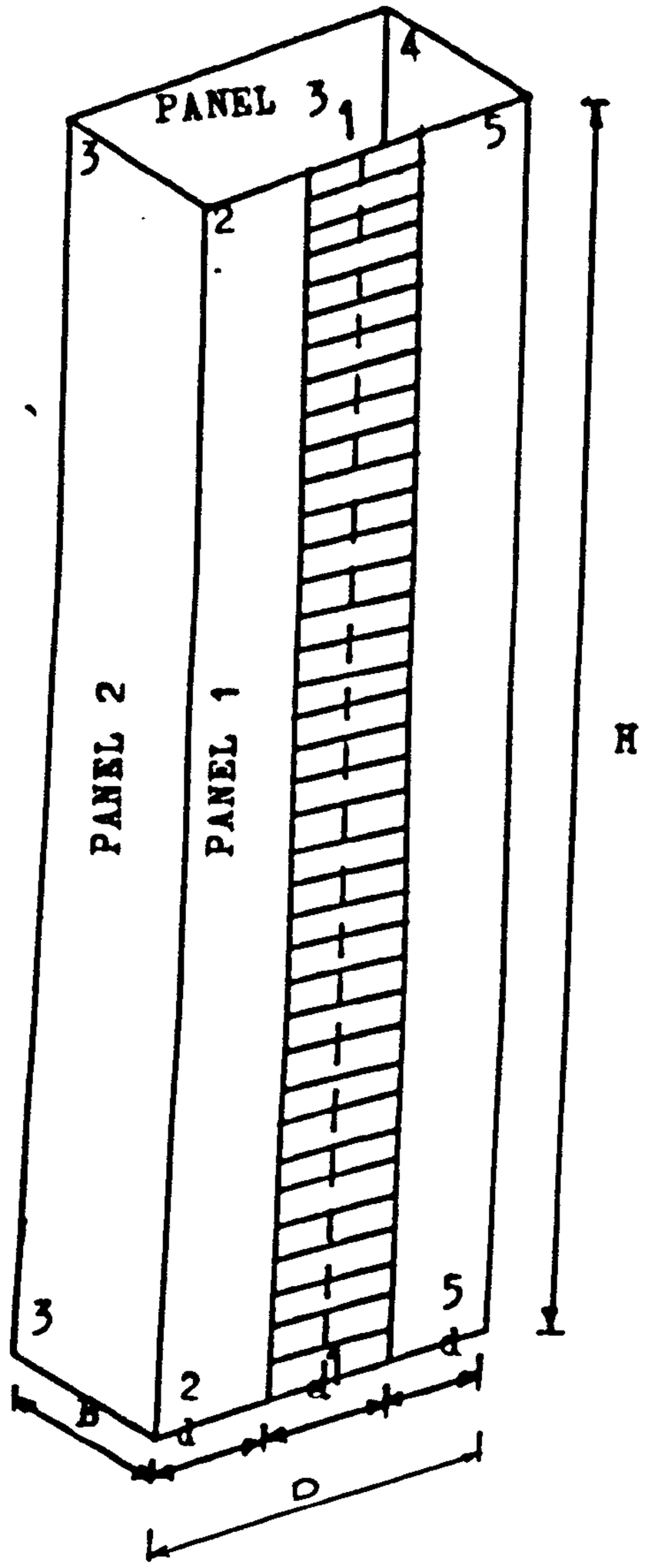

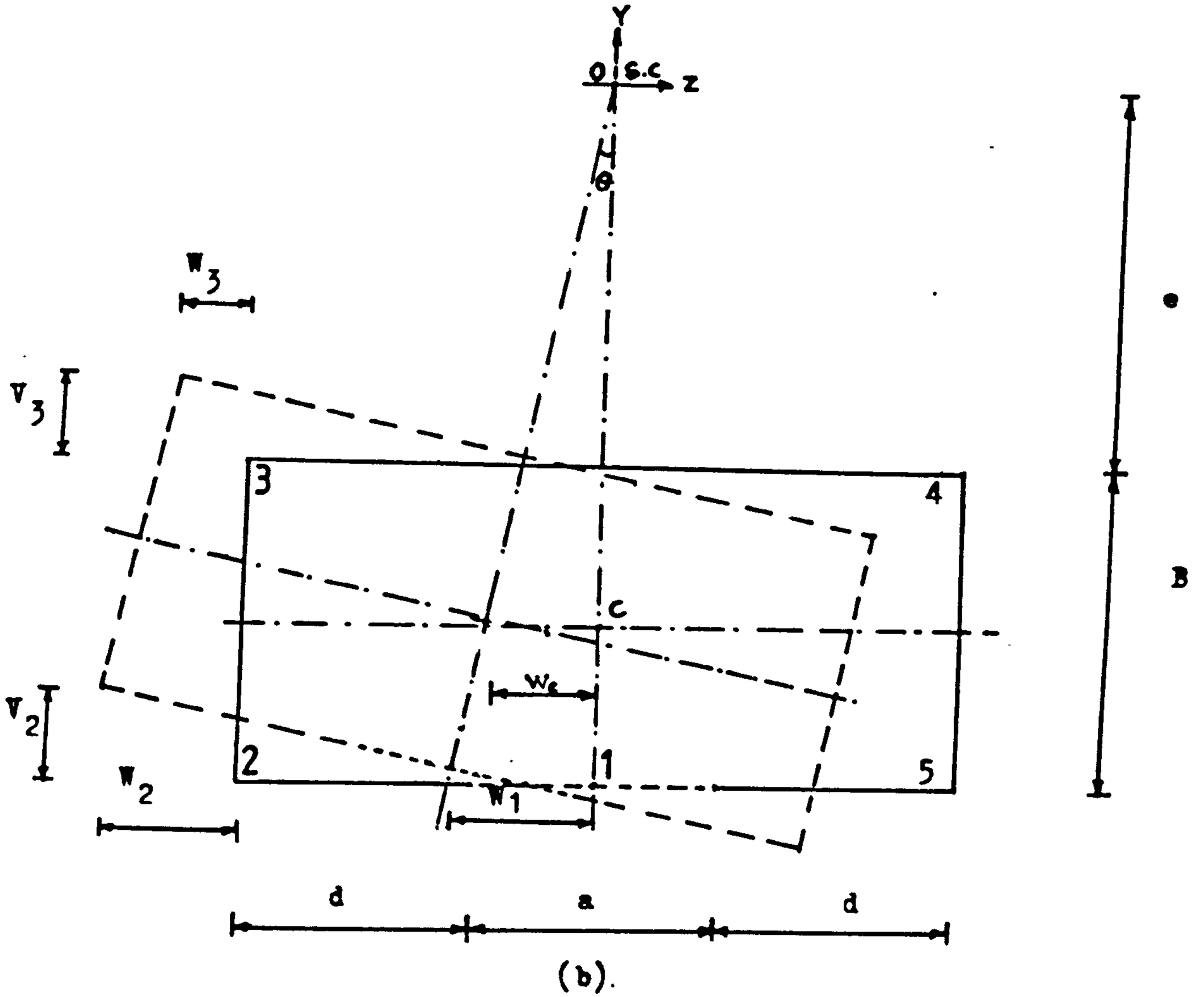

Fig. 5.4 Singly-symmetrical core structure

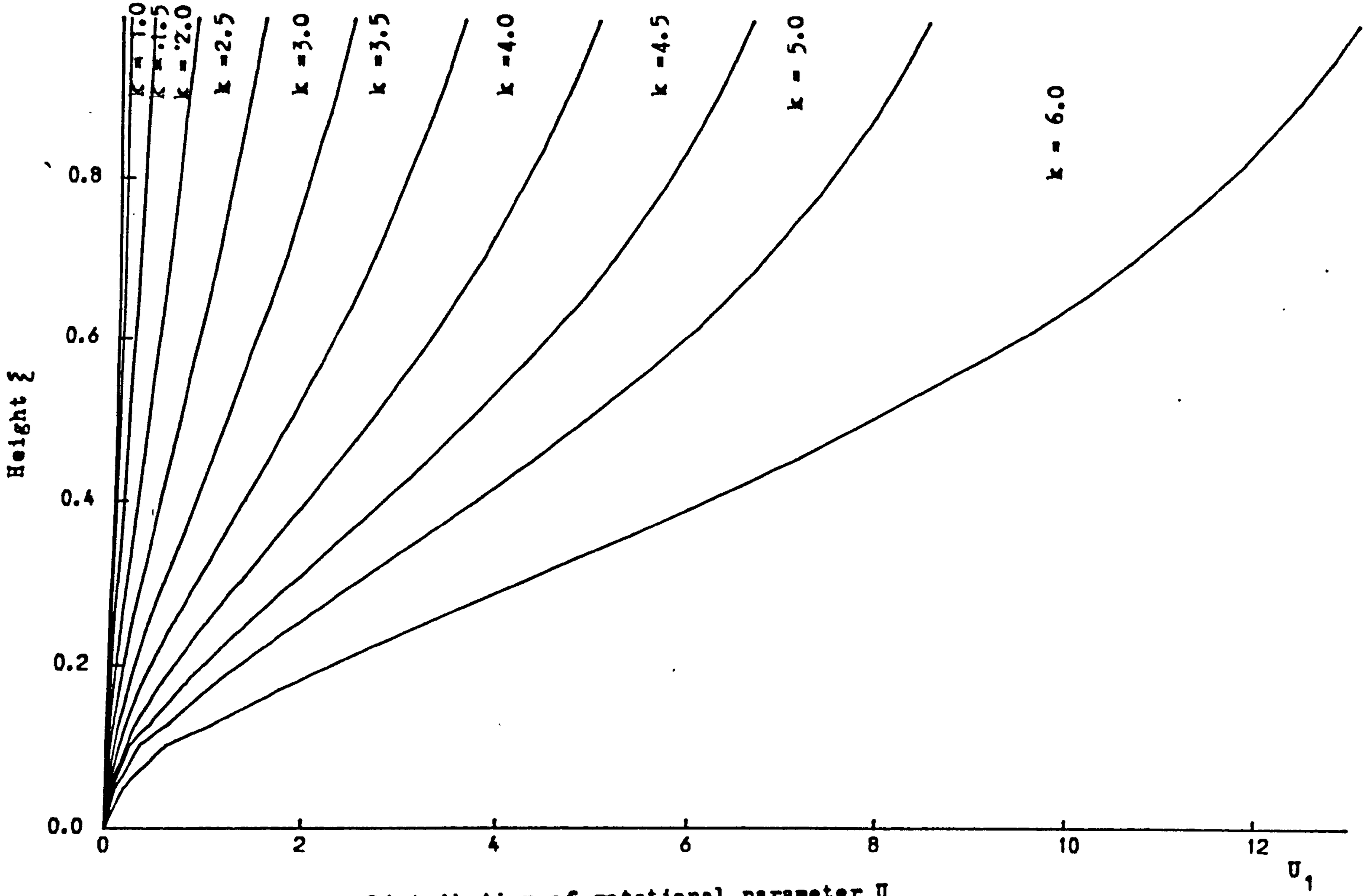

Fig. 5.5 Distribution of rotational parameter U_1

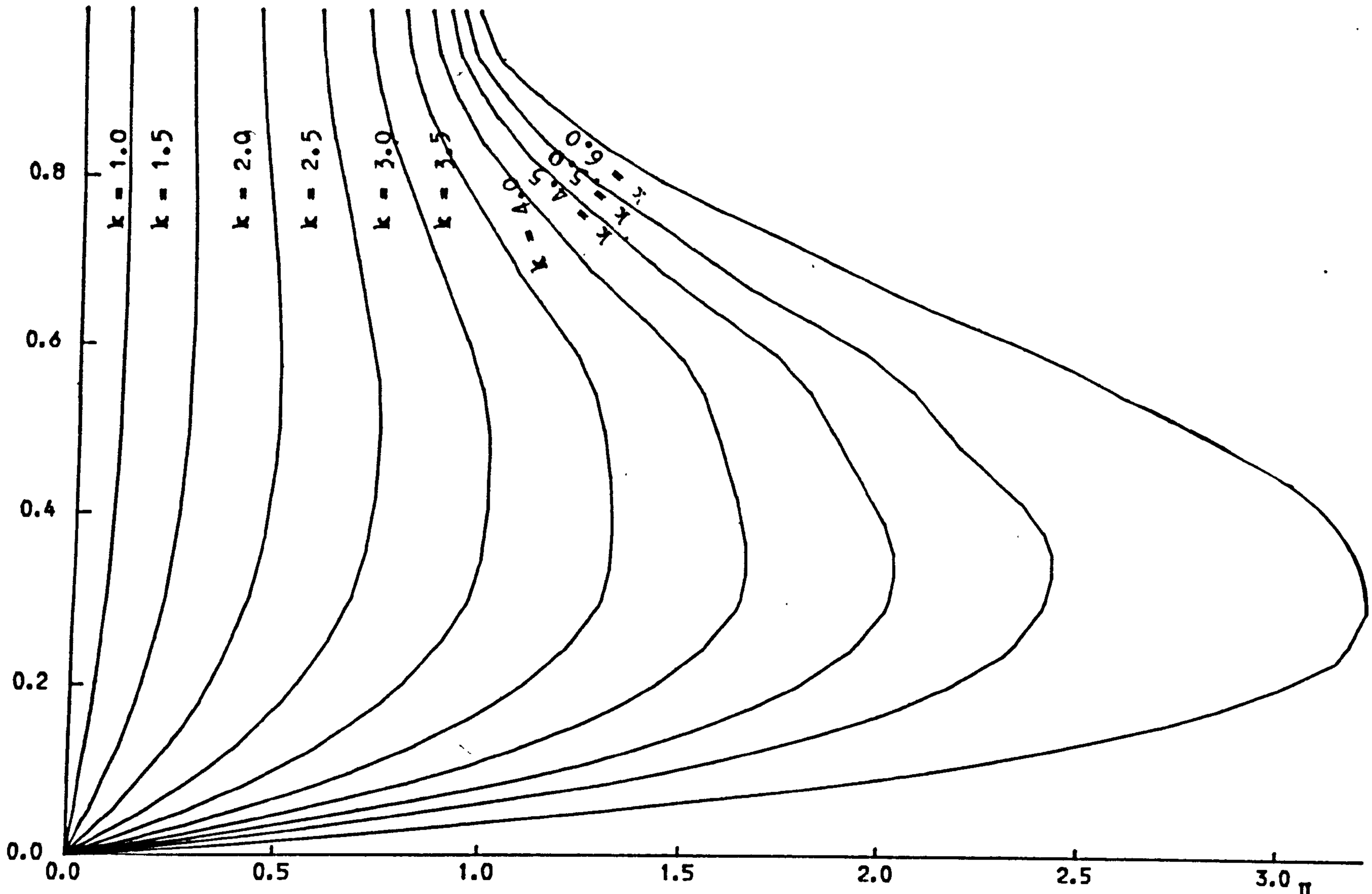

Fig. 5.6 Distribution of rotational derivative parameter U_2

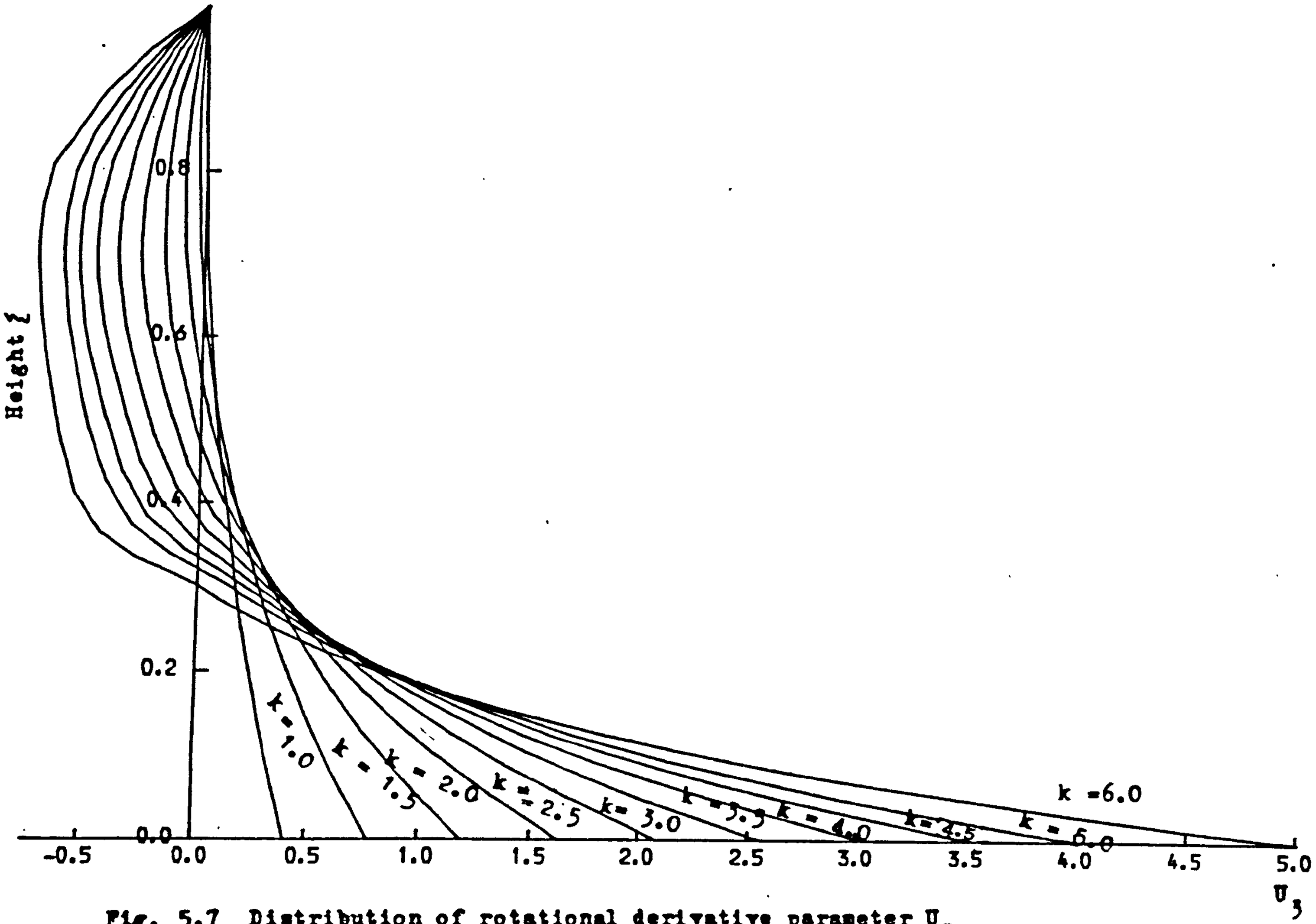

Fig. 5.7 Distribution of rotational derivative parameter U_3

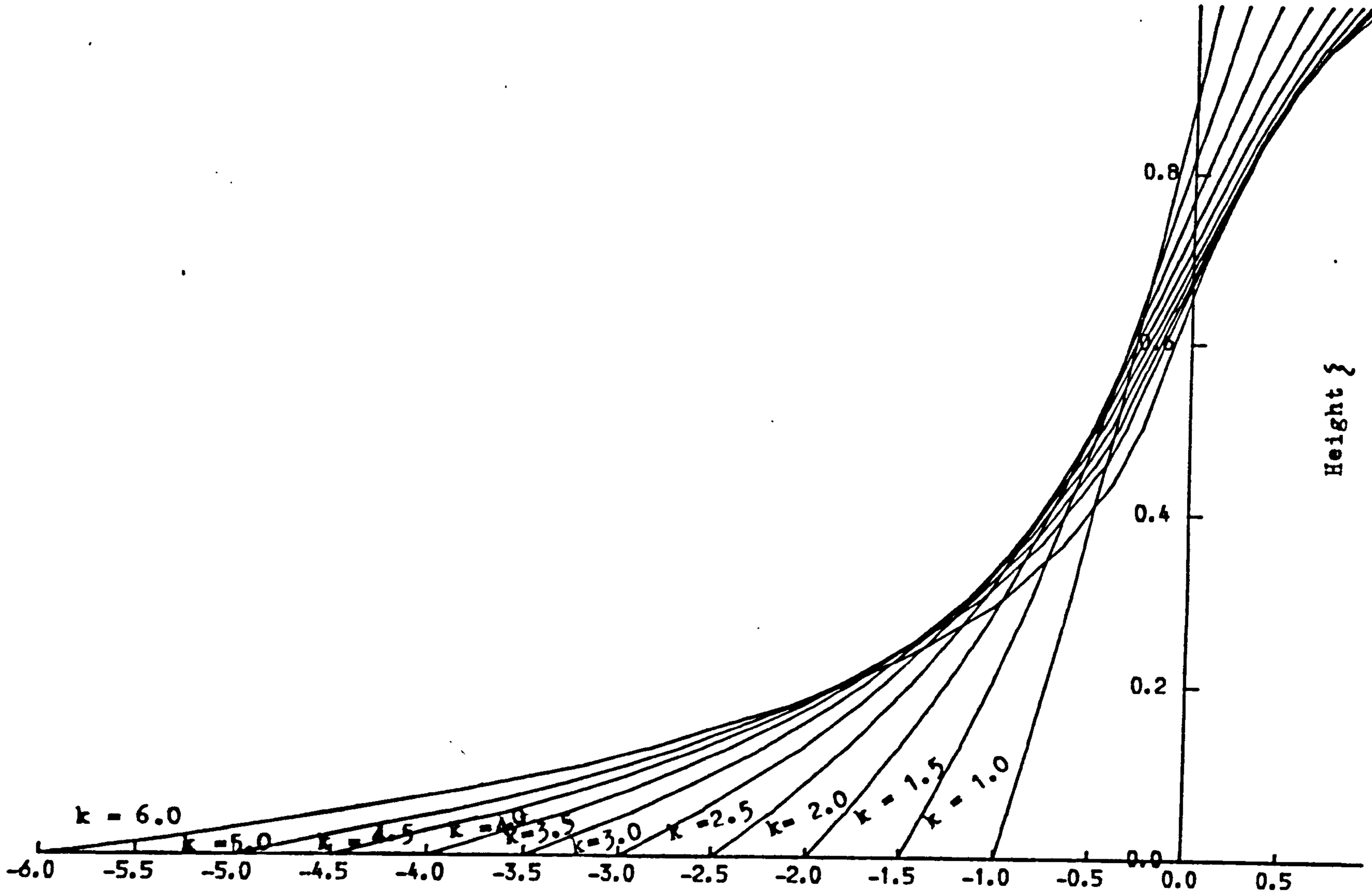

Fig. 5.8 Distribution of rotational d erivative parameter U_4

C H A P T E R 6

TORSIONAL ANALYSIS OF SYMMETRIC BUILDING STRUCTURES

NOTATION

A_1 A_2	cross-sectional areas of coupled shear walls.
b	clear opening between coupled walls.
E	elastic modulus.
GA	effective shearing rigidity of shear cantilever.
h	storey height.
I	second moment of area.
I_c	second moment of area of connecting beams.
l	distance between centroidal axes of coupled walls.
M	bending moment.
N	axial force in coupled walls.
q	shear flow in connecting medium of coupled walls.
S	shear force.
T	applied twisting moment.
t	intensity of applied twisting moment
ω	lateral force intensity on transformed structure.
x	height above base.
y	horizontal deflection.
z_{1i}, z_{2i}	distance of i^{th} wall, frame, core or coupled wall
z_{3i}, z_{4i}	from central axis.
α, β, γ	structural parameters.
θ	angle of rotation of building.
c,w,f,s	suffices denoting core, wall, frame or coupled wall.
i	suffix denoting i^{th} component.
o	suffix denoting datum plane.
'	prime denoting actions referred to transformed structure.

C H A P T E R 6

TORSIONAL ANALYSIS OF SYMMETRIC BUILDING STRUCTURES

6.1 Introduction

In chapter 3, an "exact" analysis based on the continuum approach was presented for symmetrical structures consisting of assemblies of coupled shear walls, cores, and rigidly-jointed frames, subjected to lateral forces which produce bending. The frame components were represented by equivalent shear cantilevers. Due to the high in-plane rigidity of the floor slabs, it was assumed that each horizontal cross-section of the building underwent only a rigid body movement. A solution could then be achieved by replacing the three-dimensional structure by an equivalent plane system in which the components were constrained to act in series by a set of rigid pin-ended links which simulate the action of the floor slabs. The continuum approach, leading to a sixth order governing differential equation, enabled a closed solution to the problem to be achieved, and formulae were presented for the evaluation of the lateral deflections and forces (shears and moments on each component, and axial forces and lintel shears in the coupled shear walls) throughout the structure for the particular case of a uniformly distributed leading.

If the symmetrical structure is subjected to eccentric loads, the analysis may be treated as a superposition of a symmetrical pure bending action, and a skew-symmetric pure torsional action. The former may be treated by the theory presented in chapter 3.

In the latter case, each horizontal cross-section undergoes rigid body rotations about the central axis, and the deflection of each component is proportional to its distance from the axis of rotation. It is then possible to transform the real three-dimensional structure into an equivalent plane located in any datum plan in the cross-section. This equivalent structure may be analysed "exactly" using the theory developed earlier, and the same formulae presented in chapter 3 used to obtain the deflections and forces in the substitute system. These actions may subsequently be transformed back into the original structure. A closed solution to the problem of eccentrically loaded symmetrical structures is thus possible.

When using the continuum approach, the transformation factors are very simple and rapid solutions are possible. The object of this chapter is to demonstrate the technique and show how the earlier solution may be used directly for the torsional analysis of symmetrical structures.

TRANSFORMATIONS

6.2 Transformations for wall, core and frame assemblies.

Consider a symmetrical structure which consists of 2M assemblies of independent shear walls, 2N rigidly-jointed frames and 2Q service cores, as shown in Fig. 6.1, a typical wall 'i', a typical frame 'i' and a typical core (i) being located respectively at distances z_{1i}, z_{2i} and z_{3i} from the central axis of symmetry of the building. Due to the

symmetry of the structure, only one-half need be considered.

Under the action of an applied twisting moment T, the structure will rotate about the central vertical axis Ox, each cross-section undergoing a rigid-body rotation in the horizontal plane due to the in-plane rigidity of the floor slabs. It is convenient to express all deformations in terms of the lateral deflection y_o at some arbitrarily chosen datum plane, normally in the plane of one of the structural assemblies, at distance z_o from the axis of rotation, so that $\Theta = y_o/z_o$. The lateral deflection of the i^{th} wall, the i^{th} frame and i^{th} core then become, respectively,

$$y_{wi} = z_{1i}\Theta = \frac{z_{1i}}{z_o} y_o$$

$$y_{fi} = z_{2i}\Theta = \frac{z_{2i}}{z_o} y_o \qquad (6.1)$$

$$y_{ci} = z_{3i}\Theta = \frac{z_{3i}}{z_o} y_o$$

Since the torsional stiffness of shear walls and frames, are small compared with their bending stiffnesses, it may be assumed that the twisting moment is resisted entirely by differential shearing actions of these elements. For the core assemblies, the internal torsional resistance consists of the warping resistance and the St. Venant torsional resistance. The condition of overall torsional equilibrium of the structure then become

$$T = 2\left\{\sum_{i=1}^{M} S_{wi}\, z_{1i} + \sum_{i=1}^{N'} S_{fi}\, z_{2i} + \sum_{i=1}^{Q} S_{ci}\, z_{3i} - \sum_{i=1}^{Q} T_w + \sum_{i=1}^{Q} T_s\right\} \qquad (6.2)$$

in which S_{wi}, S_{fi} and S_{ci} are the shear forces in wall 'i' frame 'i' and core 'i' and T_w and T_s are the warping resistance and St. Venant resistance (including effect of beams) of the core respectively, (chapter 5), where

$$T_w = (EI_\omega)_{ci} \left(\frac{d^3\theta}{dx^3}\right)$$

$$T_s = (GJ_o)_{ci} \left(\frac{d\theta}{dx}\right)$$

Substituting for T_w and T_s in equation (6.2) from above, T becomes,

$$T = 2\left\{\sum_{i=1}^{M} s_{wi}\, z_{1i} + \sum_{i=1}^{N} s_{fi}\, z_{2i} + \sum_{i=1}^{Q} s_{ci}\, z_{3i} - \sum_{i=1}^{Q} (EI_\omega)_{ci} \frac{d^3\theta}{dx^3} + \sum_{i=1}^{Q} (CJ_Q)_{ci} \frac{d\theta}{dx}\right\} \qquad (6.3)$$

On expressing the shears in the walls, frames and cores in terms of their flexural and shearing rigidities, equation (6.3) becomes, on using equation (6.1),

$$T = 2\left\{-\sum_{i=1}^{M} (EI)_{wi} \frac{(z_{1i})^2}{z_o} \frac{d^3y_o}{dx^3} + \sum_{i=1}^{N} (GA)_{fi} \frac{(z_{2i})^2}{z_o} \frac{dy_o}{dx} - \sum_{i=1}^{Q} (EI)_{ci} \frac{(z_{3i})^2}{z_o} \frac{d^3y_o}{dx^3} - \sum_{i=1}^{Q} (EI_\omega)_{ci} \frac{d^3\theta}{dx^3} + \sum_{i=1}^{Q} (GJ_o)_{ci} \frac{d\theta}{dx}\right\} \qquad (6.4)$$

where $(EI)_{wi}$ and $(EI)_{ci}$ are the flexural rigidities of wall 'i' and core 'i' respectively, and $(GA)_{fi}$ is the equivalent shearing rigidity of the frame 'i' when represented by a shear cantilever, $(GJ_o)_{ci}$ and $(EI_\omega)_{ci}$ are the torsional and warping rigidities, of the core 'i'.

From equation (6.1), $\Theta = \frac{1}{z_o} y_o$

and $$\frac{d\Theta}{dx} = \frac{1}{z_o} \frac{dy_o}{dx}$$

$$\frac{d^3\Theta}{dx^3} = \frac{1}{z_o} \frac{d^3y_o}{dx^3}$$

hence, equation (6.4) becomes,

$$T = \frac{2}{z_o}\left\{-\left[\sum_{i=1}^{M}(EI)_{wi}\,(z_{1i})^2 + \sum_{i=1}^{Q}(EI)_{ci}(z_{3i})^2 + \sum_{i=1}^{Q}(EI_\omega)_{ci}\right]\frac{d^3y_o}{dx^3} + \left[\sum_{i=1}^{N}(GA)_{fi}\,(z_{2i})^2 + \sum_{i=1}^{Q}(GJ_o)_{ci}\right]\frac{dy_o}{dx}\right\} \qquad (6.5)$$

An alternative procedure is to assume that all assemblies are transformed into an equivalent plane structure in the datum plane, the transformed components being constrained to act together in series by rigid pin-ended links which simulate the floor slabs. (Fig. 6.2). The applied torque T

at any level may then be replaced by two equal and opposite shear forces S_o of magnitude $T/2z_o$ at the datum positions. Since the building will normally be subjected to a distribution of twisting moment of intensity $t(x)$ per unit height due to the wind pressures acting on the facade, in which each plane equivalent structure will be subjected to a load intensity $\omega(x)$ of magnitude $t/2z_o$, then,

$$S_o = \int_x^H \omega \, dx \tag{6.6}$$

The equation of horizontal shear equilibrium in the equivalent transformed structure is then,

$$S_o = \frac{T}{2z_o} = \sum_{i=1}^{M} S'_{wi} + \sum_{i=1}^{N} S'_{fi} + \sum_{i=1}^{Q} S'_{ci} \tag{6.7}$$

where S'_{wi}, S'_{fi} and S'_{ci} are the shear forces at any level in the substitute wall 'i', frame 'i' and core 'i' respectively, given by,

$$S'_{wi} = -(EI)'_{wi} \frac{d^3 y_o}{dx^3}$$

$$S'_{fi} = (GA)'_{fi} \frac{dy_o}{dx}$$

$$S'_{ci} = -(EI)'_{ci} \frac{d^3 y_o}{dx^3}$$

Equation (6.7) may be expressed in terms of the lateral deflection y_o of the substitute structure as,

$$S_o = \frac{T}{2z_o} = \left\{ -\sum_{i=1}^{M} (EI)'_{wi} \frac{d^3y_o}{dx^3} + \sum_{i=1}^{N} (GA)'_{fi} \frac{dy_o}{dx} \right.$$

$$\left. - \sum_{i=1}^{Q} (EI)'_{ci} \frac{d^3y_o}{dx^3} \right\} \qquad (6.8)$$

in which $(EI)'_{wi}$, $(GA)'_{fi}$ and $(EI)'_{ci}$ are the transformed flexual and shear rigidities of wall 'i', frame 'i' and core 'i' respectively.

A comparison of equations (6.8) and (6.5) shows that the transformed stiffnesses are related to the real stiffness by

$$\sum_{i=1}^{M} (EI)'_{wi} = \sum_{i=1}^{M} (EI)_{wi} \left(\frac{z_{1i}}{z_o}\right)^2$$

$$\sum_{i=1}^{Q} (EI)'_{ci} = \sum_{i=1}^{Q} \left[(EI)_{ci} \left(\frac{z_{3i}}{z_o}\right)^2 + (EI_\omega)_{ci} \frac{1}{z_o^2} \right]$$

$$\sum_{i=1}^{N} (GA)'_{fi} = \sum_{i=1}^{N} (GA)_{fi} \left(\frac{z_{2i}}{z_o}\right)^2 + \sum_{i=1}^{Q} (GJ_o)_{ci} \frac{1}{z_o^2}$$

The above equations can be written as,

$$(EI)'_{wi} = \left(\frac{z_{1i}}{z_o}\right)^2 (EI)_{wi}$$

$$(EI)'_{ci} = \left(\frac{z_{3i}}{z_o}\right)^2 (EI)_{ci} + \frac{1}{z_o^2}(EI_\omega)_{ci} \qquad (6.9)$$

$$\sum_{i=1}^{N} (GA)'_{fi} = \frac{1}{z_o^2}\left[\sum_{i=1}^{N} (z_{2i})^2 (GA)_{fi} + \sum_{i=1}^{Q} (GJ_o)_{ci}\right]$$

The elastic and shear moduli may of course be omitted from equations (6.9) to give the corresponding transformation, for the second moments of area and effective shear area. The transformations are simpler if the torsional rigidity GJ_o is relatively small and may be neglected, hence

$$(GA)'_{fi} = \left(\frac{z_{2i}}{z_o}\right)^2 (GA)_{fi}.$$

On substituting equation (6.6) into (6.8), and differentiating, the governing differential equation for the substitute structure becomes,

$$(EI)' \frac{d^4 y_o}{dx^4} - (GA)' \frac{d^2 y_o}{dx^2} = \omega \qquad (6.10)$$

which is identical in form to that obtained from a pure bending analysis of a composite core, wall and frame structure. (This may be obtained from equation 3.12 with the effect of the coupled walls omitted (i.e. the term in the shear flow q is neglected)). In equation 6.10

$$(EI)' = \sum_{i=1}^{M} (EI)'_{wi} + \sum_{i=1}^{Q} (EI)'_{ci} \qquad (6.11)$$

$$(GA)' = \sum_{i=1}^{N} (GA)'_{fi}$$

The solution of equation (6.10) yields the lateral deflection y_o and hence the shears S'_{wi}, S'_{fi} and S'_{ci}, and moments M'_{wi}, M'_{fi} and M'_{ci} in the various wall, frame and core elements of the substitute structure (cf. from equations (2.64) to (2.68)). The corresponding forces in the real structure may be obtained simply by transforming back using the relationships,

$$S_{wi} = \frac{z_o}{z_{1i}} S'_{wi} \qquad M_{wi} = \frac{z_o}{z_{1i}} M'_{wi}$$

$$S_{fi} = \frac{z_o}{z_{2i}} S'_{fi} \qquad M_{fi} = \frac{z_o}{z_{2i}} M'_{fi} \qquad (6.12)$$

$$S_{ci} = \frac{z_o}{z_{3i}} S'_{ci} \qquad M_{ci} = \frac{z_o}{z_{3i}} M'_{ci}$$

6.3 Transformations for coupled shear wall assemblies

Coupled shear walls are subjected in addition to axial forces caused by the coupling actions of the lintel beams or floor slabs at each storey level, and the required transformations may be derived by considering a symmetrical structure consisting of 2R identical coupled wall assemblies as shown in Fig.6.3(a), with a typical wall 'i' being located

at a distance z_{4i} from the central axis. As in the earlier chapters, it is assumed that the discrete set of connecting beams may be replaced by a uniform equivalent connecting medium, to give the same effective stiffness per unit height, and the corresponding set of discrete shear forces in the beams are replaced by a shear flow q in the substitute medium.

The equation of torsional equilibrium is then given by,

$$T = 2\left\{\sum_{i=1}^{R} S_{si} \quad z_{4i}\right\} \qquad (6.13)$$

where S_{si} is the shear force in the i^{th} pair of coupled walls, which is related to the moment M_{si} on the walls and the internal shear flow q_i by the relationship (chapters 2 and 3)

$$S_{si} = -\frac{dM_{si}}{dx} + lq_i = -(EI)_{si}\ \frac{d^3y_{si}}{dx^3} + lq_i \qquad (6.14)$$

where l is the distance between the centroids of the walls, I_{si} is the sum of the second moments of area of the two walls, and y_{si} is the lateral deflection.

Since the lateral deflection y_{si} of wall 'i' is proportional to the distance z_{4i} from the central axis, it follows that all internal forces are also proportional to that distance. That is,

$$q_i = \frac{z_{4i}}{z_o}\ q_o\ ;\ S_{si} = \frac{z_{4i}}{z_o}\ S_{so}\ ;\ M_{si} = \frac{z_{4i}}{z_o} M_{so} \qquad (6.15)$$

It is again assumed that all coupled walls may be transformed into an equivalent plane system at an arbitrary distance z_o from the axis of symmetry. The transformed walls are connected in series by a set of rigid pin-ended links, or equivalent continuous medium, to simulate the floor slabs as shown in Fig. 6.3(b). The equation of horizontal equilibrium is,

$$S_o = T/2z_o = \sum_{i=1}^{R} S'_{si} = \sum_{i=1}^{R} \left[-(EI)'_{si} \frac{d^3 y_o}{dx^3} + l'_i\ q'_i \right] \qquad (6.16)$$

where I'_{si} is the sum of the second moments of area, q'_i is the shear flow in the connecting medium, and l'_i is the distance between centroidal axes in the transformed i^{th} pair of coupled walls.

On substituting equations (6.9), (6.14) and 6.15) into (6.13), and comparing with equation (6.16), it may be shown that when,

$$l'_i = l$$

then,

$$q'_i = \left(\frac{z_{4i}}{z}\right)^2 q_o \qquad (6.17)$$

Hence,

$$q_i = \frac{z_o}{z_{4i}}\ q'_i\ ;\ S_{si} = \frac{z_o}{z_{4i}}\ S'_{si}\ ;\ M_{si} = \frac{z_o}{z_{4i}}\ M'_{si} \qquad (6.18)$$

For the general case of structures consisting of coupled shear walls, cores and frames, consider the idealized structure shown in Fig. 6.4. Following the same procedure as above, all assemblies may be transformed into the plane of the outermost coupled shear walls, distance z_o from the central axis. The compatibility equation of the coupled shear walls located at the datum plane at any level x may be shown to be

$$1\,\frac{dy_o}{dx} - \frac{b^3 h}{12EI_c}\,q_o - \frac{1}{E}\left(\frac{1}{A_1} + \frac{1}{A_2}\right)\int_o^x N_o\,dx = o \qquad (6.19)$$

The axial force N_o in each wall is givenby

$$N_o = \int_x^H q_o\,dx \qquad (6.20)$$

On using equations (6.9) and (6.17), the equations governing the behaviour of the structure (Fig. 6.5) become

$$(EI)_1\,\frac{d^4y_o}{dx^4} = \frac{d^2M}{dx^2} + \left(\frac{b}{2} + d_1\right)\frac{dq_o}{dx} - n_1 \qquad (6.21)$$

$$(EI)_2\,\frac{d^4y_o}{dx^4} = \left(\frac{b}{2} + d_2\right)\frac{dq_o}{dx} + n_1 - n_2 \qquad (6.22)$$

$$-\left(\frac{z_{41}}{z_o}\right)^2 (GA)_1\,\frac{d^2y_o}{dx^2} = n_2 - n_3 \qquad (6.23)$$

$$\left[\left(\frac{z_{31}}{z_o}\right)^2 (EI)_3 + \left(\frac{1}{z_o}^2\right)(EI_\omega)_1\right]\frac{d^4y_o}{dx^4} - \left(\frac{1}{z_o}^2\right)(GJ_o)_1\,\frac{d^2y_o}{dx^2} = n_3 - n_4 \qquad (6.24)$$

$$\left(\frac{z_{11}}{z_o}\right)^2 (EI)_1 \frac{d^4y_o}{dx^4} = \left(\frac{z_{11}}{z_o}\right)^2 \left(\frac{b}{2} + d_1\right) \frac{dq_o}{dx} + n_4 - n_5 \quad (6.25)$$

$$\left(\frac{z_{11}}{z_o}\right)^2 (EI)_2 \frac{d^4y_o}{dx^4} = \left(\frac{z_{11}}{z_o}\right)^2 \left(\frac{b}{2} + d_2\right) \frac{dq_o}{dx} + n_5 - n_6 \quad (6.26)$$

$$-\left(\frac{z_{42}}{z_o}\right)^2 (GA)_2 \frac{d^2y_o}{dx^2} = n_6 - n_7 \quad (6.27)$$

$$\left[\left(\frac{z_{32}}{z_o}\right)^2 (EI)_4 + \left(\frac{1}{z_o^2}\right) (EI_\omega)_2\right] \frac{d^4y_o}{dx^4} \quad (6.28)$$

$$-\left(\frac{1}{z_o^2}\right) (GJ_o)_2 \frac{d^2y_o}{dx^2} = n_7$$

Where M is the static applied moment and $n_i (i = 1\text{-}7)$ are the axial forces in the connecting media (1-7).

The addition of equations (6.21) to (6.28) yields

$$EI \frac{d^4y_o}{dx^4} - GA \frac{d^2y_o}{dx^2} = \frac{d^2M}{dx^2} + L \frac{dq_o}{dx} \quad (6.29)$$

where

$$I = (I_1 + I_2)\left[1 + \left(\frac{z_{11}}{z_o}\right)^2\right] + \left(\frac{z_{31}}{z_o}\right)^2 (I_3)$$

$$+ \left(\frac{z_{32}}{z_o}\right)^2 I_4 + \left(\frac{1}{z_o^2}\right)\left[(I_\omega)_1 + (I_\omega)_2\right]$$

$$GA = \left(\frac{z_{41}}{z_o}\right)^2 (GA)_1 + \left(\frac{z_{42}}{z_o}\right)^2 (GA)_2 + \left(\frac{1}{z_o^2}\right)\left[(GJ_o)_1 + (GJ_o)_2\right]$$

$$L = \left[1 + \left(\frac{z_{11}}{z_o}\right)^2\right] l$$

On eliminating the terms in q_o and N_o from equations (6.19), (6.20) and (6.29), the governing differential equation finally become

$$\frac{d^6 y_o}{dx^6} - m^2 \frac{d^4 y_o}{dx^4} + n_2 \frac{d^2 y_o}{dx^2} = \frac{1}{EI}\left(\frac{d^4 M}{dx^4} - \gamma^2 \frac{d^2 M}{dx^2}\right) \qquad (6.30)$$

where

$$m^2 = \alpha^2 + \beta^2 + \gamma^2 \qquad n^2 = \alpha^2 \gamma^2$$

$$\alpha^2 = \frac{GA}{EI} \qquad \beta^2 = \left[\left(1 + \left(\frac{z_{11}}{z_o}\right)^2\right]\frac{12 I_c l^2}{b^3 h\ I}\right.$$

$$\gamma^2 = \frac{12 I_c}{b^3 h}\left(\frac{1}{A_1} + \frac{1}{A_2}\right)$$

Equation (6.30) is identical in form to the equation derived in chapter 3 for a set of cores, frames and coupled walls subjected to a uniformly distributed loading ω, where $\omega = {}^{t}/_{2z_o}$. The parameters α^2, β^2 and γ^2 must now be defined for the transformed structure as shown in Table 1.

The boundary conditions are the same as before, and so the solution of equation (6.30) will be identical to that given in chapter 3. The complete set of formulae will again apply, giving explicit expressions for the deflection y_o (and hence angle of rotation ${}^{y_o}/_{z_o}$) and all internal forces (shear flows, axial forces, shear forces and bending moments) in the cores, frames and coupled walls of the transformed structure.

The corresponding forces in the real structure are derived by transforming back using the simple relationships of equations (6.12) and (6.18). The axial forces in the slabs and the top concentrated interactive forces may be obtained from the equilibrium conditions for the individual components as in chapter 3.

COMPUTATIONAL PROCEDURE

The steps in the analysis are:-

(1) Transform all elements into any datum plane at a distance z_o from the central axis, by factoring all flexural and shearing rigidities according to equation

(6.11). Although the datum plane may be chosen in any suitable position, it is probably most convenient to use the plane of the outermost set of coupled walls to relate most closely to chapter 3.

(2) Calculate the effective distributed loading $\omega(=^{t}/2z_{o})$ at this position.

(3) Evaluate the structural parameters α^2, β^2 and γ^2 using Table 1. The lateral deflection y_o, the shear flow in the connecting medium the axial force in each coupled wall, and the bending moments and shear forces in all components follow from equations (3.22) to (3.28) of chapter 3.

(4) Calculate the corresponding forces in the components of the real structure by factorisation according to equations (6.12) and (6.18).

PURE BENDING Parameter (Chapter 3)	PURE TORSION Transformed parameter
$\alpha^2 = \frac{GA}{EI}$	$\alpha^2 = \frac{GA}{EI}$
$GA = \sum_{i=1}^{N} (GA)_{fi}$	$GA = \sum_{i=1}^{N} (\frac{z_{2i}}{z_o})^2 (GA)_{fi} + \sum_{i=1}^{Q} \frac{1}{z_o^2} (GJ_o)_{ci}$
$I = RI_s + \sum_{i=1}^{M} I_{wi}$	$I = I_s \sum_{i=1}^{R} (\frac{z_{4i}}{z_o})^2 + \sum_{i=1}^{M} (\frac{z_{1i}}{z_o})^2 I_{wi} + \sum_{i=1}^{Q} (\frac{z_{3i}}{z_o})^2 I_{ci} + \sum_{i=1}^{Q} (\frac{1}{z_o^2}) (I_\omega)_{ci}$
$\beta^2 = R \frac{12 I_c l^2}{b^3 h I}$	$\beta^2 = \sum_{i=1}^{R} (\frac{z_{4i}}{z_o})^2 \frac{12 I_c l^2}{b^3 h I}$
$\gamma^2 = \frac{12 I_c}{b^3 h} (\frac{1}{A_1} + \frac{1}{A_2})$	$\gamma^2 = \frac{12 I_c}{b^3 h} (\frac{1}{A_1} + \frac{1}{A_2})$
$L = l$	$L = l \sum_{i=1}^{R} (\frac{z_{4i}}{z_o})^2$ *

(* Note that L must be used in place of l in equations (23) and (24) of chapter 3).

Table 1. Definition of structural parameters for cases of pure bending and transformed pure torsion.

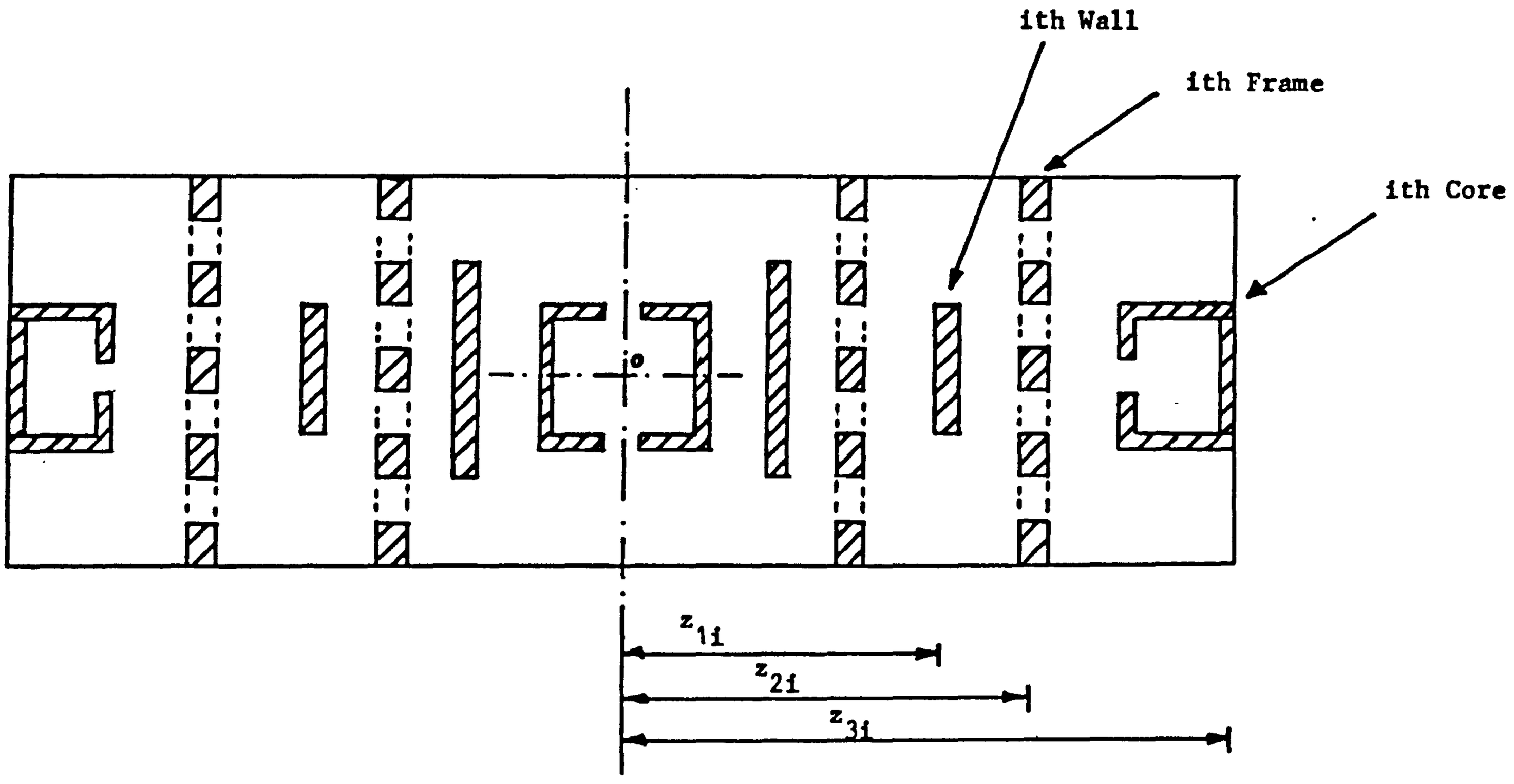

Fig. 6.1. Symmetrical structure consisting of independent walls, cores and rigidly jointed frames.

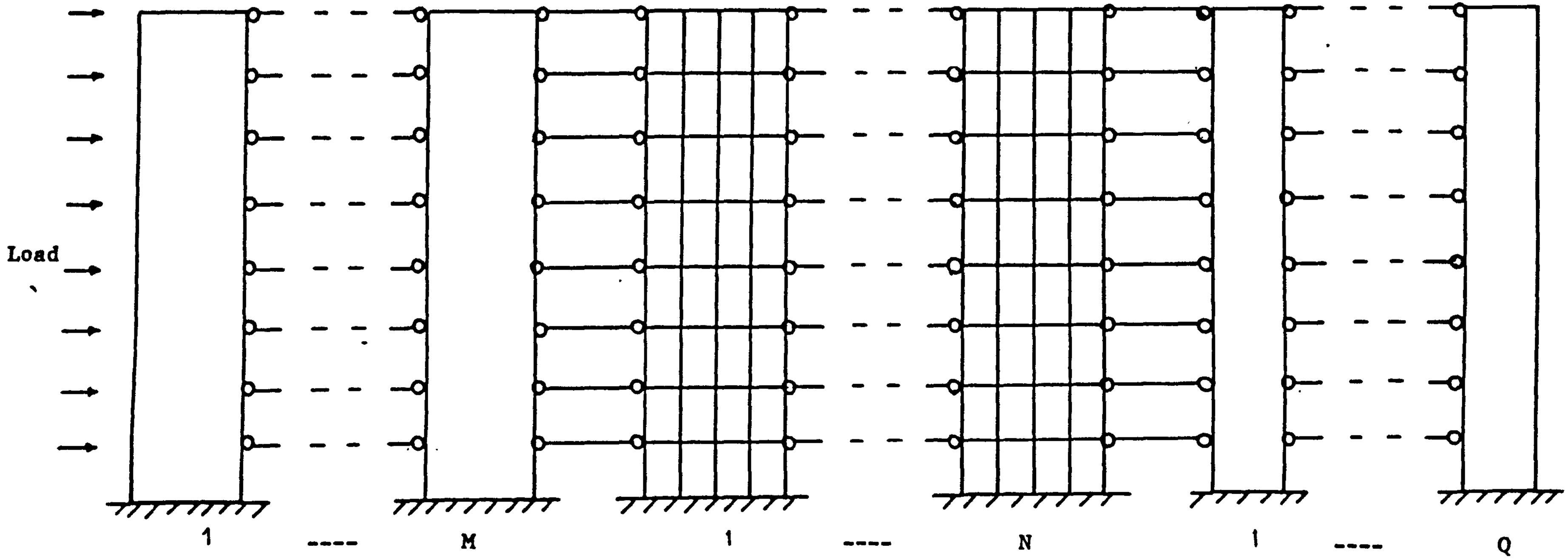

Fig. 6.2. Representation of three-dimensional symmetrical core-wall-frame structure by equivalent plane system.

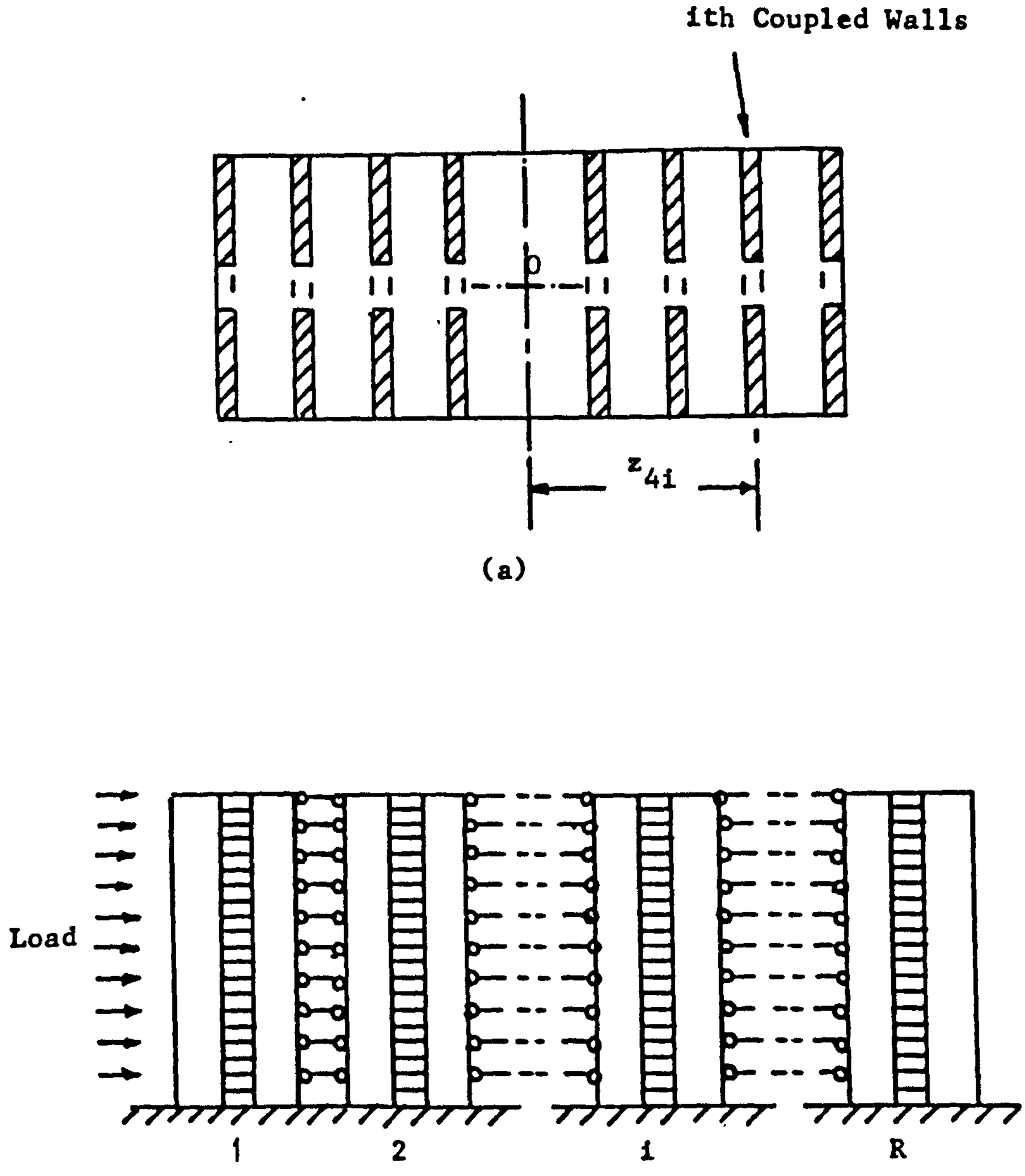

Fig. 6.3. Representation of three-dimensional symmetrical coupled shear wall structure by equivalent plane system.

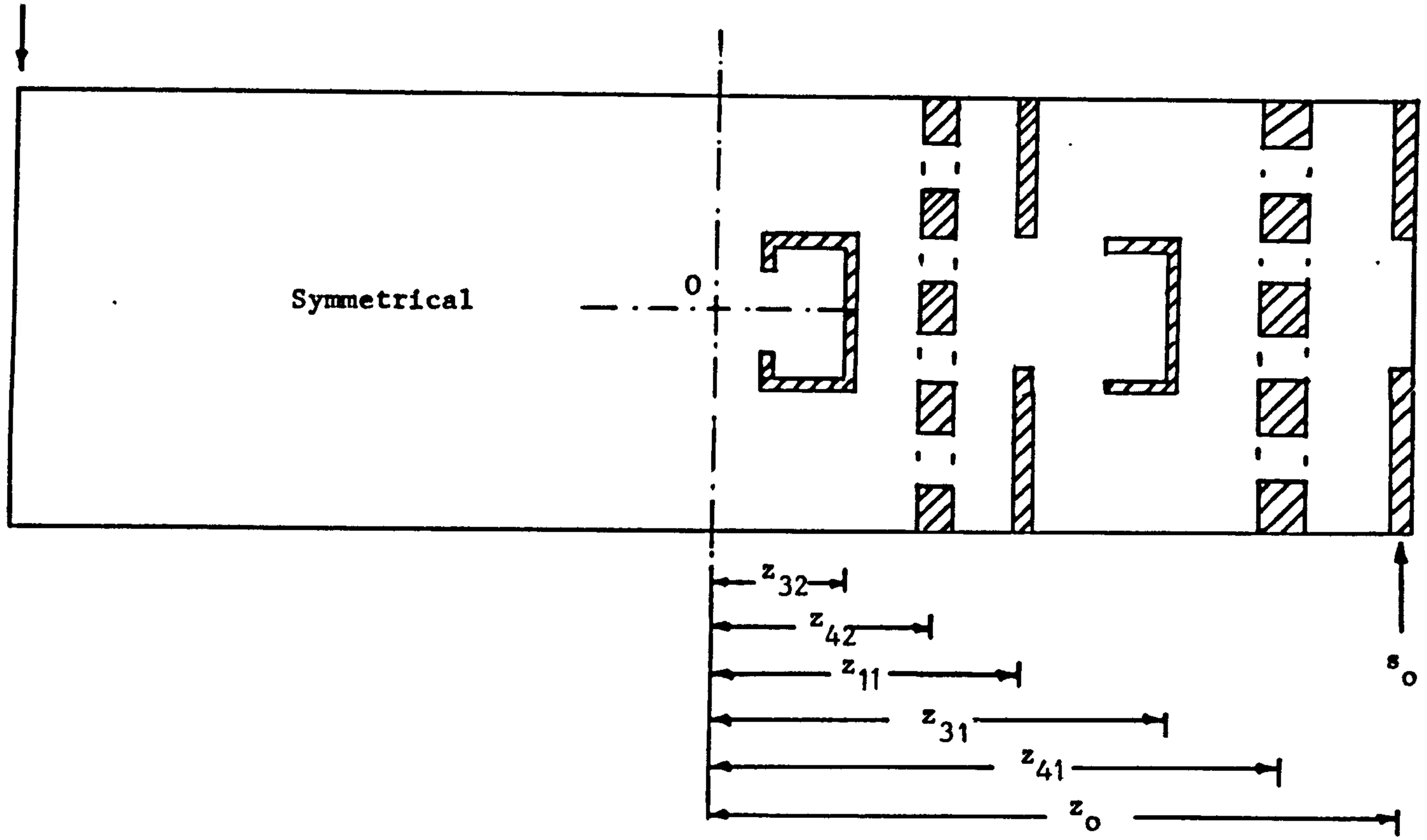

Fig. 6.4. Symmetrical structure consisting of coupled shear walls, cores and rigidly jointed frames.

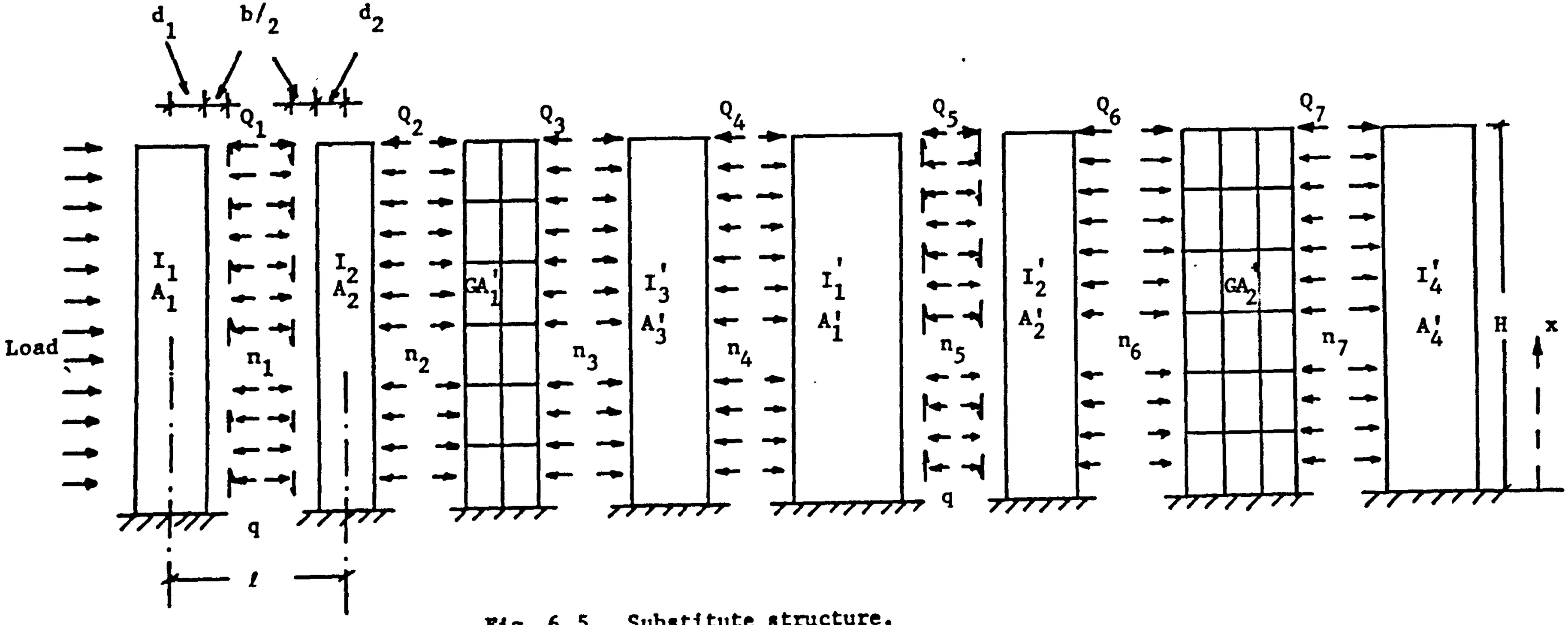

Fig. 6.5. Substitute structure.

C H A P T E R 7

ANALYSIS OF THREE-DIMENSIONAL ASYMMETRIC STRUCTURES CONSISTING OF ASSEMBLIES OF CORES, SHEAR WALLS AND RIGIDLY-JOINTED FRAMEWORKS SUBJECTED TO BENDING AND TORSION.

NOTATION

$O(x,y,x)$	set of orthogonal reference axes
E	elastic modulus
y_i	deflection of the element 'i' in the Oy direction
z_i	deflection of the element 'i' in the Oz direction
θ	rotation about vertical Ox axis
y_o, z_o,	co-ordinates of the origin O
w,f,c	suffices denoting frame, shear wall and core assemblies
l_{wi}, l_{fi}, l_{ci}	horizontal distances between the centroids of shear wall, frame and core 'i' and the datum axis Oy
r_{wi}, r_{fi}, r_{ci}	perpendicular distances between the centroids of shear wall, frame and core 'i' and the datum axis Oz
S_{wi}, S_{fi}, S_{ci}	Shear forces in shear wall, frame and core 'i' in the Oy direction
$S'_{wi}, S'_{fi}, S'_{ci}$	shear forces in shear wall, frame and core 'i' in the Oz direction
$(I_z)_{wi}, (I_z)_{ci}, (I_y)_{wi}$	second moment of areas of shear wall
$(I_y)_{ci}$	and core 'i' in two orthogonal directions
$(I_y)_{fi}$	second moment of area of the columns
$(GA)_{fi}$	effective shearing rigidity of the frame 'i' located in the Oxy plane
G	shear modulus
J_o, J	torsional constants

W	distributed lateral load
I_ω	warping constant
D	operator d/dx
H	total height
ω	unformly distributed lateral force intensity
a_i	structural parameters (i = 1 - 9)
b_i	structural parameters (i = 1 - 6)
B_i	constants of integration (i = 0 - 5)
C_i	constants of integration (i = 0 - 5)
ξ	non-dimensional height (x/H)
0	suffix denoting base of structure
z	eccentricity of lateral load relative to x axis
M_{wi}, M_{fi}, M_{ci}, $M'_{wi}, M'_{fi}, M'_{ci}$	bending moments in the shear wall, frame and core 'i' in two orthogonal directions
$\bar{y}_{fi}$, $\bar{z}_{fi}$	deflections of frame 'i' located in the Oxz plane in two orthogonal directions Oy and Oz
$\bar{I}_{fi}$, $\bar{l}_{fi}$,	horizontal and perpendicular distances between the centoid of the i^{th} frame (in Oxz plane) and the datum axes yz respectively
$(\bar{I}_z)_{fi}, (\overline{GA})_{fi}$	second moment of area and effective shearing rigidity of the i^{th} frame in the Oxz plane

CHAPTER 7

ANALYSIS OF THREE-DIMENSIONAL ASYMMETRIC STRUCTURES CONSISTING OF ASSEMBLIES OF CORES, SHEAR WALLS AND RIGIDLY JOINTED FRAMEWORKS SUBJECTED TO BENDING AND TORSION.

7.1 Introduction

The analyses of three-dimensional symmetrical structures consisting of assemblies of cores, shear walls and rigidly-jointed frameworks, subjected to lateral forces which produce bending and torsion were presented in chapters 2 and 6 respectively. As described in chapter 2, considerable load redistribution can occur between assemblies which deform with a primarily bending configuration (e.g. box cores and shear walls) and those which deform with a primarily shear configuration (e.g. frames) when coupled together and subjected to distributed horizontal loading. It is therefore important to consider the distribution of load between the various assemblies in the complete structure.

Practically all recent studies have been devoted to the planar interaction of flexural walls and frames. However, in many tall building structures the architectural and building services requirements result in the asymmetric location of core, shear wall and frame assemblies. Lateral forces resulting from wind and/or earthquake action produce a complex behaviour, involving both torsional and bending

deformations. A combined bending and torsional analysis is therefore required.

As described in chapter 1, many investigators have presented methods which deal with this type of problem, using methods of analysis which require access to a digital computer for even the simplest loadings. None of the methods presented is suitable for rapid hand calculations for the initial proportioning of components at the preliminary stages of the design process. In particular, the warping behaviour of the core assemblies has often been neglected. However, if from structural asymmetry or eccentric loading the building is subjected to torsion, the core may be expected to play a useful part in resisting the twist.

In this chapter a relatively simple hand method is presented for the static analysis of uniform asymmetric structures consisting of cores, shear walls and parallel assemblies of rigidly jointed frameworks. The analysis is later extended to include frame assemblies in two orthogonal directions.

By using the general equilibrium conditions for the structure, and solving the three generated differential equations simultaneously, closed form solutions may be achieved for standard load cases, enabling the complete distribution of forces, deflections and rotations to be determined rapidly.

7.2 Assumptions

The proposed method is based on the following basic assumptions:

1 - The distributed wind loading acts at an angle α to the longitudinal axis.

2 - The columns, independent shear walls and box cores have uniform (sectional) properties and dimensions throughout the height of the building and are rigidly fixed at the base.

3 - Diaphragm action of the floors is assumed, so that the whole structural assembly moves as a rigid body in each horizontal plane.

4 - The rigidly-jointed frameworks are treated as vertical shear cantilevers.

ANALYSIS OF STRUCTURES CONSISTING OF CORES, SHEAR WALLS AND PARALLEL ASSEMBLIES OF RIGIDLY-JOINTED FRAME-WORKS

7.3 Analysis

Consider an asymmetrical building structure which consists of M assemblies of independent shear walls, N rigidly-jointed frameworks and R service cores as shown

in Fig. 7.1 . Under the action of wind forces which act at a distance z from the left hand corner O at an angle α to the longitudinal axis, the structure will undergo translational displacements y_i and z_i in the y and z directions, and the floors will undergo a rotational displacement Θ in the Oyz plane. For convenience O is chosen as datum point, and all displacements are referred to O, therefore, the displacements of any element (e.g. i^{th} element) at level x in two orthogonal directions y and z may be expressed as

$$y_{wi} = y_o + l_{wi}\Theta \qquad z_{wi} = z_o - r_{wi}\Theta$$

$$y_{fi} = y_o + l_{fi}\Theta \qquad z_{fi} = z_o - r_{fi}\Theta \qquad (7.1)$$

$$y_{ci} = y_o + l_{ci}\Theta \qquad z_{ci} = z_o - r_{ci}\Theta$$

where f, w and c are suffices denoting frame, shear wall and core assemblies respectively, y_o and z_o are the deflections of point O in the Ozy plane and l_{fi}, l_{wi}, l_{ci}, r_{fi}, r_{wi} and r_{ci} are the horizontal and perpendicular distances between the centroids of frame, shear wall and core assemblies and the datum axes yz respectively (Fig.7.1).

Using the notation of Fig. 7.1 and transferring the distributed lateral load W to the datum position O, the equations governing the static equilibrium of the structure become

for equilibrium in Oy direction

$$V = \sum_{i=1}^{M} S_{wi} + \sum_{i=1}^{N} S_{fi} + \sum_{i=1}^{R} S_{ci} \qquad (7.2)$$

for equilibrium in Oz direction

$$P = \sum_{i=1}^{M} S'_{wi} + \sum_{i=1}^{N} S'_{fi} + \sum_{i=1}^{R} S'_{ci} \qquad (7.3)$$

for rotational equilibrium

$$T = -\sum_{i=1}^{M} S_{wi}\, l_{wi} - \sum_{i=1}^{N} S_{fi}\, l_{fi} - \sum_{i=1}^{R} S_{ci}\, l_{ci} - \sum_{i=1}^{M} T_{wi} - \sum_{i=1}^{N} T_{fi}$$

$$(7.4)$$

$$- \sum_{i=1}^{R} T_{ci} + \sum_{i=1}^{M} S'_{wi}\, r_{wi} + \sum_{i=1}^{N} S'_{wi}\, r_{wi} + \sum_{i=1}^{R} S'_{ci}\, r_{ci}$$

where $V = W \sin\alpha$, $P = W \cos\alpha$, $T = -Wz \sin\alpha$ and S_{wi} , S_{fi} and S_{ci} are the shear forces in the various elements in the Oy direction and S'_{wi}, S'_{fi}, and S'_{ci} are the shear forces in the Oz direction. These forces act through the centroids and shear centre of the shear wall, frame and core assemblies

respectively and are given by

$$S_{wi} = - E(I_z)_{wi} \frac{d^3 y_{wi}}{dx^3}$$

$$S_{fi} = (GA)_{fi} \frac{dy_{fi}}{dx} \qquad (7.5)$$

$$S_{ci} = - E(I_z)_{ci} \frac{d^3 y_{ci}}{dx^3}$$

and

$$S'_{wi} = - E(I_y)_{wi} \frac{d^3 z_{wi}}{dx^3}$$

$$S'_{wi} = - E(I_y)_{fi} \frac{d^3 z_{fi}}{dx^3} \qquad (7.6)$$

$$S'_{ci} = - E(I_y)_{ci} \frac{d^3 z_{ci}}{dx^3}$$

where $(I_z)_{wi}$, $(I_z)_{ci}$, $(I_y)_{wi}$ and $(I_y)_{ci}$ are the second moment of areas of the shear wall and core 'i' in the two orthogonal directions. $(I_y)_{fi}$ is the second moment of area of the columns and $(GA)_{fi}$ is the equivalent shearing rigidity of the frame 'i'.

In equation (7.4) T_{wi}, T_{fi} and T_{ci} are the internal torsional moments on the wall, frame and core 'i'. For core assemblies, T_{ci} consists of warping as well as

St. Venant torsional resistance given by equation (5.33), and for walls $T_{wi} = (GJ)_{wi} \frac{d\theta}{dx}$ and the torsional resistances of the frame elements are given by $T_{fi} = (GJ)_{fi} \frac{d\theta}{dx}$.

Substituting for S_{wi}, S_{fi} and S_{ci} from equations (7.5) into (7.2), V becomes

$$V = - \sum_{i=1}^{M} E(I_z)_{wi} \frac{d^3 y_{wi}}{dx^3} + \sum_{i=1}^{N} (GA)_{fi} \frac{dy_{fi}}{dx} - \sum_{i=1}^{R} E(I_z)_{ci} \frac{d^3 y_{ci}}{dx^3} \qquad (7.7)$$

On experiencing the deflections in the various elements in terms of the datum deflection y_o and the rotation θ , equation (7.7) becomes, on using equations (7.1)

$$V = - \sum_{i=1}^{M} E(I_z)_{wi} \frac{d^3}{dx^3} (y_o + l_{wi}\theta) + \sum_{i=1}^{N} (GA)_{fi} \frac{d}{dx} (y_o + l_{fi}\theta) - \sum_{i=1}^{R} E(I_z)_{ci} \frac{d^3}{dx^3} (y_o + l_{ci}\theta) \qquad (7.8)$$

or

$$V = a_1 \frac{dy_o}{dx} + a_2 \frac{d\Theta}{dx} - a_3 \frac{d^3y_o}{dx^3} - a_4 \frac{d^3\Theta}{dx^3} \qquad (7.9)$$

where

$$a_1 = \sum_{i=1}^{N} (GA)_{fi}$$

$$a_2 = \sum_{i=1}^{N} (GA)_{fi}\, l_{fi}$$

$$a_3 = E \left(\sum_{i=1}^{M} (I_z)_{wi} + \sum_{i=1}^{R} (I_z)_{ci} \right)$$

$$a_4 = E \left(\sum_{i=1}^{M} (I_z)_{wi}\, l_{wi} + \sum_{i=1}^{R} (I_z)_{ci}\, l_{ci} \right)$$

Using equations (7.1) and (7.6) and following the same procedure as above, equation (7.3) becomes

$$P = - \sum_{i=1}^{M} E(I_y)_{wi} \frac{d^3}{dx^3} (z_o - r_{wi}\Theta) - \sum_{i=1}^{N} E(I_y)_{fi} \frac{d^3}{dx^3} (z_o - r_{fi}\Theta) - \sum_{i=1}^{R} E(I_y)_{ci} \frac{d^3}{dx^3} (z_o - r_{ci}\Theta) \qquad (7.10)$$

or

$$P = - a_5 \frac{d^3 z_o}{dx^3} + a_6 \frac{d^3\Theta}{dx^3} \qquad (7.11)$$

where

$$a_5 = E\left(\sum_{i=1}^{M} (I_y)_{wi} + \sum_{i=1}^{N} (I_y)_{fi} + \sum_{i=1}^{R} (I_y)_{ci}\right)$$

$$a_6 = E\left(\sum_{i=1}^{M} (I_y)_{wi}\, r_{wi} + \sum_{i=1}^{N} (I_y)_{fi}\, r_{fi} + \sum_{i=1}^{R} (I_y)_{ci}\, r_{ci}\right)$$

In an analogous manner, on substituting for the shear forces S_{wi}, S_{fi}, S_{ci}, S'_{wi}, S'_{fi}, S'_{ci} and the internal torsional moments T_{wi} and T_{ci} from equations (7.5), (7.6) and (5.33), and expressing the deflections interms of the datum deflections y_o and z_o, and rotation Θ , equation (7.4) becomes, on using equations (7.1)

$$T = \sum_{i=1}^{M} E(I_z)_{wi}\, l_{wi}\, \frac{d^3}{dx^3}\, (y_o + l_{wi}\Theta)$$

$$- \sum_{i=1}^{N} (GA)_{fi}\, l_{fi}\, \frac{d}{dx}\, (y_o + l_{fi}\Theta)$$

$$+ \sum_{i=1}^{R} E(I_z)_{ci}\, l_{ci}\, \frac{d^3}{dx^3}\, (y_o + l_{ci}\Theta)$$

$$- \sum_{i=1}^{M} (GJ)_{wi}\, \frac{d\Theta}{dx} - \sum_{i=1}^{R} (GJ_o)_{ci}\, \frac{d\Theta}{dx}$$

$$- \sum_{i=1}^{N} (GJ)_{fi} \frac{d\theta}{dx} + \sum_{i=1}^{R} E(I_\omega)_{ci} \frac{d^3\theta}{dx^3}$$

$$- \sum_{i=1}^{M} E(I_y)_{wi} r_{wi} \frac{d^3}{dx^3} (z_o - r_{wi}\theta)$$

$$- \sum_{i=1}^{N} E(I_y)_{fi} r_{fi} \frac{d^3}{dx^3} (z_o - r_{fi}\theta)$$

$$- \sum_{i=1}^{R} E(I_y)_{ci} r_{ci} \frac{d^3}{dx^3} (z_o - r_{ci}\theta) \qquad (7.12)$$

or

$$T = - a_2 \frac{dy_o}{dx} + a_7 \frac{d\theta}{dx} + a_4 \frac{d^3y_o}{dx^3} + a_8 \frac{d^3\theta}{dx^3} - a_6 \frac{d^3z_o}{dx^3} \qquad (7.13)$$

where

$$a_7 = -\left(\sum_{i=1}^{M} (GJ)_{wi} + \sum_{i=1}^{N} (GA)_{fi} l_{fi}^2 + \sum_{i=1}^{R} (GJ_o)_{ci} + \sum_{i=1}^{N} (GJ)_{fi} \right)$$

$$a_8 = E \left(\sum_{i=1}^{M} (I_z)_{wi} l_{wi}^2 + \sum_{i=1}^{R} (I_z)_{ci} l_{ci}^2 + \sum_{i=1}^{R} (I_\omega)_{ci} \right.$$

$$\left. + \sum_{i=1}^{M} (I_y)_{wi} r_{wi}^2 + \sum_{i=1}^{N} (I_y)_{fi} r_{fi}^2 + \sum_{i=1}^{R} (I_y)_{ci} r_{ci}^2 \right)$$

On substituting for $\frac{d^3 z_o}{dx^3}$ from equation (7.11) into (7.13) the latter equation becomes

$$T - \frac{a_6}{a_5} P = -a_2 \frac{dy_o}{dx} + a_7 \frac{d\theta}{dx} + a_4 \frac{d^3 y_o}{dx^3} + a_9 \frac{d^3\theta}{dx^3} \quad (7.14)$$

where

$$a_9 = a_8 - \left(\frac{a_6}{a_5}\right)^2$$

Equations (7.9) and (7.14) may be expressed as

$$(a_1 D - a_3 D^3)\ y_o + (a_2 D - a_4 D^3)\theta = V \quad (7.15)$$

and

$$(-a_2 D + a_4 D^3)\ y_o + (a_7 D + a_9 D^3)\theta = T - \frac{a_6}{a_5} P \quad (7.16)$$

where D is the operator $\frac{d}{dx}$.

On eliminating the terms in θ and y_o from equations (7.15) and (7.16) respectively, the governing differential equations finally become

$$\frac{d^6 y_o}{dx^6} - m^2 \frac{d^4 y_o}{dx^4} + n^2 \frac{d^2 y_o}{dx^2} = \phi_1 (x) \quad (7.17)$$

$$\frac{d^6\theta}{dx^6} - m^2 \frac{d^4\theta}{dx^4} + n^2 \frac{d^2\theta}{dx^2} = \phi_2 (x) \quad (7.18)$$

where

$$m^2 = \frac{a_3\, a_7 - a_1\, a_9 + 2a_2\, a_4}{a_4^{\,2} - a_3\, a_9}$$

$$n^2 = \frac{a_1\, a_7 + a_2^{\,2}}{a_4^{\,2} - a_3\, a_9}$$

and

$$\phi_1(x) = \frac{1}{a_4^{\,2} - a_3\, a_9}\left[a_7 \frac{dV}{dx} + a_9 \frac{d^3V}{dx^3} + \frac{a_2\, a_6}{a_5}\frac{dP}{dx} - \frac{a_4\, a_6}{a_5}\frac{d^3P}{dx^3} - a_2 \frac{dT}{dx} + a_4 \frac{d^3T}{dx^3}\right] \qquad (7.19)$$

$$\phi_2(x) = \frac{1}{a_4^{\,2} - a_3\, a_9}\left[a_2 \frac{dV}{dx} - a_4 \frac{d^3V}{dx^3} - \frac{a_1\, a_6}{a_5}\frac{dP}{dx} + a_3 \frac{a_6}{a_5}\frac{d^3P}{dx^3} + a_1 \frac{dT}{dx} - a_3 \frac{d^3T}{dx^3}\right] \qquad (7.20)$$

The general solutions of equations (7.17) and (7.18) for any form of lateral loading may be expressed in the form

$$y_o = B_o + B_1\, x/_H + B_2 \cosh(k\, x/_H) + B_3 \sinh(k\, x/_H) + B_4 \cosh(r\, x/_H) + B_5 \sinh(r\, x/_H) + y_{oPI} \qquad (7.21)$$

and

$$\Theta = C_o + C_1 \, x/_H + C_2 \cosh(k \, x/_H) + C_3 \sinh(k \, x/_H)$$

$$+ C_4 \cosh(r \, x/_H) + C_5 \sinh(r \, x/_H) + \Theta_{PI} \qquad (7.22)$$

where B_i (i=0-5) and c_i (i=0-5) are constants of integration to be determined from the necessary boundary conditions, and $y_{o\,PI}$ and Θ_{PI} are the particular integral solutions, i.e. solutions for a specific form of loading.

In equations (7.21) and (7.22) $k = pH$ and $r = \frac{nH}{p}$

where

$$p^2 = \left[m^2 + (m^4 - 4n^2)^{1/2} \right] /2$$

$$\frac{n^2}{p^2} = \left[m^2 - (m^4 - 4n^2)^{1/2} \right] /2$$

In this analysis p and $\frac{n}{p}$ are assumed to be real, but the same procedure applies even if they were complex, though the mathematical calculations would be lengthier and more laborious to deal with.

Boundary conditions

In order to determine the constants B_i and c_i of equations (7.21) and (7.22), it is necessary to derive six

independent boundary conditions for each equation. If the structure is rigidly built in at the base, then at $x = o$

$$y_o = o \qquad \text{and} \qquad \frac{dy_o}{dx} = o \tag{7.23}$$

and

$$\Theta = o \qquad \text{and} \qquad \frac{d\Theta}{dx} = o \tag{7.24}$$

At the top, the bending moment in each element is equal to zero, and so, at $x = H$

$$\frac{d^2y_o}{dx^2} = o \tag{7.25}$$

and

$$\frac{d^2\Theta}{dx^2} = o \tag{7.26}$$

At $x = o$, equations (7.9) and (7.14) become, on using equations (7.23) and (7.24)

$$(V)_o = -a_3\left(\frac{d^3y_o}{dx^3}\right)_o - a_4\left(\frac{d^3\Theta}{dx^3}\right)_o \tag{7.27}$$

$$(\Gamma)_o - \frac{a_6}{a_5}(P)_o = a_4\left(\frac{d^3y_o}{dx^3}\right)_o + a_9\left(\frac{d^3\Theta}{dx^3}\right)_o \tag{7.28}$$

Solution of equations (7.27) and (7.28) simultaneously yields the following boundary consitions, at $x = o$,

$$\frac{d^3y_o}{dx^3} = \frac{1}{a_4^2 - a_3 a_9}\left[a_9 (V)_o - \frac{a_4 a_6}{a_5}(P)_o + a_4(T)_o \right] \tag{7.29}$$

$$\frac{d^3\theta}{dx^3} = \frac{1}{a_4^2 - a_3 a_9}\left[-a_4 (V)_o + \frac{a_3 a_6}{a_5}(P)_o - a_3 (T)_o \right] \tag{7.30}$$

Differentiation of equations (7.9) and (7.14) once, followed by substitution of equations (7.25) and (7.26), gives, at $x = H$

$$\left(\frac{dV}{dx}\right)_H = - a_3 \left(\frac{d^4y_o}{dx^4}\right)_H - a_4 \left(\frac{d^4\theta}{dx^4}\right)_H \tag{7.31}$$

and

$$\left(\frac{dT}{dx}\right)_H - \frac{a_6}{a_5}\left(\frac{dP}{dx}\right)_H = a_4\left(\frac{d^4y_o}{dx^4}\right)_H + a_9 \left(\frac{d^4\theta}{dx^4}\right)_H \tag{7.32}$$

Hence, from equations (7.31) and (7.32), at $x = H$

$$\frac{d^4y_o}{dx^4} = \frac{1}{a_4^2 - a_3 a_9}\left[a_9 \left(\frac{dV}{dx}\right)_H - \frac{a_4 a_6}{a_5}\left(\frac{dP}{dx}\right)_H + a_4 \left(\frac{dT}{dx}\right)_H \right] \tag{7.33}$$

and

$$\frac{d^4\Theta}{dx^4} = \frac{1}{a_4^2 - a_3\, a_9}\left[-a_4\left(\frac{dV}{dx}\right)_H + \frac{a_3\, a_6}{a_5}\left(\frac{dP}{dx}\right)_H - a_3\left(\frac{dT}{dx}\right)_H\right] \tag{7.34}$$

On differentiation of equations (7.9) and (7.11) twice, followed by substitution of equations (7.29) and (7.30), the remaining boundary conditions become, at x=o

$$\frac{d^5 y_o}{dx^5} = \frac{1}{a_4^2 - a_3\, a_9}\left[-a_{10}(V)_o + a_9\left(\frac{d^2V}{dx^2}\right)_o - a_{12}(P)_o - \frac{a_4\, a_6}{a_5}\left(\frac{d^2P}{dx^2}\right)_o + a_{11}(T)_o + a_4\left(\frac{d^2T}{dx^2}\right)_o\right] \tag{7.35}$$

and

$$\frac{d^5\Theta}{dx^5} = \frac{1}{a_4^2 - a_3\, a_9}\left[a_{13}(V)_o - a_4\left(\frac{d^2V}{dx^2}\right)_o + a_{15}(P)_o + \frac{a_3\, a_6}{a_5}\left(\frac{d^2P}{dx^2}\right)_o - a_{14}(T)_o - a_3\left(\frac{d^2T}{dx^2}\right)_o\right] \tag{7.36}$$

where

$$a_{10} = \frac{a_1 (a_9)^2 - 2a_2\, a_4\, a_9 - (a_4)^2\, a_7}{a_4^2 - a_3\, a_9}$$

$$a_{11} = \frac{-a_1\, a_4\, a_9 + a_2 (a_4)^2 + a_2\, a_3\, a_9 + a_3\, a_4\, a_7}{a_4^2 - a_3\, a_9}$$

$$a_{12} = a_{11} \frac{a_6}{a_5}$$

$$a_{13} = \frac{a_1 a_4 a_9 - a_2 a_3 a_9 - a_2 (a_4)^2 - a_3 a_4 a_7}{a_4^2 - a_3 a_9}$$

$$a_{14} = \frac{-a_1(a_4)^2 + 2a_2 a_3 a_4 + (a_3)^2 a_7}{a_4^2 - a_3 a_9}$$

$$a_{15} = a_{14} \frac{a_6}{a_5}$$

Uniformly distributed wind loading

In order to achieve a solution, the particular case of a uniformly distributed wind loading of intensity ω per unit height is considered. In that case

$$V = \omega \sin \alpha (H-x)$$

$$P = \omega \cos \alpha (H-x)$$

$$T = -\omega z \sin \alpha (H-x)$$

hence

$$\frac{dv}{dx} = -\omega \sin \alpha$$

$$\frac{dP}{dx} = -\omega \cos \alpha \qquad (7.37)$$

$$\frac{dT}{dx} = \omega z \sin \alpha$$

and

$$\frac{d^2V}{dx^2} = \frac{d^2P}{dx^2} = \frac{d^2T}{dx^2} = 0$$

On substituting for the load functions $\phi_1(x)$ and $\phi_2(x)$ in equations (7.17) and (7.18), the simplest particular integrals y_{oPI} and Θ_{PI} become

$$y_{oPI} = \frac{\omega \gamma_1^2 x^2}{2n^2} \tag{7.38}$$

and

$$\Theta_{PI} = \frac{\omega \gamma_2^2 x^2}{2n^2} \tag{7.39}$$

where

$$\gamma_1^2 = \frac{1}{a_4^2 - a_3 a_9}\left[-a_7 \sin\alpha - a_2 \frac{a_6}{a_5} \cos\alpha - a_2 z \sin\alpha\right]$$

$$\gamma_2^2 = \frac{1}{a_4^2 - a_3 a_9}\left[-a_2 \sin\alpha + a_1 \frac{a_6}{a_5} \cos\alpha + a_1 z \sin\alpha\right]$$

Substitution of equations (7.37) into the boundary conditions (7.29) - (7.36), yields the following conditions for the uniformly distributed load of ω per unit height.

at x = o

$$\frac{d^3 y_o}{dx^3} = \Delta_1 \omega H$$

$$\frac{d^3 \theta}{dx^3} = \beta_1 \omega H \qquad (7.40)$$

and

$$\frac{d^5 y_o}{dx^5} = \Delta_2 \omega H$$

$$\frac{d^5 \theta}{dx^5} = \beta_2 \omega H \qquad (7.41)$$

at x = H

$$\frac{d^4 y_o}{dx^4} = -\Delta_1 \omega$$

$$\frac{d^4 \theta}{dx^4} = -\beta_1 \omega \qquad (7.42)$$

where

$$\Delta_1 = \frac{1}{a_4^2 - a_3 a_9} \left[a_9 \sin\alpha - a_4 \frac{a_6}{a_5} \cos\alpha - a_4 z \sin\alpha \right]$$

$$\Delta_2 = \frac{1}{a_4^2 - a_3 a_9} \left[-a_{10} \sin\alpha - a_{12} \cos\alpha - a_{11} z \sin\alpha \right]$$

$$\beta_1 = \frac{1}{a_4^2 - a_3 a_9}\left[-a_4 \sin\alpha + a_3 \frac{a_6}{a_5} \cos\alpha + a_3 z \sin\alpha\right]$$

$$\beta_2 = \frac{1}{a_4^2 - a_3 a_9}\left[a_{13} \sin\alpha + a_{15} \cos\alpha + a_{14} z \sin\alpha\right]$$

The remaining boundary conditions are as expressed by equations (7.23)- (7.26).

Then on substituting equations (7.21) and (7.22) into the above boundary conditions, and solving for the integration constants, it is found that

$$B_o = -B_2 - B_4$$

$$B_1 = \frac{\omega H^2}{p^2 n^2}\left[p^2 \Delta_2 - (n^2 + p^4)\Delta_1\right]$$

$$B_2 = \frac{\omega}{p^4(n^2-p^4)\cosh k}\left[(p^2\Delta_2 - n^2\Delta_1)\, k \sinh k + p^2(p^2\Delta_1 - \gamma_1^2)\right]$$

$$B_3 = \frac{\omega H (n^2\Delta_1 - p^2\Delta_2)}{p^3(n^2 - p^4)}$$

$$B_4 = \frac{\omega p^4}{n^4(n^2 - p^4)\cosh r}\left[p^2(p^2\Delta_1 - \Delta_2)\, r \sinh r + (p^2\gamma_1^2 - n^2\Delta_1)\right]$$

$$B_5 = \frac{\omega H p^5(\Delta_2 - p_2\Delta_1)}{n^3(n^2 - p4)}$$

The constants C_i $(i = o - 5)$ may be obtained simply, by substituting β_1, β_2, and γ_2 for Δ_1, Δ_2 and γ_1 respectively in the above relationships. Hence, the general solutions for y_o and Θ become

$$y_o = \frac{\omega}{p^4(n^2 - p^4)\cosh k}\left[(p^2\Delta_2 - n^2\Delta_1)k \sinh k + p^2(p^2\Delta_1 - \gamma_1^2)\right]\times$$

$$(\cosh k\xi - 1) + \frac{\omega H(n^2\Delta_1 - p^2\Delta_2)}{p^3(n^2 - p^4)} \sinh k\xi$$

$$+ \frac{\omega H p^5(\Delta_2 - p^2\Delta_1)}{n^3(n^2 - p^4)} \sinh r\xi + \frac{\omega p^4}{n^4(n^2 - p^4)\cosh r}\left[p^2(p^2\Delta_1 - \Delta_2)\times\right.$$

$$\left. r \sinh r \right] + (p^2\gamma_1^2 - n^2\Delta_1)\Big](\cosh r\xi - 1) + \frac{\omega H^2}{p^2n^2}\left[p^2\Delta_2 - (n^2 + p^4)\Delta_1\right]\xi$$

$$+ \frac{\omega\gamma_1^2 H^2}{2n^2}\xi^2 \qquad (7.43)$$

and

$$\Theta = \frac{\omega}{p^4(n^2 - p^4)\cosh k}\left[(p^2\beta_2 - n^2\beta_1)k \sinh k + p^2(p^2\beta_1 - \gamma_2^2)\right](\cosh k\xi - 1) + \frac{\omega H(n^2\beta_1 - p^2\beta_2)}{p^3(n^2 - p^4)} \sinh k\xi$$

$$+ \frac{\omega H p^5(\beta_2 - p^2\beta_1)}{n^3(n^2 - p^4)} \sinh r\xi + \frac{p^4\omega}{n^4(n^2 - p^4)\cosh r}\left[p^2(p^2\beta_1 - \beta_2)\right.$$

$$\left. r \sinh r \right.$$

$$+ (p^2\gamma_2^2 - n^2\beta_1)\Big] (\cosh r\xi - 1) + \frac{\omega H^2}{p^2 n^2}\left[p^2\beta_2 - (n^2 + p^4)\beta_1\right]\xi$$

$$+ \frac{\omega\gamma_2^2 H^2}{2n^2}\xi^2 \qquad (7.44)$$

where ξ is the non-dimensional height ($= x/_H$) and k and r are the relative stiffness parameters .

On integrating equation (7.11) thrice, the datum deflection z_o becomes

$$z_o = \frac{a_6}{a_5}\Theta + \frac{\omega\cos\alpha}{24a_5}(H - x)^4 + A_o\frac{x^2}{2} + A_1 x + A_2 \qquad (7.45)$$

where A_i ($i = o - 2$) are the constants of integration to be determined from the necessary boundary conditions, i.e. at

$x = o$

$$z_o = o \qquad (7.46)$$

$$\frac{dz_o}{dx} = o$$

and, at $x = H$

$$\frac{d^2 z_o}{dx^2} = o \qquad (7.47)$$

On substituting equation (7.45) into the boundary conditions (7.46) - (7.47), and solving for the integration constants, it is found that

$$A_o = 0$$

$$A_1 = \frac{\omega H^3 \cos\alpha}{6a_5}$$

$$A_2 = -\frac{\omega H^4 \cos\alpha}{24\, a_5}$$

Hence, the general solution for z_o becomes

$$z_o = \frac{a_6}{a_5}\Theta + \frac{\omega H^4 \cos\alpha}{24a_5}\left[(1-\xi)^4 + 4\xi - 1)\right] \quad (7.48)$$

Substitution of equations (7.43), (7.44) and (7.48) into equations (7.1) and using equations (7.5) and (7.6) yields closed-form solutions for the shear forces in the various elements in the two orthogonal directions. The shear forces in the i^{th} wall, frame and core assemblies become

$$S_{wi} = -E(Iz)_{wi}(K_1 + K_2) \quad (7.49)$$

$$S_{fi} = (GA)_{fi}(K_3 + K_4) \quad (7.50)$$

$$S_{ci} = -E(Iz)_{ci}(K_5 + K_6) \quad (7.51)$$

$$S'_{wi} = -E(I_y)_{wi}\left[\left(\frac{a_6}{a_5} - r_{wi}\right)K_7 - \frac{\omega H \cos\alpha}{a_5}(1-\xi)\right] \quad (7.52)$$

$$S'_{fi} = - E(I_y)_{fi} \left[\left(\frac{a_6}{a_5} - r_{fi} \right) K_7 - \frac{\omega H \cos\alpha}{a_5} (1 - \xi) \right] \quad (7.53)$$

$$S'_{ci} = - E(I_y)_{ci} \left[\left(\frac{a_6}{a_5} - r_{ci} \right) K_7 - \frac{\omega H \cos\alpha}{a_5} (1 - \xi) \right] \quad (7.54)$$

where

$$K_1 = p^3 \left[(B_2 + l_{wi} C_2) \sinh k\xi + (B_3 + l_{wi} C_3) \cosh k\xi \right]$$

$$K_2 = \frac{n^3}{p^3} \left[(B_4 + l_{wi} C_4) \sinh r\xi + (B_5 + l_{wi} C_5) \cosh r\xi \right]$$

$$K_3 = \frac{1}{H} (B_1 + l_{fi} C_1) + p \left[(B_2 + l_{fi} C_2) \sinh k\xi \right.$$

$$\left. + (B_3 + l_{fi} C_3) \cosh k\xi \right]$$

$$K_4 = \frac{n}{p} \left[(B_4 + l_{fi} C_4) \sinhr \xi + (B_5 + l_{fi} C_5) \coshr \xi \right]$$

$$K_5 = p^3 \left[(B_2 + l_{ci} C_2) \sinh k\xi + (B_3 + l_{ci} C_3) \cosh k\xi \right]$$

$$K_6 = \frac{n^3}{p^3} \left[(B_4 + l_{ci} C_4) \sinhr \xi + (B_5 + l_{ci} C_5) \coshr \xi \right]$$

$$K_7 = p^3 (C_2 \sinh k\xi + C_3 \cosh k\xi) + \frac{n^3}{p^3} (C_4 \sinhr \xi + C_5 \cosh r\xi)$$

The bending moments M_{wi}, M_{ci}, M'_{wi}, and M'_{ci} in the shear wall 'i' and core 'i' are given by

$$M_{wi} = E\,(I_z)_{wi}\ \frac{d^2 y_{wi}}{dx^2}$$

$$M_{ci} = E\,(I_z)_{ci}\ \frac{d^2 y_{ci}}{dx^2} \qquad (7.55)$$

and

$$M'_{wi} = E\,(I_y)_{wi}\ \frac{d^2 z_{wi}}{dx^2}$$

$$M'_{ci} = E\,(I_y)_{ci}\ \frac{d^2 z_{ci}}{dx^2} \qquad (7.56)$$

The bending moments M_{fi} and M'_{fi} in the frame 'i' are related to the deflections y_{fi} and z_{fi} by the following relationships

$$\frac{dM_{fi}}{dx} = -\,(GA)_{fi}\ \frac{dy_{fi}}{dx} \qquad (7.57)$$

$$M'_{fi} = E(I_y)_{fi}\ \frac{d^2 z_{fi}}{dx^2} \qquad (7.58)$$

Integrating equation (7.57) once and using the condition that $M_{fi} = 0$ at the top ($\xi = 1$), M_{fi} becomes

$$M_{fi} = -(GA)_{fi}\left[y_{fi} - y_{fi}(H)\right] \qquad (7.59)$$

where $y_{fi}(H)$ is the deflection at the top of the frame 'i' for the specified loading.

Substitution of equations(7.43), (7.44) and (7.48) into equations (7.1) and using equations (7.55), (7.56), (7.58) and (7.59) yields closed form solutions for the

bending moments in the various elements in the two orthogonal directions. It is found that

$$M_{wi} = E\,(I_z)_{wi}\left[K8 + K9 + \frac{\omega}{n^2}\,(\gamma_1^2 + l_{wi}\,\gamma_2^2)\right] \quad (7.60)$$

$$M_{fi} = (GA)_{fi}\left[K_{10} + K_{11} + (B_1 + l_{fi}\,C_1)(1 - \xi) + \frac{\omega H^2}{2n^2}\,(\gamma_1^2 + l_{fi}\,\gamma_2^2)(1 - \xi^2)\right] \quad (7.61)$$

$$M_{ci} = E\,(I_z)_{ci}\left[(K_{12} + K_{13} + \frac{\omega}{n^2}\,(\gamma_1^2 + l_{ci}\gamma_2^2)\right] \quad (7.62)$$

$$M'_{wi} = E\,(I_y)_{wi}\left[(\frac{a_6}{a_5} - r_{wi})\,K_{14} + \frac{\omega H^2 \cos\alpha}{2a_5}(1 - \xi)^2\right] \quad (7.63)$$

$$M'_{fi} = E\,(I_y)_{fi}\left[(\frac{a_6}{a_5} - r_{fi})\,K_{14} + \frac{\omega H^2 \cos\alpha}{2a_5}\,(1 - \xi)^2\right] \quad (7.64)$$

$$M'_{ci} = E\,(I_y)_{ci}\left[(\frac{a_6}{a_5} - r_{ci})\,K_{14} + \frac{\omega H^2 \cos\alpha}{2a_5}\,(1 - \xi)^2\right] \quad (7.65)$$

where

$$K_8 = p^2\left[(B_2 + l_{wi}\,C_2)\cosh k\xi + (B_3 + l_{wi}\,C_3)\sinh k\xi\right]$$

$$K_9 = \frac{n^2}{p^2}\left[(B_4 + l_{wi}\,C_4)\cosh r\xi + (B_5 + l_{wi}\,C_5)\sinh r\xi\right]$$

$$K_{10} = \Big[(B_2 + l_{fi} C_2) (\cosh k - \cosh k\xi) +$$

$$(B_3 + l_{fi} C_3) (\sinh k - \sinh k\xi) \Big]$$

$$K_{11} = \Big[(B_4 + l_{fi} C_4) (\cosh r - \cosh r\xi) +$$

$$(B_5 + l_{fi} C_5) (\sinh r - \sinh r\xi) \Big]$$

$$K_{12} = p^2 \Big[(B_2 + l_{ci} C_2) \cosh k\xi + (B_3 + l_{ci} C_3) \sinh k\xi \Big]$$

$$K_{13} = \frac{n^2}{p^2} \Big[(B_4 + l_{ci} C_4) \cosh r\xi + (B_5 + l_{ci} C_5) \sinh r\xi \Big]$$

$$K_{14} = \Big[p^2 (C_2 \cosh k\xi + C_3 \sinh k\xi)$$

$$+ \frac{n^2}{p^2} (C_4 \cosh r\xi + C_5 \sinh r\xi) + \frac{\omega \gamma_2^2}{n^2} \Big]$$

ANALYSIS OF STRUCTURES CONSISTING OF CORE, SHEAR WALL AND RIGIDLY JOINTED FRAME ASSEMBLIES IN TWO ORTHOGONAL DIRECTIONS

7.4 Analysis

In many tall building structures the architectural and/or structural requirements may necessitate the inclusion of

structural assemblies in two orthogonal directions. Fig. 7.2 shows the plan form of a structure which consists of M assemblies of independent shear walls, R service cores, N rigidly jointed-frames in the Oxy plane and Q rigidly jointed frames in the Oxz plane.

Although the mathematical formulation for such structures is considerably more laborious, the analytical procedure is similar to that presented in section 7.3.

The displacements of any element (e.g. i^{th} element) at level x in two orthogonal directions y and z are given by equations (7.1) and the following equations

$$\bar{y}_{fi} = y_o + \bar{I}_{fi}\theta \qquad \bar{z}_{fi} = z_o - \bar{r}_{fi}\theta \qquad (7.66)$$

where $\bar{y}_{fi}$, $\bar{z}_{fi}$, $\bar{I}_{fi}$ and $\bar{r}_{fi}$ are the deflections and horizontal and perpendicular distances between the centroid of the i^{th} frame (in Oxz plane) and the datum axes yz respectively.

The equilibrium equations may now be expressed as

$$V = \sum_{i=1}^{M} S_{wi} + \sum_{i=1}^{N} S_{fi} + \sum_{i=1}^{Q} \bar{S}_{fi} + \sum_{i=1}^{R} S_{ci} \qquad (7.67)$$

$$P = \sum_{i=1}^{M} S'_{wi} + \sum_{i=1}^{N} S'_{fi} + \sum_{i=1}^{Q} \bar{S}'_{fi} + \sum_{i=1}^{R} S'_{ci} \qquad (7.68)$$

$$T = -\sum_{i=1}^{M} S_{wi}\, l_{wi} - \sum_{i=1}^{N} S_{fi}\, l_{fi} - \sum_{i=1}^{Q} \bar{S}_{fi}\, \bar{l}_{fi}$$

$$- \sum_{i=1}^{R} S_{ci}\, l_{ci} - \sum_{i=1}^{N} T_{fi} - \sum_{i=1}^{Q} \bar{T}_{fi} \qquad (7.69)$$

$$- \sum_{i=1}^{M} T_{wi} - \sum_{i=1}^{R} T_{ci} + \sum_{i=1}^{M} S'_{wi}\, r_{wi} + \sum_{i=1}^{N} S'_{fi}\, r_{fi}$$

$$+ \sum_{i=1}^{Q} \bar{S}'_{fi}\, \bar{r}_{fi} + \sum_{i=1}^{R} S'_{ci}\, r_{ci}$$

where $\bar{T}_{fi}$ is the torsional resistance and $\bar{S}_{fi}$ and $\bar{S}'_{fi}$ are the shear forces in the y and z directions corresponding to the i^{th} frame located in the Oxz plane, given by

$$\bar{T}_{fi} = (\overline{GJ})_{fi} \frac{d\theta}{dx}$$

$$\bar{S}_{fi} = - E (\bar{I}_z)_{fi} \frac{d^3 \bar{y}_{fi}}{dx^3} \qquad (7.70)$$

$$\bar{S}_{fi} = (\overline{GA})_{fi} \frac{d\bar{z}_{fi}}{dx}$$

in which $(\bar{I}_z)_{fi}$ and $(\overline{GA})_{fi}$ are the second moment of area and equivalent shearing rigidity of the i^{th} frame in the Oxz plane respectively.

Using the same procedure as in section (7.3), equations (7.67) - (7.69) may be expressed as

$$V = a_1 \frac{dy_o}{dx} + a_2 \frac{d\Theta}{dx} - b_1 \frac{d^3y_o}{dx^3} - b_2 \frac{d^3\Theta}{dx^3} \qquad (7.71)$$

$$P = b_3 \frac{dz_o}{dx} - b_4 \frac{d\Theta}{dx} - a_5 \frac{d^3z_o}{dx^3} + a_6 \frac{d^3\Theta}{dx^3} \qquad (7.72)$$

$$T = - a_2 \frac{dy_o}{dx} + b_4 \frac{dz_o}{dx} + b_5 \frac{d\Theta}{dx} + b_2 \frac{d^3y_o}{dx^3} - a_6 \frac{d^3z_o}{dx^3} + b_6 \frac{d^3\Theta}{dx^3} \qquad (7.73)$$

where a_1, a_2, a_5 and a_6 are as described in section (7.3), and b_i (i = 1 - 6) are given by

$$b_1 = a_3 + E \sum_{i=1}^{Q} (\bar{I}_z)_{fi}$$

$$b_2 = a_4 + E \sum_{i=1}^{Q} (\bar{I}_z)_{fi} \bar{I}_{fi}$$

$$b_3 = \sum_{i=1}^{Q} (\overline{GA})_{fi}$$

$$b_4 = \sum_{i=1}^{Q} (\overline{GA})_{fi}\ \bar{r}_{fi}$$

$$b_5 = a_7 - \sum_{i=1}^{Q} (G\bar{A})_{fi}\ \bar{r}_{fi}^{\,2}$$

$$b_6 = a_8 + E \sum_{i=1}^{Q} (\bar{I}_z)_{fi}\ \bar{l}_{fi}^{\,2}$$

Equations (7.71) - (7.73) may be expressed as

$$(a_1D - b_1D^3)\ y_o + (a_2D - b_2D^3)\Theta = V \qquad (7.74)$$

$$(b_3D - a_5D^3)z_o + (-b_4D + a_6D^3)\Theta = P \qquad (7.75)$$

$$(-a_2D + b_2D^3)y_o + (b_4D - a_6D^3)z_o + (b_5D + b_6D^3)\Theta = T \qquad (7.76)$$

On eliminating the terms in Θ, y_o and z_o from equations (7.74) - (7.76) respectively, the governing differential equations finally become

$$\frac{d^7 y_o}{dx^7} + m_1^2 \frac{d^5 y_o}{dx^5} - n_1^2 \frac{d^3 y_o}{dx^3} + q_1^2 \frac{dy_o}{dx} = \phi_3(x) \quad (7.77)$$

$$\frac{d^7 z_o}{dx^7} + m_1^2 \frac{d^5 z_o}{dx^5} - n_1^2 \frac{d^3 z_o}{dx^3} + q_1^2 \frac{dz_o}{dx} = \phi_4(x) \quad (7.78)$$

$$\frac{d^7 \theta}{dx^7} + m_1^2 \frac{d^5 \theta}{dx^5} - n_1^2 \frac{d^3 \theta}{dx^3} + q_1^2 \frac{d\theta}{dx} = \phi_5(x) \quad (7.79)$$

where

$$m_1^2 = \frac{1}{b_7}\left[b_2^2 b_3 + 2a_2 a_5 b_2 + a_1 (a_6)^2 + 2a_6 b_1 b_4 + a_5 b_1 b_5 - a_1 a_5 b_6 - b_1 b_3 b_6\right]$$

$$n_1^2 = \frac{1}{b_7}\left[2a_2 b_2 b_3 + (a_2)^2 a_5 + 2a_1 a_6 b_4 + b_1 (b_4)^2 + a_1 a_5 b_5 + b_1 b_3 b_5 - a_1 b_3 b_6\right]$$

$$q_1^2 = \frac{1}{b_7}\left[(a_2)^2 b_3 + a_1 (b_4)^2 + a_1 b_3 b_5\right]$$

and

$$\phi_3(x) = \frac{1}{b_7}\Big\{(b_3 + a_5 D^2)(a_2 - b_2 D^2) T + (a_2 - b_2 D^2)(b_4 - a_6 D^2) P + \left[(b_4 - a_6 D^2)^2 + (b_3 - a_5 D^2)(b_5 + b_6 D^2)\right] V\Big\} \quad (7.80)$$

$$\phi_4(x) = \frac{1}{b_7}\Big\{(a_1 - b_1D^2)\,(b_4 - a_6D^2)\,T + (-b_4 + a_6D^2)\,(-a_2 + b_2D^2)\,V + \Big[(-a_2 + b_2D^2)^2 + (b_5 + b_6D^2)\,(a_1 - b_1D^2)\Big]P\Big\} \tag{7.81}$$

$$\phi_5(x) = \frac{1}{b_7}\Big\{\Big[a_1\,b_3 - (a_1\,a_5 + b_1b_3)D^2 + a_5\,b_1D^4\Big]T + \Big[a_2\,b_3 - (a_2\,a_5 + b_2\,b_3)D^2 + a_5\,b_2\,D^4)\Big]V + \Big[-a_1\,b_4 + (b_1\,b_4 + a_1\,a_6)D^2 - a_6\,b_1\,D^4)\Big]P\Big\} \tag{7.82}$$

where

$$b_7 = a_5\,a_6\,b_1 - (a_6)^2\,b_1 - a_5\,(b_2)^2$$

A consideration of equations (7.77) - (7.79) might suggest that these equations may be reduced to sixth order differential equations if integrated once, but due to the difficulty involved in finding the integration constant generated this process was ruled out.

The complete solutions of the seventh order differential equations are given by the addition of the complementary functions and the particular integrals. The characteristic equation is

$$\lambda^7 + m_1^2\lambda^5 - n_1^2\lambda^3 + q_1^2\lambda = o \tag{7.83}$$

A numerical solution of equation (7.83) yields seven real and/or complex roots, zero, $\pm\lambda_1$, $\pm\lambda_2$ and $\pm\lambda_3$. Hence, the general solution of equations (7.77) - (7.79) for any form of lateral loading may be expressed in the form

$$y_o = D_o + D_1 \cosh\lambda_1 x + D_2 \sinh\lambda_1 x + D_3 \cosh\lambda_2 x + D_4 \sinh\lambda_2 x + D_5 \cosh\lambda_3 x + D_6 \sinh\lambda_3 x + y_{oPI} \quad (7.84)$$

$$z_o = E_o + E_1 \cosh\lambda_1 x + E_2 \sinh\lambda_1 x + E_3 \cosh\lambda_2 x + E_4 \sinh\lambda_2 x + E_5 \cosh\lambda_3 x + E_6 \sinh\lambda_3 x + z_{oPI} \quad (7.85)$$

$$\Theta = F_o + F_1 \cosh\lambda_1 x + F_2 \sinh\lambda_1 x + F_3 \cosh\lambda_2 x + F_4 \sinh\lambda_2 x + F_5 \cosh\lambda_3 x + F_6 \sinh\lambda_3 x + \Theta_{PI} \quad (7.86)$$

where D_i $(i = o - 6)$, E_i $(i = o - 6)$ and F_i $(i = o - 6)$ are the constants of integration to be determined from the necessary boundary conditions, and y_{oPI}, z_{oPI} and Θ_{PI} are the particular integral solutions.

Boundary conditions

The first three boundary conditions are as expressed by equations (7.23) - (7.26) and (7.46) - (7.47). A consideration of equations (7.71) - (7.73) then yields the following conditions, at $x = o$

$$\frac{d^3y_o}{dx^3} = -\frac{1}{b_1 b_7}\left\{(b_7\,(V)_o + a_5\,b_2\left[b_1(T)_o + b_2(V)_o - a_6\,b_1\,b_2(P)_o\right]\right\}$$

$$\frac{d^3z_o}{dx^3} = \frac{1}{a_5 b_7}\left\{a_5\,a_6\left[b_1(T)_o + b_2(V)_o\right] - \left[(a_6)^2\,b_1 + b_7\right](P)_o\right\}$$

$$\frac{d^3\theta}{dx^3} = \frac{1}{b_7}\left\{a_5\left[b_1(T)_o + b_2(V)_o\right] - a_6 b_1(P)_o\right\} \qquad (7.87)$$

Differentiating equations (7.71) - (7.73) once, and using the boundary conditions (7.25), (7.26) and (7.47) yields the following conditions, at $x = H$

$$\frac{d^4y_o}{dx^4} = -\frac{1}{b_1 b_7}\left\{b_7\,(\frac{dV}{dx})_H + a_5\,b_2\left[b_1(\frac{dT}{dx})_H + b_2\,(\frac{dV}{dx})_H - a_6\,b_1 b_2(\frac{dP}{dx})_H\right]\right\}$$

$$\frac{d^4z_o}{dx^4} = \frac{1}{a_5 a_7}\left\{a_5\,a_6\left[b_1\,(\frac{dT}{dx})_H + b_2\,(\frac{dV}{dx})_H\right] - \left[(a_6)^2\,b_1 + b_7\right](\frac{dP}{dx})_H\right\}$$

$$\frac{d^4\theta}{dx^4} = \frac{1}{b_7}\left\{a_5\left[b_1\,(\frac{dT}{dx})_H + b_2\,(\frac{dV}{dx})_H\right] - a_6\,b_1\,(\frac{dP}{dx})_H\right\}$$

(7.88)

Differentiating equations (7.71) - (7.73) twice, and using the boundary conditions (7.87) yields the following conditions, at $x = o$

$$\frac{d^5 y_o}{dx^5} = -\frac{1}{b_1 b_7}\left\{ b_7 (L_1)_o + a_5 b_2 \left[b_1 (L_3)_o + b_2 (L_1)_o - a_6 b_1 b_2 (L_2)_o \right] \right\}$$

$$\frac{d^5 z_o}{dx^5} = \frac{1}{a_5 a_7}\left\{ a_5 a_6 \left[b_1 (L_3)_o + b_2 (L_1)_o \right] - \left[(a_6)^2 b_1 + b_7 \right] (L_2)_o \right\}$$

$$\frac{d^5 \theta}{dx^5} = \frac{1}{b_7}\left\{ a_5 \left[b_1 (L_3)_o + b_2 (L_1)_o \right] - a_6 b_1 (L_2)_o \right\} \qquad (7.89)$$

where

$$(L_1)_o = \left(\frac{d^2 V}{dx^2}\right)_o - a_1 \left(\frac{d^3 y_o}{dx^3}\right)_o - a_2 \left(\frac{d^3 \theta}{dx^3}\right)_o$$

$$(L_2)_o = \left(\frac{d^2 P}{dx^2}\right)_o - b_3 \left(\frac{d^3 z_o}{dx^3}\right)_o + b_4 \left(\frac{d^3 \theta}{dx^3}\right)_o$$

$$(L_3)_o = \left(\frac{d^2 T}{dx^2}\right)_o + a_2 \left(\frac{d^3 y_o}{dx^3}\right)_o - b_4 \left(\frac{d^3 z_o}{dx^3}\right)_o - b_5 \left(\frac{d^3 \theta}{dx^3}\right)_o$$

Finally, on differentiating equations (7.71) - (7.73) thrice, and using the boundary conditions (7.88), the seventh boundary conditions become, at $x = H$

$$\frac{d^6 y_o}{dx^6} = -\frac{1}{b_1 b_7}\left\{ b_7 (L_4)_H + a_5 b_2 \left[b_1 (L_6)_H + b_2 (L_4)_H \right] - a_6 b_1 b_2 (L_5)_H \right\}$$

$$\frac{d^6 z_o}{dx^6} = \frac{1}{a_5 b_7}\left\{a_5\, a_6\left[b_1(L_6)_H + b_2(L_4)_H\right] - \left[(a_6)^2 b_1 + b_7\right](L_5)_H\right\}$$

$$\frac{d^6\Theta}{dx^6} = \frac{1}{b_7}\left\{a_5\left[b_1(L_6)_H + b_2(L_4)_H\right] - a_6\, b_1(L_5)_H\right\}$$

(7.90)

where

$$(L_4)_H = \left(\frac{d^3 V}{dx^3}\right)_H - a_1\left(\frac{d^4 y_o}{dx^4}\right)_H - a_2\left(\frac{d^4\Theta}{dx^4}\right)_H$$

$$(L_5)_H = \left(\frac{d^3 P}{dx^3}\right)_H - b_3\left(\frac{d^4 z_o}{dx^4}\right)_H + b_4\left(\frac{d^4\Theta}{dx^4}\right)_H$$

$$(L_6)_H = \left(\frac{d^3 T}{dx^3}\right)_H + a_2\left(\frac{d^4 y_o}{dx^4}\right)_H - b_4\left(\frac{d^4 z_o}{dx^4}\right)_H - b_5\left(\frac{d^4\Theta}{dx^4}\right)_H$$

For any specific loading, the particular integrals y_{oPI} z_{oPI} and Θ_{PI} may readily be obtained. Then, on substituting equations (7.84) - (7.86) into the boundary conditions (7.23) - (7.26), (7.46) - (7.47), (7.87), (7.89) and (7.90), the constants of integration D_i(i= o - 6), E_i(i= o -6)and F_i (i = o - 6) may be obtained. Therefore, closed form solutions for deflections and rotation are possible. On following the same procedure as described in section (7.3), closed-form solutions may be achieved for the moments and shear forces in the various shear wall, frame and core

assemblies. As mentioned previously, the characteristic equations regarding the general differential equations can only be solved numerically, hence, general solutions can not be obtained. For any specific structure the parameters m_1^2, n_1^2 and q_1^2 may be calculated and used to solve the general equations (7.77) - (7.79).

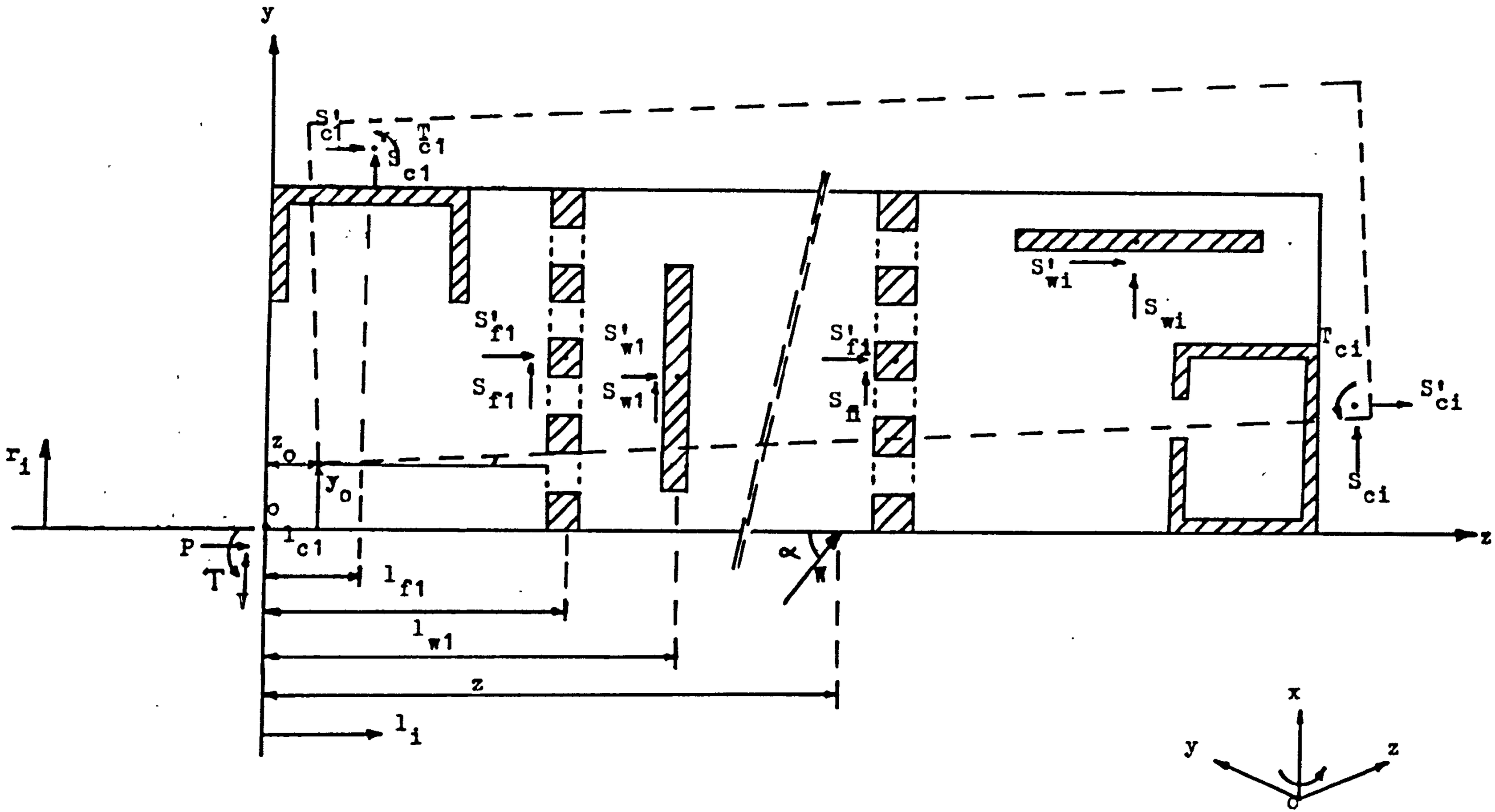

Fig. 7.1 Asymmetrical structure consisting of cores, shear walls and parallel assemblies of frames

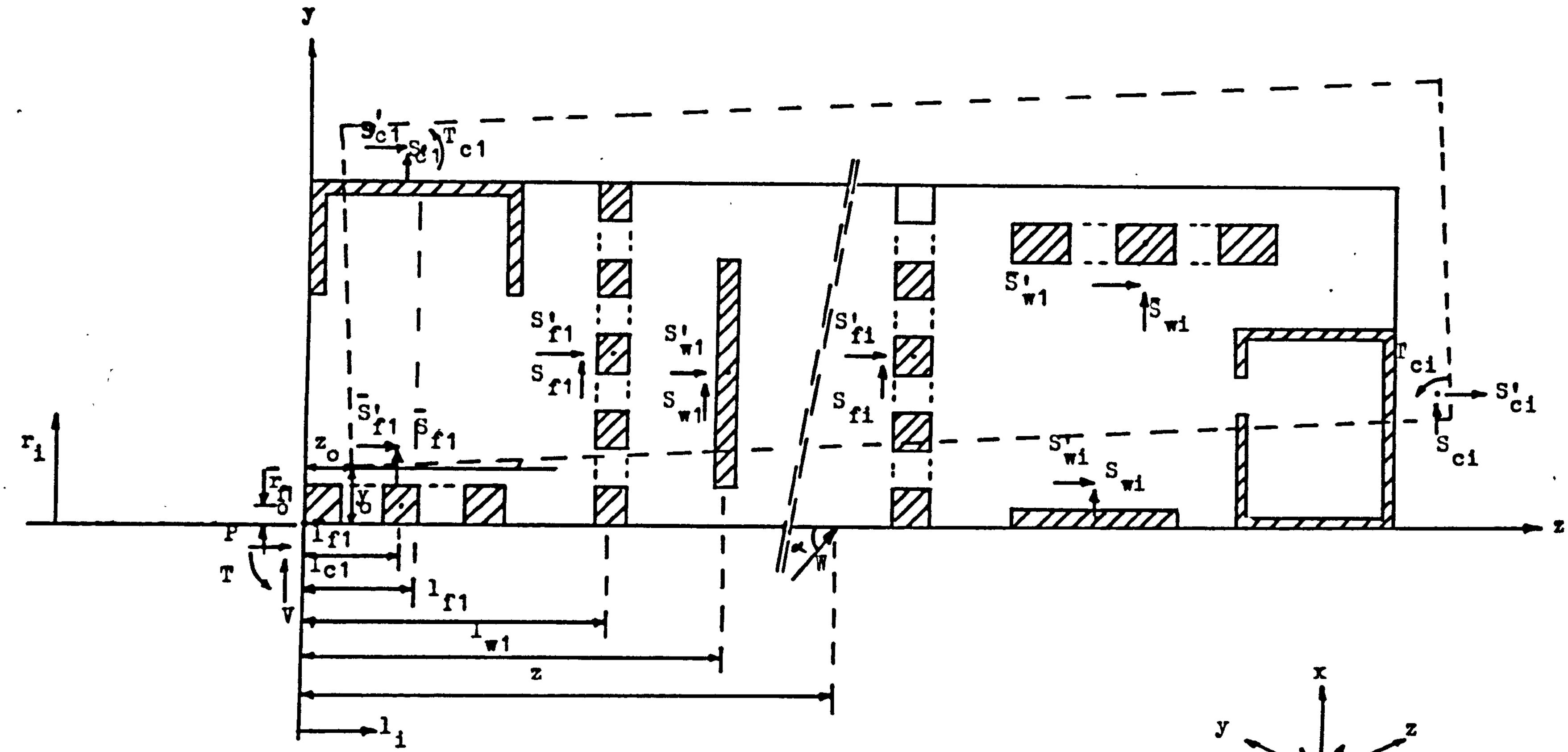

Fig. 7.2 Asymmetrical structure consiting of cores, shear walls and assemblies of frames in two orthogonal directions

C H A P T E R 8

COMPARISON WITH RELEVANT PUBLISHED DATA AND NUMERICAL PARAMETER STUDIES

CHAPTER 8

COMPARISON WITH RELEVANT PUBLISHED DATA AND NUMERICAL PARAMETER STUDIES

8.1 Introduction

In order to substantiate the accuracy of the methods of analysis presented in chapter 3 and 7 for the analysis of symmetric and asymmetric structures consisting of different load bearing elements, comparison of these methods with relevant published work is essential. In view of the limited number of published data on structures of the forms considered, it has proved possible to compare the results from the present analysis with only three typical example structures which have been taken from different publications[23,30,34]. The comparisons between the various methods are presented graphically, relevant conclusions are drawn and the differences are discussed. A numerical parameter study of the structural behaviour of a three-dimensional symmetric structure consisting of cores, coupled shear walls and rigidly-jointed frames considered in chapter 3 is carried out. As described previously, the closed-form solutions for deflections and internal forces are dependent on three variables, the non-dimensional height ξ and the relative stiffness parameters k and r. Parameters k and r are in turn functions of the parameters αH, βH and γH which are given by

$$\alpha^2 = \frac{GA}{EI}$$

$$\beta^2 = \frac{12 I_c l^2}{b^3 h I}$$

$$\gamma^2 = \frac{12 I_c}{b^3 h} \left(\frac{1}{A_1} + \frac{1}{A_2}\right)$$

where GA is the equivalent shearing rigidity of the frames, E is the elastic modulus, I is the combined second moment of area of the coupled shear walls and cores, I_c is the second moment of area of the connecting beams, l is the distance between centroidal axes of the coupled walls, b is the clear span between the coupled walls, h is the storey height, A_1 and A_2 are the cross-sectional areas of the coupled shear walls and H is the total building height.

The above formulae shows that:

(i) the stiffness parameter α^2 is equal to the ratio of the shearing rigidity of the frames to the combined flexural rigidities of the coupled walls and cores.

(ii) the stiffness parameter β^2 is a function of the ratio of the flexural rigidity of the connecting beams to the combined flexural rigidities of the coupled shear walls and cores.

(iii) the stiffness parameter γ^2 is a function of the ratio of the flexural rigidity of the connecting beams to the flexural rigidity /

of the coupled shear walls only. The effects of varying the parameters αH, βH and γH on the top deflection, the maximum bending moments in the walls and frames and axial forces on the coupled walls are then considered.

8.2 Comparison with previous research

In order to examine the accuracy and validity of the methods, three examples which were analysed by previous investigators are considered. One of these examples is applicable to the theory presented in chapter 3 and the other two to that of chapter 7. These examples have been taken as presented in the various publications, i.e. the unit of the applied load in example I is in Mp and in example II all units are imperial. There are results described as being obtained from the discrete matrix method. The author has been unable to determine precisely what this method is, but it appears that this refers to a standard matrix frame analysis.

EXAMPLE I

In this example, a ten-storey plane structure of the form shown in Fig. 8.1(a) was considered. The structure consists of a pair of symmetrical coupled shear walls and

a one-bay frame with identical columns and horizontal beams and a constant storey height throughout the structure.

The relevant structural data are:

Storey height	$h = 3$ m
Total building height	$H = 30$ m
For coupled shear walls,	$I_1 = I_2 = 0.5$ m^4
	$A_1 = A_2 = 0.5$ m^2
	$I_c = 8.523 \times 10^{-4}$ m^4
	$l = 4$ m
	$b = 1$ m
	$E = 2 \times 10^6$ M p/m^2

and for the frame

$$I_h = 4 \times 10^{-3} \text{ m}^4$$
$$I_b = 1.6 \times 10^{-2} \text{ m}^4$$
$$l' = 4 \text{ m}$$

This example was analysed by Arvidsson[23] using four methods; the equivalent shear wall frame method, the discrete matrix method, Rosman's method and his own proposed method. Arvidsson's method is based on the continuum approach and the complementary energy theory, and a solution was obtained by Euler's formula. In the equivalent shear wall frame method the coupled shear wall is represented by a homogeneous shear wall of an equivalent stiffness, so that, the lateral deflection

obtained is the same as that of the prototype system under a lateral distributed load. In Rosman's method, the connecting beams and frames are replaced by a continuous shear medium. By assuming that the shear force distribution in the connecting beams is similar to that of the frames the problem is reduced to a continuous shear wall-frame system. This assumption applies only when the areas of the coupled walls and frames are infinite.

In order to analyse the example structure using the method presented in chapter 3, the equivalent shearing rigidity of the frame was first calculated by using the formula given in section (2.3). It was found that

$$GA = 12800\ M_p$$

Hence, the relevant structural parameters became

$$\alpha H = 2.4$$

$$\beta H = 7.0$$

$$\gamma H = 3.5$$

which are fairly typical values for these parameters.

Figs. 8.3 and 8.4 show the distribution of the shear force in the frame assembly, and the shear force in the connecting beams per storey height. The results from the method presented differ by less than 5% from the Arvidsson's and discrete matrix methods, but the

differences are much higher when compared to more approximate solutions, i.e. Rosman's and the equivalent shear wall-frame method. This is basically due to the simplifying assumptions made in the latter analyses. Rosman's method results in an over-estimation of the forces in the connecting beams and an under-estimation of the shear force in the frame. On the contrary, the equivalent shear wall-frame method results in an under-estimation of the shear force in the connecting beams and an over-estimation of the shear force in the frame.

The structure was reanalysed by Arvidsson and the present method by changing the frame properties to

$$I_h = 2.5 \times 10^{-2} \text{ m}^4$$

$$I_b = 0.1 \text{ m}^4$$

The equivalent shearing rigidity is then found to be,

$$GA = 80000 \text{ Mp}$$

hence,

$$\alpha H = 6.0$$

and the parameters βH and γH remain the same.

Figs. 8.5 and 8.6 show the distributions of the shear forces in the frame and the connecting beams. In this case the differences between the various methods are almost the same as before.

From the above examples it can be deduced that the present method agrees favourably with Arvidsson's and the discrete matrix methods. Compared to Arvidsson's method it has the advantage that core assemblies may also be included in the analysis. Earlier work has confirmed the accuracy of the continuum approach for uniform coupled shear walls[44], and that of the shear cantilever concept for wall-frame structures[20]. Consequently, since no further approximations or assumptions have been introduced, it must be expected that the present analysis of combinations of all three components will be of comparable accuracy, and acceptable for design purposes.

EXAMPLES II and III

In order to compare the method of analysis presented in chapter 7 with other published work two example structures are considered. These examples are the only available published data which could be used for comparison purposes. Example II has been analysed by Stamato and Mancini[30] using a method of analysis which is based on the continuum approach and matrix analysis. A corresponding model made in perpex with the structural form of example II had previously been tested by Stamato. Example III has been analysed by Mortelmans et al[34] using an approximate frame method of analysis which is based on the following assumptions

(i) the rotations at all the junction nodes of one beam have the same size.

(ii) the beams are of constant stiffness.

(iii) the bending moments concentrated in the nodes and exerted by the beams may be spread over the height of a floor.

(iv) the horizontal wind load on the plane, elastic system, is constant.

In both of the above examples it has been assumed that the structure rotates about the Ox axis, and deflects in the Oy direction only (Fig. 8.2). Hence, the governing differential equation (7.11) may be neglected and equations (7.9) and (7.14) become

$$V = -a_3 \frac{d^3 y_o}{dx^3} + a_1 \frac{dy_o}{dx} + a_2 \frac{d\theta}{dx}$$

$$T = -a_2 \frac{dy_o}{dx} - a_7 \frac{d\theta}{dx} \qquad (8.1)$$

where

$$V = \omega (H - x)$$

$$T = -\omega z (H - x)$$

$$a_1 = \sum_{i=1}^{N} (GA)_{fi}$$

$$a_2 = \sum_{i=1}^{N} (GA)_{fi} \, l_{fi}$$

$$a_3 = E \sum_{i=1}^{M} (I_z)_{wi}$$

$$a_7 = -\left(\sum_{i=1}^{N} (GA)_{fi}\, l_{fi}^2 + \sum_{i=1}^{N} (GJ_o)_{fi} + \sum_{i=1}^{M} (GJ_o)_{wi} \right)$$

in which, ω is the uniformly distributed load, z is the eccentricity of the lateral load relative to the x axis, N is the number of frames, M is the number of cores or shear walls, fi and wi are suffices denoting frame and core or shear wall assemblies, l_{fi} is the horizontal distance between centroids of frame 'i' and the datum axis Oy, GJ_o is the torsional rigidity and I_z is the second moment of area of the core or shear wall.

On following the same procedure as described in chapter 7 the general solutions of the deflections y_o and the rotation θ become

$$y_o = C_o + C_1 \cosh m x + C_2 \sinh mx + \frac{\omega}{m^2 a_3} \left(1 - \frac{za_2}{a_7}\right) \left(Hx - \frac{x^2}{2}\right) \qquad (8.2)$$

and

$$\theta = - \frac{a_2}{a_7} y_o - \frac{z\omega}{a_7} \left(\frac{x^2}{2} - Hx\right) \qquad (8.3)$$

where

$$m^2 = \frac{a_1}{a_3} - \frac{a_2^2}{a_3 a_7}$$

$$C_1 = \frac{\omega}{m^4 a_3} \left(1 - \frac{z a_2}{a_7}\right) \left(\frac{mH \sinh m H + 1}{\cosh m H}\right)$$

$$C_2 = - \frac{\omega H}{m^3 a_3} \left(1 - \frac{z a_2}{a_7}\right)$$

$$C_o = - C_1$$

and

m is the relative stiffness parameter.

For the analyses of examples II and III the datum axes have been chosen as the centroidal axes of the shear-wall and core assemblies respectively. The choice of datum axes becomes important for these two particular examples where there is only one core or shear wall assembly in each structure. If the origin O is chosen as the left-hand corner of the example structure, m^2 is then given by (chapter 7)

$$m^2 = \frac{a_3 a_7 - a_1 a_9 + 2 a_2 a_4}{a_4^2 - a_3 a_9}$$

where a_1, a_2, a_3 and a_7 as described above and a_4 and a_9 are given by

$$a_4 = E \sum_{i=1}^{M} (I_z)_{wi} \, l_{wi}$$

$$a_9 = E \sum_{i=1}^{M} (I_z)_{wi} \, l_{wi}^2$$

From a consideration of the denominator of m^2 it can be deduced that this quantity becomes zero when there is only one core or shear wall component in the structure which leads to an infinity value for m^2 and hence a solution becomes impossible. Therefore, for structures which contain none or more than one shear wall and/or core assemblies the choice of datum axes becomes arbitrary. However, for structures which contain only one shear wall or core element, their local centroidal axes should be chosen as the datum axes for the overall structure.

EXAMPLE II

This example is a ten-storey model structure of the plan form shown in Fig. 8.2(a) which was first considered by Stamato and Mancini[30]. The model of this structure was first tested by Stamato and analysed by his proposed method and also by a discrete matrix method. All the columns were $\frac{3}{4}$ in. in both y and z directions, the beams were $\frac{1}{4}$ in. thick and 5/4 in. deep and the wall was $\frac{1}{4}$ in. and 4 in. in z and y directions respectively, and have a constant cross-section throughout the height of the building. The horizontal uniformly distributed load was $\omega = 0.2$ lb applied in the plane of frame 2.

The relevant structural data are :

Storey height	$h = 5$ in.
Total model height	$H = 50$ in.
For shear wall	$I_z = 1.3333$ in.^{4} /

$J_o = 1.3385$ in.^{4}

$E = 4.2 \times 10^5$ lb/sq.in.

$G_o = 1.5 \times 10^5$ lb/sq. in.

For each frame $GA = 2960$ lb

$J_{column} = 0.05273$ in.^{4}

Then on adding the properties of the two groups of elements, the relevant structural parameters become

$a_1 = 5919$ lb

$a_2 = 88791$ lb in.

$a_3 = 560000$ lb. in.^{2}

$a_7 = 1627840$ lb.in.^{2}

Hence

$$m = 0.04384 \text{ in.}^{-1}$$

The distributions of the deflection of frame 2 (Fig.8.2(a)), rotation, bending moments in the wall, and shear forces in frame 2,3,4 and 5 are shown in Figs. 8.7 to 8.12. These figures also include the results obtained from Stamato and Mancini's[30] analysis, the discrete matrix analysis and experimental data. As the figures show there is close agreement between the results obtained by the various methods of analysis and the experimental data. The differences between the results obtained by the present method and Stamato's analysis for the deflection, rotation, bending moment and shear forces are less than 6%, while compared to

the discrete matrix analysis the difference between the results is about 10%.

In view of lack of any other published data on structures of the form considered, it is not possible to compare the results from the present analysis with those from other more sophisticated techniques (e.g. Finite element methods). However, earlier work has confirmed the accuracy of the continuum approach for the structural components of the forms considered. As a result, since no further approximation or assumptions have been introduced it must be expected that the present analysis will be of comparable accuracy, and may be used for design purposes.

EXAMPLE III

Fig. 8.2(b) shows the plan form of a ten-storey building which has been analysed by Mortelmans et al[34]. It consists of nine frames and a lift shaft. The dimensions of the columns were 0.28m and 0.7 m in z and y directions,horizontal beams were 0.2 m thick and 0.4 m deep, and the dimensions of the lift shaft were 6.5 m and 4m in z and y directions. The wall thickness of the lift shaft was 0.18, and the lateral uniformly distributed wind load was $\omega = 1\ KN/m^2$.

The relevant structural data are:

Storey height	$h = 3\ m$
Total building height	$H = 30\ m$
For core	$I_z = 9.9897\ m^4$
	$J_o = 31.3172\ m^4$
	$E = 2.5 \times 10^7\ KN/m^2$
	$G_o = 1.0417 \times 10^7\ KN/m^2$
For each frame	$GA = 60194\ KN$
	$J_{column} = 9.2839 \times 10^{-3}\ m^3$

Then, on adding the properties of the two groups of elements the relevant structural parameters become

$a_1 = 521681\ KN$

$a_2 = 5417460\ KN\ m$

$a_3 = 249743208\ KN\ m^2$

$a_7 = 474177878\ KN\ m^2$

Hence,

$$m = 0.04291 \quad m^{-1}$$

Figs. 8.13 and 8.14 show respectively the distributions of the lateral deflection in frame 1 (Fig.8.2(b)) and the rotation. In order to investigate the influence of the building height, the example structure was analysed successively by Mortelmans et al[34] for buildings of 4,6,8 and 10 storeys. The comparison between the results obtained by the present method and Mortelmans' method is close and the higher the building the lower the differences between the results obtained by the two methods. This is expected since an analysis based on the continuum approach is generally more accurate for taller buildings.

For a ten-storey building the differences between the results obtained by the present and Mortelmans' methods for the top deflection in frame 1, top rotation and the base moment in the lift shaft are about 6%, 7% and 8%, indicating that close agreement exists between these two methods of analysis.

In many tall buildings box cores play an important role in providing both bending and torsional stiffness for the structure. Mortelmans et al have assumed that, due to crack formation, the bending and torsional rigidities of the lift shaft are reduced to one third and one tenth of the original value respectively. Figs. 8.16

and 8.17 show respectively, the distributions of the deflections in frame 1 (Fig. 8.2(b)) and the rotations for various stiffnesses. For cases I and II there is close agreement between the two methods, while there are significant differences for cases III and IV. These differences were expected since, in their analysis Mortelmans et al have assumed that at the base of the structure $\frac{dy_o}{dx} = \frac{d\theta}{dx} = 0$. However, a consideration of equation (8.1) indicates that for the present analysis at $x = 0$ if $\frac{dy_o}{dx} = 0$, then, $\frac{d\theta}{dx} = \frac{\omega z H}{a_7}$. Consequently, the larger the value of a_7 the smaller the value of $\frac{d\theta}{dx}$, and hence a closer agreement between the boundary conditions assumed for the two methods of analysis.

If the torsional effects of the columns are considered negligible, the parameter a_7 may be expressed as

$$a_7 = -\left(\sum_{i=1}^{8} (GA)_{fi}\, l_{fi}^2 + G_o\, J_o\right)$$

where

$$\sum_{i=1}^{8} (GA)_{fi}\, l_{fi}^2 = 1.44465 \times 10^8 \text{ KN m}^2$$

and

$$G_o\, J_o = 3.2623 \times 10^8 \text{ KN m}^2$$

From above it is obvious that for this particular example, including a somewhat unrealistic closed box core, G_oJ_o is

a more important constituent part of a_7 and any reduction of its value will in turn result in a higher value for $\frac{d\theta}{dx}$ and hence the overall analysis.

For case I where G_oJ_o is unaltered $\frac{d\theta}{dx} = 2.5 \times 10^{-5}$ while when G_oJ_o is reduced to one tenth of its original value $\frac{d\theta}{dx} = 6.8 \times 10^{-5}$, i.e. almost three times larger. Therefore, it may be deduced that the large differences between the results obtained by the two methods for cases III and IV are mainly due to the boundary conditions chosen, and this is also true for case I where these differences are relatively small. It must be mentioned that as EI does not play any role regarding the boundary condition $(\frac{d\theta}{dx})_o$, as expected (case II), its reduction to one third of its original value does not have any significant effects on the results obtained by the two methods.

Figs. 8.18 and 8.19 illustrate the distribution of the torsional moments in the lift shaft for cases I and III respectively. There are significant differences at the base of the lift shaft due to the boundary conditions chosen as explained above.

8.3 Numerical parameter studies

In chapters 3 and 6 the explicit formulae used for the analysis purposes are basically the same. In both chapters the closed-form formulae used to determine the

deflections and the internal forces have all stemmed from a single sixth order differential equation with constant coefficients which are in turn dependent on three non-dimensional structural parameters αH, βH and γH.

In order to investigate the effects of these structural parameters on the deflections and the internal forces it is necessary to establish an appropriate range for each of these parameters. By considering some typical dimensions of a modern apartment building, some idea may be gained of the effects of the various building dimensions on these parameters. The parameters α^2, β^2 and γ^2 are given in section 8.1 where

$$l = \frac{1}{2}(2b + d_1 + d_2)$$

$$A_1 = d_1 t$$

$$A_2 = d_2 t$$

in which d_1 and d_2 are the distances from the inner edges of walls 1 and 2 to their centroids, and t is the thickness of the walls.

Since a number of dimensions are involved, it is convenient to consider a single corridor opening b of 2m, and a constant storey height h of 2.8 m, which are fairly typical of modern apartment buildings.

The width of a building will generally lie

within the range of 14 and 22 m, so that $(d_1 + d_2)$ will be between 12 and 20 m. If the two walls are assumed equal ($d_1 = d_2 = d$) the range of d will be between 6 and 10 m. For apartment buildings with floor slabs of say, 0.15 to 0.25 m thickness, the depths of the connecting beams varies from 0.3 to 0.6 m and have the same thickness as the shear walls, i.e., between 0.2 and 0.5 m.

Taking a possible height range of 30-100 m the values of the parameters $\alpha H, \beta H$ and γH then become

αH	0.1 - 8.0
βH	0.5 - 15.0
γH	0.5 - 6.0

The above values for the range of parameters αH, βH and γH are of course approximate, as they depend on many variables. However, they do correspond to a fairly wide range of modern building structures.

In order to assess the relative importance of the structural parameters $\alpha H, \beta H$ and γH the distributions of the top deflections, the maximum axial forces in the coupled walls and the maximum bending moments in the coupled shear walls, cores and frames are sketched for representative values of αH, βH and γH. The distributions may be expressed in terms of a series of functions F_1 to F_4 as follows, related where appropriate to the applied load

intensity ω , and the total base statical moment $\omega H^2/2$. These functions are defined as

$$y_{max} = (\omega H^4/EI)F_1$$

$$N_{max} = (\omega H^2/2)F_2$$

$$M_{1\ max} = M_{2\ max} = (1/2)\ (\omega H^2/2)\ \frac{I_{1+2}}{I}\ F_3$$

$$M_{3\ max} = (\omega H^2/2)\ \frac{I_3}{I}\ F_3$$

$$M_{4\ max} = (\omega H^2/2)F_4$$

Figs. 8.20 to 8.23 show the distributions of the deflection and the internal force functions F_1, F_2, F_3 and F_4. A consideration of these figures indicates that, the maximum values of function F_1 occurs when αH and βH are minimum regardless of the value of γH, and F_1 has its minimum value when αH and βH are maximum and γH has its lowest value. This suggests that, in order to have a stiff structure;

(i) the value of GA relative to EI should be large so that the parameter αH has a relatively large value

(ii) to include multiple coupled walls or coupled walls with relatively large cross-sectional areas in the building so that the relative values of γ H and β H are small and large respectively.

As β^2 and γ^2 are interrelated it seems that an increase in the cross sectional areas of the coupled walls would also decrease the value of β^2, but this can effectively be counteracted by the increase in the value of l in the case of larger walls or the factor which should be multiplied by β^2 if multiple coupled walls are used (i.e. for n pairs of coupled shear walls $\beta^2 = n \frac{12 I_c l^2}{b^3 h I}$, while γ^2 always remains the same).

In order to assess the order of the relative importance of the structural parameters α H, β H and γ H the particular case is considered when, α H and γ H have their lowest value, and β H has its highest value, in this case the value of function F_1 is about 3×10^{-3}, while when β H has its lowest value and α H has its highest value function F_1 is about 6.1×10^{-3}, regardless of the value of γ H. The same tendencies are found for other relative values of these parameters. Hence, it can be concluded that in order to stiffen a stucture both α H and β H should be increased but the latter plays a relatively more important role. The effect of γ H on the overall structure is minimum,

although if only coupled walls are considered it can become significant. Similarly, a consideration of Figs. 8.21 to 8.23 suggest that;

(i) the axial force function F_2 is a minimum when βH has its lowest value , regardless of the values of αH and γH, and F_2 is a maximum when βH has its highest value and αH and γH have their lowest values. As expected, αH does not play a significant role since function F_2 is almost wholly related to the action of the coupled shear walls. However, the role of βH is relatively more significant than that of γH.

(ii) since the moments in the walls are functions of the second derivative of the deflection, the effects of the parameters αH, βH and γH on the function F_3 are the same as on F_1, as explained previously.

(iii) the function F_4 is a minimum (= 6×10^{-5}) when αH and γH have their lowest values and βH has its highest value, and F_2 is a maximum (= 0.78) when αH and βH have their highest and lowest values respectively, regardless of the value of γH. It may therefore be deduced that αH plays a more significant role than βH and γH.

In Appendix 2 design curves are included for the functions F_1, F_3 and F_4 which cover the full range of parameters αH, βH and γH.

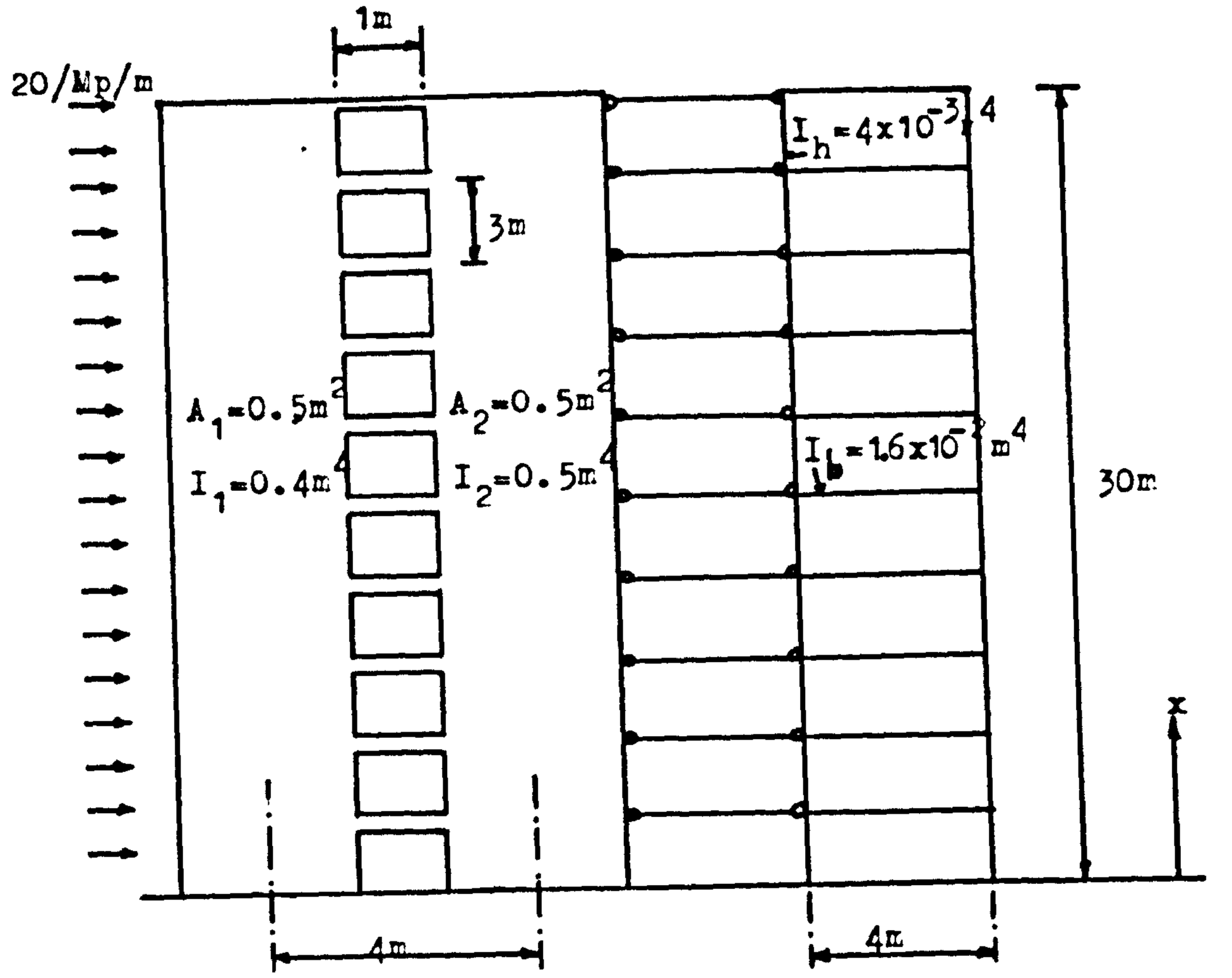

(a)

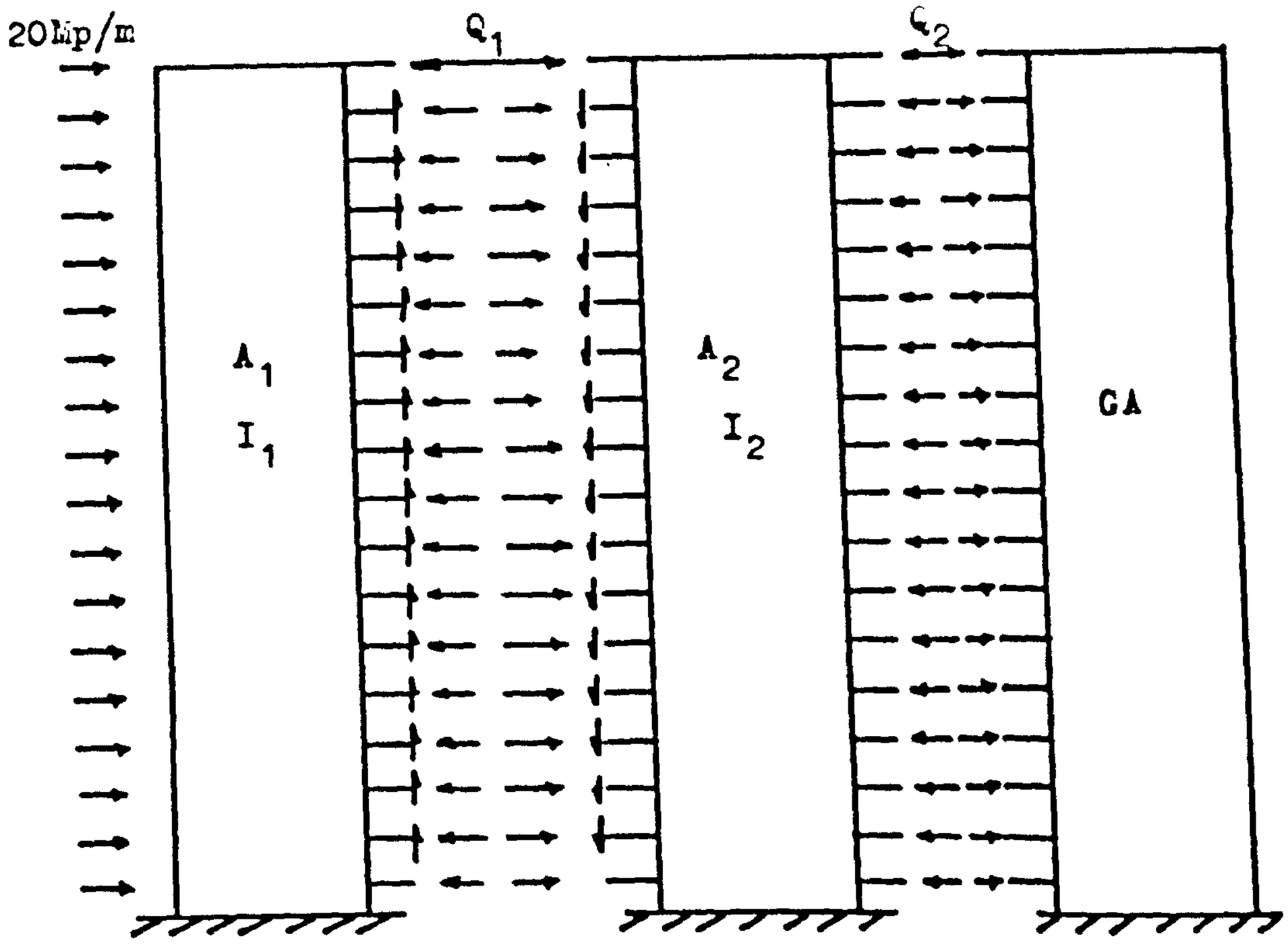

(b)

Fig. 8.1 Real and Substitute structures of example I

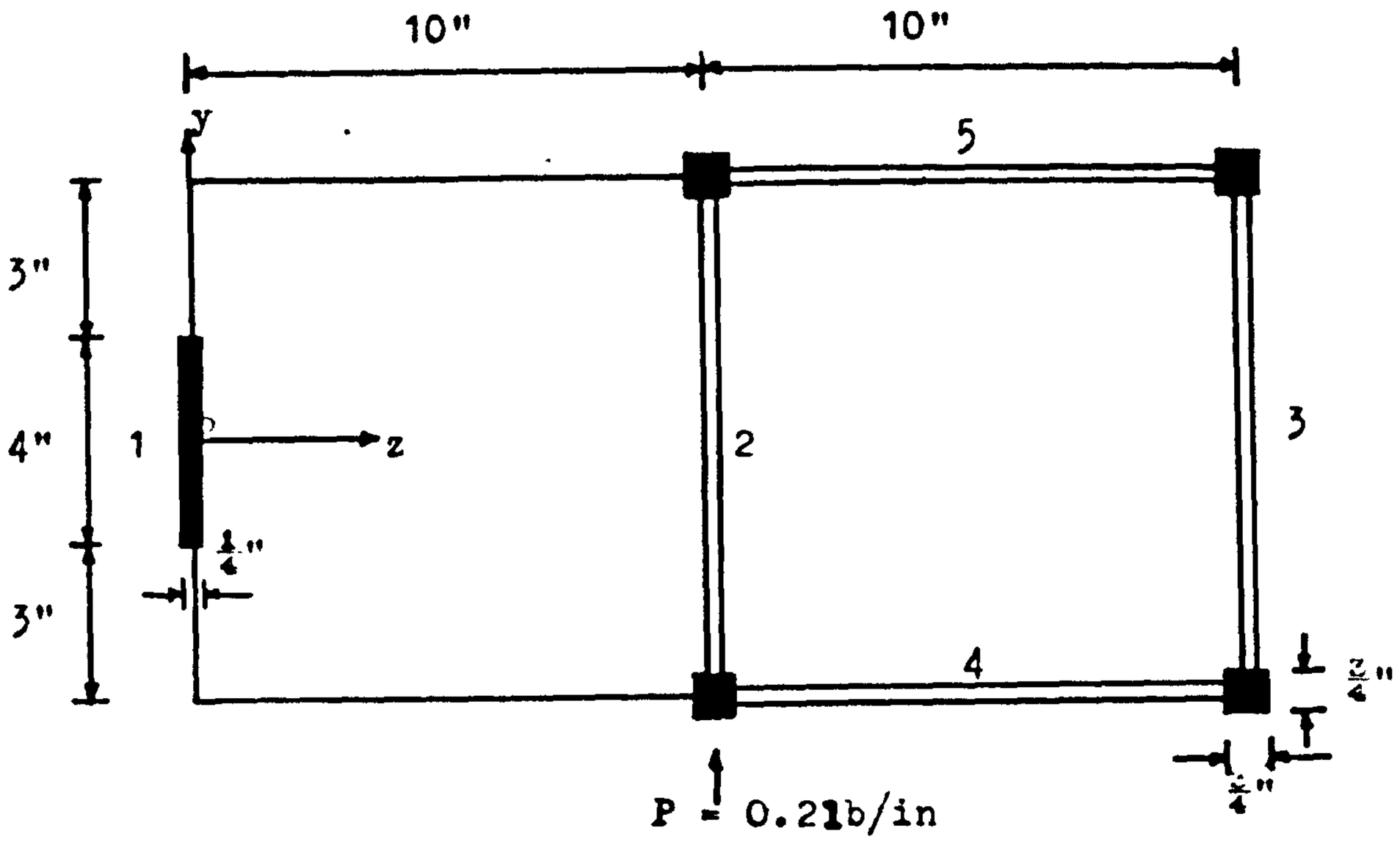

(a)

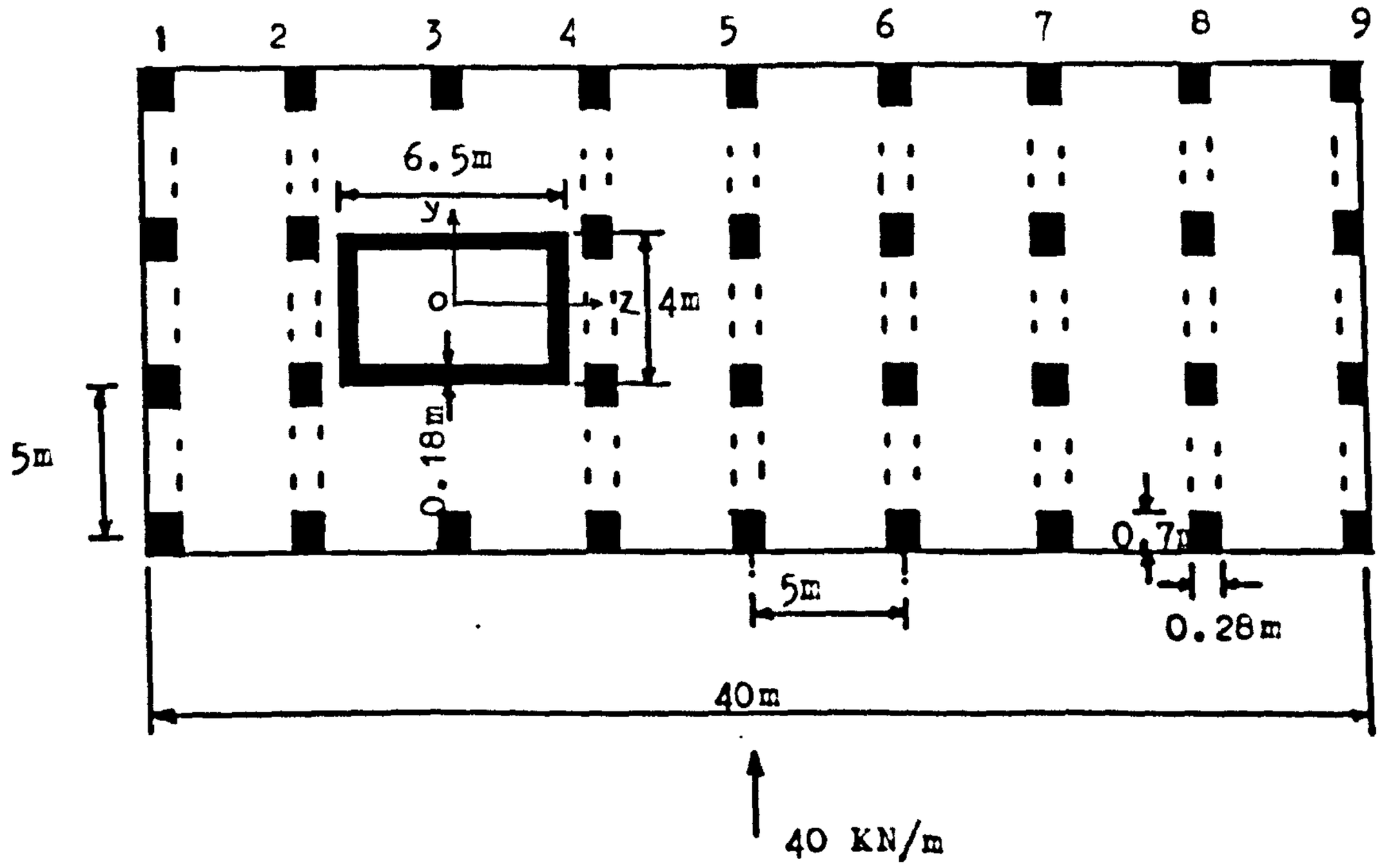

(b)

Fig. 8.2 Plan forms of example structures II and III

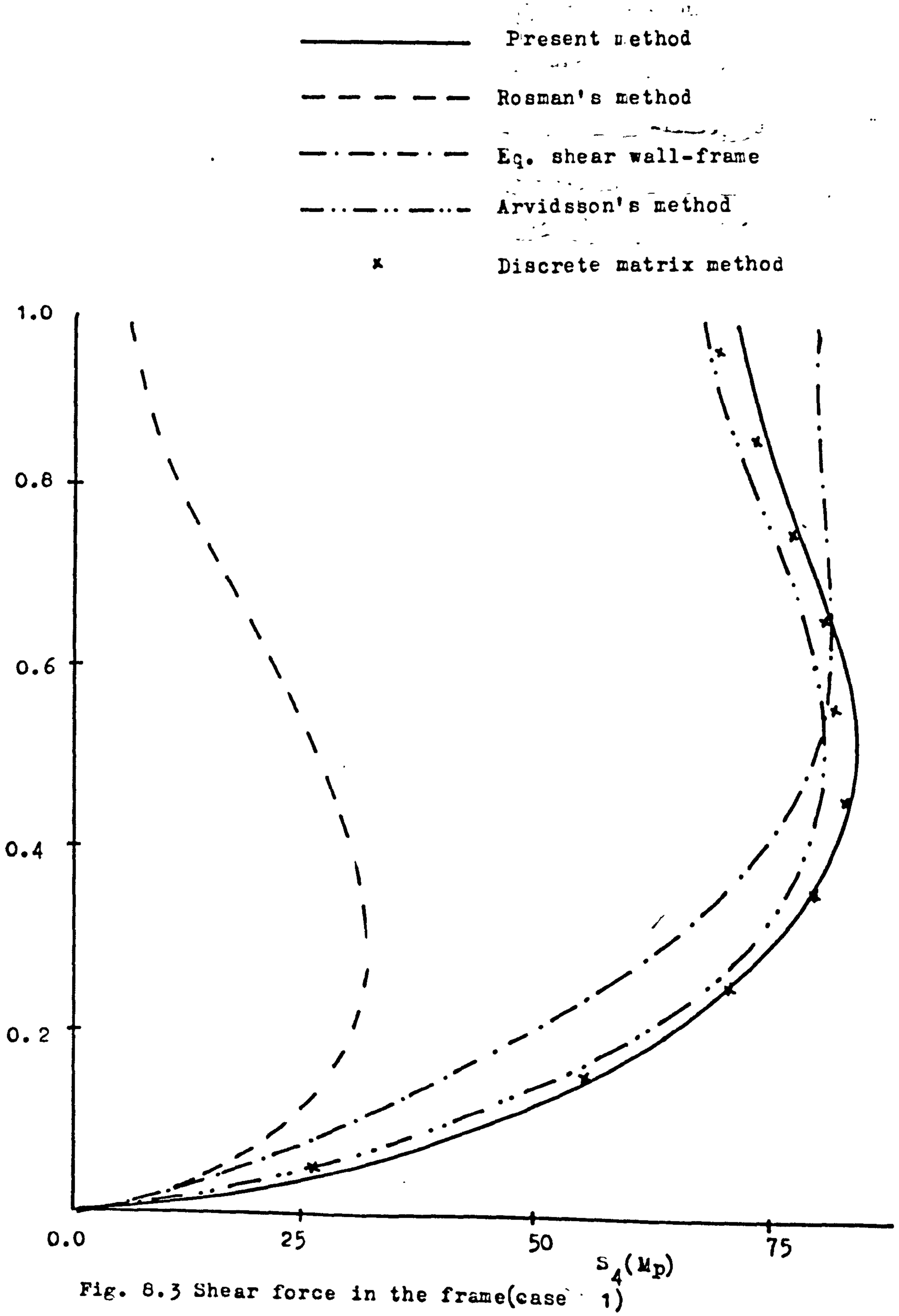

Fig. 8.3 Shear force in the frame(case 1)

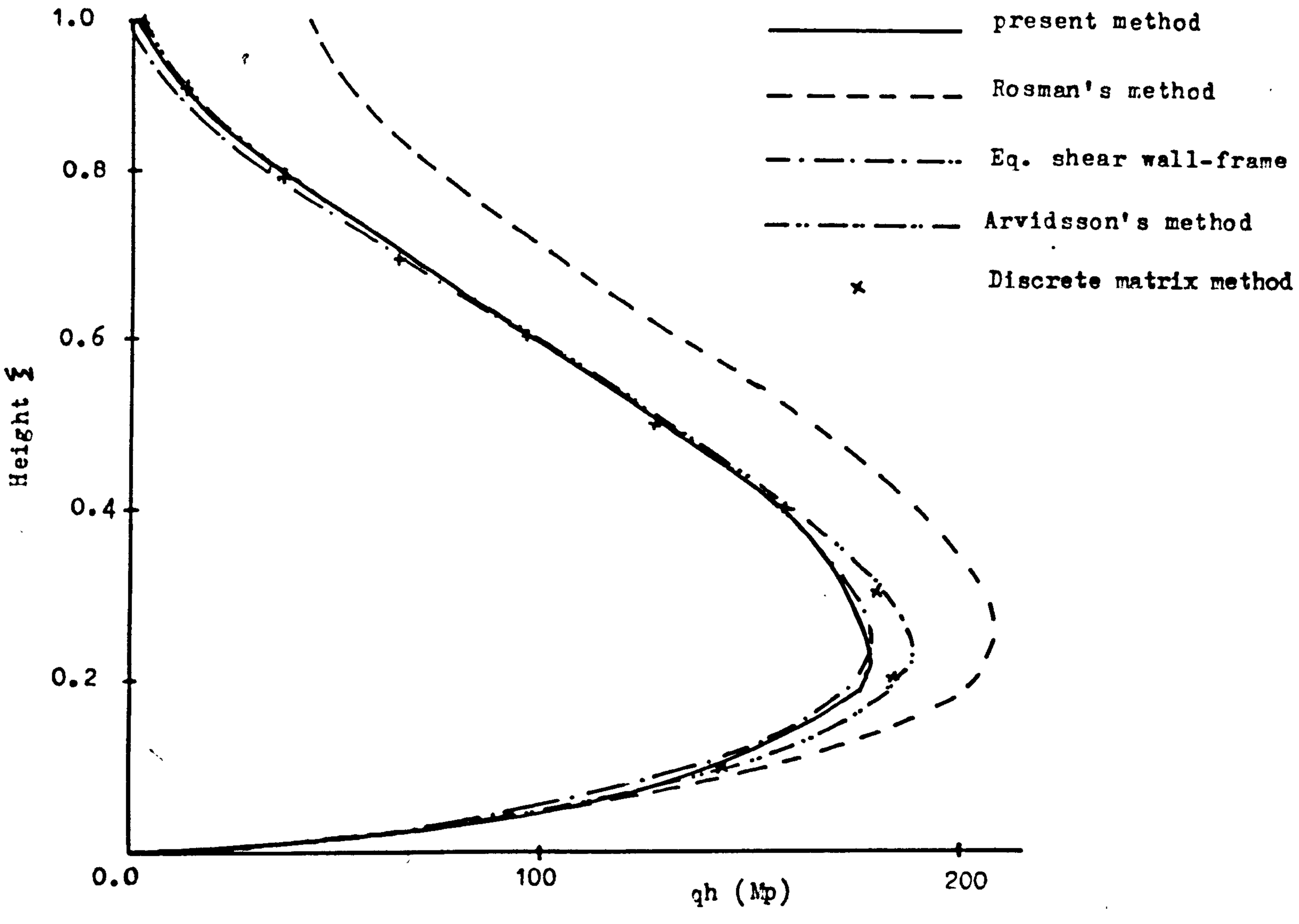

Fig. 8.4 Shear flow (qh) in connecting beams (case 1)

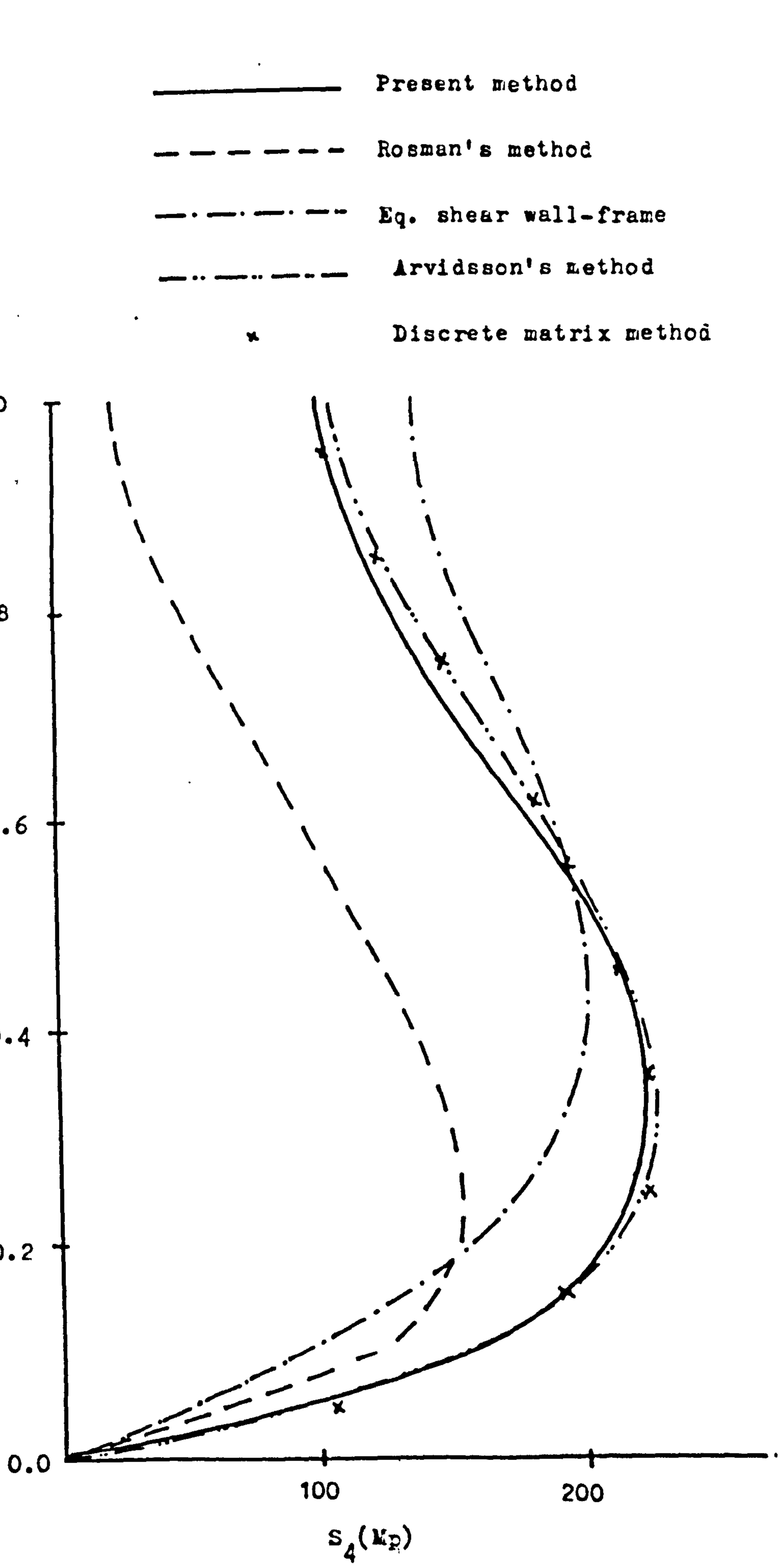

Fig. 8.5 Shear force S_4 in frame (case 2)

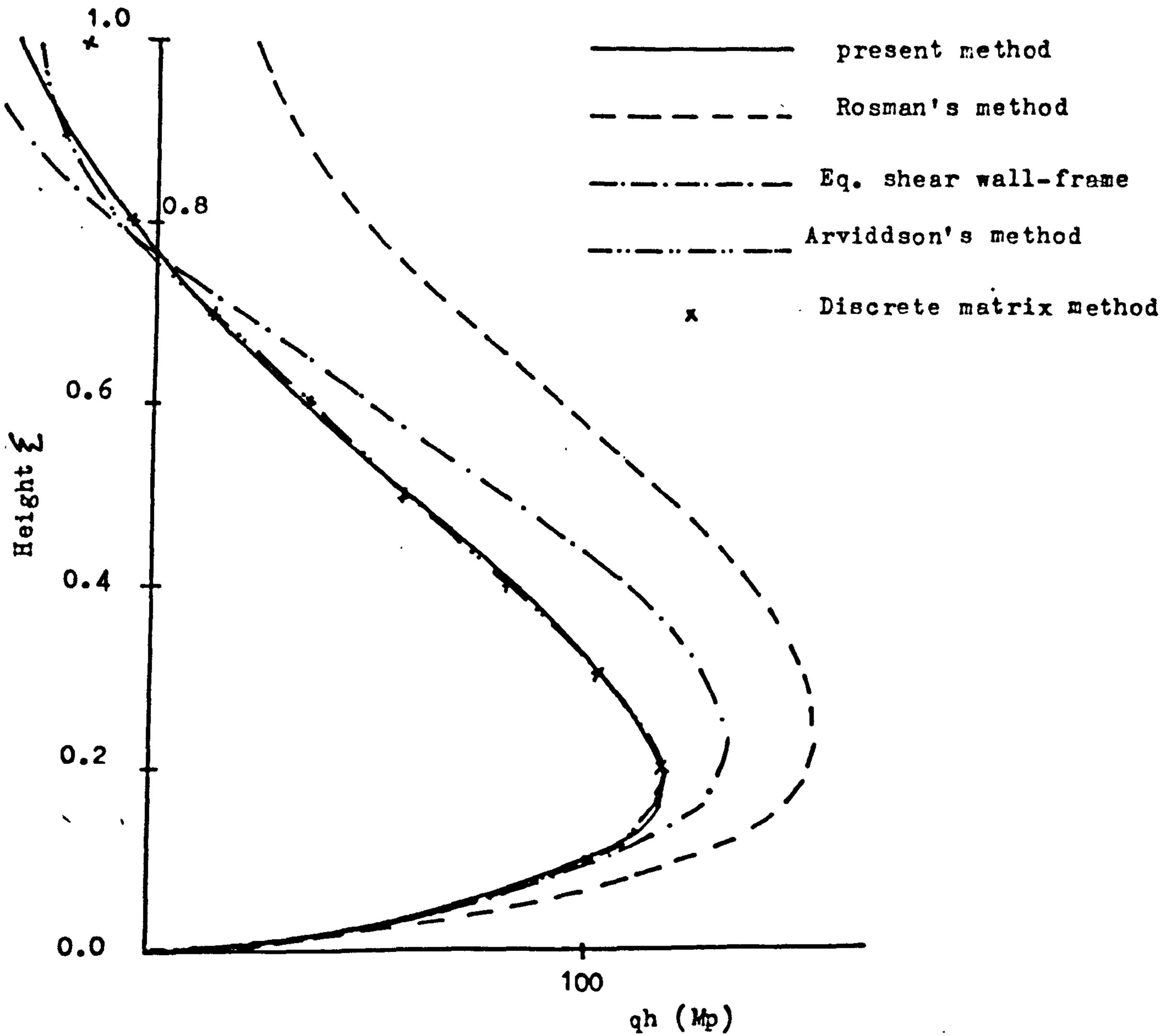

Fig. 8.6 Shear flow (qh) in connecting beams (case 2)

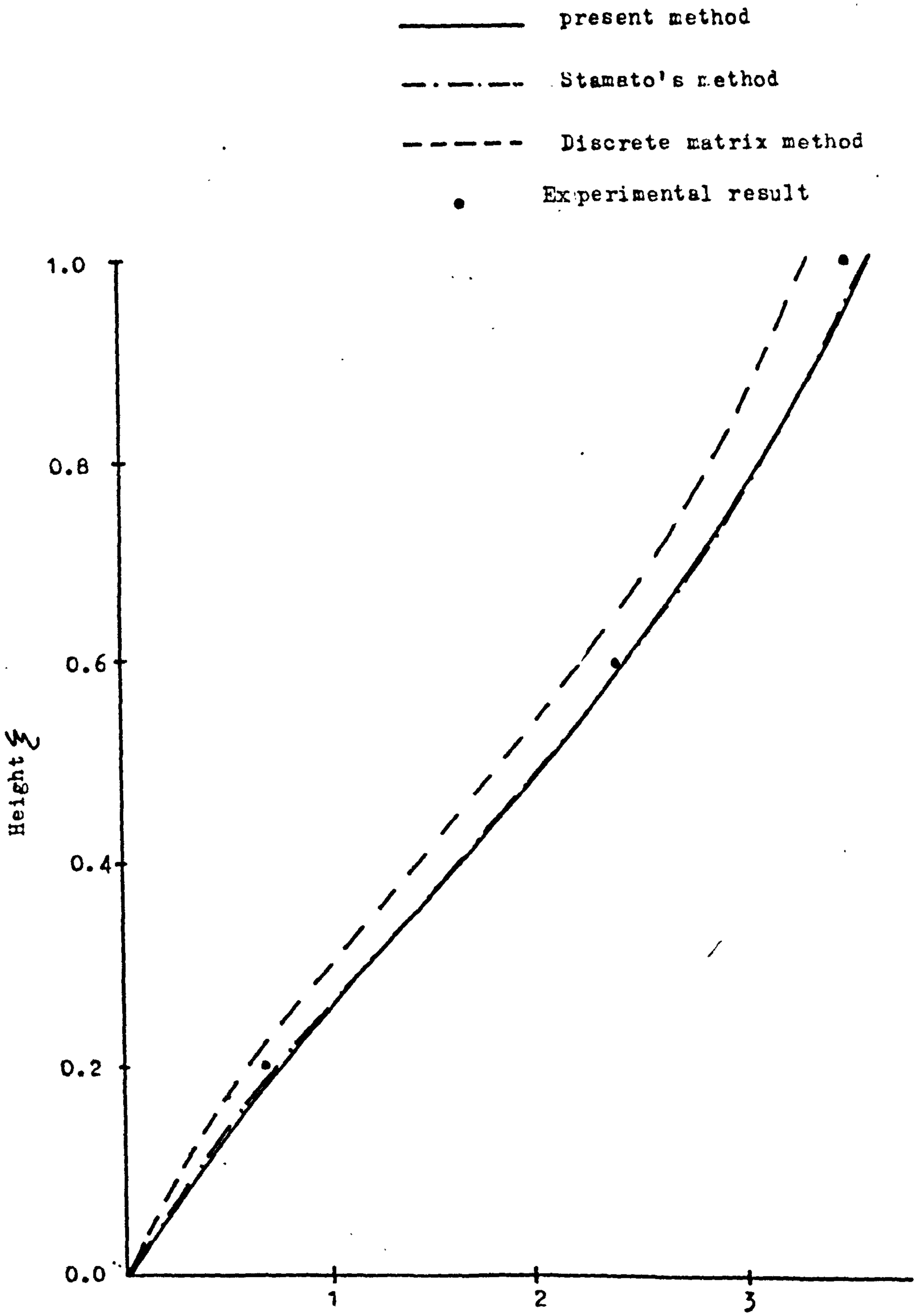

Fig. 8.7 Distribution of lateral deflection of frame 2.

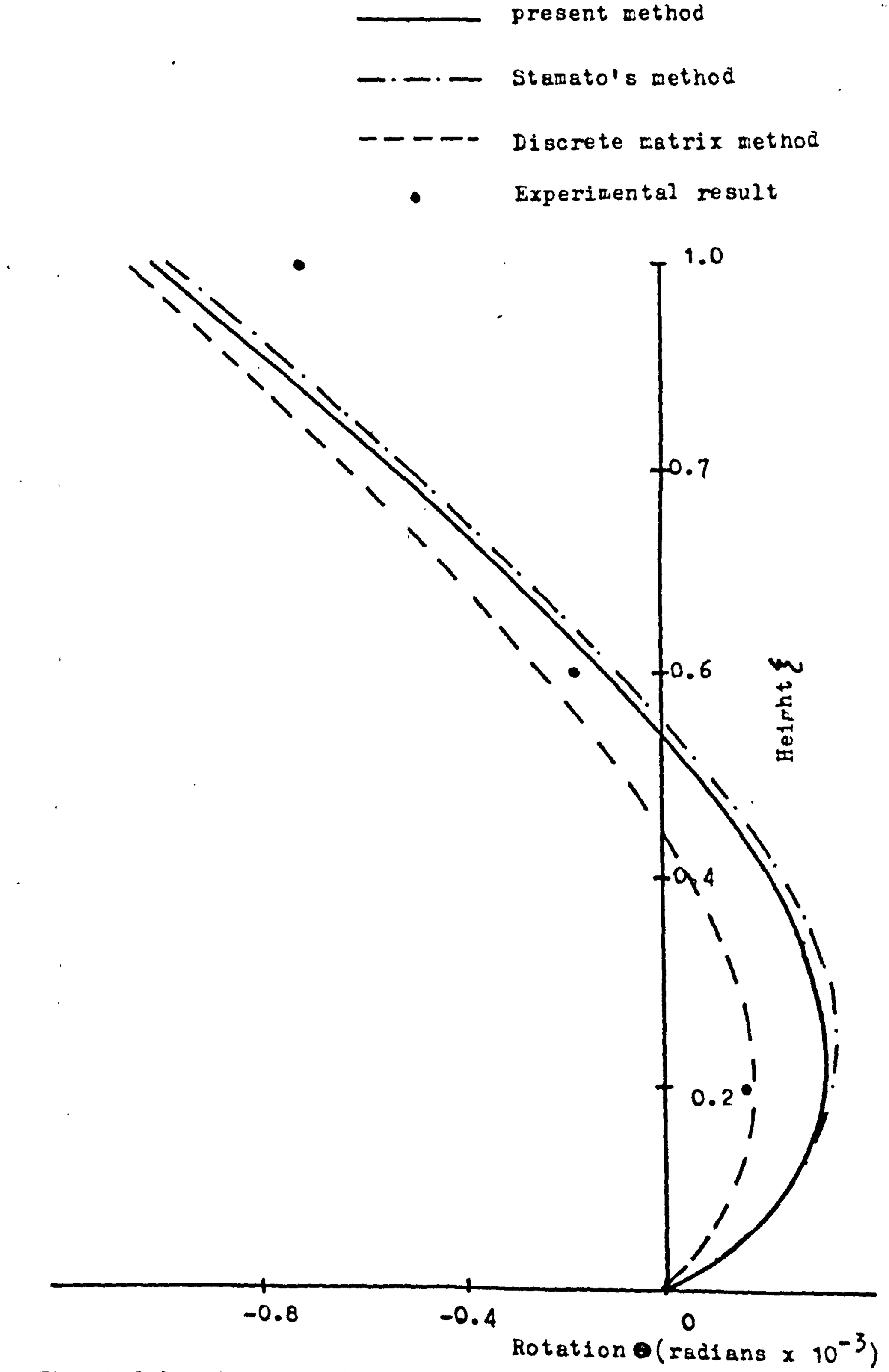

Fig. 8.8 Rotations of Diaphragms

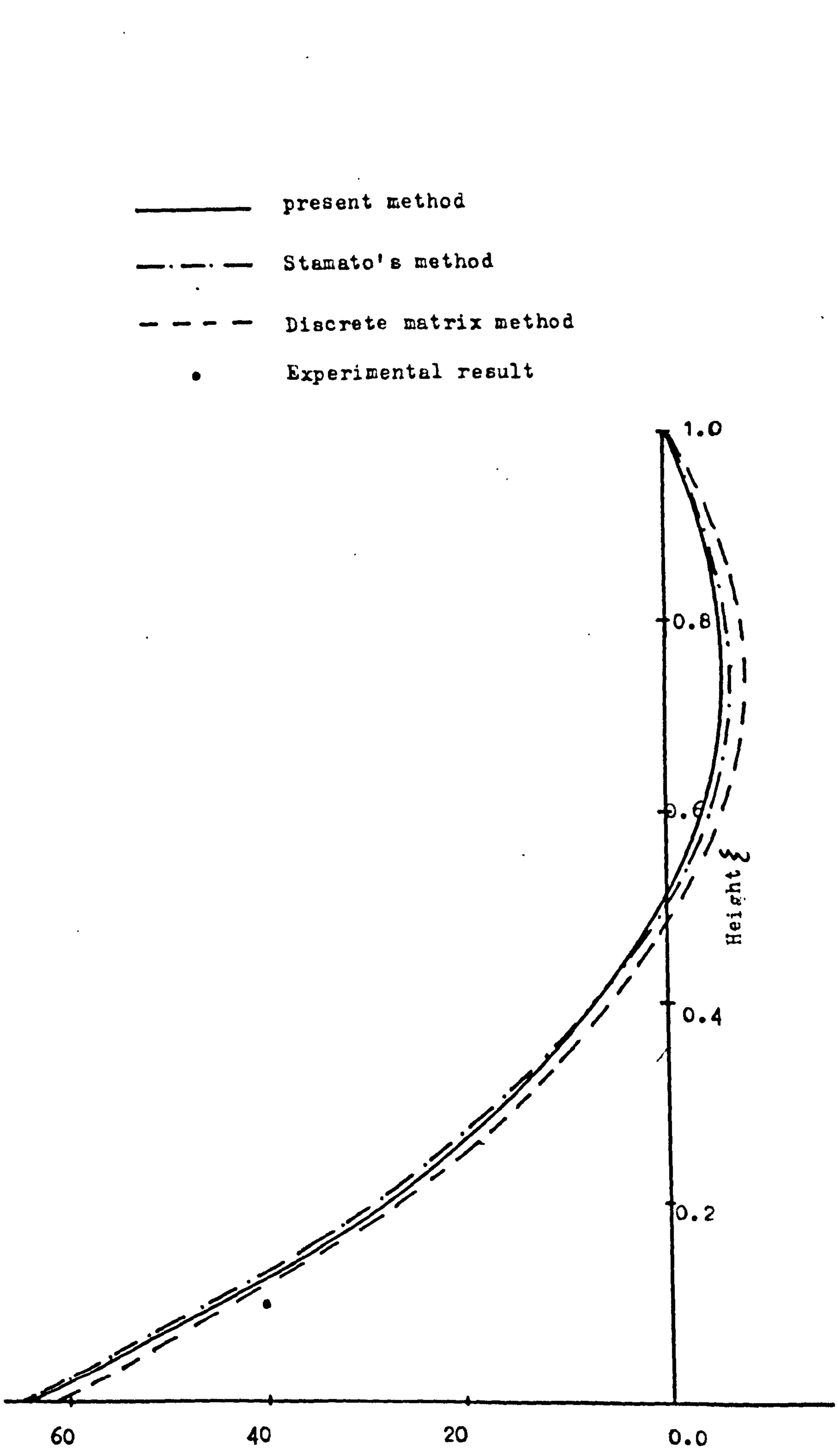

Fig. 8.9 Distribution of bending moment in wall (Example II)

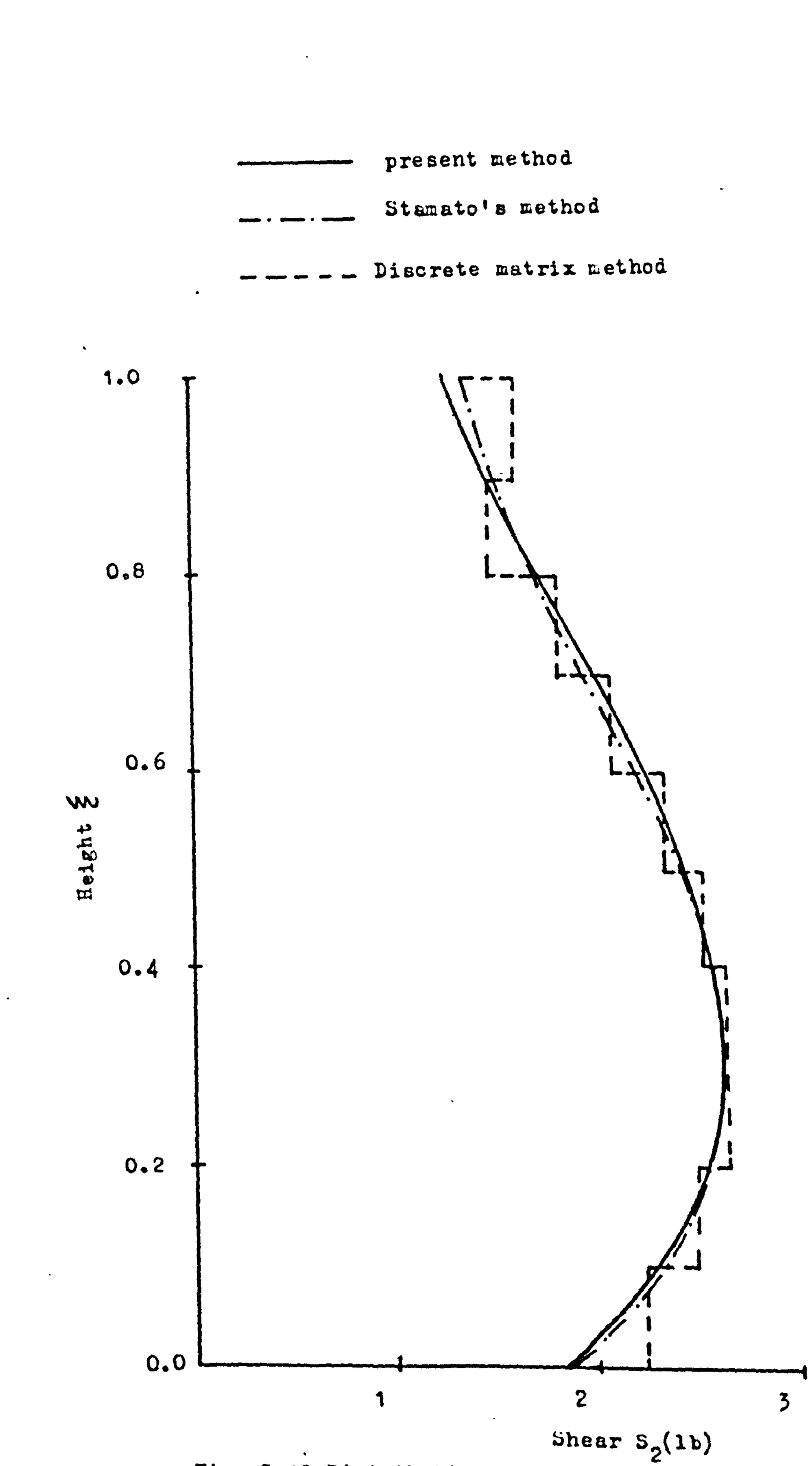

Fig. 8.10 Distribution of total shear force in Frame 2 (Example II)

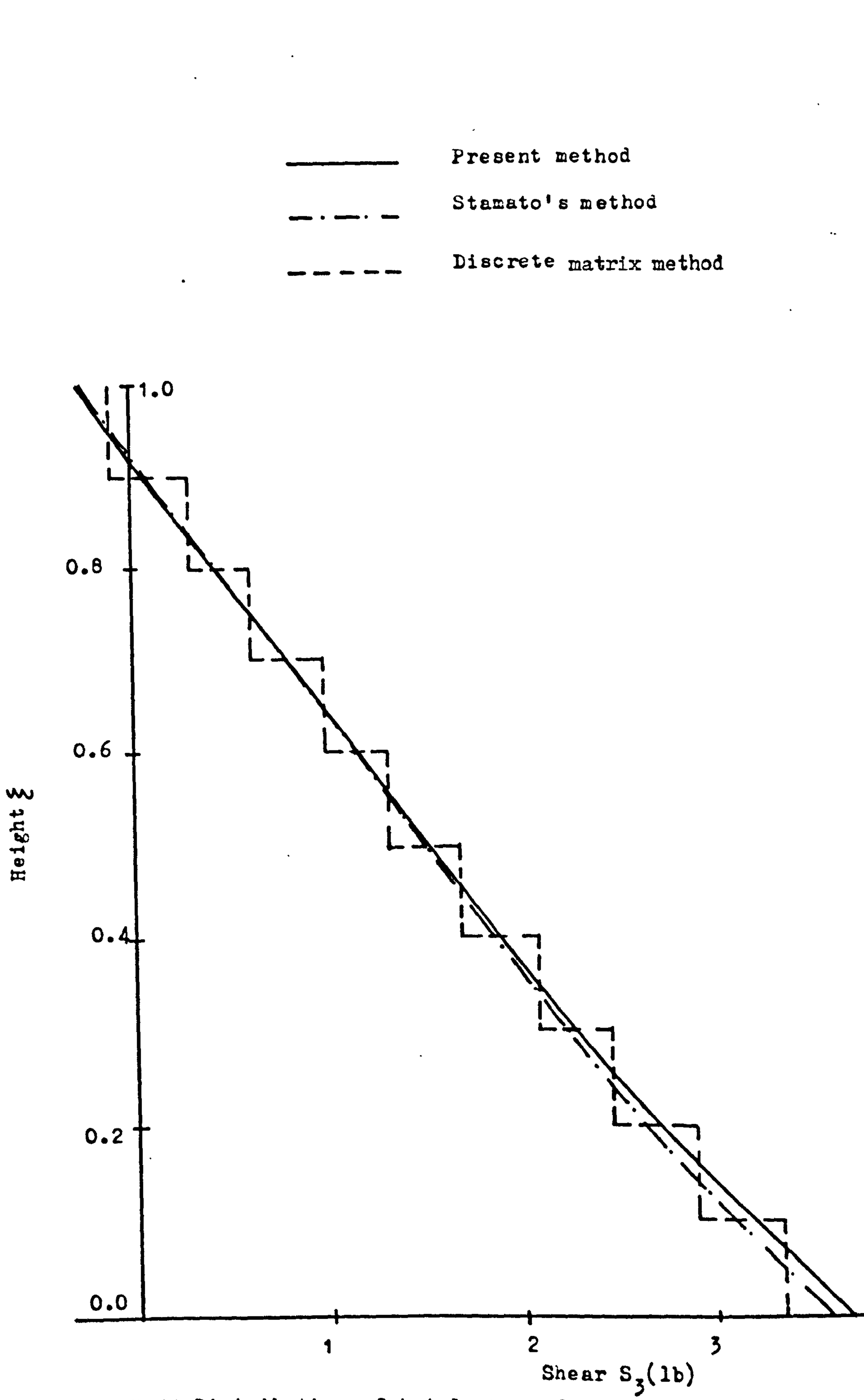

Fig. 8.11 Distribution of total shear force in frame 3 (Example II)

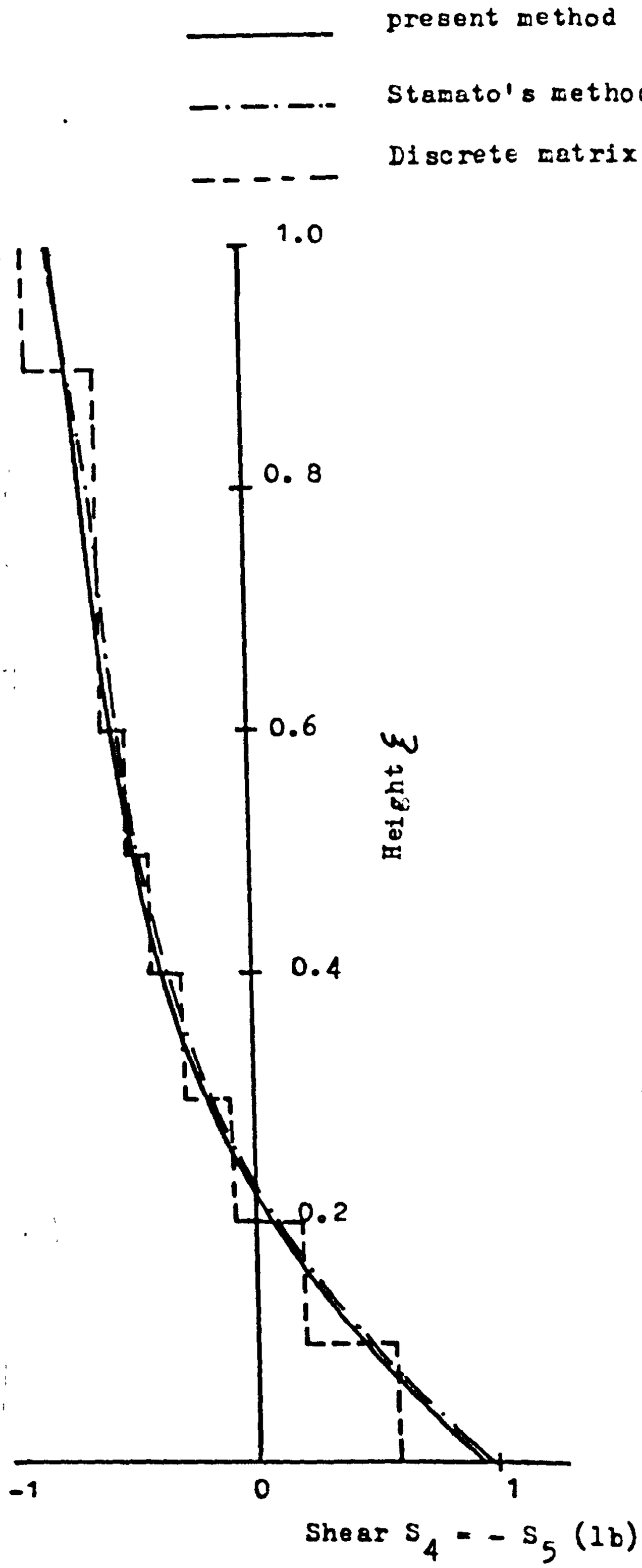

Fig. 8.12 Distribution of total shear force in Frames 4,5 (Example II)

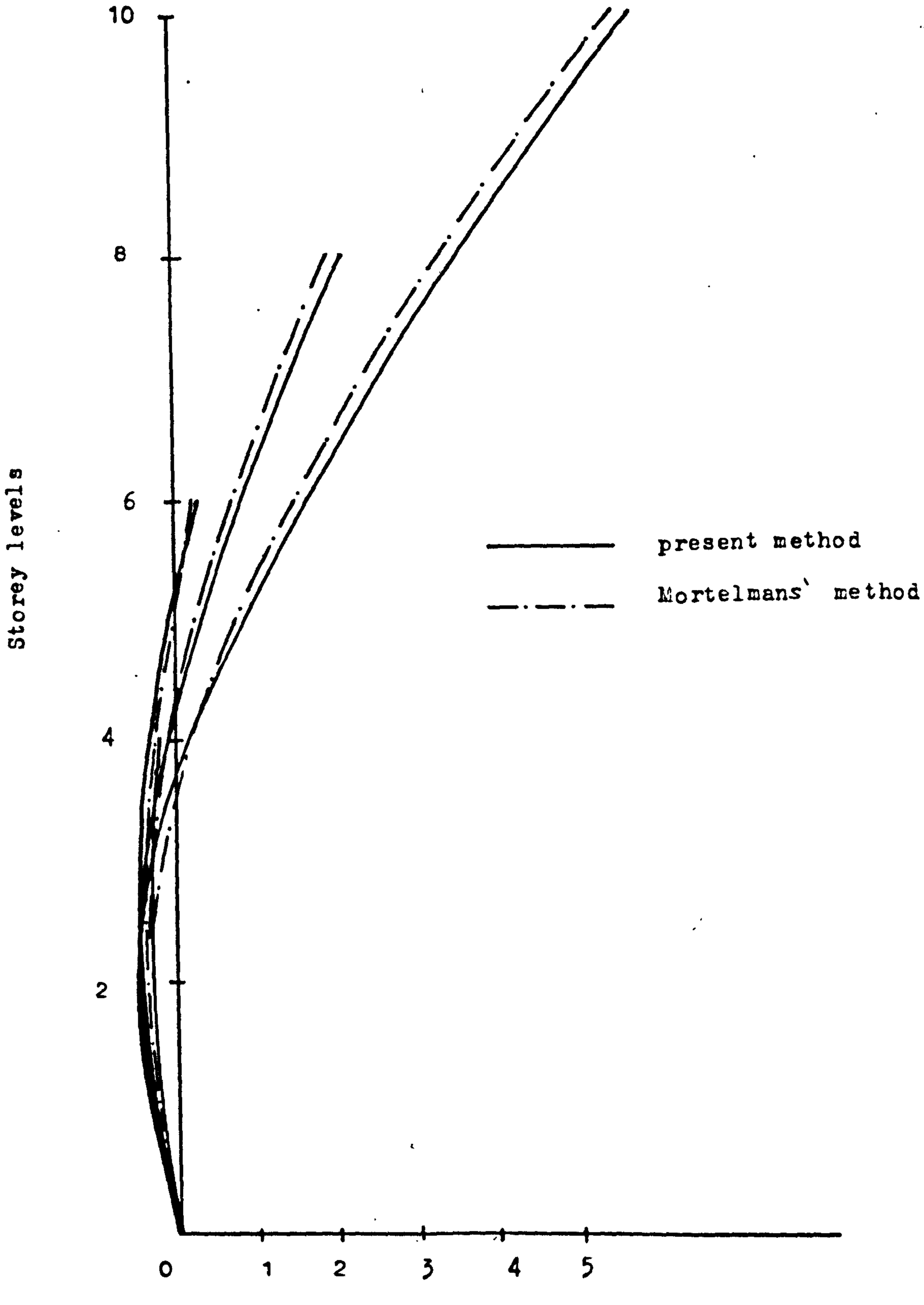

Fig. 8.13 Distributions of lateral deflections in Frame 1 for buildings of 4,6, 8 and 10 storey levels of plan form shown in Fig. 8.2(b) (Example III)

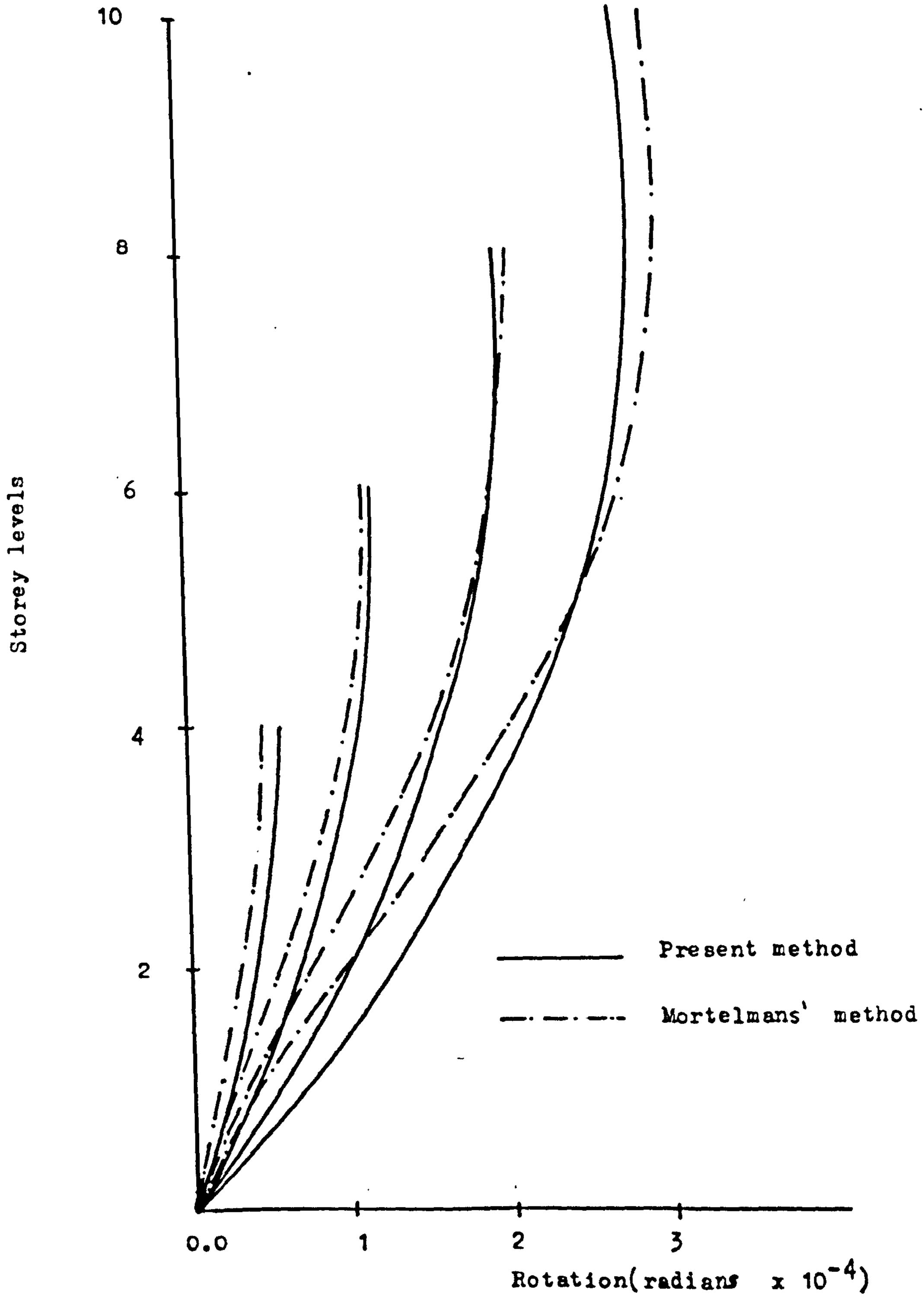

Fig. 814 Distributions of rotations for buildings of 4,6,8 and 10 storey levels of plan form shown in Fig. 8.2(b) (Example III)

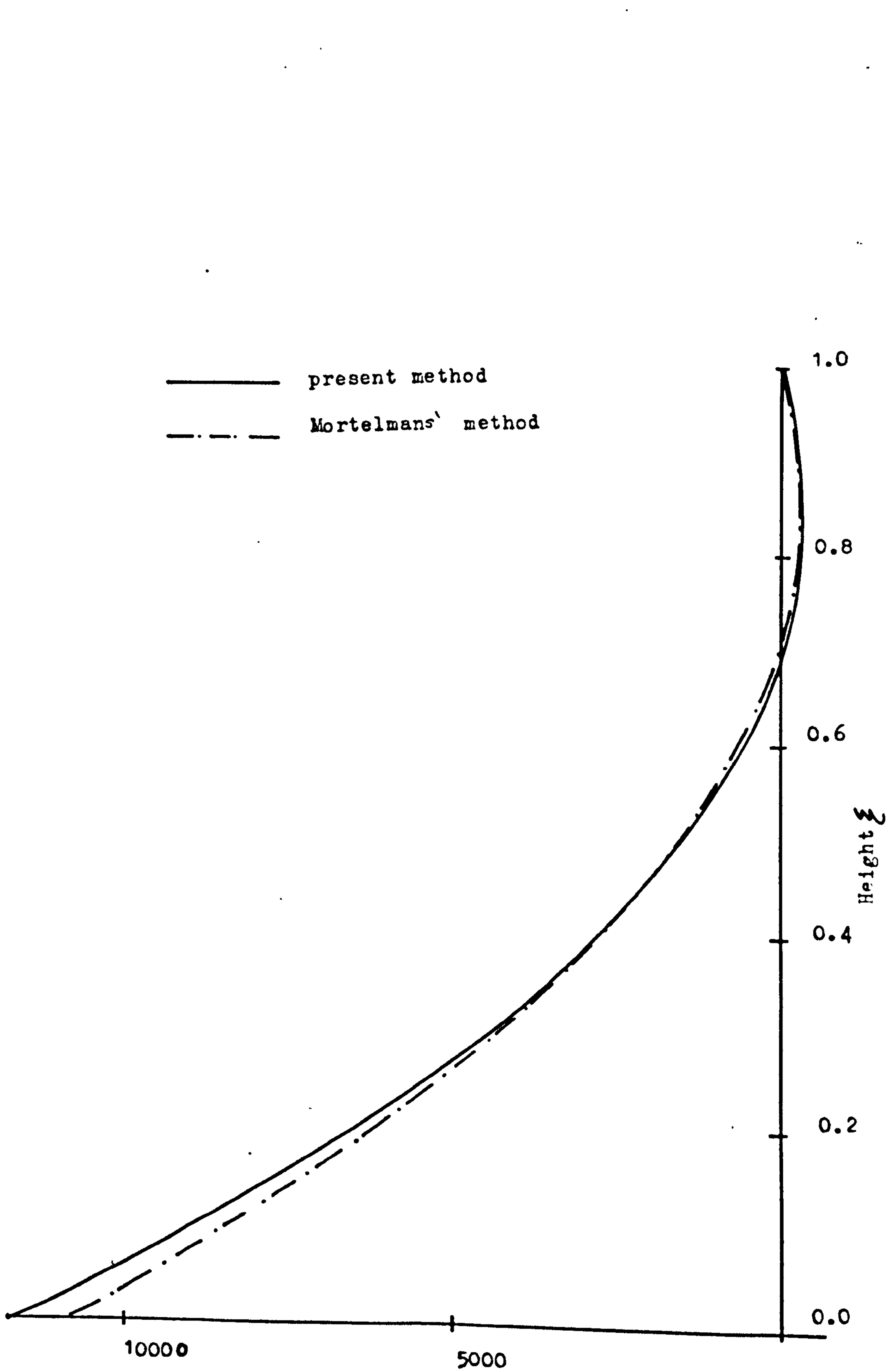

Fig. 8.15 Distribution of bending moment in lift shaft (Example III)

———— present method

—·—·—·— Mortelmans' method

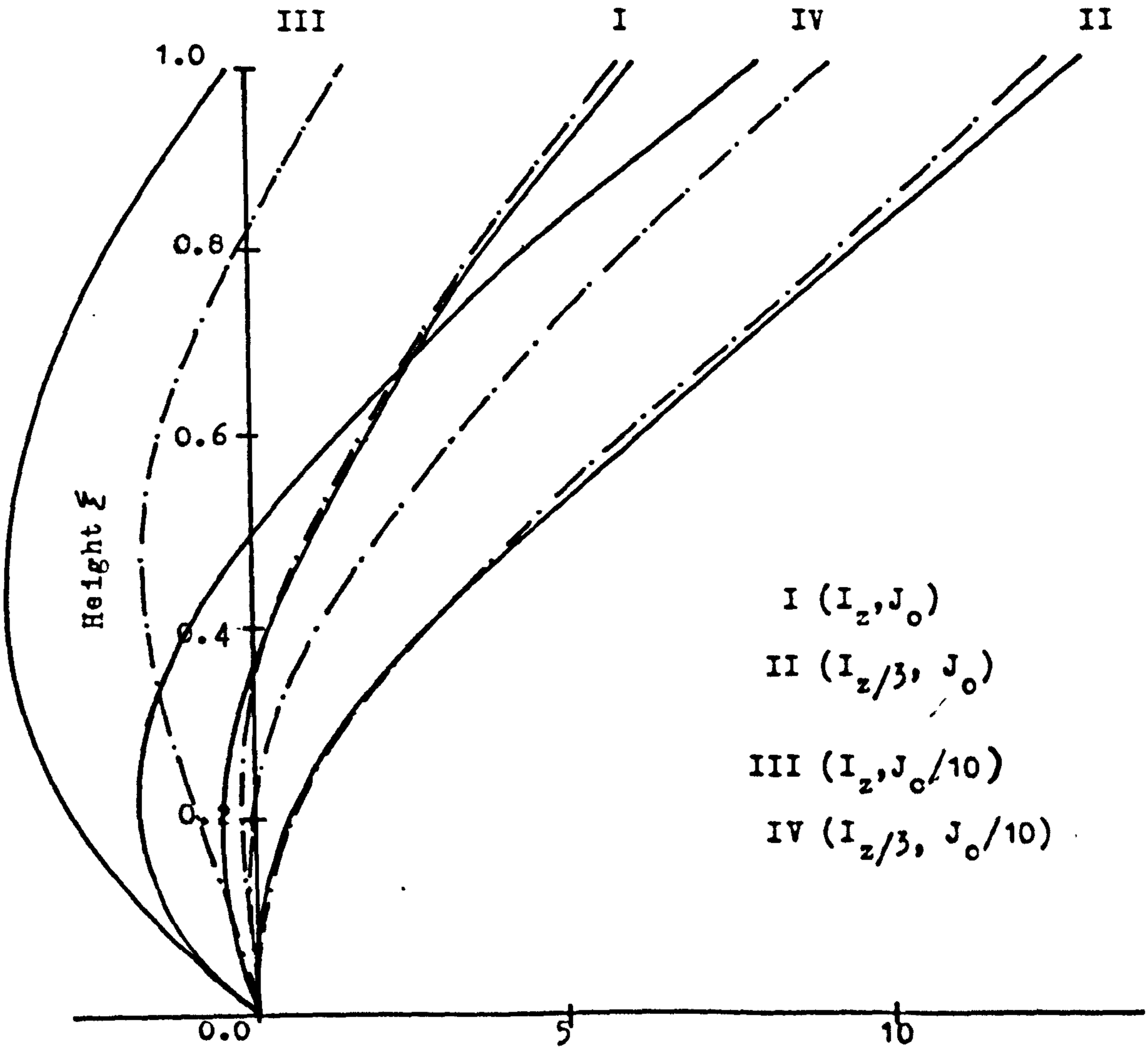

Fig. 8.16 Distributions of lateral deflections in frame 1 for various internal stiffnesses (Example III)

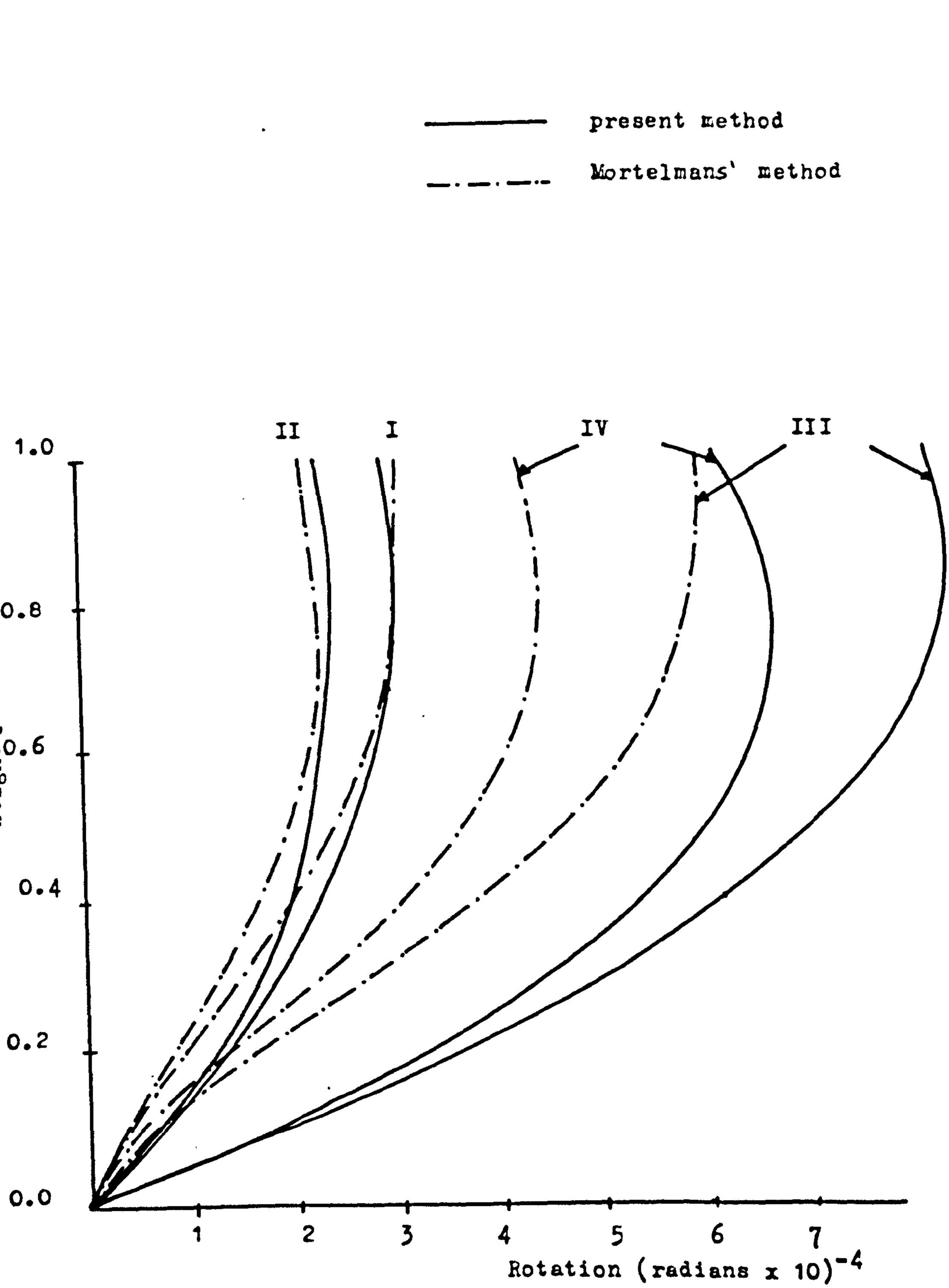

Fig. 8.17 Distributions of rotations for various internal stiffnesses (Example III)

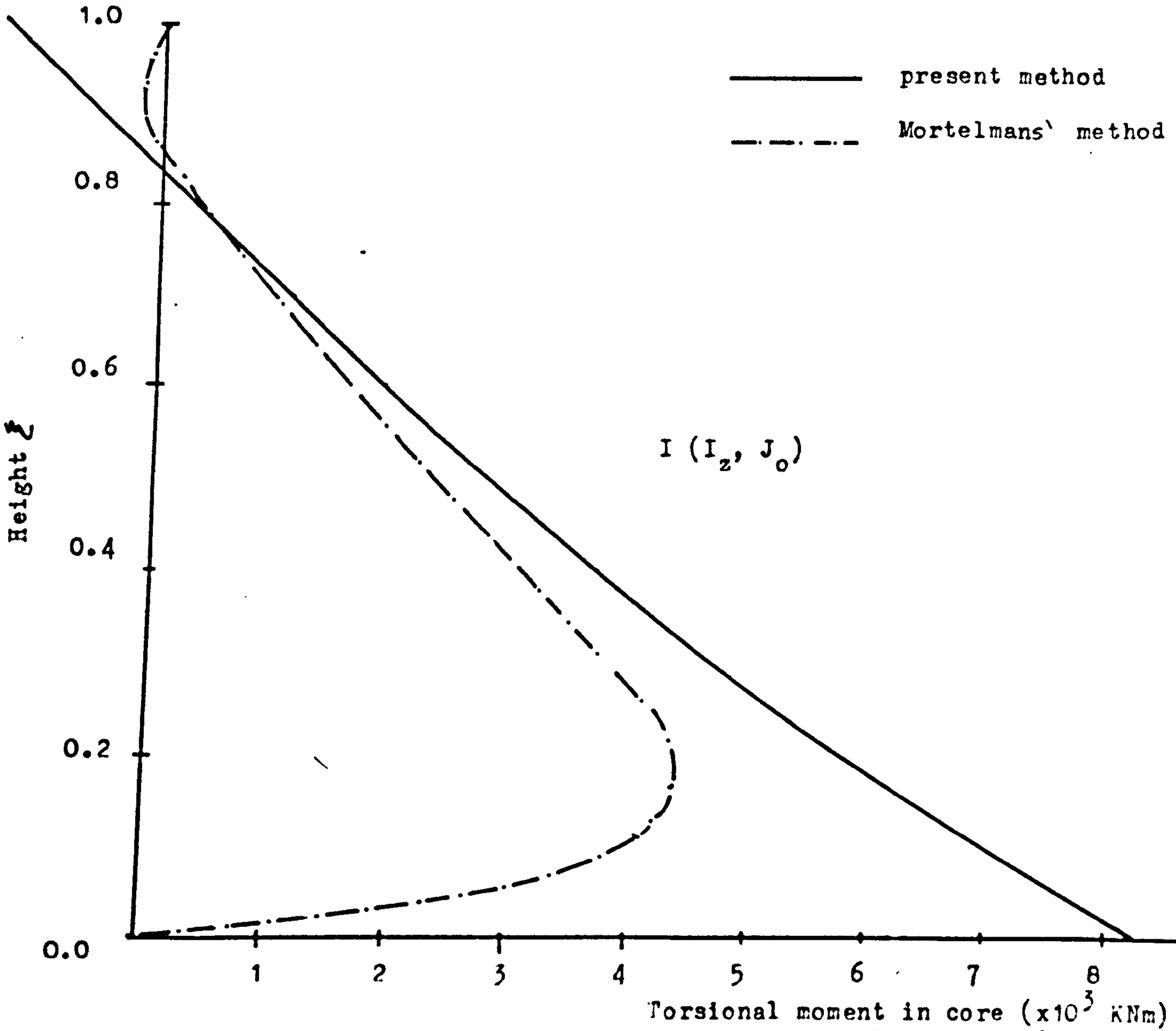

Fig. 8.18 Distribution of the torsional moment in lift shaft (case I)
(Example III)

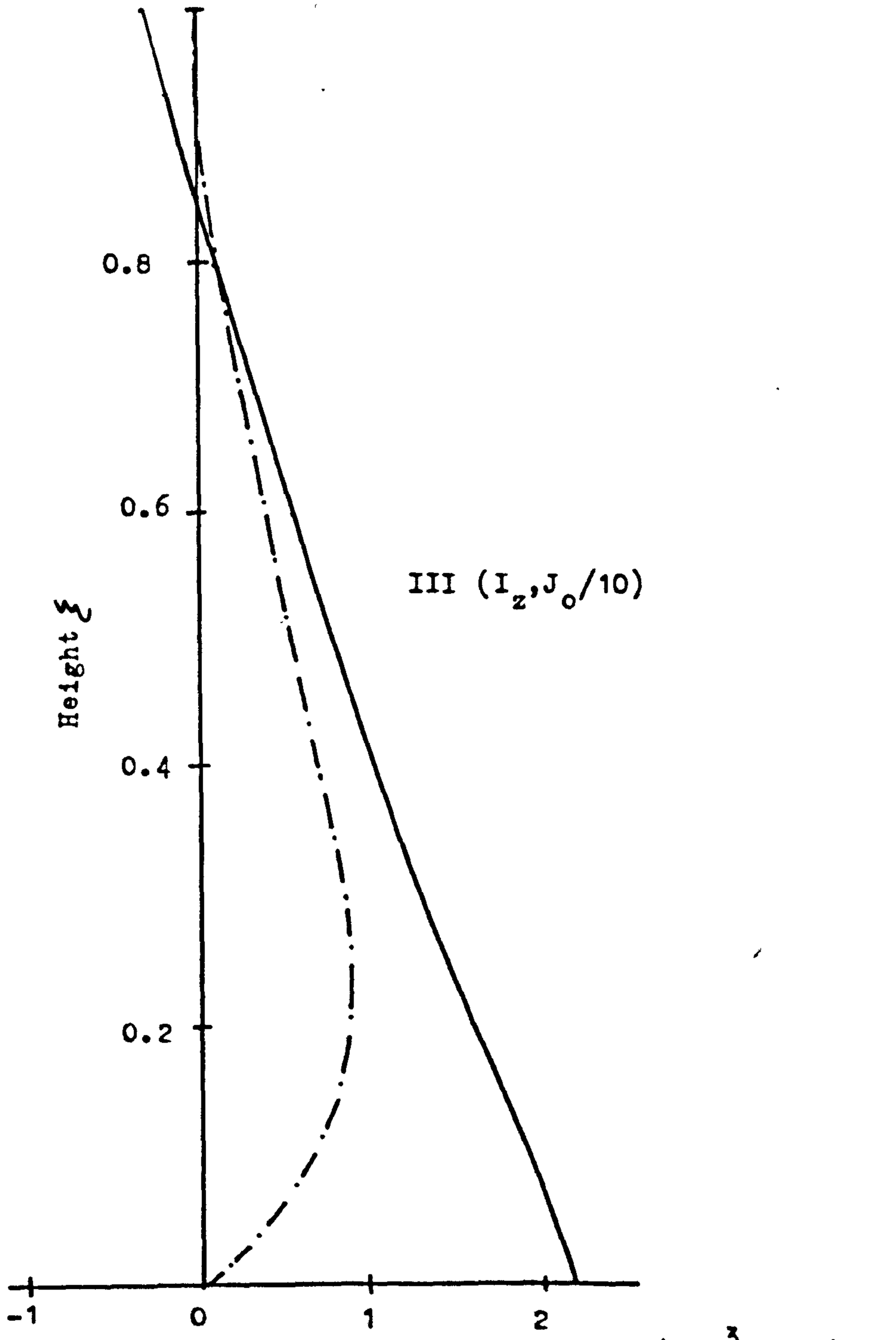

Fig. 8.19 Distribution of torsional moment in lift shaft (case III)

(Example III)

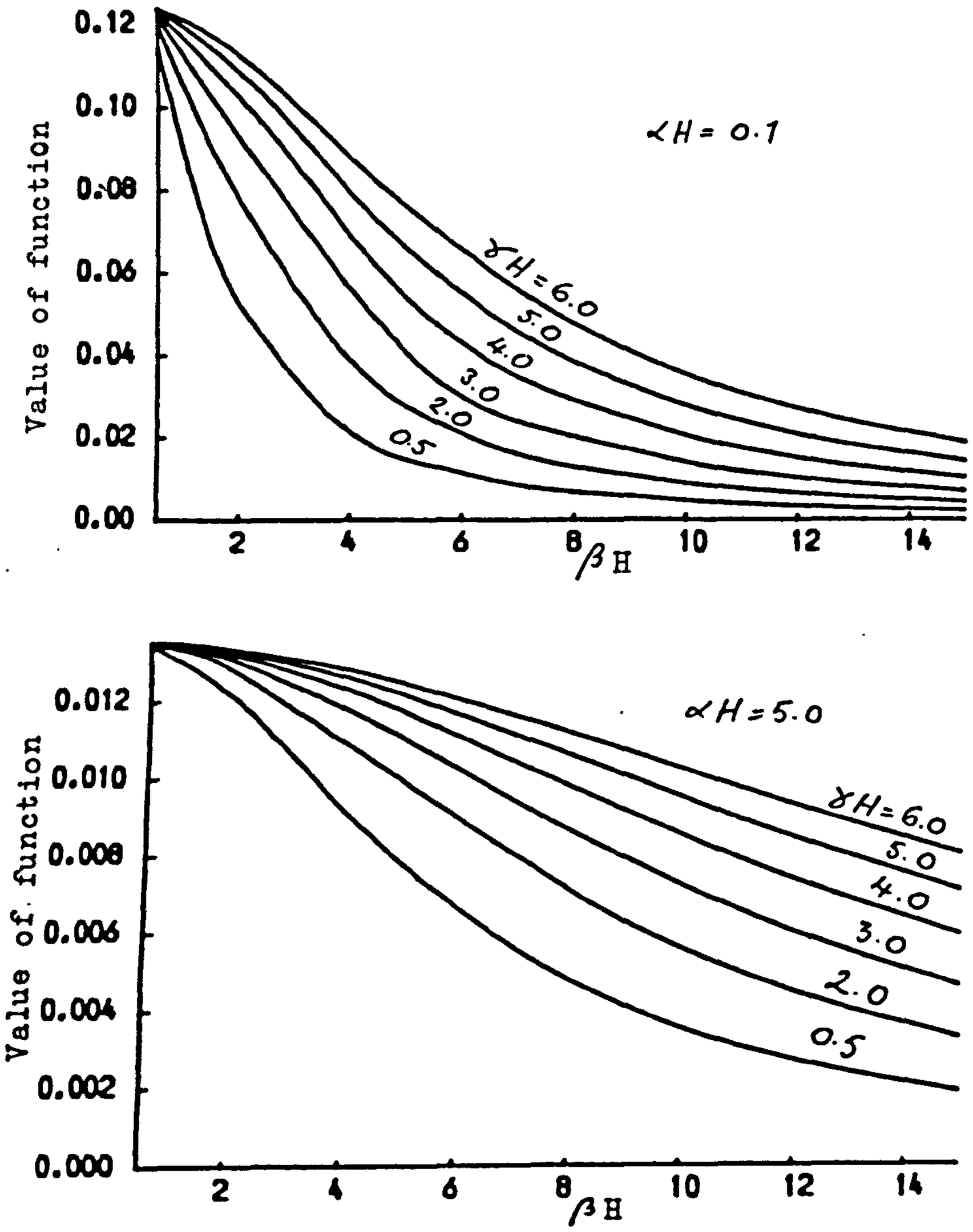

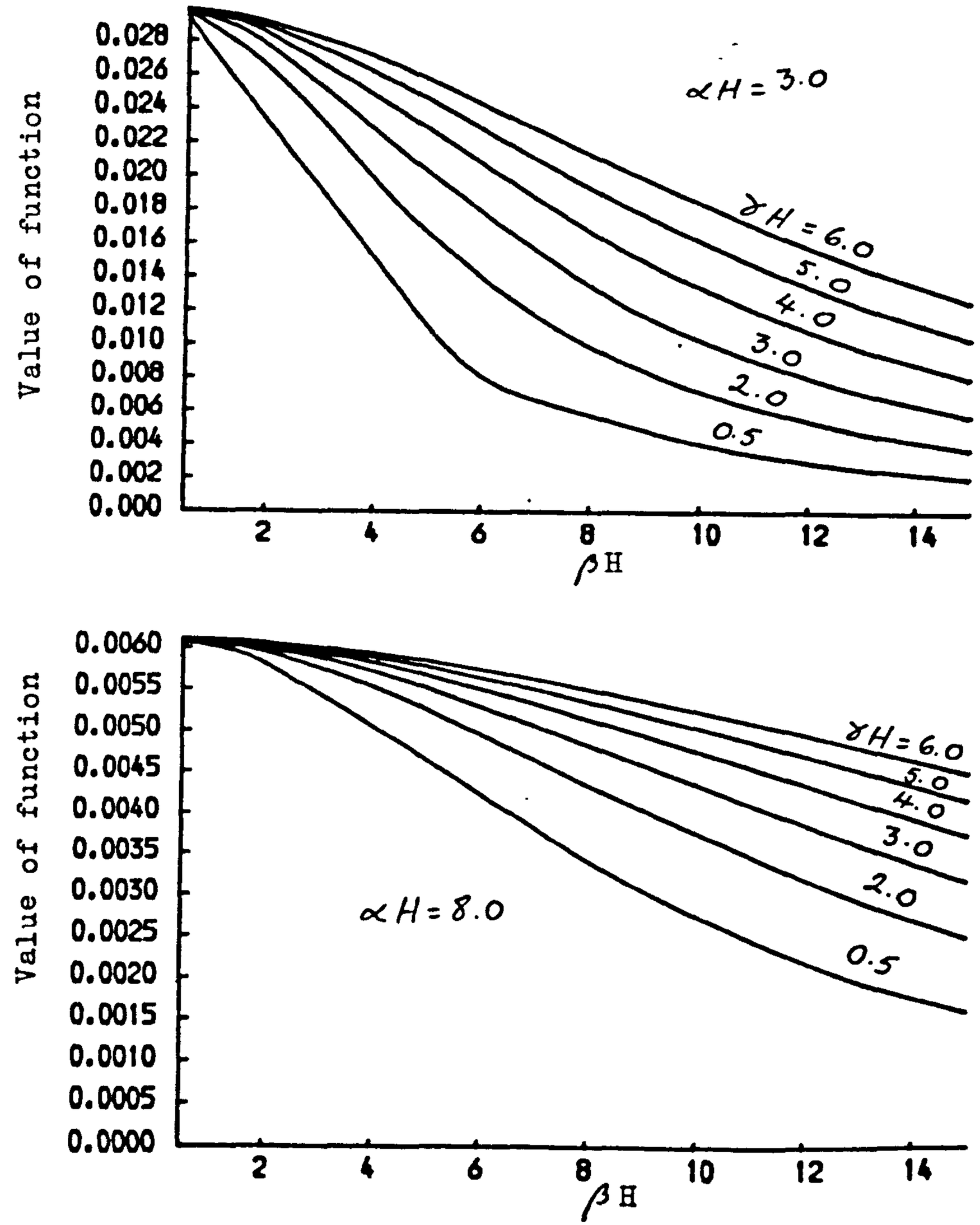

Fig. 8.20 Distributions of deflection function F_1

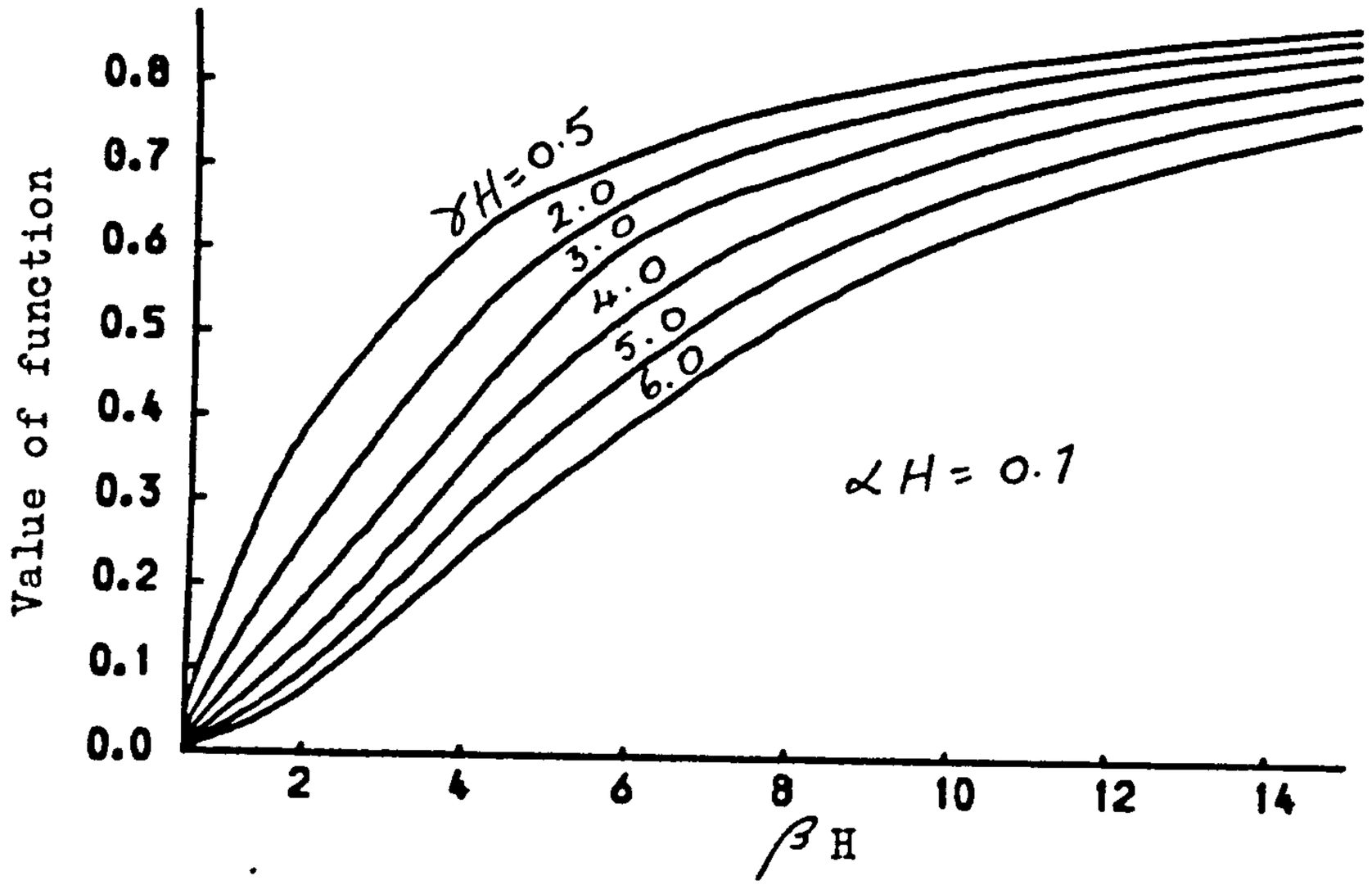

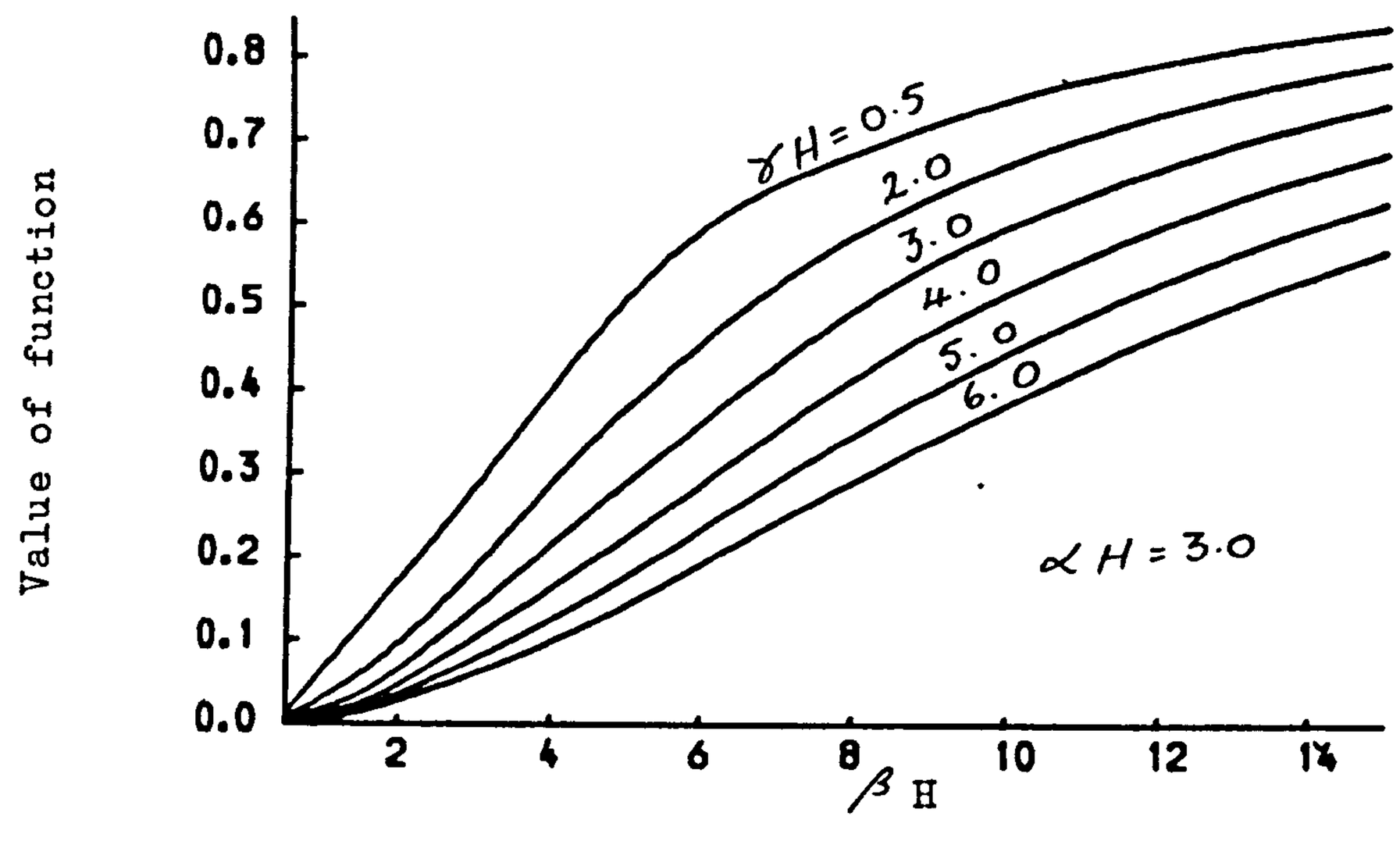

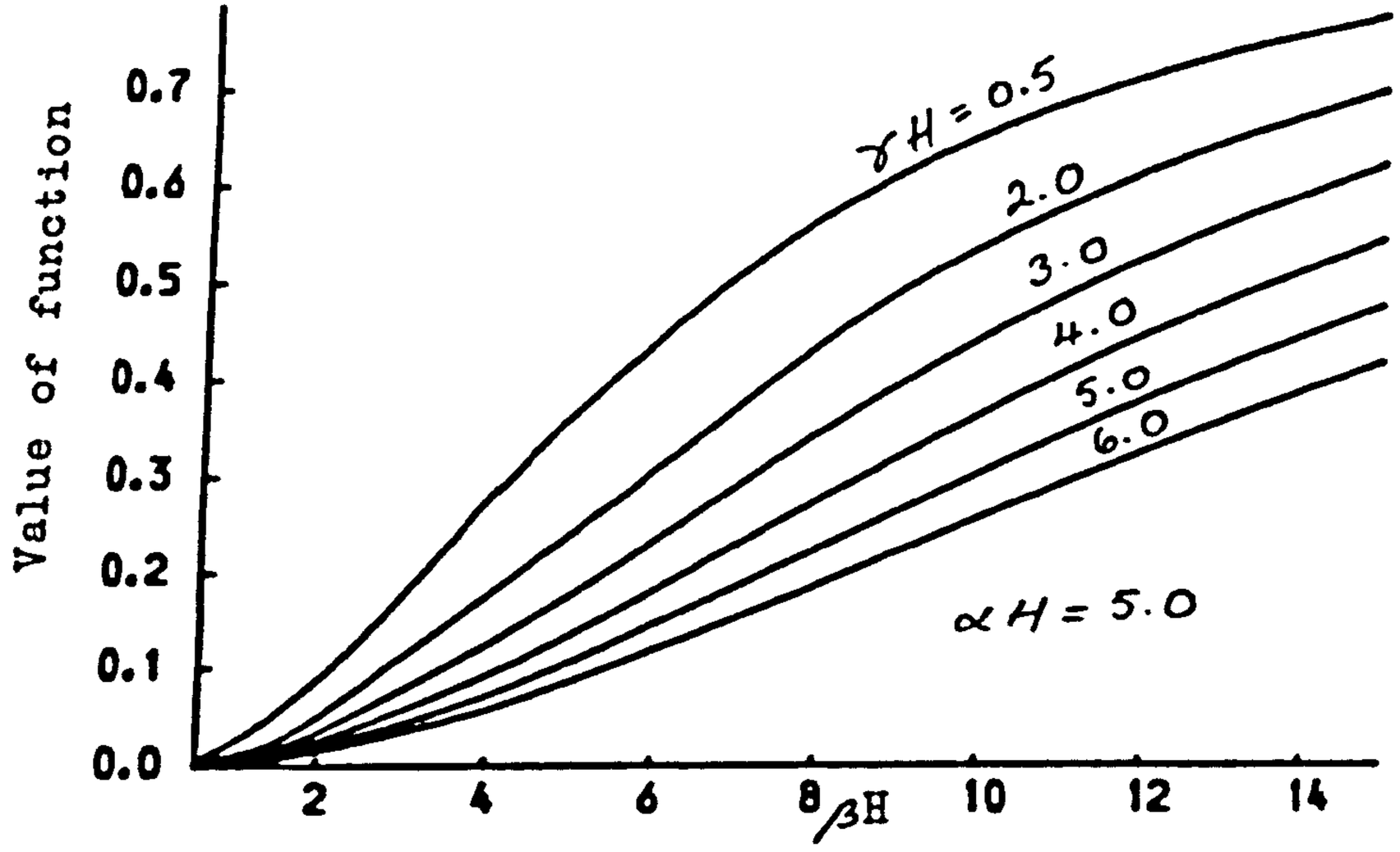

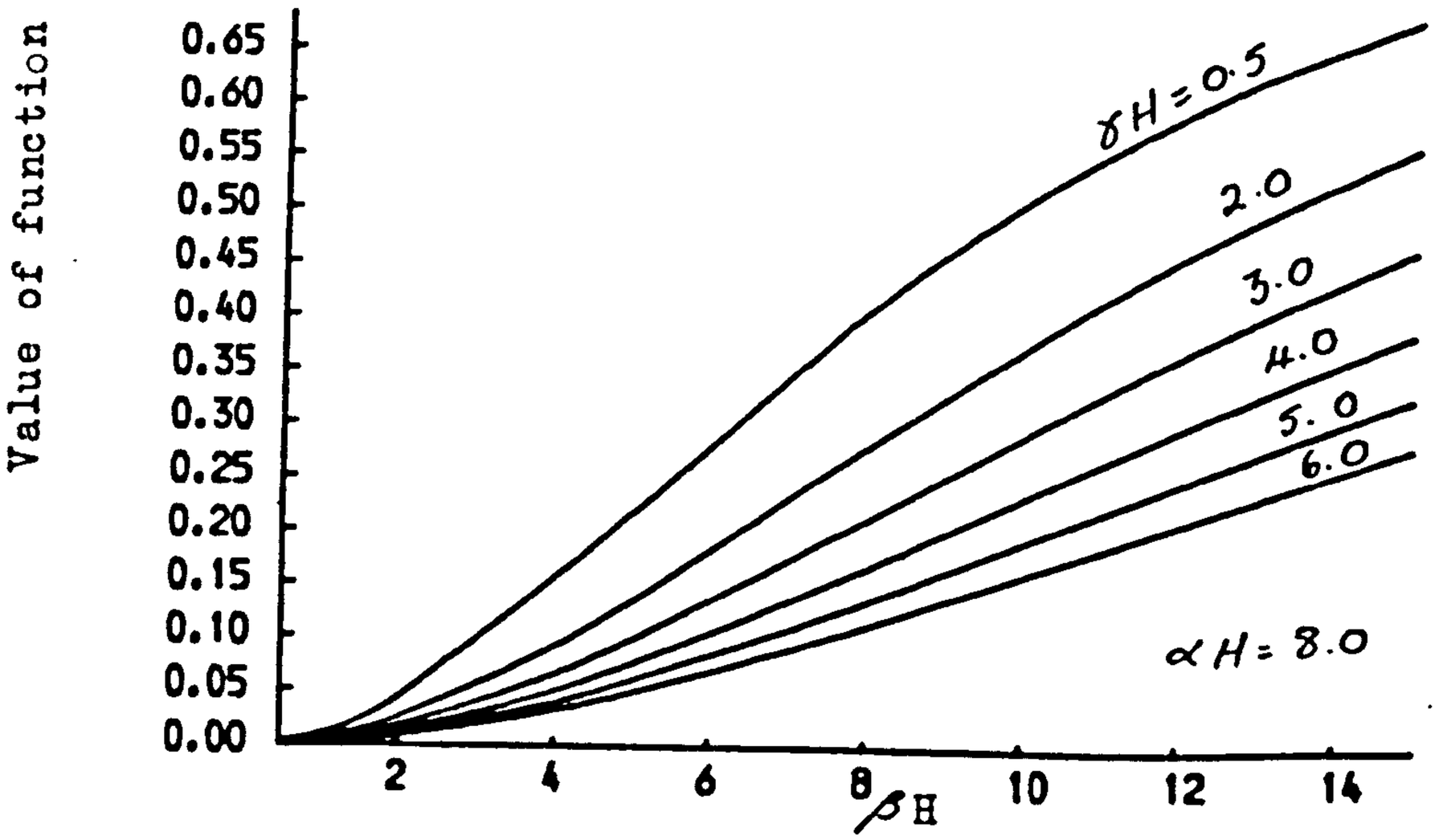

Fig. 8.21 Distributions of axial force function F_2

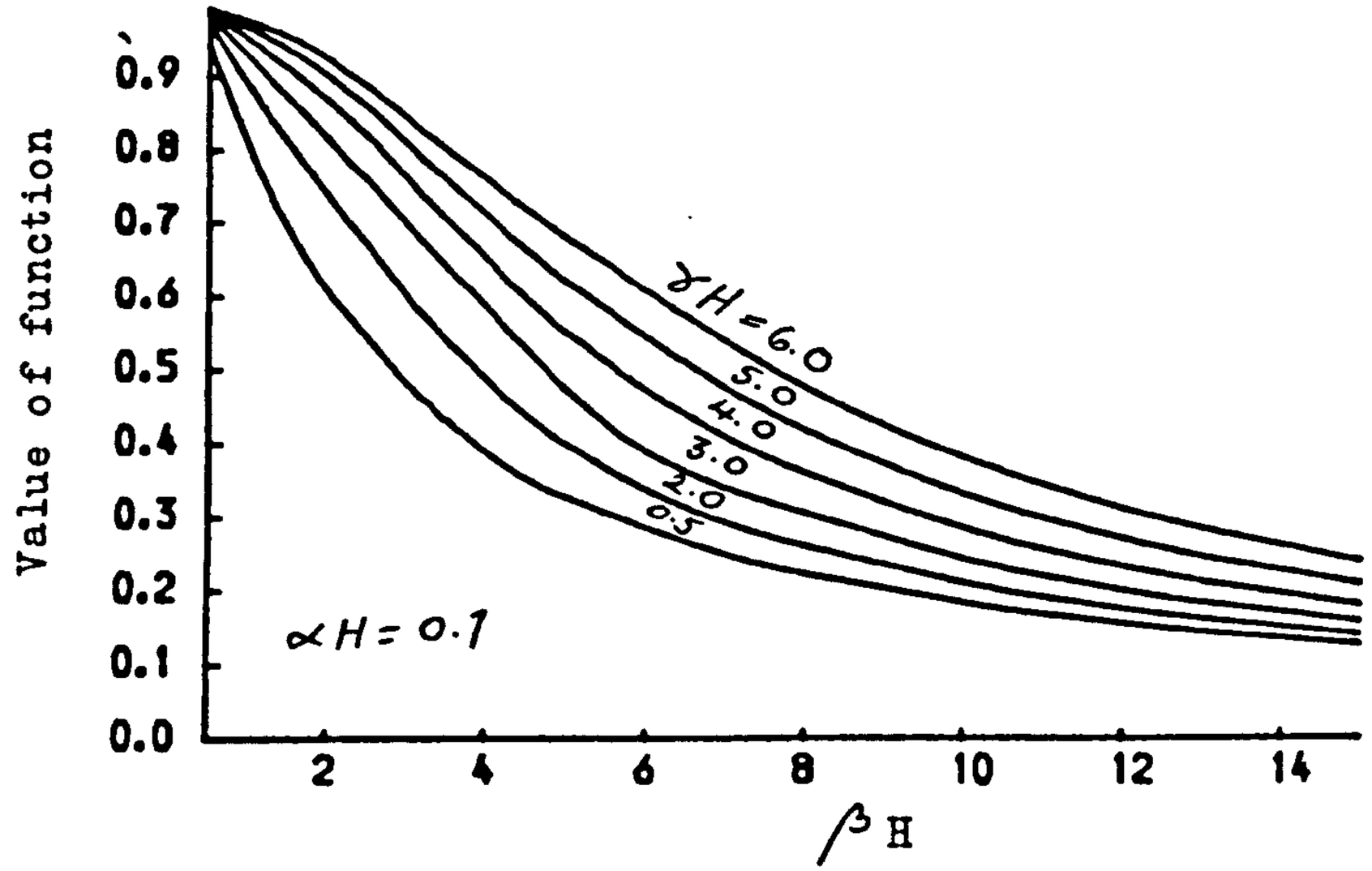

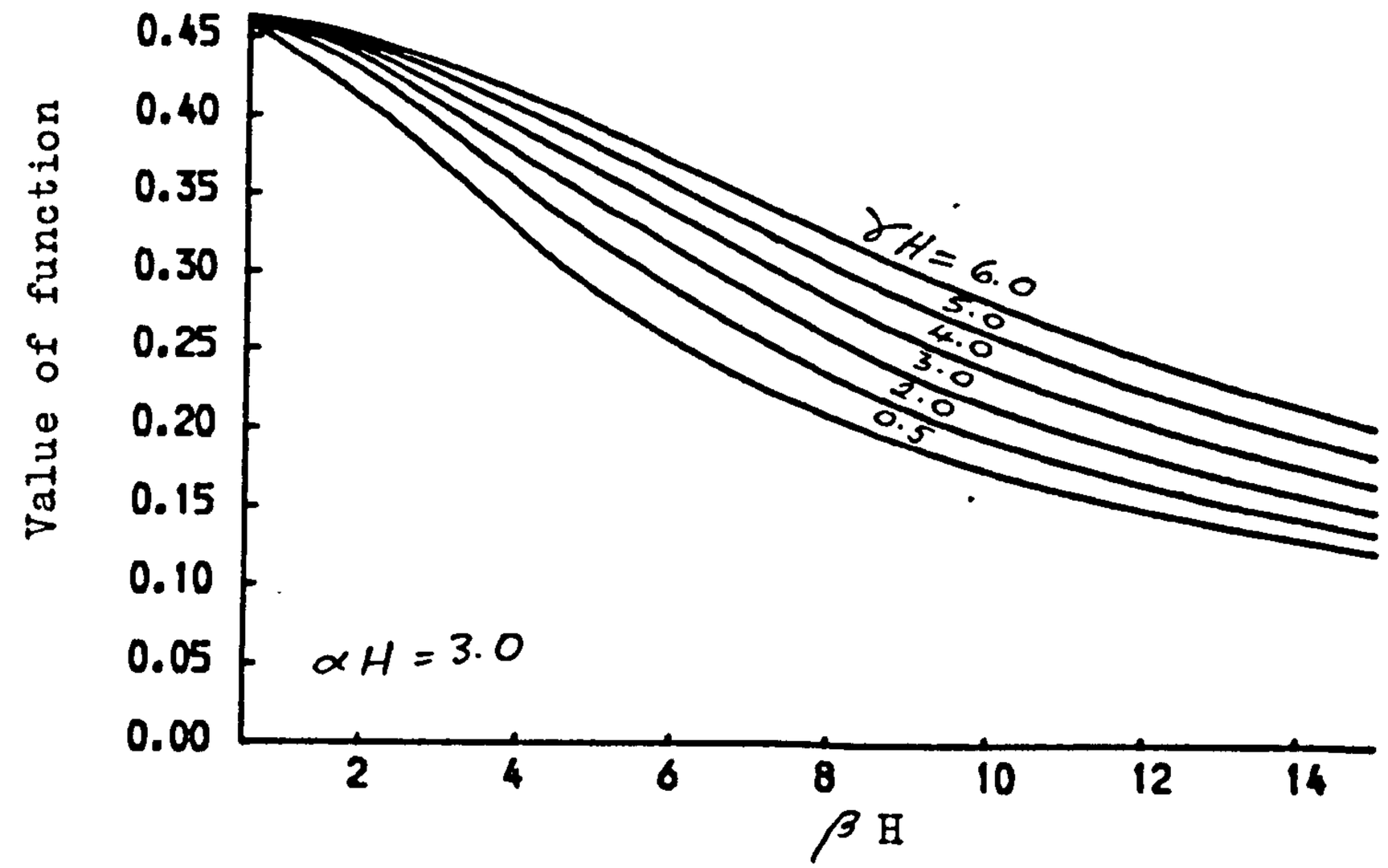

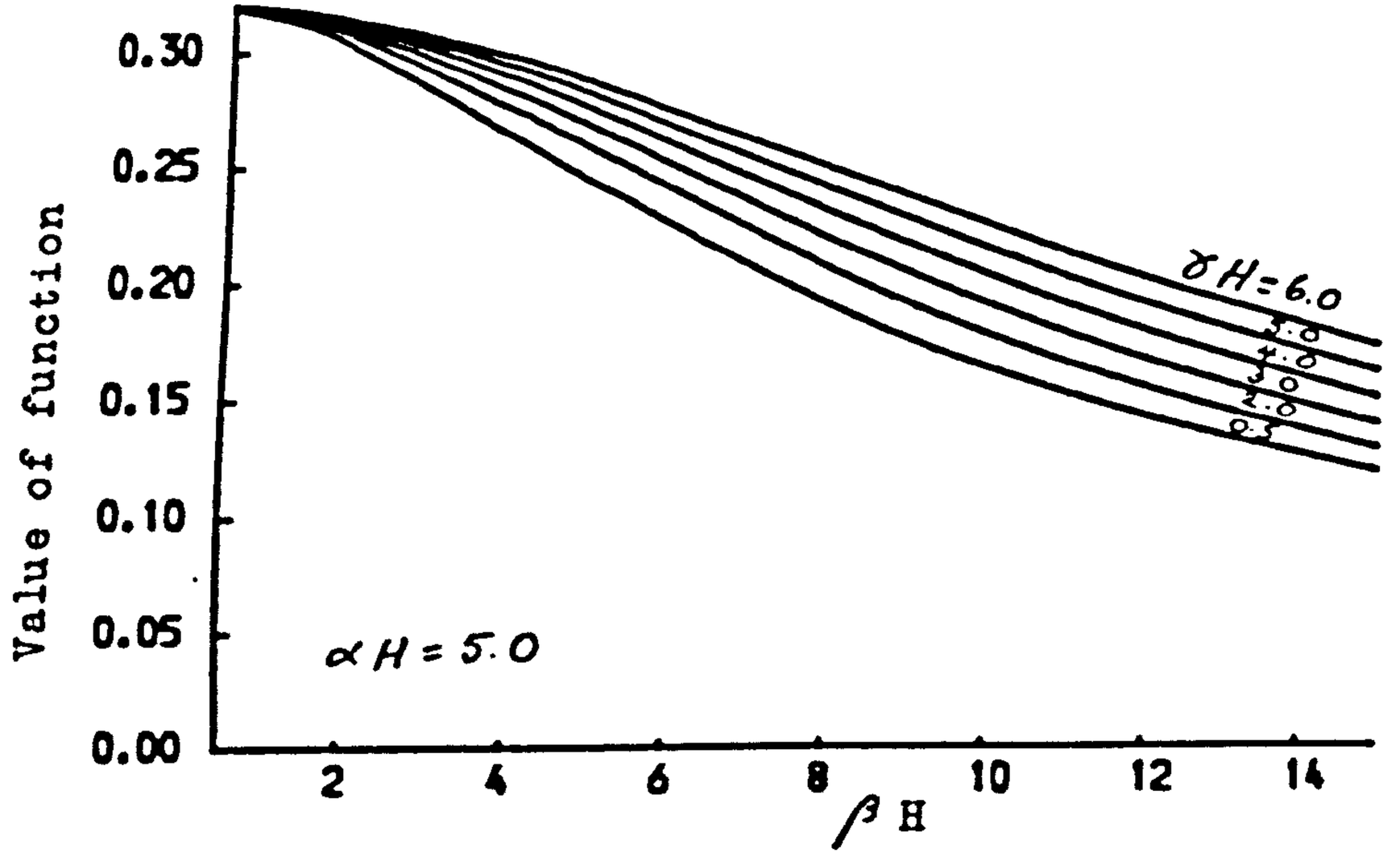

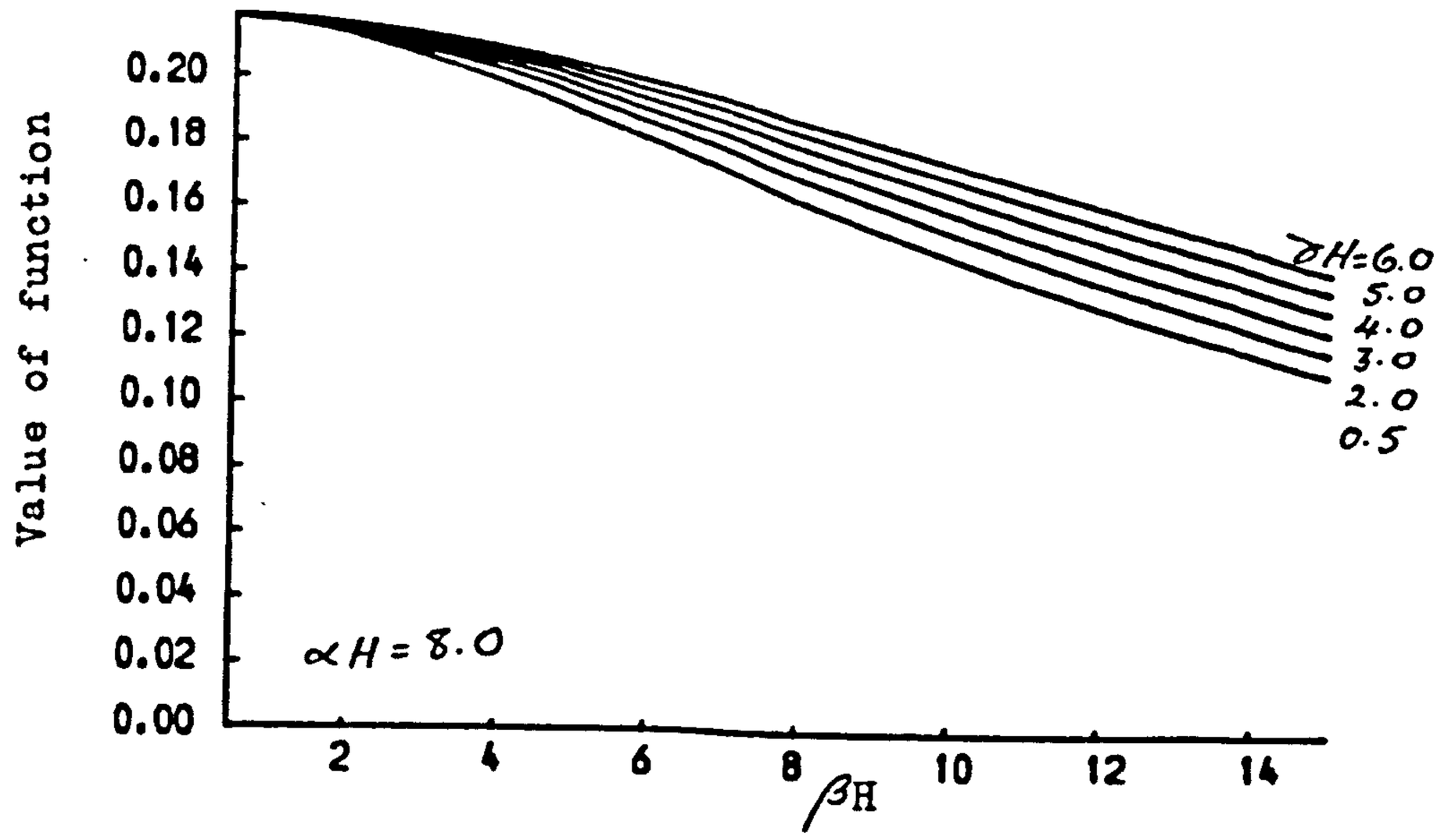

Fig. 8.22 Distributions of moment function F_3

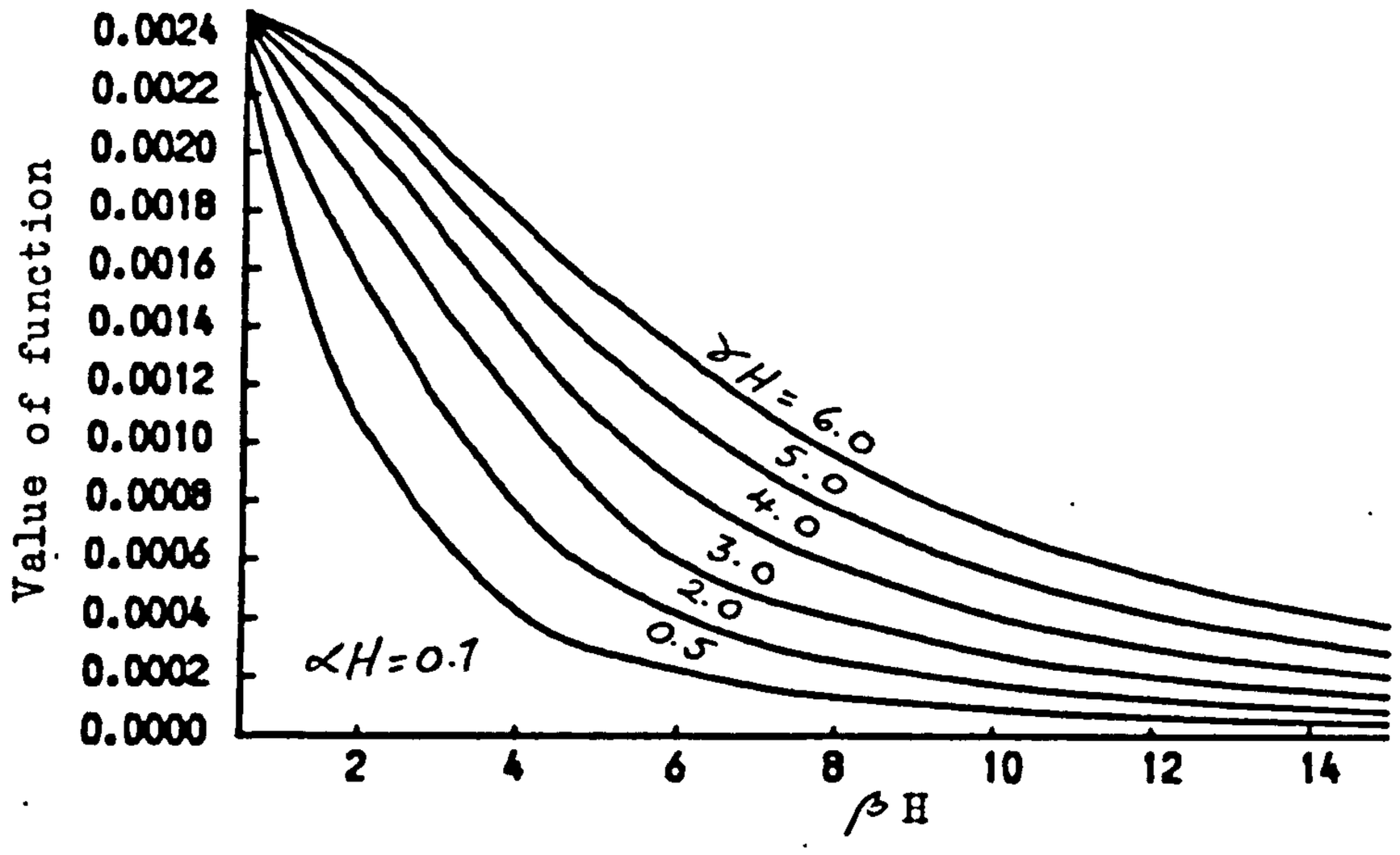

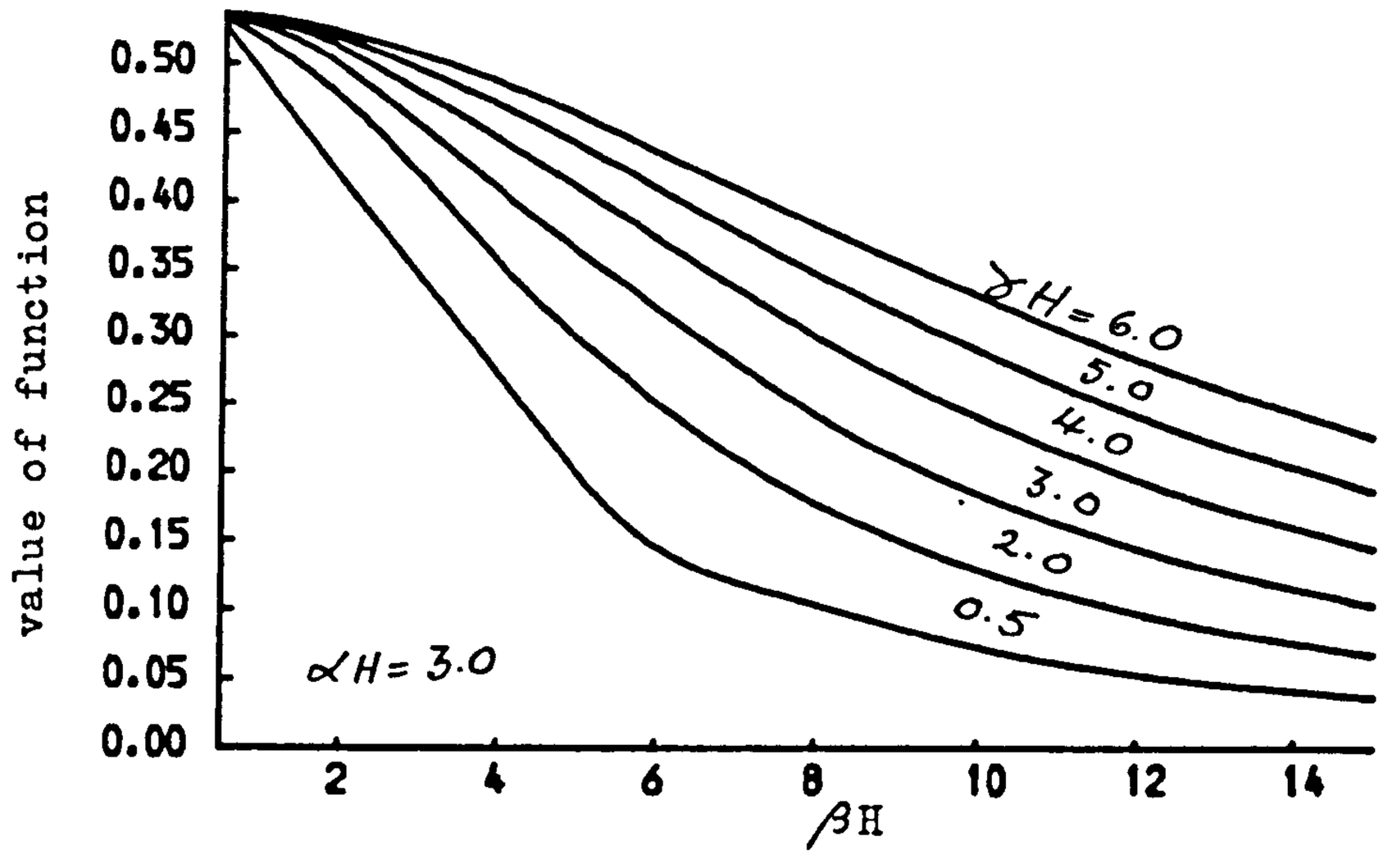

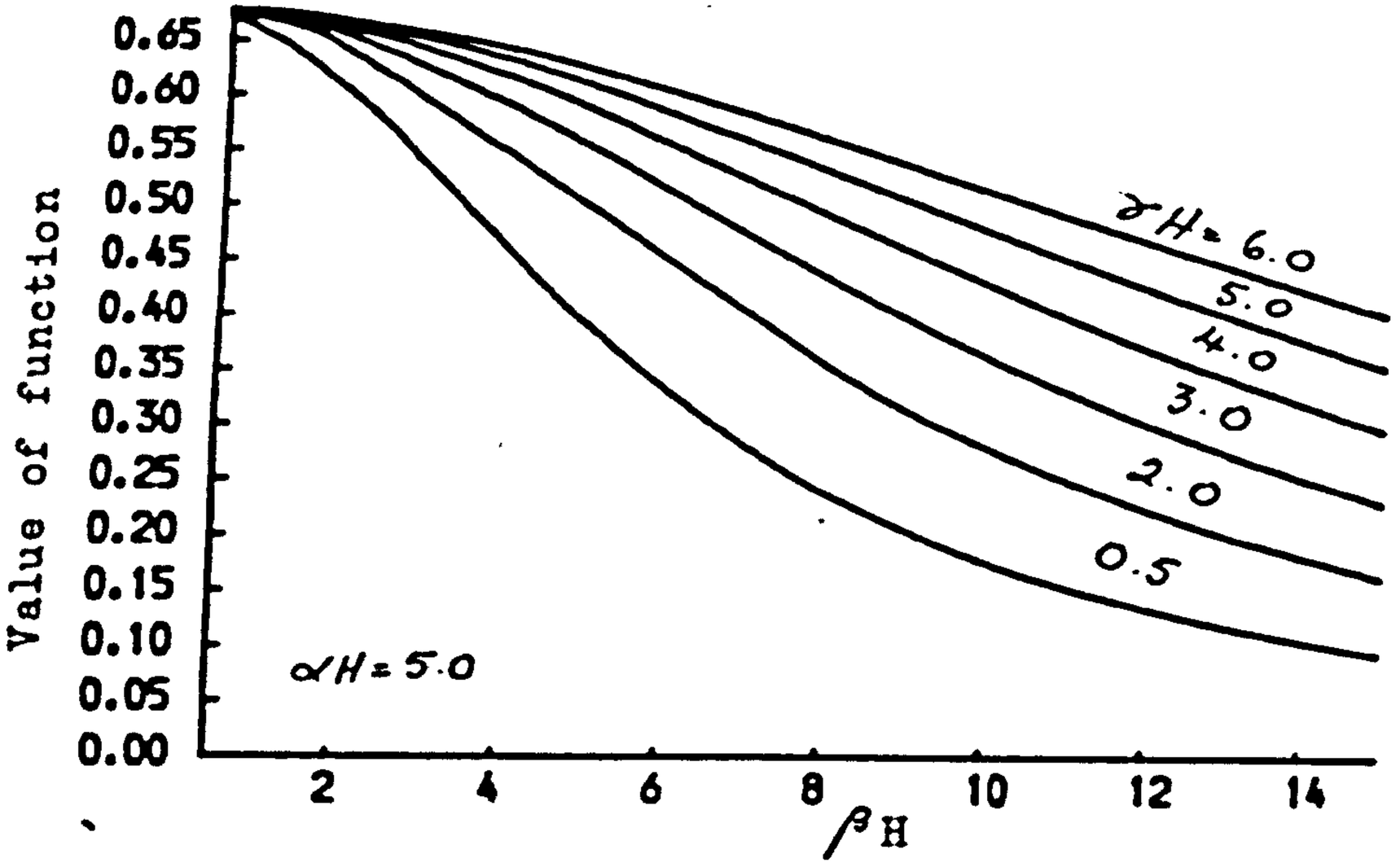

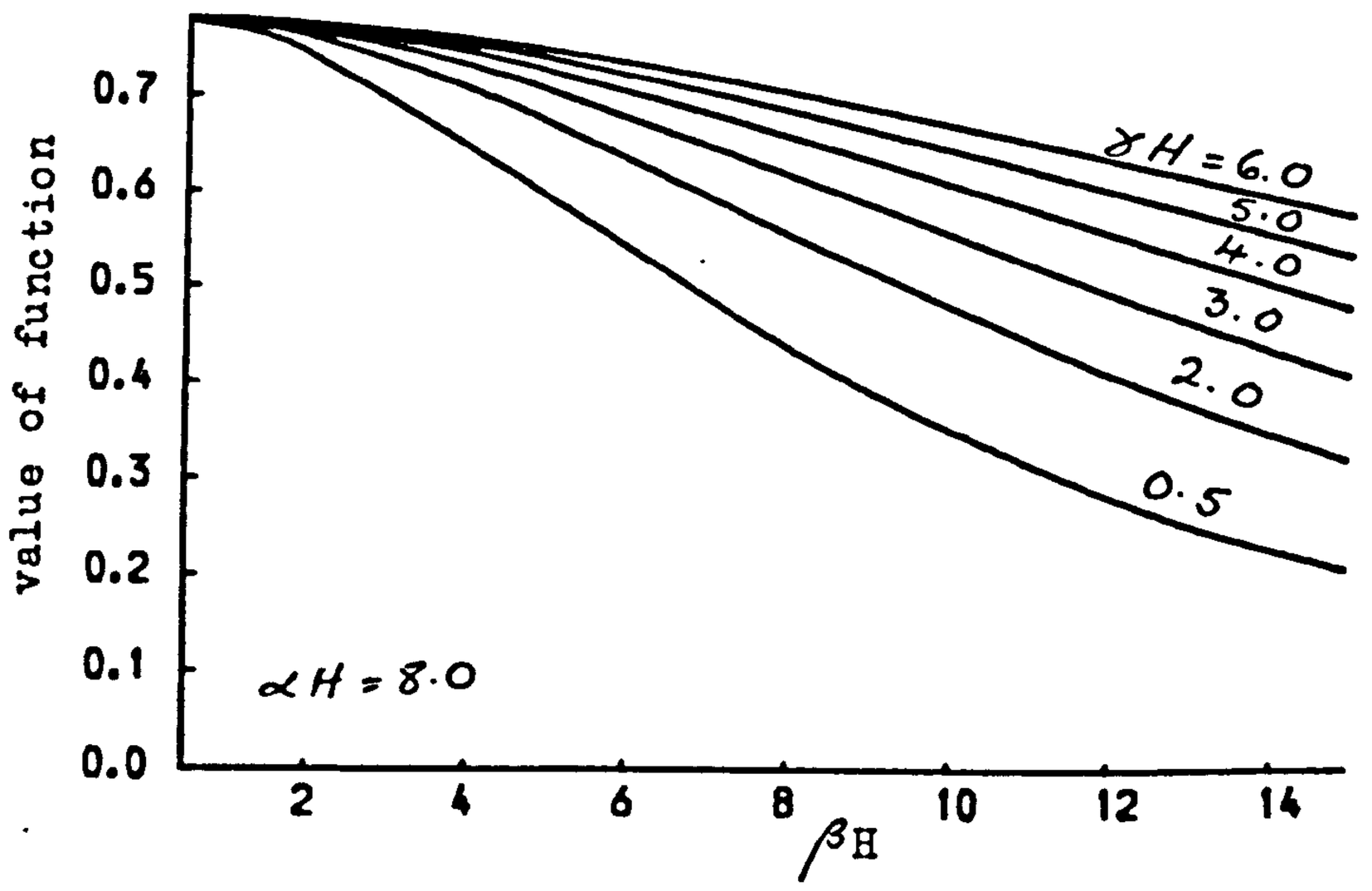

Fig. 8.23 Distributions of moment function F_4

C H A P T E R 9

CONCLUSIONS AND SUGGESTIONS FOR FUTURE WORK

CHAPTER 9

CONCLUSIONS AND SUGGESTIONS FOR FUTURE WORK

9.1 Conclusions

"Exact" methods of analyses leading to closed-form solutions have been presented for three-dimensional symmetric and asymmetric structures, consisting of box cores, independent shear walls, coupled shear walls and rigidly-jointed frameworks. The analyses have been based on the continuous connection technique and lead to sixth order governing differential equations in terms of deflections or rotation. The solutions are then functions of the relative structural stiffness parameters. In the analyses, the frame assemblies have been represented by equivalent shear cantilevers of infinite flexural rigidities with the same overall shear stiffness as the frames.

The governing differential equations were formulated for any general load case, but in order to achieve closed-form solutions for the deflections and the internal forces the particular case of a uniformly distributed wind loading was considered. Solutions in similar forms may be obtained for any other form of loading which can be expressed as an integrable function of height.

The methods of analyses presented may be used for both the preliminary and final stages of the design process to obtain solutions for three-dimensional tall building

structures subjected to any form of lateral loads which may produce bending and torsion of the structure.

It has been shown that for buildings consisting of various load bearing elements, the commonly applied design rule of assuming that the lateral forces are distributed among the walls and frames in proportion to the top deflection of each component can lead to substantial errors in the lateral loads in each assembly as a result of the load redistribution which may occur. If this simple design rule is adopted the results obtained indicate that considerable errors may be incurred in the deflection and the internal forces.

General theories were presented for the analyses of the particular cases of regular symmetrical cross-wall and wall-frame structures subjected to lateral forces which produce bending. The structures were analysed by transforming them into equivalent plane continuous systems. After the analyses of the simple structures were performed, the results were transformed back into the real three-dimensional systems. The closed solutions enabled the complete distributions of the forces and deflections throughout the structures to be determined, and the relative importance of the structural parameter k to be assessed quickly in the early stages of the design (for cross-wall structures k is a function of the ratio of the flexural rigidity of the connecting beams to the combined flexural rigidities

of the coupled shear walls and cores, and for wall-frame structures k is equal to the ratio of the shearing rigidity of the frames to the combined flexural rigidities of the combined walls and cores). Once the actions in the continuous systems have been established, the corresponding forces in any element of the real discrete structure may be determined. The forces in the columns and beams of the frame may be evaluated approximately by making assumptions regarding the positions of the points of contraflexure in each, as practised in the well-established Portal method of analysis. Complete solutions were presented for the particular case of a uniformly distributed wind load. There is little difficulty in deriving solutions for the other common load cases, the only difference lying in the particular integral term of the general solution of the equations.

A number of non-dimensional design curves for the deflections and the internal forces were presented. It was shown that for cross-wall structures the coupled shear walls carry a larger proportion of the lateral loads in the upper levels and less in the lower levels. The curves also indicate that as the stiffness variable k increases, the redistribution of the lateral loads between coupled shear walls and core elements become more significant at the lower levels. The above conclusions also apply to wall-frame structures with the exception that in this case the independent shear wall or core assemblies carry the

larger proportion of the lateral loads in the upper levels and less in the lower levels. In order to illustrate the theoretical results two numerical examples were considered.

A modification of the continuum method of analysis of wall-frame structures was made to allow the base flexibility of the two components to be included. Curves were presented to illustrate the influence of the relative shear stiffness ratio $\emptyset$ on the main structural actions for a wide range of component stiffness ratios. The shear stiffness ratio $\emptyset$ is the ratio of the shearing rigidity of the wall to the combined rigidities of the wall and frame. The curves indicate that the influence of $\emptyset$ on the base moments and top shears varies with k, being greatest at lowest values of the relative stiffness parameter k. It was also shown that the influence of $\emptyset$ on the top deflection is similar at all values of k.

The above general theories were later combined to produce an approximate theory for the analysis of regular symmetrical structures consisting of cores, coupled shear walls and rigidly-jointed frames subjected to lateral forces which produce bending. In order to demonstrate the typical structural behaviour of such systems a representative numerical example was considered. It was shown that the lateral forces were small in the upper levels of both cores and frames, but they increased rapidly in the lower

levels. The lateral forces were carried largely by the coupled shear walls, and were roughly uniform throughout the height, giving rise to a roughly linear distribution of shearing forces. The top concentrated force on the frame was of the order of about 10% of the total lateral load, and produce an approximately linear distribution of bending moments throughout the height. The bending moments in both coupled walls and cores were both small and negative in sense in the upper levels, owing to the coupling actions of the connecting beams and the top concentrated interactive forces, but increased rapidly in the lower levels owing to the redistribution of lateral forces. In order to compare the present method with other published data an example was considered which was first analysed by Arvidsson using his proposed method, Rosman's method, the equivalent shear wall-frame method and the so called discrete matrix method. The present method agreed favourably with Arvidsson's and computer-based discrete matrix methods but there were significant differences compared to the more approximate methods (Rosman's and equivalent shear wall-frame methods).

The solutions mentioned above are not applicable to structures which contain two different sets of coupled shear walls. However, these solutions were extended to include the effects of two different sets of coupled shear walls. The distribution and structural actions of such

three-dimensional structures were illustrated by considering a typical example structure subjected to uniformly distributed lateral loads. It was shown that, in the upper levels the lateral loads on the two different sets of coupled shear walls were small and relatively large in the core assembly, but due to the load redistribution they increase and decrease respectively in the lower levels.

In order to extend the earlier analysis to take into account the torsional behaviour of the structures mentioned, it was found necessary to consider the behaviour of asymmetric partially closed core structures. The analysis was achieved by using the folded plate theory in conjunction with the continuous connection technique, and lead to a third order governing differential equations in terms of a single variable θ, the angle of rotation and a single non-dimensional parameter k, the core relative stiffness. Design curves were presented for the rotation and its derivatives for any single cell partially closed core structures to enable solutions to be achieved for the resulting internal forces.

It was then possible to extend the earlier analyses to consider the torsional behaviour of symmetrical structures. Simple transformations were derived to allow the equations developed for a continuum-based bending analyses for symmetrical structures to be used directly for torsion analyses also. Structures subjected to eccentric loading

producing bending and torsion may then be treated by a superposition of the two cases, the same explicit form of solution being valid for each.

A relatively simple method of analyses was then presented for three-dimensional uniform asymmetric structures consisting of cores, independent shear walls, and parallel assemblies of rigidly-jointed frameworks. The analysis was extended to include frame assemblies in two orthogonal directions. By considering the general equilibrium conditions of the structure and solving the three generated governing differential equations simultaneously, closed-form solutions were obtained for the deflections, rotation, and the internal forces. The choice of the datum axes in the analysis is arbitrary with the exception that, for structures consisting of frames and only one core or an independent shear wall assembly, the local centroidal axes of the latter assembly should be chosen as the datum axes for the overall structure. Otherwise the governing stiffness parameter (which is a function of the torsional and bending properties of the various components) becomes infinity and a solution becomes impossible. In order to examine the validity and accuracy of the method of analysis presented, two example structures which had been previously analysed by various investigators were considered. One of these asymmetric example structures which consisted of a shear wall, and four frame assemblies located in two orthogonal directions was

first analysed by Stamato and Mancini using their proposed method and a so called discrete matrix method. The agreement between the results obtained using the present method and Stamato and Mancini's method was very close but compared to the discrete matrix method the differences were slightly higher.

The second asymmetric example structure which consisted of nine frames and a box core was analysed successively by Mortelmans for buildings of 4, 6, 8 and 10 storeys.

The agreement between the results obtained using the present method and Mortelmans' method was close, especially for the higher buildings of 8 and 10 storeys. This confirms the common belief that continuum-based techniques are more suitable for taller buildings. In their analysis Mortelmans et al assumed that due to crack formations the flexural and torsional rigidities of the lift shaft were reduced to one third and one tenth of the original value respectively. In this case there were significant discrepancies between the two methods which were due to the assumptions made in the present and Mortelmans' analyses.

In view of the limited number of published data on structures of the form considered in this thesis, it was not possible to compare the results from the analyses presented with those from other more sophisticated techniques (e.g. Finite element methods), and the example

structures considered for comparison purposes were the only ones available in the literature. However, earlier work has confirmed the accuracy of the continuum approach for uniform coupled shear wall structures, partially closed box core structures, and that of the shear cantilever concept for wall-frame structures. Consequently, since no further approximations or assumptions have been introduced, it must be expected that the present analyses of combinations of all of these components will be of comparable accuracy, and acceptable for design purposes.

In order to assess the relative importance of the structural parameters αH, βH and γH a numerical parameter study was carried out. The parameters α, β and γ were defined as

$$\alpha = f\left(\sqrt{\frac{GA}{EI}}\right)$$

$$\beta = f\left(\sqrt{\frac{EI_c}{EI}}\right)$$

$$\gamma = f\left(\sqrt{\frac{EI_c}{EI_s}}\right)$$

where GA is the effective shearing rigidity of the frames, EI_c is the flexural rigidity of the connecting beams, EI is the flexural rigidity of the combined coupled walls and cores, EI_s is the combined flexural rigidity of the coupled walls, and H is the total building height.

From the curves presented for the top deflections, maximum axial forces in the coupled walls, and maximum bending moments in the walls and frames it was established that in order to have a stiff structure both α H and β H should have relatively large values and γ H should have a relatively small value, but the effect of β H in increasing the stiffness was more significant than that of α H while the role of γ H was less significant. Regarding the axial forces in the coupled shear walls the role of β H is more pronounced than that of γ H, and α H does not play a significant role. Since moments in the walls are functions of the second derivative of the deflection, the effects of parameters α H, β H and γ H on the wall moments are the same as their effects on deflection. However, with respect to moments in the frames α H plays a more significant role than β H and γ H.

Finally, attempts were made to obtain general solutions for:

(i) symmetric structures consisting of two sets of different coupled shear walls, cores and frames subjected to bending

(ii) Asymmetric structures consisting of cores, independent shear walls and rigidly-jointed frames place in two orthogonal directions subjected to bending and torsion.

Since the characteristic equations regarding the general

differential equations of such structures could only be solved numerically, general solutions were not possible, though for specific structural parameters solutions may be obtained.

An attempt was also made to obtain a solution for the asymmetric structures consisting of cores,.independent shear walls, frames and coupled shear walls subjected to bending and torsion. However, no results were obtained. The difficulties encountered were mainly due to the coupling actions of the connecting beams which made it impossible to express the shear forces in the coupled walls in terms of the lateral deflection only.

9.2 Suggestions for Future Work

In this thesis simple methods have been presented for the analysis of three-dimensional symmetric and asymmetric structures subjected to bending and torsional loads. Clearly there is scope for further refinement and extension of the present study. Some of these possible investigations are given below:

1- The extension of the present method to include the action of dynamic loadings arising from wind gusts and earthquakes.

2- The methods presented deal with structures consisting of various structural elements in two orthogonal directions. An investigation/

into the behaviour of structures consisting of obliquely placed load bearing elements is desirable.

3- The methods presented are applicable to uniform regular structures. An extension of these methods to structures with variable configuration along the height needs further research.

4- The methods presented relate to elastic analyses only, a need therefore exists to include the elasto-plastic behaviour of reinforced concrete elements in the analyses.

5- An analysis for regular symmetrical structures consisting of two different sets of coupled shear walls cores and frames was presented in chapter 4. The analysis could be extended to include three or more sets of coupled shear wall assemblies.

6- Construction of simple nomograms for the deflections, rotation, and the internal forces for the analyses presented is highly desirable. This would be very useful for the proportioning of the components in the early stages of the design.

REFERENCES

1. Monographs on the planning and design of tall buildings, 5 vols. : PC, planning and environmental criteria for tall buildings; SC, tall building systems and concepts; CL, tall building criteria and loadings; CB, Structural design of tall concrete and masonary buildings; SB, Structural design of tall steel buildings, published separately. ASCE, 1978-1981.

2. Proceedings of the International Conference on Planning and Design of Tall buildings, Lehigh University, Bethlehem, Pennsylvania, U.S.A, 5 vols., ASCE/IABSE, 1972.

3. "The quiet revolution in skyscraper design", ASCE/Civil Eng., May, 1983, pp. 54-59.

4. Fintel, M. Et al "Response of Buildings to Lateral Forces" ACI Committee 442, Title No. 68-11, Feb. 1971, pp.81-106.

5. MacLeod, I.A. "Lateral stiffness of shear walls with openings", Tall buildings, Pergamon Press, London, 1967, pp.233-244.

6. MacLeod, I.A. "Analysis of shear wall buildings by the frame method", Proc. Ins. Civ. Engrs, London, vol.55, pp. 593-603.

7. Kratky, R.J. and puri, s.p.s. "Discussion of modified beam method for analysis of symmetrical interconnected shear walls", by B.Stafford Smith, ACI Journal, ACI, Vol.68, No.6, p.472.

8. Schwaighofer, J. and Microys, H.F. "Analysis of shear wall structures using standard computer programs," ACI Journal, ACI, vol. 66, No.12, pp.1005-1008.

9. Beck, H. "Contribution to the analysis of coupled shear walls", Journal of ACI, proc. vol.59, No.8, 1962, pp.1055-1070.

10. Rosman, R. "Approximate analysis of shear walls subjected to lateral loads", ACI Journal, proc. vol. 61, No.6, June,1964, pp.717-732.

11. Rosman, R. "An approximate method of analysis of walls in multistorey buildings", Civil Engineering and Public works review (London), vol.59,1964, pp.67-69.

12. Coull, A. "Distribution of shear form in coupled shear wall structures", "Response of multistorey concrete structures to lateral forces", ACI publication sp-36, 1973, pp.217-224.

13.Coull, A. and Choudhury, J.R. "Stresses and deflections in coupled shear walls", Journal of ACI, Proc. vol.64, No.2, Feb. 1967, pp.65-72.

14.Coull, A. and Choudhury, J.R. "Analysis of coupled shear walls", Journal of the Struct. Div., Proc., ASCE, ST1, Jan. 1968, pp.71-82.

15.Coull, A. and Puri, R.D. "Analysis of coupled shear walls of variable thickness", Building Science, Vol.2, 1967, pp.181-188.

16.Coull, A. and Puri, R.D. "Analysis of coupled shear walls of variable cross-sections", Building Science, Vol.2, 1968, pp.313-320.

17.Tso, W.K. and Chan, P.C. "Flexible foundation effect on coupled shear walls", Journal of ACI, proc., vol.69, Nov. 1972, pp.678-683.

18.Coull, A. "Interaction of coupled shear walls with elastic foundations", Journal of ACI., proc., vol. 68, 1971, pp.456-461.

19.Coull, A. "Coupled shear walls subjected to differential settlement", Building Science, vol.6, 1971, pp.209-212.

20.Heidebrecht, A.C.and Stafford Smith, B. "Approximate analysis of tall wall-frame structures", Journal of the Struct.Div., ASCE, 99, No.ST2, Feb.1973, pp.199-221.

21.Coull, A. "Interactions between coupled shear walls and cantilevered cores in three-dimensional regular symmetric cross-wall structures", proc. ICE, 55, 1973, pp.827-840.

22.Stafford Smith B. and Abergel, D.P. "Approximate analysis of high-rise structures comprising coupled walls and shear walls", Building and Environment, vol.18, No.1/2, pp.91-96, 1983.

23.Arvidsson, K. "Interaction between coupled shear walls and frames", proc. ICE, part 2, 1979, 67, Sept., pp.589-596.

24.Stafford Smith, B.and Taranath, B.S. "The analysis of tall core-supported structures, subjected to torsion", proc. ICE, vol.53, part 2, Sept.,1972, pp.173-187.

25.Tso, W.K. and Biswas, J.K. "Analysis of core wall structures subjected to applied torque", Building science, vol. 8, 1973, pp.251-257.

26.Tawfik, S.Y. "Torsional analysis of core structures in tall buildings", Ph.D. thesis University of Glasgow, 1980.

27.Stamato, M.C. "Three dimensional analysis of tall buildings", Report No.24-4, proc. of ASCE-IABSE International Conference on Planning and Design of Tall buildings, Lehigh University, Bethlehem, pa. vol.3, p.683-699.

28. Clough, R.W. and King, I.P. "Analysis of three-dimensional building frames", publications of IABSE, Zurich, Switzerland, vol.24, 1964, pp.15-30.

29.Winokur, A. and Gluck, J. "Lateral loads in asymmetric multi-storey structures", Journal of the Struct. Div., ASCE, vol.94, No.ST3, proc., paper 5842, pp.645-656.

30.Stamato, M.C. and Mancini, E. "Three-dimensional interaction of walls and frames", J.Struct.Div., ASCE, 99, No. ST12, proc., paper No. 10193, pp. 2375-2390.

31.Wynhoven, J.H.and Adams, P.F. "Analysis of three-dimensional structures", J. Struct. Div., ASCE, Vol.98, ST1, Jan. 1972, pp.233-248.

32.Wynhoven, J.H. and Adams, P.F. "Torsional displacements in multi-storey structures", publications of IABSE, Zurich, Switzerland, vol.33-II, 1973, pp.209-219.

33. Rutenberg, A. and Heidebrecht, A.C. "Approximate analysis of asymmetric wall-frame structures", Building Science, London, vol.10, pp.27-35.

34. Mortelmans, F.K., De Roeck, G.P. and Van Gemert, D.A. "Approximate method for lateral load analysis of high-rise buildings", J.Struct.Div., ASCE, vol.107, No.ST8, August, 1981, pp.1589-1610.

35. Haris, A. "Approximate stiffness analysis of high-rise buildings", J.Struct. Div., ASCE, vol. 104, No. ST4, proc., paper 13700, April, 1978, pp.681-696.

36. Coull, A. and Irwin, A.W. "Torsional analysis of multistorey shear wall structures", ACI publication SP-35, 1973 AC A W I, pp.211-238.

37. Coull, A. and Adams, N.W. "A simple method of analysis of the load distribution in multistorey shear wall structures", "Response of multistorey concrete structures to lateral forces", publication SP-36, ACI, 1973, pp.187-216.

38. Coull, A. and Mohammed, T.H. "Simplified analysis of lateral load distribution in structures consisting of frames, coupled shear walls, and cores, Struct. Engr. vol. 61B, No.1, March, 1983, pp. 1-8.

39.Coull, A. and Stafford Smith, B. "Tall Buildings", proc. of a symposium on tall buildings, University of Southampton, April 1966, Pergamon Press.

40. "Response of multistorey concrete structures to lateral forces", publication Sp -36, ACI, Detroit, Mich., USA, 1973.

41.Galambos, T.V. Structural members and frames, Prentice-Hall, 1968.

42.Khan, M.A. H. and Stafford Smith, B. "Restraining action of bracing in thin-walled open section beams", proc. ICE, part 2, vol.59, 1975, March, pp.67-78.

43.Stafford Smith B. and Abate, A. "The effects of shear deformations on the shear centre of open-section thin-walled beams", proc. ICE, part 2, vol. 77, 1984, March, pp.57-66.

44.MacLeod, I.A. "Connected shear walls of unequal width", J. Am. Concr. Inst., 1970, 67, May, pp.408-412.

PUBLICATIONS

45.Coull, A. and Khachatoorian, H. "Distribution of lateral forces in structures consisting of cores, coupled shear walls and rigidly-jointed-frames", proc. Ins. Civ. Engrs, Part 2, Vol. 73, Dec. 1982, pp.731-745.

46. Coull, A. and Khachatoorian, H. "Analysis of laterally loaded wall-frame structures", accepted for publication by ASCE.

47. Coull, A. and Khachatoorian, H. "Torsional analysis of symmetric building structures", accepted for publication in the Third International Conference on Tall Buildings, Hong Kong, Dec. 1984.

APPENDIX 1

Proof that the roots of the characteristic equation of the differential equations (3.13) are real.

APPENDIX 1

Proof that the roots of the characteristic equation of the differential equation (3.13) are real

The characteristic equation of the differential equation (3.13) is given by,

$$\lambda^6 - m^2 \lambda^4 + n^2 \lambda^2 = 0 \qquad (1)$$

The roots of equation (1) are given by,

$$\lambda_1 = \lambda_2 = 0$$

and

$$\lambda^2_{3,4} = \frac{m^2}{2} \pm \frac{1}{2} (m^4 - 4n^2)^{1/2} \qquad (2)$$

where

$$m^2 = \alpha^2 + \beta^2 + \gamma^2$$

$$n^2 = \alpha^2 \gamma^2$$

in which

$$\alpha^2 = \frac{GA}{EI}$$

$$\beta^2 = \frac{12 I_c l^2}{b^3 h I}$$

$$\gamma^2 = \frac{12 I_c}{b^3 h} \left(\frac{1}{A_1} + \frac{1}{A_2}\right)$$

For the differential equation (3.13) to have real roots,

$$m^4 - 4n^2 \not< 0 \qquad (3)$$

Consider the left-hand side of the inequality (3)

$$m^4 - 4n^2 = (\alpha^2 + \beta^2 + \gamma^2)^2 - 4\alpha^2\gamma^2$$

$$= \alpha^4 + \beta^4 + \gamma^4 + 2\alpha^2\beta^2 + 2\alpha^2\gamma^2 + 2\beta^2\gamma^2 - 4\alpha^2\gamma^2$$

$$= \alpha^4 + \beta^4 + \gamma^4 + 2\alpha^2\beta^2 - 2\alpha^2\gamma^2 - 2\beta^2\gamma^2 + 4\beta^2\gamma^2$$

$$= (\alpha^2 + \beta^2 - \gamma^2)^2 + 4\beta^2\gamma^2$$

Since the right-hand side of the above equation contains the sum of the squares, it must always be positive, hence

$$m^4 - 4n^2 \not< 0$$

APPENDIX 2

Design curves for deflection function F_1 and moment functions F_3 and F_4 in coupled shear walls, cores and frames respectively as described in chapter 8

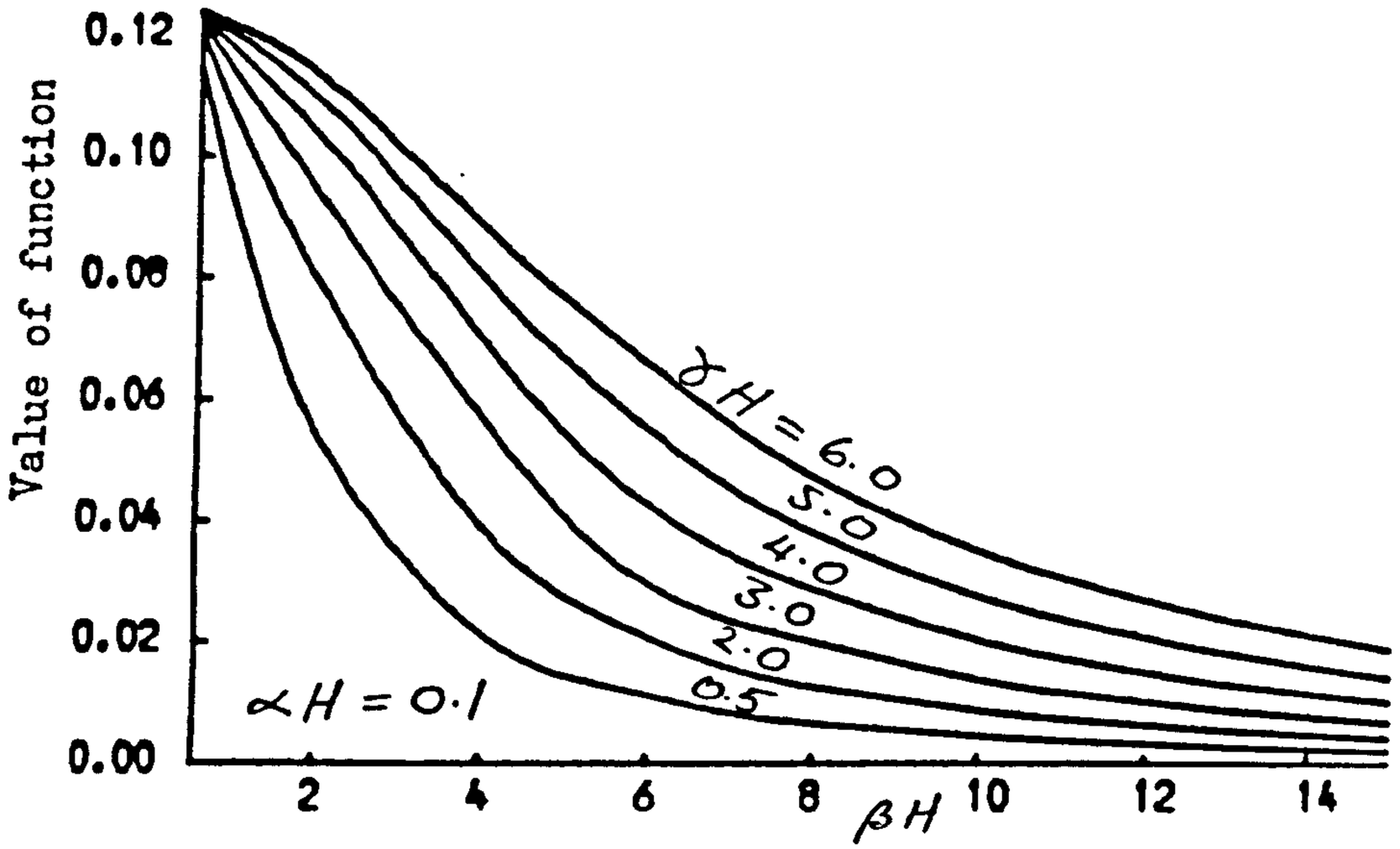

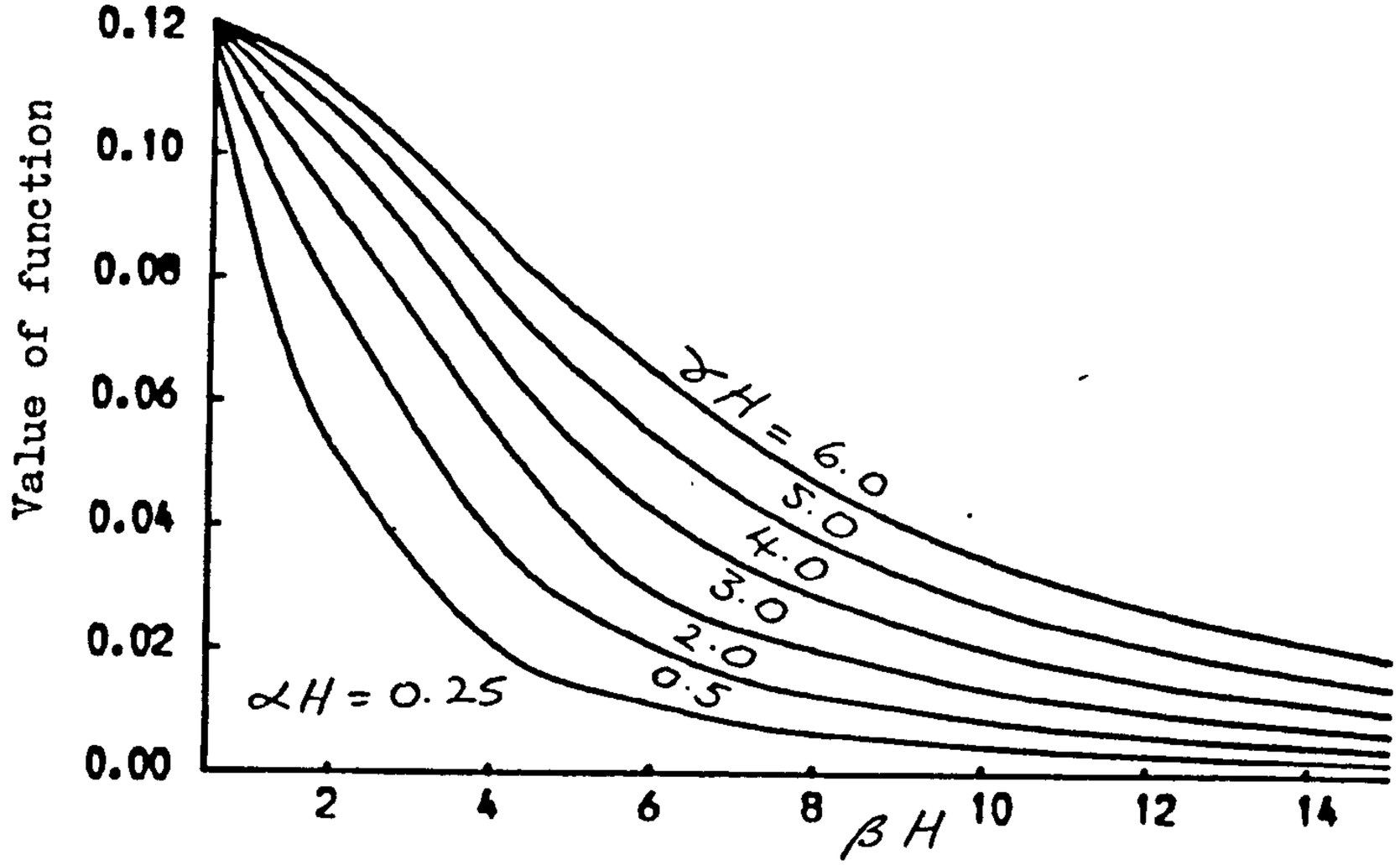

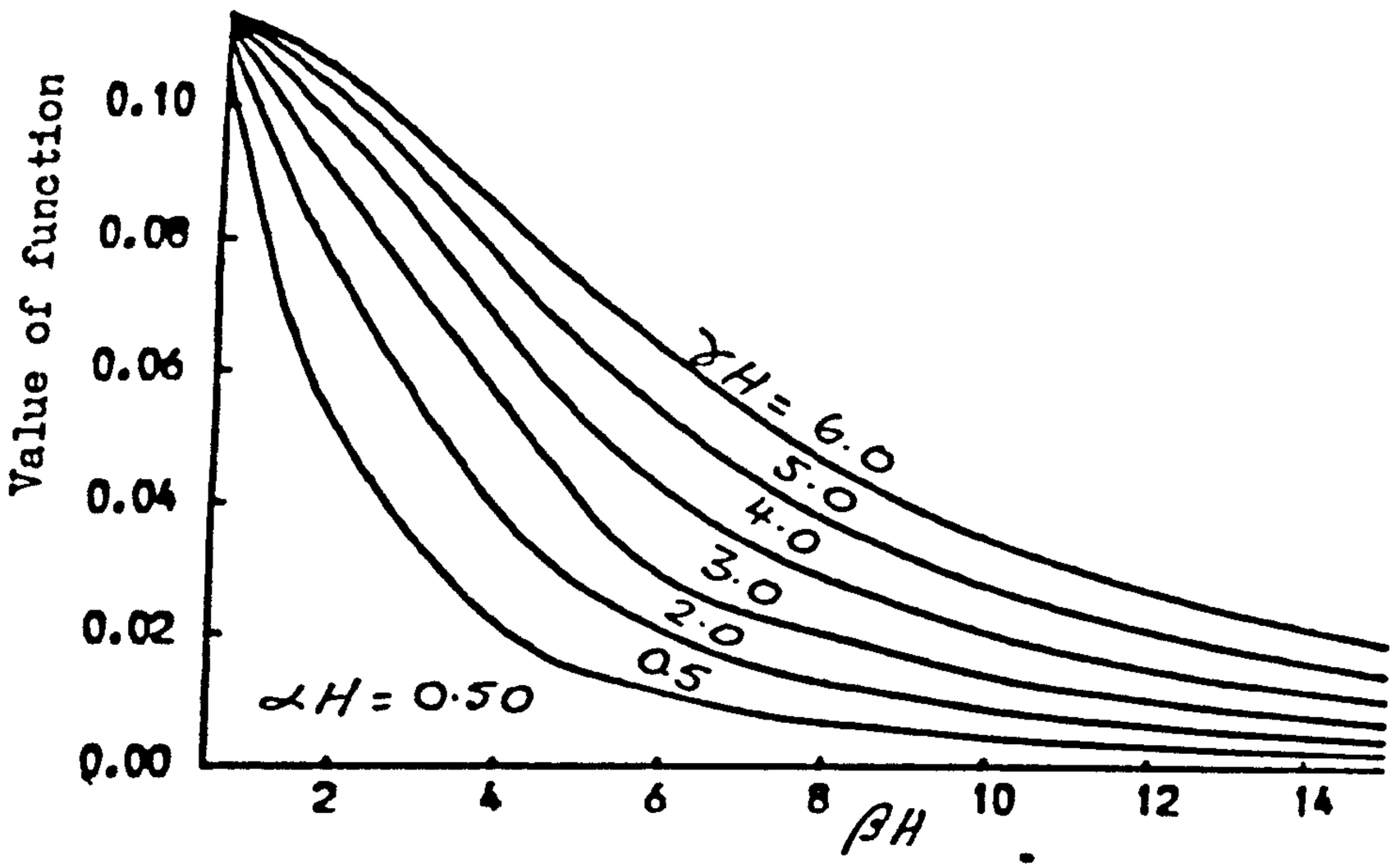

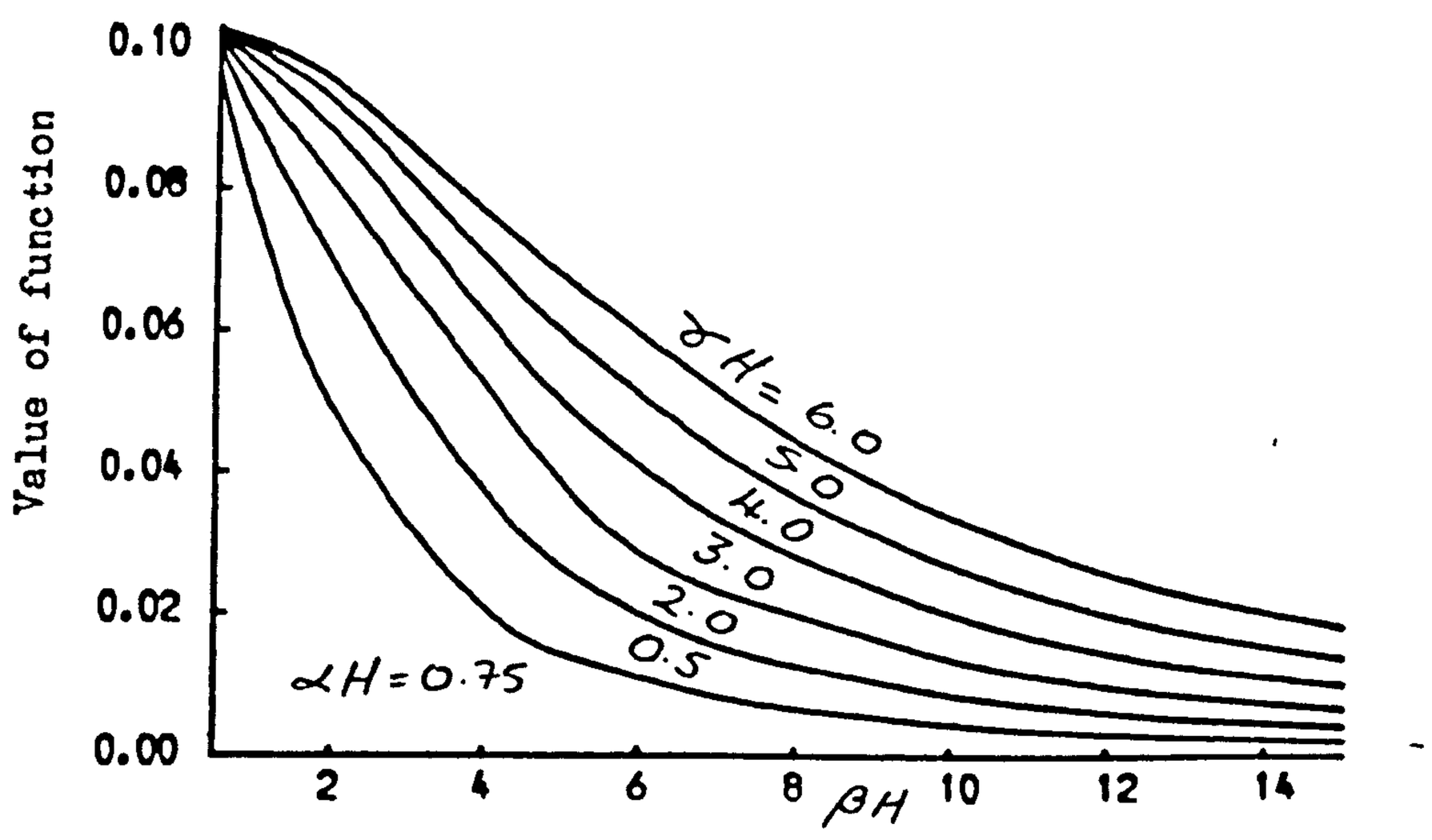

Fig. 2.1 Distributions of deflection function F_1

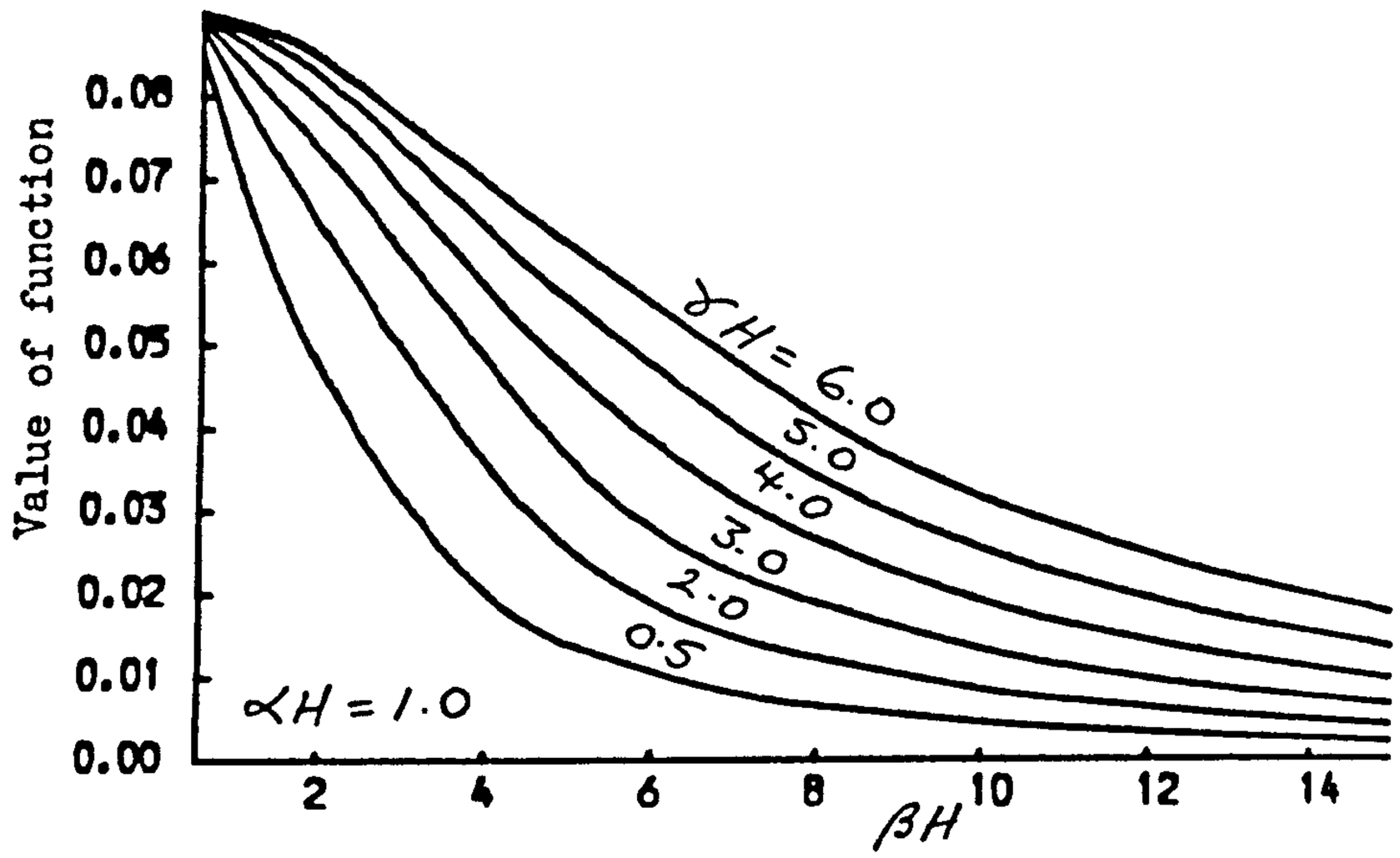

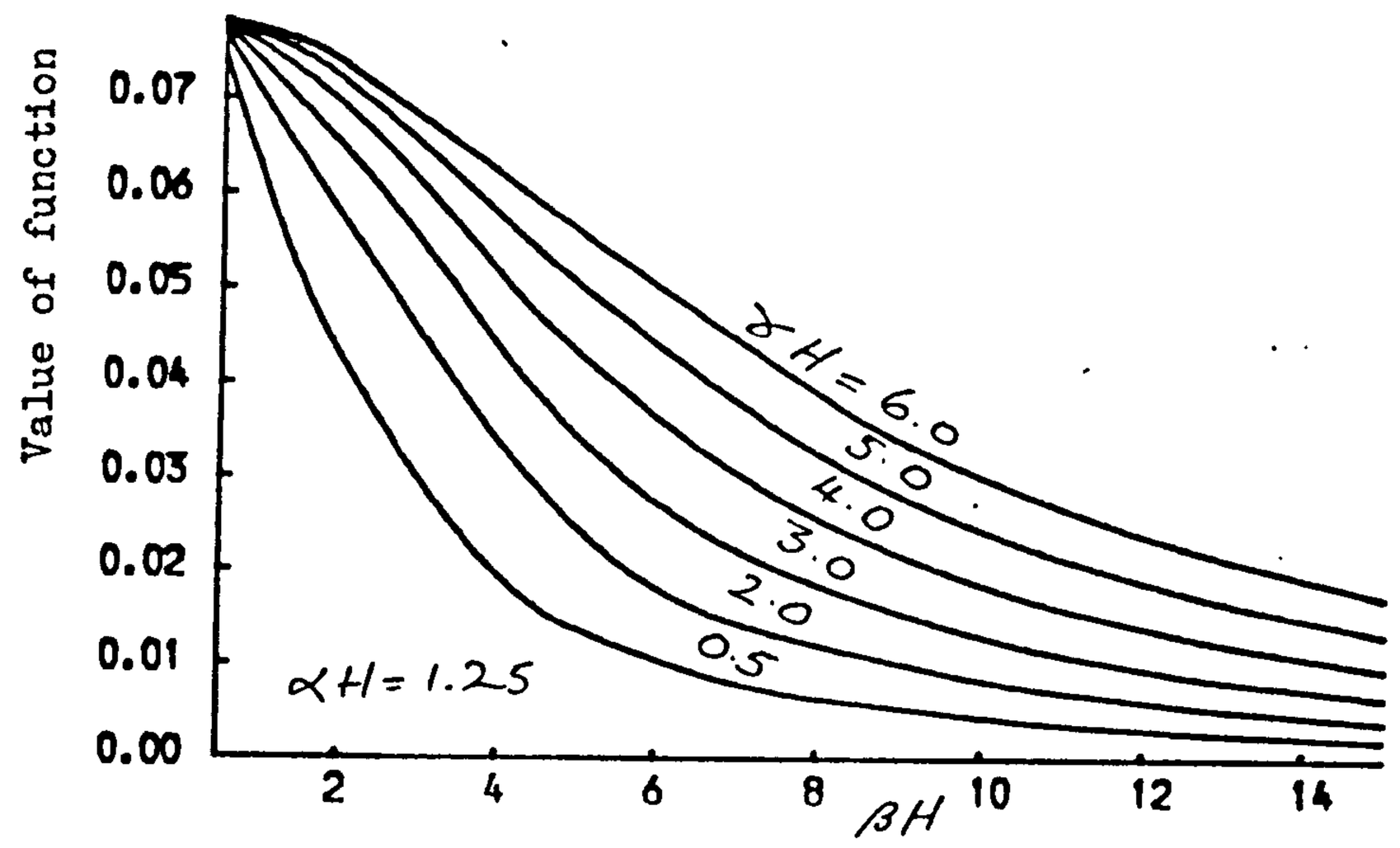

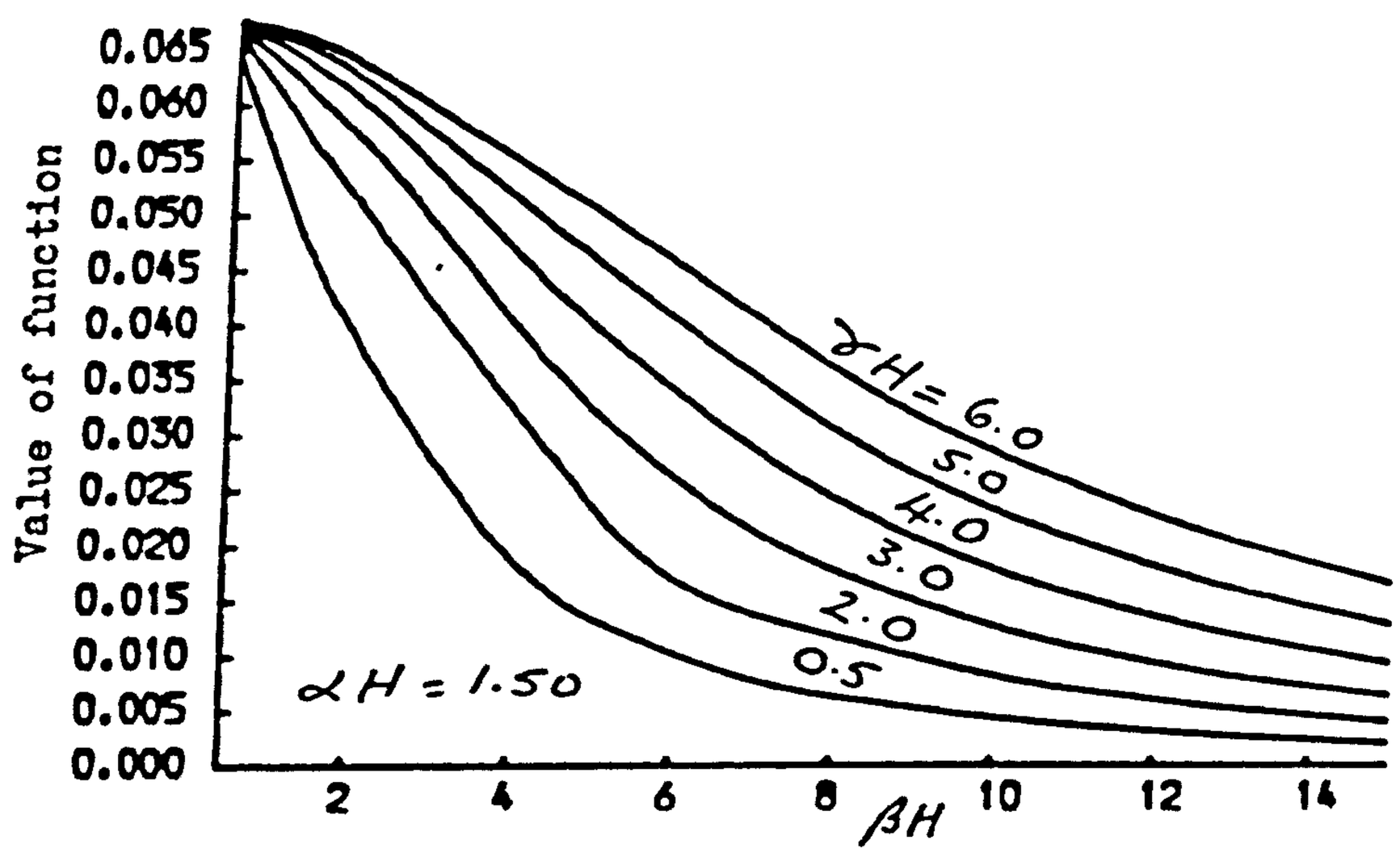

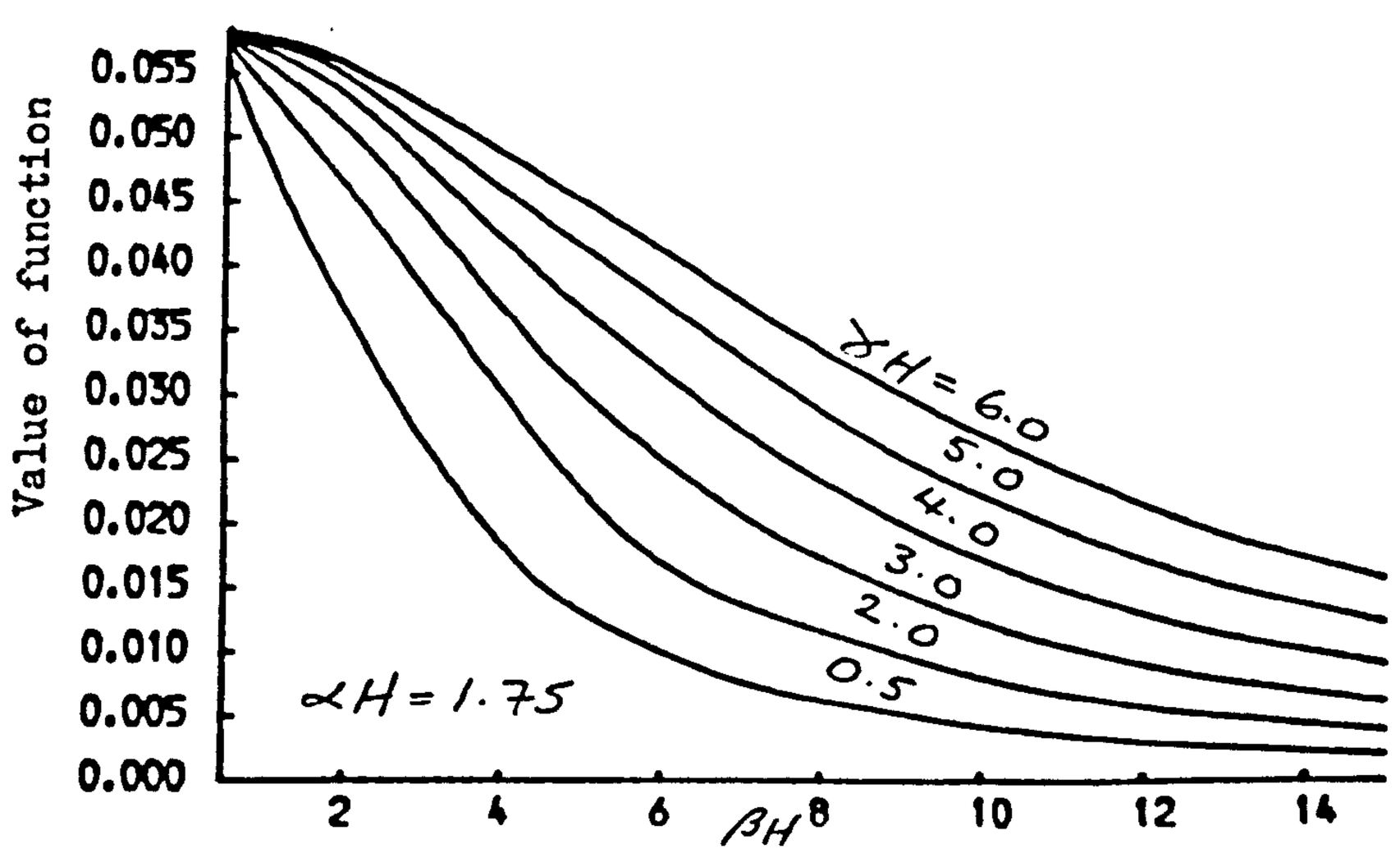

Fig. 2.2 Distributions of deflection function F_1

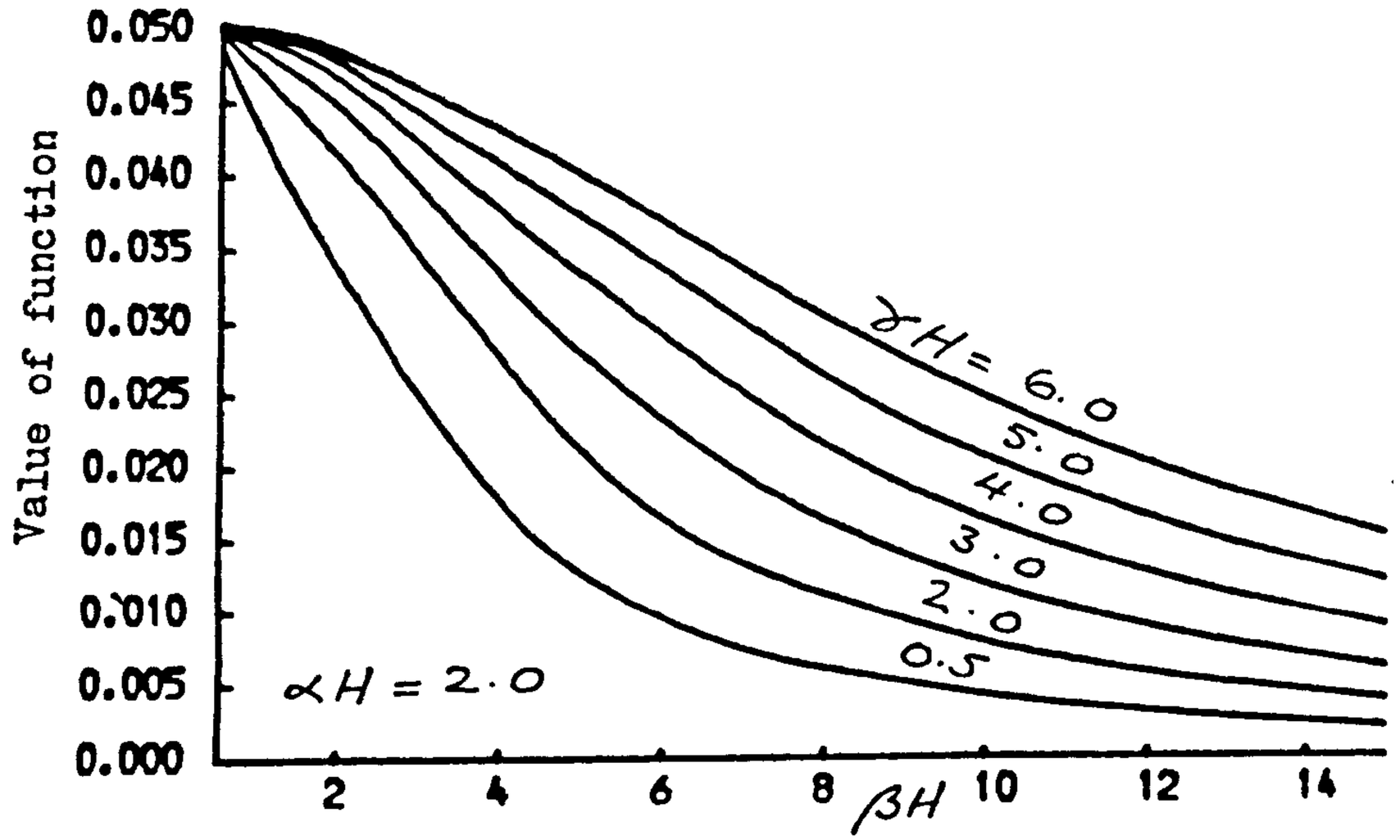

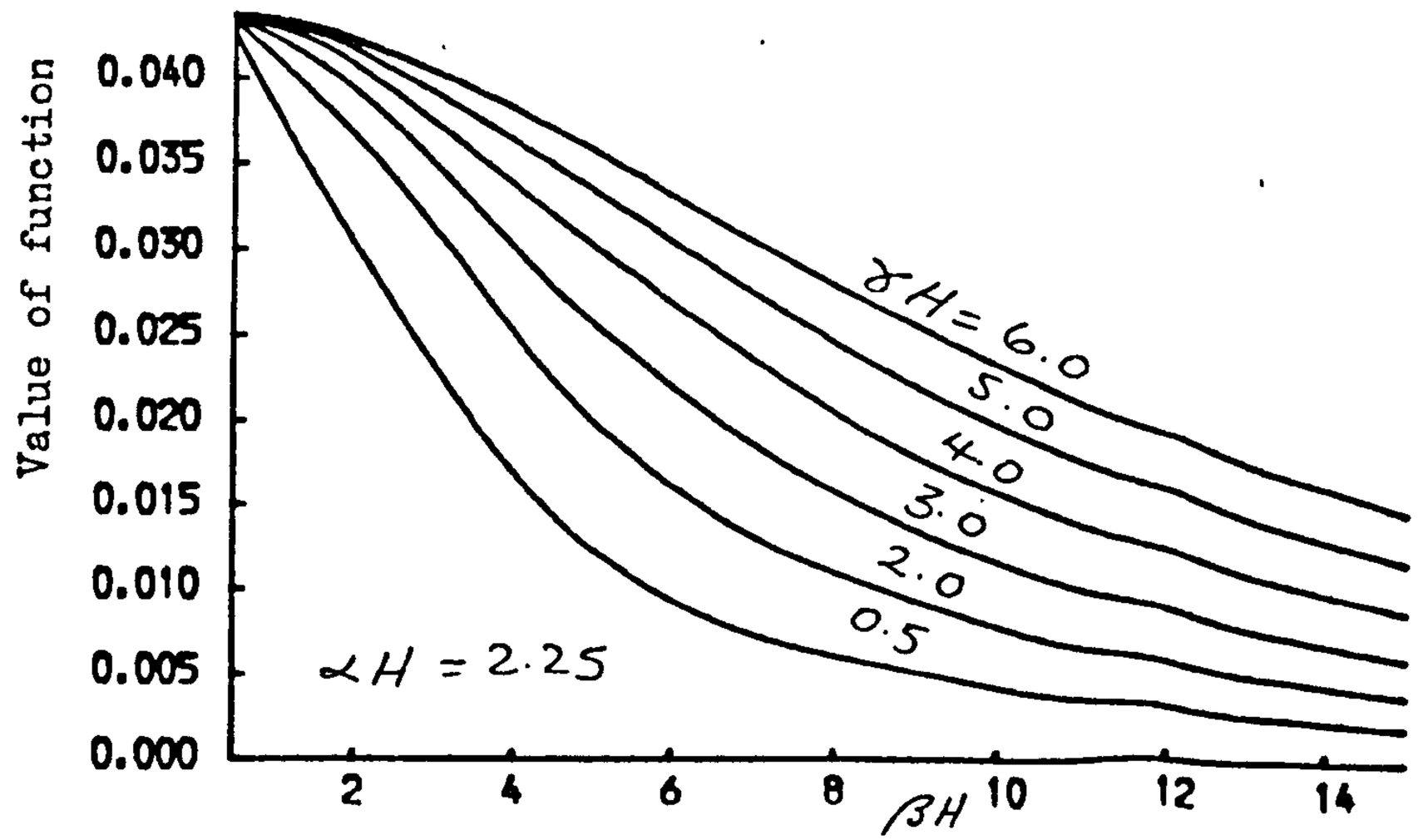

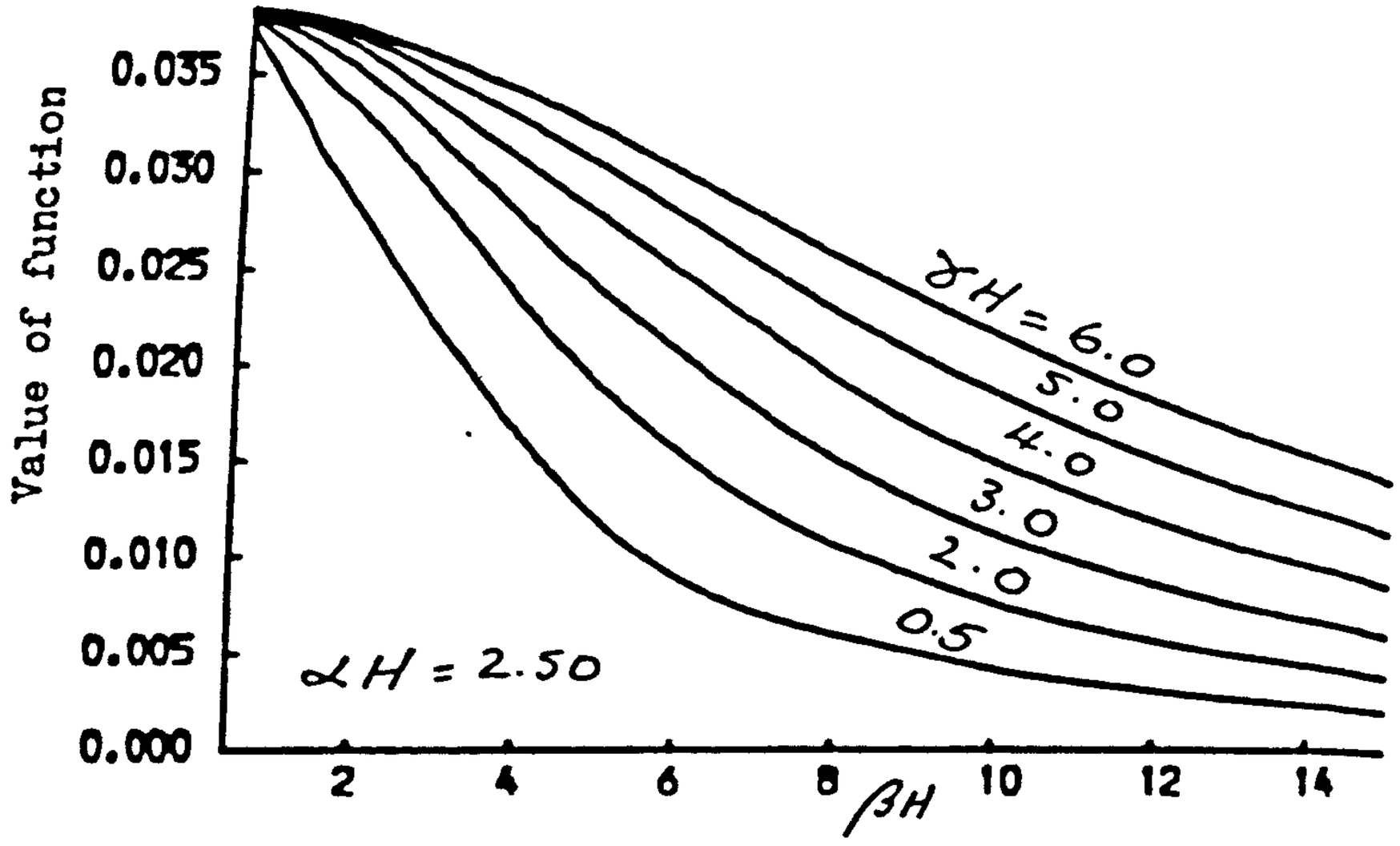

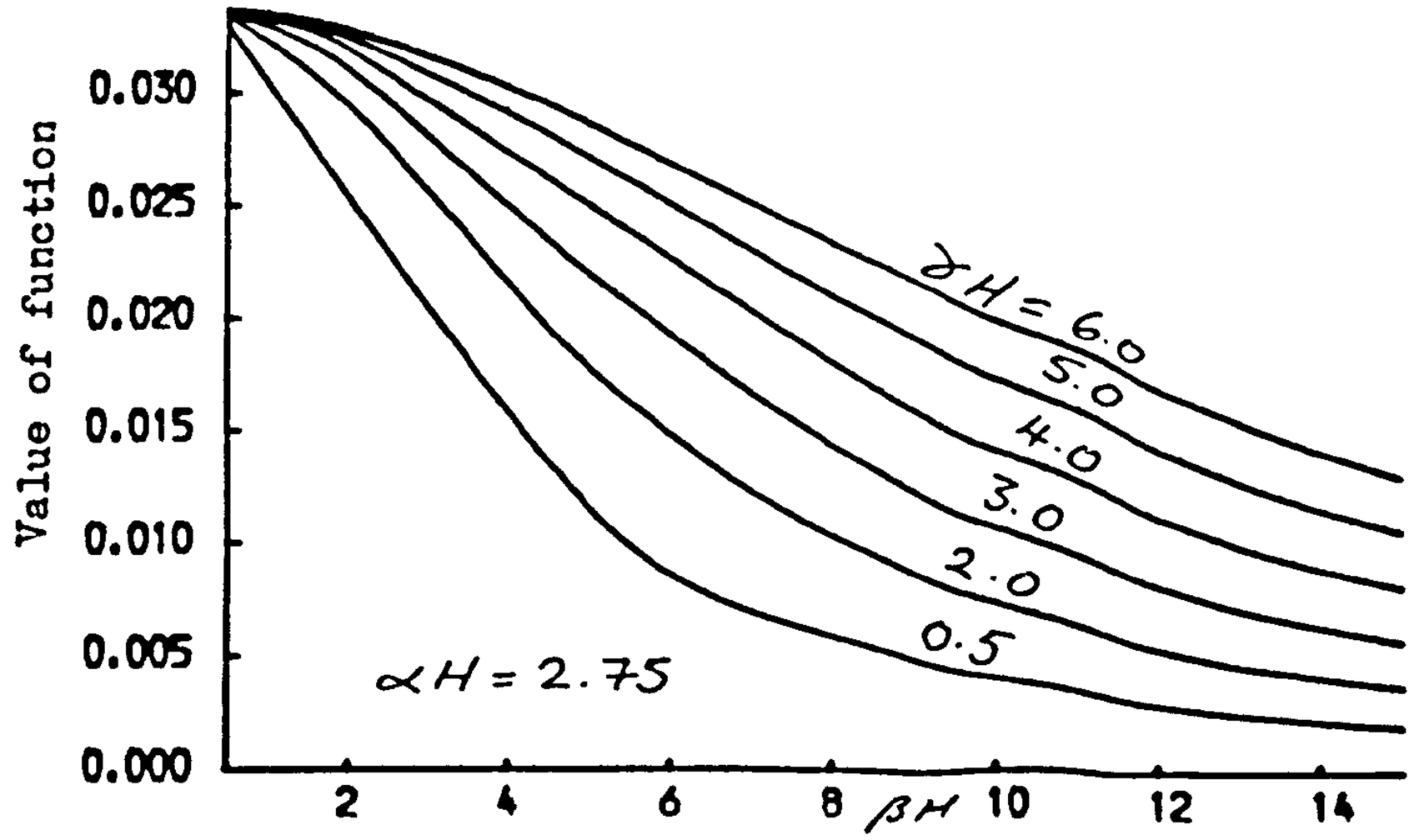

Fig. 2.3 Distributions of deflection function F_1

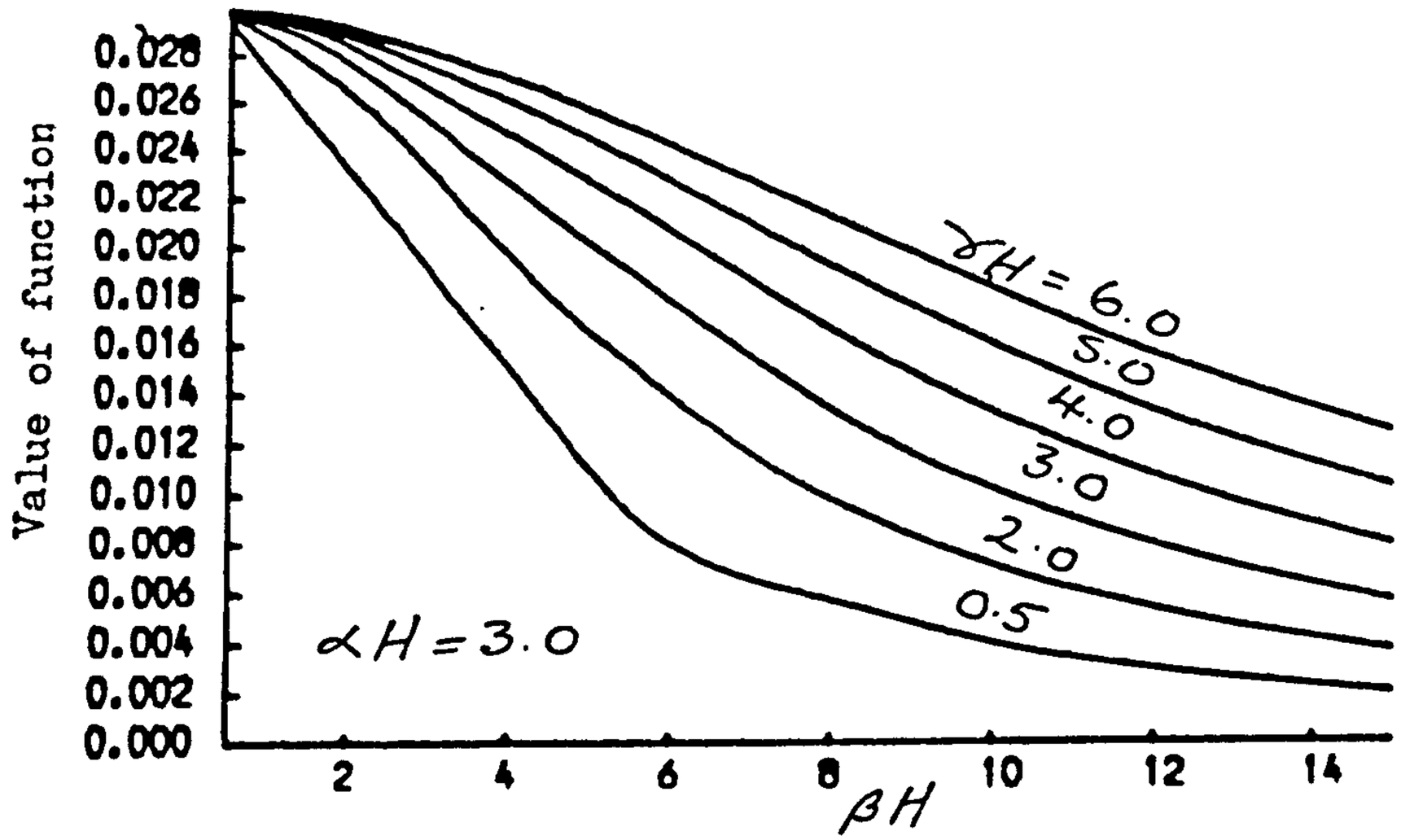

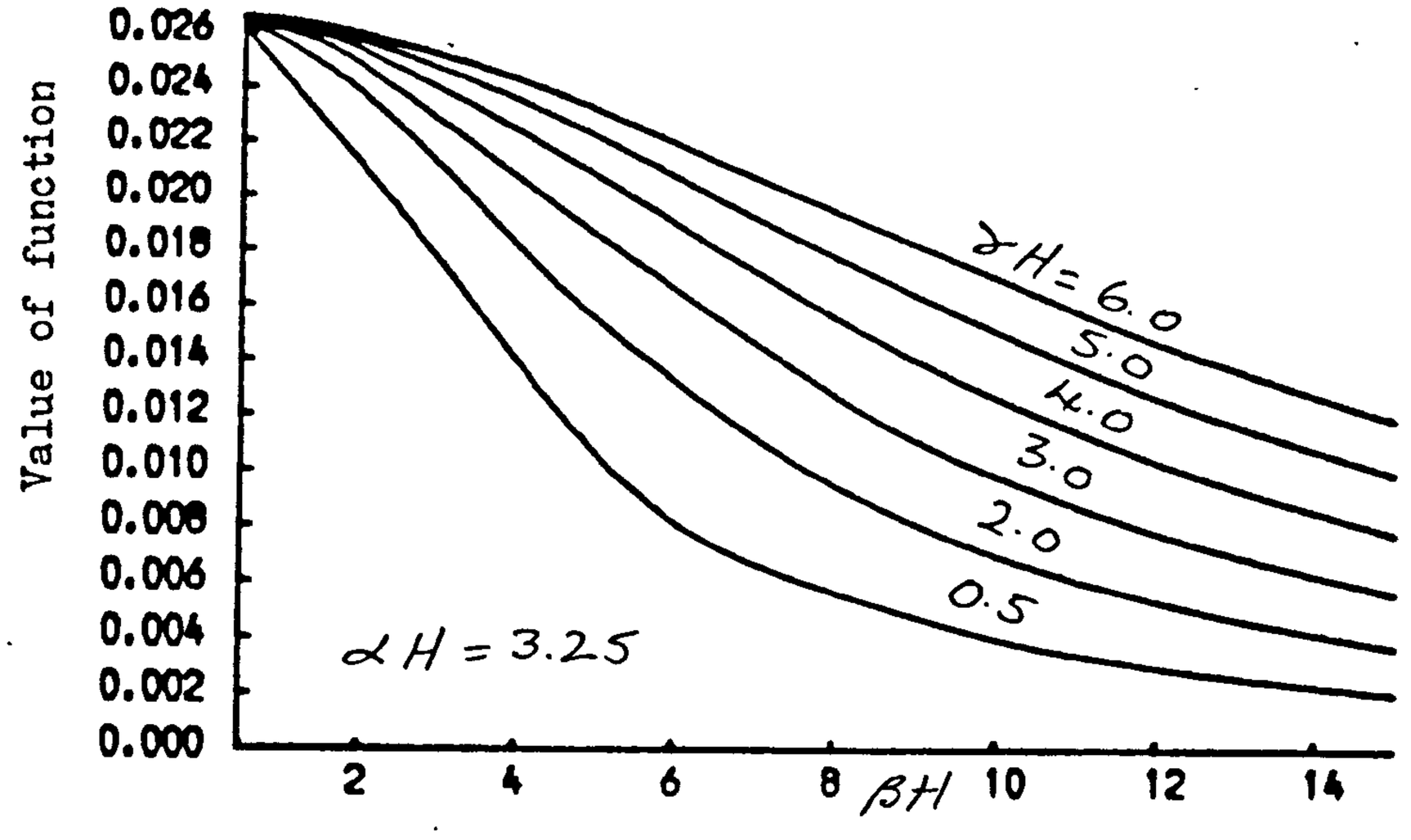

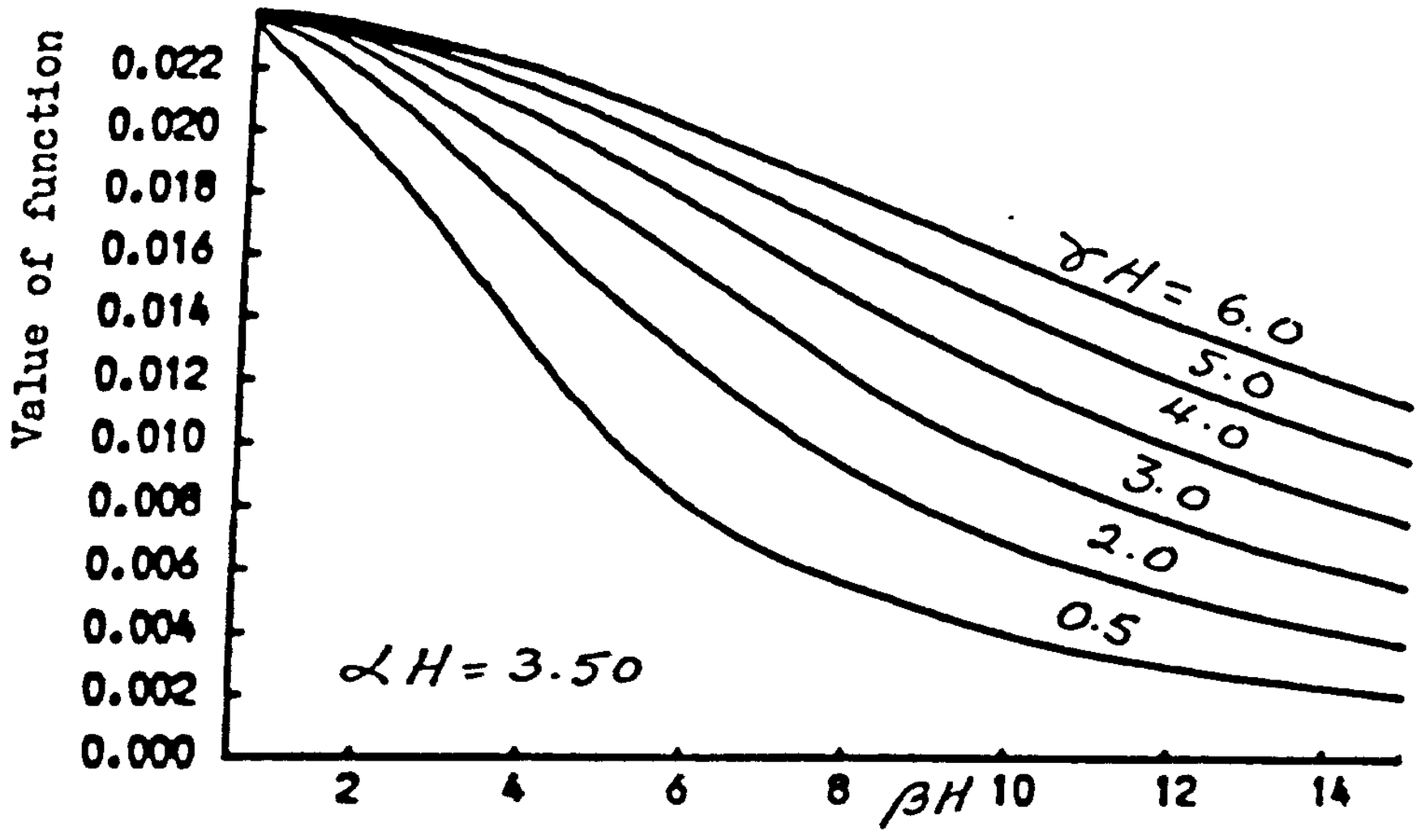

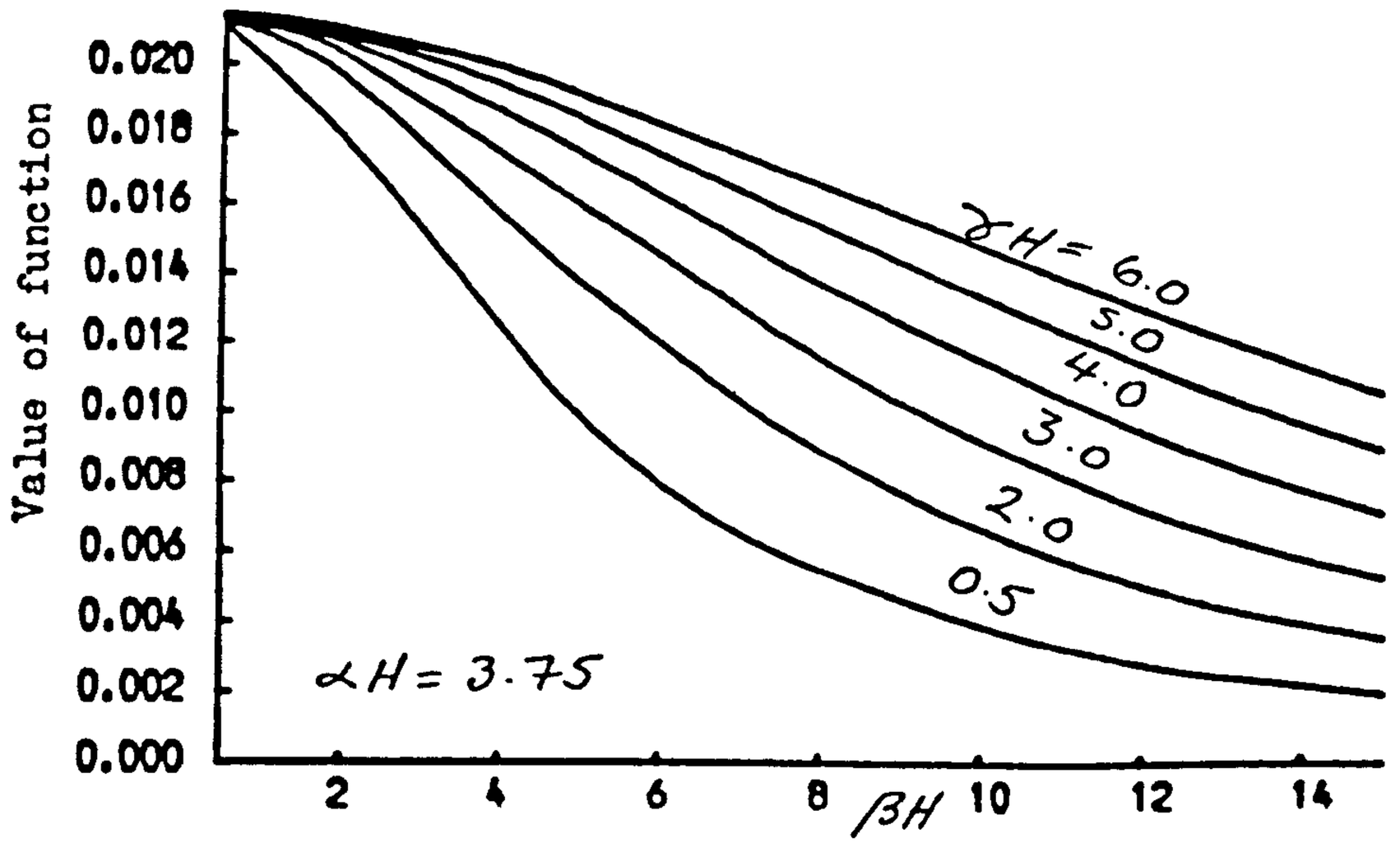

Fig. 2.4 Distributions of deflection function F_1

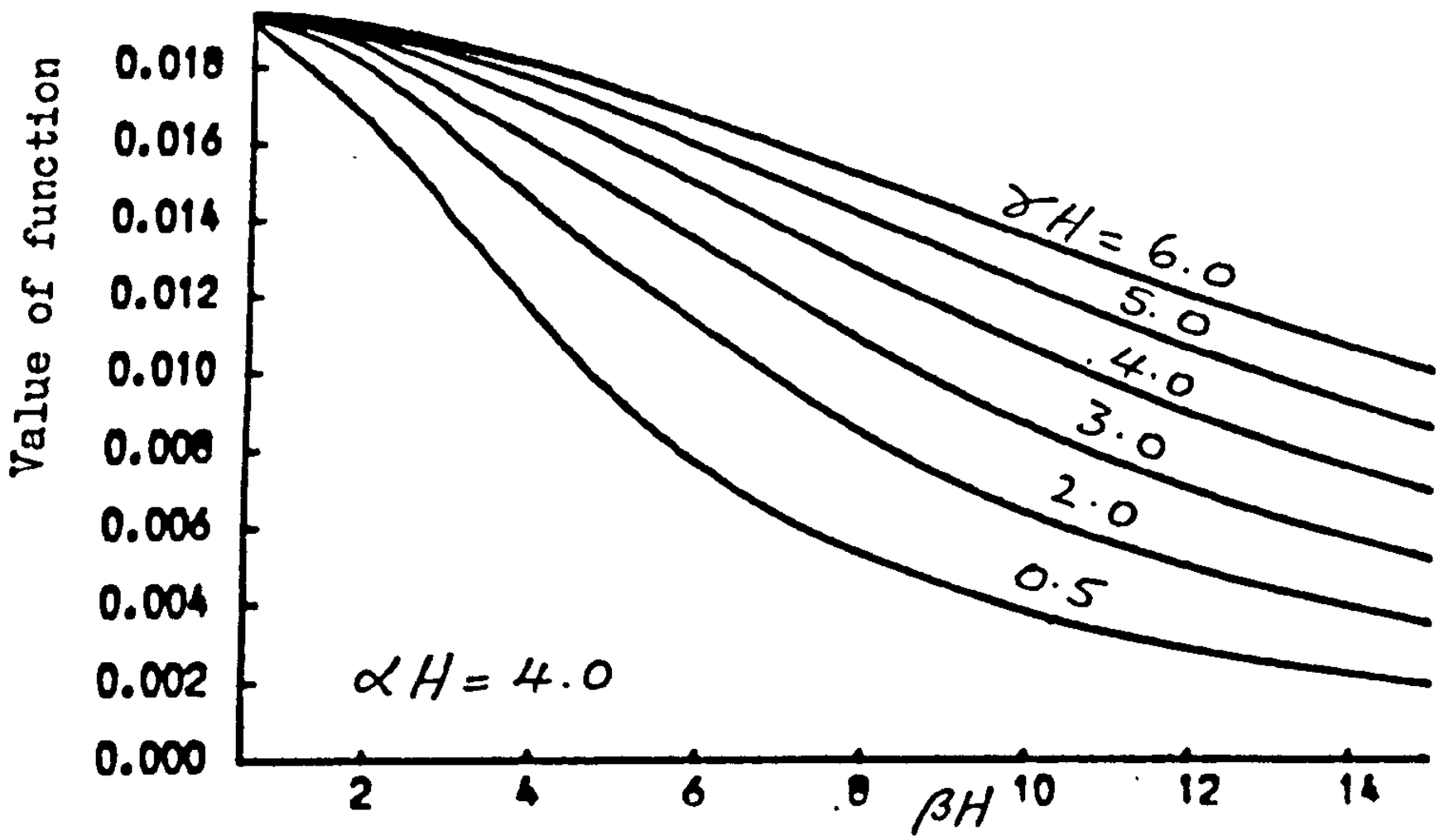

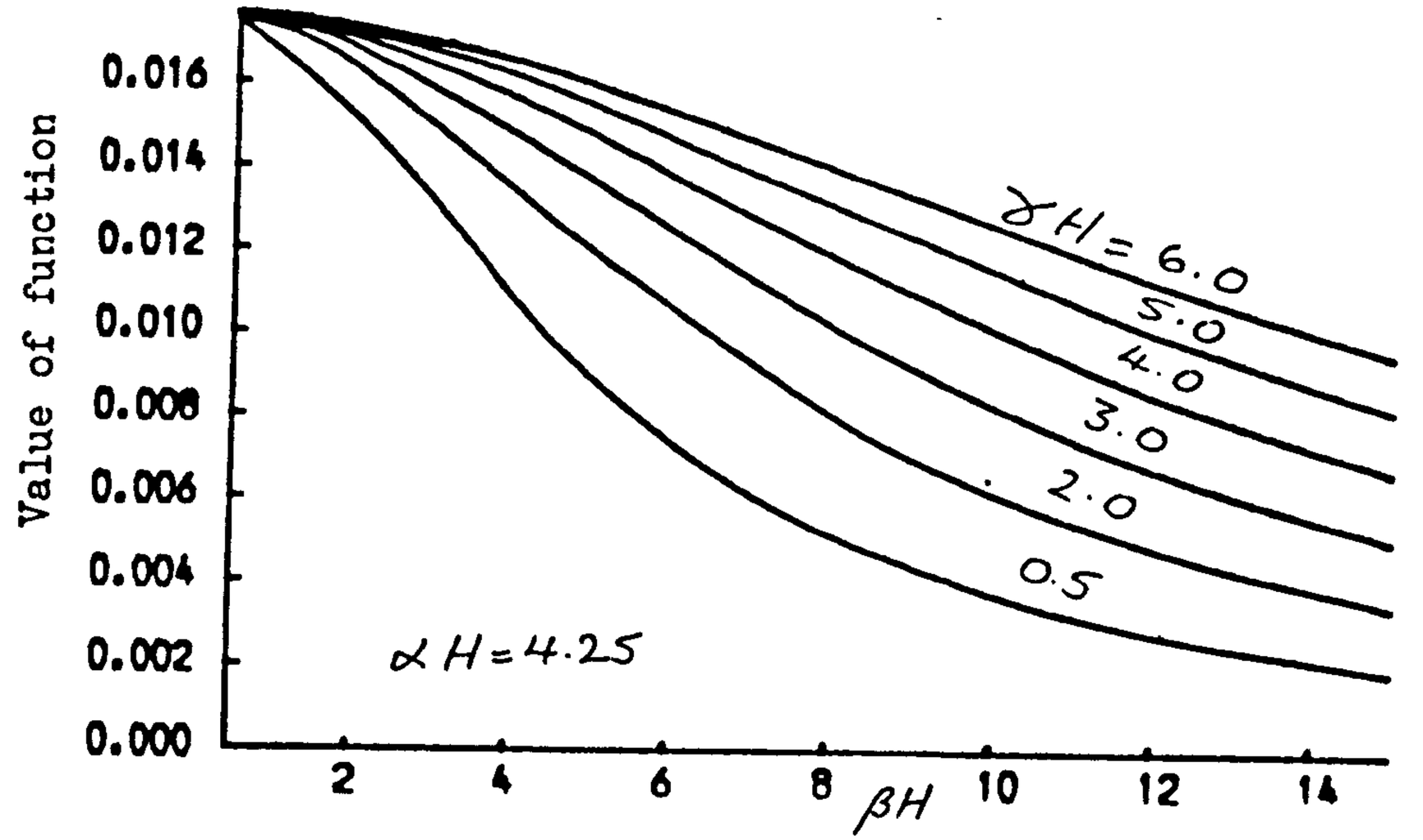

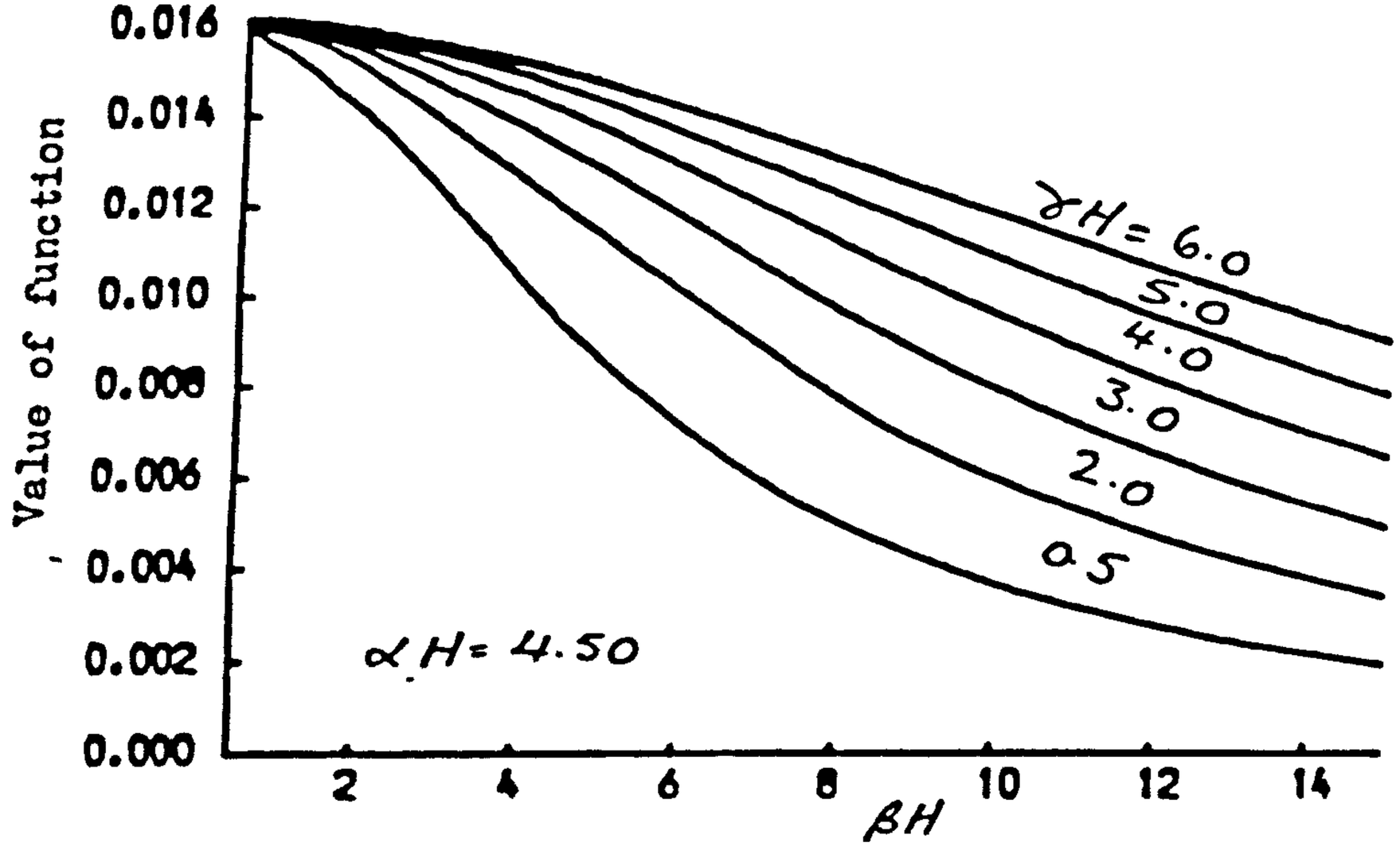

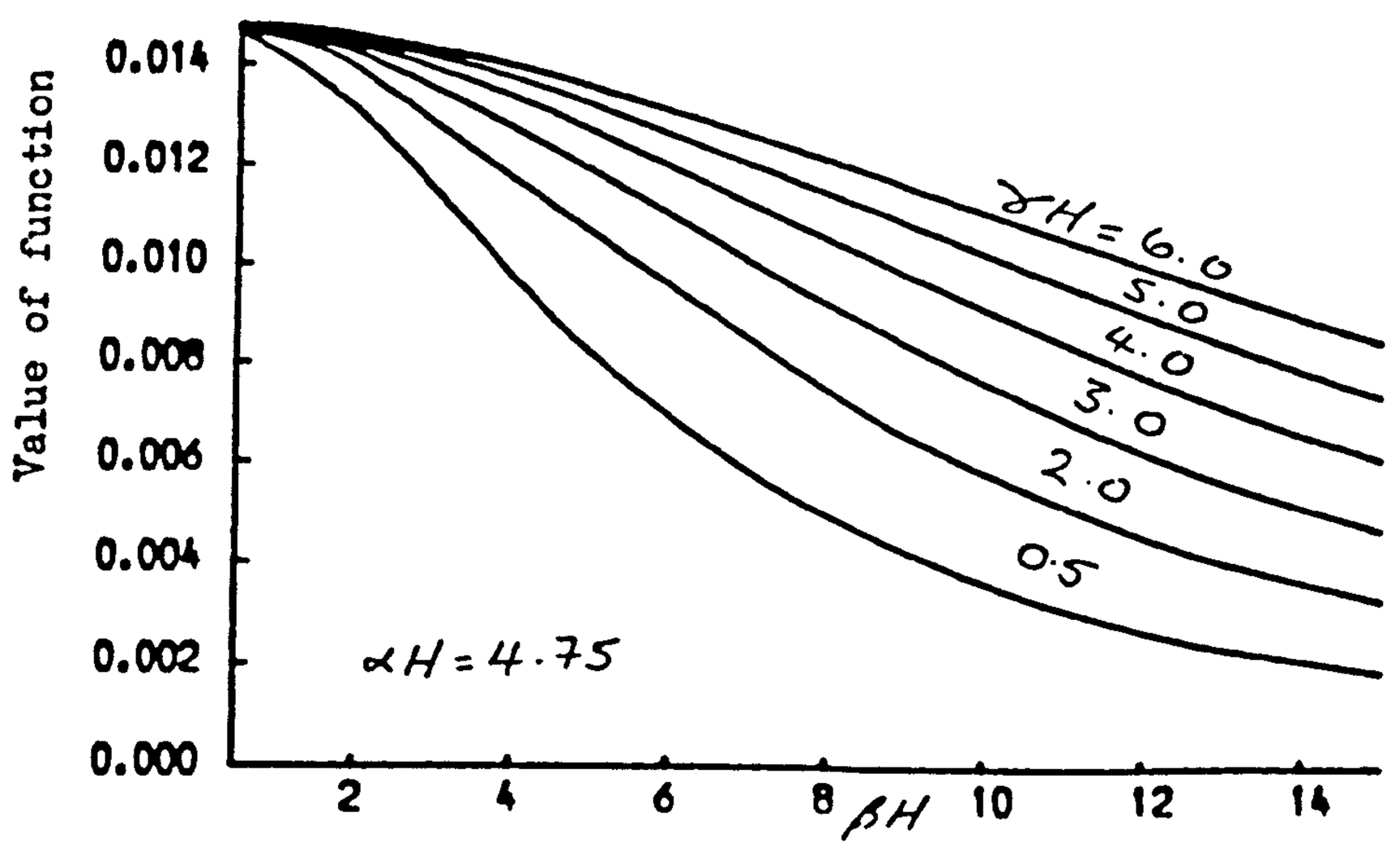

Fig. 2.5 Distributions of deflection function F_1

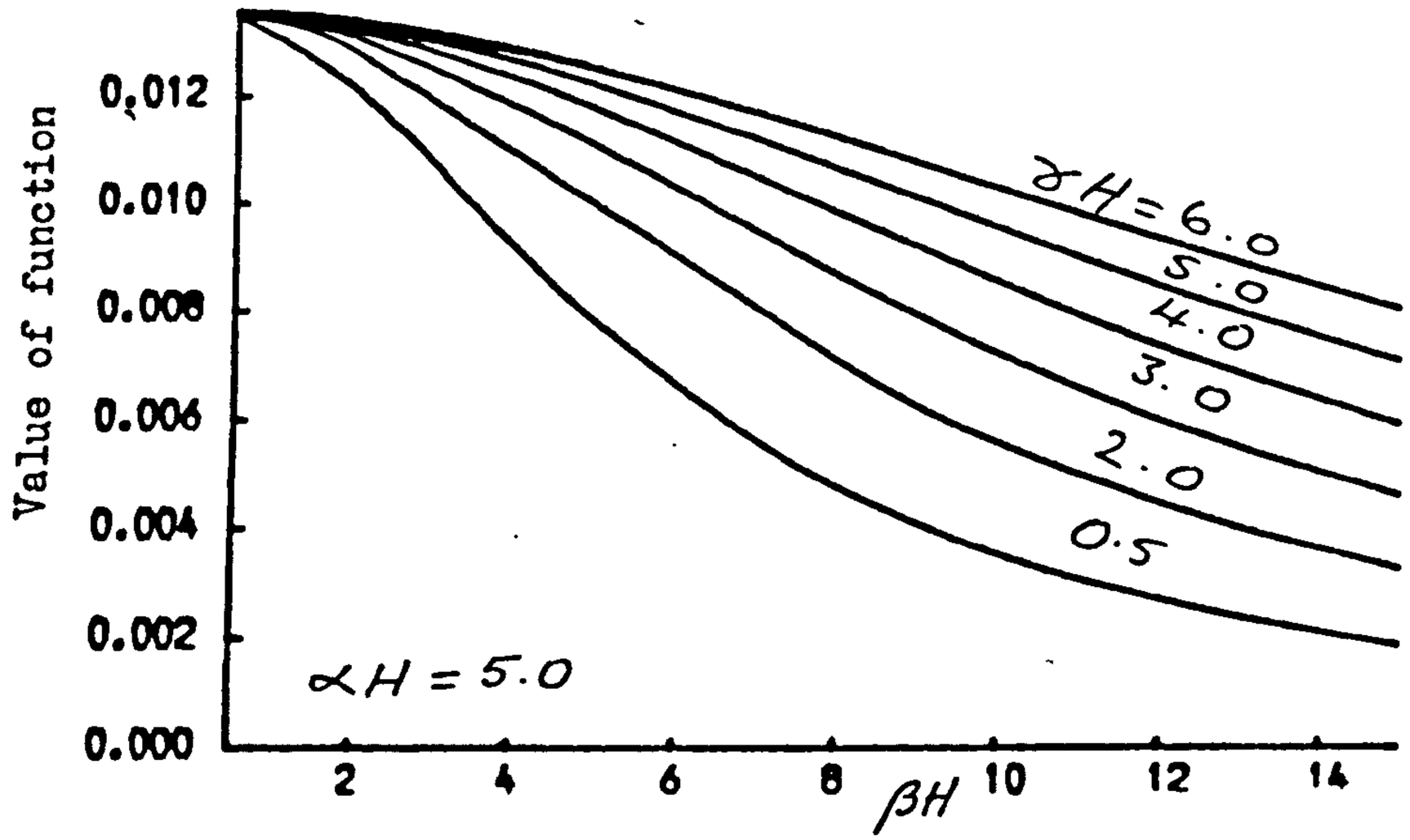

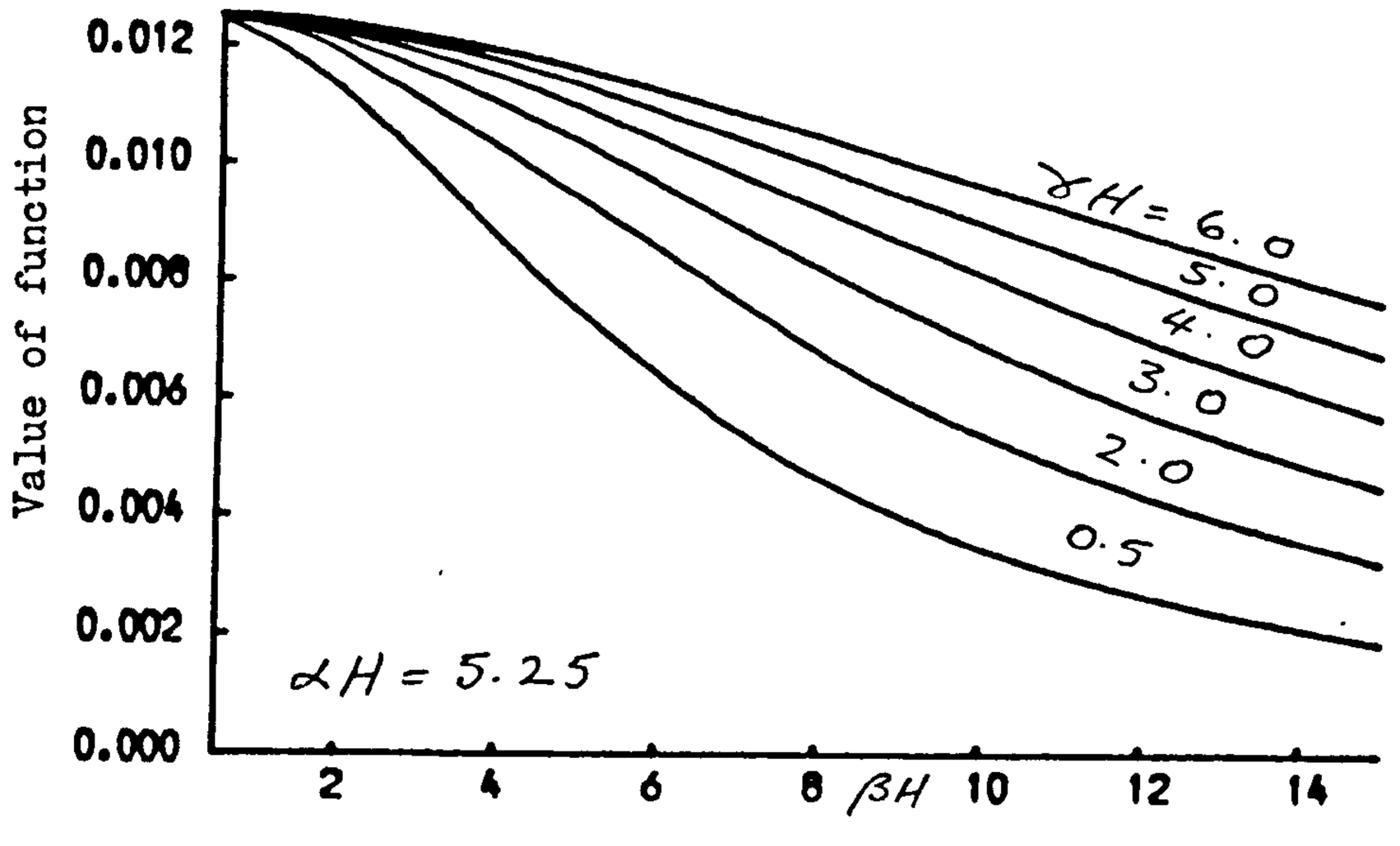

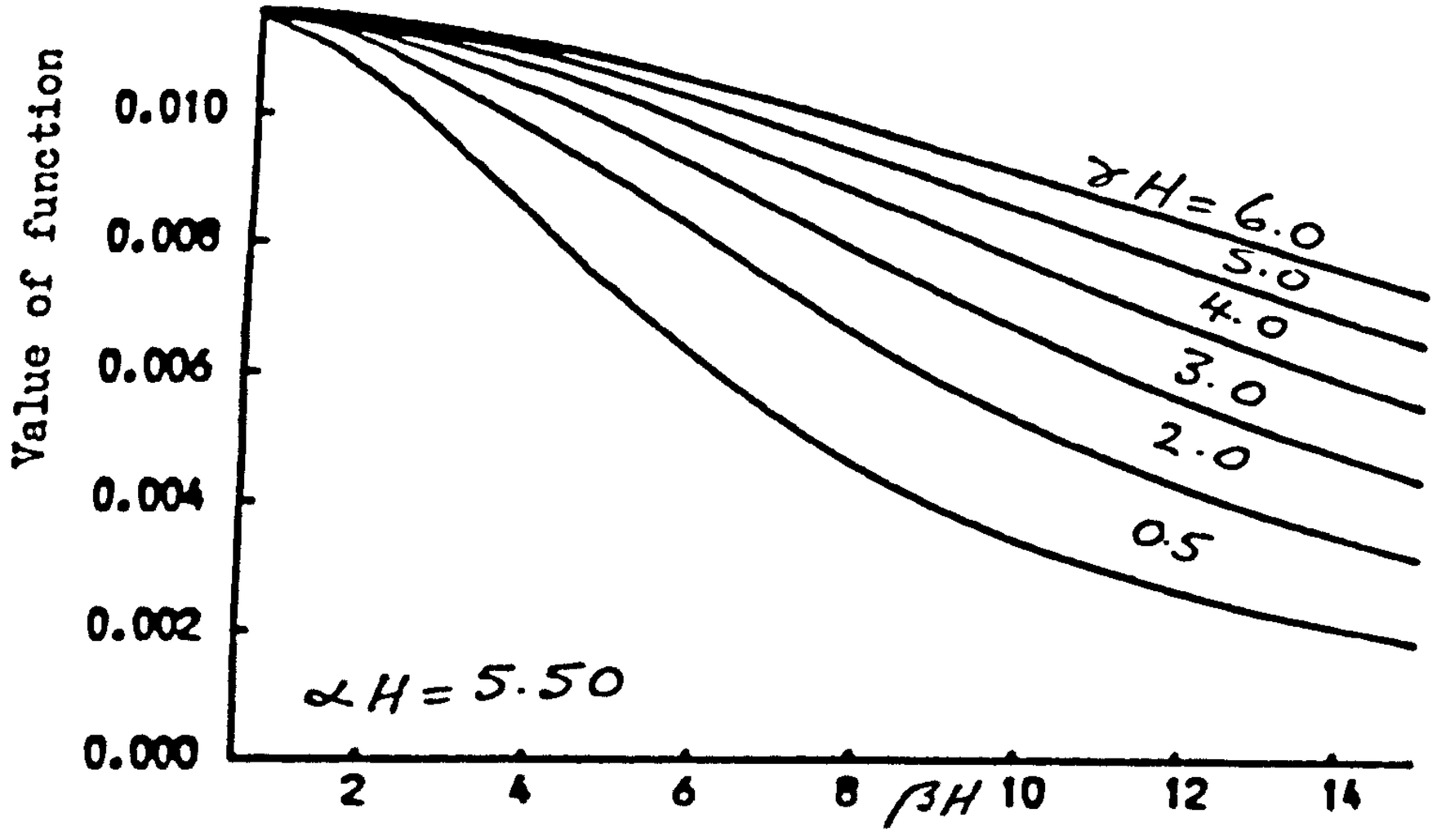

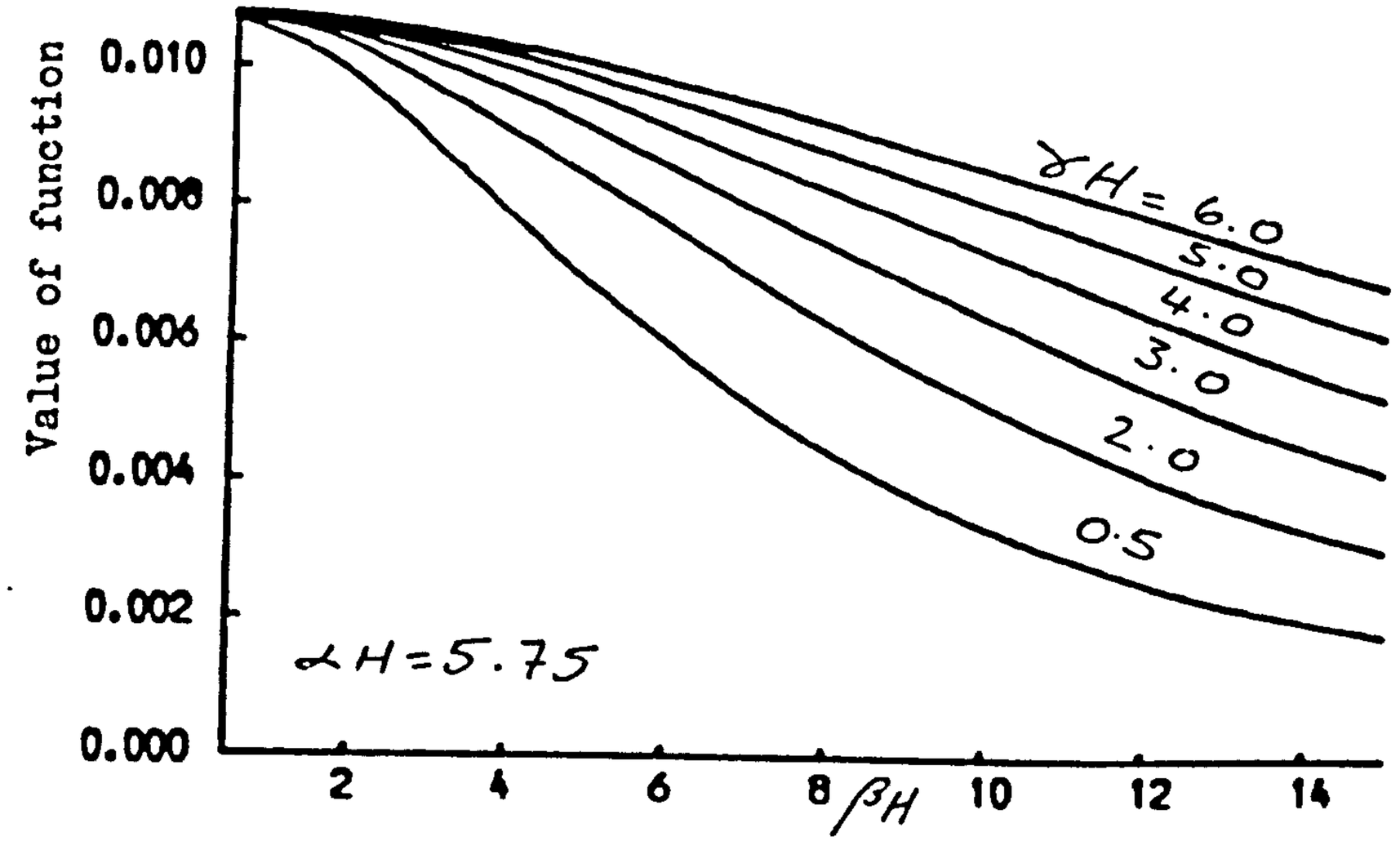

Fig. 2.6 Distributions of deflection function F_1

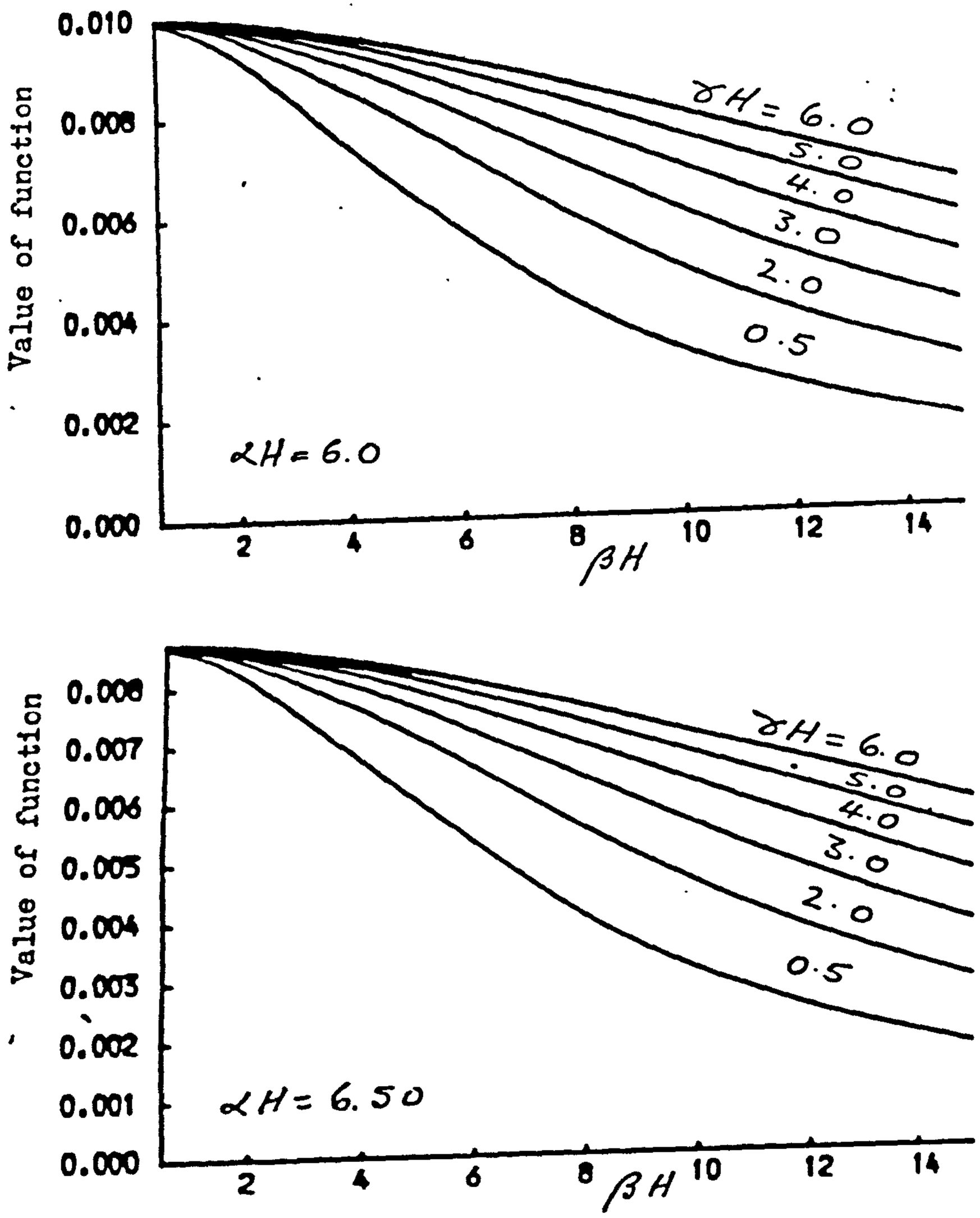

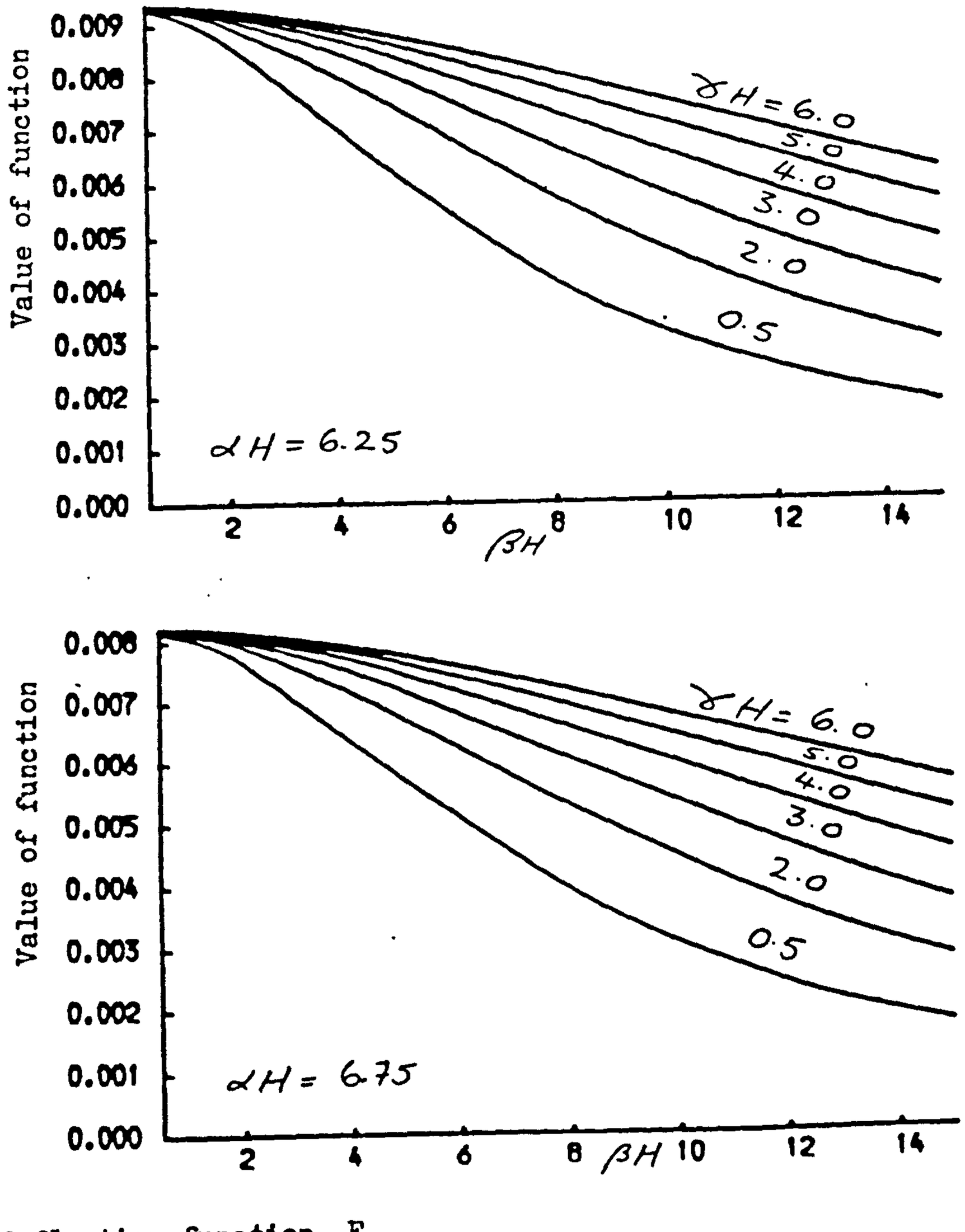

Fig. 2.7 Distributions of deflection function F_1

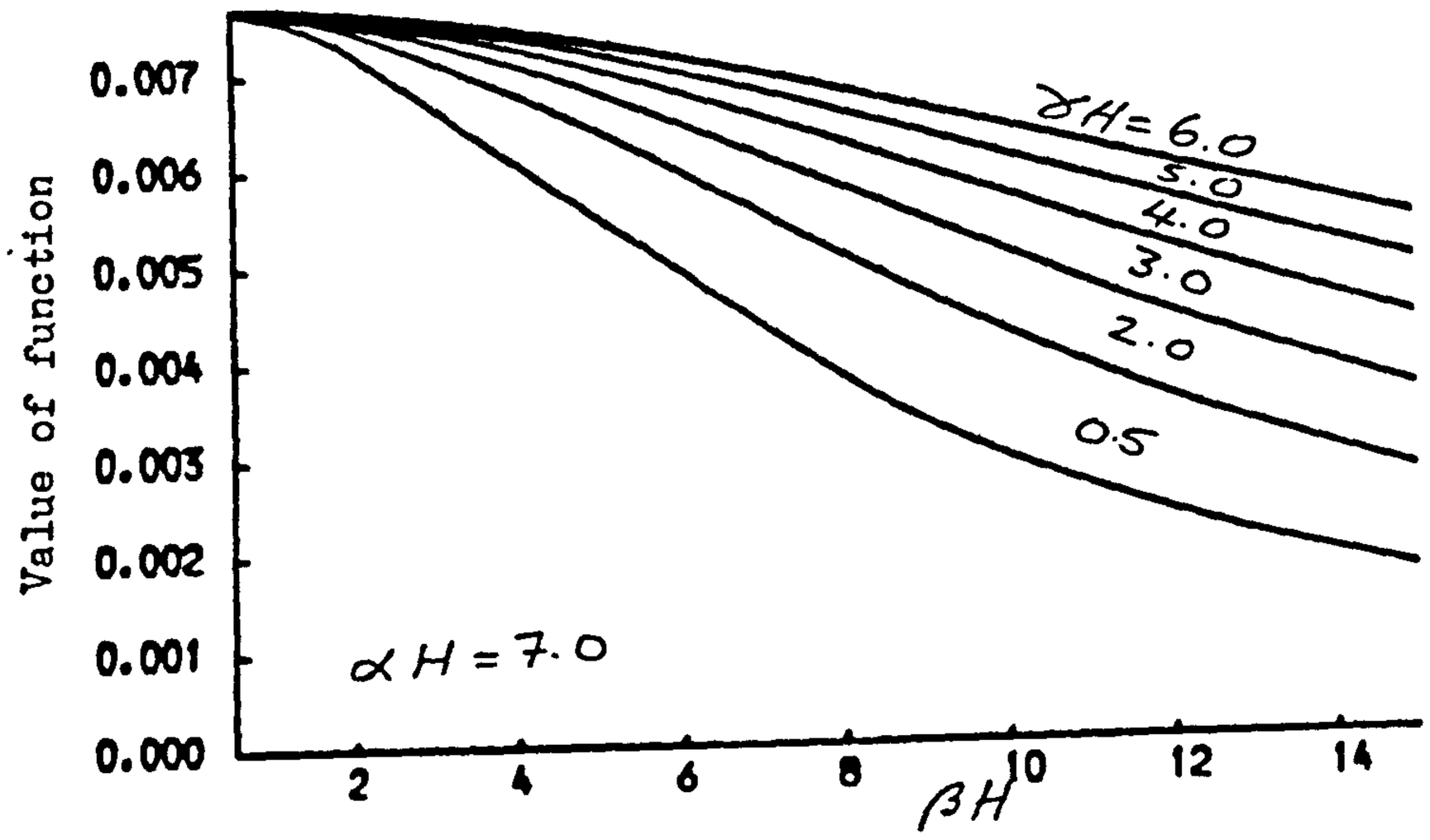

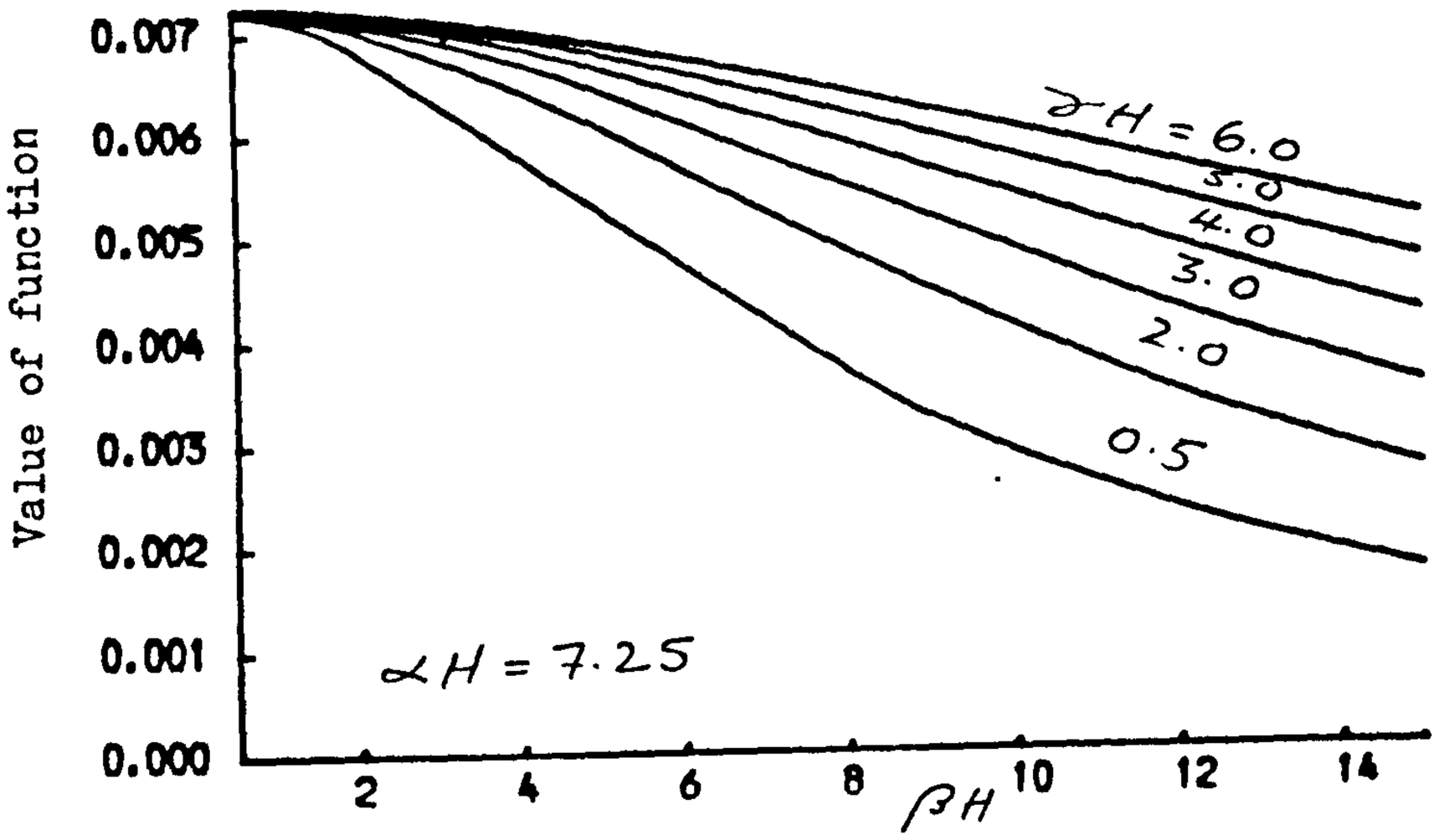

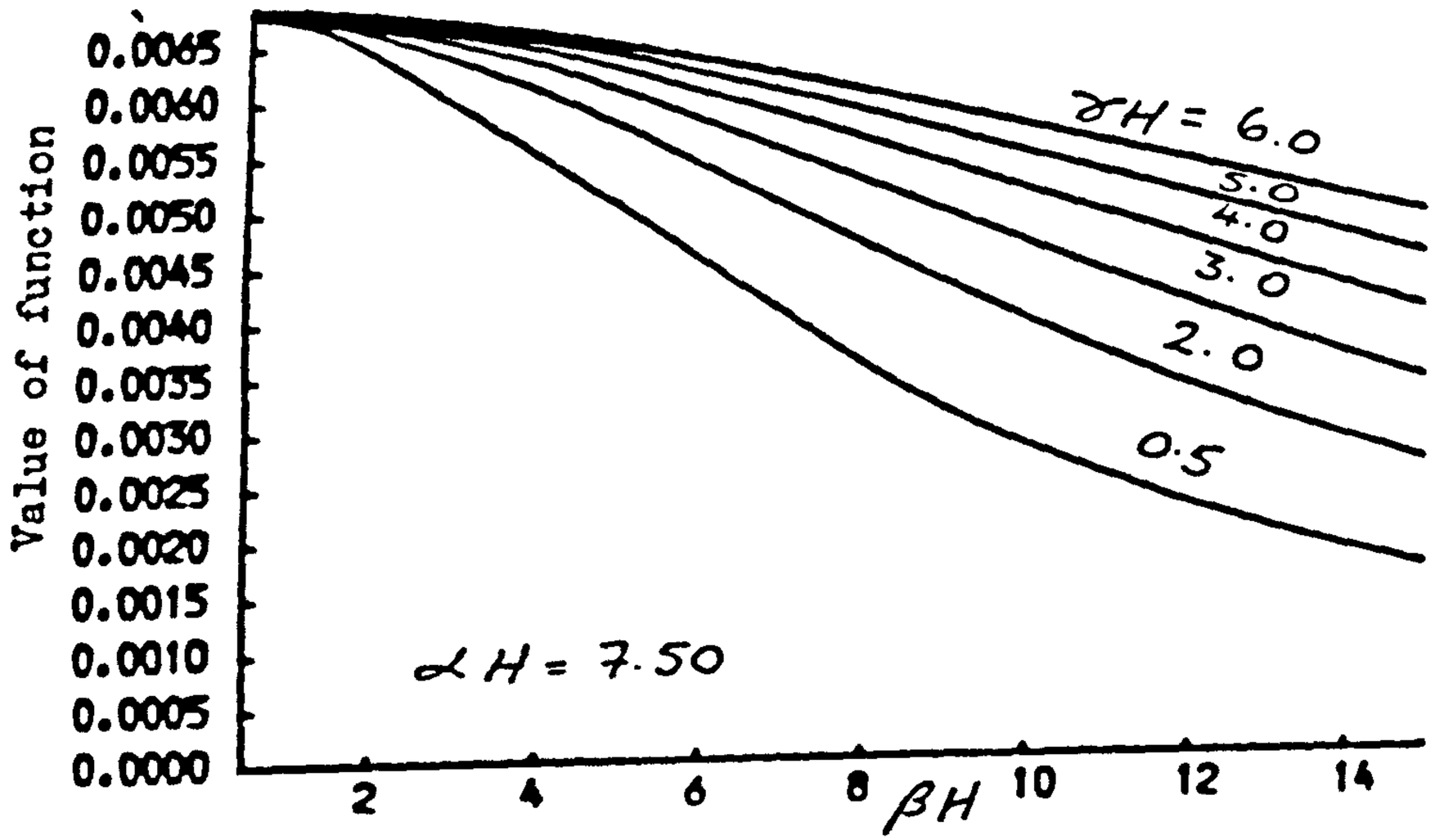

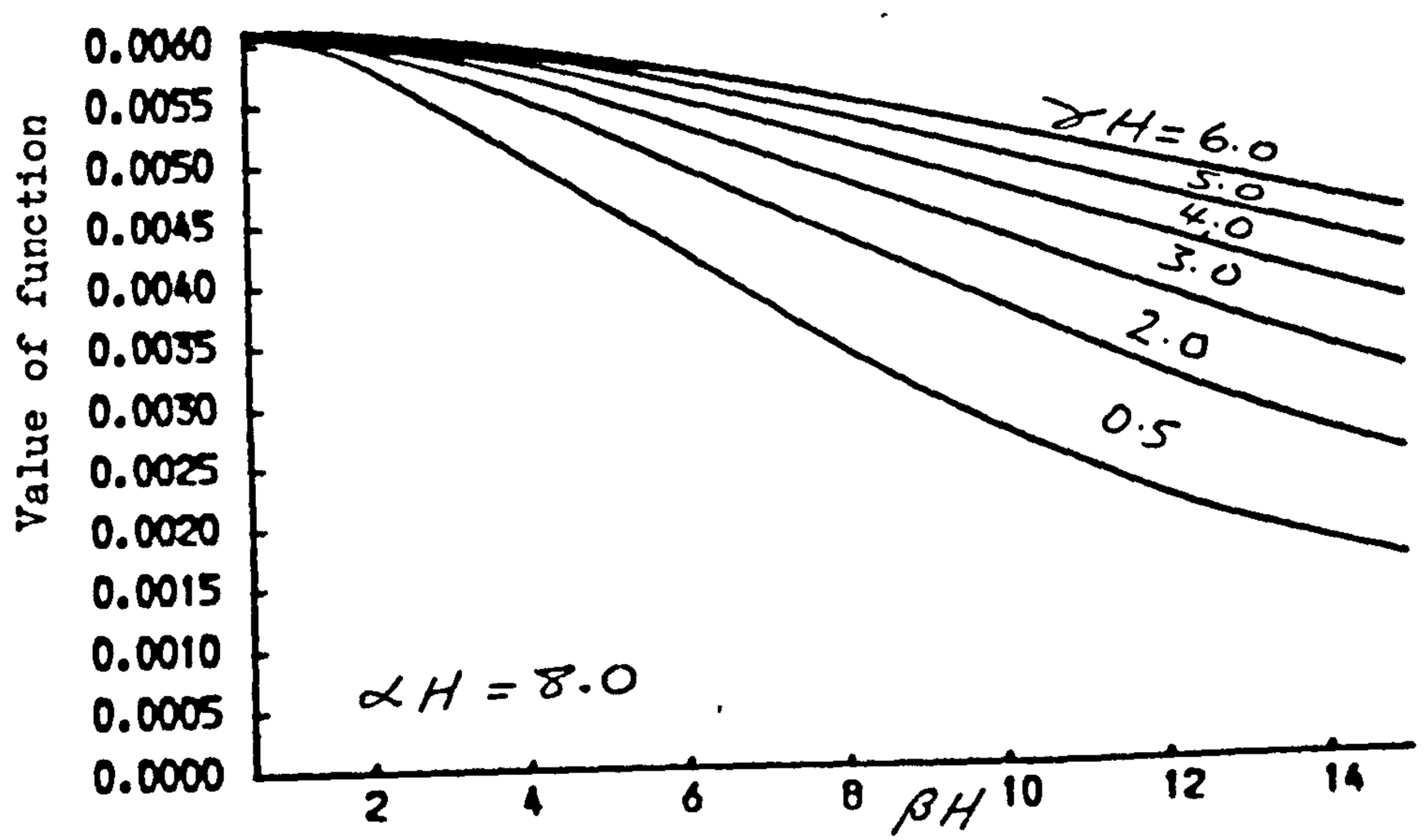

Fig. 2.8 Distributions of deflection function F_1

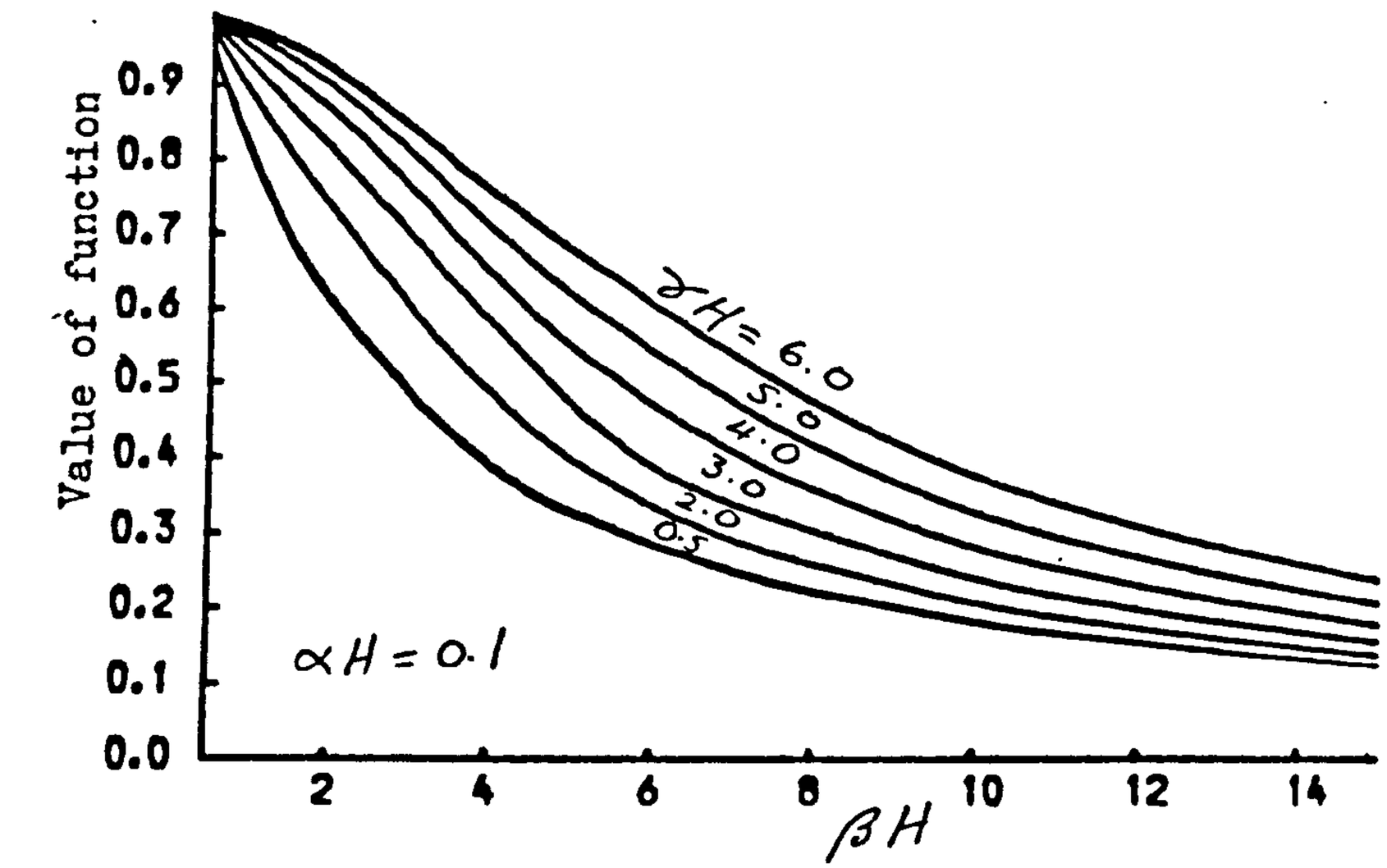

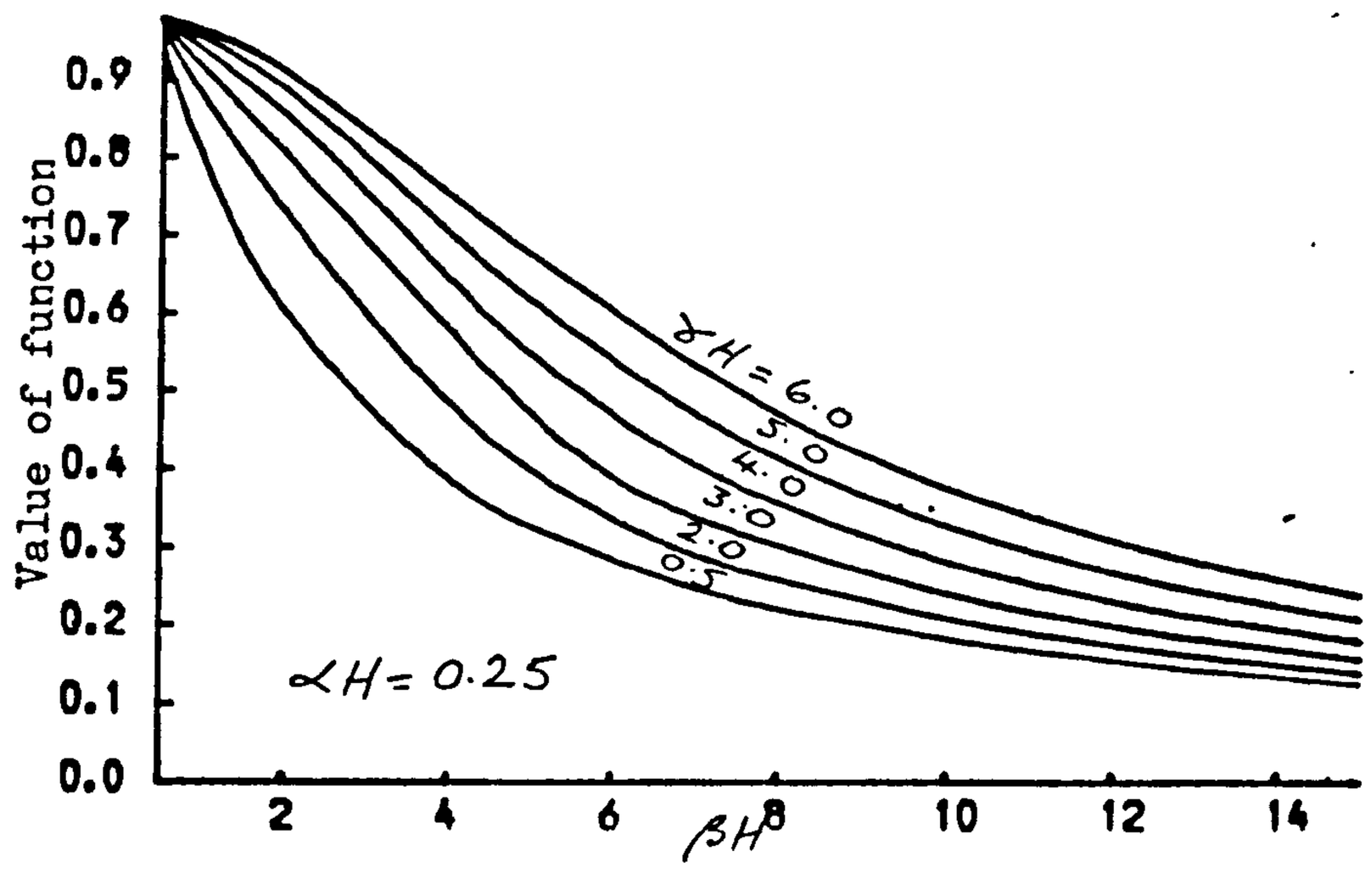

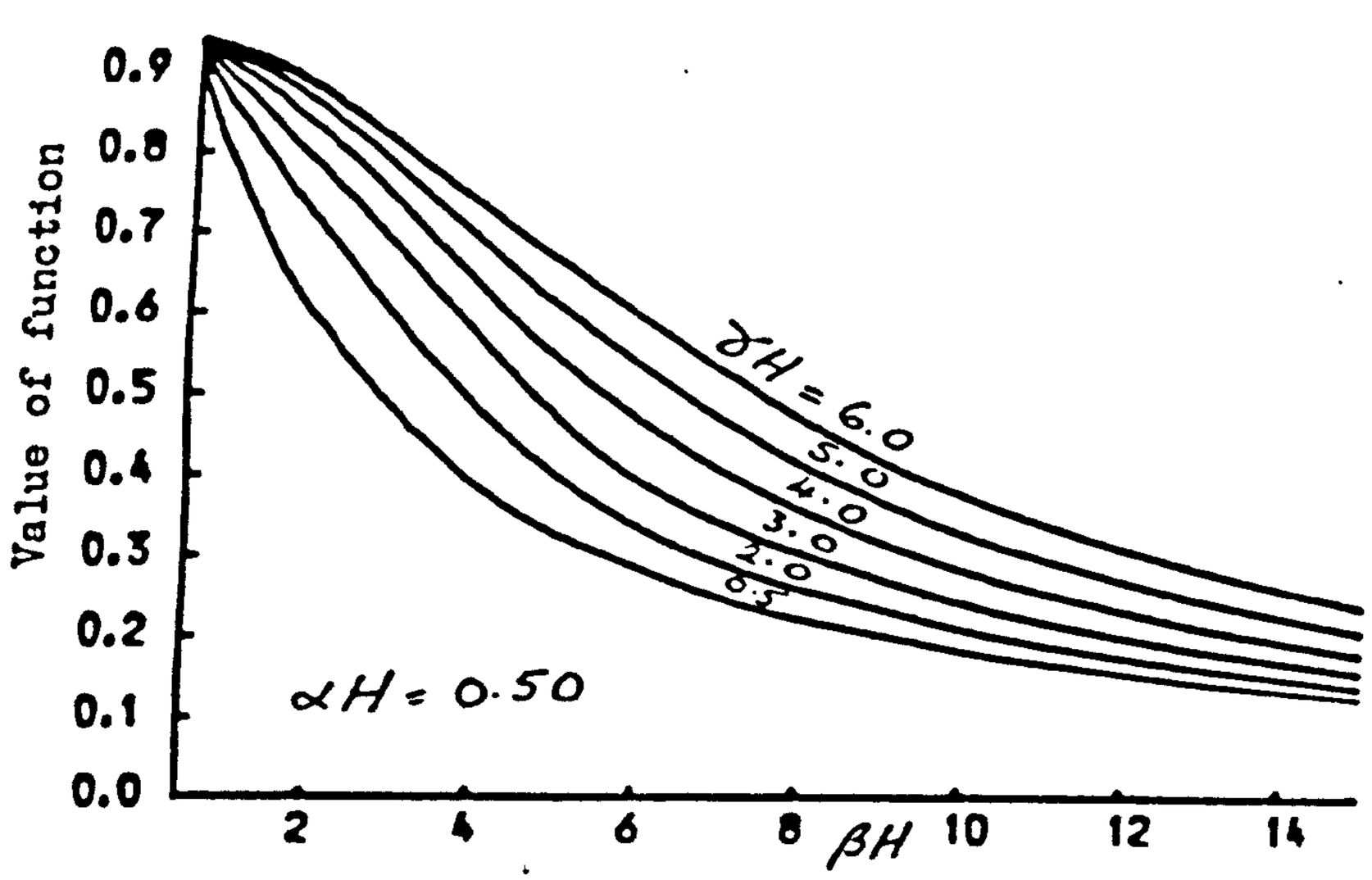

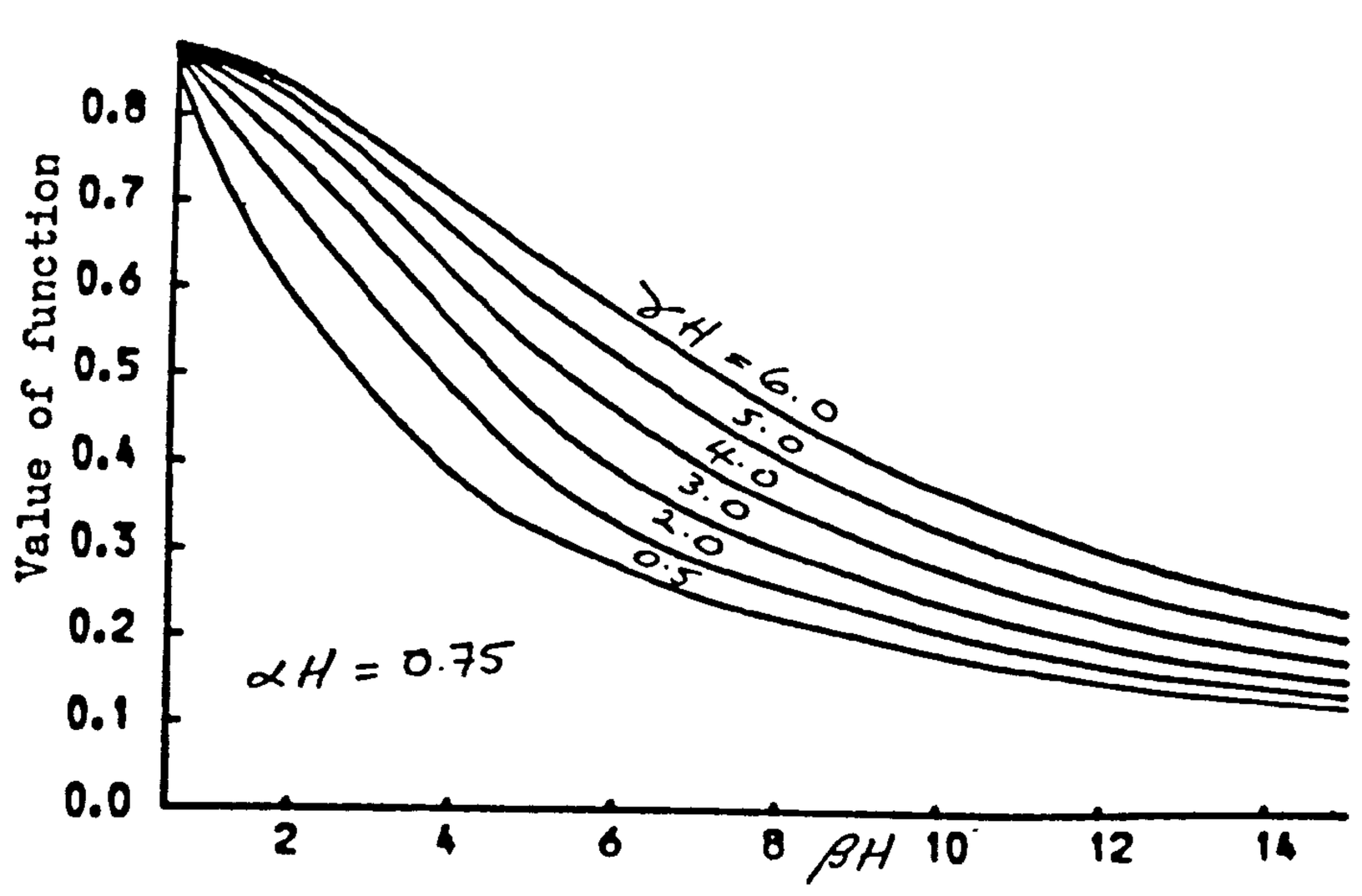

Fig. 2. 9 Distributions of moment function F_3

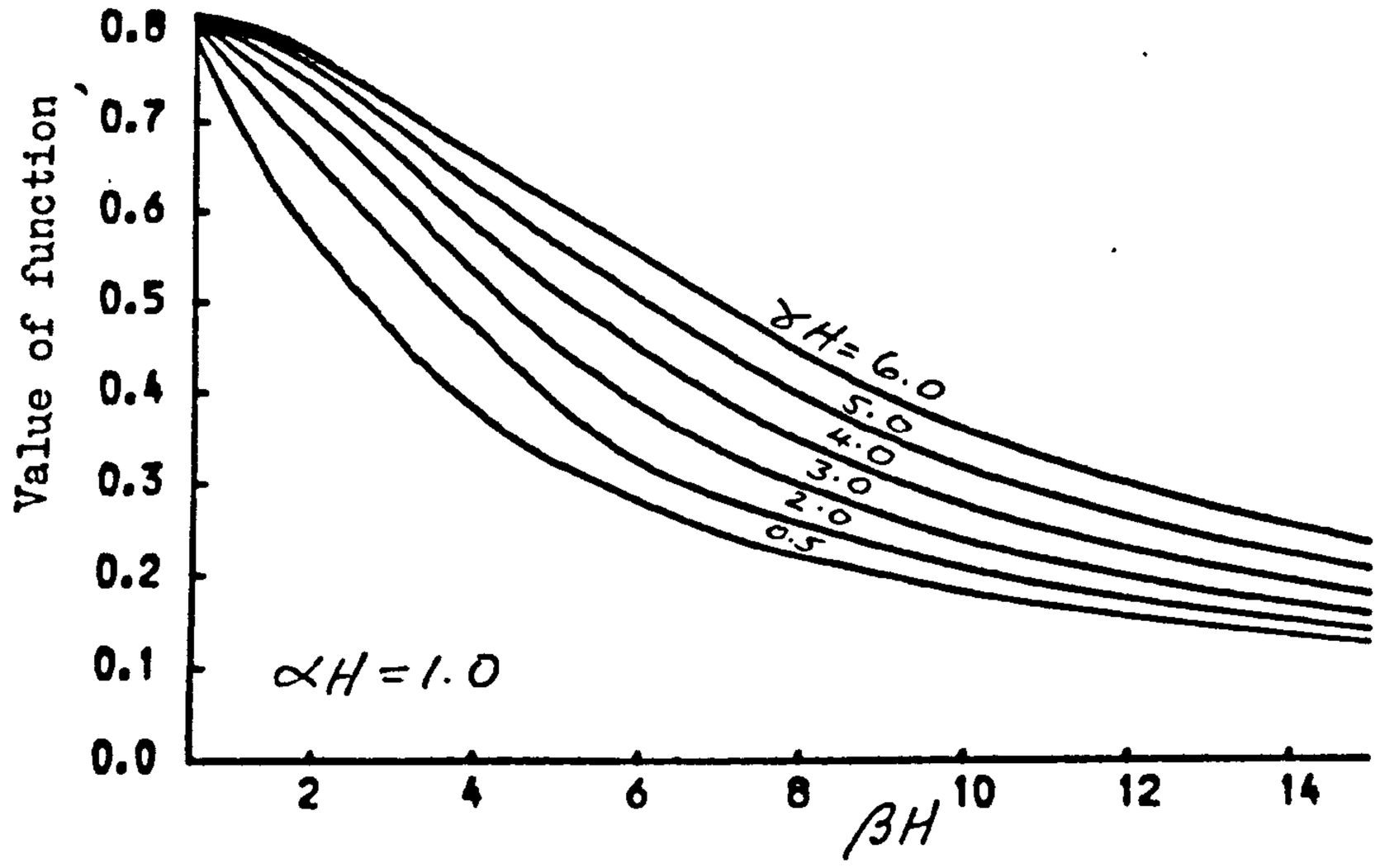

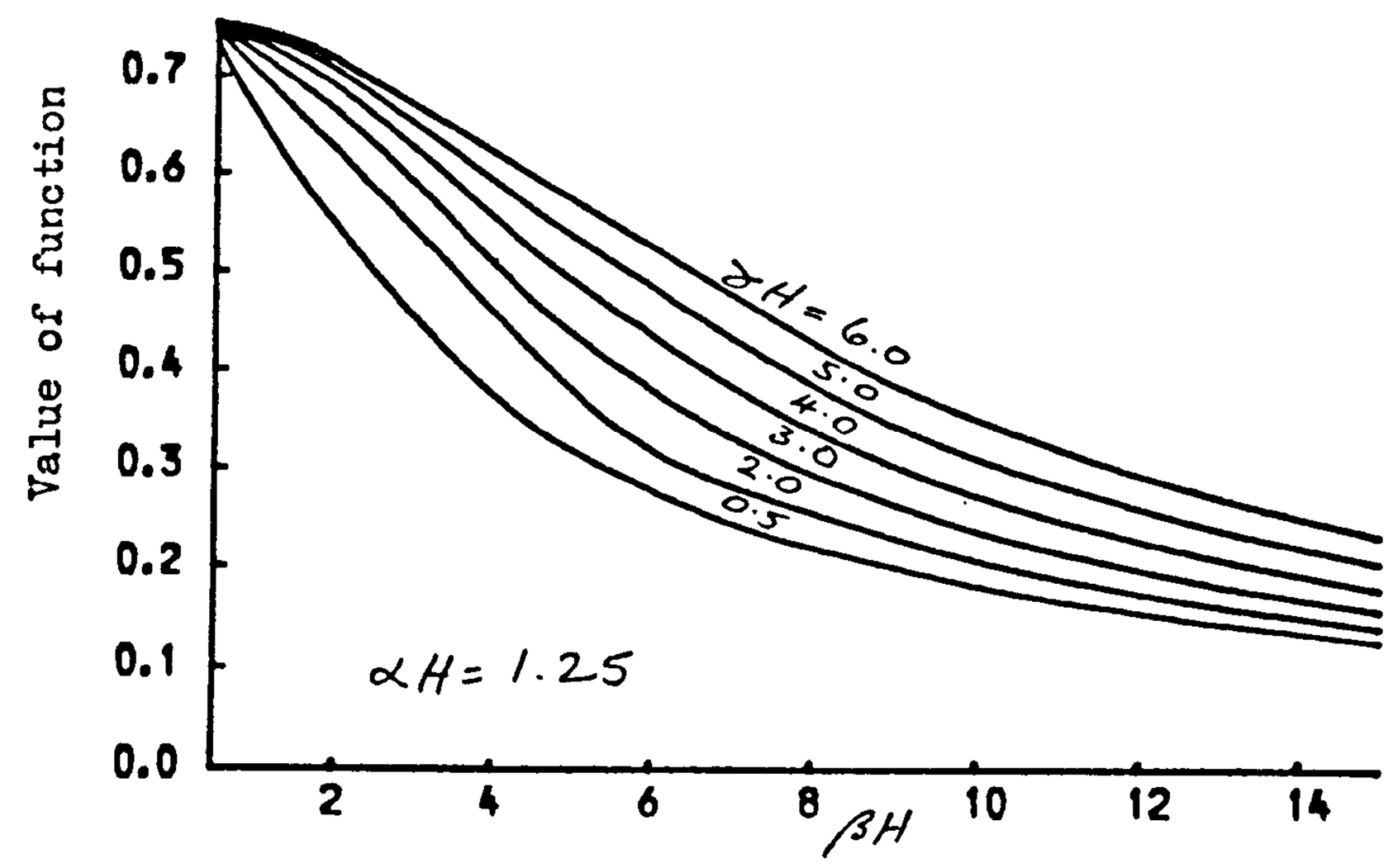

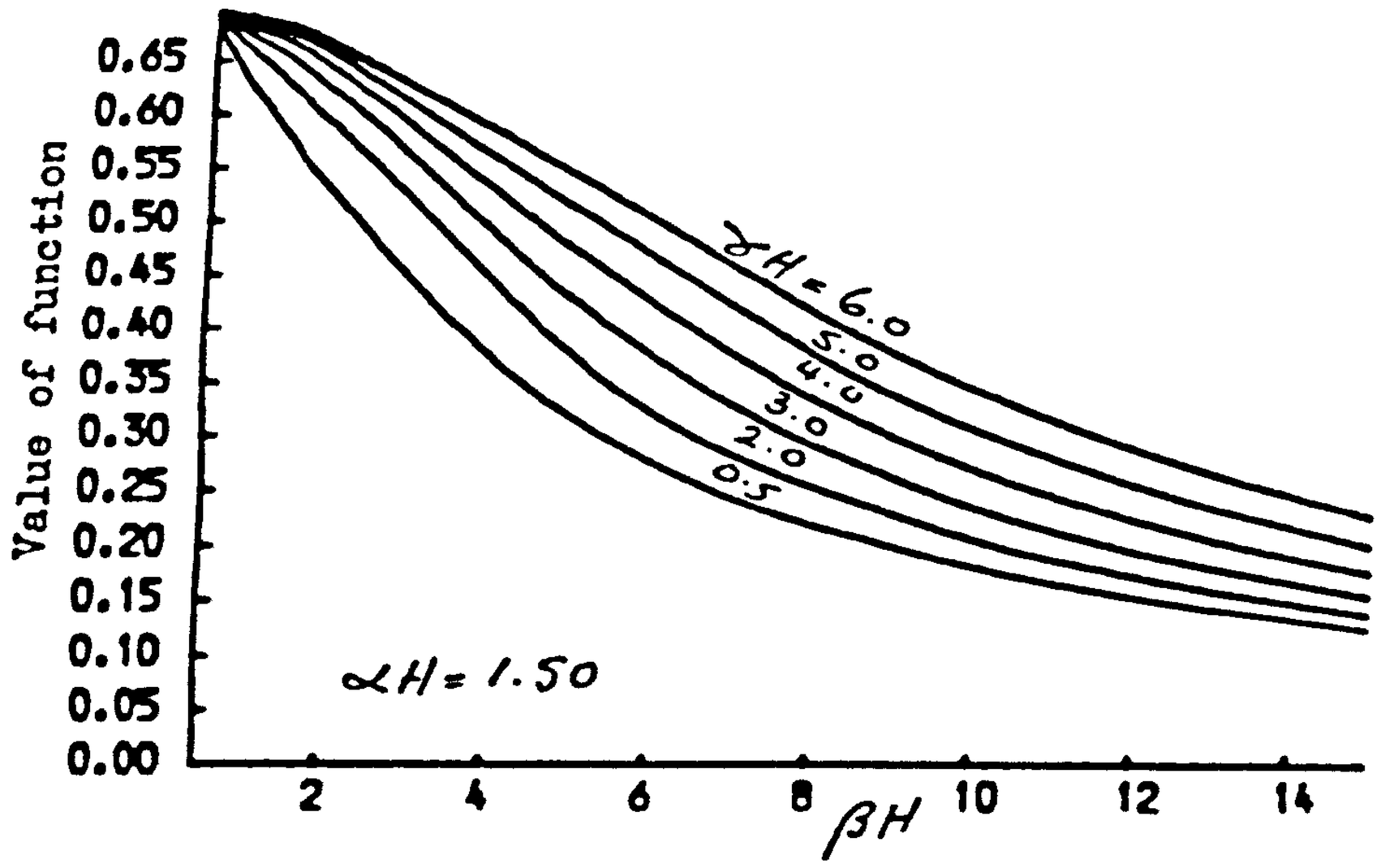

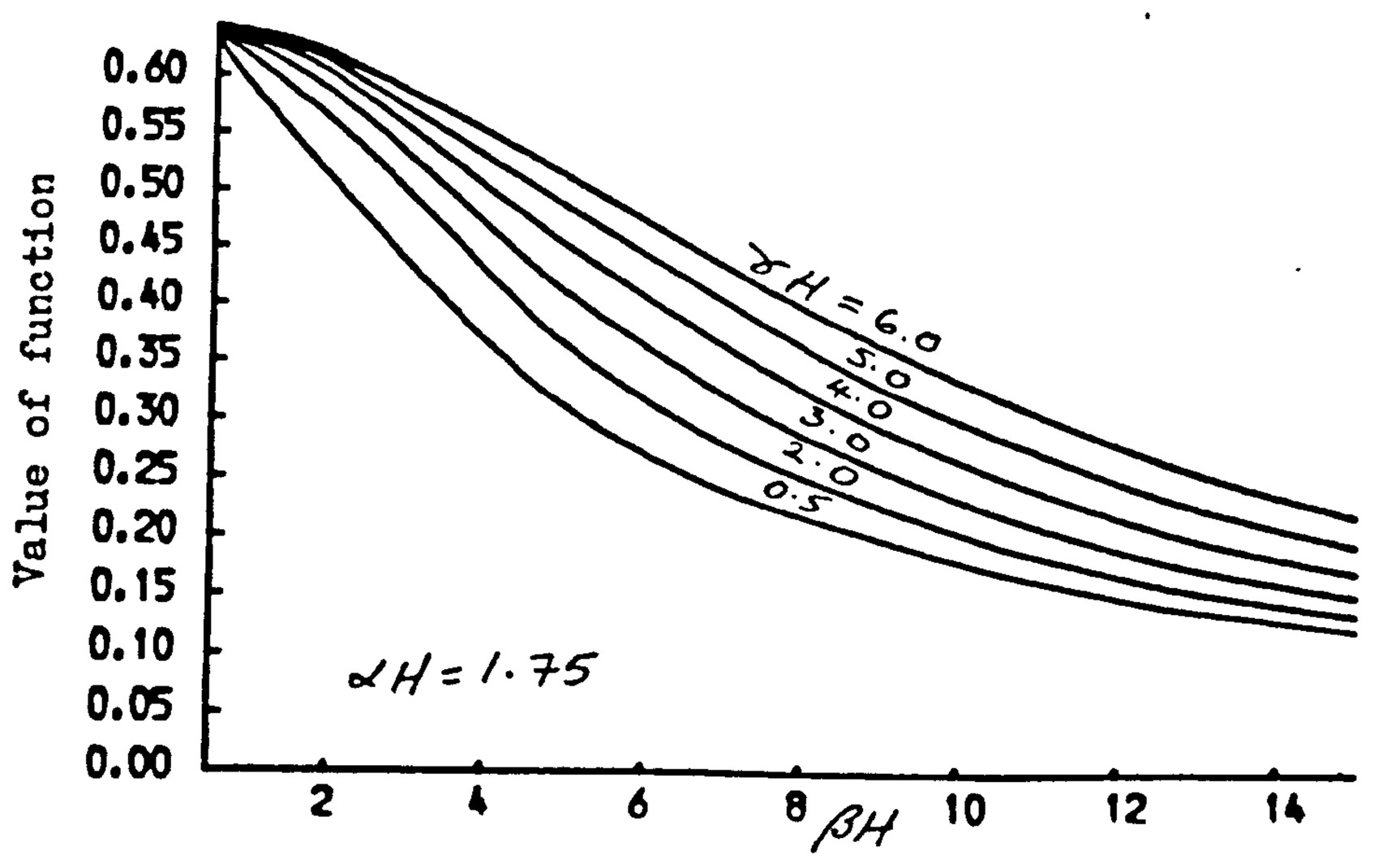

Fig. 2.10 Distributions of moment function F_3

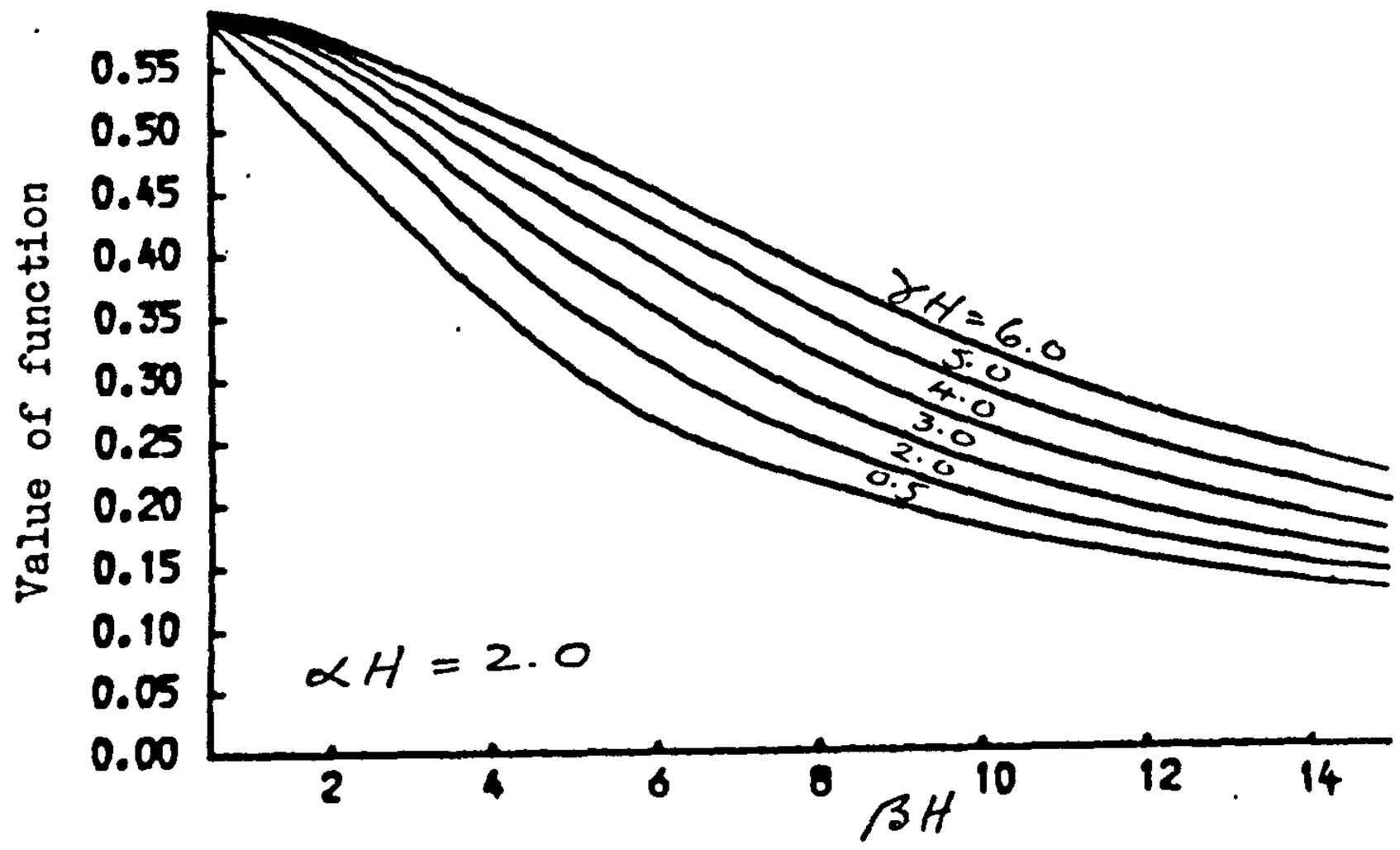

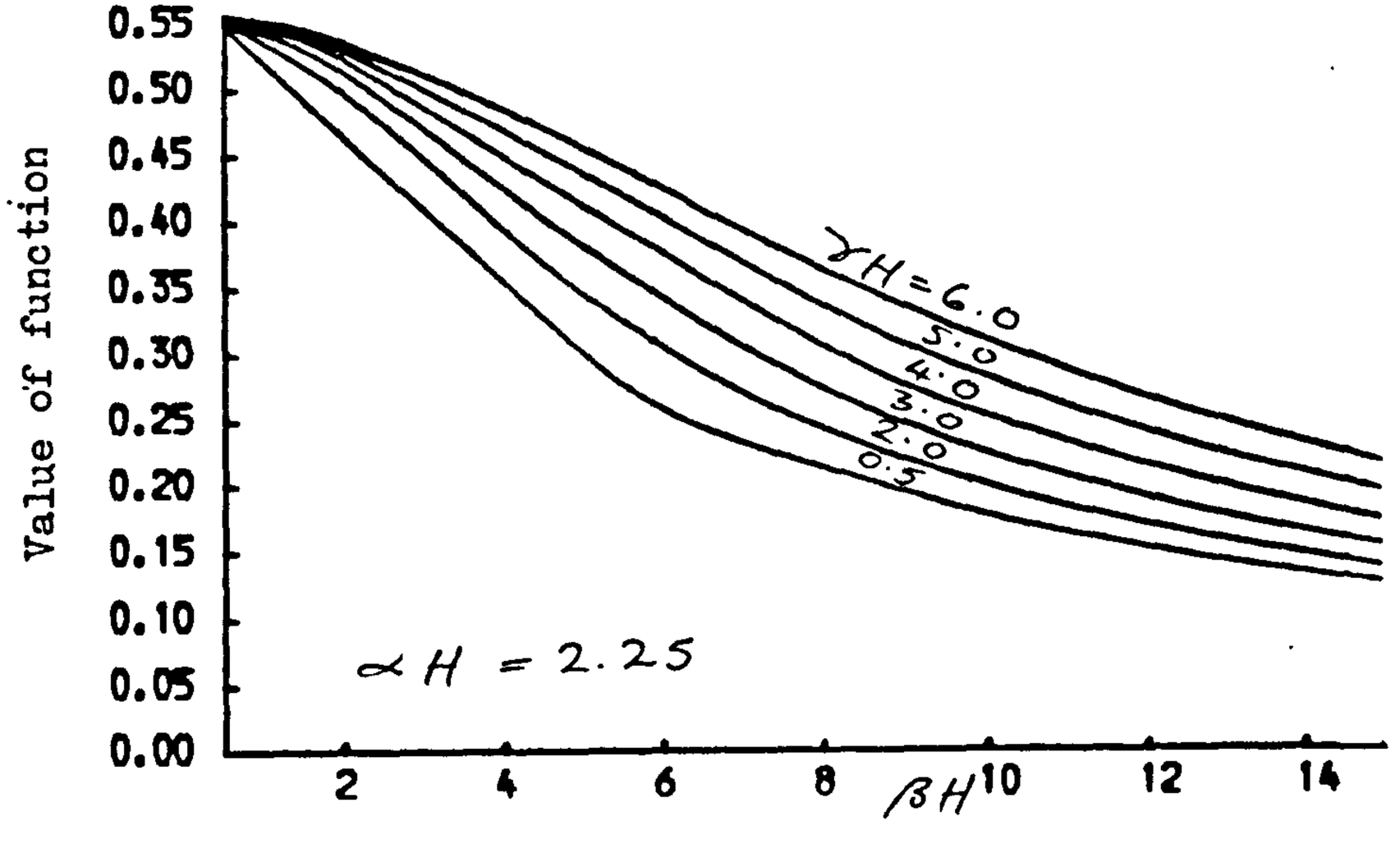

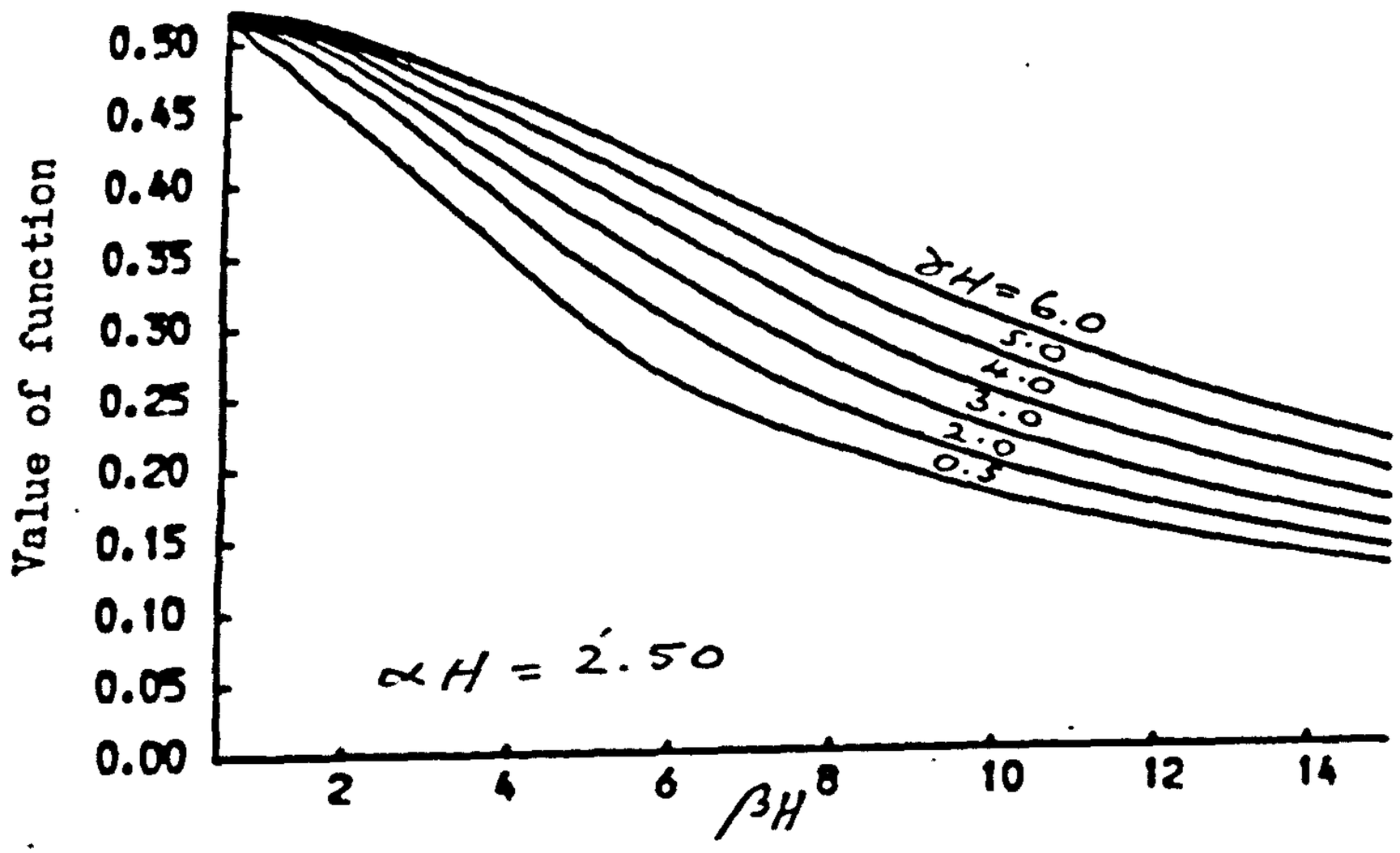

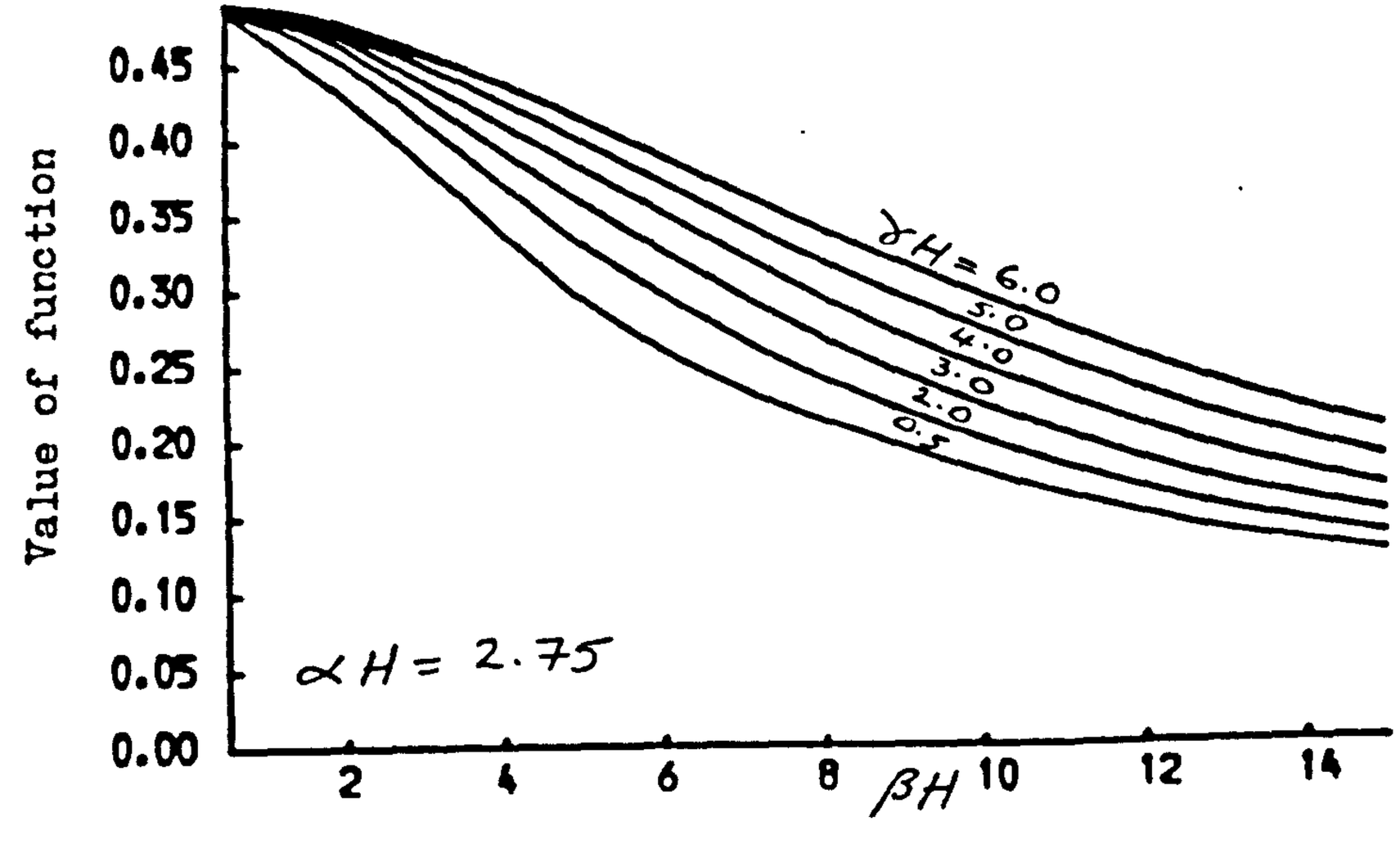

Fig. 2.11 Distributions of moment function F_3

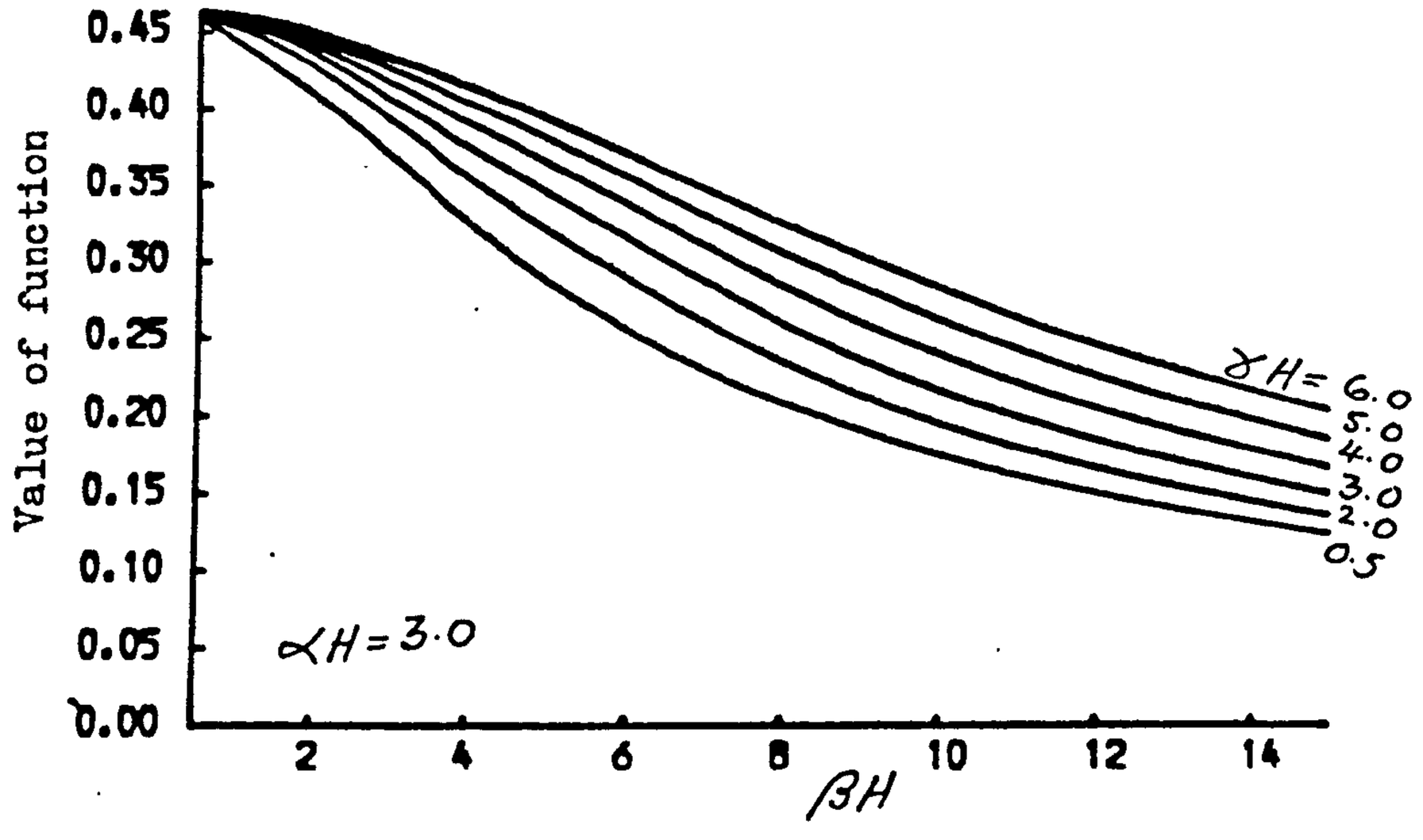

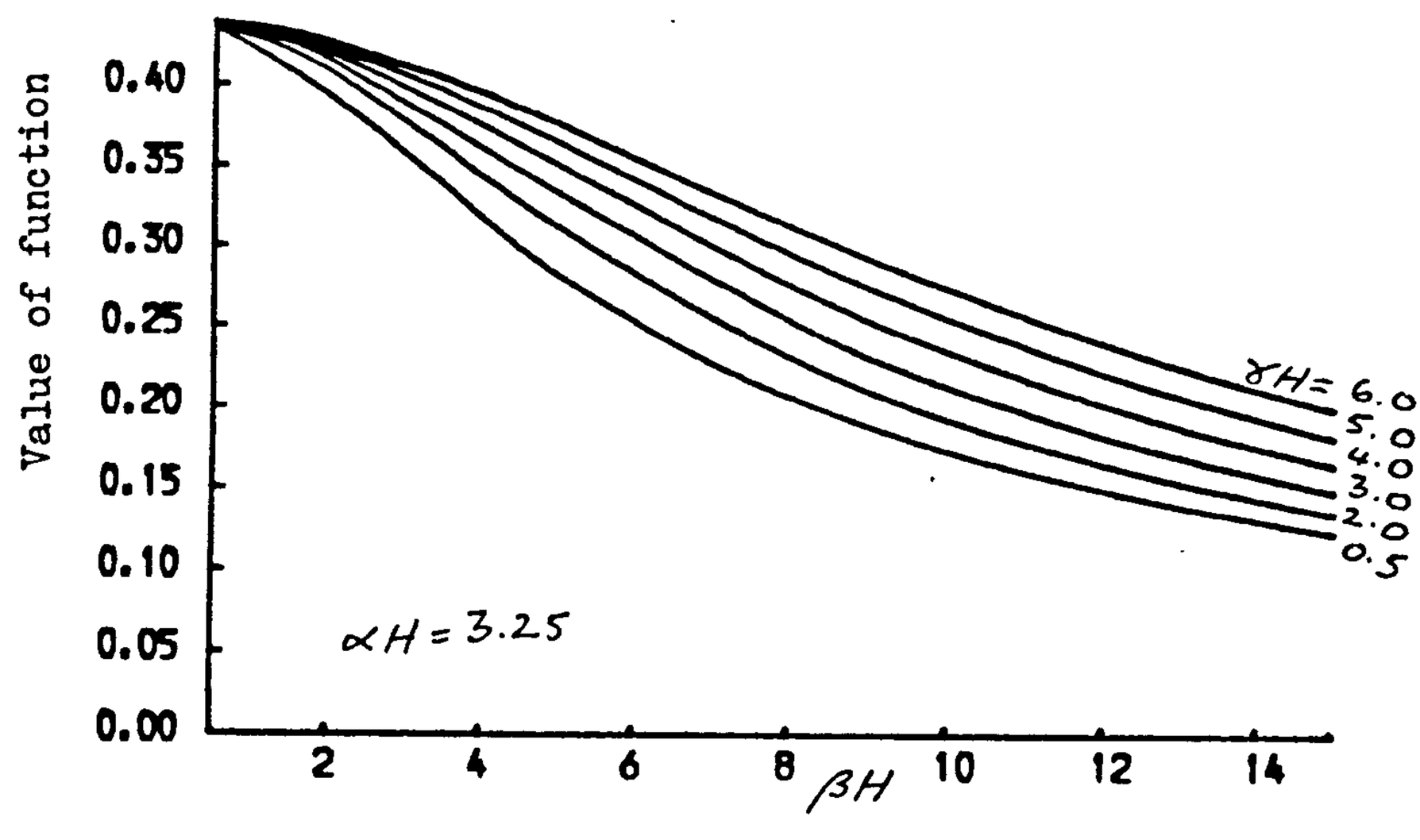

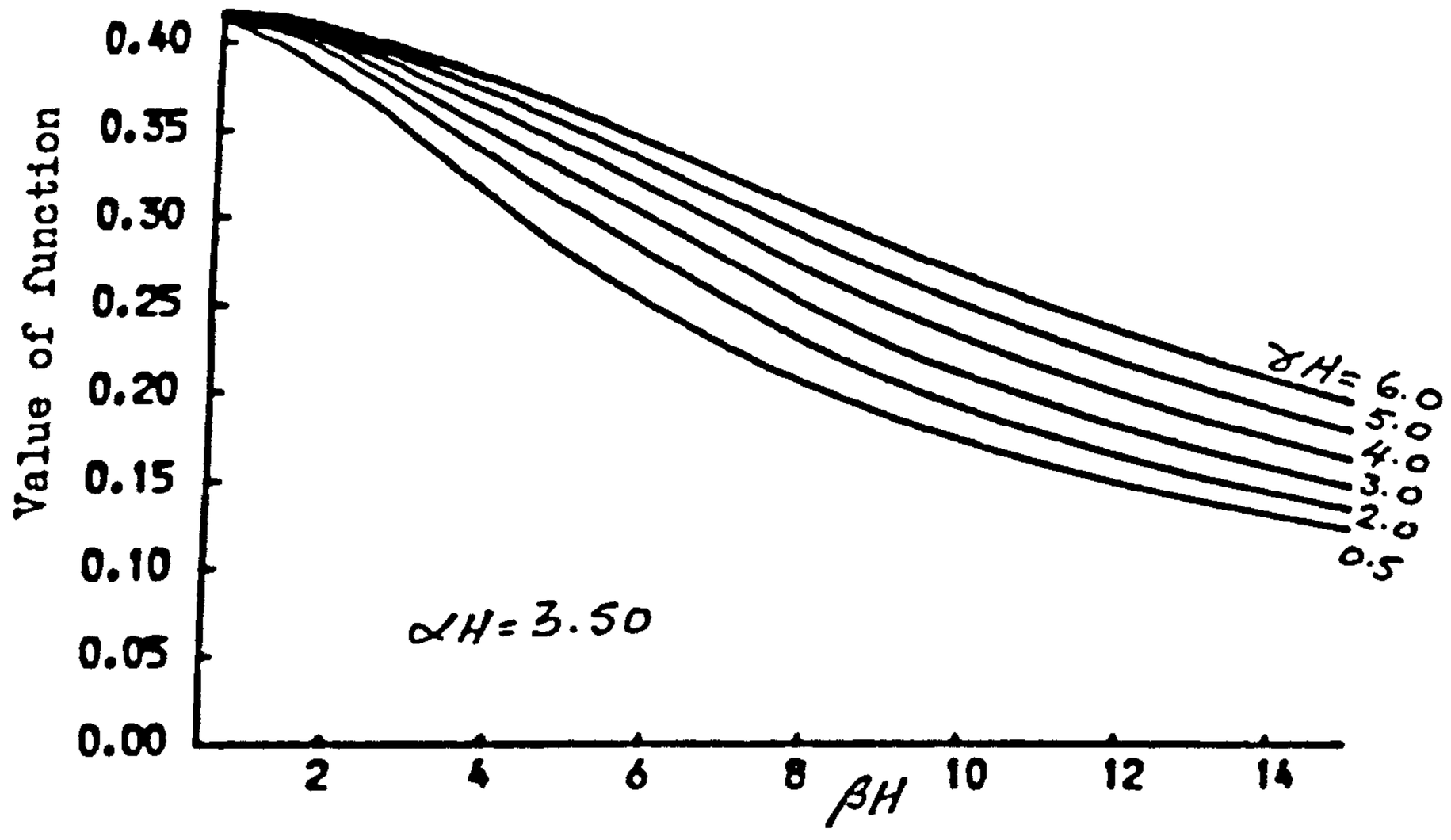

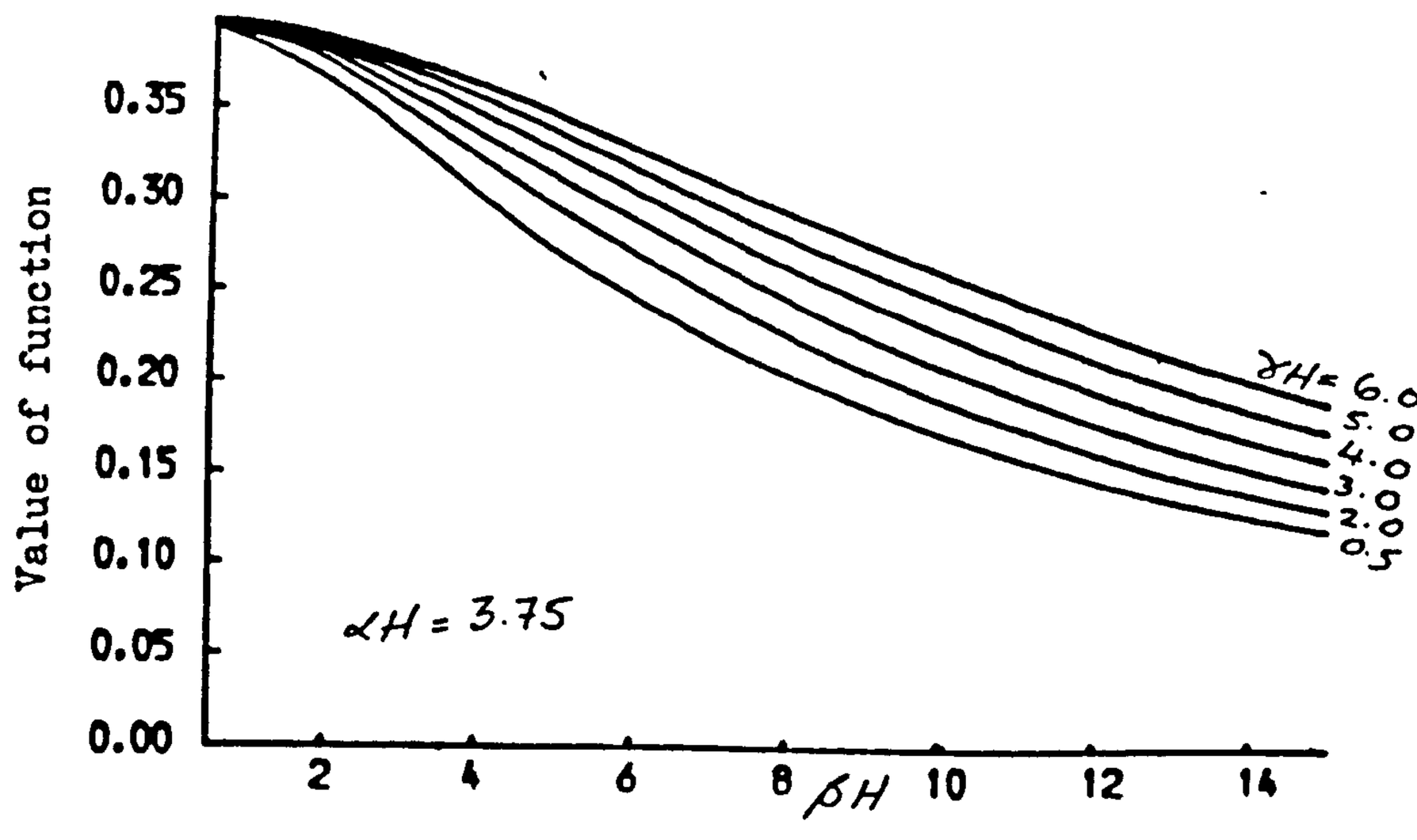

Fig. 2.12 Distributions of moment function F_3

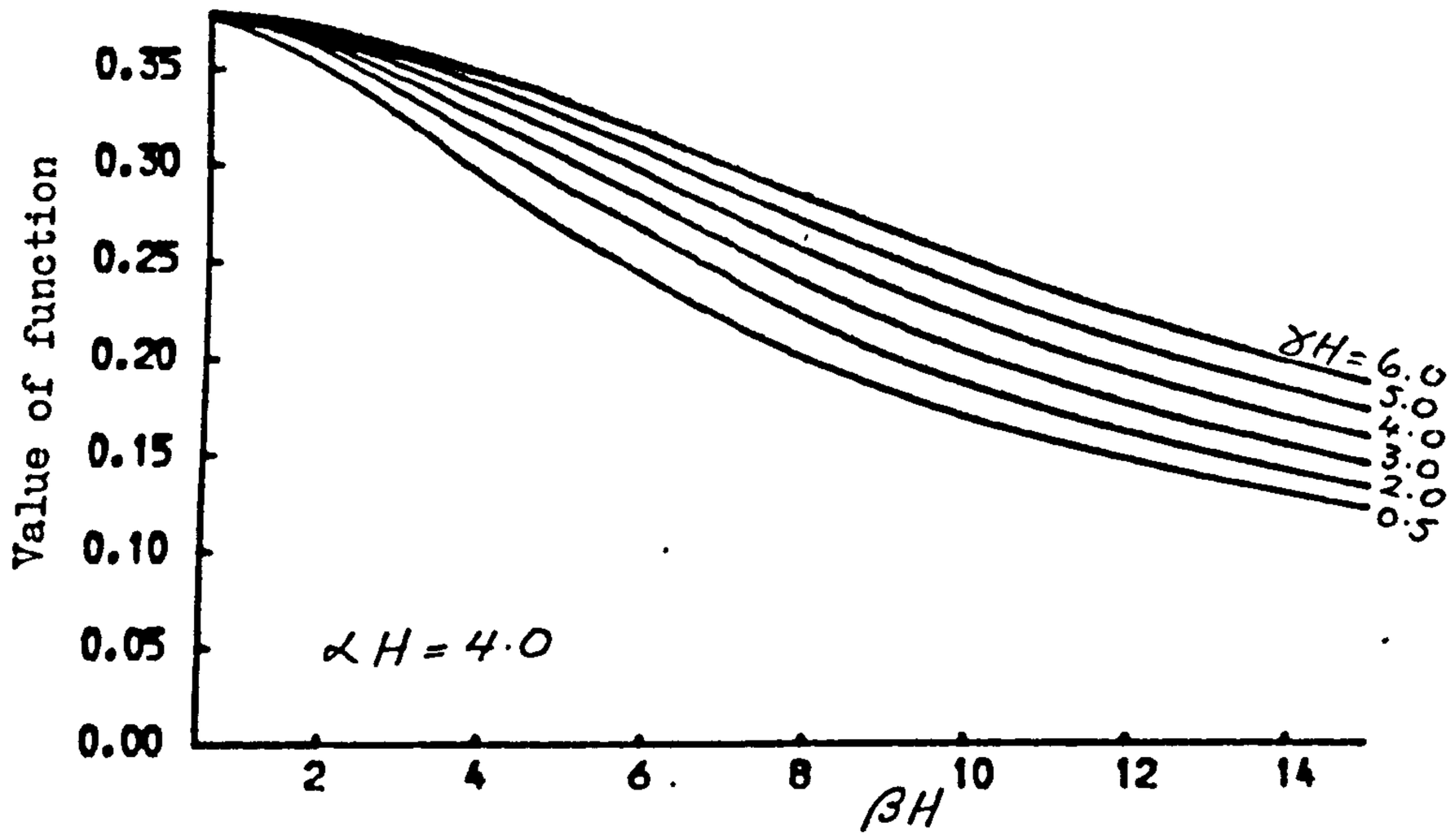

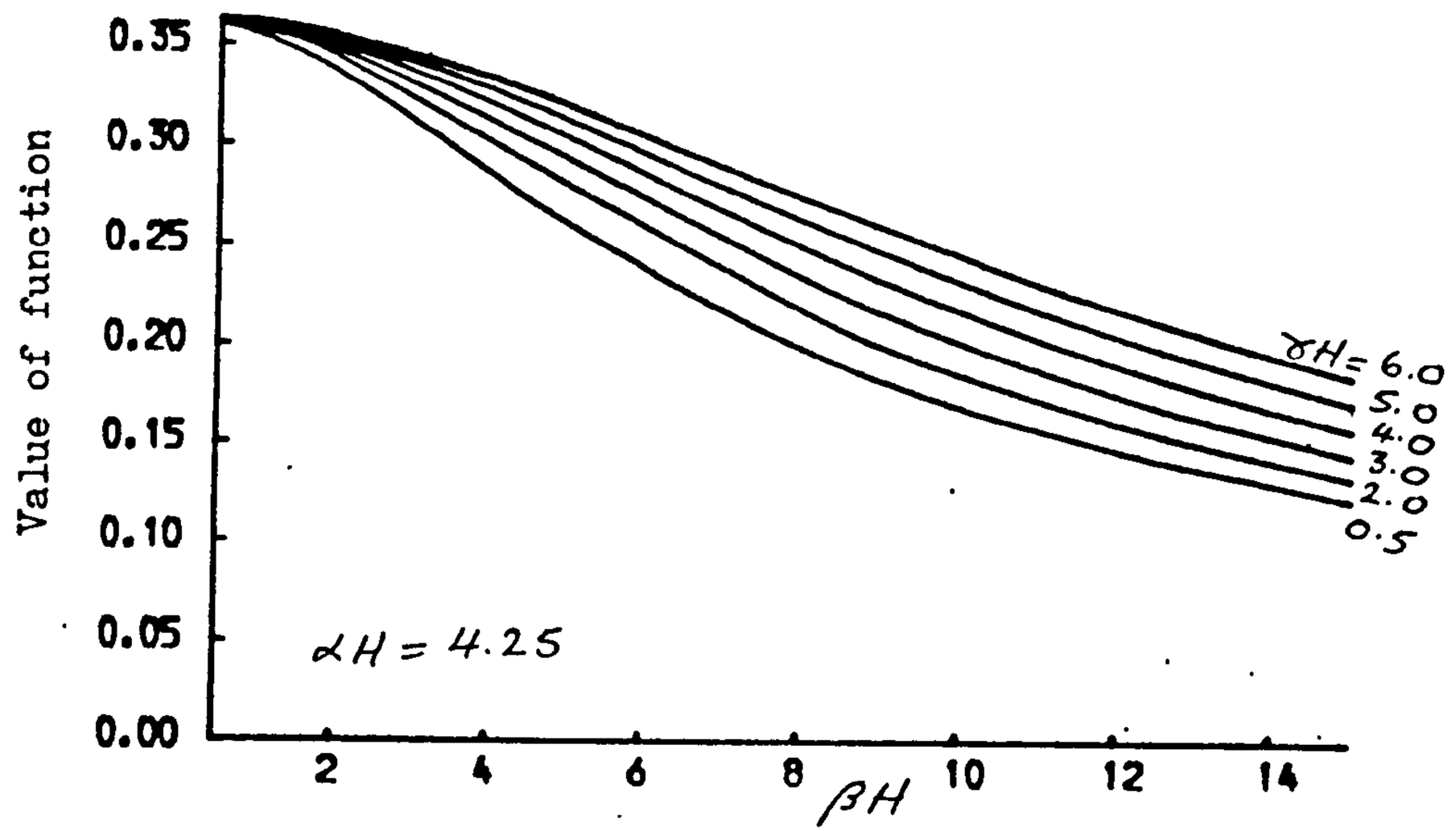

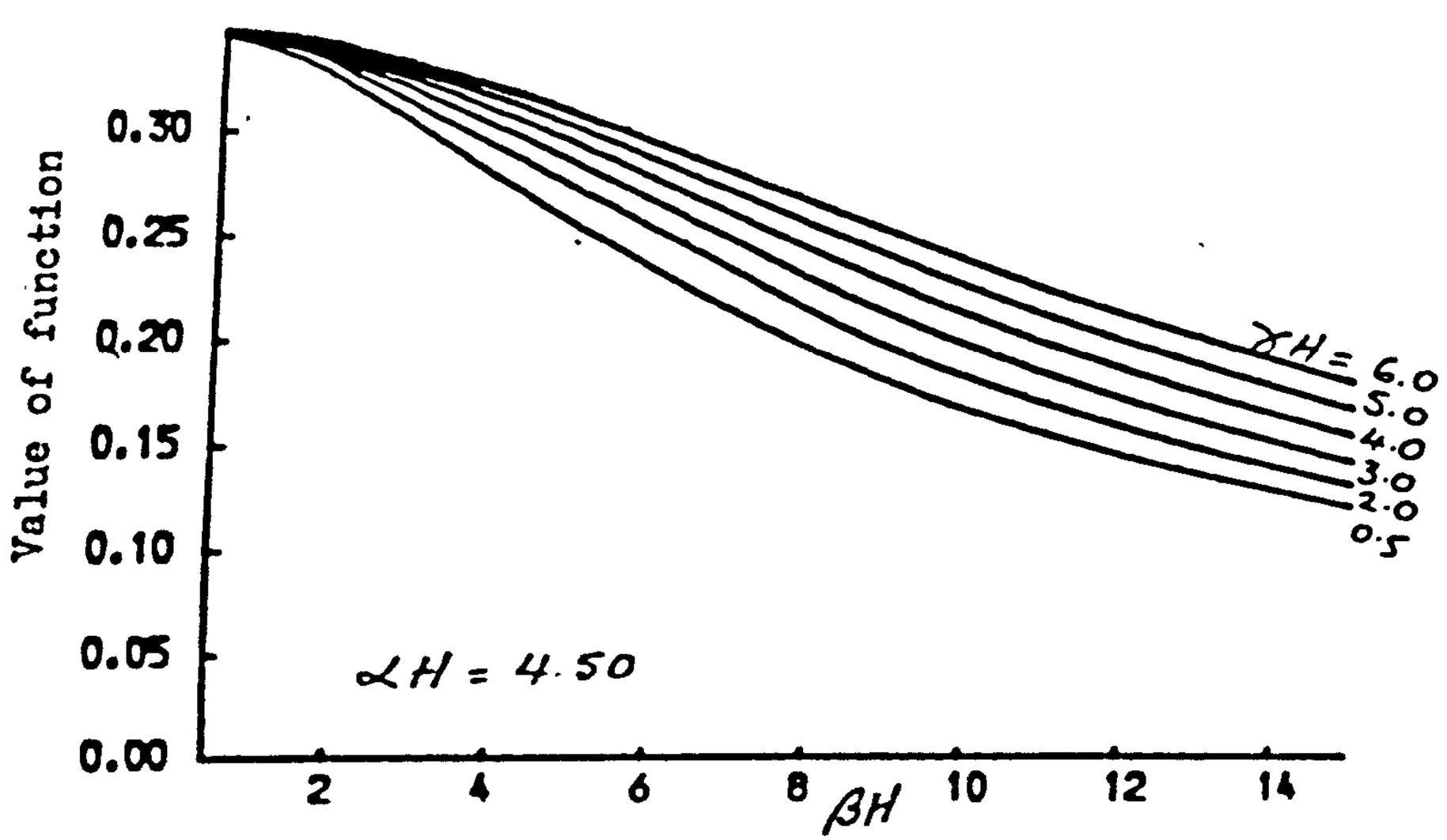

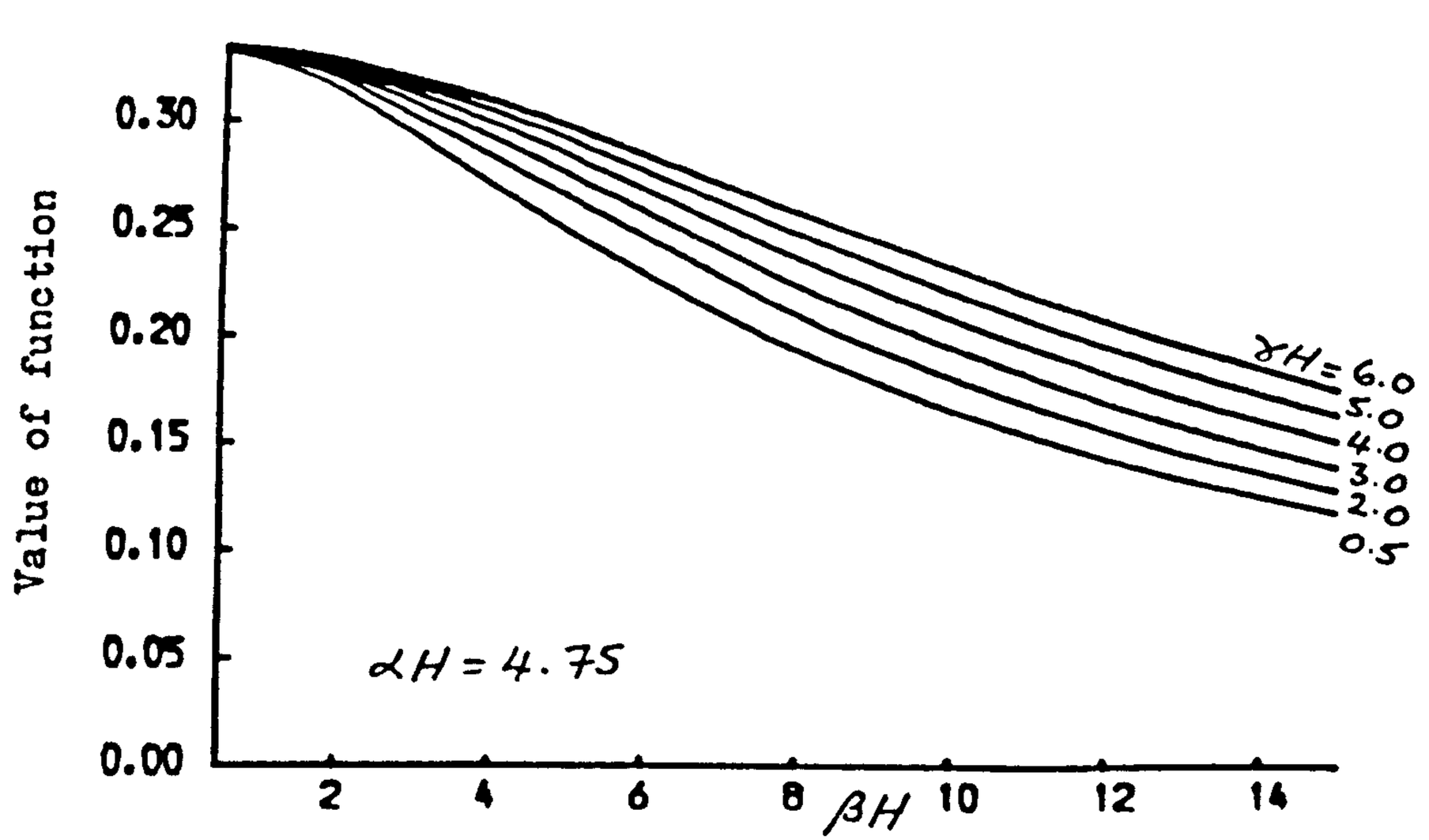

Fig. 2.13 Distributions of moment function F_3

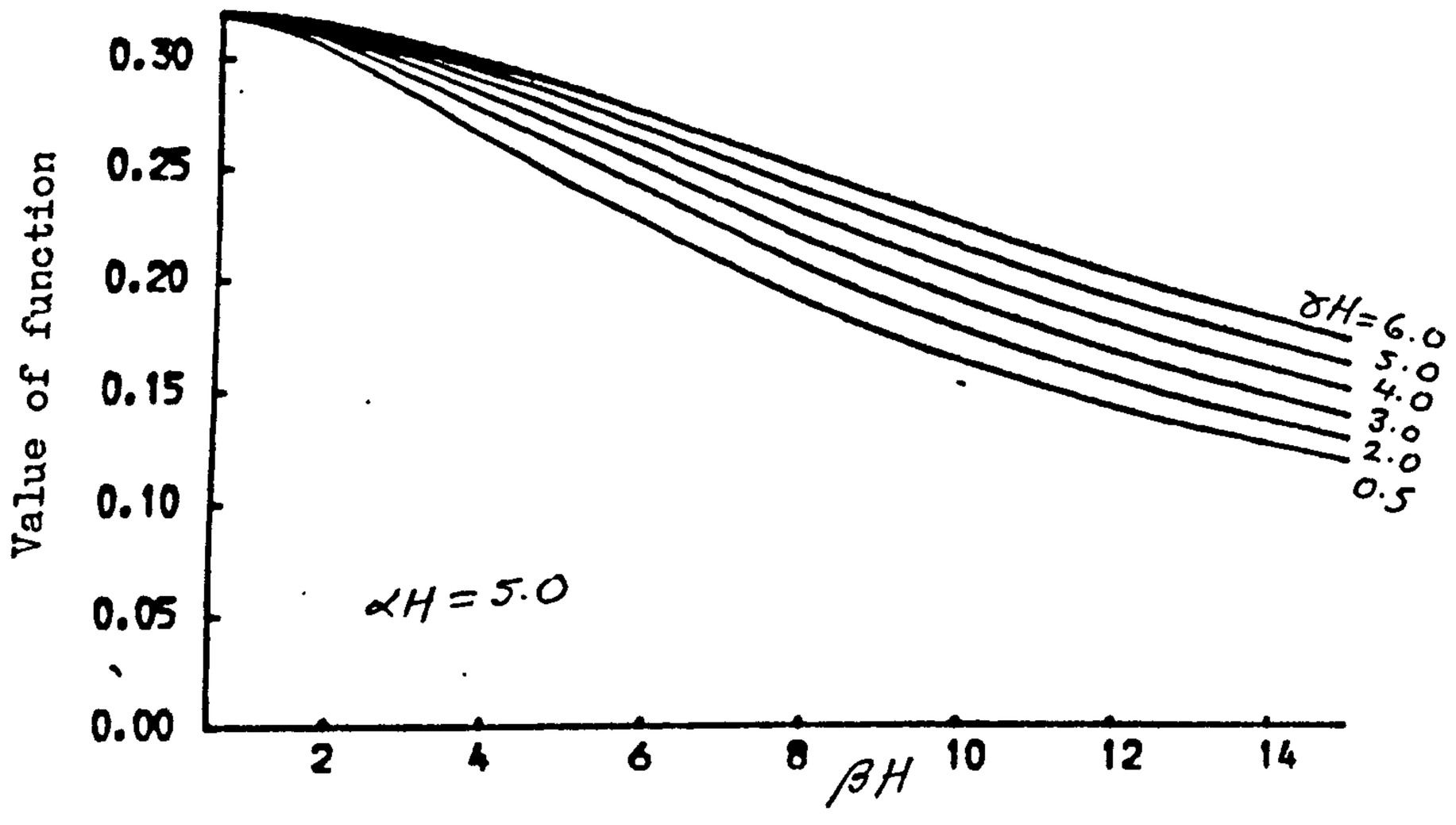

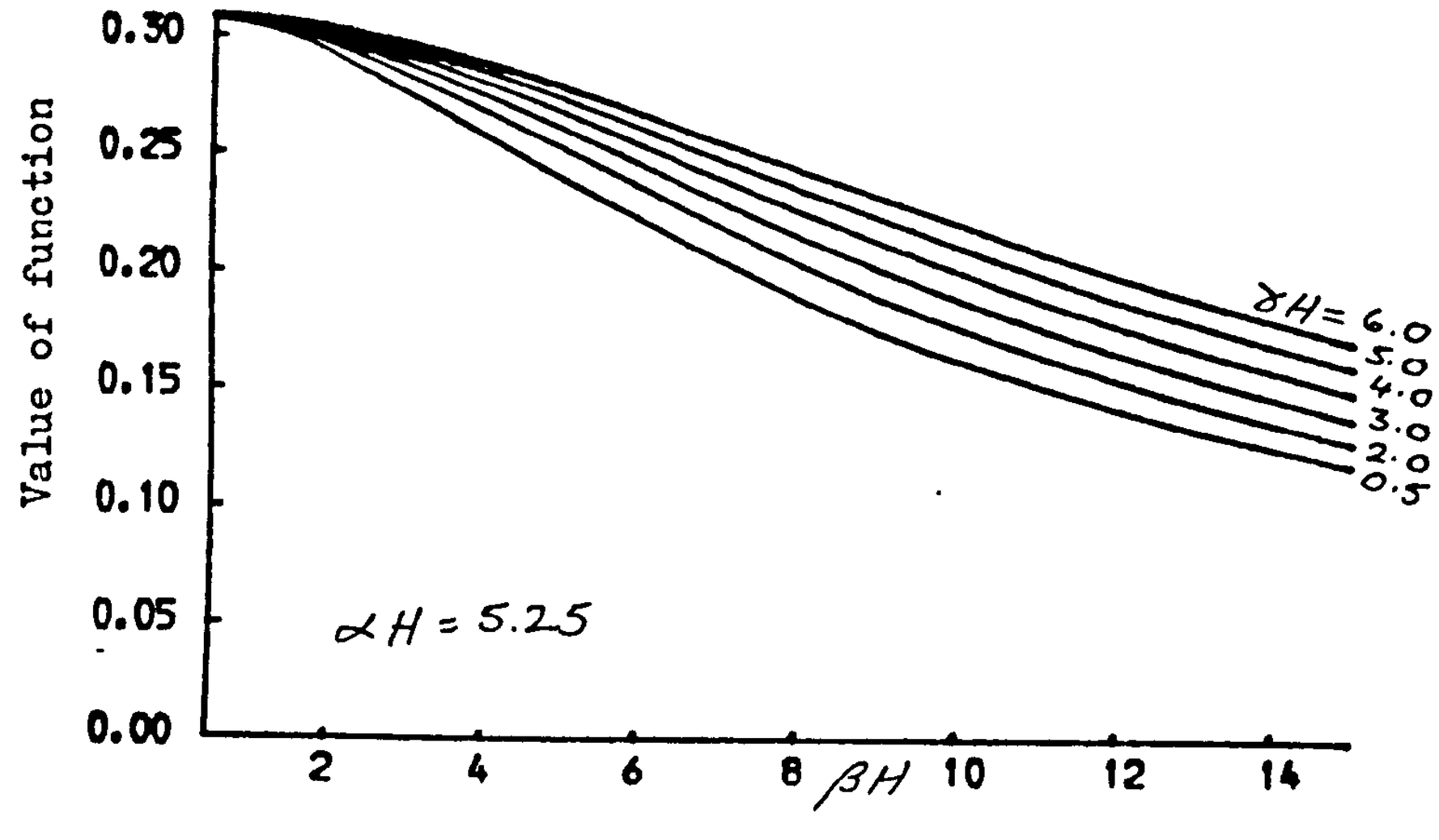

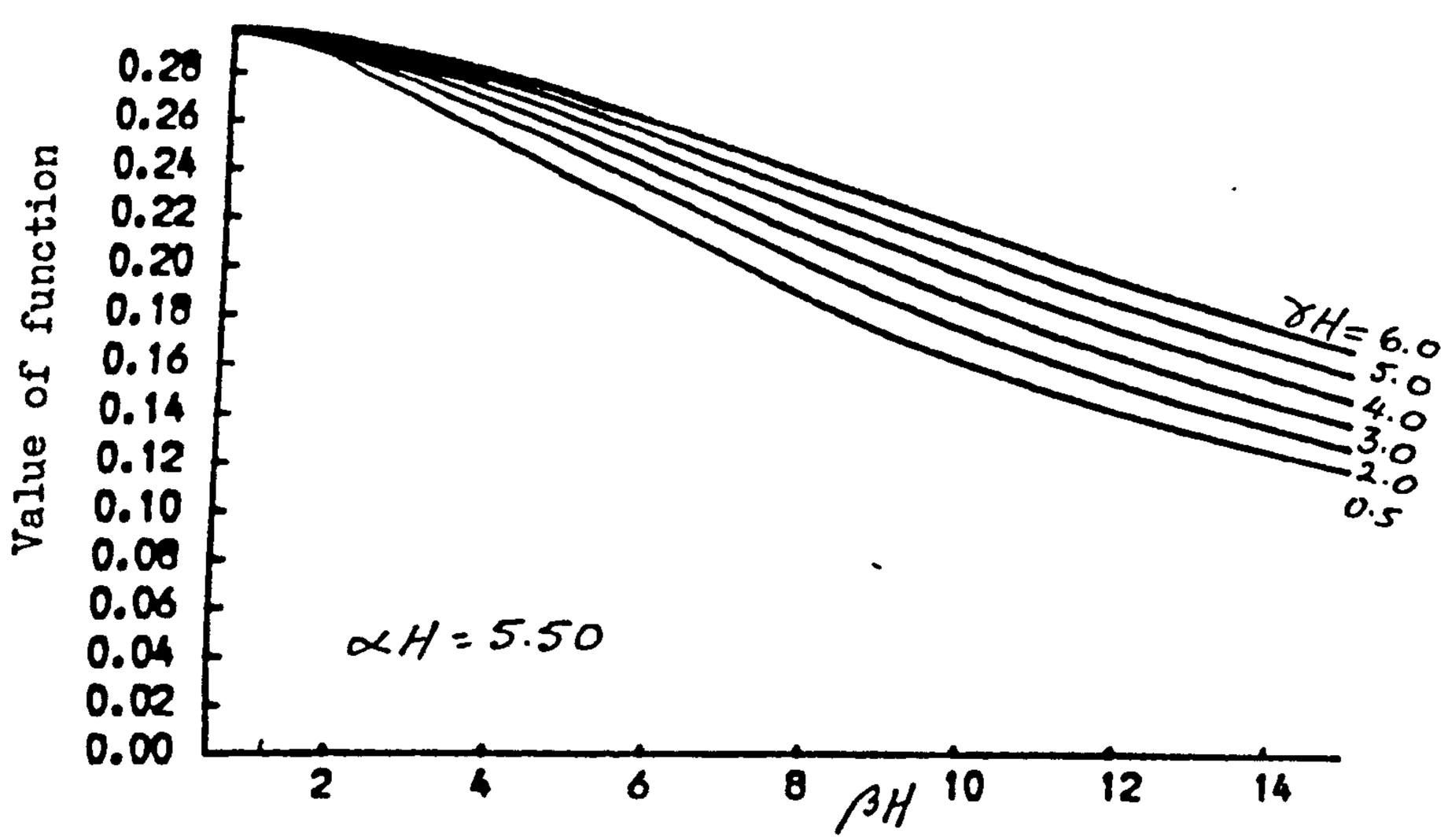

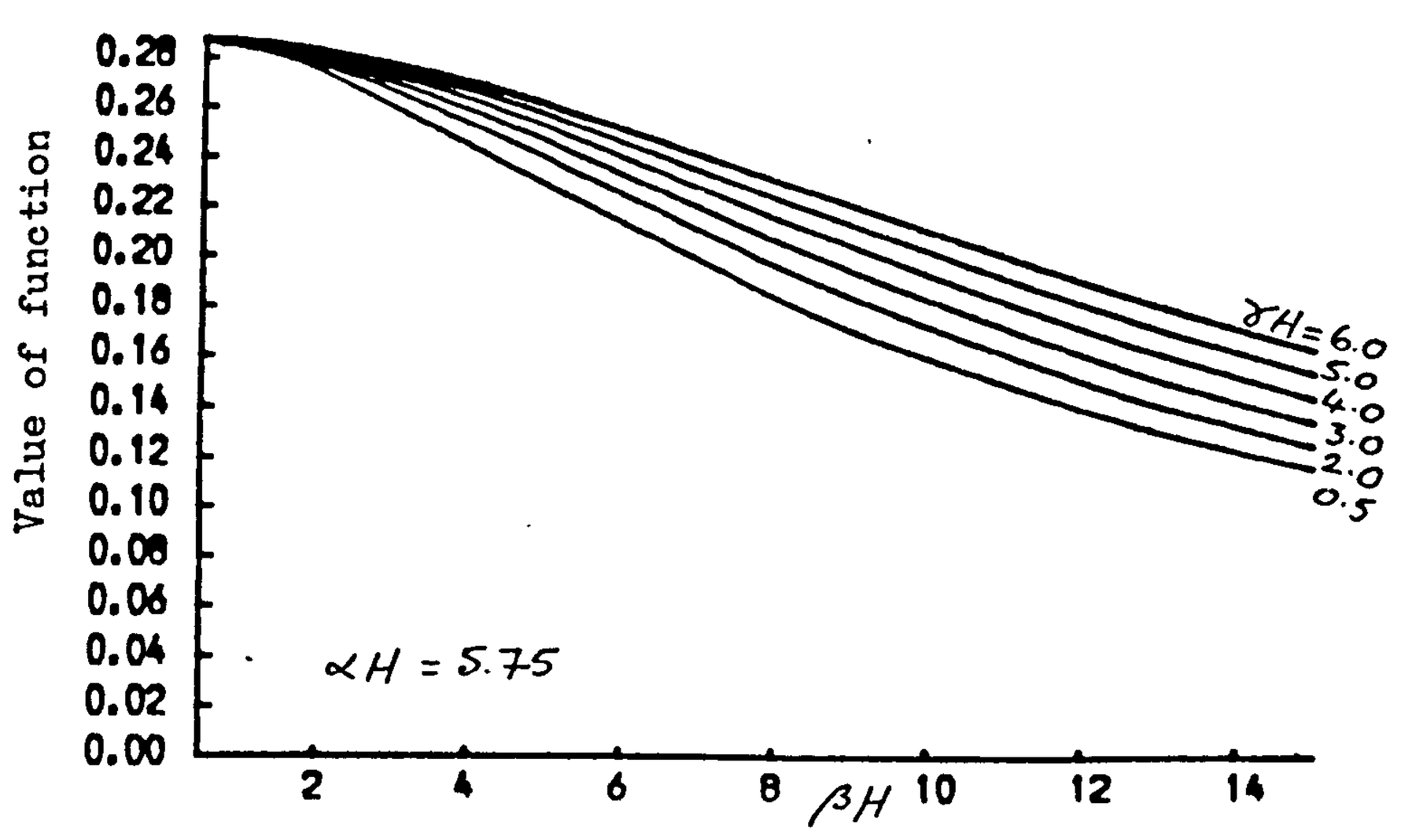

Fig. 2.14 Distributions of moment function F_3

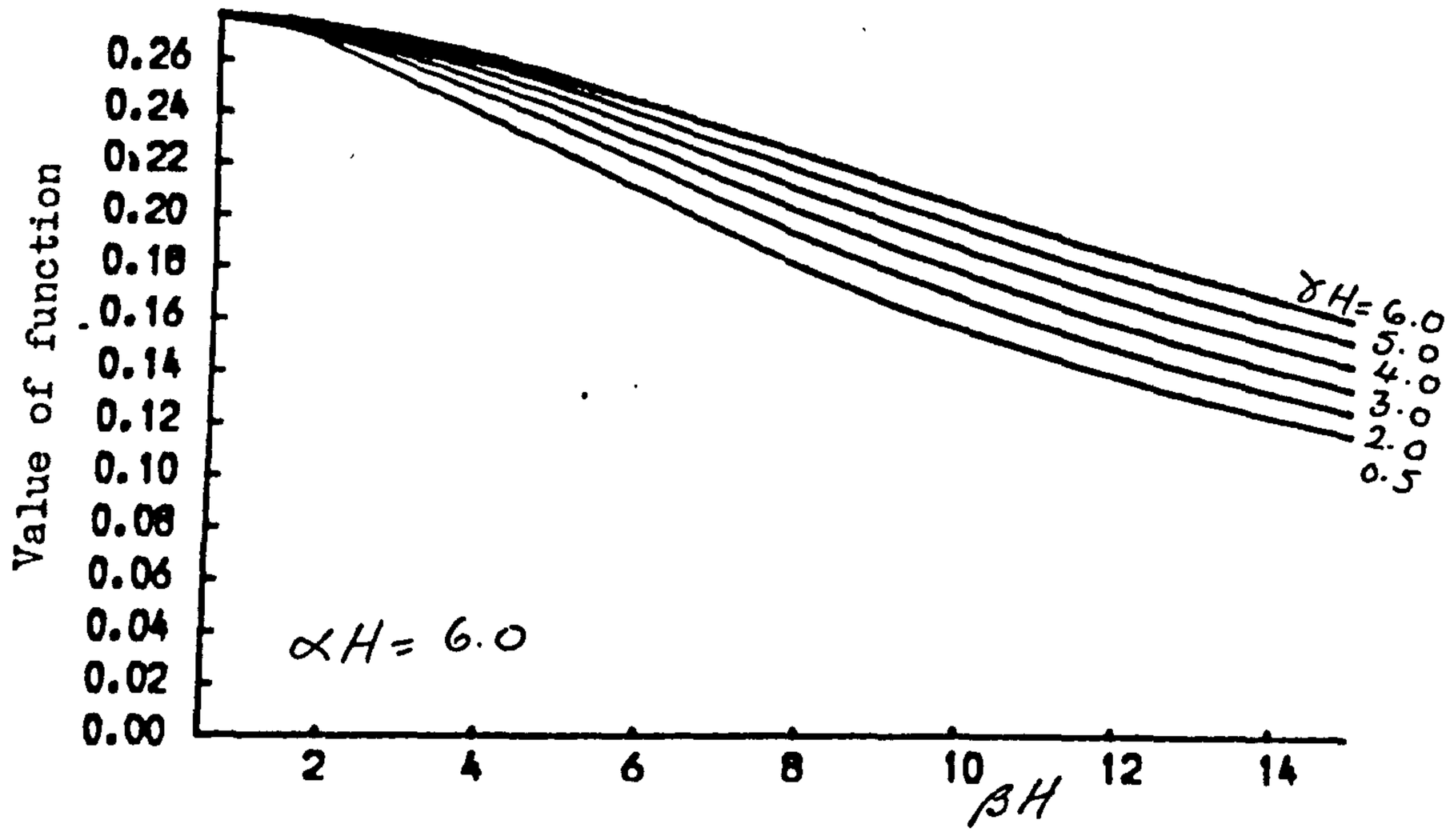

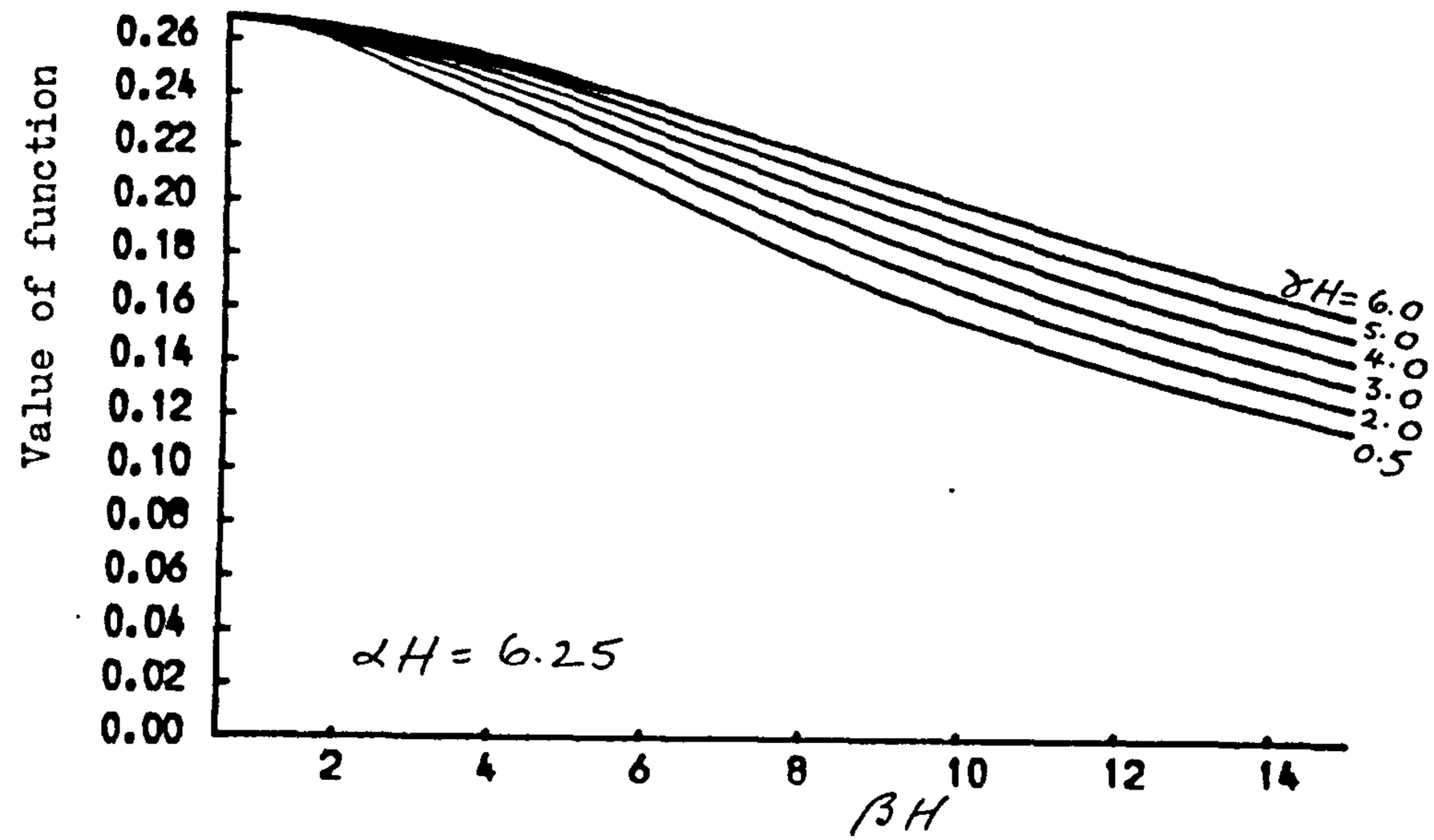

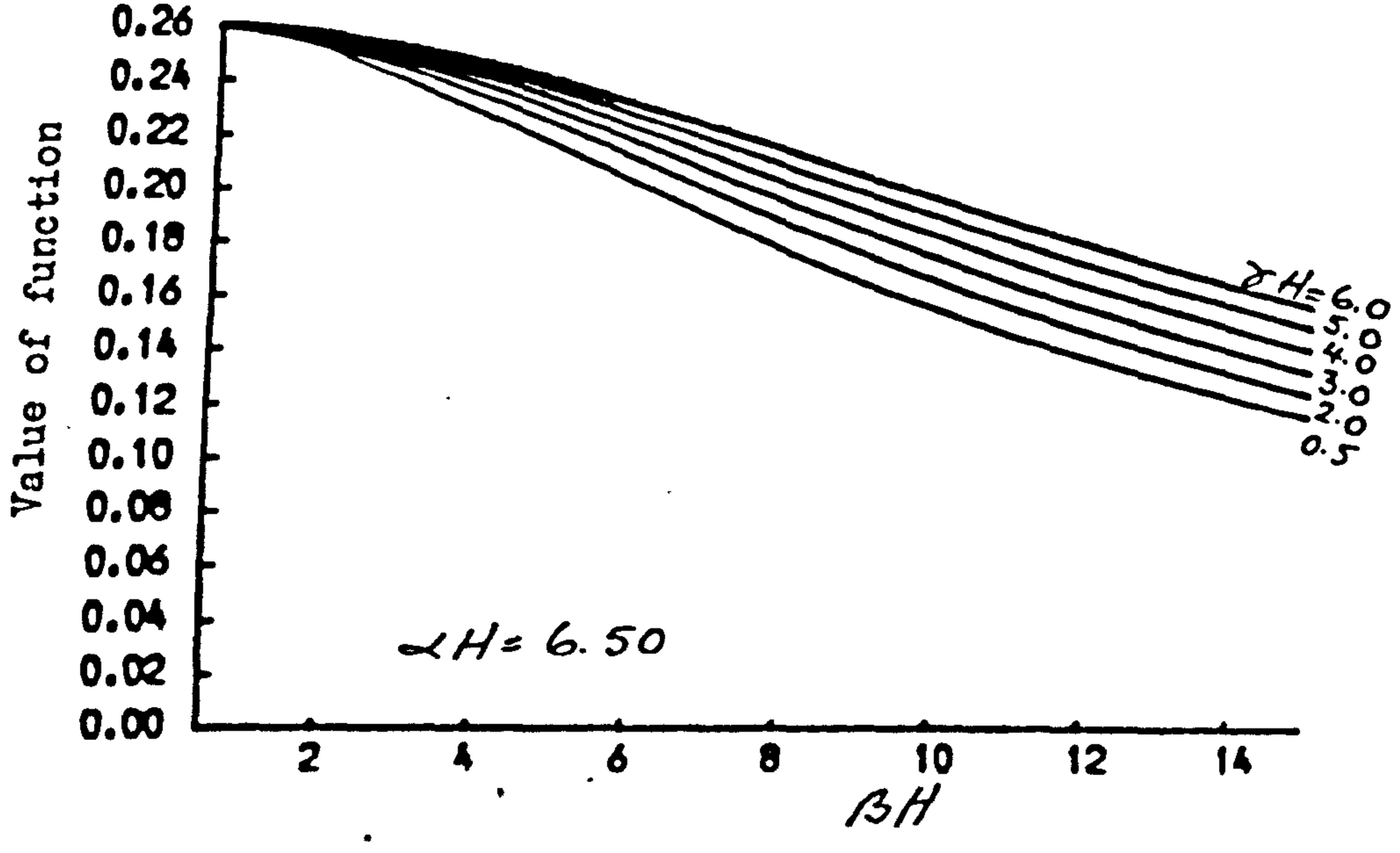

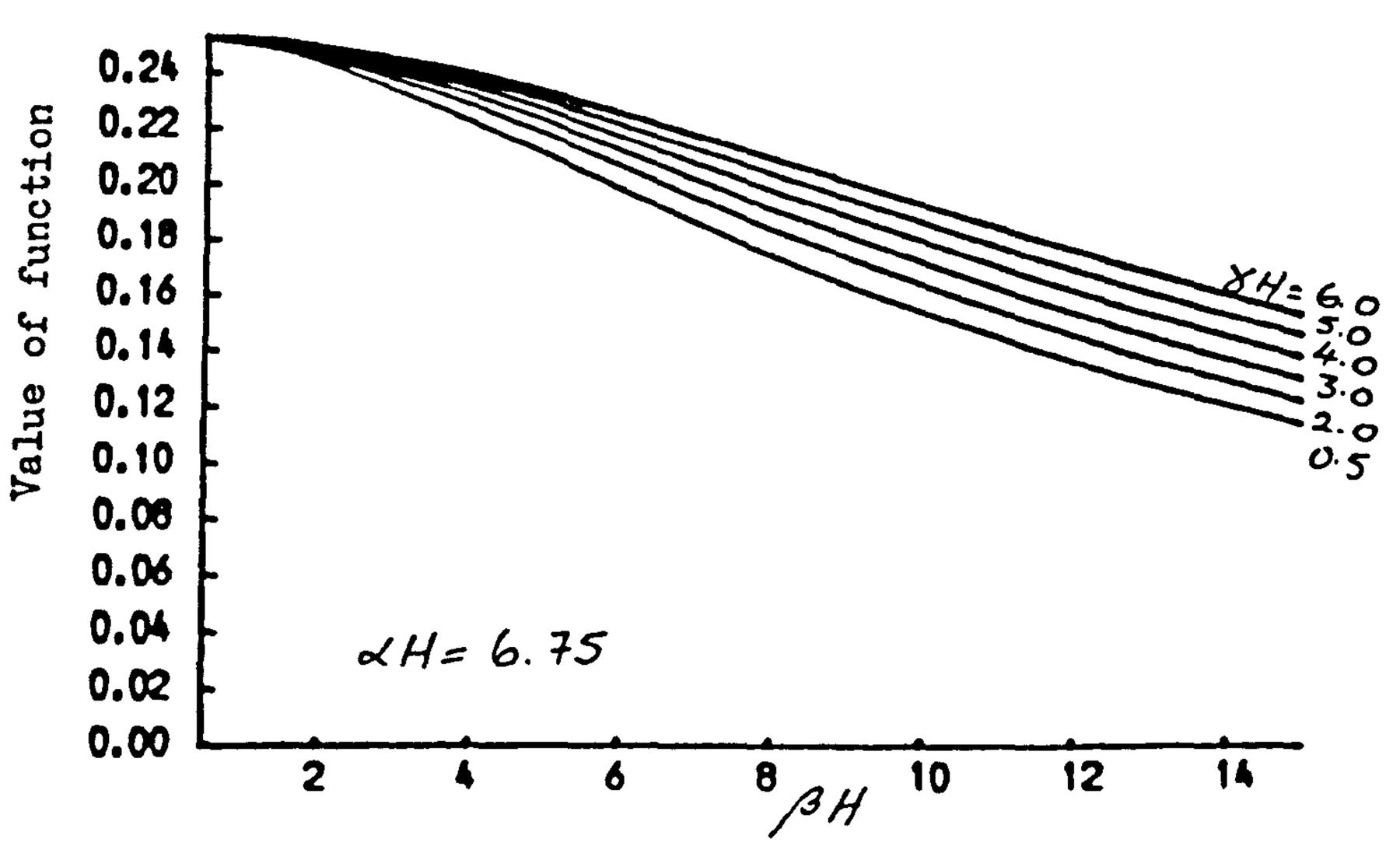

Fig. 2.15 Distributions of moment function F_3

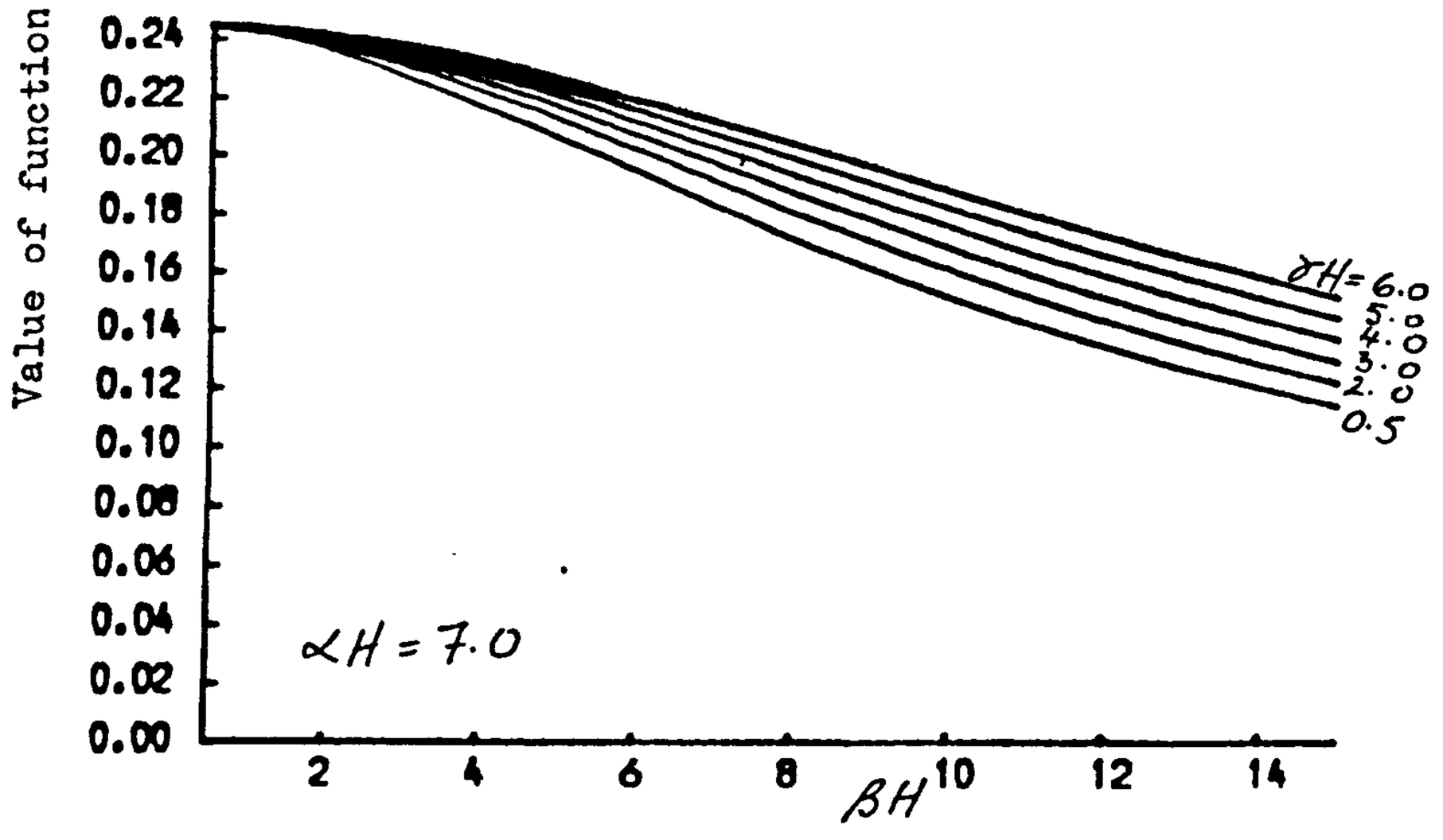

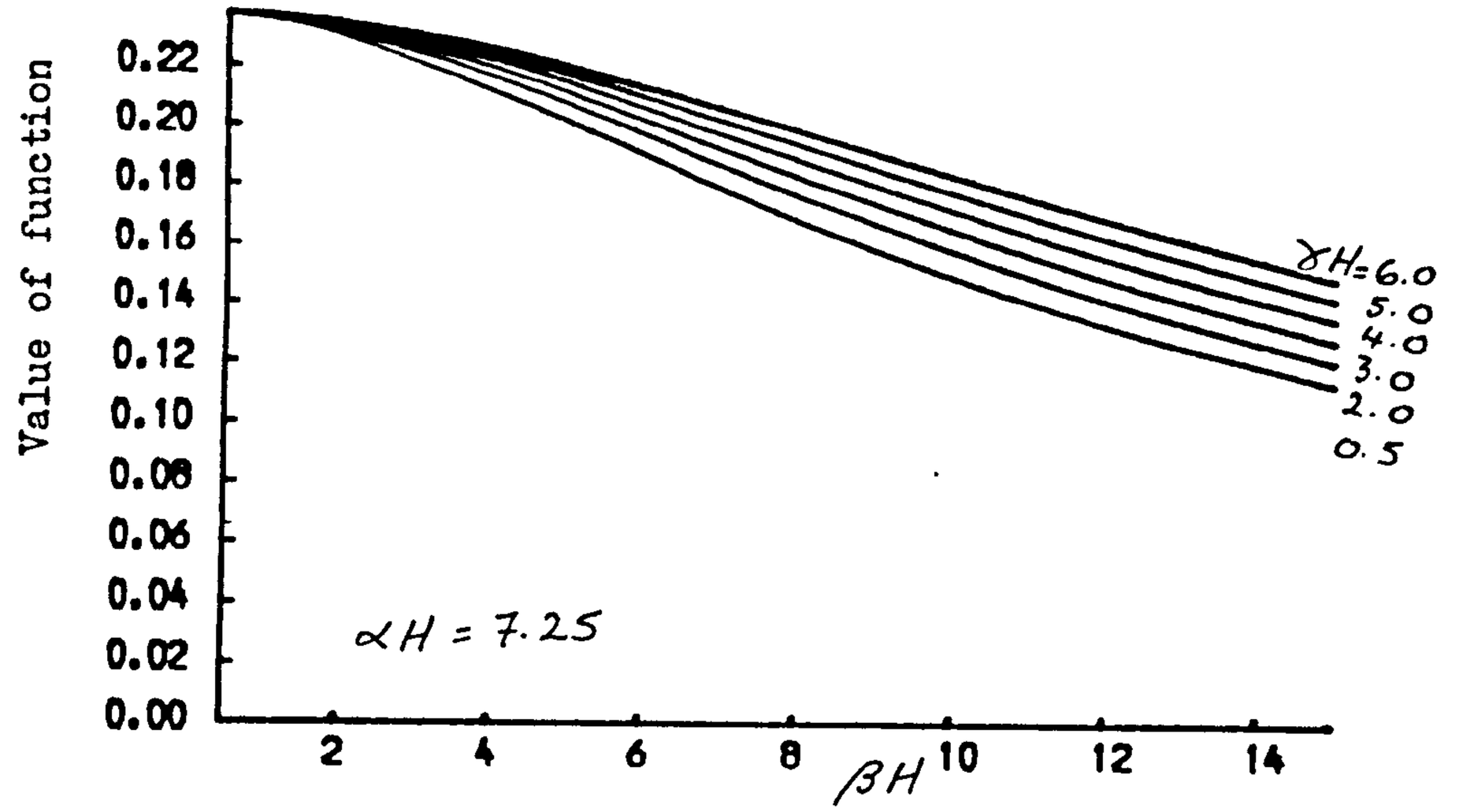

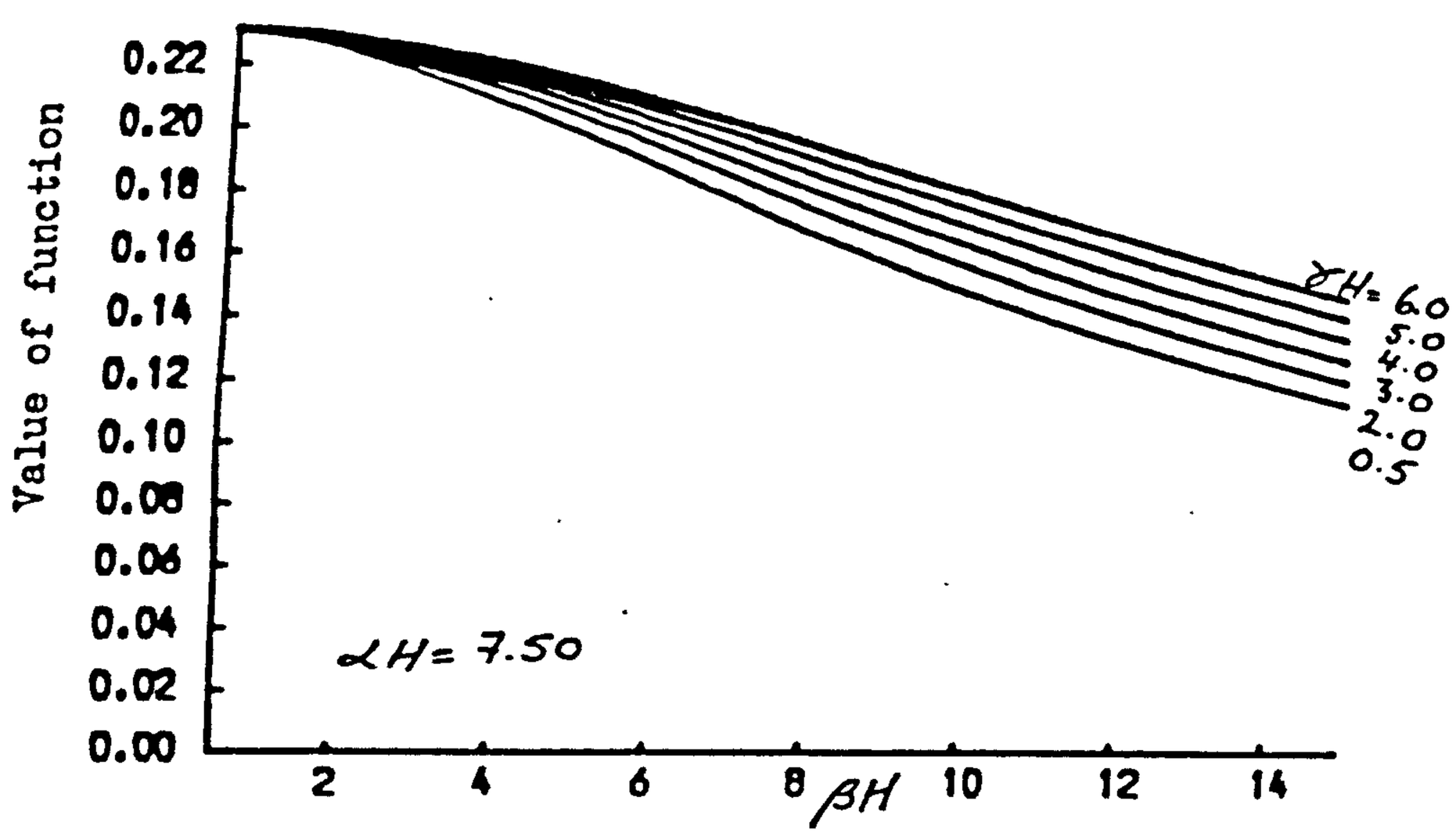

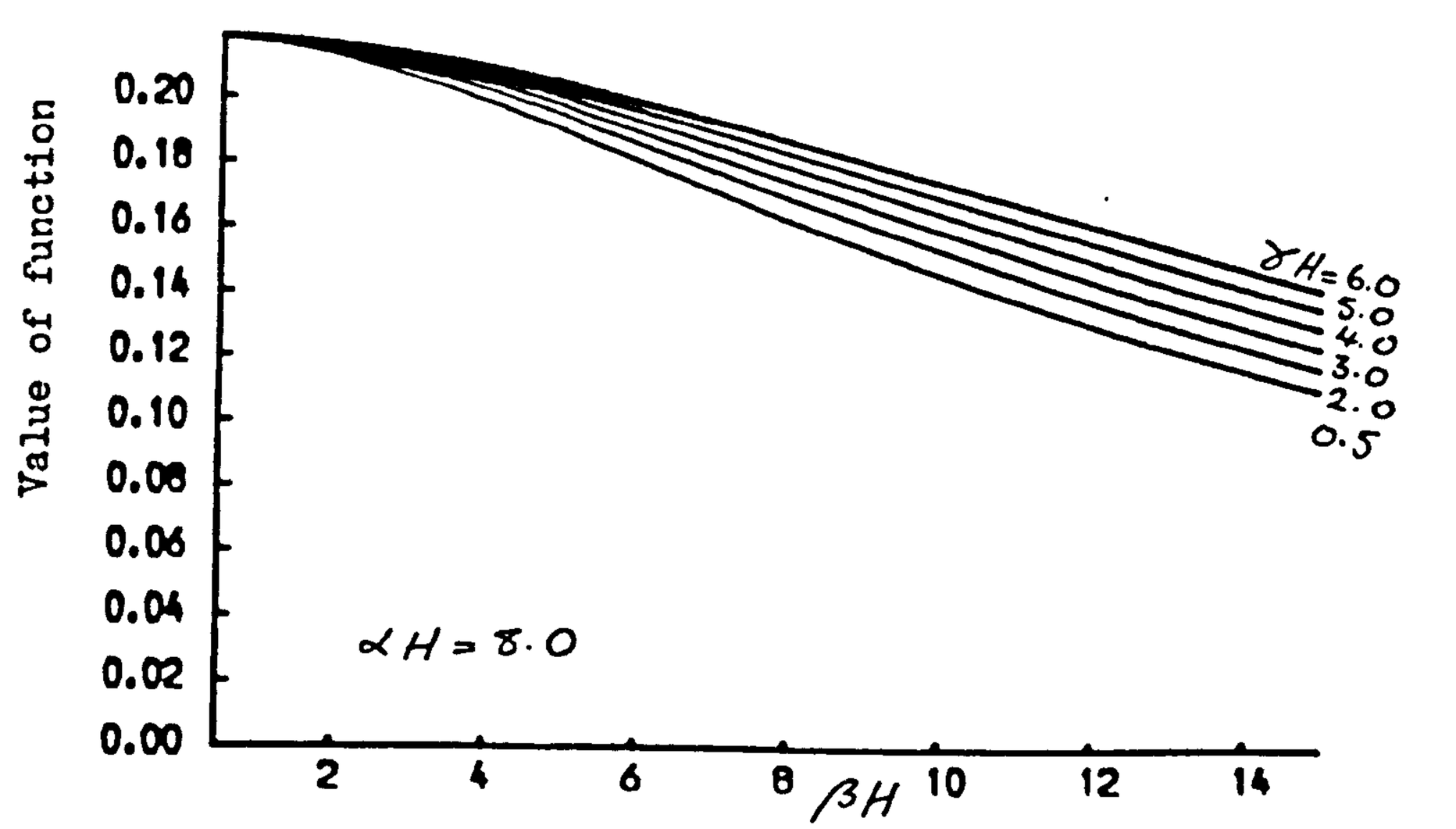

Fig.2.16 Distributions of moment function F_3

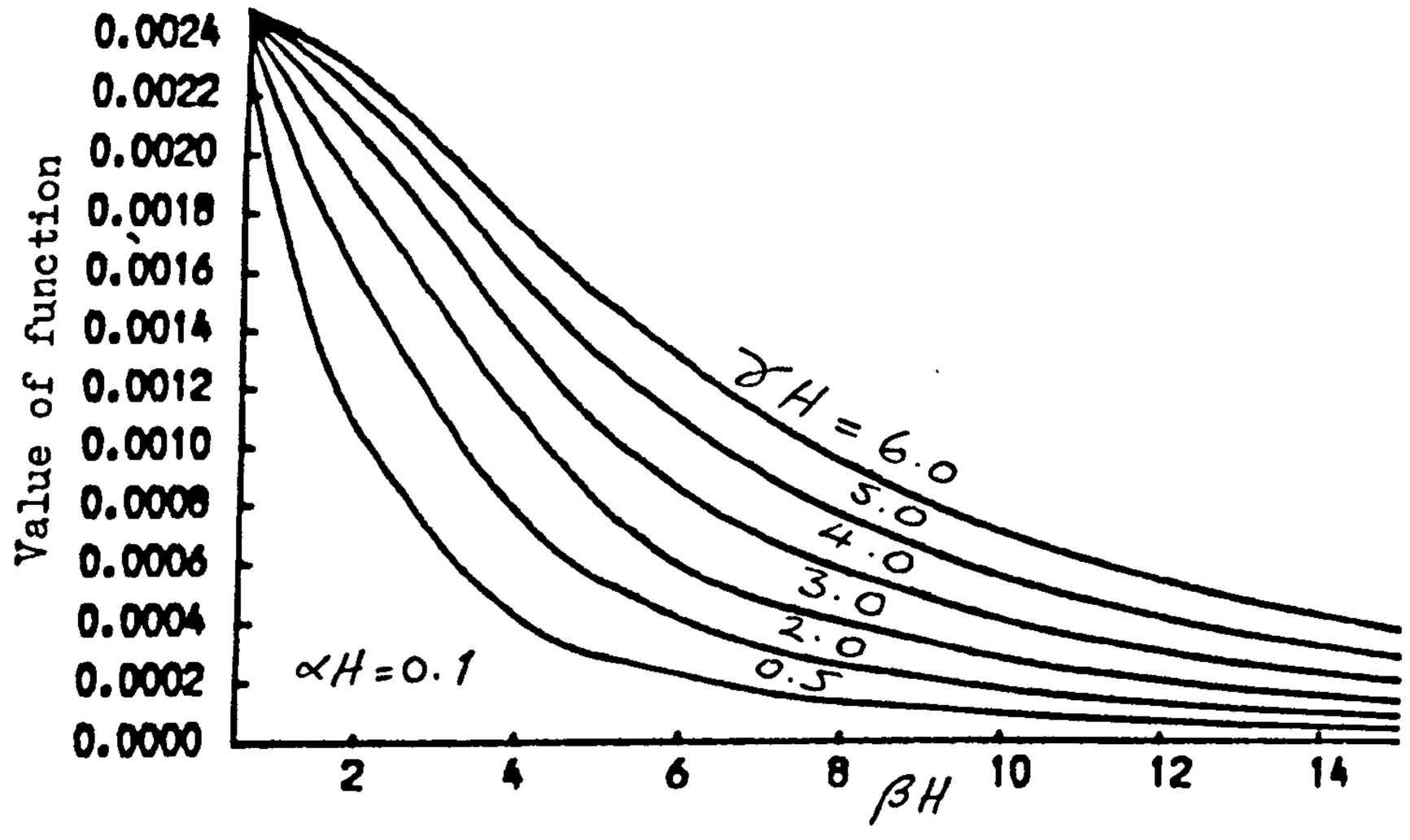

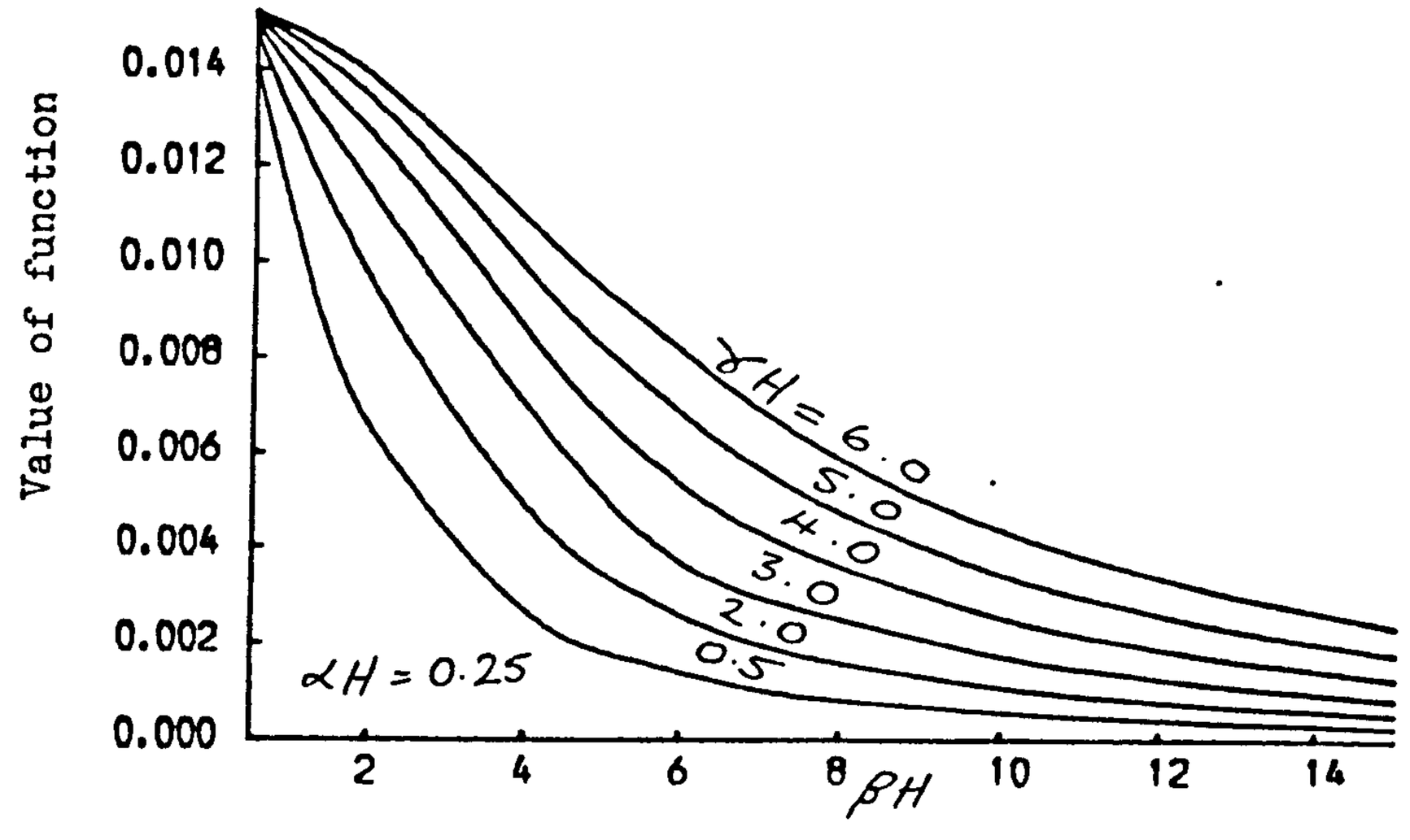

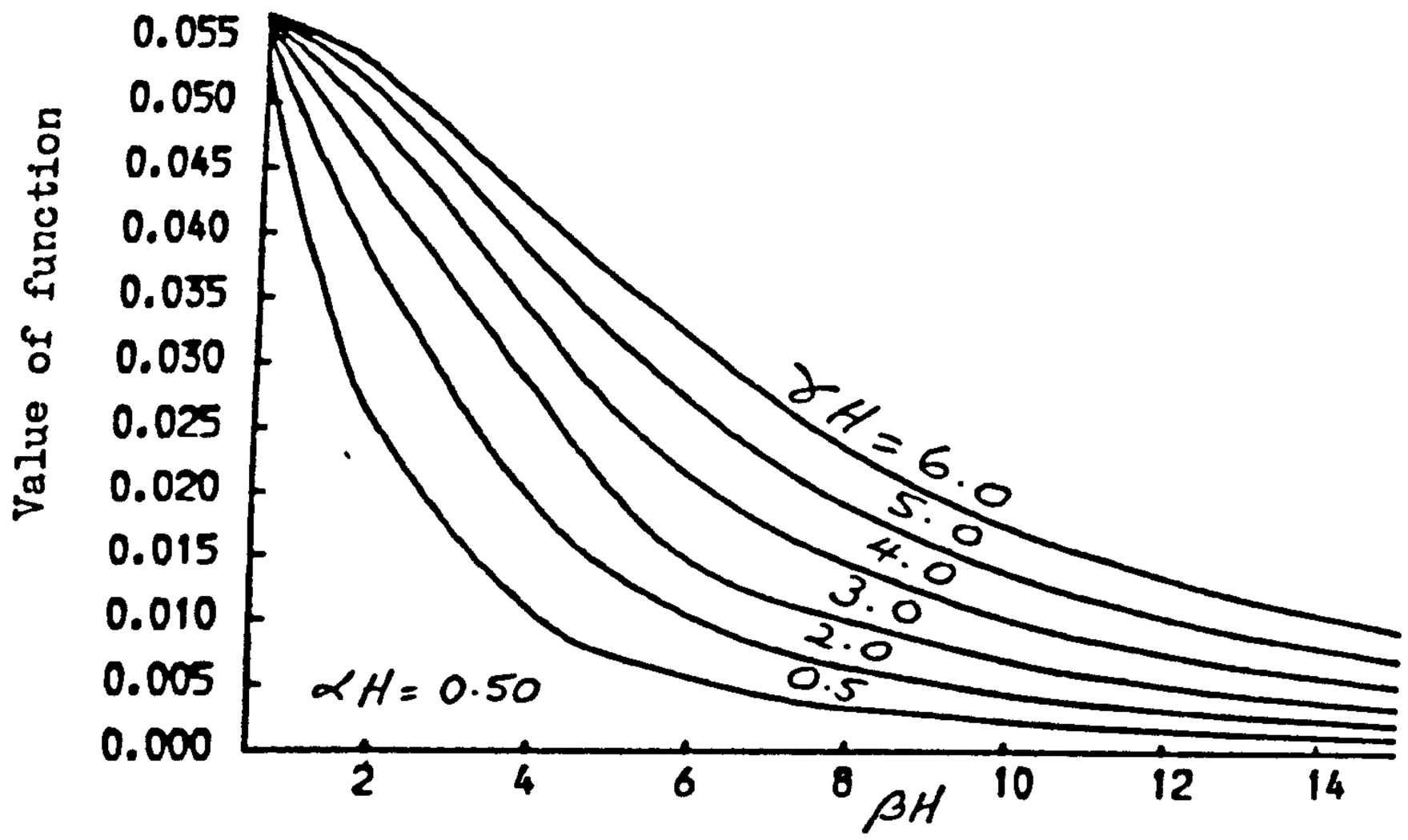

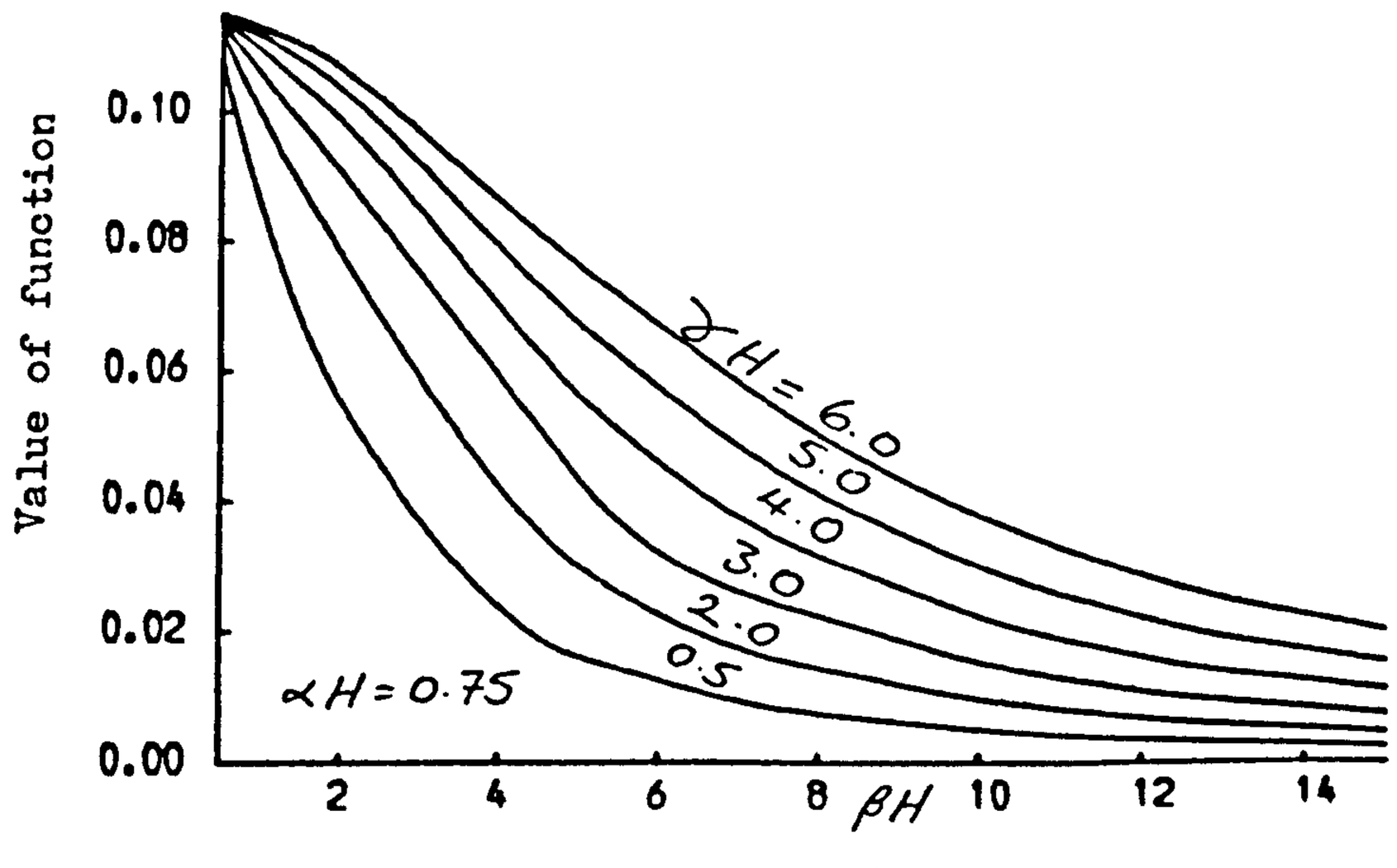

Fig. 2.17 Distributions of moment function F_4

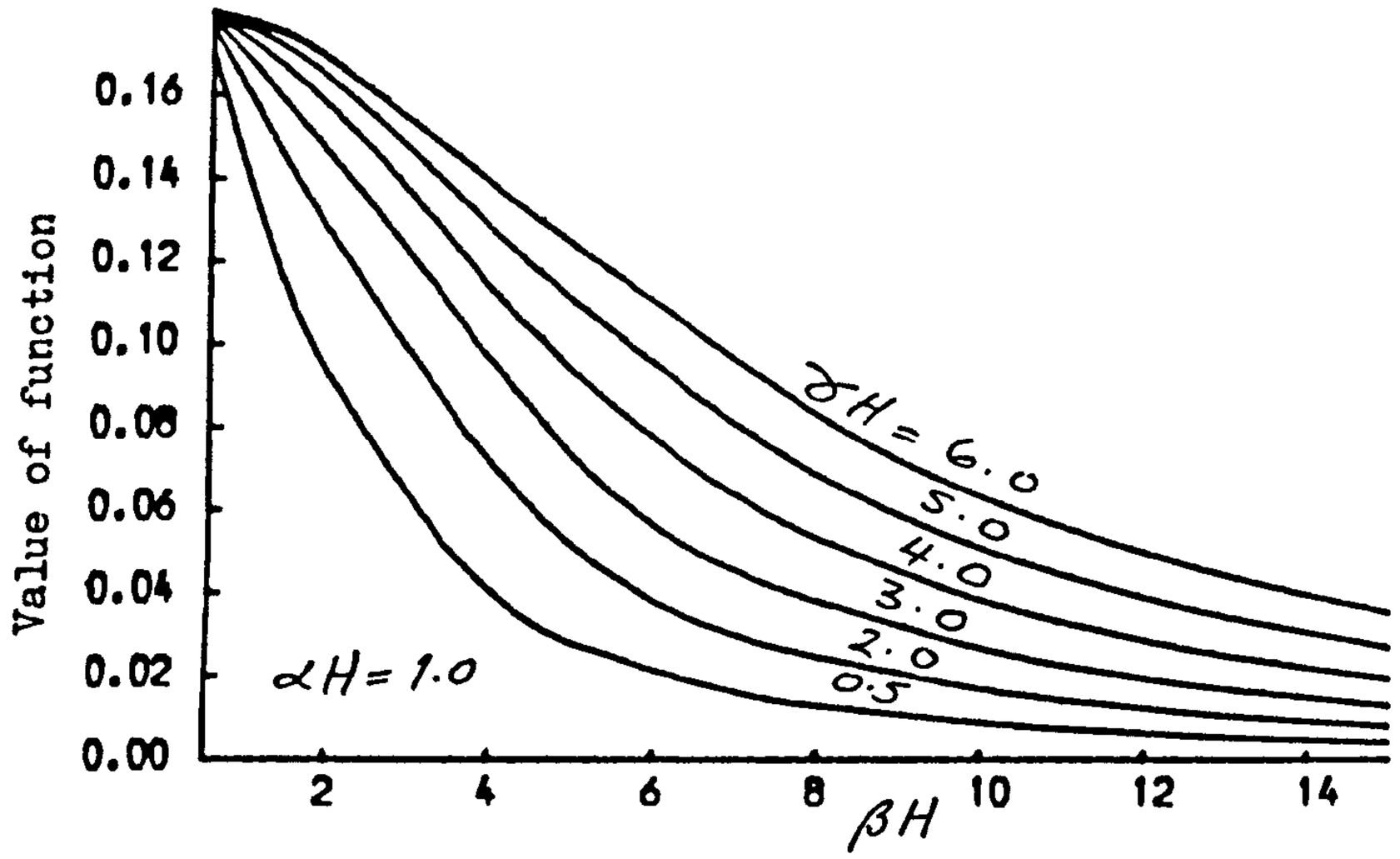

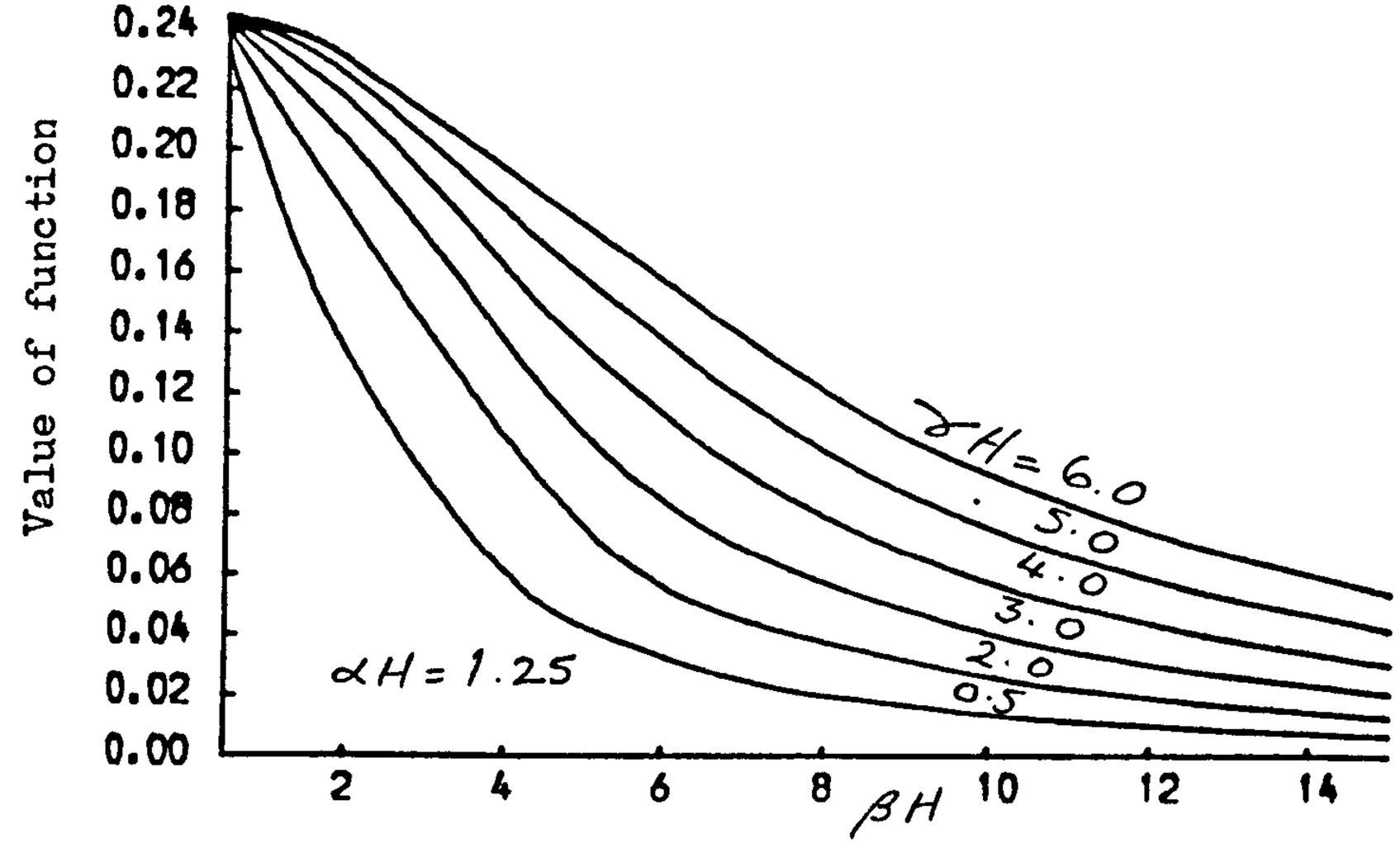

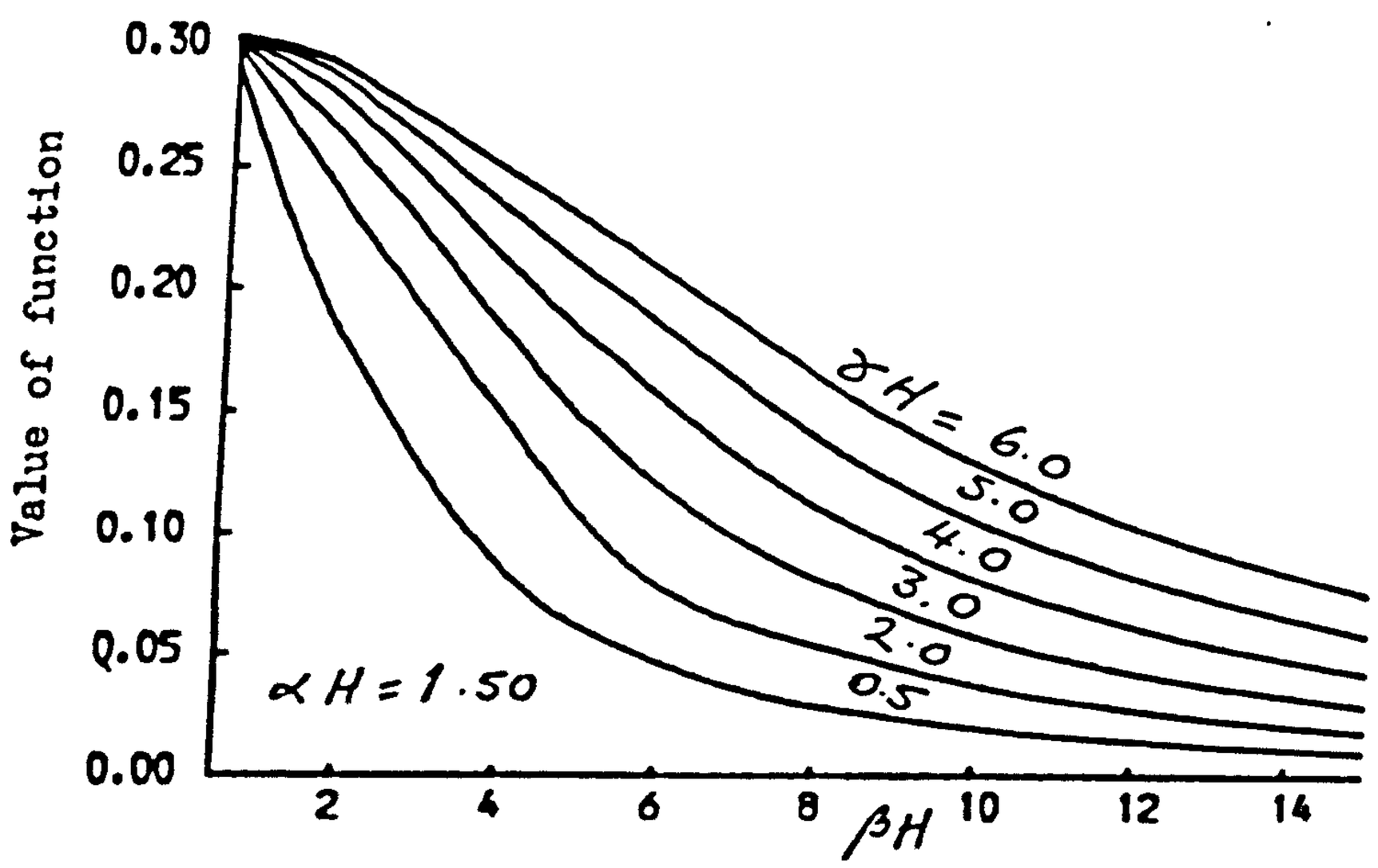

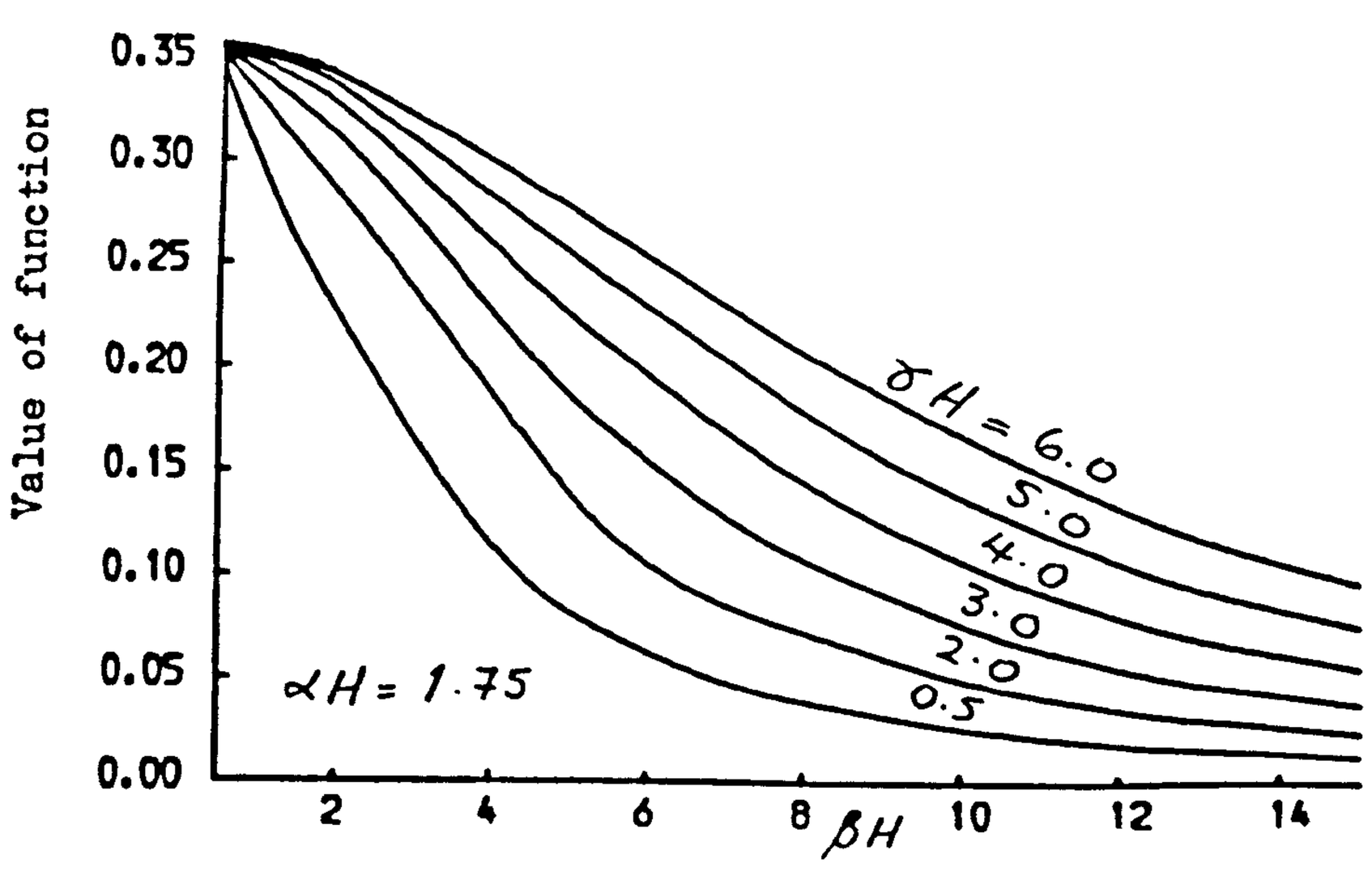

Fig. 2.18 Distributions of moment function F_4

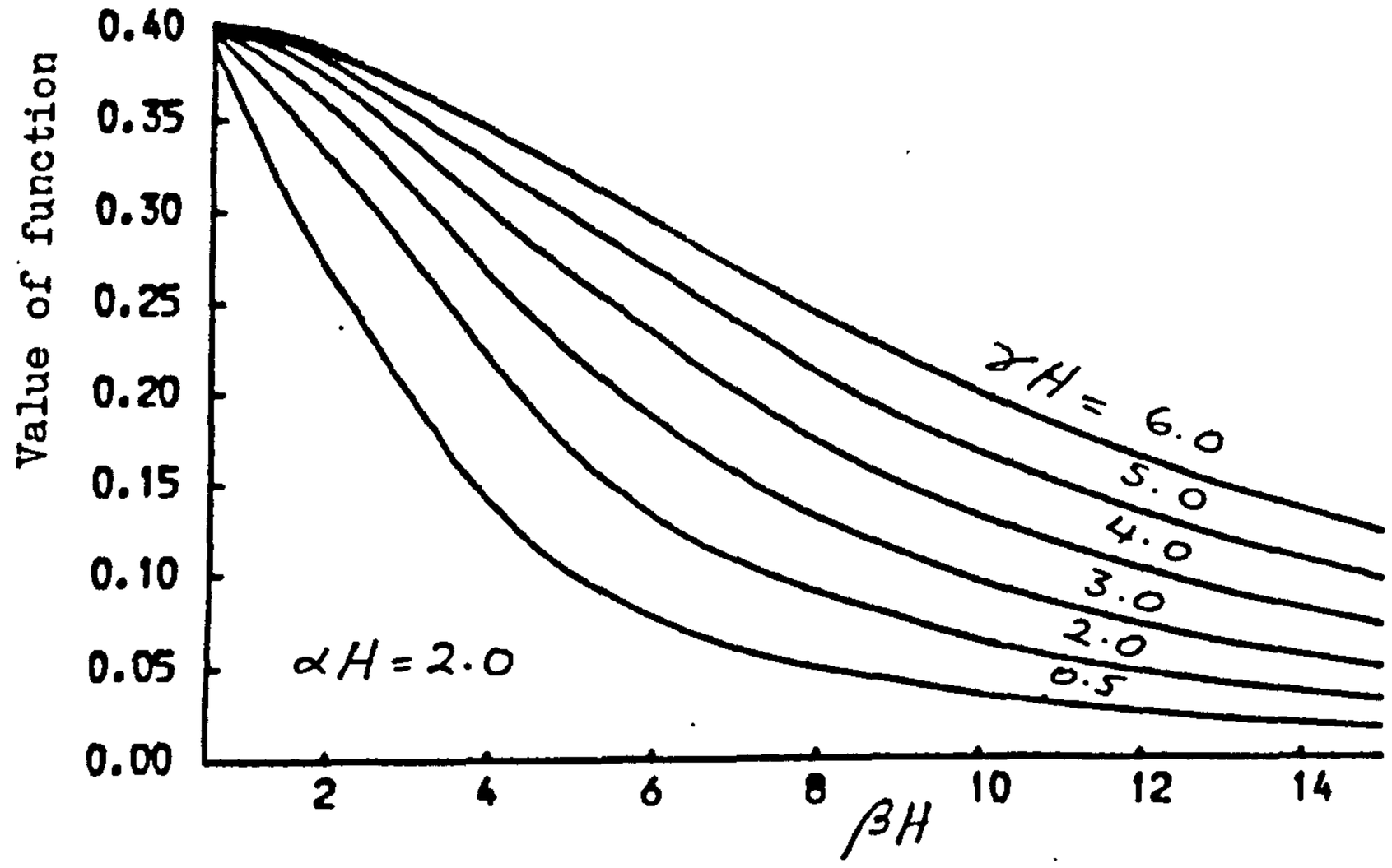

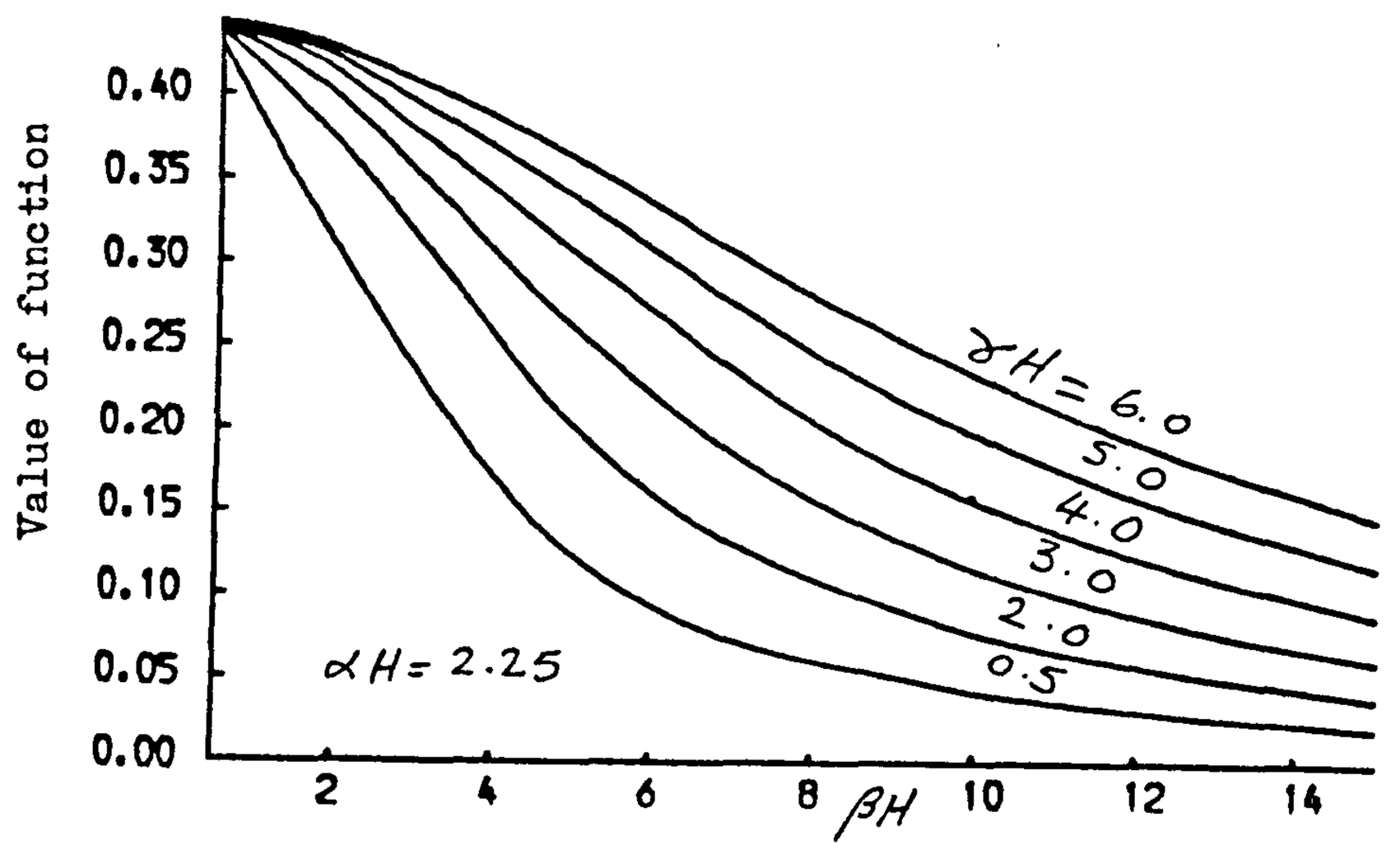

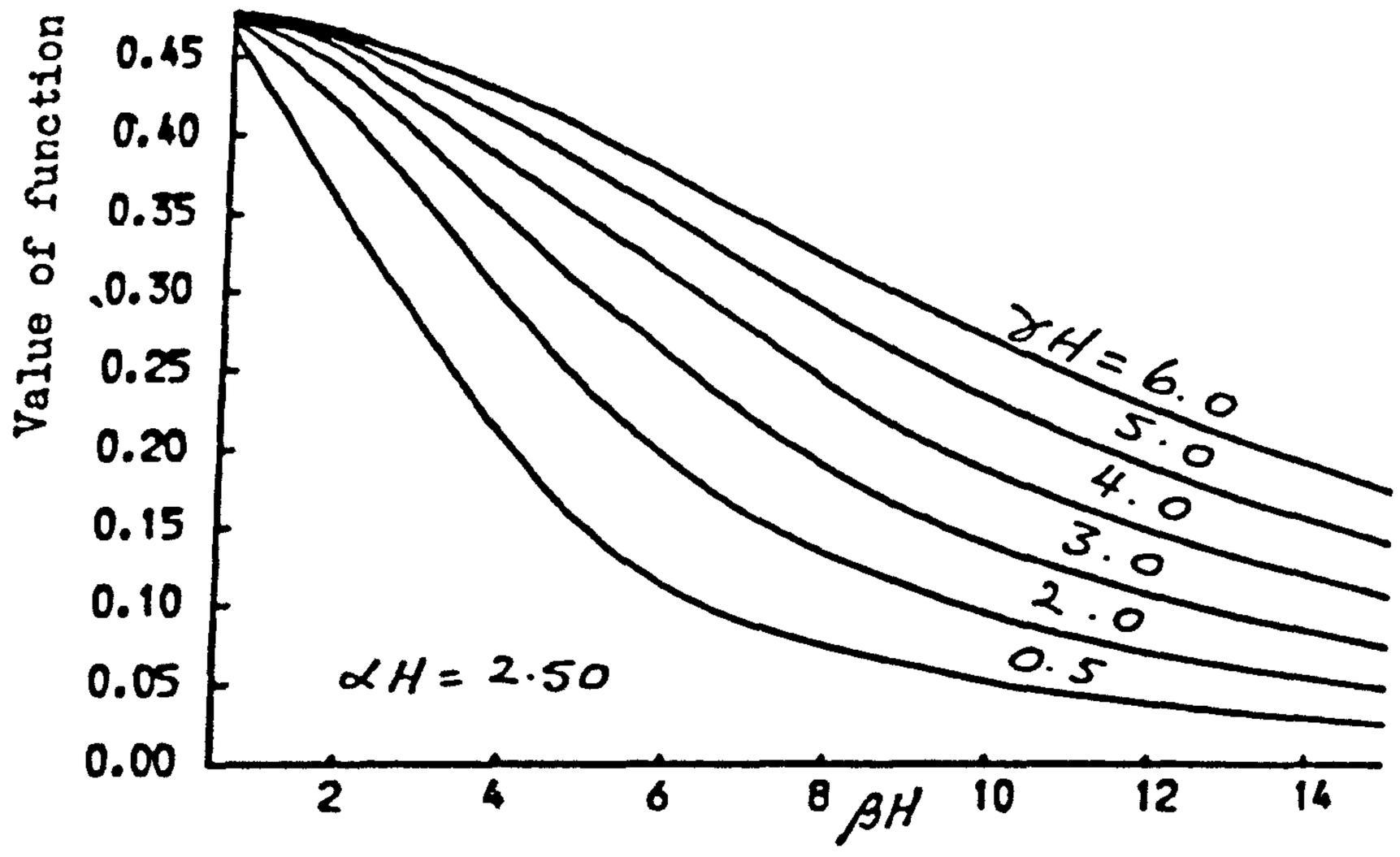

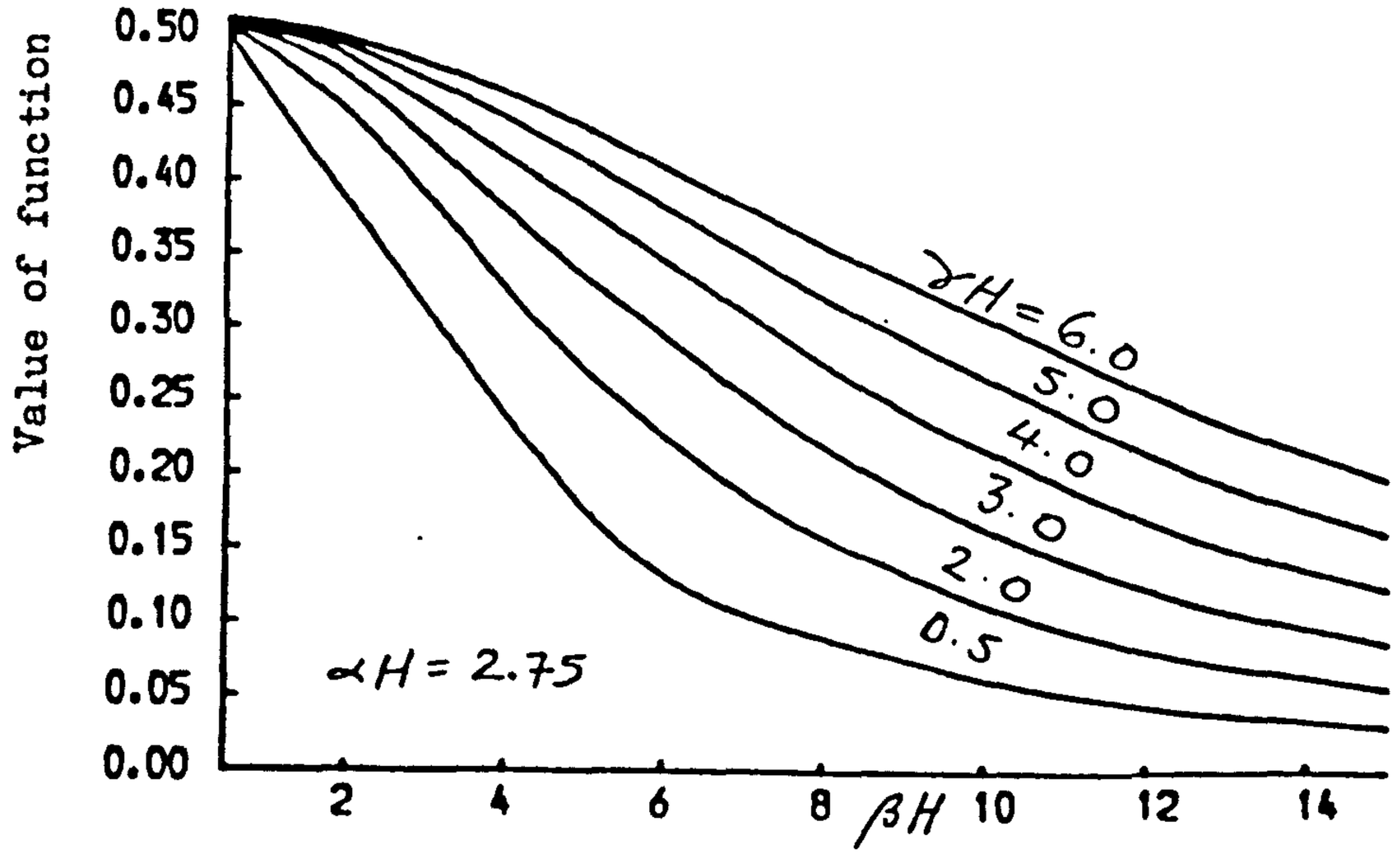

Fig. 2.19 Distributions of moment function F_4

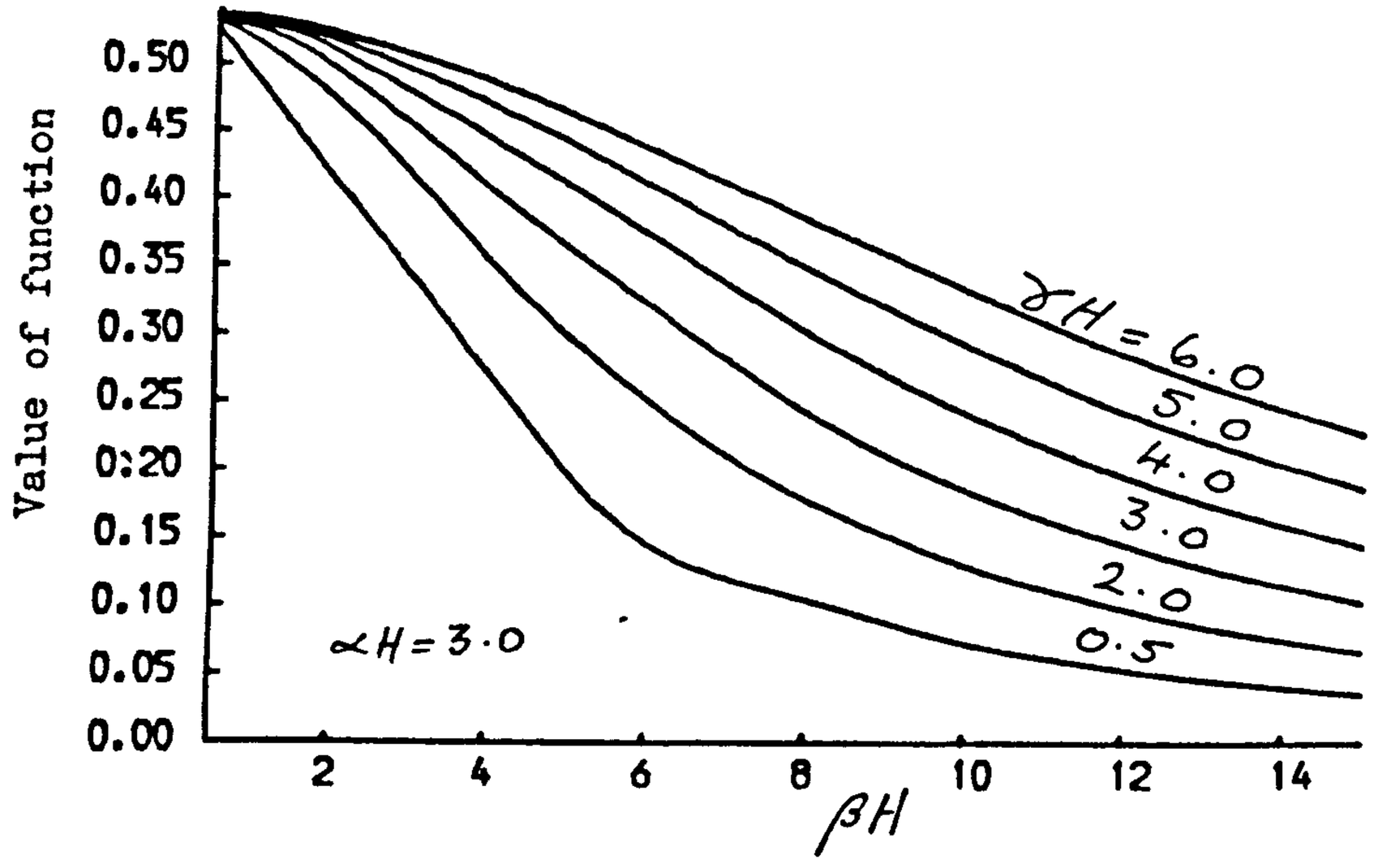

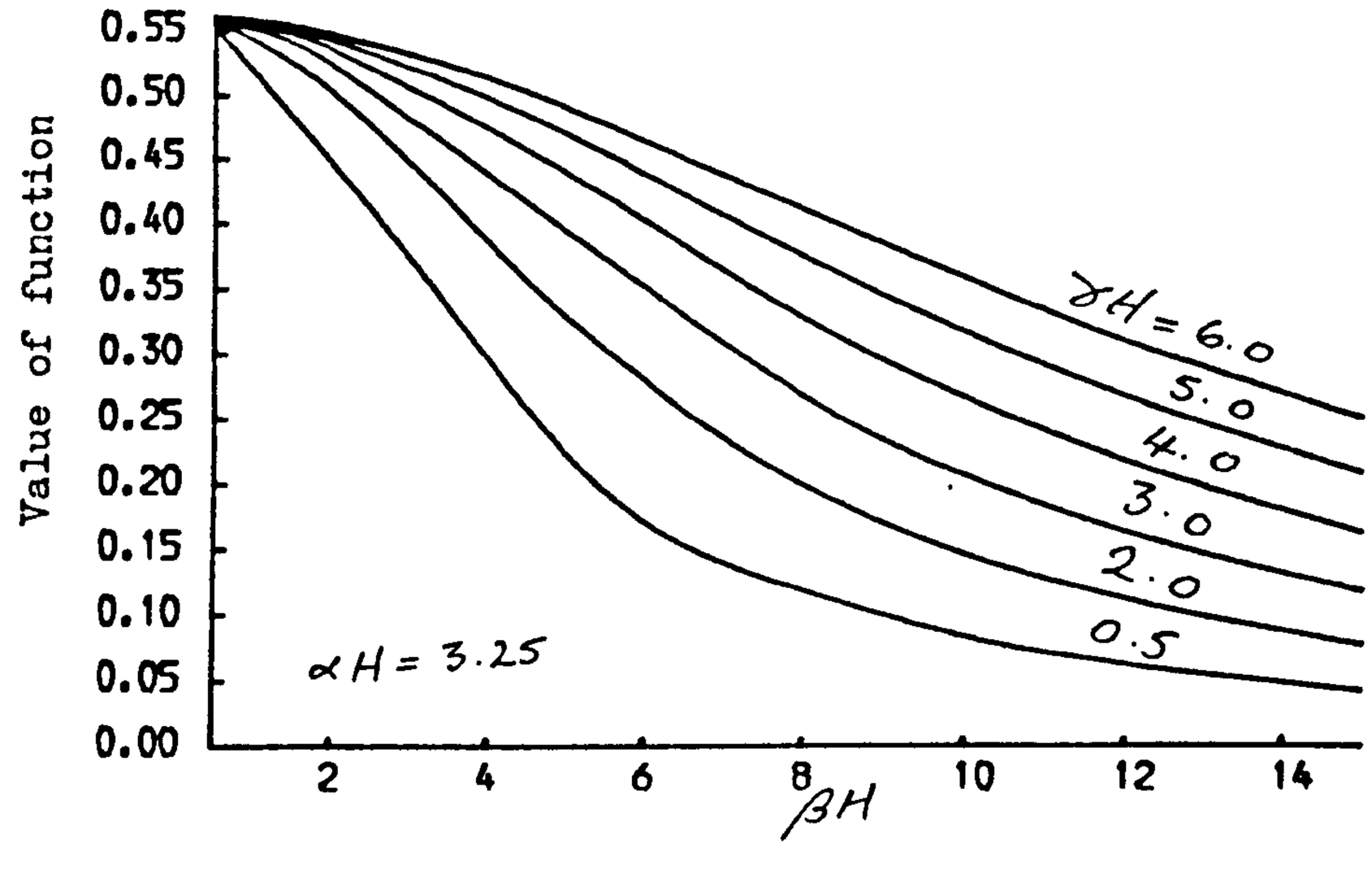

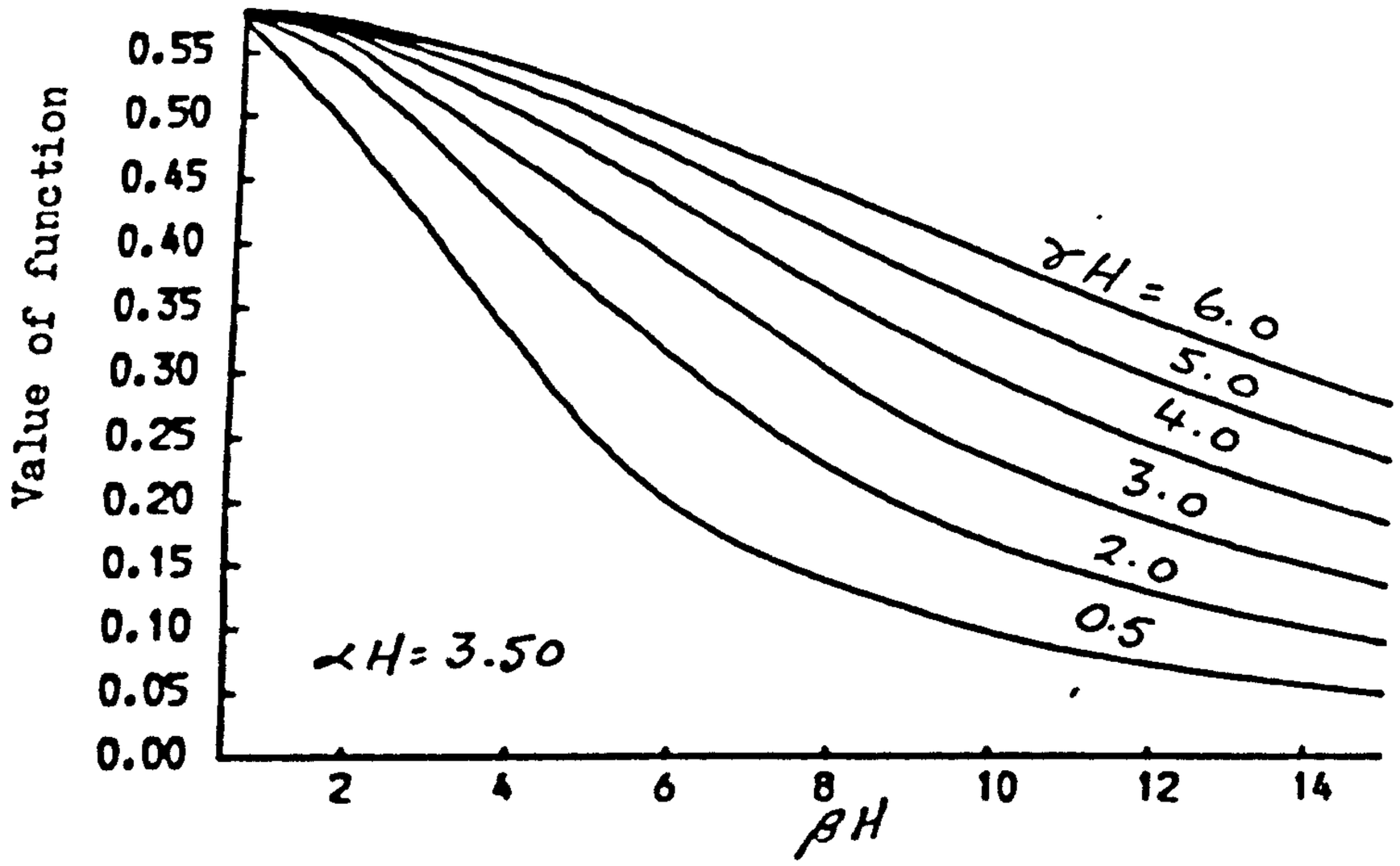

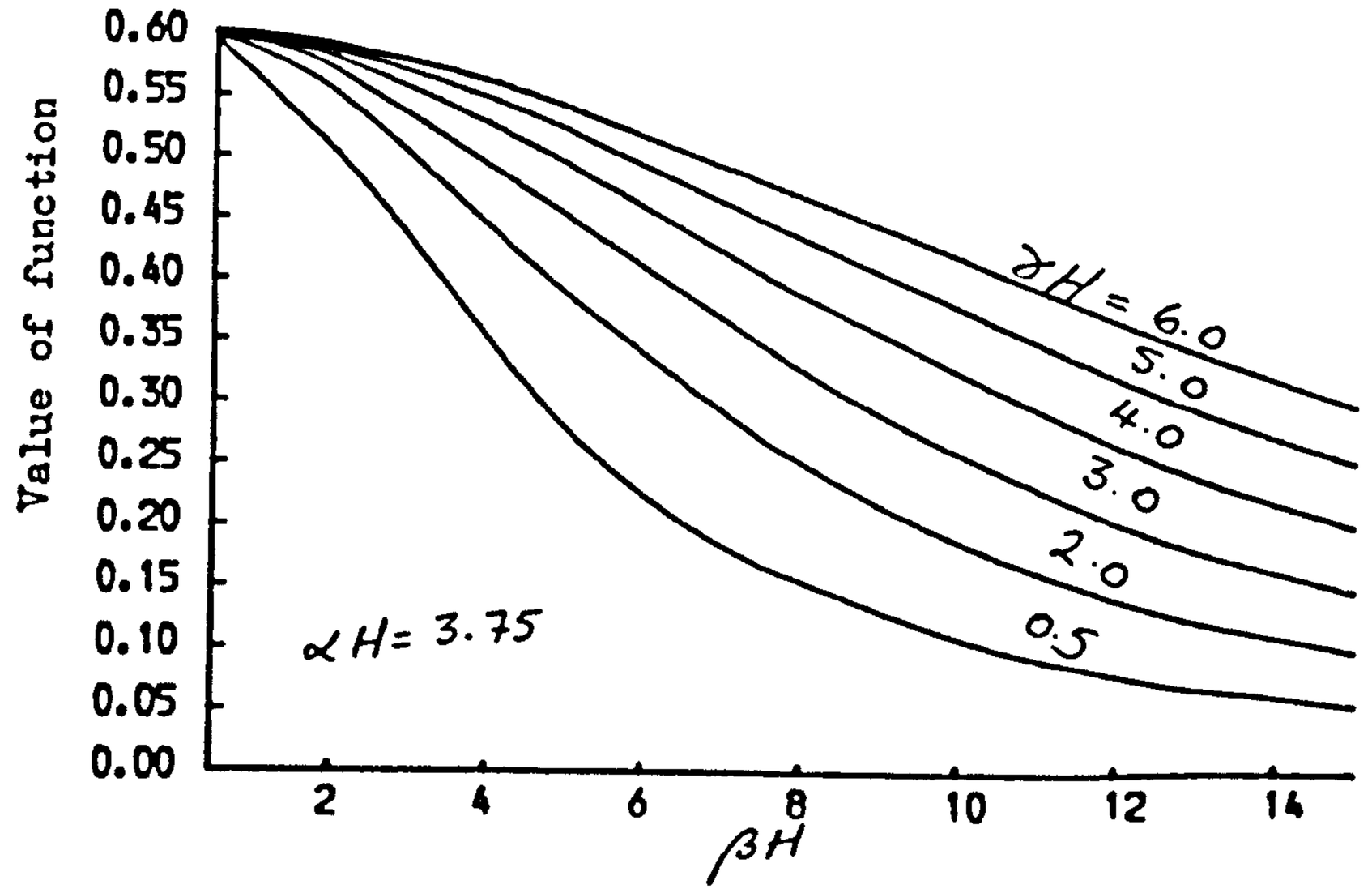

Fig. 2.20 Distributions of moment function F_4

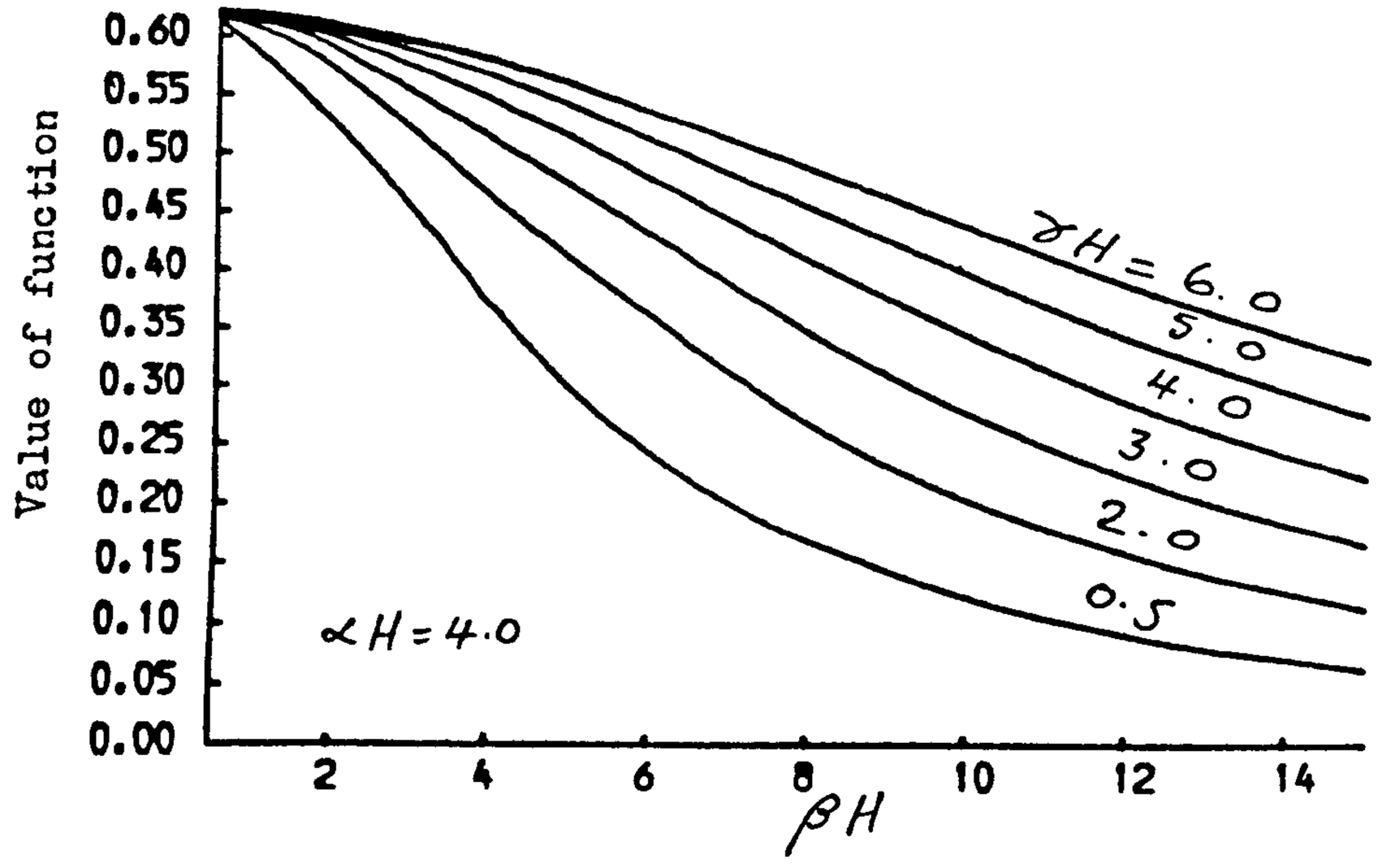

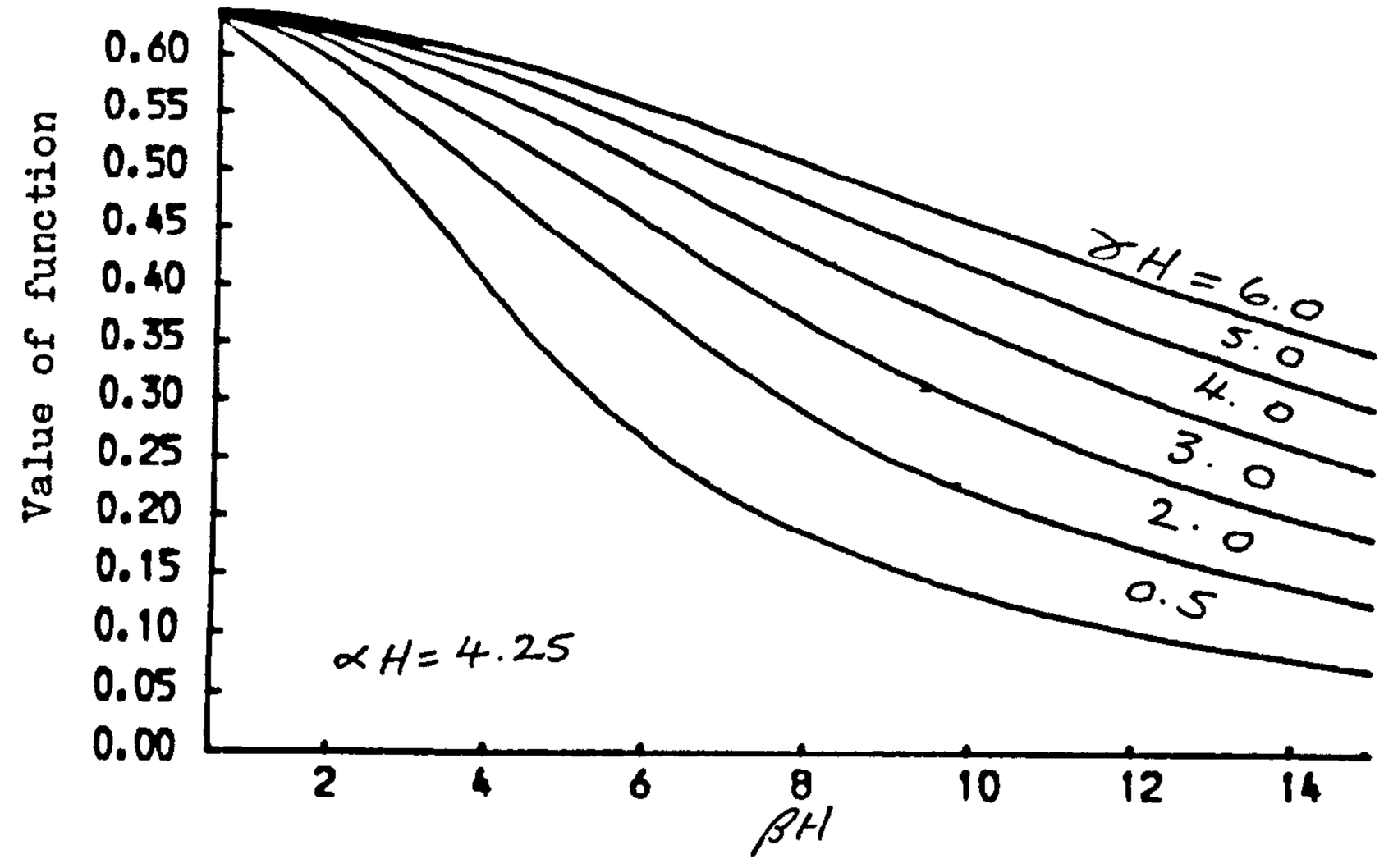

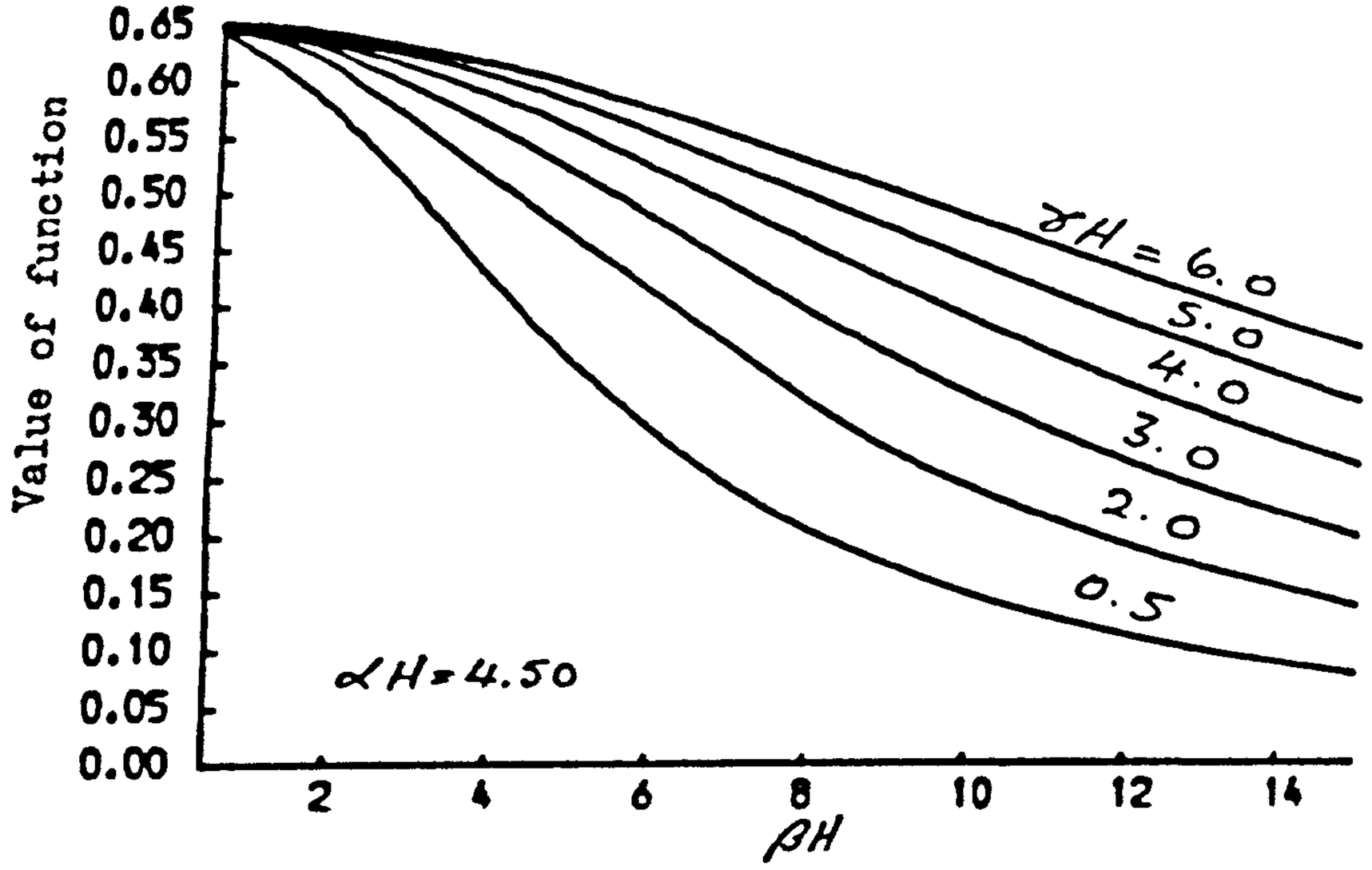

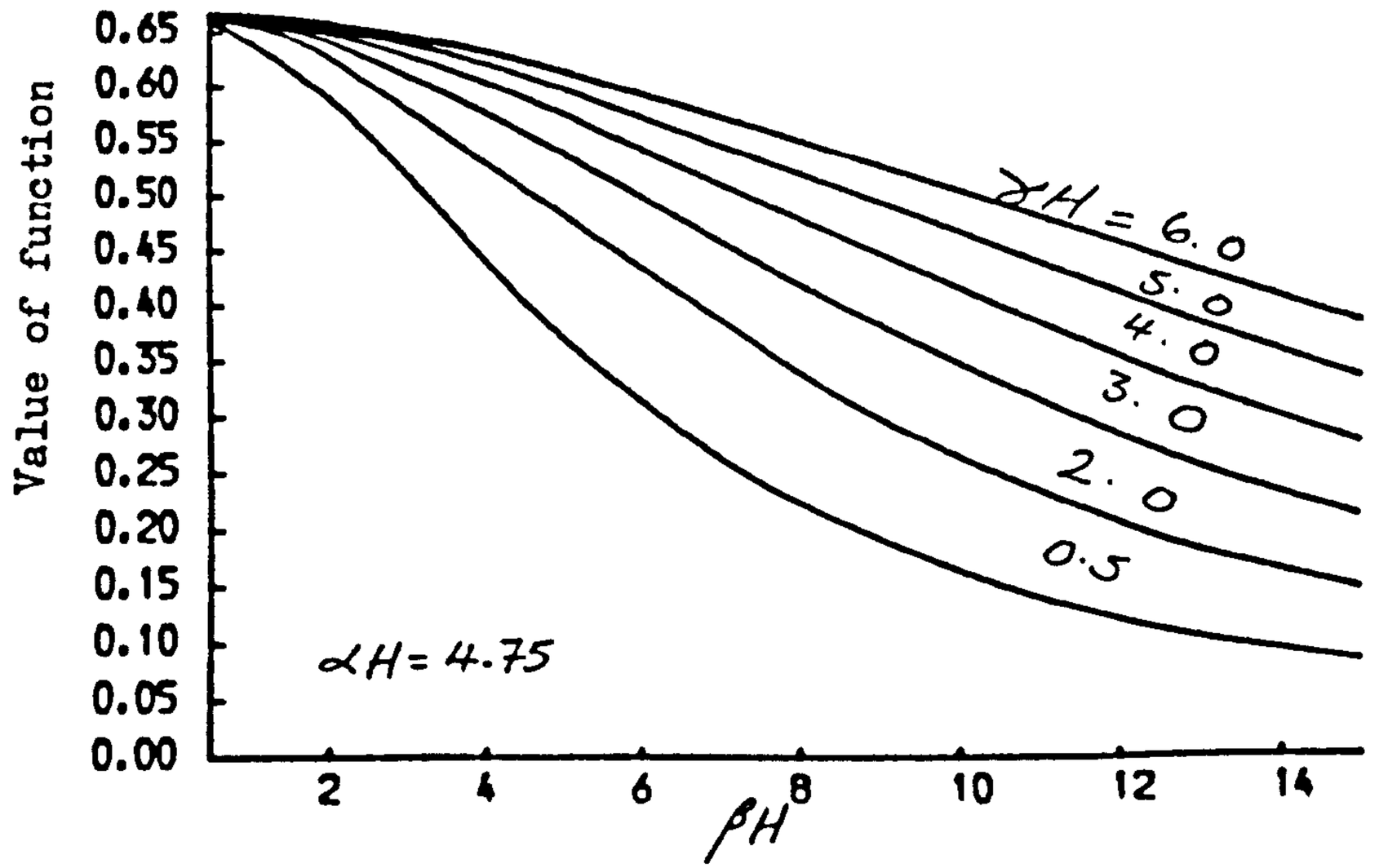

Fig. 2.21 Distributions of moment function F_4

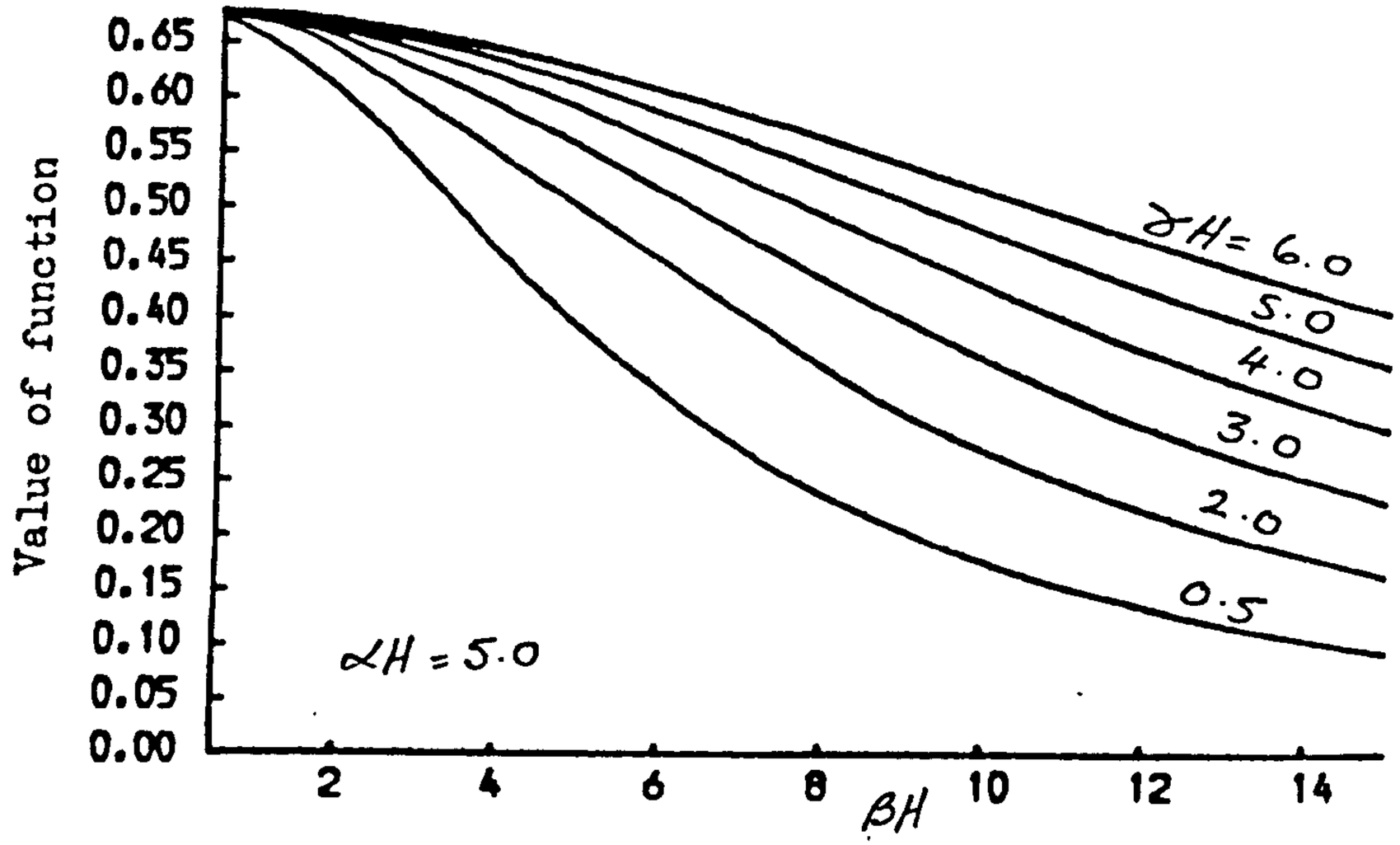

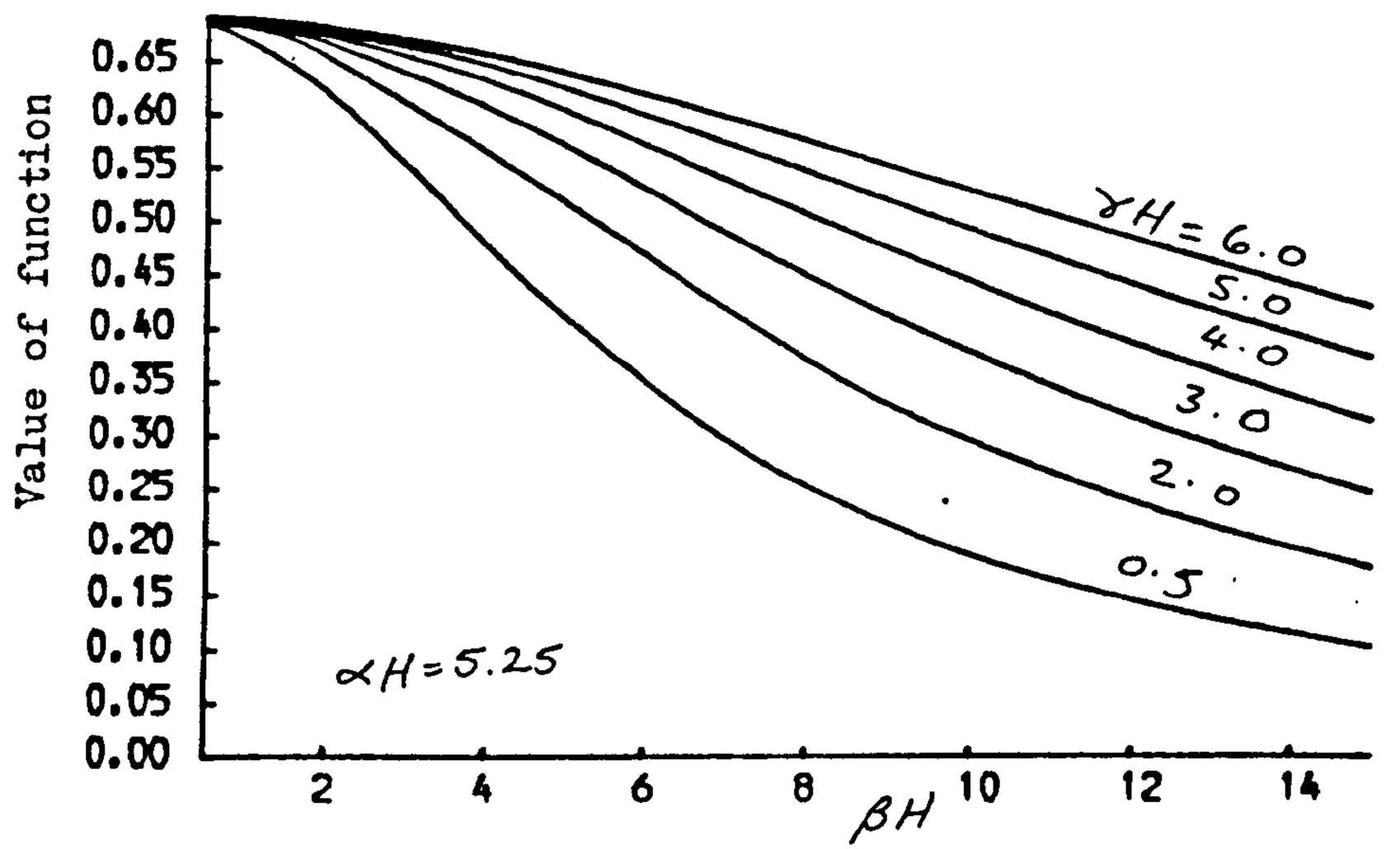

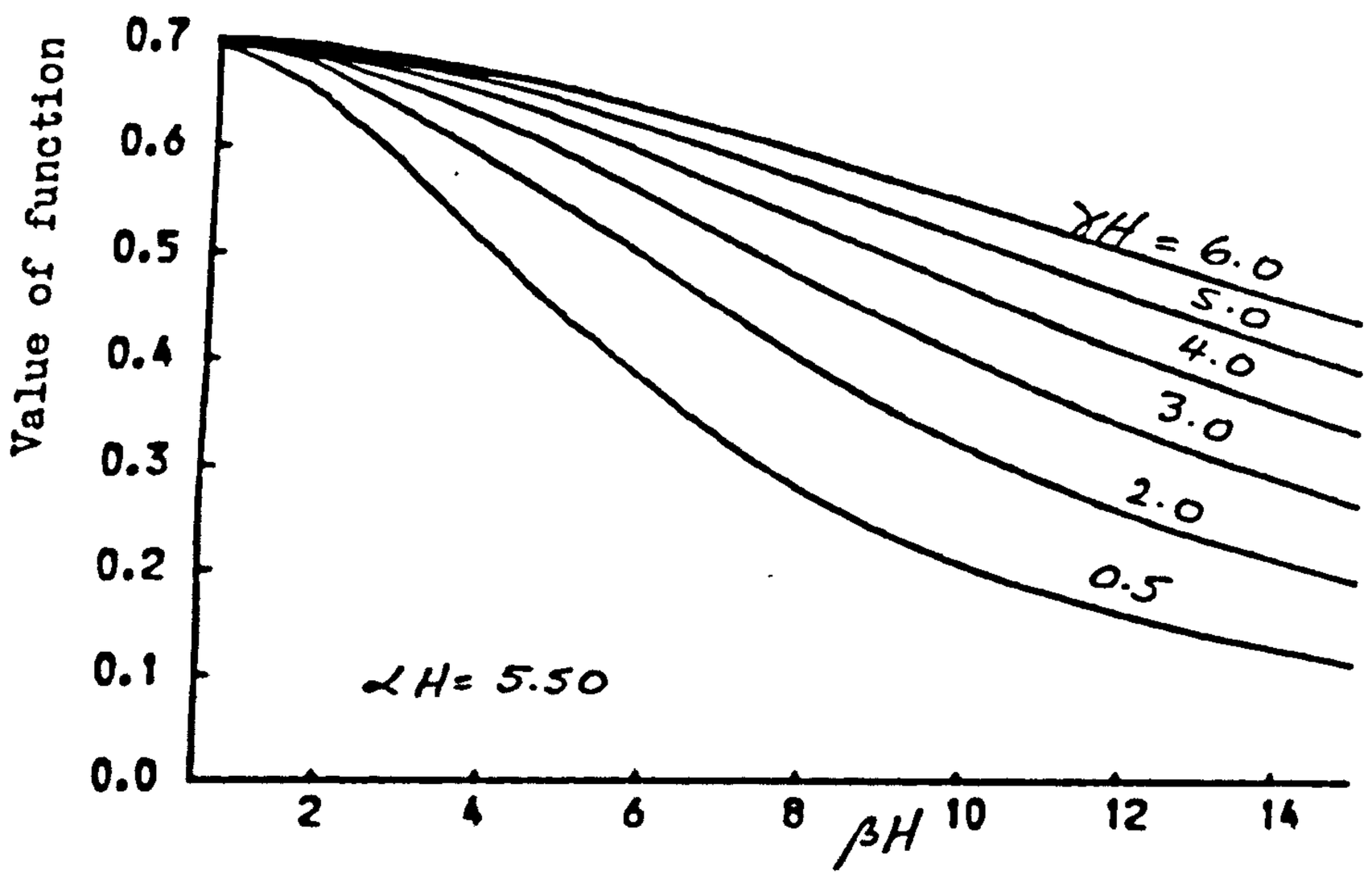

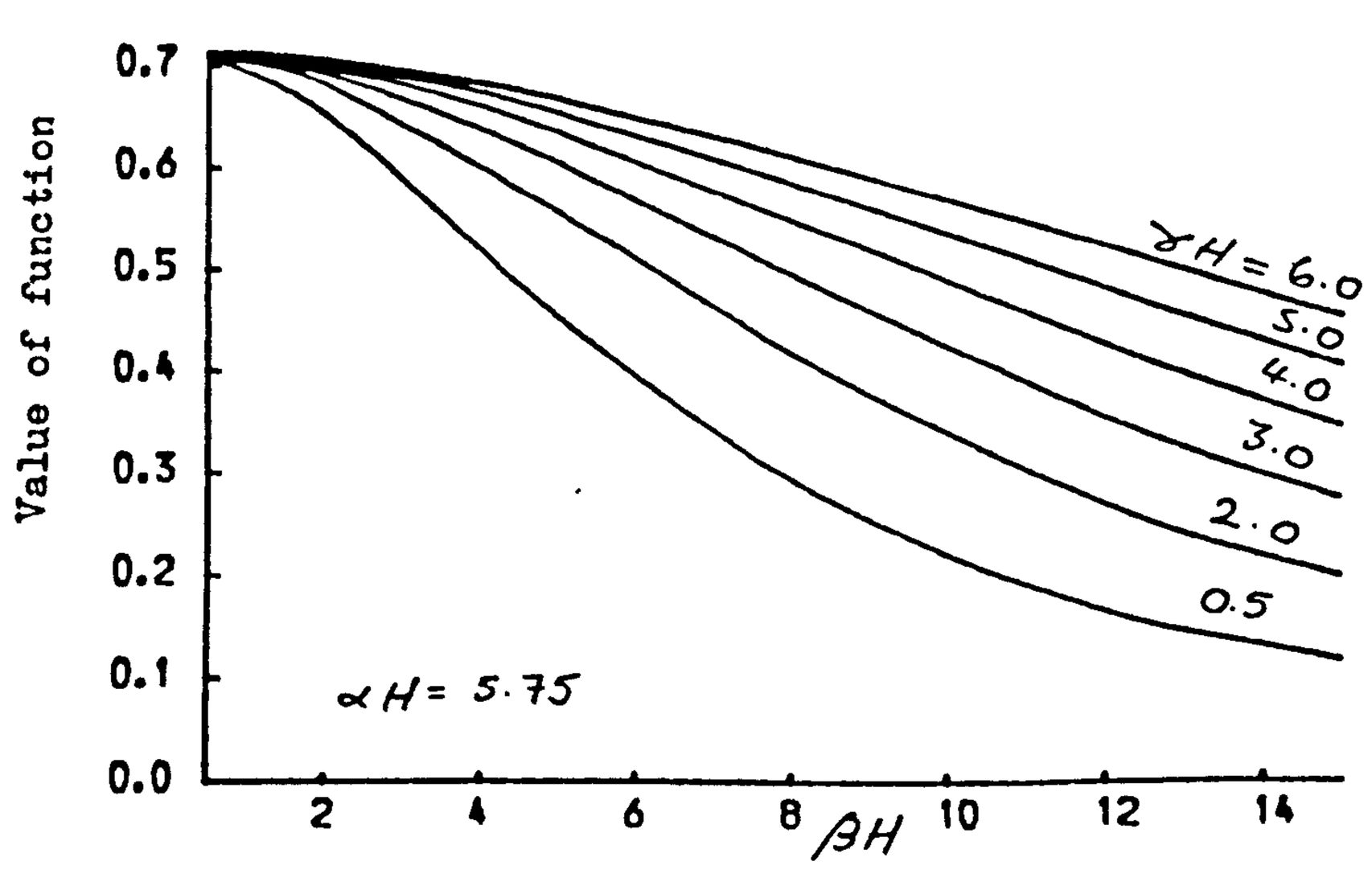

Fig. 2.22 Distributions of moment function F_4

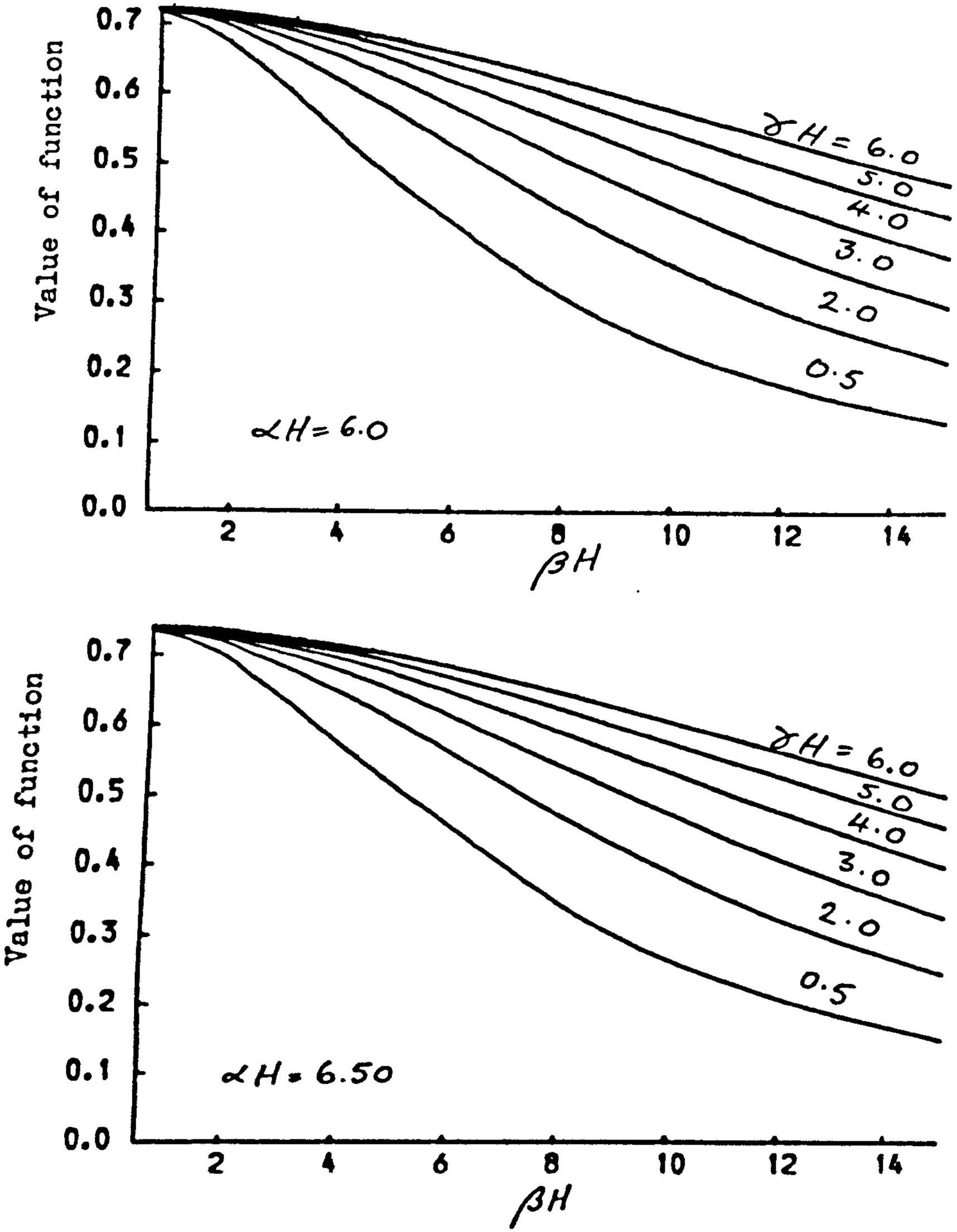

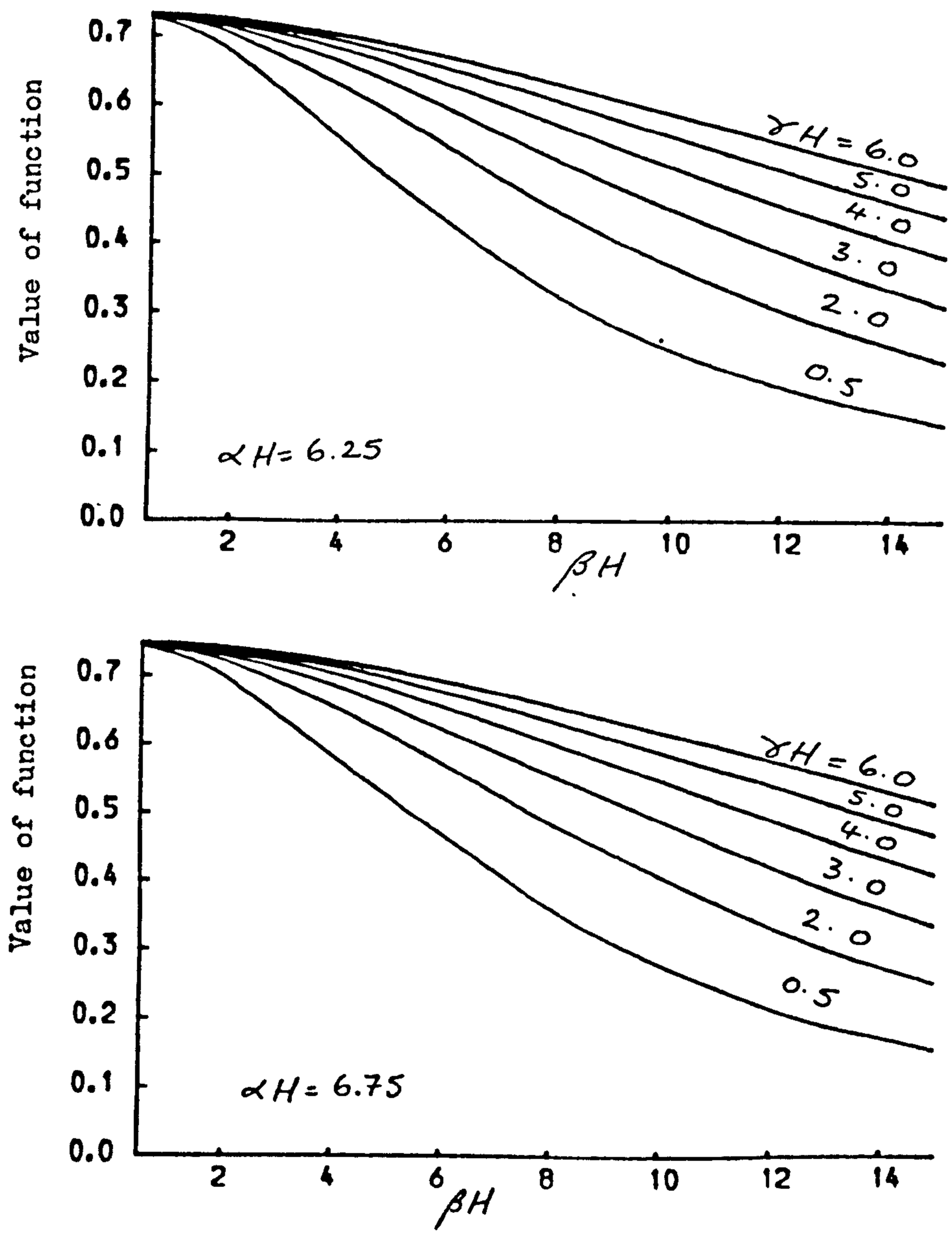

Fig. 2.23 Distributions of moment function F_4

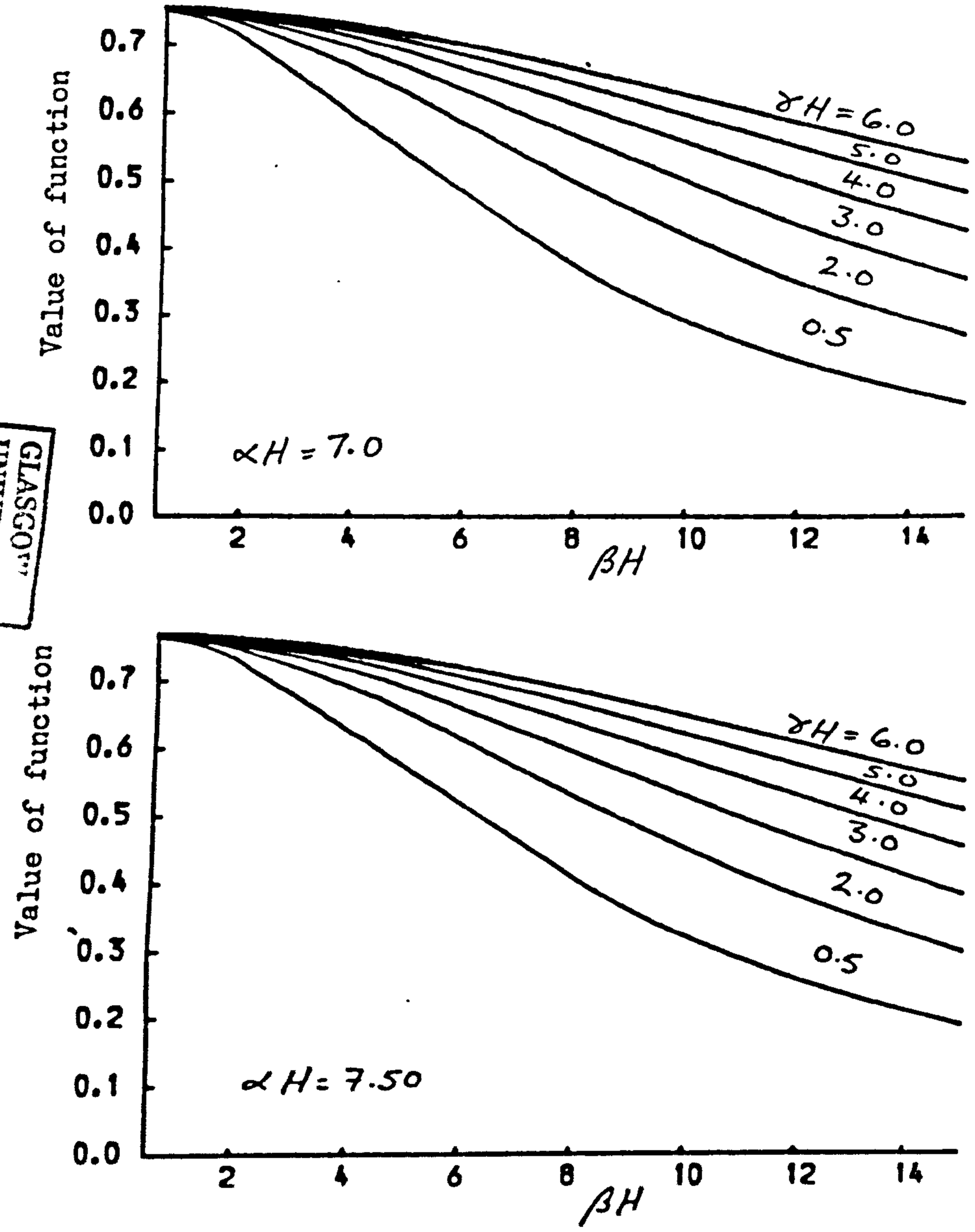

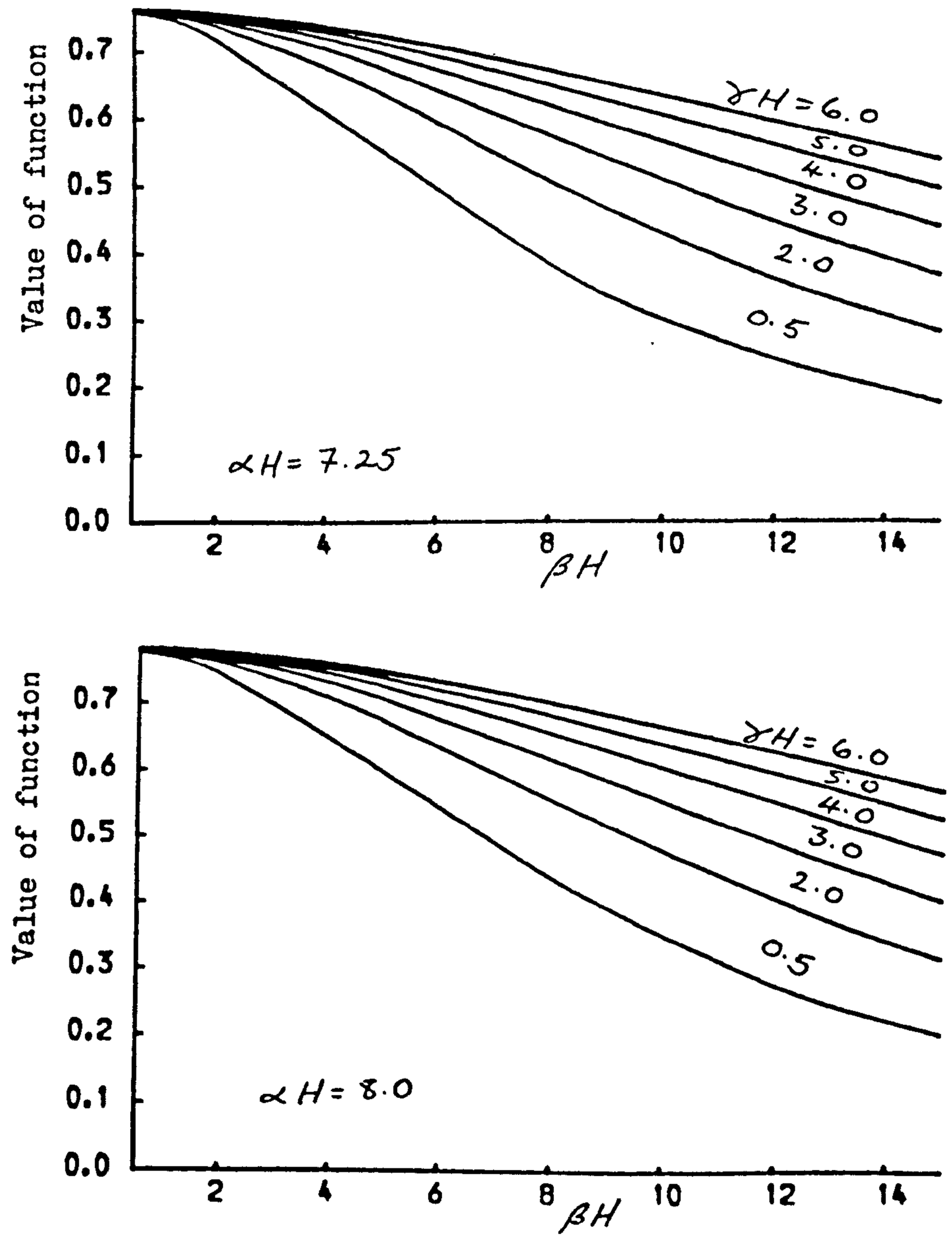

Fig. 2.24 Distributions of moment function F_4